



Universitat
de les Illes Balears

DOCTORAL THESIS
2022

**STUDY OF POTENTIAL ALTERNATIVES TO HUMAN
DIGESTIVE ENZYMES AND PREDICTION OF
DIGESTIBILITY AND BIOACCESSIBILITY OF
STARCH CONTAINING MEALS**

Francina Maria Payeras Perelló



Universitat
de les Illes Balears



**FRESENIUS
KABI**

caring for life

DOCTORAL THESIS
2022

Doctoral Programme of Chemical Science and Technology

**STUDY OF POTENTIAL ALTERNATIVES TO HUMAN
DIGESTIVE ENZYMES AND PREDICTION OF
DIGESTIBILITY AND BIOACCESSIBILITY OF
STARCH CONTAINING MEALS**

Francina Maria Payeras Perelló

Thesis Supervisor: Nadja Siegert

Thesis Supervisor: Susana Simal Florindo

Thesis tutor: Susana Simal Florindo

Doctor by the Universitat de les Illes Balears



Universitat
de les Illes Balears

Dr Susana Simal Florindo, of Universitat de les Illes Balears

I DECLARE:

That the thesis titles Study of potential alternatives to human digestive enzymes and prediction of digestibility and bioaccessibility of starch containing meals, presented by Francina Maria Payeras Perelló to obtain a doctoral degree, has been completed under my supervision and meets the requirements to opt for an International Doctorate.

For all intents and purposes, I hereby sign this document.

Signature

Palma de Mallorca, 26 Jan 2022

ACKNOWLEDGEMENTS

First of all, I would like to express my sincere gratitude to my directors, Dr Susana Simal and specially Dr Nadja Siegert, for your valuable guidance throughout my studies, for your encouragement, support and for all the opportunities I was given to complete this thesis.

The author and directors would like to acknowledge Grant PID2019-106148RR-C43 funded by MCIN/AEI/ 10.13039/501100011033 for the financial support.

I would like to acknowledge Prof. Crispulo Gallegos for giving me the opportunity to join I&D Complex Formulations department at Fresenius Kabi.

Many thanks also to my colleagues/friends, Lucia, Laura, Nadja, Seba and Miga for your patient support, but mainly for all the great moments.

Finalment, m'agradaria agrair a la familia i amics per la seva paciència i suport durant aquests anys, però sobretot per els moments de diversió i desconexió.



INDEX

Abstract	Page 10
Resum	Page 12
Resumen	Page 14
Chapter 1: Introduction	Page 20
1. Clinical nutrition	Page 22
2. Human digestion	Page 22
3. In vitro digestion methods	Page 31
4. Digestive enzymes	Page 38
5. Bile	Page 61
6. Electrolytes present in gastrointestinal tract	Page 62
7. pH throughout gastrointestinal tract	Page 65
8. Carbohydrates	Page 68
9. In vitro digestion of carbohydrates	Page 79
10. References	Page 82
Chapter 2: Objectives	Page 96
Chapter 3: Materials and methods	Page 101
1. Chemicals	Page 103
2. Simulated digestive fluids	Page 104
3. Enzyme activity methods	Page 105
4. Determination of bile acids concentration	Page 123
5. Determination of the mixing speed	Page 125
6. Method to stop digestion	Page 125
7. Buffer for static digestion method	Page 125
8. Meal	Page 126
9. In vitro digestion method	Page 137
10. Static digestion method	Page 137
11. Dynamic digestion method	Page 142
12. In vitro digestion runs	Page 161
13. Analytical methods	Page 163
14. References	Page 171

Chapter 4: Results and discussion**Page 177**

1. Introduction Page 179
2. Enzyme activity methods Page 179
3. Adaptation of enzymes used in in vitro methods to physiological levels Page 192
4. Adaptation of non-enzymatic key parameters of in vitro methods Page 209
5. Verification of carbohydrate adapted in vitro methods with real foods Page 217
6. In vitro digestion of starch Page 234
7. Impact of protein on starch digestion Page 243
8. Impact of fat on starch digestion Page 254
9. Impact of food matrix on starch digestion Page 267
10. References Page 279

Chapter 5: Conclusions**Page 284**

ABSTRACT

This PhD thesis investigates the adaptation of two in vitro digestion methods for glycaemic index prediction and also outlines the effect of the macronutrients on the digestion of two starch sources.

Potential alternatives to the main digestive human enzymes (α -amylase, pepsin, trypsin, lipase), which are expensive or not commercially available, have been studied based on their pH and temperature profiles to build a strong in vivo–in vitro correlation. This is important, as commonly used enzyme activity methods are often performed at non-physiological conditions such as 20°C, in the absence of digestive electrolytes and without considering the pH variations that occur during digestion. Therefore, the effect of digestive electrolytes on enzyme activity was also studied. Moreover, the storage stability of enzymatic solutions was studied and the maximum storage time at constant enzyme activity was defined.

The alternative sources found in this study mimic the pH profile of the human enzymes at 37°C. The results demonstrated that, for the alternative sources, the effect of the temperature on the activity was similar to that of the human enzyme. In the presence of digestive electrolytes, the results revealed that each enzyme reacts differently. While α -amylase increased its activity in the presence of electrolytes, trypsin activity decreased and for lipase and pepsin no change in activity was found. Furthermore, enzymatic solutions can be used in in vitro digestion methods for a long period when stored at specific conditions (temperature, solvent).

The digestion of carbohydrates and the effect of other macronutrients (protein and fat) was studied by determining the amount of glucose released from the different sources. The released glucose represents glucose available for intestinal absorption and in vivo, these glucose levels would impact blood glucose levels, thus being of special interest for products intended for patients with diabetes.

The digestion of three foods (rice, potato, cocoa cream) was studied with two in vitro digestion methods (static and dynamic). With the aim of demonstrating that the selected in vitro digestion methods could provide reliable results, the measured glycaemic index (GI) was compared with reported values. The obtained results showed that the in vitro GI measured with both methods was slightly lower than the reported values. However, the reported GI for those meals was reached for most of the meals by applying a correction factor (with the exception of the cacao cream) when the dynamic digestion method was performed.

To identify the digestion pattern of different carbohydrate sources, the digestion of two commercial starch sources (starch from rice and starch from potato) was studied with both methods (static and dynamic), the degree of hydrolysis (DH) and GI being measured. Then, the effect of the other macronutrients on the starch digestion was studied by adding protein (egg whites from chicken) or fat (olive oil or butter) to the starch. In general, clinical nutrition products for enteral route include the three macronutrients, thus, the digestion of meals that contains starch, protein and fat was also studied. The main differences obtained in the digestion of the different meals were due to their disintegration and solubilisation profiles, which would affect the time needed for the meal to be reached by the enzymes and subsequent enzymatic starch hydrolysis.

Finally, the obtained results (DH and GI) with both in vitro digestion methods were compared, leading to the conclusion that there were no differences between the DH and GI obtained with the adapted static or adapted dynamic digestion methods.

RESUM

Aquesta tesi investiga l'adaptació de dos mètodes de digestió in vitro per a la predicció de l'índex glicèmic (GI) i descriu l'efecte dels macronutrients a la digestió de dos tipus de midó.

S'han estudiat potencialment alternatives als principals enzims digestius humans (α -amilasa, pepsina, tripsina, lipasa), que són cars o no estan disponibles comercialment, en funció dels seus perfils de pH i temperatura per a la obtenció d'una bona correlació in vivo-in vitro. Això és rellevant, ja que els mètodes per a mesurar l'activitat enzimàtica es solen dur a terme en condicions que no són fisiològiques, com podria ser a 20°C, absència d'electròlits digestius o sense considerar les variacions de pH que ocorren durant la digestió. Per aquest motiu, també s'ha estudiat l'efecte dels electròlits digestius a l'activitat enzimàtica. S'ha estudiat l'estabilitat de les dissolucions enzimàtiques durant el seu magatzematge i s'ha definit el temps de magatzematge màxim a activitat enzimàtica constant.

Les alternatives trobades en aquest estudi imiten el perfil de pH dels enzims humans a 37°C. Els resultats han demostrat que, per a les alternatives d'aquests enzims, l'efecte de la temperatura a l'activitat enzimàtica és similar als enzims humans. Els resultats han revelat que en la presència d'electròlits digestius cada enzim reacciona de manera diferent. Mentre l' α -amilasa augmenta la seva activitat amb la presència d'electròlits, la tripsina disminueix la seva activitat i en el cas de la lipasa i pepsina no es varen observar canvis en la seva activitat. S'ha trobat que les dissolucions enzimàtiques es poden usar en els mètodes de digestió in vitro durant un llarg període de temps quan aquestes es guarden en condicions específiques (temperatura i dissolvent).

S'ha estudiat la digestió dels carbohidrats i l'efecte d'altres macronutrients (proteïna i grassa), determinant la quantitat de glucosa alliberada dels carbohidrats. La glucosa alliberada representa la glucosa disponible per a la seva absorció intestinal i in vivo, aquests nivells de glucosa tendrien un impacte en els nivells de glucosa en sang, el que és d'especial interès per a productes per a pacients amb diabetis.

S'ha estudiat la digestió de tres menjars (arròs, patata i crema de cacau) amb dos mètodes de digestió in vitro (estàtic i dinàmic). Amb l'objectiu de demostrar que els mètodes de digestió in vitro seleccionats poden proporcionar resultats fiables, els GI obtinguts s'han comparat amb els valors publicats (in vivo). Els resultats obtinguts demostren que els GI in vitro mesurats amb ambdós mètodes són més baixos comparats amb els valors publicats. No obstant, aplicant un factor de correcció (excepte per la crema de cacau en el mètode dinàmic) es varen obtenir els GI publicats per a gairebé tots els menjars.

Per a la identificació del patró de digestió d'alguns carbohidrats, s'ha estudiat la digestió de dos tipus de midó (d'arròs i patata) usant ambdós models in vitro i s'ha mesurat el grau d'hidròlisis (DH) i el GI. Es va estudiar l'efecte dels altres macronutrients en la digestió dels midons afegint proteïna (clares d'ou de pollastre) o grassa (oli d'oliva o mantega) al midó. En general, els productes de nutrició clínica enteral inclouen els tres macronutrients, i per aquest motiu també es va estudiar la digestió de menjars que contenen midó, proteïna i grassa. Les diferències principalment obtingudes es deuen als perfils de solubilització dels diferents menjars, el que afectaria el temps necessari per als enzims per arribar al menjar i la posterior hidròlisis enzimàtica del midó.

Es varen comparar els resultats obtinguts amb ambdós mètodes de digestió in vitro. Aquesta comparació va conduir a la conclusió que no hi havia diferències entre el DH i GI obtinguts amb els models estàtic o dinàmic.

RESUMEN

Esta tesis investiga la adaptación de dos métodos de digestión in vitro para la predicción del índice glucémico (GI) i describe el efecto de los macronutrientes en la digestión de dos tipos de almidón.

Se han estudiado potencial alternativas a los principales enzimas digestivos humanos (α -amilasa, pepsina, tripsina, lipasa), que son caros o no están disponibles comercialmente, en función de sus perfiles de pH y temperatura para la obtención de una buena correlación in vivo-in vitro. Esto es relevante, ya que los métodos para medir la actividad enzimática se suelen llevar a cabo en condiciones no fisiológicas, como a 20°C, ausencia de electrolitos digestivos o sin considerar los cambios de pH que ocurren durante la digestión. Por este motivo, se ha estudiado el efecto de los electrolitos digestivos a la actividad enzimática. Se ha estudiado la estabilidad de las disoluciones enzimáticas durante su almacenamiento y se ha definido el tiempo de almacenaje máximo a actividad enzimática constante.

Las alternativas encontradas en este estudio imitan el perfil de pH de los enzimas humanos a 37°C. Los resultados han demostrado que, para las alternativas de estos enzimas, el efecto de la temperatura a la actividad enzimática es similar a los enzimas humanos. Se ha revelado que en la presencia de electrolitos cada enzima reacciona de manera diferente. La α -amilasa aumenta su actividad con la presencia de electrolitos, la tripsina disminuye su actividad y en el caso de la lipasa y pepsina no se observaron cambios en su actividad. Se ha encontrado que las disoluciones enzimáticas se pueden usar en los métodos de digestión in vitro durante un largo periodo de tiempo cuando estas se guardan en condiciones específicas (temperatura y disolvente).

Se ha estudiado la digestión de los carbohidratos y el efecto de otros macronutrientes (proteína y grasa), determinando la cantidad de glucosa liberada de los carbohidratos. La glucosa liberada representa la glucosa disponible para su absorción intestinal y in vivo, estos niveles de glucosa tendrían un impacto en los niveles de glucosa en sangre, lo que es de especial interés para productos para pacientes con diabetes.

Se ha estudiado la digestión de tres comidas (arroz, patata y crema de cacao) con dos métodos de digestión in vitro (estático y dinámico). Con el objetivo de demostrar que los métodos de digestión in vitro seleccionados pueden proporcionar resultados fiables, los GI obtenidos se han comparado con los valores publicados. Los resultados demostraron que los GI in vitro medidos con ambos métodos son más bajos comparados con los valores publicados. No obstante, aplicando un factor corrector (excepto para la crema de cacao en el método dinámico) se obtuvieron los GI publicados.

Para la identificación del patrón de digestión de algunos carbohidratos, se ha estudiado la digestión de dos tipos de almidón (arroz y patata) usando ambos métodos in vitro y se ha medido el grado de hidrólisis (DH) y el GI. Se estudió el efecto de los otros macronutrientes en la digestión de los almidones añadiendo proteína (claras de huevo de pollo) o grasa (aceite de oliva o mantequilla) al almidón. Los productos de nutrición clínica enteral suelen incluir los tres macronutrientes, por lo tanto, se estudió la digestión de comidas que contenían almidón, proteína y grasa. Las diferencias se deben principalmente a los perfiles de solubilización de las comidas, lo que afectaría el tiempo necesario de los enzimas para llegar a la comida y la posterior hidrólisis del almidón.

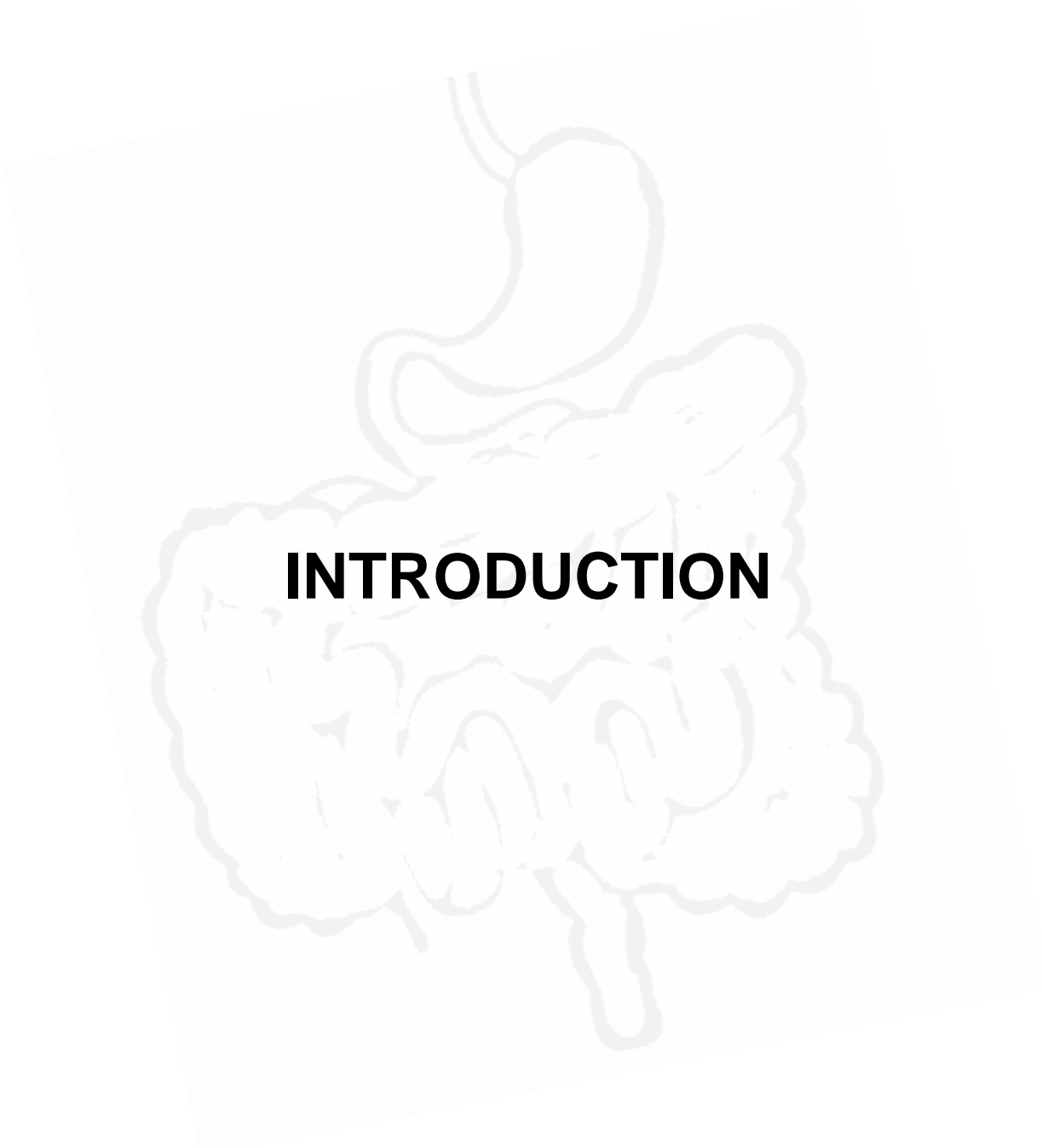
Se compararon los resultados obtenidos con ambos métodos de digestión in vitro y se concluyó que no había diferencias entre el DH y GI medidos con ambos métodos de digestión in vitro.

ABBREVIATIONS

3- α HSD	3 α -hydroxysteroid dehydrogenase
ACW	Antral contractions waves
ARCOL	Artificial colon
ATP/ADP	Adenosine triphosphate/Adenosine diphosphate
AU	α -amylase units (mg maltose \cdot 3 min ⁻¹)
AUC	Area under the curve
BioAcc	Bioaccessible fraction
BP	British pharmacopeia
BPNP-G7	Non-reducing-end blocked p-nitrophenyl maltoheptaoside
BU	Bernfeld units
CA	Cellulose acetate
CH	Carbohydrates
CNT-G3	2-chloro-4-nitrophenyl alpha-maltotrioside
COST	European Cooperation in Science and Technology
CV	Coefficient of variation
DGE	German Nutrition Society
DGM	Dynamic gastric model
DH	Degree of hydrolysis
DI water	Deionized water
DIDGI	Dynamic gastrointestinal digester
DNA	Deoxyribonucleic acid
E	Enzyme
EDTA	Ethylenediaminetetraacetic acid
End res.	End residues
ESIN	Engineered stomach and small intestine
ESL	Extended shelf life
F	Fats
F6P	Fructose-6-phosphate
FAO	Food and agriculture organization
FDA	Food and drug administration
FIP	International pharmaceutical federation
G6P/G69-DH	Glucose-6-phosphate/Glucose-6-phosphate dehydrogenase suspension
GDS	Gastric digestion simulator
GI	Glycaemic index
GIT	Gastrointestinal tract
GL	Glycaemic load
GLUT2S	Glucose transporter
GP	Gastric phase
HEPES	2-(4-(2-hydroxyethyl)piperazin-1-yl) ethanesulfonic acid
HEPES	N-(2-Hydroxyethyl)piperazine-N'-(2-ethanesulfonic acid)
HGL	Human gastric lipase
HGS	Human gastric simulator
HK	Hexokinase

HPL	Human pancreatic lipase
HPSEC	High pressure size exclusion chromatography
HTST I/ HTST II	High temperature – short time I/High temperature – short time II
IDDM/NIDDM	Insulin-dependent diabetes mellitus/Non-insulin-dependent diabetes mellitus
IP-1	Intestinal phase – 30 min
IP-2	Intestinal phase – 60 min
IP-3	Intestinal phase – 90 min
IP-4	Intestinal phase – 120 min
IU	International units ($\mu\text{mol product} \cdot \text{min}^{-1}$)
IViDiS	In vitro digestion system
Kat	Katal
LTLT	Low temperature – long time
LU	Lipase units ($\mu\text{mol product} \cdot \text{min}^{-1}$)
Max/Min	Maximum/Minimum
MMC	Migrating myoelectric cycle
NAD ⁺ /NADH	Nicotinamide adenine dinucleotide
NADP ⁺ /NADPH	Nicotinamide adenine dinucleotide phosphate
NBT	Nitro blue tetrazolium chloride
OP	Oral phase
P	Proteins
P1	Pancreatic enzyme for cats and dogs (Pfizer)
P2	Pancreatic enzyme for cats and dogs (Zoetis)
P3	Pancreatin from porcine pancreas 4xUSP (Sigma Aldrich)
P4	Pancreatin from porcine pancreas 8xUSP (Sigma Aldrich)
P5	PancZyme (American Laboratories inc.)
P6	Pancreatin powder (Nordmark)
PES	Polyethersulfone
PGI	Phosphoglucose isomerase
PhEur	European pharmacopeia
PTFE	Polytetrafluoroethylene
PU	Pepsin units ($\Delta A_{280} 0.001 \cdot \text{min}^{-1}$)
PVP	Polyvinylpyrrolidone
RD-IV-HSM	Rope-driven in vitro human stomach model
RGE	Lyophilized rabbit gastric extracts
RM	Reaction mixture
RT	Room temperature
S	Substrate
SBP	Substrate binding pocket
SDF	Simulated digestive fluid
SGF	Simulated gastric fluid
SGF/GELS	Simulated gastric fluid/Diluted simulated gastric fluid (Dynamic system)
SGLT1	Sodium glucose transporter 1
SHIME	Simulator of the human intestinal microbial ecosystem
SIF	Simulated intestinal fluid
SIF/SIES	Simulated intestinal fluid/Diluted simulated intestinal fluid (Dynamic system)

SIMGI	Simulator gastrointestinal
SSF	Simulated salivary fluid
ST	Sterilization
SU	Somogyi unit
TAME	N α -p-tosyl-L-arginine methyl ester hydrochloride
TCA	Trichloroacetic acid
TIM	TNO intestinal model
TIM-1/TIMagc	TNO gastro-intestinal model 1/Advanced gastric compartment
Tris-HCl	Trizma hydrochloride
TS	Thermoshaker
TSI	The smallest intestine
TU	Trypsin units ($\mu\text{mol product} \cdot \text{min}^{-1}$)
U	Enzyme activity unit
UB	Ultrasonic bath
UHT	Ultra-high temperature
USP	United States Pharmacopeia
V _{sphere}	Volume of sphere
WG4	Working group 4
WHO	World health organization



INTRODUCTION

INTRODUCTION

1. Clinical nutrition

The science of nutrition deals with the processes by which components of food are made available to an organism for meeting energy requirements, for building and maintaining tissues, and, in a more general sense, for maintaining the organism in optimal functional health (1).

The German Nutrition Society (DGE) has recommended the intake goals of macronutrients that are depicted in figure 1 in order to fulfil the energy requirements of humans. DGE is an official incorporated society, which is not influenced by economic or political interests. It is a non-profit organization committed to scientific facts and has been engaged in topics on nutrition and nutritional research (2).

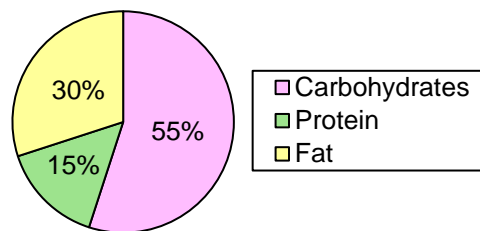


Figure 1. Nutrient intake goals on % energy (2)

Public health nutrition focuses on health promotion and disease prevention in the general population, in contrast to clinical nutrition, which focuses on the nutritional management of patients with established disease. Then clinical nutrition is the medical specialty dealing with the relationship between disease and nutrition (3). Clinical nutrition can be divided into 2 specialties, enteral and parenteral nutrition.

Enteral nutrition feeding is indicated in patients with a normal gastrointestinal tract (GIT) who cannot or will not eat or in whom oral consumption is inadequate. Nutrients are delivered in a suitable form through feeding tubes introduced at various points into the alimentary tract or through the mouth.

On the other hand, parenteral nutrition is the administration of nutrients by the intravascular route. Parenteral feeding is initiated when the GIT should not be used or when because of GIT dysfunction adequate enteral nutrition cannot be achieved. It should be noted that nutrients have to be in a form that normally enters the blood circulation after digestion and absorption (1).

2. Human digestion

Digestion is the mechanical and chemical breaking down of food into a form that can be transferred to the body's internal environment, where it can be distributed to cells by the circulatory system. Mechanical transformations, that reduce the size of the food particles, take place in the mouth and stomach; and the enzymatic transformations, where macromolecules are hydrolysed into smaller constituents, take place mainly in the intestine (4,5).

The digestive system includes the GIT, a tube extending from the mouth to the anus and its associated accessory organs, primarily glands, which secrete fluids into the GIT. The main parts of the human GIT are depicted in figure 2 (6):

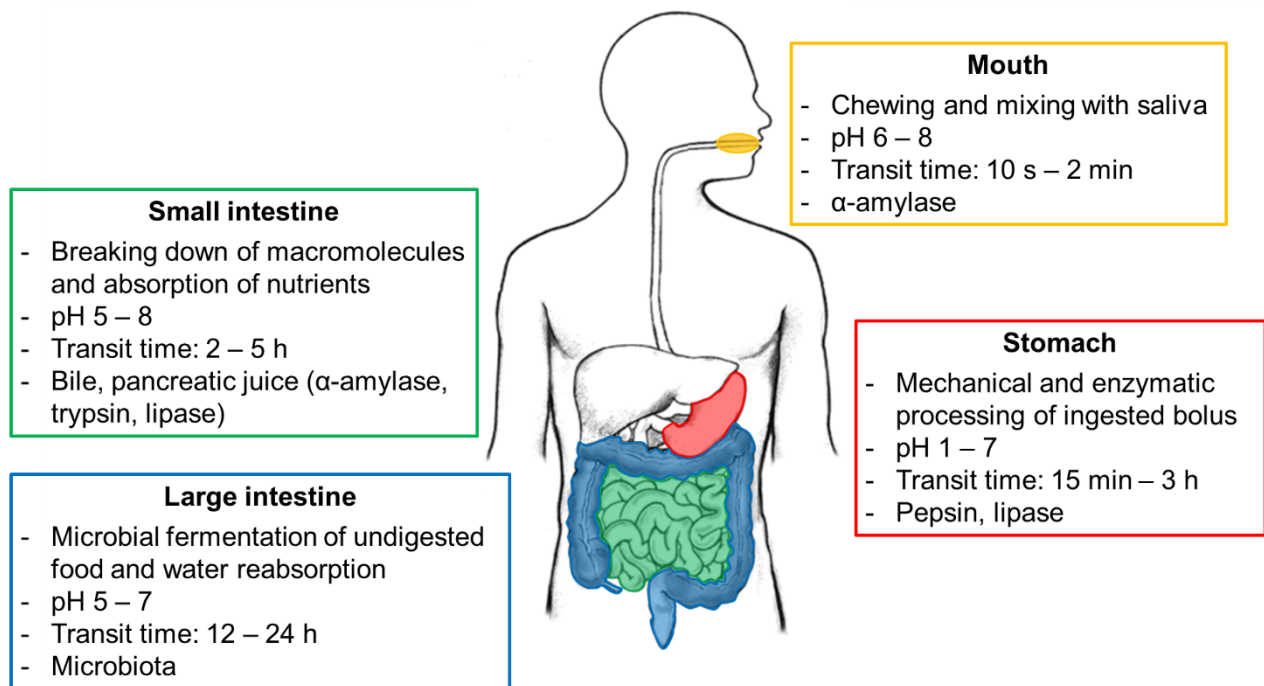


Figure 2. Main parts of GIT and general functions (4)

The lumen of the GIT is continuous with the external environment, which means that its contents are technically outside the body. The molecules released by digestion then move from the lumen of the GIT across a layer of epithelial cells and enter the blood, this process is called absorption.

The faeces are material that leaves the body via the anus and consists of water and solid matter, that is composed of about 30% dead bacteria, 10 – 20% fat, 10 – 20% inorganic matter, 2 – 3% protein and 30% undigested roughage from the blood and dried constituents of digestive juices such as bile pigment and sloughed epithelial cells. The undigested food present in the faeces is material that was never actually part of the internal environment (7,8).

2.1. Mouth

The oral cavity acts as the entrance of the digestive pathway. Chewing is the first step in the process of digestion and is meant to prepare the food for swallowing and further processing in the digestive system. Mastication breaks up food into small particles, increasing the surface area for digestion and absorption. Mastication has a considerable influence on the digestive process such as gastric emptying rates (5,9,10).

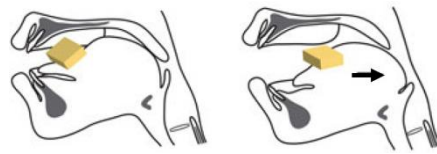
The presence of food in the mouth initiates mechanical and chemical stimuli via neuronal reflexes that result in an increased secretion of fluid (saliva) into the oral cavity. When the saliva is secreted, the food flavours are released; taste and texture of the food are perceived and thus influencing the chewing process (10,11).

During food processing, food particles are reduced in size by mastication and softened by saliva until the food consistency is appropriate for swallowing (9).

During mastication the food mixes with the saliva to form a bolus, which is a rounded, smooth, and lubricated portion of mechanically broken-down food. The water in saliva moistens the food particles, whereas the salivary mucins bind masticated food into a coherent and slippery bolus. The enzymatic digestion of carbohydrates is also initiated in the food bolus due to the presence of α -amylase (11).

In healthy subjects, the duration of bolus aggregation in the oropharynx ranges from a fraction of a second to about 10 seconds, and it has substantial interindividual variation. The bolus aggregation in the pharynx ends when a swallow is initiated (figure 3) (9,10).

a) *Stage I*: food particles are reduced in size and softened by saliva



b) *Stage II*: bolus aggregation in the pharynx

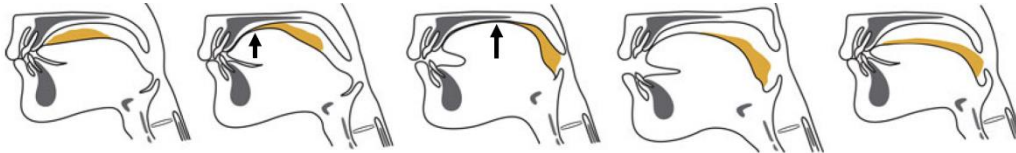


Figure 3. Mastication process (arrows indicate the direction of tongue movement) (9)

Swallowing will happen after approximately 20-30 chews. Delayed swallowing causes excessive salivary secretion, which reduces cohesion between food particles and dissolves the bolus, resulting in reduced swallowing efficiency (11).

Saliva plays a critical role in oral homeostasis, as it modulates the ecosystem within the oral cavity. The multiple functions of saliva relate both to its fluid characteristics and specific components (9,11,12).

Saliva is derived from 3 paired major salivary glands (90% of the fluid production) as well as from the minor salivary glands in the oral mucosa. A schematic representation of the salivary glands in the mouth are depicted in figure 4. In healthy individuals the daily production and swallowing of saliva normally ranges from 0.5 to 1.5 L and it is composed of more than 99% water and less than 1% solids, mostly proteins and salts (11).

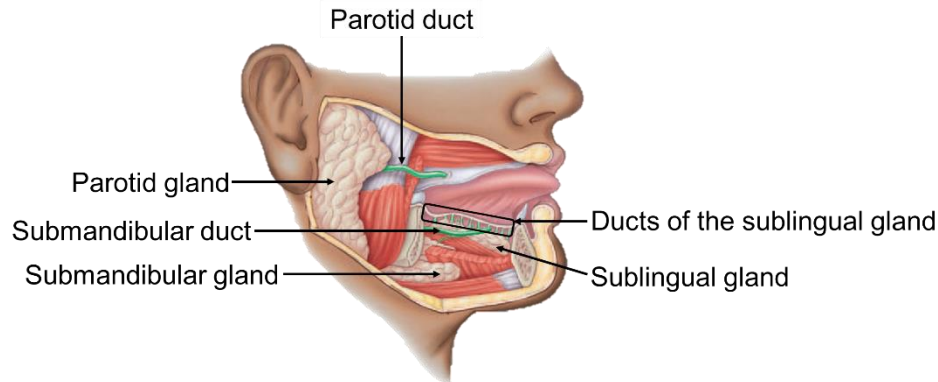


Figure 4. Salivary glands (6)

The final composition of saliva secreted to the oral cavity strongly depends on the flow rate. As flow rate increases, the concentrations of total protein, sodium, calcium, chloride and bicarbonate increase to varying extents, while the concentration of total phosphate decreases.

Taste is a main stimulant for formation of saliva, the highest saliva stimulation is obtained with sour taste, which can easily result in salivary flow rates between 5 and 10 mL·min⁻¹, followed by salt, sweet and bitter tastes (5,13).

The salivary flow rate and their composition also may be influenced by the state of hydration, nutritional state, the time of collection, nature and duration of stimulus, emotional state and gender. However, it is generally believed that age per se does not reduce the salivary function in healthy, non-medicated adults. Salivary secretion increases with the hardness and the size of the object being chewed as well as the chewing force by the chewing muscles (5,13).

The food bolus is conveyed from the mouth to the stomach by the process of peristalsis, which is an advancing contractile wave of the walls of a flexible conduit that forces the contents of the conduit forward (5,13). Figure 5 is a representation of the peristaltic waves that helps the food bolus to travel through the oesophagus.

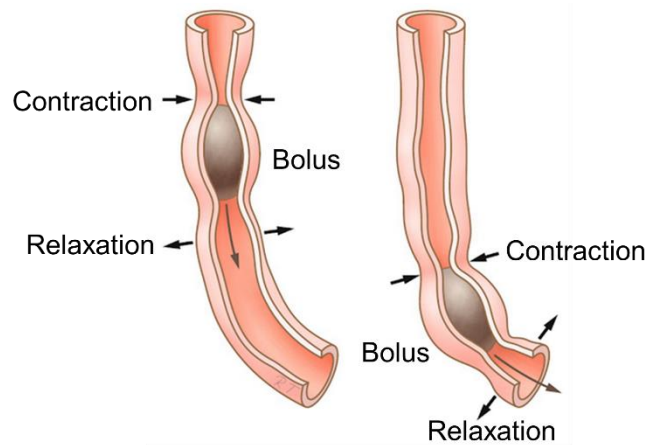


Figure 5. Schematic representation of a peristaltic wave (14)

Therefore, the major functions of the oral phase in response to a meal are the mechanical disruption of food into smaller particles by chewing and addition of saliva which aids in taste, bolus formation for swallowing (water and mucin), and initiates digestion of carbohydrates (α -amylase) (11).

2.2. Stomach

The stomach is the major compartment for food disintegration in the human body, where both biochemical reactions and mechanical size reduction occur contributing to breakdown of chewed solid food into small size (5,13).

The human stomach is a “J”-shaped and is divided into 4 major regions: fundus, corpus, antrum and pylorus (figure 6). The stomach has 3 main motor functions: storage, mixing, and emptying. The proximal part made of fundus and corpus acts as a reservoir for undigested material, responsible for the emptying of liquids, whereas the distal stomach (antrum) is the grinder, mixer and sieve of solid food, and acts as a pump for gastric emptying of solids by propelling actions (5,15).

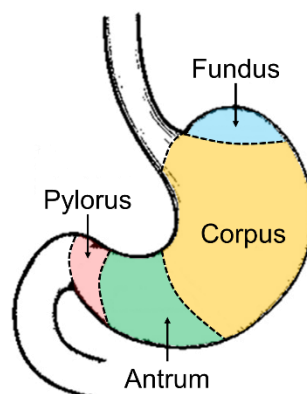


Figure 6. Schematic diagram of human stomach (15)

The reservoir function of the stomach is achieved through the flexible walls of the stomach. It is capable of dilating to accommodate more than 1 L meal without a significant increase in its luminal pressure. The normal capacity of the human stomach varies from 0.25 to about 1.7 L (5,13,15).

The geometry of the stomach not only changes from one individual to another, but it is also significantly influenced by the position of the body, the condition of surrounding viscera and organs, the amount and

type of meal ingested, and the digestion time. After a typical meal, an average-sized human stomach is about 10 cm wide at its widest point, its greater curvature is about 30 cm long, has a pyloric ring diameter of 1.1 cm or less, and its average capacity is about 0.94 L (5, 13, 15).

The motor activity that develops in response to the ingestion of a meal has a critical role in gastric digestion. It not only develops the fluid-mechanical forces promoting the mechanical and chemical digestion of the food, but it also allows the stomach to act as a holding chamber by receiving and storing the ingested meal. It controls the release of gastric contents into the duodenum, once their physicochemical properties render suitable for the next phase of digestion. The motility pattern of the gastric wall can be characterized by 3 types of muscle contractions.

- The first type of motor activity originates and develops in the upper part of the stomach. It is characterized by slow and weak wave activities.
- The second type of motor activity is characterized by a series of regular-peristaltic antral contractions waves (ACW) that originate at the middle of the stomach and propagate circumferentially toward the pylorus.
- The third type of motor activity can be described as a tonic contraction of the entire gastric wall, which allows the stomach to accommodate itself to varying volumes (5, 13, 15).

In the stomach, peristaltic contractions are initiated by tonic contractions on the upper surface of the stomach and continue down to the pyloric valve. The contraction frequency is ~3 cycles per minute and each contraction takes about 1 min to advance from the fundus to the pylorus.

The peristaltic contraction mixes oral bolus with gastric juice and propels this mixture to the antrum. The antrum is where foods receive the most intense squeezing and crushing forces, causing efficient food breakdown. Liquids and small particles (< 1 to 2 mm) flow continuously from the stomach through the pyloric opening into the duodenum, while indigestible particles greater in size are squirted back into the stomach, by an action called retropulsion. Repeated propulsion, grinding, and retropulsion reduce the size of food particles and convert the mixture into emulsion-like digesta. This mechanical destruction combined with chemical reactions change the food mixture into a softer consistency in a suspension form that is called "chyme" and expelled into the duodenum (5, 13, 15).

Gastric juice contains water, mineral salts, mucus, hydrochloric acid, pepsinogen, lipase and intrinsic factor. The stomach secretes 2 to 3 L of gastric juice per day, and the rate of secretion may increase from 1 mL·min⁻¹ under fasted conditions to 10 to 50 mL·min⁻¹ immediately after food ingestion. Increase in food amount, protein content, and meal viscosity increases the secretion (5, 16).

Water in the gastric juice further liquefies the swallowed food. Hydrochloric acid acidifies the food and reduces the action of salivary α -amylase. It also converts pepsinogen to the active enzyme pepsin and kills many microbes which may be harmful to the body. Pepsin starts the hydrolysis of proteins and lipase starts the hydrolysis of fats. The intrinsic factor is necessary for the absorption of vitamin B12. The mucus in the gastric juice prevents mechanical injury to the stomach wall by lubricating the contents, it also prevents chemical injury by acting as a barrier between the stomach wall and other constituents of gastric juice (8, 16–18).

2.2.1. Gastric emptying

Gastric emptying results from the net effects of propulsive forces within the stomach and the resistance to flow offered by the narrowed gastroduodenal pylorus. Liquids, digestible solids and indigestible solids are emptied by different mechanisms.

Liquid and semi-liquids contents, as well as particles with a size of 1 to 2 mm, are emptied from the stomach into the duodenum during fed motility, whereas the contents of size > 2 mm are emptied during fasting motility.

After ingestion, liquids are rapidly distributed throughout the entire stomach and they empty from the stomach according to 1st order kinetics, thus the speed is directly proportional to the volume present in the stomach (figure 7).

It has an initial gastric emptying rate up to 10 to 40 mL·min⁻¹, followed by a slower emptying rate of 2 to 4 mL·min⁻¹. The halftime, indicating when 50% ingested meal is emptied, ranges from 10 to 60 min (5).

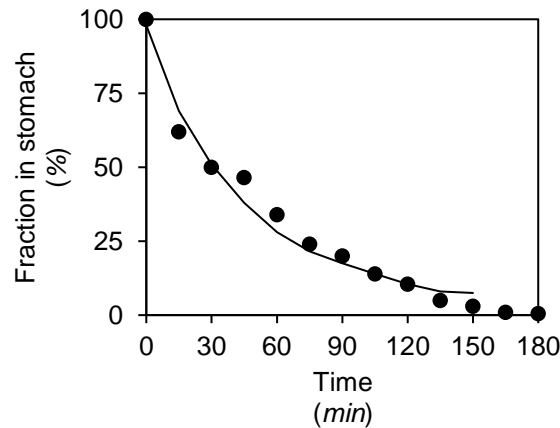


Figure 7. Gastric emptying curve after a liquid meal intake in a healthy volunteer (5)

Ingested solids are stored initially in the proximal stomach and move gradually into the distal stomach. Solids are ground to particles of a size less than 1 to 2 mm before they are able to go through the pyloric opening.

The gastric emptying rate of solids shows a biphasic pattern (figure 8): a lag phase where little emptying occurs, followed by a linear emptying phase during which solids particles empty from the stomach by mainly zero-order kinetics, that is, independent of gastric volume (5).

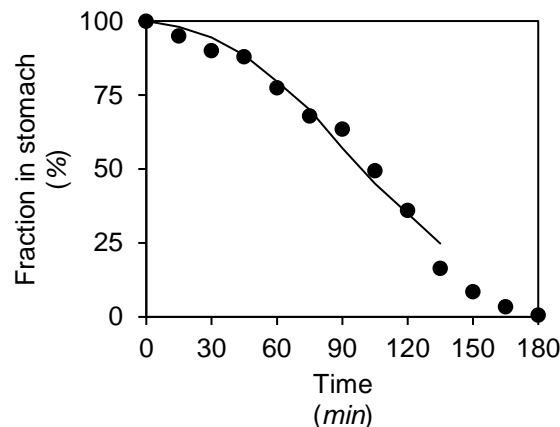


Figure 8. Gastric emptying curve after a solid meal intake in a healthy volunteer (5)

During the fasting state an inter-digestive series of electrical events take place, however these immediately cease upon the ingestion of food. This is called inter-digestive myoelectric cycle or migrating myoelectric cycle (MMC), which is divided into following 4 phases as it is shown in figure 9 (5,19,20).

- Phase I (basal phase) lasts from 40 to 60 min with rare contractions.
- Phase II (pre-burst phase) lasts from 40 to 60 min with intermittent action potential and contractions. As the phase progresses the intensity and frequency also increase gradually.
- Phase III (burst phase) lasts for 4 to 6 min it includes intense and regular contractions for short period. It is due to this wave that all the undigested material (> 2 mm) is swept out of the stomach down to the small intestine. It is also known as the housekeeper wave.
- Phase IV lasts for 0 – 5 min is a transition period of decreasing activity until the next cycle begins (5,19,20).

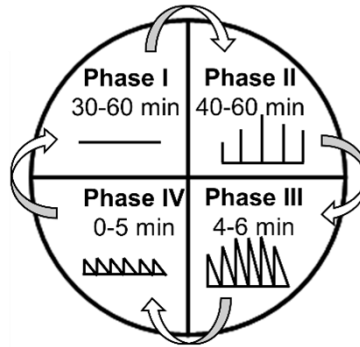


Figure 9. Inter-digestive Myoelectric Cycle or Migrating Myoelectric Cycle (MMC) (21)

Gastric emptying is regulated by both gastric and duodenal factors. Gastric factors include the food volume, fluid viscosity, caloric content, acidity, and food physical properties such as texture and density. Duodenal gastric feedback is the major control mechanism for gastric emptying. The duodenum contains receptors that respond to distention, the presence of acid, carbohydrate, fat, and protein digestion products. Therefore, chemical composition of the meal and the physical nature of the food remain crucial in regulating emptying rate.

Biological factors such as age, body mass index, posture, stress or depression also influence gastric emptying. For example, gastric emptying is slower in elders and females, which could be related to their weaker antrum contractions (5).

However, gastric emptying generally delivers about 2 to 4 kcal·min⁻¹ caloric content to the duodenum through a negative feedback mechanism mediated by the duodenal receptors. Meals of larger weight and caloric content are associated with longer emptying time for both solids and liquids.

Among the major components of foods, fat is emptied more slowly than carbohydrates and proteins. This is primarily because of its high caloric density. Density difference causes phase separation of chyme in the stomach, leading to the layering of fat above water that may also contribute to the longer emptying time of fat. Different sugars empty from the stomach at different rates. Complex interactions occur when different types of solids and liquids are consumed simultaneously.

Increasing the viscosity of liquid meals delays gastric emptying and increases satiety. However, it should be noted that after ingestion of a high viscosity meal, the increase in the chyme viscosity is not proportional to the meal viscosity. A rapid intragastric dilution in the stomach occurs after a high viscosity meal is ingested to reduce the meal viscosity and minimize delay in gastric emptying (5).

2.3. Small intestine

Final stages of digestion occur in the next section of the GIT, the small intestine. The small intestine is the longest and most important section of the tract because most of the chemical and mechanical digestion takes place there (6,8).

The small intestine is approximately 2.5 cm in diameter, and 6 m long and it is coiled and folded to fit inside the abdomen. It is divided into 3 segments, as it is shown in figure 10: an initial short segment, the duodenum (~25 cm), is followed by the jejunum (~2.5 m) and then by the longest segment, the ileum (~3.5 m). Normally, most of the chyme entering from the stomach is digested and absorbed in the first quarter of the small intestine, in the duodenum and jejunum (6,8,22).

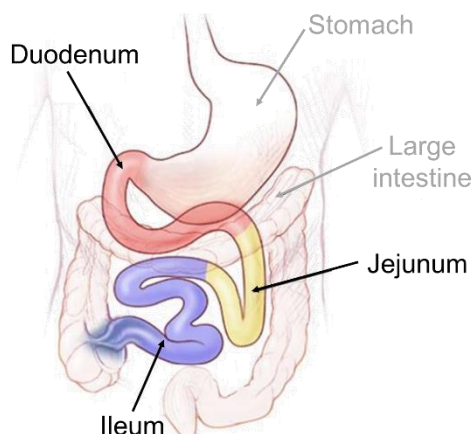


Figure 10. Schematic representation of small intestine (23)

The duodenum nearly completes a 180-degree arc as it curves within the abdominal cavity, and the head of the pancreas lies within this arc. The duodenum begins with a short superior part, which is where it exits the pylorus of the stomach, and ends in a sharp bend, which is where it joins the jejunum. The jejunum and ileum are similar in structure to the duodenum, except that a gradual decrease occurs in the diameter of the small intestine, in the thickness of the intestinal wall, in the number of circular folds, and in the number of villi as one progresses through the small intestine. The junction between the ileum and the large intestine is the ileocecal junction, it has a ring of smooth muscle, the ileocecal sphincter, and one-way ileocecal valve (6).

The small intestine is where almost all of the nutrients that are present in the food are absorbed. Each day ~9 L of water enters the digestive system (ingested water but also the water from the secretions), from which ~8 L are absorbed in the small intestine and only ~1 L enters in the colon (6,22).

In the small intestine carbohydrates, fats, and proteins are broken down by hydrolytic enzymes into monosaccharides, fatty acids, and amino acids. Some of these enzymes are on the luminal surface of the intestinal lining cells, while others are secreted by the pancreas and enter the intestinal lumen at the duodenum. Vitamins, minerals and water, which do not require enzymatic digestion, are also absorbed in the small intestine (6,8).

The small intestine is lined with a mucosal layer and that mucosa maximizes digestion and absorption. The mucosal layer of the small intestine has many ridges and folds, these folds are called plicae and they have tiny finger-like branches that stick out to grab even more food particles and these little projections are called villi. The villi themselves is covered by a forest of even smaller hairs called microvilli (figure 11) (22).

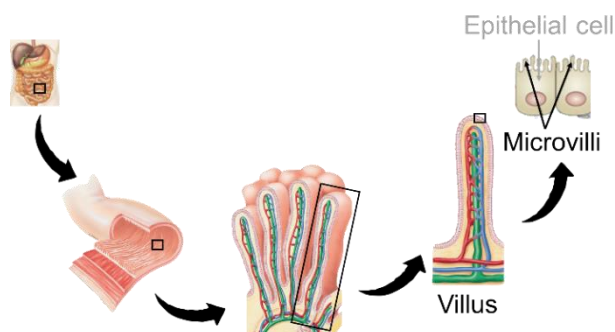


Figure 11. Diagram of villi and microvilli (6)

Mixing and propulsion of chyme are the primary mechanical events that occur in the small intestine. These functions are the result of segmental (figure 12) or peristaltic contractions (figure 5), which are accomplished by the smooth muscle in the wall of the small intestine and which are only propagated

for short distances. Segmental contractions mix the intestinal contents, and peristaltic contractions propel the intestinal contents along the digestive tract. Frequently, intestinal peristaltic contractions are continuations of peristaltic contractions that begin in the stomach (6).

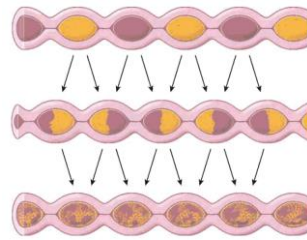


Figure 12. Segmentation consists of ring-like contractions along the length of the small intestine, within a matter of seconds the contracted segments relax and the previously relaxed areas contract (24)

The contractions move at a rate of about $1 \text{ cm}\cdot\text{min}^{-1}$, the movements are slightly faster at the proximal end of the small intestine and slightly slower at the distal end. It usually takes 3 – 5 h for chyme to move from the pyloric region to the ileocecal junction.

The ileocecal sphincter at the juncture between the ileum and the large intestine remains mildly contracted most of the time, but peristaltic waves reaching it from the small intestine cause it to relax and allow movement of chyme from the small intestine into the cecum. Closure of the sphincter facilitates digestion and absorption in the small intestine by slowing the rate of chyme movement from the small intestine into the large intestine and prevents material from returning to the ileum from the cecum (6).

2.3.1. Pancreatic juice

The pancreas and liver secrete substances that flow via ducts into the duodenum. The pancreas, an elongated gland located behind the stomach, has both endocrine and exocrine functions, but only the latter are directly involved in gastrointestinal function. The exocrine portion of the pancreas secretes digestive enzymes and a fluid rich in bicarbonate ions. The high acidity of the chyme coming from the stomach would inactivate the pancreatic enzymes in the small intestine if the acid was not neutralized by the bicarbonate ions in the pancreatic fluid (8).

A diagram of the liver, gallbladder and pancreas is shown in figure 13:

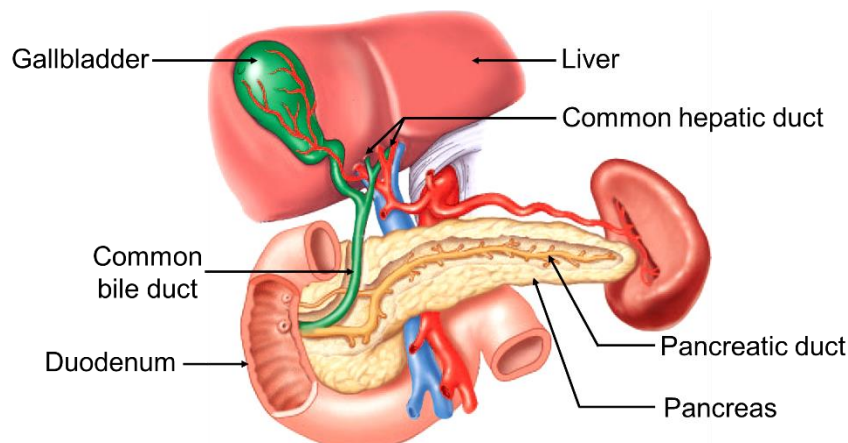


Figure 13. Diagram of liver, gallbladder and pancreas (6)

2.4. Large intestine

The large intestine is about 1.5 m long and consists of 4 regions: cecum, appendix, colon, and rectum. Normally 18 – 24 h are required for material to pass through the large intestine, in contrast to the 3 – 5 h required for movement of chyme through the small intestine (6).

A schematic representation of the different parts of the large intestine is depicted in figure 14:

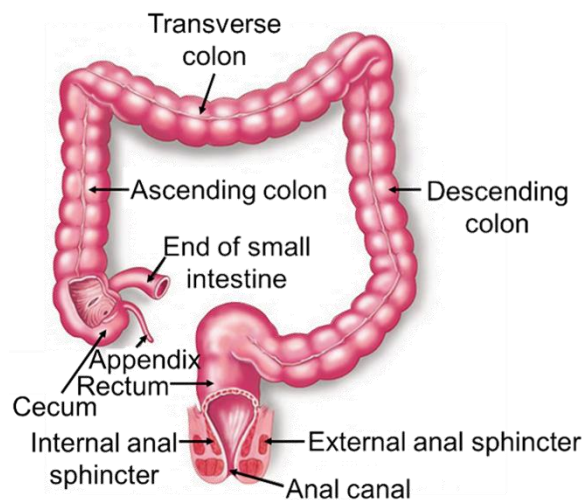


Figure 14. Large intestine (25)

Unlike the small intestine, which is coiled and packed in a small volume, the colon consists of 3 relatively straight portions, the ascending colon, the transverse colon, and the descending colon. The colon empties into the rectum.

The colon absorbs ~90% of water, sodium and potassium that enter it. The undigested or unabsorbed nutrients feed a large population of bacteria, which synthesize several key vitamins (B12, thiamine, riboflavin, vitamin K) that are also absorbed by the large intestine (25).

Little enzymatic activity is associated with secretions of the colon when mucus is the major secretory product. Mucus lubricates the wall of the colon and helps the faecal matter stick together (6).

The contents of the large intestine (after water and salt have been removed) are known as the faeces. The faeces consist primarily of undigested food, indigestible materials, and bacteria (25).

Segmental mixing movements occur in the colon much less often than in the small intestine. Peristaltic waves are largely responsible for moving chyme along the ascending colon. At widely spaced intervals (normally 3 or 4 times each day), large parts of the transverse and descending colon undergo several strong peristaltic contractions, called mass movements. Mass movements are very common after meals because the presence of food in the stomach or duodenum initiates them (6).

3. In vitro digestion methods

In many developed countries, a segment of the population exhibits malnutrition (low micronutrient intake) while simultaneously being overweight (excess energy consumption). Moreover, specific food consumption patterns have been shown to increase or decrease risk for type II diabetes, cardiovascular disease, obesity, and certain cancers. These links have driven increased consumer awareness to the functional properties of the foods they consume and have prompted the food industry to develop innovative “functional food” products, or food products with functional ingredients (4,26).

To develop these innovative food products, it is necessary to understand the behaviour of food during the digestion process, from its initial physical breakdown, to the transformation and absorption of its constituent nutrient molecules.

Therefore, the interest in simulating digestion to understand food behaviour in the GIT is growing. Moreover, the digestive system is also central to numerous questions in other fields such as toxicology, pharmacology, and microbiology (4,26).

Food digestion is a complex series of dynamic processes and can be modified by numerous stimuli (e.g., the food itself), therefore in vivo feeding methods (using animals or humans) provide the most accurate results, but they are costly, time consuming and imply ethical constraints.

Compared with in vivo studies, in vitro techniques can save labour and time, reduce cost, improve reproducibility and there is no ethical constraint.

An important area of food and pharmaceutical research is the study of bioavailability, which is the fraction of ingested component that reaches the target organ or systemic circulation. In vitro models provide a suitable alternative to in vivo assay by determining the bioaccessibility of an ingested substance as an indicator of bioavailability (figure 15). Bioaccessibility is the fraction of ingested component available for intestinal absorption (4,5,27–29).

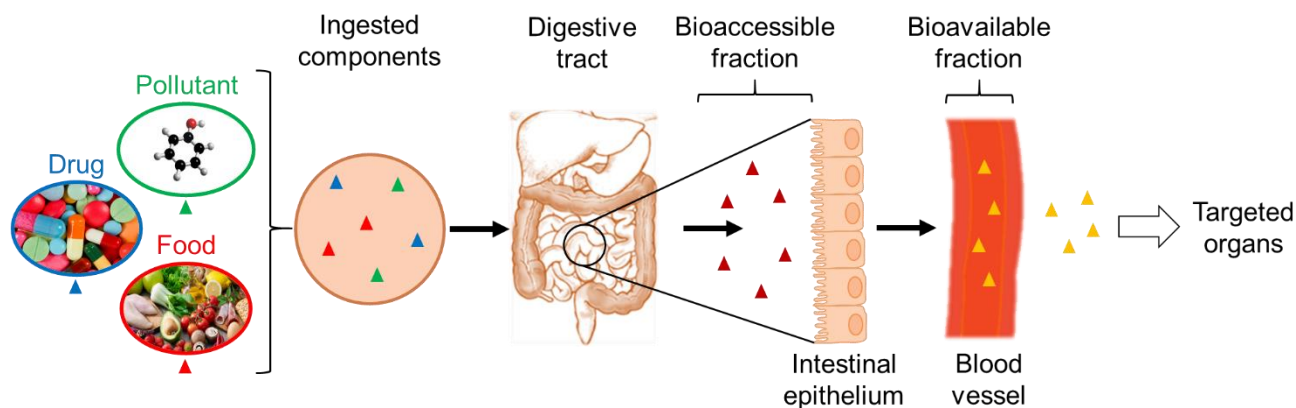


Figure 15. Bioaccessible and bioavailability fraction of ingested components (4)

According to Longland 1991 (30), an adequate gastrointestinal in vitro model should have the following characteristics:

- Sequential use of enzymes in physiological amounts.
- The pH should allow the activation of enzymes and cofactors (e.g., bile salts and coenzymes).
- Digestive end products should be removed from the system.
- Appropriate mixing at each stage of digestion.
- Physiological transit times for each step of digestion.

The appropriate system to evaluate a substance is dependent on the chemical composition of the substance, for example, if it contains hydrolytic and fermentatively digestible components, a system capable of both types of digestion should be used (31).

The models that are available can be divided into models to study digestion and models to study microorganisms. The methods described to study digestion generally involve a single, two- or three-step digestion, simulating gastric digestion, gastric/small intestinal digestion, and occasionally oral/gastric/small intestinal digestion (32,33).

There are 3 types of GIT models: static, semi-dynamic and dynamic. Most models are static gastrointestinal models, which simulate transit through the human digestive tract by sequential exposure of the food to simulated mouth, gastric and small intestinal conditions. Dynamic gastrointestinal models mimic the gradual transit of ingested compounds through the digestive tract. Whereas the more complex models can simulate more aspects of human physiology, the simple models are easy to perform and allow simultaneous determination of large numbers of samples (5,34).

3.1. Static digestion methods

In a common static digestion model, the oral phase is mimicked by a short incubation with α -amylase then the gastric phase is reproduced by a pepsin hydrolysis of homogenized food bolus, under fixed pH and temperature, for a set period of time. This step may be followed, in the same bioreactor, by an intestinal phase involving pancreatic enzymes with or without bile (4).

One of the main drawbacks of static in vitro digestion models is that they are oversimplified and do not take into account the dynamic aspects of the digestive process. Therefore, these models have been used to compare the digestion of related foods under the same conditions, to study the digestion of pure compounds or to unravel the interactions between constituents at the molecular level (28).

Static in vitro digestion methods are particularly popular because they are easy to use, cheap and do not require specific equipment. However, a huge number of protocols differing in the experimental conditions (pH, duration of the different steps, amount of digestive enzymes and bile etc) have been proposed making the comparison of results between studies impossible (28). Recently, an international consensus was reached within the COST Action Infogest (35) and a protocol published (33) that has since been widely used internationally.

The United States Pharmacopeia (USP) apparatus also provides a static, closed environment, widely used in the characterization of drugs and in quality control of drug dosage forms and nutritional supplements. According to USP, dissolution refers to the process by which the active ingredient is dissolved into a liquid assay medium, and the result provides the approximate time required for full solubilization of the drug under the test conditions.

Four basic types of dissolution apparatus are specific by the USP and recommended in the FDA guidance (chapter <711>, USP (36)):

- Apparatus 1 (rotating basket) using 40-mesh wire basket rotated in a dissolution medium at a constant speed between 25 and 150 rpm (figure 16a).
- Apparatus 2 (paddle method) is similar to apparatus 1 except that the rotating basket is substituted with a paddle (figure 16b).
- Apparatus 3 (reciprocating cylinder) involves enclosing the dosage form in a transparent cylinder that is reciprocated up and down in the medium contained by a glass tube in a water bath.
- In apparatus 4, the dissolution medium is continuously pumped through a flow-through cell that contains the dosage form and is immersed in a water bath (5).

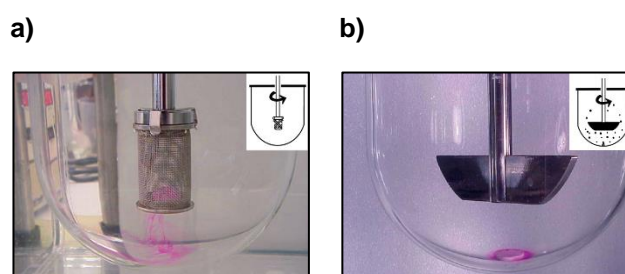


Figure 16. Representation of drug release process using a) apparatus 1 and b) apparatus 2 (37,38)

Main factors that influence release of drug ingredients include pH, surfactant, bile, movement, ionic strength, buffer capacity, enzymes, and the presence of foods. The dissolution medium can be varied to suit different test purposes. An aqueous dissolution medium composed of 0.1 N HCl is often employed to simulate gastric medium. The commonly used agitation speed is 50 to 100 rpm for basket method and 25 to 75 rpm for paddle method.

The USP definition of drug disintegration is “that state in which any residue of the unit, except fragments of insoluble coating or capsule shell, remaining on the screen of the test apparatus is a soft mass having no palpably firm core”. Researchers have tried to correlate in vivo results with those from USP dissolution testing, and the correlation seems to be possible to establish in some cases. However, the estimation of in vivo drug release from in vitro dissolution tests often ends in failure (5).

Another kind of static digestion method was designed by Oomen et al (39) to study the bioaccessibility of soil contaminants (figure 17). In that model the digestion started by introducing 9 ml of saliva of pH 6.5 (± 0.2) to 0.6 g of soil, this mixture was rotated head-over-heels for 5 min at 55 rpm. Subsequently, 13.5 mL of gastric juice (pH 1.07 ± 0.07) was added, and the mixture was rotated for 2 h.

Finally, 27 mL duodenal juice (pH 7.8 ± 0.2) and 9 mL bile (pH 8.0 ± 0.2) were added simultaneously, and the mixture was rotated for another 2 h. All digestive juices were heated to $37 \pm 2^\circ\text{C}$. Mixing was done in a rotator that was also heated to $37 \pm 2^\circ\text{C}$. At the end of the in vitro digestion process, the digestion tubes were centrifuged for 5 min at 3,000 g, yielding the chyme (supernatant) with a pH of at least 5.5 and the digested soil (pellet).

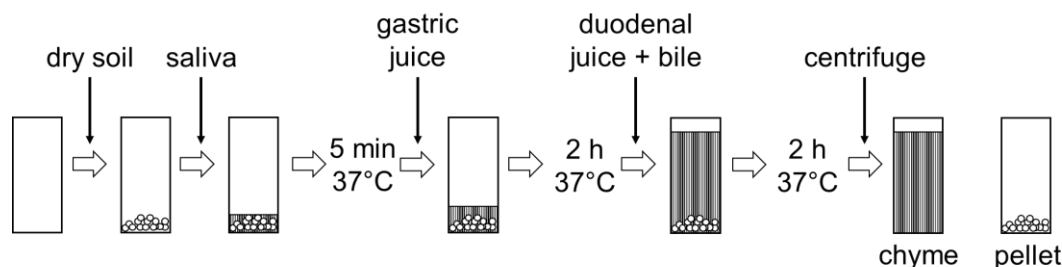


Figure 17. Schematic representation of the in vitro digestion procedure (39)

3.2. Semi-dynamic digestion methods

The semi-dynamic digestion model mimics gastric digestion, it is simple to handle and more physiologically relevant than a static model as it simulates the gradual pH decrease, and it has the novelty to include emptying, and the sequential addition of digestive enzymes and gastric fluid.

A freshly prepared sample is placed into 70 mL glass v-form vessel thermo-stated at 37°C after the addition of gastric solution simulating the gastric fluid residue in the stomach (figure 18). Then, 3 solutions are added at a constant rate:

- Gastric solution using pH-stat dosing device: $0.09 \text{ mL}\cdot\text{min}^{-1}$
- Enzymatic mixture (lipase, pepsin) using a syringe pump: $0.003 \text{ mL}\cdot\text{min}^{-1}$
- Pepsin using a syringe pump: $0.003 \text{ mL}\cdot\text{min}^{-1}$

A 3D action shaker at 35 rpm is used for agitation. Gastric emptying is simulated by taking 9 different volumes according to a pre-set curve based on in vivo study data. Samples are taken from the bottom of the vessel using a pipette with a tip internal diameter of 2 mm because it approximates the upper limit of particle size that has been seen to pass through the pyloric opening into the duodenum.



Figure 18. Glass v-form vessel during semi-dynamic digestion method (40)

After that, small intestinal digestion is simulated using static digestion method. The intestinal digestion is performed for 60 min in a shaking incubator at 37°C , 190 rpm.

This method was developed because the static digestion model is easy to use on a daily basis but it does not mimic many relevant factors such as progressive emptying, and on the other hand the dynamic digestion models can closely mimic human digestion but they are not a routine tool due to their complexity. Therefore, semi-dynamic digestion model is an intermediate between sophistication of the dynamic models and easy to use of static models (40).

3.3. Dynamic digestion methods

Digestion is a dynamic process; food entering the GIT will be transferred from one compartment to another at variable rates depending on its structure, caloric content, osmolarity, and rheological properties. Physicochemical conditions occurring in the different compartments will evolve with time (41).

The simplistic approach of the static methods is often not a realistic simulation of the more complex in vivo conditions, where the biochemical environment encountered is constantly changing and physical parameters such as shear and grinding forces can have a large impact on the breakdown of larger food particles and the release of nutrients.

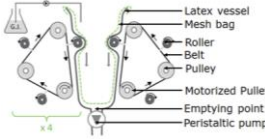
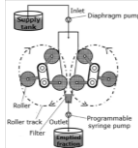
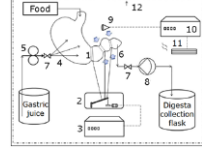
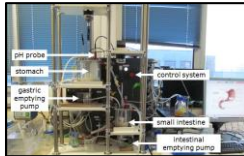
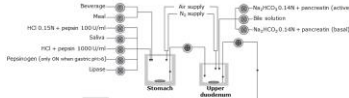
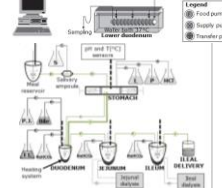
Body position may also have an influence on some aspects of gastric digestion, especially, gastric sieving of larger particles and pharmaceuticals. Several dynamic digestion models have been developed in recent years to address these complex aspects of digestions.

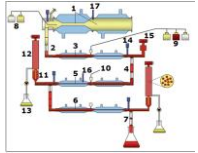
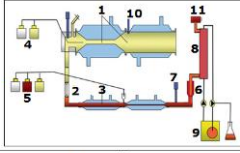
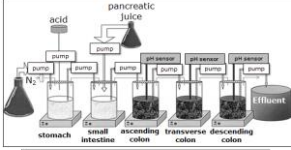
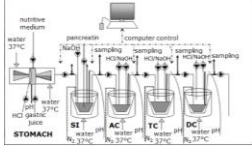
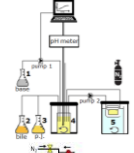
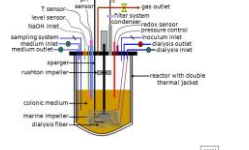
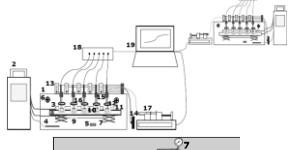
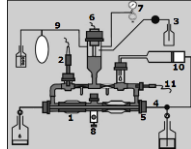
Three main approaches have been followed in the design of the models' gastric compartments, each with their own advantages and disadvantages: vertical alignment, horizontal alignment and beaker. Vertical alignment of the gastric model allows phase separation to occur during digestion, as in vivo, but has the disadvantage of gravity influencing the sedimentation of larger particles towards the bottom opening. Horizontal alignment may be more suitable for the simulation of gastric sieving, but it does not provide a realistic representation of the low mixing environment of the gastric fundus. A beaker is used in some models and is reminiscent of most static models.

In contrast to the stomach, the peristaltic movements and tube-like structure of the small intestine may reduce the impact of body position on its function. Several dynamic digestion models use a horizontal, tube-like alignment to represent the small intestine. In these models, the peristaltic movements of the small intestine are simulated either by alternating pressure on the flexible wall of the compartment or constrictions within the wall of the compartment. Other models use one or more thermostated beakers to simulate the small intestine. The design of the stomach and intestinal parts of digestion models has a direct impact on the physical forces exerted on the chyme, and how realistically the model simulates in vivo shear forces (42).

Table 1 is a comparison of some dynamic digestion methods, its different compartments, mixing processes, the sampling and a schematic representation.

Table 1. Dynamic in vitro digestion methods

Model	Compartments	Mixing process	Sampling	Scheme	Ref.
Dynamic gastric model (DGM)	Fundus Antrum	3 contractions·min ⁻¹	Sieve		4,43
Human gastric simulator (HGS)	Stomach	3 contractions·min ⁻¹	Mesh bag		4,13
Gastric digestion simulator (GDS)	Antrum				44
Rope-driven in vitro human stomach model (RD-IV-HSM)	Stomach	3 contractions min ⁻¹			45
DIDGI system	Stomach Small intestine				42
In vitro digestion system (IViDiS)	Stomach Duodenum				46
Engineered stomach and small intestine (ESIN)	Stomach Duodenum Jejunum Ileum	Pistons (3 movements min ⁻¹)	Dialysis (jejunum, ileum)		47

TNO intestinal model (TIM-1)	Stomach Duodenum Jejunum Ileum	Water from inside glass jacket with a flexible wall inside	Dialysis (jejunum, ileum)		48,49
Tiny TIM	Stomach Small intestine	Water from inside glass jacket with a flexible wall inside	Dialysis (small intestine)		42
Simulator of the human intestinal microbial ecosystem (SHIME)	Stomach Small intestine Ascending, transverse and descending colon	Magnetic stirrer			42
Simulator gastrointestinal (SIMGI)	Stomach Small intestine Ascending, transverse and descending colon	<i>Stomach:</i> Water from inside glass jacket with a flexible wall inside <i>Intestine:</i> magnetic stirrer (150 rpm)			50
The smallest intestine (TSI)	Small intestine (5 reactors for 5 samples)	Magnetic stirrer (170 rpm)	Dialysis (cut off: 10 kDa)		51
Artificial colon (ARCOL)	Large intestine	Rushton and marine impeller (400 rpm)	Dialysis (cut off: 30 kDa)		52
Copenhagen MiniGut	Colon (5 vessels)	Magnetic stirrer			53
TNO large-intestinal model (TIM-2)	Colon	Water from inside glass jacket with a flexible wall inside	Dialysis		54

4. Digestive enzymes

4.1. α -amylase

The term “amylase” can be generally defined as the enzyme which hydrolyses the O-glycosyl linkage of starch, being α -amylase (α -1,4-glucan-4-glucanohydrolase) the one that catalyse the endogenous hydrolysis of α -1,4-glycosidic linkages (55). An example of a glycosidic linkage is shown in figure 19.

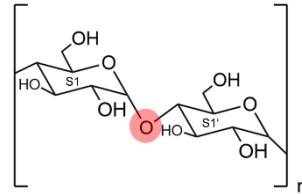


Figure 19. Glycosidic linkage

In humans, α -amylase is present in salivary and pancreatic secretions. Salivary α -amylase initiates carbohydrate digestion in the mouth, then the pre-digested carbohydrates pass through the stomach and travels to the small intestine where they are highly digested with the pancreatic α -amylase (56–58).

4.1.1. Structure

All mammalian amylases appear to be secreted with the N-terminal blocked by a pyrrolidone acid (figure 20). This unusual N-terminal structure may be a defensive mechanism against amino-peptidases and other digestive enzymes that are present in the medium in which human amylase must function (59).

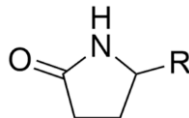


Figure 20. Pyrrolidone at the N-terminal of α -amylase

The overall topology of amylase consists of 3 domains, which has been structurally conserved in amylases from other sources as well. A schematic representation is depicted in figure 21:

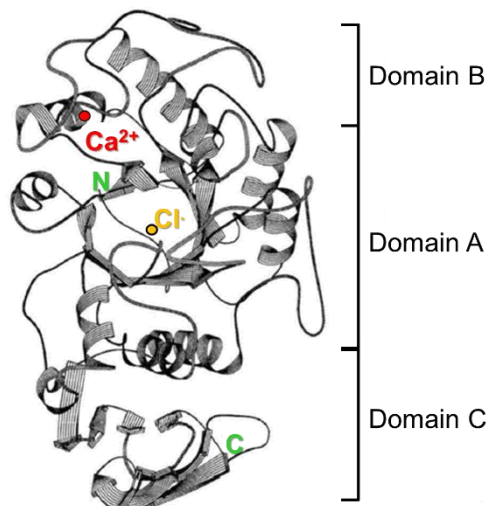


Figure 21. Stereo drawing of a schematic representation of the polypeptide chain fold of human pancreatic amylase. Also indicated the 3 structural domains present in this protein along with location of the calcium (red) and chloride (yellow) binding sites. N- and C- terminal ends of the polypeptide chain have also been labelled N and C (green), respectively (59)

- **Domain A:** domain that forms (β/α)8-barrel structure from residues 1 to 99 and 169 to 404. The cleft present in domain A is the site of polysaccharide binding and contains the putative catalytic sites of α -amylase. The 3 catalytic residues Asp197, Glu233 and Asp300 are clustered next to each other in the central portion of the cleft (60). Nagamine et al (58) have proposed the presence of at least seven, and possibly 9 binding subsites for glucose residues in the substrate-binding cleft amylase. The aromatic residues Trp58 – Trp59 are part of a large substrate-binding site involving residues from the A and B domains.

There is a loop that is formed by the residues 304 – 310 that consists of 4 glycine, 2 alanine and 1 histidine and is used to anchor the substrate. Upon substrate binding and during hydrolysis, the segment may help in holding the substrate in place in the catalytic site. After the reaction, the products are released by the movement of the glycine-rich segment to the open position.

- **Domain B:** it is a long protruding loop as an excursion from domain A that goes from residues 100 to 168 and contains the tight bond calcium ion.
- **Domain C:** this domain consists of 92 residues (residues 405 – 496) and is found to be the most variable domain between amylases of different origins (57,59,60).

4.1.2. Mechanism of action

The 3 acidic amino acid residues that have been identified for the catalytic site of the α -amylase are Asp197, Glu233 and Asp300, and all of them are essential for efficient hydrolysis of polysaccharides (55). However, only 2 of the 3 conserved catalytic residues directly play a role, the Glu233 that act as acid/base catalyst and the Asp197 that act as the nucleophile. The third conserved residue, Asp300, binds to 2 OH groups of the substrate through hydrogen bonds and plays an important role in the distortion of the substrate.

Other conserved amino acids residues play a role in positioning the substrate into the correct orientation into the active site, proper orientation of the nucleophile, transition state stabilization, and polarization of the electronic structure of the substrate (61–63).

Figure 22 shows the orientation of a substrate in the active site of the enzyme:

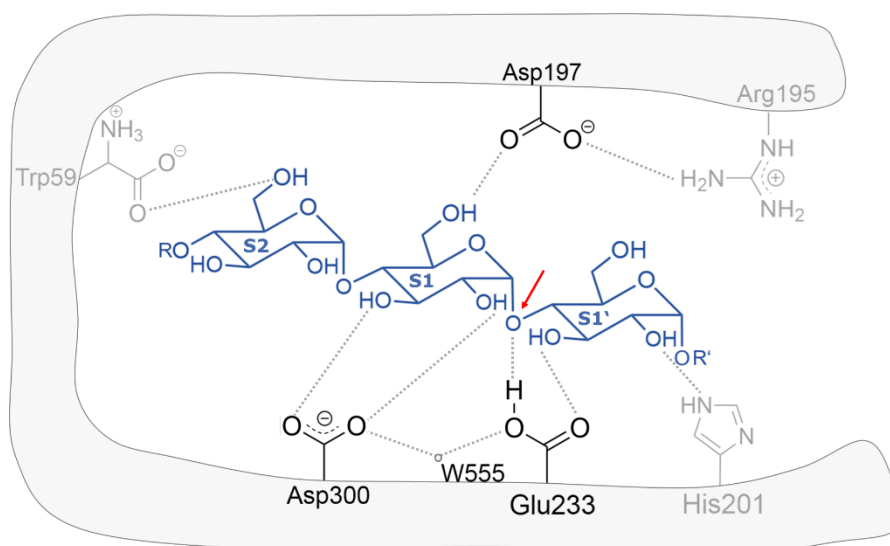


Figure 22. Interaction between the active site of α -amylase and a possible substrate (black: active site, grey: amylase residues that orient the substrate, blue: substrate, red arrow: scissile bond) (57,65,66,63)

The generally accepted catalytic mechanism of the α -amylase is that of the α -retaining double displacement and it involves 6 steps, which are represented in figure 23.

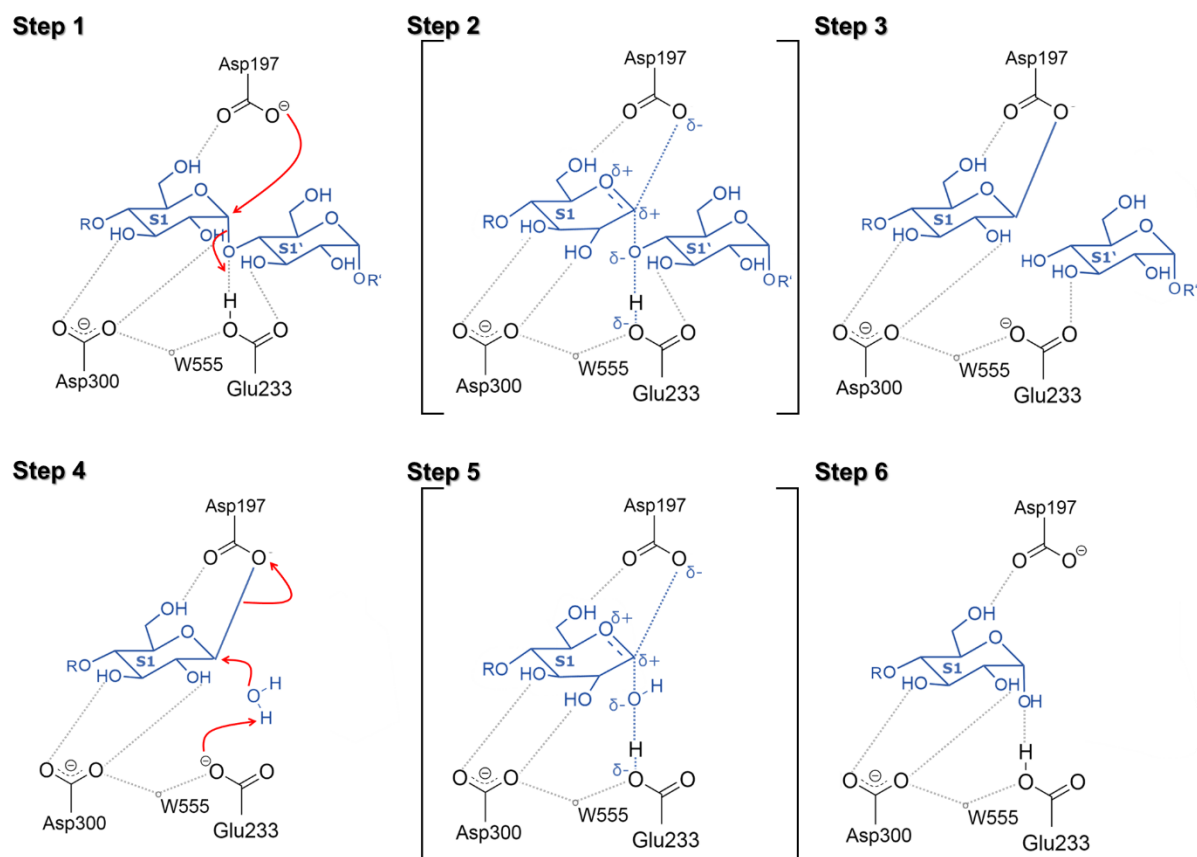


Figure 23. Schematic representation of the mechanism of action of α -amylase (66,61,62)

In this mechanism, a covalent glycosyl-enzyme intermediate forms as a consequence of a nucleophilic displacement of the aglycon by a catalytic carboxylic acid (Asp197). The covalent intermediate is then hydrolysed through another nucleophilic displacement, this time by a water molecule, to result in the release of the product with net retention of configuration at the anomeric carbon. Both the glycosylation and deglycosylation steps are thought to proceed through oxocarbenium ion-like transition states. These transition states are stabilized by another active site carboxylic acid that acts first as a general acid and then as a general base catalyst (56,66,62,64).

4.1.3. Role of calcium and chloride

Structural studies have led to the detection of a chloride binding site in amylases from human saliva, pig, human pancreas, and other sources. Moreover, it has been seen that the removal of chloride results in a significant decrease in activity.

The chloride binding site is located on the same side of the catalytic site, in fact the ligands of chloride form an extensive hydrogen bond network in which the catalytic residues are also involved. A schematic representation of the interactions between chloride ion and its environment in α -amylase is depicted in figure 24.

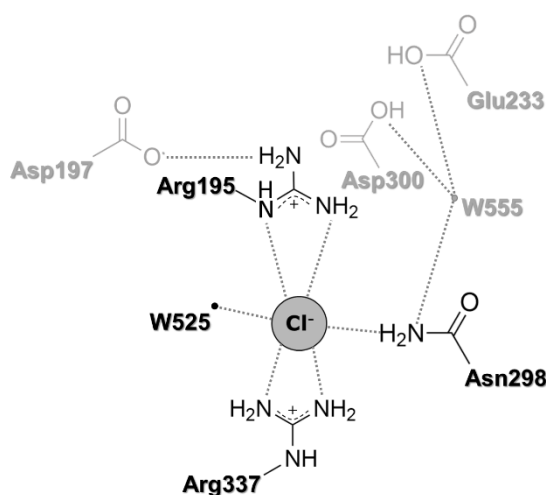


Figure 24. Schematic representation of the network of interactions within the chloride binding site (black) and the neighbouring catalytic centre (grey) (57,60–66)

The binding of chloride ion to mammalian amylases leads to an increase in the activity and a shift in the optimum pH from acidic values to neutrality. This shift in the pH-optimum may be attributable to the repulsion between the anion and the residue Glu233 (residue of the active site). The chloride is required to increase the pKa of the acid/base catalyst Glu233, which would otherwise be lower due to the presence of Arg337, a positively charged residue. The direct effects of chloride ion on the key catalytic glutamic acid carboxyl group are attributable to the fact that the chloride orients the sidechain of Glu233 to optimize the catalytic process (57,60–67).

Table 2 compares the distances of the chloride ion with the enzyme in human and porcine amylases.

Table 2. Chloride ion binding site interactions in human and porcine amylases (59)

Interaction	Atom	Distances (Å)	
		Human	Porcine
Arg195	NE	3.47	3.27
	NH2	3.32	3.37
Asn298	ND2	3.25	3.26
Arg337	NH1	3.35	3.39
	NH2	3.16	3.06
Water	O	3.32	3.21

Mammalian amylases have also one essential calcium ion per molecule of amylase. The calcium ion is tightly bound to residues located in the A (His201) and the B domains (Asn100, Arg158, Asp167). His201 is essential for mammalian amylases to exert their optimum activity at neutral pH.

Table 3 compares the distances of the calcium ion with the enzyme in human and porcine amylases.

Table 3. Calcium ion binding site interactions in human and porcine amylases (59)

Interaction	Atom	Distances (Å)	
		Human	Porcine
Asn100	OD1	2.31	2.31
Arg158	O	2.51	2.32
Asp167	OD1	2.58	2.67
	OD2	2.49	2.64
His201	O	2.41	2.28
Water	O	2.46	2.44
Water	O	2.49	2.49
Water	O	2.65	2.62

Although the calcium ion is far from the chloride ion, it is still near the substrate-binding site, it is 12.4 Å apart from the point of the catalytic attack.

The B domain is rendered partially rigid by the calcium ion, a disulphide between Cys141 and Cys160, and an interdomain disulphide bond between Cys70 of the A domain and Cys115 of domain B. The results of some studies suggest that one role of the calcium binding site of human amylase is to stabilise the structure of domain B. The calcium binding may be instrumental providing an asymmetric environment for the substrate such that the reducing and non-reducing ends of the carbohydrates are properly oriented (57,59,60,67).

Therefore, the calcium ion is essential for catalytic activity as it stabilizes the structural integrity of the A and B domains, orients the His201 in the substrate-binding cleft and provides an asymmetric environment for substrate binding. Figure 25 is a schematic representation of the interactions between calcium and the residues of α -amylase.

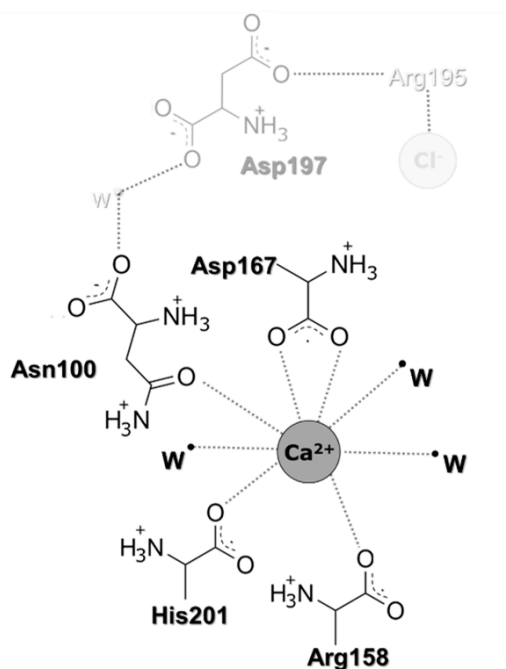


Figure 25. Schematic representation of the network of interactions within the calcium binding site (black), catalytic centre and the chloride ion (grey) (57,60)

4.1.4. Salivary vs pancreatic amylase

The complete amino acid sequence for the human amylase shows that the homology of salivary and pancreatic cDNA is 97%, being only 14 out of the 496 residues different between them (60,68,69). However, although the amino acid sequence is similar, they differ in their product formation and substrate utilization (70).

In terms of the active site region, 2 substitutions in salivary amylase could have implications on substrate binding. The first, involves the replacement of Thr163 by a serine, in a second replacement, Leu196 is exchanged for isoleucine in the middle of a highly conserved region of primary sequence. In the direct vicinity of this substitution are Arg195, which binds a chloride ion, Asp197 (which is a catalytic residue) and His201, which is part of the calcium binding site (59).

4.1.5. “Gastric” amylase

Salivary amylase is generally thought to be completely destroyed during the gastric passage due to the low pH values of the gastric juice. However, due to the fact that the gastric pH depends on the buffer capacity of the ingested meal, it could be possible that highly buffered protein meals could facilitate the intact gastric of salivary amylase. Skude et. al. reported that more than 75% of duodenal aspirates in healthy human volunteers after a Lundh meal were contaminated by active salivary amylase (71,102).

When the gastric pH is below 3, salivary amylase activity is not detected anymore in the stomach. However, it takes a while until the pH reach these low values, and by that time a significant amount of amylase could continue with the carbohydrate digestion and reach the small intestine.

On the other hand, starchy meal doesn't have a high buffer capacity, but even in those cases it has been seen that some salivary amylase also reaches the small intestine. And this could be explained with the fact that polysaccharides are able to protect human salivary amylase from the inactivation at low pH. Not only do carbohydrates protect amylase, but the simplest end products of amylolytic hydrolysis also serve to protect salivary amylase at pH 3 (72,73).

4.1.6. Physiological levels

The physiological levels of α -amylase are reported in different units depending on the used method for the activity determination. For that reason, in this thesis, the units of the reported activities were homogenised to the same unit.

For the unit conversion, the following was taken into consideration: the unit definition, the effect of pH and temperature and the substrate used to measure the enzyme activity.

- *Unit definition:* the selected unit definition to express α -amylase activity (AU) was the definition made by Bernfeld et al, which is “amount of enzyme needed to release 1 mg of maltose in 3 min”. This definition is analogue to international units (eq. 1):

$$1 \text{ AU} = \frac{1 \text{ mg maltose}}{3 \text{ min}} \cdot \frac{10^3 \mu\text{g maltose}}{1 \text{ mg maltose}} \cdot \frac{1 \mu\text{mol maltose}}{342.3 \mu\text{g maltose}} = 0.97 \sim 1 \frac{\mu\text{mol product}}{\text{min}} = 1 \text{ IU} \quad \text{Eq. 1}$$

The equivalence of the most used unit definitions for α -amylase activity to the Bernfeld units are described in table 4:

Table 4. Unit conversion (74–80)

Unit	Definition	Conversion to IU
BU (Bernfeld unit)	$\frac{1 \text{ mg maltose}}{3 \text{ min}}$	1 IU
Standard unit	$\frac{1 \text{ nmol product}}{1 \text{ min}}$	10^{-3} IU
USP (United States Pharmacopeia)	$\frac{0.16 \text{ } \mu\text{Eq Glycosidic linkage}}{1 \text{ min}}$	0.24 IU
BP (British Pharmacopeia)	$\frac{1 \text{ } \mu\text{Eq Glycosidic linkage}}{1 \text{ min}}$	1 IU
PhEur (European Pharmacopeia)	$\frac{1 \text{ } \mu\text{Eq Glycosidic linkage}}{1 \text{ min}}$	1 IU
FIP (International Pharmaceutical Federation)	$\frac{1 \text{ } \mu\text{Eq Glycosidic linkage}}{1 \text{ min}}$	1 IU
Kat (Katal unit)	$\frac{1 \text{ mol product}}{1 \text{ s}}$	$6 \cdot 10^7$ IU
SU (Somogyi unit)	$\frac{1 \text{ mg glucose}}{30 \text{ min}}$	0.185 IU

- The pH and temperature of the enzyme environment affect in different ways the ability of α -amylase to catalyse the carbohydrate hydrolysis. Therefore, the measured activity when an enzyme activity method is performed at one pH or temperature or another would be different. For that reason, the pH/temperature curves must be taken into account in order to express the activity at the same conditions.
- The substrate used to determine enzyme activity also affect to the final value, as for the enzyme it would be different to catalyse the hydrolysis of a carbohydrate rich in amylopectin or amylose. Henry et al measured amylase activity using different substrates; thus, its results could be used to determine the effect of that substrates on the determination of amylase activity (81).

Besides the effect of different sources of starch, a comparison of further substrates is described in table 5:

Table 5. Substrate comparison

Method	Substrate	Factor (vs potato starch)
Salimetrics	CNP-G3	3.9
Ceralpha	BPNP-G7	0.3

Once the reported activities were homogenised to the same unit, the found average of the physiological α -amylase activities in saliva and small intestine are depicted in figure 26:

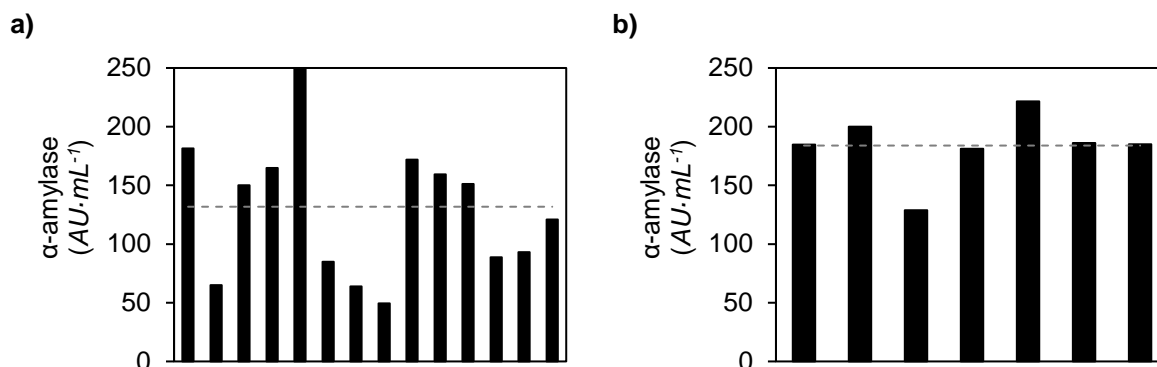


Figure 26. Physiological α -amylase activity found in a) saliva and, b) small intestine (69,82–100)
(x-axis: different references)

4.2. Pepsin

Pepsin is a digestive enzyme that catalyses the hydrolysis of the peptide bonds (figure 27) adjacent to hydrophobic or aromatic amino acids, leading to the breaking down of proteins into smaller units to enable the digestive process (101,102).

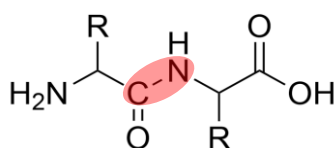


Figure 27. Peptide bond between 2 amino acids

Pepsin is secreted in the stomach as pepsinogen, that is the inactive form of the pepsin. The stability of pepsinogen in neutral and slightly alkaline solutions, as well as its catalytic inactivity, distinguishes it from the enzyme pepsin (103).

Upon ingestion of food, the zymogen (proenzyme) is secreted into the lumen of the stomach and is converted into its respective active form in the acidic gastric juice of the lumen (pH < 5). This conversion process is initiated by the acidic conditions in the lumen, is carried out by the enzyme itself and is accompanied by conformational changes in both the zymogen and the active enzyme moieties (figure 28).

Ile.Met.Tyr.Lys.Val.Pro.Leu.Ile.Arg.Lys.Lys.Ser.Leu.Arg.Arg.Thr.Leu.Ser.Glu.Arg.Gly.Leu.Leu↓Lys.
Asp.Phe.Leu.Lys.Lys.His.Asn.Leu.Asn.Pro.Ala.Arg.Lys.Tyr.Phe.Pro.Gln.Trp.Glu.Ala.Pro.Thr.Leu↓Val.
Asp.Glu.Gln.Pro.Leu...

Figure 28. Major cleavage sites in human pepsinogen during activation at pH 2 (104)
(red arrows: cleavage sites, italic: pro-segment, bold: pepsin)

The substrate binding cleft is covered and occupied by the pro-segment, which serves to block the entry of the substrate to the active site and is critical to maintain the zymogen in its inactive form at neutral pH. The pro-segment is bound to the active enzyme mainly through electrostatic interactions, although hydrogen bonds and hydrophobic interactions also play a role.

The cleavage of the pro-segment is carried out by the enzyme itself, occurs by a sequential pathway. There is a cleavage of one or more peptide bonds within the pro-segment, followed by a cleavage of the peptide bond connecting the pro-segment to the active enzyme (104).

In general, when the pH is lowered to 2.0, the protonation of acidic residues in the active enzyme moiety initiates a number of conformational changes, including the unmasking of the active site and the placement of the scissile bond of the pro-segment into the active site. These conformational changes are followed by the proteolytic cleavage of the pro-segment and, finally, the dissociation of the pro-segment from the active enzyme and the rearrangement of residues at the N-terminus of the active enzyme.

The rate of activation is sensitive to pH, temperature, ionic strength and zymogen concentration (104).

4.2.1. Structure

Pepsin is an aspartic protease, which belongs to the A1 family of peptidases. And the single molecular chain of these enzymes forms 2 domains with different amino acid sequences. The catalytic site (figure 30) is formed at the junction of the domains and contains 2 aspartic acid residues (figure 29), Asp32 and Asp215, one in each domain. The pKa values of the aspartic acid is shown in table 6.

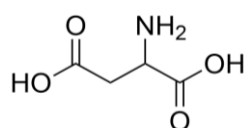


Figure 29. Aspartic acid

Table 6. pKa values of aspartic acid (pI 2.98) (105)

	pKa
α -CO ₂ H	2.10
NH ₃	9.82
R-group	3.86

The hydroxyl groups of Ser35 and Thr218 are near the active carboxyl of Asp32 and Asp215, respectively. The hydroxyl of the Thr218 can make only one hydrogen bond with the outer oxygen of the Asp215 carboxyl, and this interaction protects the aspartic acid to be protonated at low pH values (105,106).

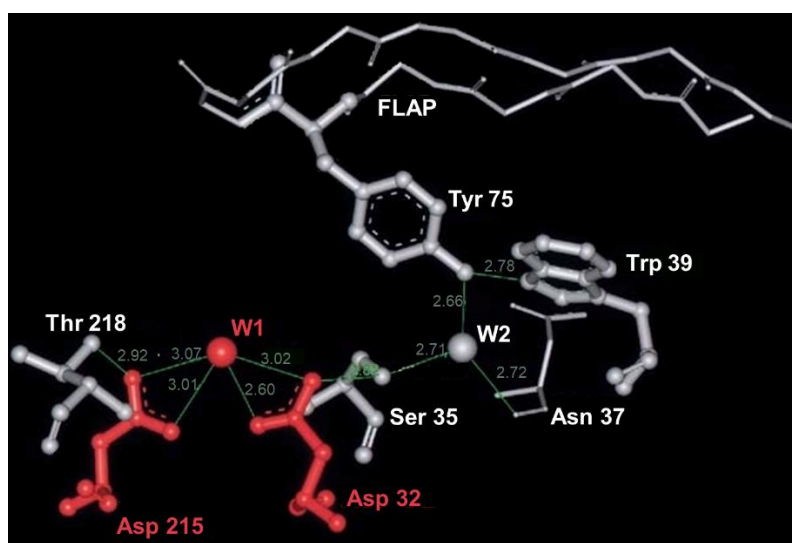


Figure 30. The catalytic site and the surrounding region of unbound pepsin in monoclinic crystals (106)

4.2.2. Mechanism of action

The accepted mechanism of pepsin assumes that one of the aspartic acid residues, acting as a general base (Asp215), must be charged, whereas the other one, acting as a general acid (Asp32), must be protonated. The first important role of residues adjacent to the catalytic centre of pepsin is to preserve the charged state of Asp215 and the protonated state of Asp32.

The Thr218 takes up a guard position near the Asp215 carboxyl at a distance of a hydrogen bond. This hydrogen bond utilizes the anti-lone pair electrons of the outer oxygen, while the syn-lone pair of this oxygen is engaged in the hydrogen bond with the water molecule W1. The efficiency of such a mechanism of charge protection is shown by the activity of pepsin at low pH values.

When the pepsin is secreted as pepsinogen, the hydrogen bond between Thr218 and Asp215 is not possible to be formed because Asp215 is involved in hydrogen bonds with Lys37 and Tyr38 of the propart (figure 31). The hydroxyl group of Thr218 can form only a weak hydrogen bond with the water molecule 540, although is close to Ser219 NH group. Then, the rearrangement of the Thr218 hydroxyl group by changing the χ_1 torsion angle and the formation of the hydrogen bond with the Asp215 carboxyl is an important step in the activation of pepsinogen (106).

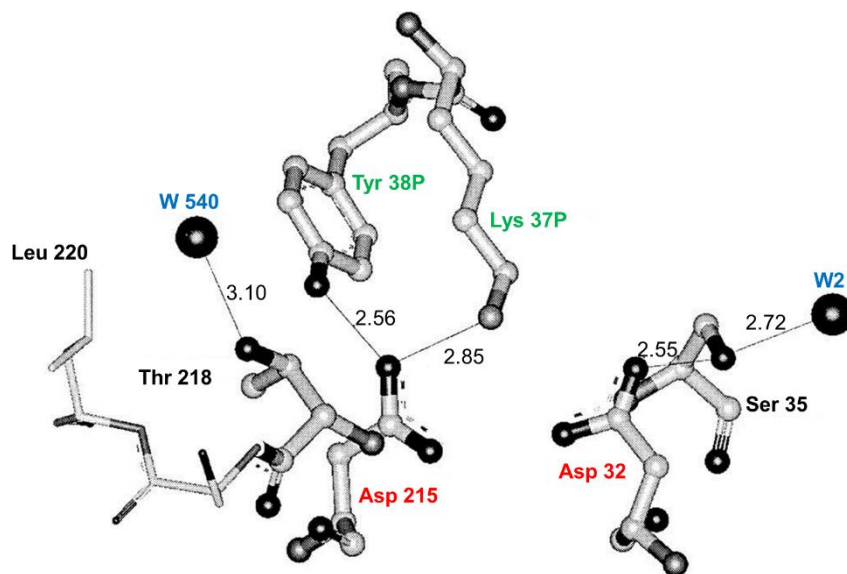


Figure 31. Conformation of the residues in the pepsinogen (106)

When the flap takes up the closed conformation, the hydroxyl of Tyr75 approaches the Trp39 N1 atom and W2. The hydrogen bond formed between the Tyr75 hydroxyl and W2 fixes the orientation of this water molecule. As Trp39 donates its proton to the Tyr75 hydroxyl, it forces Tyr75 to become a proton donor to W2, making this water donate protons to the Ser35 hydroxyl and the carbonyl oxygen of the Asn37.

Figure 32 shows the interactions present in the active site of pepsin and a susceptible substrate (106).

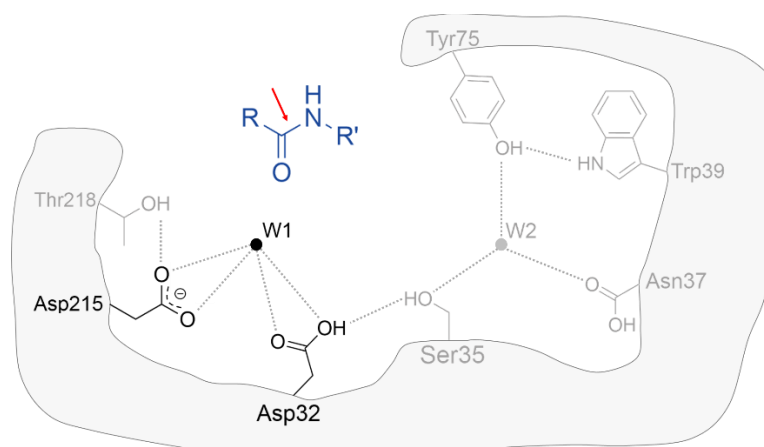


Figure 32. Interaction of pepsin active site with a possible substrate (106)
(black: active site, grey: other pepsin residues, blue: substrate, red arrow: scissile bond)

The Ser35 hydroxyl, approaching the Asp32 carboxyl after substrate binding, turns to donate a proton to the O1 carboxyl oxygen of Asp32, enhancing its acidic properties and assisting the transfer of a proton from the Asp32 carboxyl to the carbonyl oxygen of the scissile bond. This bond is concomitantly attacked by W1 polarized into a nucleophilic state by the charged Asp215 carboxyl. The chain of the hydrogen bonds, Trp39 – Tyr75 – W2 – Ser35, acts as a bridge for transmitting a signal from the flap to the active site (figure 33).

After substrate cleavage, a proton should be accepted by the Asp32 carboxyl to return the active site to its initial state. The Ser35 hydroxyl can assist this process if it alters a proton orientation toward W2. It is possible that W2 also changes its orientation, which may be initiated by the movement of the flap (Tyr75) after substrate cleavage and release of the C-terminal part of the product (106).

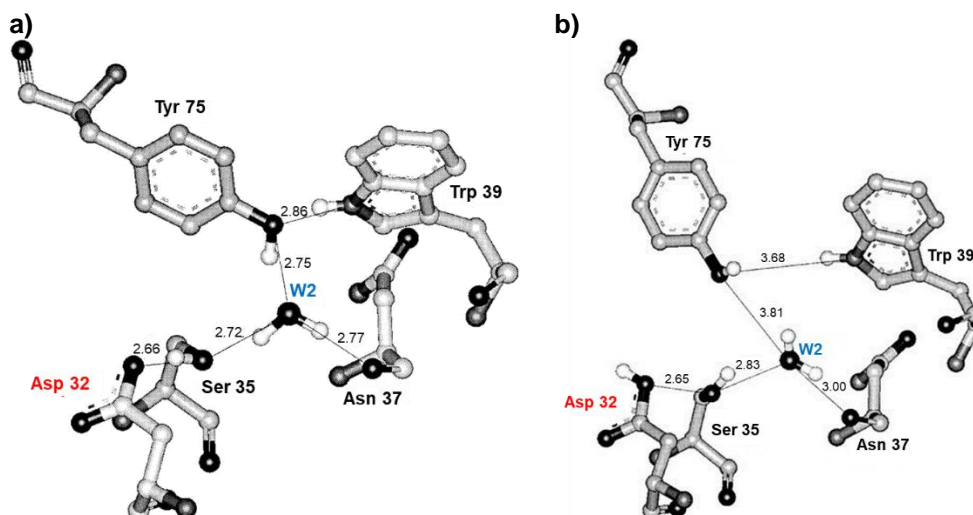


Figure 33. a) Scheme showing the arrangement of hydrogen bonds in the active site area of pepsin during formation of enzyme-substrate complex, b) scheme showing a possible reorientation of water molecule W2 after moving of Tyr75 out of the interior of a molecule (106)

The W2 molecule, returning a rotational degree of freedom, may act as a switch, utilizing consecutively its donor and acceptor properties in a hydrogen bond with Ser35 during the catalytic cycle. Analogously, Thr218 can assist proton acceptance by the Asp215 carboxyl from the gem-diol unit of the tetrahedral intermediate if the hydrogen bond Thr218 – Asp215 becomes weaker after substrate binding. This consideration shows that the formation of a chain of hydrogen-bonded residues Trp39 – Tyr75 – W2 – Ser35 – Asp32 can be an important step for the reaction catalysed by pepsin (106).

A schematic representation of the mechanism of action of pepsin is depicted in figure 34.

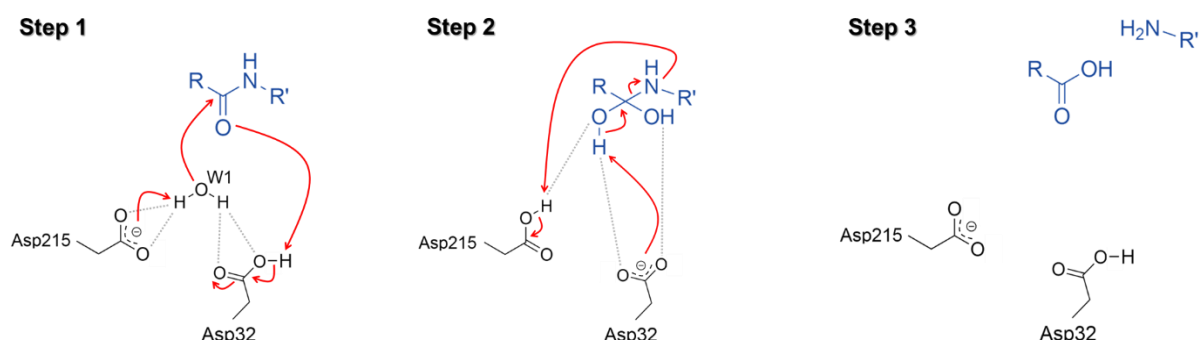


Figure 34. Schematic representation of the mechanism of action of the pepsin (107 – 109)

4.2.3. Stability of pepsin at low pH

For most proteins the ratio of positively charged groups to negatively charged groups at neutral pH values is close to 1. Thus, at the extremes of the pH scale, as the net charge on the protein is increased, the increasing charge repulsion will destabilize the folded state. The greater charge density on the folded protein can be relieved so the unfolded state should have a lower electrostatic free energy component.

The pepsin contains some residues that are negatively charged at high pH, and due to the presence of short hydrogen bonds, their carboxyl group does not move during the activation process (pepsinogen degradation), which means that the charged state is unlikely to change during the conversion from alkaline to acid media. Then, there are sufficient carboxyl groups with depressed pKa values, due to their special microenvironment, to account for the net negative charge of the enzyme (110).

Pepsin has such an extraordinary high ratio of potentially negatively charged groups to positively charged groups and because some of them remain negatively charged when the pH decreases, it has an unusually stable native structure at low pH values.

However, increasing the pH to values that are greater than the average pKa values of most carboxylate groups, the net negative charge on pepsin would become very large and the unfolded state would be stabilized. Indeed, at pH values greater than 6.5 the tertiary structure of pepsin becomes extremely unstable and it denatures irreversibly (110).

4.2.4. Physiological levels

An average of human gastric pepsin activity is $1573.5 \pm 402.2 \text{ PU}\cdot\text{mL}^{-1}$ (figure 35), where one unit is defined as the amount of enzyme needed to produce a ΔA_{280} of 0.001 per min, measured as TCA-soluble products, at 37°C, total volume 16 mL and pH 2.

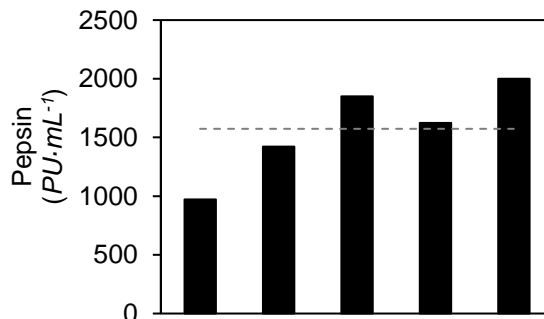


Figure 35. Reported physiological levels of pepsin (111–113,154)
(x-axis: different references)

The selected unit definition for pepsin activity in this thesis is not the international units, but the conversion of the defined PU to international units would be $80 \text{ PU} = 1 \text{ IU}$.

To calculate this factor conversion (eq. 2 – 8), the PU definition was taken in consideration ($\Delta A_{280} = 0.001$, $\epsilon_{\text{tyrosine}} = 1280 \text{ M}^{-1}\cdot\text{cm}^{-1}$, light path (b) = 1 cm, total volume = 16 mL).

$$A = \epsilon \cdot b \cdot c \quad \text{Eq. 2}$$

$$\Delta A = \epsilon_1 \cdot b_1 \cdot c_1 - \epsilon_2 \cdot b_2 \cdot c_2 \quad \text{Eq. 3}$$

$$0.001 = 1280 \cdot 1 \cdot c_1 - 1280 \cdot 1 \cdot c_2 \quad \text{Eq. 4}$$

$$0.001 = 1280 \cdot (c_1 - c_2) \quad \text{Eq. 5}$$

$$c_1 - c_2 = \frac{0.001}{1280} = 7.8 \cdot 10^{-7} \frac{\text{mol}}{\text{L}} \quad \text{Eq. 6}$$

$$16 \text{ mL} \cdot \frac{7.8 \cdot 10^{-7} \text{ mol}}{10^3} \cdot \frac{10^6 \mu\text{mol}}{1 \text{ mol}} = 0.0125 \frac{\mu\text{mol tyrosine}}{\text{min}} \quad \text{Eq. 7}$$

$$1 \text{ PU} = 0.0125 \text{ IU} \rightarrow 80 \text{ PU} = 1 \text{ IU} \quad \text{Eq. 8}$$

4.3. Trypsin

Trypsin is the main intestinal digestive enzyme responsible for the hydrolysis of food proteins. Trypsin is a serine protease and hydrolyses peptide bonds in which the carboxyl groups are contributed by the lysine and arginine residues. The serine proteases are characterized by the presence of a serine group in their active site (figure 36) (114).

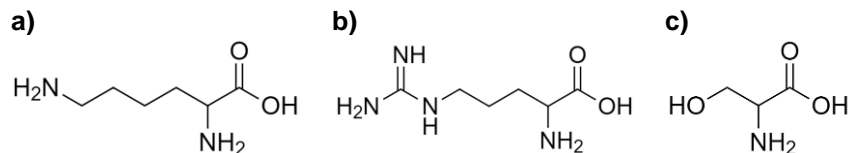


Figure 36. Structure of a) lysine, b) arginine and c) serine residues

4.3.1. Trypsinogen

Trypsin is expressed in an inactive form, known as trypsinogen. And is mainly activated by enterokinase and small amounts of trypsin that hydrolyse the peptide bond after Lys23. Enterokinase recognizes a specific sequence ($\text{H}_2\text{N} - \text{Asp} - \text{Asp} - \text{Asp} - \text{Asp} - \text{Lys} - \text{COOH}$) at the amino-terminus of trypsinogen and cleaves the peptide bond C-terminal to the Lys residue to produce the active enzyme (115 – 118).

It is important that the trypsinogen is not activated before reaching the duodenum as a premature activation can lead to pancreatitis. For that reason, the pancreas also produces a trypsin inhibitor that binds to any traces of active trypsin that might be present before it is secreted into the intestine (119).

A comparison of the structures of trypsinogen and trypsin revealed that after removal of the specific N-terminal segment, a buried aspartate (Asp199) rotates around the polypeptide backbone and forms a salt bridge with the new N-terminal amine of Ile24. This interaction stabilizes the oxyanion hole, a site on the polypeptide that is essential for catalysis. And once this region is stabilized, trypsin is irreversibly activated.

Figure 37 shows the arrangement of the key residues:

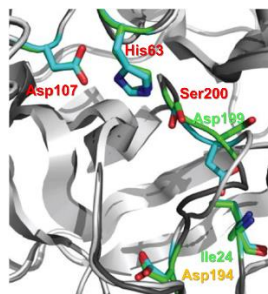


Figure 37. Arrangement of the key residues (120)

4.3.2. Role of calcium

Calcium promotes the formation of the active trypsin from trypsinogen and it also stabilizes trypsin against autolysis. But it has been shown that calcium not only protects trypsin against self-digestion, but it also slightly increased its proteolytic activity. The requirement for calcium ensures that the enzymes are not active in the cytoplasm where the calcium concentration is low (121, 122).

Figure 38 shows the environment of the calcium in the human trypsin:

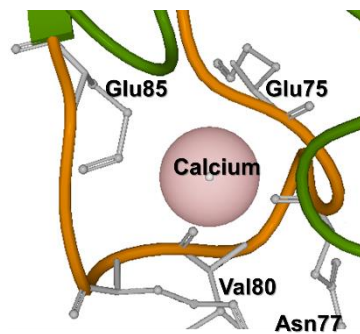


Figure 38. Environment of the calcium in the huma trypsin structure (123)

4.3.3. Structure

The general structure consists of a N-terminal peptide (15 amino acids), a short activation peptide (8 amino acids), the catalytic triad (His63, Asp107 and Ser200), the 3 key pocket specificity residues (Asp194, Gly217 and Gly227), and the 6 absolutely conserved cysteine residues necessary to build the 3 disulphide bridges observed in all vertebrate trypsins (48 – 64, 171 – 185, 196 – 220) (figure 39). Human trypsin has a similar tertiary structure to bovine, rat and porcine trypsins (120).

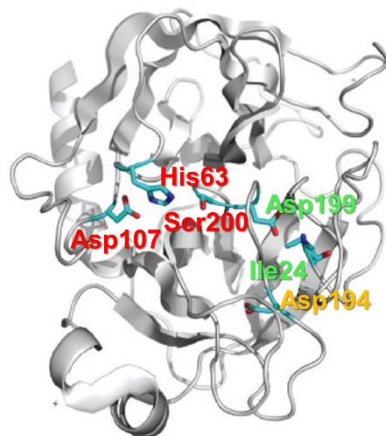


Figure 39. Global structure of trypsin, the residues that form the catalytic triad (red), and the base of the specificity pocket (yellow) are depicted (120)

The substrate specificity of trypsins is conferred by the substrate binding pocket composed of Asp194, Gly217 and Gly227. Whereas Asp194 forms a strong electrostatic band with arginine or lysine residues of the substrate, Gly217 and Gly227 permit entry of large amino acid side chains into the hydrophobic pocket (116).

4.3.4. Mechanism of action

Catalytic activity in trypsin proceeds by the utilization of an arrangement of three-amino acid side chains that constitute the catalytic triad. The δ -oxygen of Asp107 accepts a hydrogen bond from the δ 1-nitrogen of His63, this interaction highly polarizes His63 such that there is a proton on the δ 1-nitrogen and not on the ϵ 2-nitrogen. Consequently, the ϵ 2-nitrogen faces Ser200 and acts as a general base to increase the nucleophilic character of the hydroxyl group of Ser200 (figure 40).

In the accepted mechanism of catalysis (figure 41), after the initial complex between trypsin and a substrate is formed, the hydroxyl oxygen of Ser200 attacks the carbonyl carbon of the Arg or Lys residue. The histidine acts as a general acid and donates the proton abstracted from Ser200 to the newly formed amine group.

The first product then dissociates, and a covalent acyl-enzyme complex is simultaneously formed. Diacylation occurs through a similar mechanism except that solvent provides the attacking nucleophile (120).

The structural basis for recognition of Arg and Lys residues is a clearly defined region in the protein referred as the substrate binding pocket (SBP). The Asp194 occupies the base of this site and forms favourable interactions with the positively charged Arg and Lys side chains of bound substrates. Residues lining the sides of the SBP also affect substrate recognition. Glycines at positions 217 and 227 lie on opposite walls of the pocket and interact with the aliphatic portion of the long side chains of Lys and Arg. Large hydrophobic residues do not bind productively in the SBP and negatively charged residues are chemically incompatible (124).

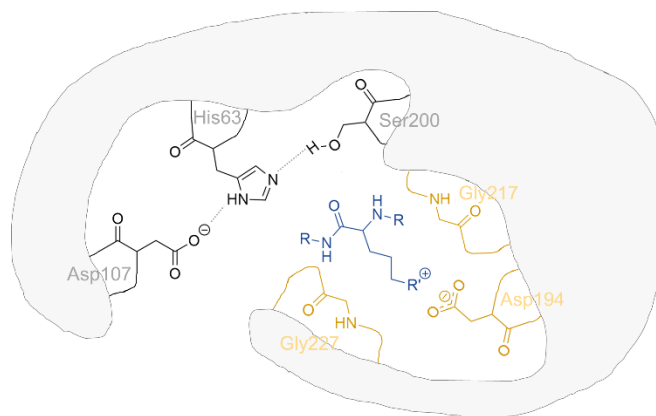


Figure 40. Schematic representation of trypsin at pH ~ 8 (black: residues of the catalytic site, brown: residues of the substrate binding pocket, blue: residue of the protein that is digested, R': side chain of lysine or arginine) (116,120)

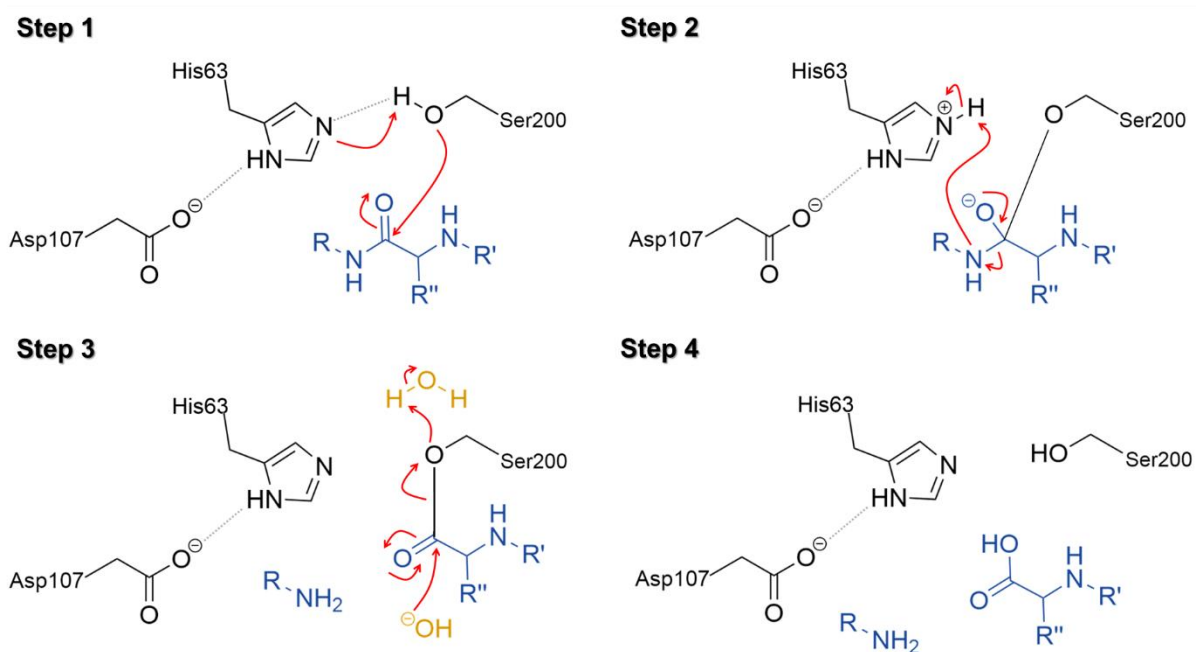


Figure 41. Schematic representation of the mechanism of action of trypsin (120)

Human trypsin works at its maximum capacity when the pH is slightly alkaline (optimal pH: 7.5 – 8.5). This could be explained by the fact that at lower pH values, the imidazole group of the His63 would be protonated and then the reaction could not start because it would not be able to take the proton from the Ser200. On the other hand, at higher pH values, the side chain of the Arg or Lys from the digestible protein, would be uncharged and could not form the strong electrostatic bond with the Asp194, that is formed at the optimal pH (125).

4.3.5. Physiological levels

An average of the reported trypsin activity present in the small intestine after meal intake is $100.8 \pm 31.7 \text{ TU}\cdot\text{mL}^{-1}$ (figure 42), where one TU is defined as the amount of enzyme needed to hydrolyse $1 \mu\text{mol}$ of substrate (TAME) per minute at 25°C and pH 8.1. These units are equivalent to international units.

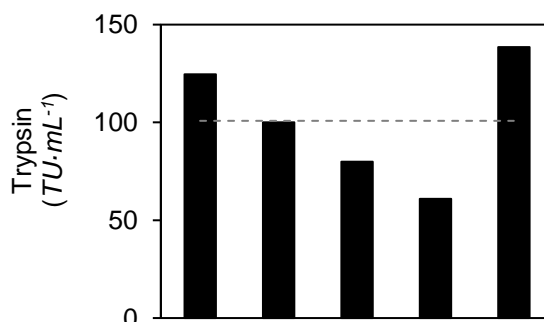


Figure 42. Physiological trypsin activities (94,95,99,115,126,127)
(x-axis: different references)

4.4. Lipase

4.4.1. Gastric lipase

Most dietary fatty acids are ingested as triglycerides and their bioavailability depends on the hydrolysis of ester bonds on the glycerol backbone. Lipases may degrade a broad range of ester compounds, however in the gastrointestinal tract, they catalyse the hydrolysis of the ester bonds in acylglycerols (figure 43) including the triglycerides that comprise greater than 95% of the dietary fats in the western diet.

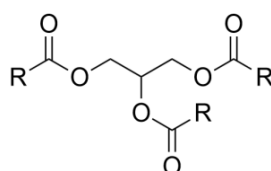


Figure 43. Acylglycerols structure

In humans, the digestion of dietary triglycerides begins in the stomach, where gastric lipase releases about 15% of the fatty acids and then the lipases secreted by pancreatic acinar cells complete fat digestion in the proximal small intestine. However, it has been shown that human gastric lipase accounts for an additional 7.5% lipolysis in the duodenum, where it acts in synergy with the pancreatic lipase (128 – 130).

Depending on the species considered the enzyme is either synthesised and secreted by the tongue tissue (lingual lipase) as in the rat, mouse and sheep, or by gastric mucosa (gastric lipase) as in the rabbit, guinea pig, dog and humans (131 – 133).

Triglyceride lipolysis (figure 44) is a heterogeneous catalysis involving soluble lipases, insoluble substrate, and the creation of a lipid-water interface. When optimal lipolysis occurs, triglycerides are transformed into one 2-monoglyceride and 2 free fatty acids (129,134).

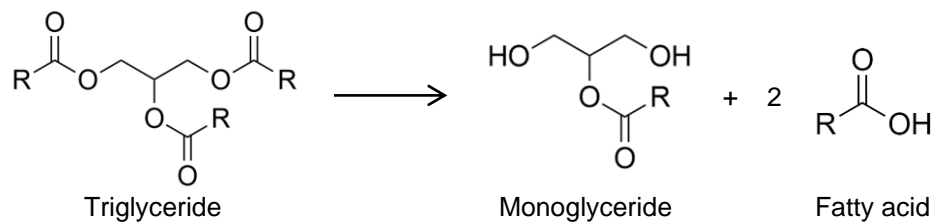


Figure 44. Lipolysis

Gastric lipolysis plays an important role in fat digestion under normal conditions, as the long-chain free fatty acids released in the stomach facilitate the subsequent intestinal hydrolysis of dietary fat by pancreatic lipase (135).

The characteristics of gastric lipase, such as optimum pH of 4 – 5.4 and its ability to function without bile salts or cofactors, are advantages in gastric lipolysis. In addition, gastric lipase is not inhibited by the bile salts present in the gastrointestinal tract, whereas pancreatic lipase requires a cofactor, namely colipase, to counteract the inhibitory effects of bile salts on lipase adsorption at lipid-water interfaces (129,135 – 137).

Gastric lipolysis is essential for an optimal digestion process in the intestine by human pancreatic lipase (HPL). Indeed, gastric lipolysis ensures:

- Lipid emulsification or lipid droplet rearrangement in the stomach to create lipid-water interface necessary for lipolysis.
- Release of long-chain free fatty acids stimulating cholecystokinin secretion, which in turn stimulates HPL secretion and slows down gastric emptying.
- Release of unsaturated long-chain free fatty acids that rapidly activates the HPL-colipase complex by increasing the colipase binding to lipid interface or by causing a conformational change of HPL via a direct interaction with free fatty acids.
- Formation of diglycerides, which are hydrolysable at much higher rates than triglycerides (129).

4.4.1.1. Structure

An important feature of lipases is the presence of a mobile subdomain lid located over the active site. If the lid is closed, the active site is protected from the environment and inaccessible to the substrates, hence the lipase is inactive. In an open conformation, substrates can enter the active site of lipases and be converted.

The presence of apolar-aqueous interphases increases lipase activity and this is known as “interfacial activation”.

Lids of lipases are amphipathic structures, in the closed conformation, their hydrophilic side faces the solvent, while the hydrophobic side is directed toward the catalytic pocket. As the enzyme shifts to the open conformation, the hydrophobic face becomes exposed and contributes to the substrate-binding region (138).

Human gastric lipase (HGL) is a highly glycosylated molecule with an N-terminal tetrapeptide (Leu-Phe-Gly-Lys). The three-dimensional structure of HGL can be considered as the superposition of 3 independent structural elements: the lid (Lys210 – Thr267), the cap (Thr184 – Asn308) and the core (Leu1 – Ala183, Val309 – Lys379) domains (129,135,136,139).

Figure 45 shows a representation of the gastric lipase and its different parts:

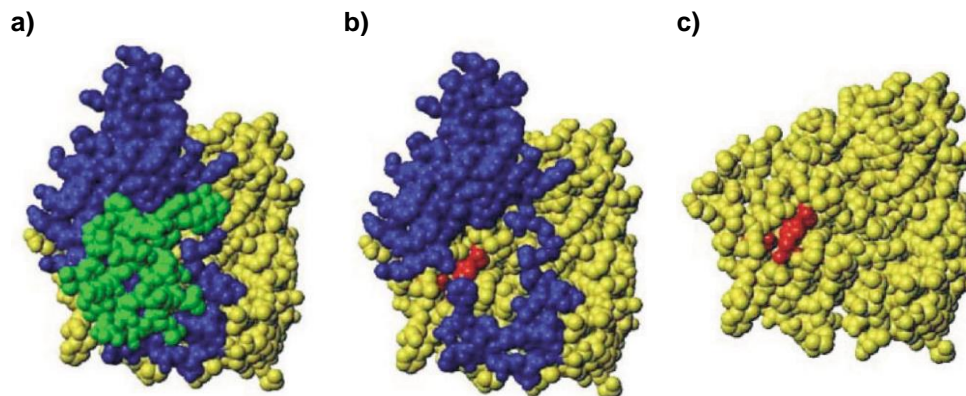


Figure 45. Representation of a) HGL, b) enzyme without lid and c) core domain and catalytic triad (139)
(green: lid domain, blue: cap domain, yellow: core domain, red: catalytic triad)

4.4.1.2. Why it has an acidic optimal pH?

Gastric lipase is active and stable in the acidic environment of the stomach, where the gastrointestinal lipolysis of dietary fat is initiated. This lipase can be said to be an extremophilic enzyme because it retains its activity in gastric juice at pH 2, in the presence of pepsin and physiological temperature (137).

Most lipases show optimum activity at pH levels above 7, which is consistent with the ionization properties of histidine and the fact that this residue is known to play an important role in the charge relay system involving the catalytic triad and the enhancement of the nucleophilic character of the serine residue.

The optimum activity of gastric lipase at acidic pH is only apparent and results from the fact that the lipase adsorption at the lipid-water interface, which is pH-dependent, must occur before the insoluble substrate is hydrolysed. For that reason, the limiting step in the overall process of insoluble substrate hydrolysis is the adsorption of the enzyme at the lipid-water interface (140).

Figure 46 shows the effect of pH on the maximum rate of the adsorption, activity and catalytic turn-over.

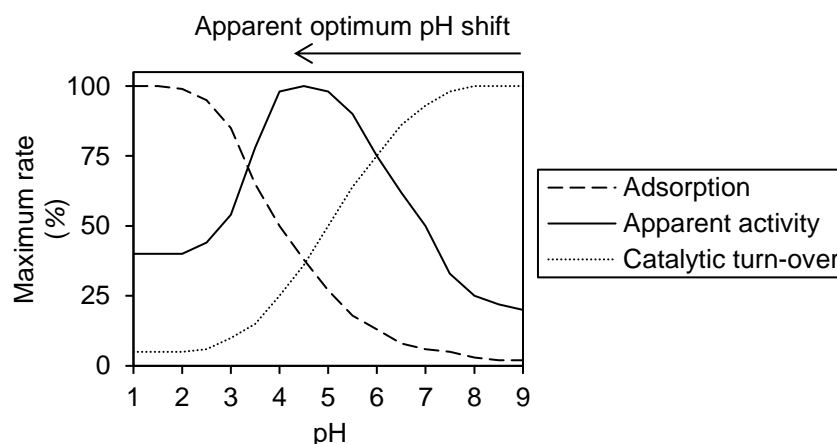


Figure 46. Simulation of gastric lipase apparent activity considering pH-dependent enzyme adsorption and catalytic turn-over (140)

The kinetic model of the lipase is depicted in figure 47:

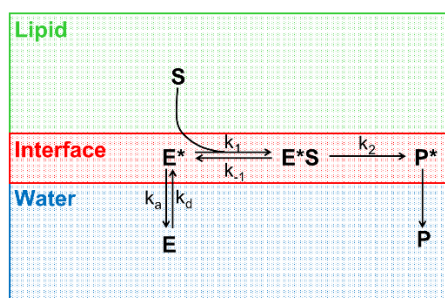


Figure 47. Kinetic model for the action of lipase on an insoluble substrate (141)

Interfacial adsorption of gastric lipase is mainly driven by hydrophobic interactions notably via a large apolar ring around the active site cavity, which is preserved on a wide range of pH, However the protein is positively charged below pH 5. Since the adsorption process of gastric lipase is pH-dependent, some electrostatic interactions are probably important, but specific amino acids or domains potentially involved in these interactions have not yet been identified.

The edges of the apolar ring surrounding the lipase active site are positively charged while a patch of negative charges is located opposite to the entrance of the active site and this specific distribution of charges, in addition to hydrophobic interactions may facilitate the orientation of the lipase close to a negatively charged lipid interface. This distribution should result in an attraction of the positively charged ring and a repulsion of the part opposite to the active site (142).

The molecular surface of HGL is represented in figure 48, where the hydrophobic regions are differentiated from the hydrophilic ones.

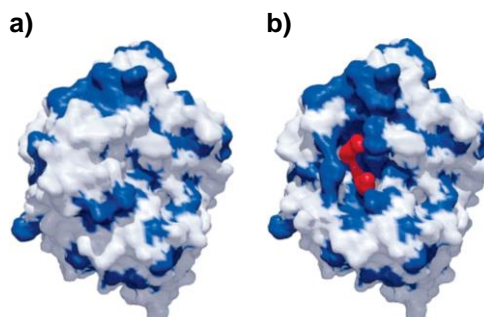


Figure 48. Molecular surface representations of HGL where the hydrophobic residues are coloured blue, a) complete enzyme, b) lipase with the putative lid depleted and an inhibitor represented in red in the active site (130)

4.4.1.3. Mechanism of action

In lipases, as well as in serine proteases, the catalytic machinery consists of a triad and an oxyanion hole. In HGL, the nucleophilic serine is located at position 153 and the other 2 residues that form the catalytic triad are His353 and Asp324. The nucleophilic serine is covered by the cap and the lid and is therefore not freely accessible to lipidic substrate molecules. However, once the lid has been removed, the rest of the cap domain forms a ring of hydrophobic residues around the active site serine, therefore the cap domain may well be involved in the affinity of gastric lipase for lipids (139,143).

The oxyanion hole is a part of the enzyme that stabilizes the oxyanion transition state via hydrogen bonds with 2 main chain nitrogens. Within HGL, one mandatory component of the oxyanion hole is the NH group of the residue following the nucleophile Ser (Gln154) and the second NH group belongs to Leu67 (130).

A schematic representation of the mechanism of action of HGL is depicted in figure 49.

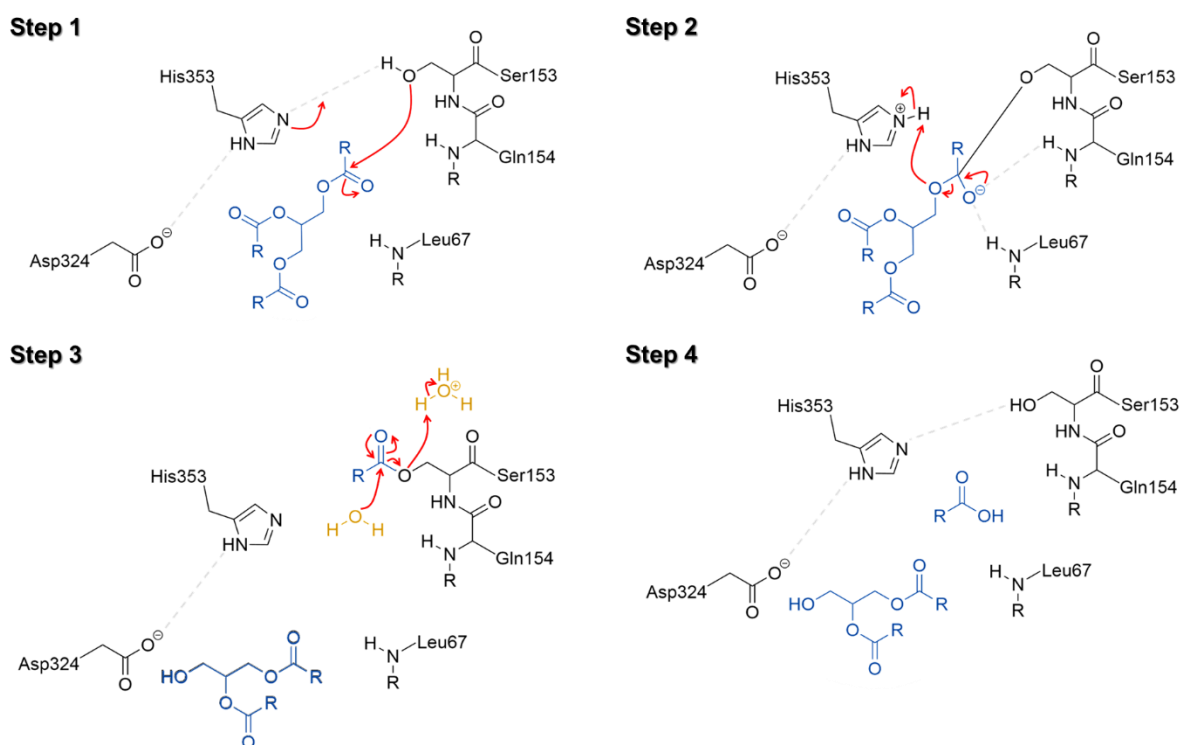


Figure 49. Schematic representation of the mechanism of action of gastric lipase (144)

The catalysis starts by an acylation, this step consists in the transfer of a proton between the aspartate, the histidine, and the serine residues of the lipase, causing the activation of the hydroxyl group of the catalytic serine. As a consequence, the hydroxyl residue of the serine, with subsequently increased nucleophilicity, attacks the carbonyl group of the substrate.

The tetrahedral intermediate is formed with a negative charge on the oxygen of the carbonyl group. The oxyanion hole stabilizes the charge distribution and reduces the state energy of the tetrahedral intermediate by forming at least 2 hydrogen bonds. The diacylation step then takes place, where a nucleophile (water) attacks the enzyme, releasing the product and regenerating the enzyme (144).

4.4.1.4. Physiological levels

The reported physiological activity of the lipase is $66.3 \pm 7.7 \text{ LU}\cdot\text{mL}^{-1}$ (figure 50) in the stomach, where one unit is defined as the amount of enzyme needed to release $1 \mu\text{mol}$ of butyric acid per min at 37°C and pH 5.5. These units are equivalent to international units.

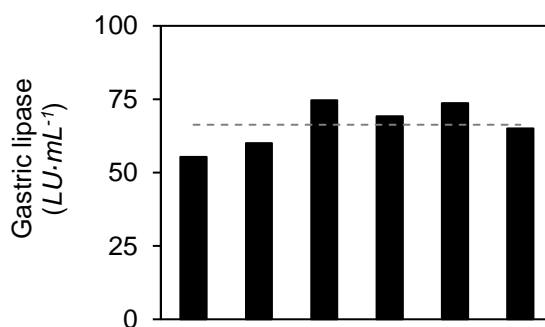


Figure 50. Physiological lipolytic activity in human stomach (129, 131, 145, 146, 151) (x-axis: different references)

4.4.2. Pancreatic lipase

Pancreatic lipase is one of the exocrine enzymes of the pancreatic juice and it is essential for the digestion of dietary fats in the intestinal lumen (134).

4.4.2.1. Structure

This lipase is divided into 2 domains: a globular N-terminal (amino acids 1 – 335) and a C-terminal domain (amino acids 336 – 465). The domains are separated by a short, unstructured stretch of amino acids and are stabilized by 7 disulphide bonds (128).

The N-terminal domain bears the catalytic triad (Ser152, Asp176, His263), the access of which is controlled by a surface loop, the lid (figure 51). While, the C-terminal domain is mainly devoted to colipase binding (147,148).

The lid domain is one of the largest loops that cover the active site however there are 2 shorter loops that also block the active site, which are formed by residues 76 – 85 (β 5 loop) and residues 204 – 224 (β 9 loop) (128).

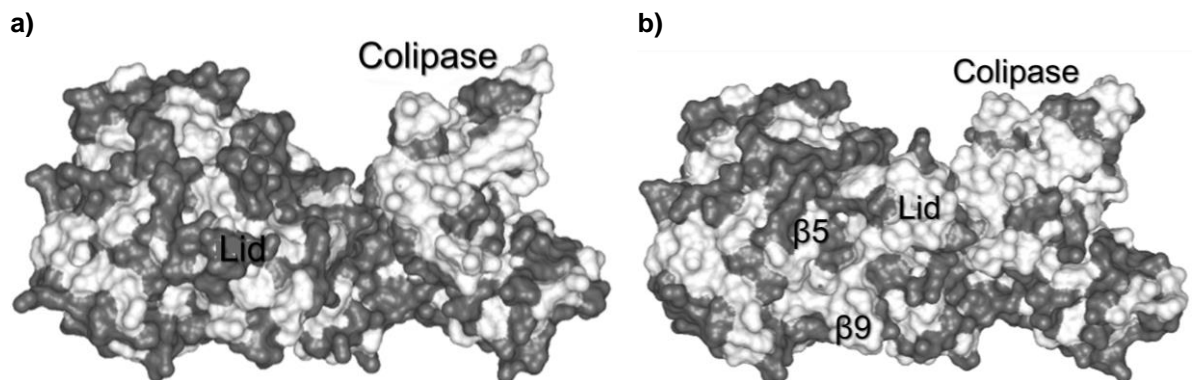


Figure 51. Surface representation of lipase-colipase complex in the a) closed and b) open conformation (149)
(hydrophobic residues are light shading)

4.4.2.2. Colipase

Efficient dietary fat digestion in the small intestine requires colipase and bile salts in addition to lipases. The importance of bile salts in fat absorption is apparent when bile flow is absent. For instance, in humans with bile fistulas and greatly decreased duodenal bile acid concentrations, the intestine only absorbs about 50 – 75% of dietary lipids. Additionally, bile salts may alter the surface of the emulsion particles by clearing dietary proteins and oligosaccharides apart from their important role in fatty acid absorption. This action removes potential inhibitors of pancreatic lipase from the lipid-water interface (149).

Pancreatic lipase is inhibited by physiological concentrations of bile salts as well as by phospholipids and proteins that are present in emulsions of dietary lipids. For that reason, it requires the colipase as a cofactor, to restore the activity to pancreatic lipase under the presence of these substances. Colipase also helps to anchor the lipase to the surface, stabilizes it in the “open”-active conformation and permits the efficient digestion of dietary fats (128,134).

The effect of bile and colipase on the lipase activity is shown in figure 52.

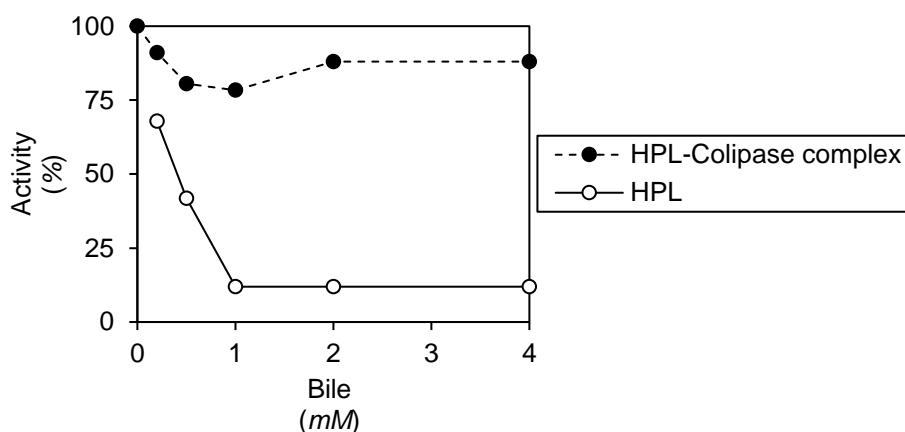


Figure 52. Effect of bile and colipase on the lipase activity of HPL (144)

The effect of bile salts on pancreatic lipase activity is related to their concentration. Below their critical micelle concentration, bile salts enhance lipase activity probably by stabilizing the enzyme at the lipid interface while above their critical micelle concentration, they induce an inhibition and the presence of colipase is an absolute requirement to restore full lipase activity (144).

The colipase is formed by 112 amino acids, it has a molecular weight of 11.6 kDa and it is secreted in an inactive form and activated in the duodenum by trypsin. The first 17 amino acids form a signal peptide, which are followed by a 5 amino acid prosegment. This hypothesis accounts for the absence of a zymogen of pancreatic lipase, as is found for many other digestive enzymes, and offers a mechanism to protect the pancreas and surrounding fat tissue from damage by lipase. On the other hand, the pro-colipase does not form any interactions with the N-terminal domain and does not alter its conformation (128,129,149).

The interaction occurs initially between colipase and the C-terminal domain through 2 salt bridges involving Asp390 and Lys400 of pancreatic lipase. At the same time, the colipase exposes its hydrophobic fingertips to bring the catalytic N-terminal domain of pancreatic lipase into close contact with the lipid interface where the opening of the lid occurs, leading to an open conformation of the active site of the lipase.

The contact with the interface causes the lid domain of pancreatic lipase to open, and new interactions are formed between colipase and lipase that increase the binding affinity of colipase, lipase and the interface. Once the lid is opened, the new interactions with colipase keep the lid in the open conformation, and lipolysis proceeds at a high rate catalysed by the Ser-His-Asp triad (128,129).

4.4.2.3. Mechanism of action

The catalytic triad is pulled together through hydrogen bonds between the hydroxyl group of serine and one imidazole nitrogen of histidine, and between the other imidazole nitrogen and the carboxylic group of the aspartic acid. It is under this conformation that the hydrolysis reaction can take place. The hydroxyl group of serine is thought to initiate the reaction through a nucleophilic attack to the first glyceryl carbon, with the fatty carboxylate being the leaving group. Consequently, the reaction would become faster the more electrophilic the glyceryl carbon is and the better the leaving group (more stable) of the carboxylate is. Therefore, the molecular mechanism of HPL is analogous to HGL, the only difference is the numbering of the residues and the oxyanion hole (150).

4.4.2.4. Physiological levels

Pancreatic lipase has been classified among the enzymes with the greatest turnover number because a molecule of lipase can release up to 500k molecules of free fatty acids per minute. It is generally recognized that the pancreas produces much greater amounts of lipase than those required for the digestion of dietary triglycerides (136).

The reported physiological activity of lipase in the small intestine is 1704.3 ± 566.7 LU·mL⁻¹ (figure 53), where one unit is the amount of lipase needed to release 1 μmol of butyric acid per min at 37°C and pH 8.

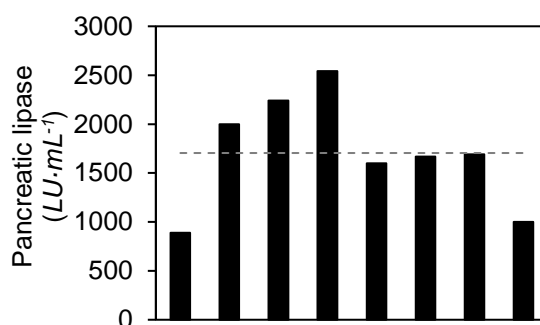


Figure 53. Physiological lipase activity in small intestine (95,99,129,145,146,151)
(x-axis: different references)

4.4.3. Parameters that affect lipolysis

For lipolysis to occur, lipases must be adsorbed to a lipid-water interface, therefore the properties of such an interface are an important factor for activity. The lipid droplet size is a key physicochemical parameter governing the lipid-water interface surface area.

Lipid droplet size governs human gastric and pancreatic lipase activity in humans. Depending on the droplet size, there is a triglyceride hydrolysis rate of 5 – 37% in the stomach and 30 – 65% in the duodenum. For the same amount of lipid, small-size droplets (0.7 μm) allow a much higher lipid-water interface surface area than large-size droplets (10 μm) leading to a higher lipolysis of the droplet triglycerides by HGL in the stomach (37% vs 16%) and also by HPL in the duodenum (73% vs 46%).

First, under physiological conditions, lipases are in excess relative to the substrate, and a larger lipid-water interface area will allow the binding of more lipase molecules to the substrate. In addition, gastric lipolysis is inhibited by the protonated long-chain generated free fatty acid that accumulates at the lipid droplet surface at acidic pH levels, forming particles that entrap HGL and stop its action when free fatty acids concentration reaches 121 – 172 μmol·m⁻² interface area, thus a greater interface surface area will delay the inhibition phenomenon.

Furthermore, food components interfering with the lipid emulsification process, such as viscous fibres, lead to a lower interface area and consequently to lower triglyceride lipolysis by HGL and HPL.

Droplet size is not the main physicochemical parameter governing lipolysis rate; thus, lipid droplet organization is another key physicochemical parameter. A lipid droplet is composed of a hydrophobic core containing most of the triglyceride molecules, esterified cholesterol and lipid-soluble vitamins, surrounded by an amphipathic surface monolayer of phospholipid. The droplet surface also contains free cholesterol and a few triglyceride molecules thereby enabling lipase action at the lipid droplet surface (129).

4.5. Introduction to alternative sources

The best approach to mimic human digestion would be the use of human enzymes. However, these enzymes are usually very expensive or not commercially available. Hence, it is necessary to find good alternatives to human enzymes for numerous in vitro methods.

The main enzymes that catalyse the hydrolysis of the macronutrients in the lumen of the gastrointestinal tract are α -amylase in the mouth, pepsin and lipase in the stomach and α -amylase, trypsin and lipase (in the secreted fluid called pancreatin) in the small intestine.

However, for pancreatin it is difficult to find an alternative source containing the same ratio of enzymes. For that reason, the described in vitro digestion methods usually only take into consideration the activity of the enzyme that catalyses the hydrolysis of the substance of interest. However, it would be more accurate to find a solution to mimic the pancreatin with the same ratio of enzymes (152).

Therefore, the suitability of different commercially available enzymes to closely mimic the human digestion in an in vitro method, evaluated according to the similarities between both enzyme activity profiles was studied in this thesis. In comparison to the human equivalent, enzyme activities were studied in dependence of pH, temperature as well as of dissolution media.

5. Bile

Bile contains bicarbonate ions, cholesterol, phospholipids, bile pigments, organic wastes and bile salts (figure 54). The bile salts solubilize dietary fats, which would otherwise be insoluble in water, and their solubilization increases the rates at which they are digested and absorbed. On the other hand, bicarbonate ions help neutralize acid from the stomach and brings the pH up to a level at which pancreatic enzymes can function.

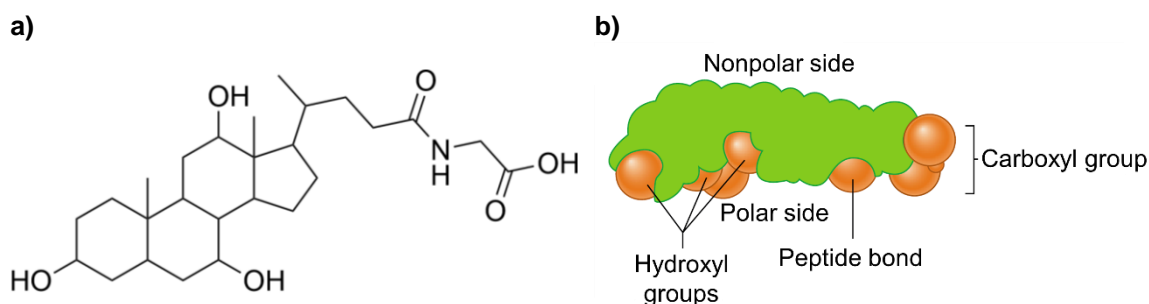


Figure 54. a) Structure of glycocholic acid, b) three-dimensional structure of bile salt (8)

Bile is secreted by the liver and flows to the gallbladder, where 40 – 70 mL of bile can be stored. The liver produces and secretes about 600 – 1000 mL of bile each day.

Most bile salts are reabsorbed in the ileum and carried in the blood back to the liver, where they contribute to further bile secretion. Bile secretion into the duodenum continues until the duodenum is emptied (6,8).

5.1. Physiological concentration

The general composition of human, bovine and porcine bile is depicted in the following graph (figure 55):

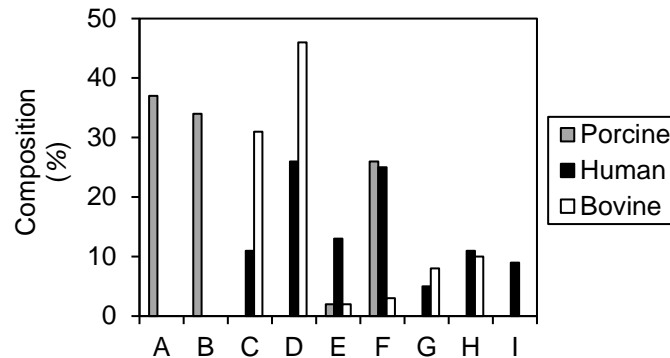


Figure 55. Comparison of different sources of bile (42)

(A: taurohyodeoxycholate, B: Glycohyodeoxycholate, C: Taurocholate, D: Glycocholate, E: Taurochenodeoxycholate, F: Glycochenodeoxycholate, G: Taurodeoxycholate, H: Glycodeoxycholate, I: Other bile acids)

An average of the physiological concentration of bile in the small intestine is depicted in the following graph (figure 56):

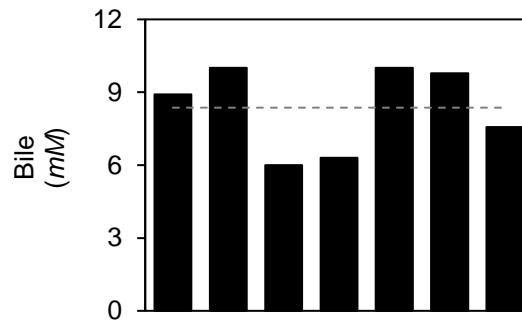


Figure 56. Postprandial bile concentration in the small intestine (153–158)
(x-axis: different references)

6. Electrolytes present in gastrointestinal tract

6.1. Saliva

Although salivary electrolytes and proteins account for only a small proportion of saliva, they play various important roles to maintain the oral health, integrity of teeth but also affect the activity of α -amylase. For example, the bicarbonate present in saliva serves as the main buffer against acid (159).

The most abundant salivary electrolytes are sodium, potassium chloride and bicarbonate and an average of the concentration of some electrolytes present in human saliva is shown in figure 57.

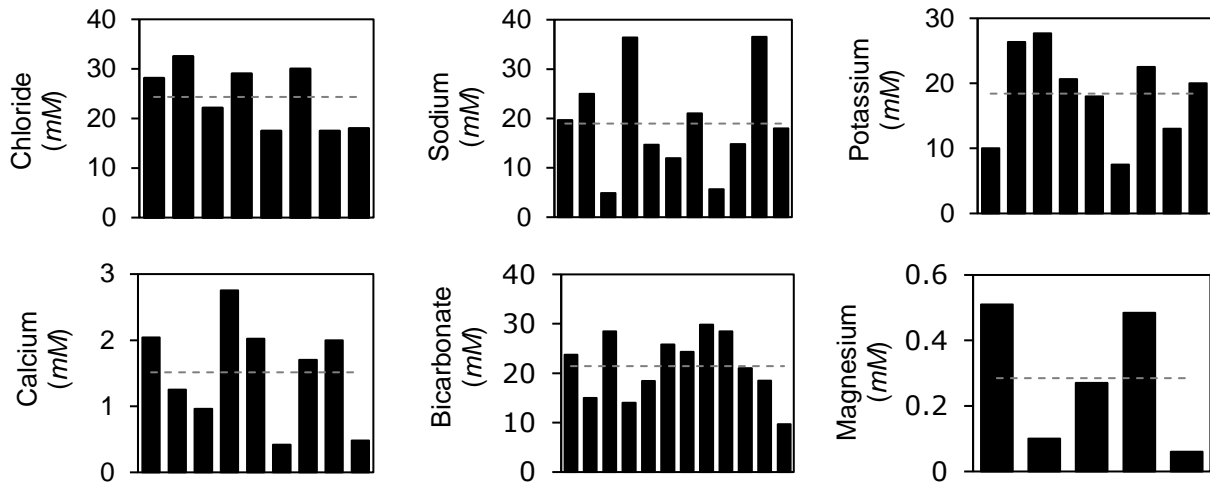


Figure 57. Physiological concentration of electrolytes in saliva (bar: reported values (160 – 172), dashed line: average, x-axis: different references)

The final composition of saliva depends, among other variables, on its flow rate, which has a high individual variability and even for the same individual the composition is not constant as it depends if the saliva is stimulated, the kind of meal that is eaten, etc.

6.2. Stomach

The most relevant electrolytes that are present in the gastric juice are chloride, sodium, potassium and calcium in a smaller extend. The ions H^+ and HCO_3^- have also an important role in the stomach as they regulate the gastric pH. The gastric content changes over time after a meal consumption, however an average of the postprandial concentration of the most important electrolytes is depicted in the following graphs (figure 58):

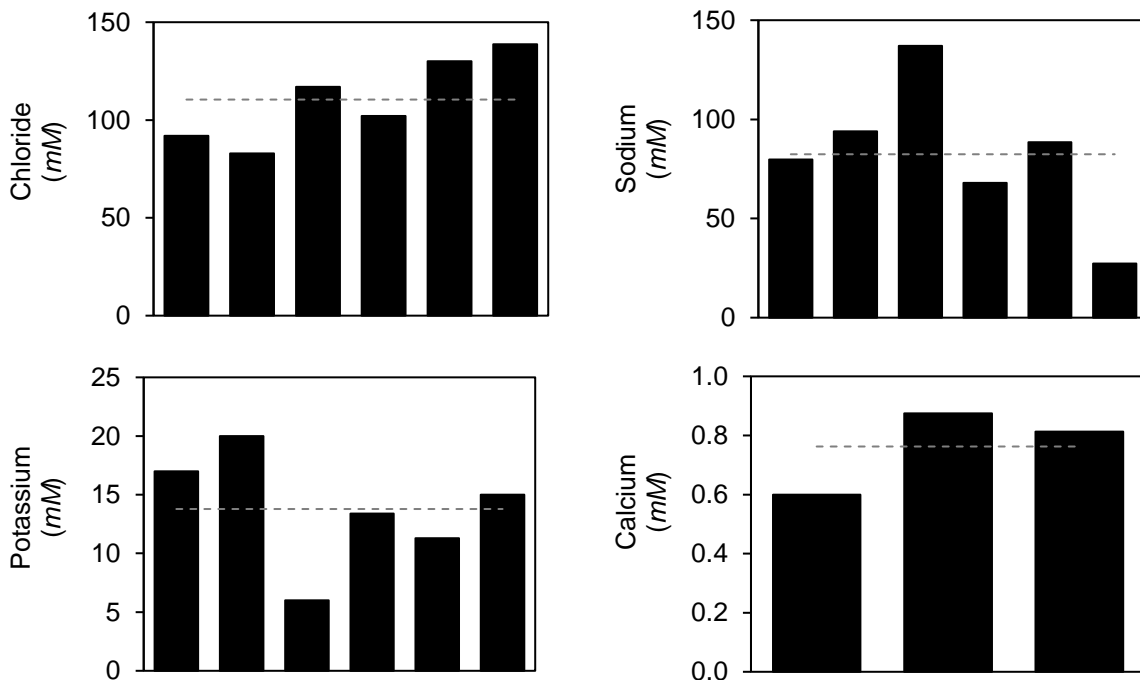


Figure 58. Concentration of some of the most important electrolytes present in the gastric juice (173 – 180) (x-axis: different references)

6.3. Small intestine

The major cations in the pancreatic juice are sodium and potassium, both are secreted at concentrations similar to their plasma concentrations. The major anions are bicarbonate and chloride, the concentrations of which depend on flow rates, as the flow rate increases, the bicarbonate concentration rises asymptotically, and the chloride concentration falls reciprocally. In humans, the pancreatic juice also contains calcium and traces of other electrolytes.

An average of the main electrolytes present in the human pancreatic juice are depicted in the following figure (figure 59):

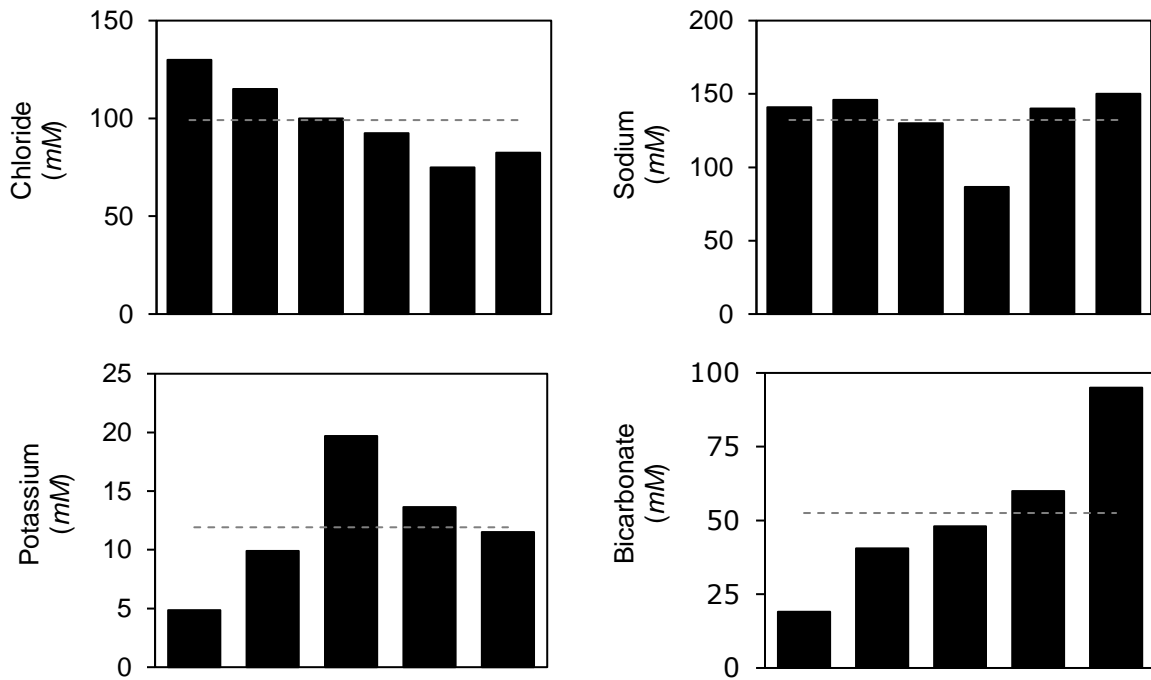


Figure 59. Average of electrolyte concentration in human pancreatic juice (181 – 186)
(x-axis: different references)

7. pH throughout gastrointestinal tract

7.1. Mouth

When no food is being eaten, saliva has a pH between 6.0 and 7.6. Once chewing begins, more saliva is produced, which contains large quantities of bicarbonate ions. Bicarbonate ions counteract the pH change due to the acid released from the foodstuff (187). Therefore, the pH of saliva depends on the kind of meal that has been eaten, and the effect of different types of meal on the postprandial pH are reflected in the following graph (figure 60):

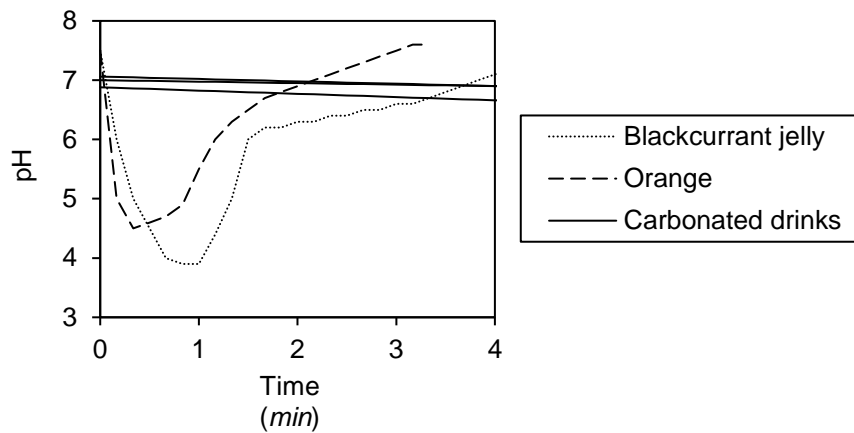


Figure 60. Effect of different kind of meals on the postprandial pH in the mouth (each line is an example of a meal) (187,188)

Therefore, the reported average of the pH in the mouth would be 6.7 ± 0.5 (figure 61):

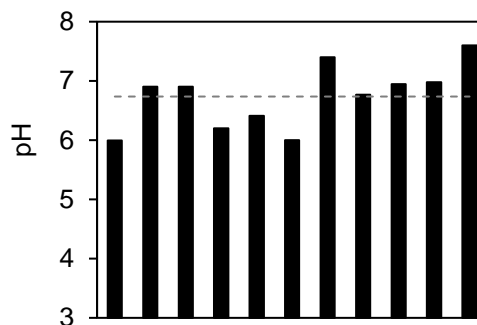


Figure 61. Reported pH values in the mouth (187–190)
(x-axis: different references)

7.2. Stomach

Gastric pH is not a constant parameter and its value changes continuously during digestion. After meal ingestion, gastric pH increases from 1-1.5 (basal fasting conditions) to 5-7 depending on the type of meal and its buffering capacity. It then decreases due to meal dilution by gastric acid secretion before returning to basal conditions after around 3 hours. Gastric emptying also contributes to this pH decrease by removing the meal components from the gastric contents and reducing their buffering effects.

Large inter-individual variations are usually observed, and the main cause of this variability is gastric emptying and the residence time of the meal in the stomach that varies with the type of food ingested. The rate of gastric emptying is known to be one of the main factors of the variability of postprandial events, including pH variations, with significant inter- and intra-individual variations in healthy volunteers (191).

Generally, and as it shown in figure 62, a pure carbohydrate meal has no detectable effect on acidity, while a protein meal of similar caloric value has a significant buffering effect. Then, after the intake of food, the buffering action of the proteins and the dilution of hydrogen ions provided by the acid bulk cause the pH to rise.

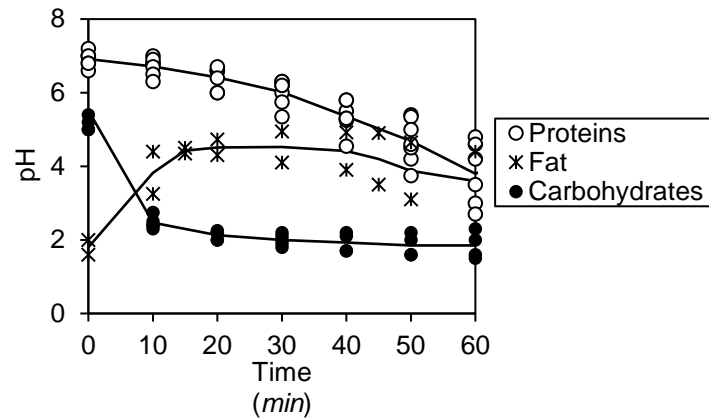


Figure 62. Postprandial gastric pH of meals rich in proteins, fat or carbohydrates (192 – 196)

On the other hand, the “viscosity” of the meal also has an impact on the gastric pH, and a liquid meal with a balance of carbohydrate and protein has a strong buffering effect but the pH rapidly returns to basal levels as the liquid is emptied (197).

The effect of the meal status on the pH is shown in figure 63.

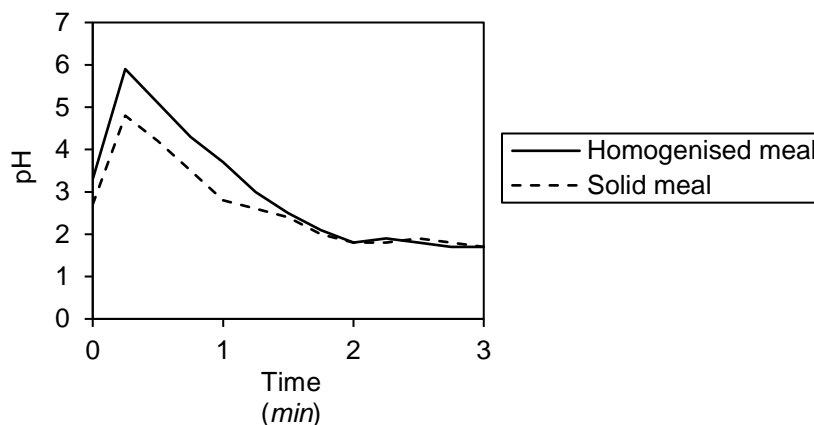


Figure 63. Effect of meal texture on postprandial gastric pH (homogenised meal: puree made in a blender) (198)

7.3. Small intestine

The gastric pH is highly influenced by the meal, this variation on the pH is then also seen in the pH of the duodenal content. However, the bicarbonate ions released counteract the acidic fluid that is emptied from the stomach, therefore the meal slightly affects the pH of the duodenum and it does not influence the jejunal/ileal pH.

An example of the pH variation due to the gastric content that is emptied into the duodenum can be seen in the following graph (figure 64):

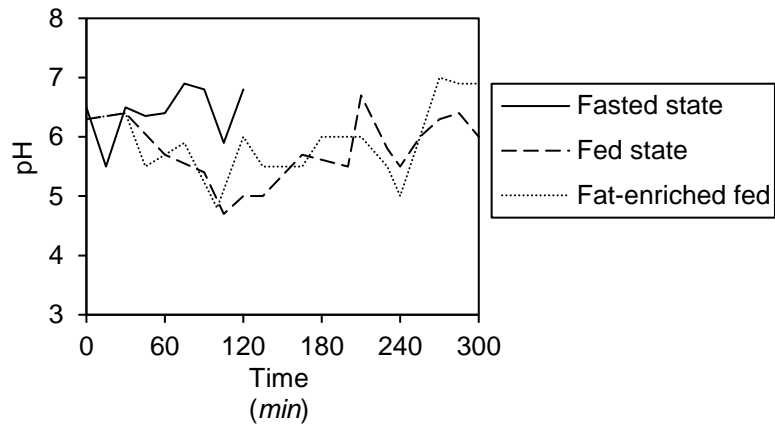


Figure 64. pH values of the duodenal content for 3 different kinds of meals (199)

The pH in the jejunum and ileum is less influenced by the meal, but varies between different individuals as a function of age, sex, among other factors. The reported average of the physiological pH values in the 3 compartments of the small intestine after a meal is shown in the following graphs (figures 65 – 67) (200):

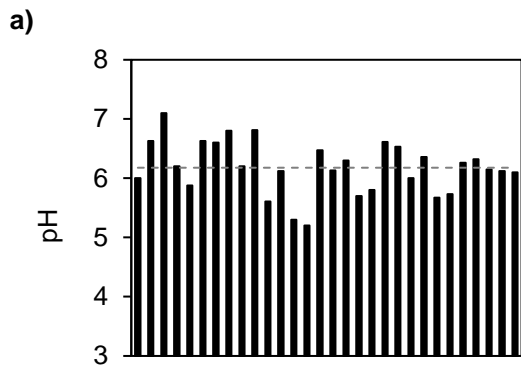


Figure 65. pH values in duodenum (x-axis: different references)

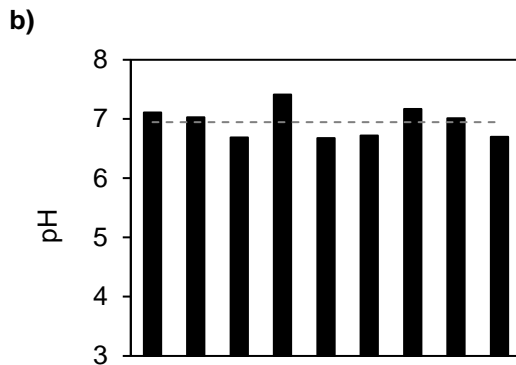


Figure 66. pH values in jejunum (x-axis: different references)

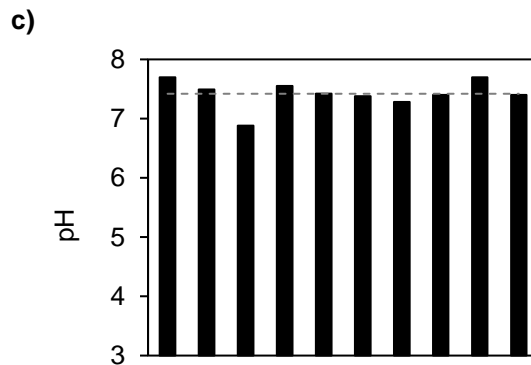


Figure 67. pH values in ileum (x-axis: different references)

7.4. Large intestine

The average of reported pH values in the large intestine is 6.5 ± 0.4 , which are depicted in the following graph (figure 68):

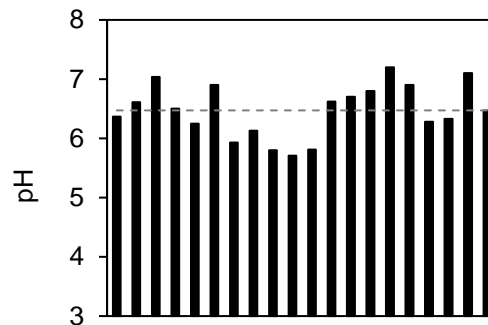


Figure 68. pH in the large intestine (200)
(x-axis: different references)

8. Carbohydrates

The macronutrients can be classified as carbohydrates, fats and proteins. They generally cannot be absorbed in their natural forms through the gastrointestinal mucosa and are useless as nutrients without preliminary digestion.

The chemistry of digestion is simple as the same basic process of hydrolysis is involved. The only difference lies in the types of enzymes required to promote the hydrolysis reactions for each type of macronutrient (7).

Dietary carbohydrates are the main source of energy in the current human diet, where is estimated that starch contributes about 50 – 70% of human total energy intake. Carbohydrates are the main determinant of postprandial blood glucose levels (26,201).

The sources of carbohydrates in the human diet are mainly the complex carbohydrates (starch, glycogen), and in a lower extend the disaccharides (lactose, sucrose) and simple sugars (glucose, fructose). The diet also contains a large amount of cellulose, which is a carbohydrate that no enzyme secreted in the human digestive tract is capable to hydrolyse.

8.1. Digestion of carbohydrates

When food is chewed, it is mixed with saliva, which contains α -amylase secreted mainly by the parotid glands. This enzyme hydrolyses starch into maltose and other small polymers of glucose that contain 3 – 9 glucose molecules. However, the food remains in the mouth only a short time, so that probably not more than 5% of all the starches will have become hydrolysed by the time the food is swallowed.

However, starch digestion sometimes continues in the stomach, before the oral bolus becomes mixed sufficiently with the stomach secretions. Then α -amylase activity is stopped due to the low pH of the gastric secretions. Nevertheless, on average, as much as 30 – 40% of the starches can be hydrolysed into simple sugars.

Pancreatic secretion contains a large quantity of α -amylase that is almost identical in its function with the α -amylase of saliva but is several times as powerful. Therefore, within 15 to 30 minutes after the chyme empties from the stomach into the duodenum and mixes with pancreatic juice, all the contained carbohydrates will have become digested. In general, the carbohydrates are almost totally converted into maltose and/or other very small glucose polymers before passing beyond the duodenum or upper jejunum.

The enterocytes lining the villi of the small intestine contain enzymes (lactase, sucrose, maltase, and α -dextrinase), which are capable of slitting the disaccharides lactose, sucrose, and maltose, plus other small glucose polymers, into their constituent monosaccharides (7,202).

8.1.1. Formation of carbohydrates from proteins and fats

The liver plays a key role in maintaining blood glucose levels during fasting by converting its stored glycogen to glucose (glycogenolysis) and by synthesizing glucose, mainly from lactate and amino acids (gluconeogenesis).

Gluconeogenesis is especially important in preventing an excessive reduction in the blood glucose concentration during fasting. Glucose is the primary substrate for energy in tissues such as the brain and the red blood cells, and adequate amounts of glucose must be present in the blood for several hours between meals.

Approximately 25% of the liver's glucose production during fasting is from gluconeogenesis, helping to provide a steady supply of glucose to the brain. During prolonged fasting, the kidneys also synthesize considerable amounts of glucose from amino acids and other precursors.

About 60% of the amino acids in the body proteins can be converted easily into carbohydrates, the remaining 40% have chemical configurations that make this difficult or impossible. Each amino acid is converted into glucose by a slightly different chemical process. Similar interconversions can change glycerol into glucose or glycogen (7).

8.1.2. Absorption of carbohydrates

Essentially all the carbohydrates in the food are absorbed in the form of monosaccharides, only a small fraction are absorbed as disaccharides and almost none as larger carbohydrate compounds. By far the most abundant of the absorbed monosaccharides is glucose, usually accounting for more than 80% of carbohydrate calories absorbed. The reason for this is that glucose is the final digestion product of our most abundant carbohydrate food, the starches. The remaining 20% of absorbed monosaccharides are composed almost entirely of galactose and fructose.

Monosaccharides are taken up by the enterocytes via specific transport proteins that facilitate the transport of the D-isomers (but not L-isomers) of hexoses. D-Glucose is taken up by the Na^+ -coupled secondary active transport symporter known as Na^+ -glucose transporter 1 (SGLT1) (figure 69). SGLT1 is a high-affinity Na^+ -glucose transporter. Its affinity constant (K_a) for sugar transport is a function of the Na^+ concentration. In the absence of Na^+ , D-glucose binds to SGLT1 with a much lower affinity ($K_a \gg 10 \text{ mM}$) but in the presence of Na^+ , a conformational change allows sugar to bind with high affinity ($K_a \ll 0.5 \text{ mM}$).

When intracellular Na^+ concentration is low ($\sim 10 \text{ mM}$), Na^+ dissociates from its binding site, causing the transporter affinity for D-glucose to decrease, and the sugar is released into the cytoplasm of the cell. The transporter must complete its cycle by undergoing a third, much slower transition to reorient the binding sites to the extracellular surface.

Subsequently, D-glucose can leave the cell on the basolateral side of the cell via facilitated diffusion transporters (glucose transporters (GLUT2s)) from a high concentration inside the cell to a low concentration outside the cell (7,202).

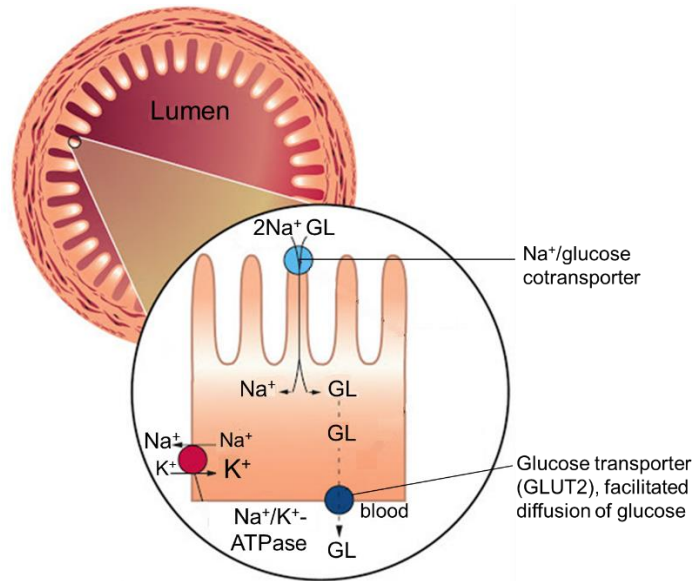


Figure 69. Secondary transport: the use of energy stored in an ionic gradient (203)

8.1.3. Metabolism and transport of carbohydrates

After absorption from the intestinal tract, much of the fructose and almost all the galactose is rapidly converted into glucose in the liver. Therefore, little fructose and galactose are present in the circulating blood. Glucose thus becomes the final common pathway for the transport of almost all carbohydrates to the tissue cells.

Before glucose can be used by the body's tissue cells, it must be transported through the tissue cell membrane into the cellular cytoplasm. However, glucose cannot easily diffuse through the pores of the cell membrane because the maximum molecular weight of particles that can diffuse readily is about $100 \text{ g}\cdot\text{mol}^{-1}$ (glucose: $180.2 \text{ g}\cdot\text{mol}^{-1}$).

Penetrating through the lipid matrix of the cell membrane are large numbers of protein carrier molecules that can bind with glucose. In this bound form, the glucose can be transported by the carrier from one side of the membrane to the other side and then released.

The rate of glucose transport as well as transport of some of other monosaccharides is greatly increased by insulin. When large amounts of insulin are secreted by the pancreas, the rate of glucose transport into most cells increases to 10 or more times the rate of transport compared to when no insulin is secreted. Conversely, the amounts of glucose that can diffuse to the insides of most cells of the body in the absence of insulin, with the exception of liver and brain cells, are far too little to supply the amount of glucose normally required for energy metabolism.

In effect, the rate of carbohydrate utilization by most cells is controlled by the rate of insulin secretion from the pancreas (7).

8.1.3.1. *Insulin*

Insulin is a small protein (MW: $5808 \text{ g}\cdot\text{mol}^{-1}$), composed of 2 amino acid chains connected to each other by disulphide linkages (figure 70). When the 2 amino acid chains are split apart, the functional activity of the insulin molecule is lost (204).

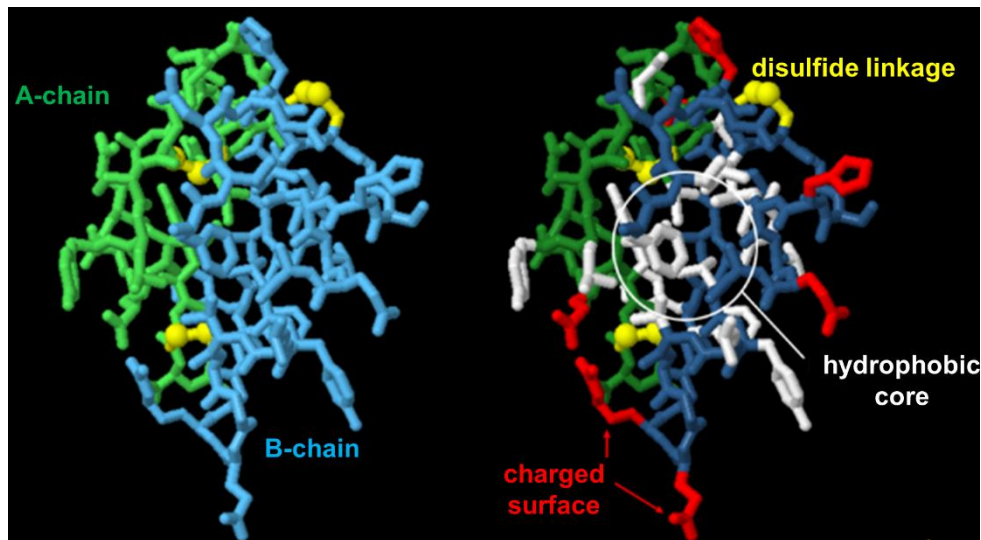


Figure 70. Insulin structure (205)

Insulin it has a plasma half-life that averages only about 6 minutes, so that it is mainly cleared from the circulation within 10 – 15 minutes.

Immediately after a high-carbohydrate meal, the glucose that is absorbed into the blood causes rapid secretion of insulin. The insulin in turn causes rapid uptake, storage and use of glucose by almost all tissues of the body.

One of the most important of all the effects of insulin is to cause most of the glucose absorbed after a meal to be stored almost immediately in the liver in the form of glycogen. Then, between meals, when food is not available and the blood glucose concentration begins to fall, insulin secretion decreases rapidly and the liver glycogen is split back into glucose, which is released back into the blood to keep the glucose concentration from falling too low.

When the quantity of glucose entering the liver cells is more than what can be stored as glycogen or can be used for local hepatocyte metabolism, insulin promotes the conversion of all this excess glucose into fatty acids.

The brain is quite different from most other tissues of the body in that insulin has little effect on uptake or use of glucose. Instead, the brain cells are permeable to glucose and can use glucose without the intermediation of insulin.

The brain cells are also quite different from most other cells of the body in that they normally use only glucose for energy and can use other energy substrates, such as fats only with difficulty. Therefore, it is essential that the blood glucose level always be maintained above a critical level, which is one of the most important functions of the blood glucose control system. When the blood glucose falls too low, into the range of 20 to 50 mg·(100·mL)⁻¹, symptoms of hypoglycaemic shock develop, characterized by progressive nervous irritability that leads to fainting, seizures, and even coma.

At the normal fasting level of blood glucose of 800 to 900 mg·L⁻¹, the rate of insulin secretion is minimal. If the blood glucose concentration is suddenly increased to a level 2 to 3 times as normal and kept at this high level thereafter, insulin secretion, increases markedly in 2 stages (figure 71).

- Plasma insulin concentration increases almost 10 times within 3 – 5 minutes after the acute elevation of the blood glucose, this results from immediate dumping of preformed insulin. However, the initial high rate of secretion is not maintained, instead the insulin concentration decreases about halfway back toward normal in another 5 – 10 minutes.
- Beginning at about 15 minutes, insulin secretion rises a second time and reaches a new plateau in 2 to 3 hours, this time usually at a rate of secretion even greater than that in the initial phase. This secretion results both from additional release of preformed insulin and from activation of the enzyme system that synthesizes and releases new insulin from the cells.

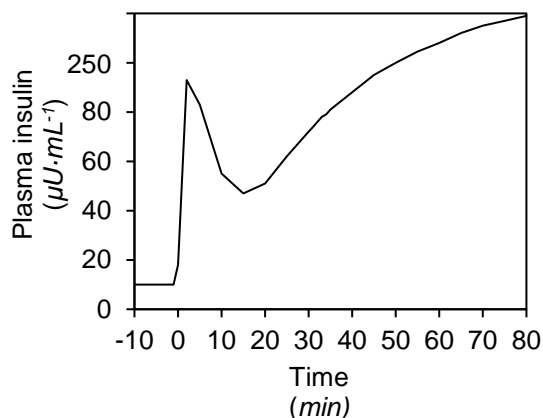


Figure 71. Increase in plasma insulin concentration after a sudden increase in blood glucose to 2 to 3 times of the normal range (204)

The turn-off of insulin secretion is almost equally as rapid, occurring within 3 to 5 minutes after reduction in blood glucose concentration back to the fasting level.

This response of insulin secretion to an elevated blood glucose concentration provides an extremely important feedback mechanism for regulating blood glucose concentration. That is, any rise in blood glucose increases insulin secretion, and the insulin in turn increases transport of glucose into liver, muscle, and other cells, thereby reducing the blood glucose concentration back toward the normal value (204).

An approximate relationship between the blood glucose levels and the insulin secretion is depicted in figure 72.

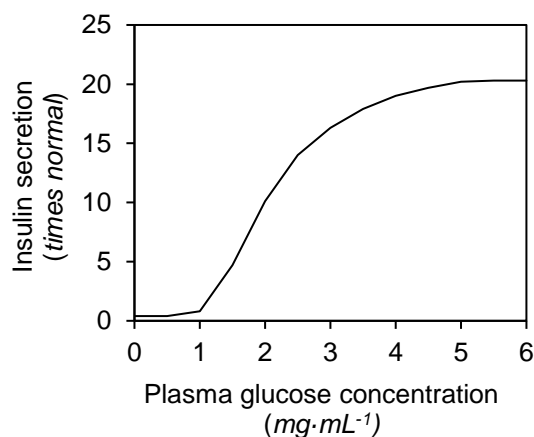


Figure 72. Approximate insulin secretion at different plasma glucose levels (204)

8.2. Diseases related to carbohydrates: Diabetes mellitus

The normal blood glucose concentration in a fasted state is about $900 \text{ mg}\cdot\text{L}^{-1}$. However, after a meal rich in carbohydrates, this level seldom rises above $1400 \text{ mg}\cdot\text{L}^{-1}$ unless the person has diabetes mellitus (7).

Diabetes mellitus is a syndrome of impaired carbohydrate, fat and protein metabolism caused by either lack of insulin secretion or decreased sensitivity of the tissues to insulin. There are 2 general types of diabetes mellitus:

- Type I diabetes, also called insulin-dependent diabetes mellitus (IDDM), is caused by lack of insulin secretion.

- Type II diabetes, also called non-insulin-dependent diabetes mellitus (NIDDM), is caused by decreased sensitivity of target tissues to the metabolic effect of insulin. This reduced sensitivity to insulin is often called insulin resistance.

In both types of diabetes mellitus, metabolism of all the main foodstuffs is altered. The basic effect of insulin lacks or insulin resistance on glucose metabolism is to prevent the efficient uptake and utilization of glucose by most cells of the body, except those of the brain. As a result, blood glucose concentration increases, cell utilization of glucose falls increasingly lower, and utilization of fats and proteins increases.

In recent decades, the prevalence of diabetes mellitus has dramatically increased in the USA and worldwide (figure 73). Globally, an estimated 422 million adults were living with diabetes in 2014, compared to 108 million in 1980. The global prevalence of diabetes has nearly doubled since 1980, rising from 4.7% to 8.5% in the adult population. Therefore, diabetes mellitus is a disease that affects a large amount of people around the world and the prevalence increases with the time (206).

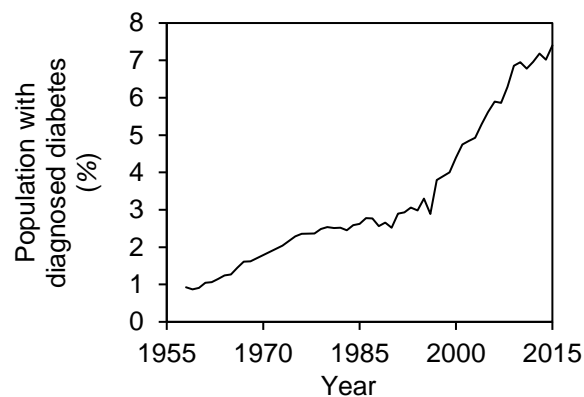


Figure 73. Percentage of USA population with diagnosed diabetes (1958 – 2015) (207)

8.2.1. Type I diabetes

The usual onset of type I diabetes occurs at about 14 years of age. Type I diabetes may develop very abruptly, over a period of a few days or weeks, with 3 principal repercussions: increased blood glucose, increased utilization of fats for energy and for formation of cholesterol by the liver and depletion of the body's proteins.

The lack of insulin decreases the efficiency of peripheral glucose utilization and augments glucose production, raising plasma glucose to 3 – 12 mg·mL⁻¹. The very high levels of blood glucose can cause severe cell dehydration throughout the body. This occurs partly because glucose does not diffuse easily through the pores of the cell membrane, and the increased osmotic pressure in the extracellular fluids causes osmotic transfer of water out of the cells. In addition, the loss of glucose in the urine causes osmotic diuresis. That is the osmotic effect of glucose in the renal tubules greatly decreases tubular reabsorption of fluid. The overall effect is massive loss of fluid in the urine, causing dehydration of the extracellular fluid, which in turn causes compensatory dehydration of the intracellular fluid. Thus, polyuria, intracellular and extracellular dehydration, and increased thirst are classic symptoms of diabetes.

8.2.2. Type II diabetes

Type II diabetes is far more common than type I, accounting for about 90% of all cases of diabetes mellitus. In most cases, the onset of type II diabetes occurs after age 30, often between the ages of 50 and 60 years, and the disease develops gradually.

Type II diabetes, in contrast to type I, is associated with increased plasma insulin concentration. This occurs as a compensatory response by the pancreatic beta cells for diminishing sensitivity of target tissues to the metabolic effects of insulin. The decrease in insulin sensitivity impairs carbohydrate utilization and storage, raises blood glucose and stimulates a compensatory increase in insulin secretion.

With prolonged and severe insulin resistance, even the increased levels of insulin are not sufficient to maintain normal glucose regulation. As a result, moderate hyperglycaemia occurs after ingestion of carbohydrates in the early stages of the disease. In the later stages of type II diabetes, the pancreatic beta cells become “exhausted” and are unable to produce enough insulin to prevent more severe hyperglycaemia, especially after the person ingests a carbohydrate-rich meal (204).

8.2.3. Glycaemic index and glycaemic load

Glycaemic index (GI) was originally (1980s) designed for people with diabetes as a guide to food selection. In 1997 a committee of experts was brought together by the Food and Agriculture Organization (FAO) of the United Nations and the World Health Organization (WHO) to review the available research evidence regarding the importance of carbohydrates in human nutrition and health. The committee approved the use of the GI method for classifying carbohydrate-rich foods and recommended that the GI values of foods be used in conjunction with information about food composition to guide food choices (208,209).

The GI is a concept that ranks the carbohydrates based on their immediate impact on blood glucose levels. It is calculated as the incremental area under the curve (iAUC) for blood glucose after consumption of a test food divided by the iAUC of a reference food (usually 50 g of glucose) containing the same amount of carbohydrate (208,210) (eq. 9).

$$GI = \frac{iAUC_{\text{glucose}}(\text{test food})}{iAUC_{\text{glucose}}(\text{reference})} \cdot 100 \quad \text{Eq. 9}$$

However, the GI concept has been extended to also take into account the effect of the total amount of carbohydrate consumed. Because, for example, watermelon has a high GI and may not be considered a good food selection as part of a low GI diet. However, watermelon only contains 5 g of carbohydrate per 100 g, thus it would have a minimal glycaemic effect.

Glycaemic load (GL) provides an indication of glucose available for energy or storage following a carbohydrate containing meal and it may be determined by indirect and direct methods:

- The indirect method involves multiplying the GI of a food by the amount of available carbohydrate (M) divided by 100 (eq. 10) (208,211).

$$GL = \frac{GI \cdot M}{100} \quad \text{Eq. 10}$$

This method implies that GL is directly proportional to the amount of the particular food eaten, and this is perhaps counterintuitive because the blood glucose AUC does not increase in direct proportion to the amount consumed. Figure 74 shows an example of the effect of an increase on the amount of granola bar to the blood glucose AUC.

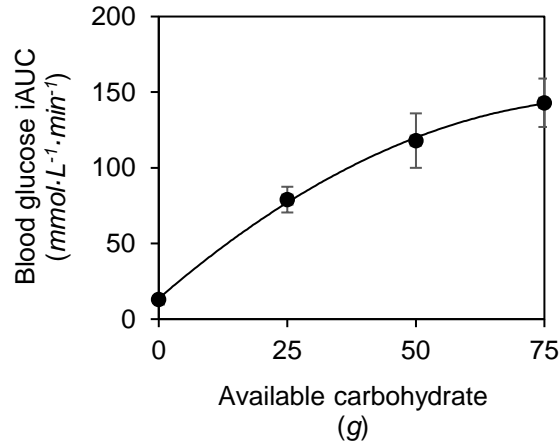


Figure 74. Blood glucose area under the curve (AUC) responses to increasing amounts of granola bar tested in 20 people (208)

- For the direct method (figure 75), an AUC for glucose is calculated for a range of doses of the reference food measured on different days. A standard curve is constructed for each subject with increasing amounts of the reference on the x axis with its corresponding AUC for blood glucose on the y axis

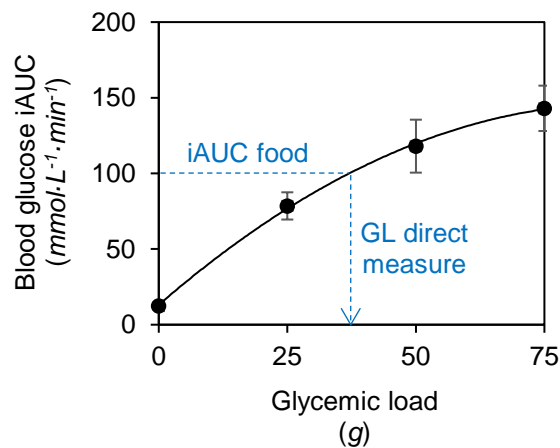


Figure 75. Example of an individual's standard glucose curve (208)

Using this technique, glycaemic equivalence is the amount of glucose that would theoretically produce the same blood glucose AUC as that particular portion size of food consumed. Major drawbacks of the direct method are increased time and cost required to determine the GL of a food. The reference must be tested at several doses in each subject and the GL of a food cannot be estimated from currently available GI values.

A GI and GL classification systems are in common use in which foods are categorized as shown in table 7 (208):

Table 7. Classification of GI and GL (208)

	<u>GI</u> (%)	<u>GL</u> (g)
Low	<55	≤10
Medium	55 – 69	10 – 20
High	>70	≥20

GI values for the same type of foods sometimes vary, this variation may reflect both methodologic factors and true differences in the physical and chemical characteristics of the foods.

One possibility is that 2 similar foods may have different ingredients (botanical differences from country to country) or may have been processed with a different method, resulting in significant differences in the rate of carbohydrate digestion and hence the GI value (209).

Foods are usually tested one at a time rather than as whole meals, therefore there is interest in determining not only the GI of meals but also the GI of whole diets. For this purpose, a formula using the GI of individual foods, weighted according to the amount of carbohydrate each food contributes to the meal (eq. 11), was devised by Dodd et al (2011).

$$\text{Meal GI} = \frac{(\text{GI}_{\text{Food A}} \cdot M_{\text{Food A}}) + (\text{GI}_{\text{Food B}} \cdot M_{\text{Food B}}) + \dots}{M_{\text{Total}}} \quad \text{Eq. 11}$$

However, the agreement between the calculated and measured GIs was poor. The main findings of that study were that the formula used to calculate the GI of mixed meals overestimated the GI of the meals and that the overestimation was unpredictable. These results could be explained taking into account that when the individual foods are incorporated into meals, the matrix has an impact on the final GI value (210).

The in vivo measurement of glycaemic response requires the recruitment of volunteers under ethical committee approval, the availability of medical personnel for blood drawing, and disposal procedures for clinical waste, therefore in vivo measurements are complicated, expensive and time consuming (212).

Measuring the rate at which carbohydrates in foods are digested in vitro has been suggested as a cheaper and less time-consuming method for predicting the GI values of foods. However, only a few foods have been subjected to both in vitro and in vivo testing, and it is not yet known whether the in vitro method is reliable indication of the in vivo postprandial glycaemic effects of all types of foods (209).

8.3. Starch

Starch is a polycrystalline polymer, consisting mainly of 2 glucan molecules, amylose and amylopectin. Amylose is a linear polymer composed of glucose residues connected via α -1,4 bonds whereas, amylopectin is a highly branched glucose polymer composed of α -1,4 and α -1,6 linked glucose units.

It is believed that amylose forms part of the amorphous regions, which are not involved in forming the ordered structures. The crystalline portion of starch is largely formed from amylopectin, where the side chains are arranged together to form a double helix structure.

The crystalline structure of starch granules can be divided into 3 types, known as A-, B-, and C-type starches.

In the native granular form, A-type polymorph starch consists in amylopectin with short branch-chains and is mainly presented in cereal or rhizome such as corn, wheat and rice. Some tubers, such as potato, lesser yam and rhizomes present the B-type, which has longer branch-chains in the amylopectin, and the C-type pattern is a mixture of A- and B-type polymorphs and naturally occurs in seeds.

However, besides the glucan molecules, lipids and proteins are also found in starch granules as minor components. Starch structure is the main factor determining the physicochemical properties, and any changes in structure will alter the physicochemical and functional properties of starch granules. The chemical composition of A-, B-, and C-type starches are presented in table 8 (213,214).

Table 8. Protein, lipid and crystallinity of starch types (213)

Starch		Protein	Lipid	Crystallinity
<i>Type</i>	<i>Example</i>	(%)	(%)	(%)
A-type	Rice	1.27 ± 0.03	0.39 ± 0.03	17.3
B-type	Potato	0.93 ± 0.05	0.62 ± 0.02	25.0
C-type	Tapioca	0.65 ± 0.02	0.25 ± 0.05	23.8

In the A-type the double helices are packed in a monoclinic unit cell ($a=2.12$ nm, $b=1.17$ nm, $c=1.07$ nm, $\gamma=123.5^\circ$) with 8 water molecules per unit cell. In the B-type structure, the double helices are packed in a hexagonal unit cell ($a=b=1.85$ nm, $c=1.04$ nm) with 36 water molecules per unit cell. A schematic representation of A- and B- type starch is shown in figure 76 (215).

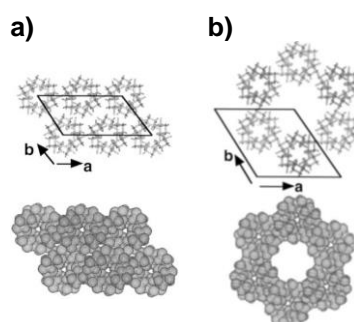


Figure 76. Crystalline packing of double helices in a) A-type and b) B-type starch (215)

Native starch is not widely used in the food industry due to its poor functional properties, therefore most starches currently incorporated into foods are chemically modified. The mean thermal transition of the starch is gelatinization, which is used to describe the molecular behaviour of starch treated with heat and moisture content. In this process the starch changes its semi-crystalline phase to an amorphous phase through the dissociation of the crystalline double-helices in the granules (214,216).

In excess of water, hydrogen bonds stabilizing the structure of the double helices in crystallites are broken and are replaced by the hydrogen bonds with water, and swelling is regulated by the crystallinity of the starch. The granules become increasingly susceptible to shear disintegration as they swell (217). And the differences on structure and the composition of starches may affect availability of molecules to interact with water (218).

The gelatinization process is affected by the size of the grains, and it is benefited for lower grain sizes. A comparison of the effect of the temperature on different starch sources is shown in table 9.

Table 9. SEM images of starch treated at different temperatures (219)
(magnification: 1000x for potato starch, 2500x for tapioca, wheat and rice starch)

Starch	40°C	50°C	60°C	70°C	80°C
Potato					
Tapioca					
Wheat					
Rice					

The energy necessary to complete the starch gelatinization is known as gelatinization enthalpy (ΔH_p) (216). The temperature of gelatinization gives a measure of crystallite quality (double helix length), the high temperature might be due to the higher proportion of longer chains in the amylopectins. These chains could form long double helices that would require a higher temperature to dissociate completely than that required for shorted double helices.

Enthalpy values are affected by molecular architecture of crystalline region, amylose-amylopectin ratio and presence of short amylopectin chains. The starch with lower and less perfect crystallinity has lower temperature and enthalpy of gelatinization. The presence of short chains decreases the stability of double helix in amylopectin molecules, which lowers the gelatinization temperature as well as the enthalpy, and this is because an increase in the short outer chain in amylopectin molecule would reduce the efficiency of packing in the starch crystallinity (217,220). High temperatures may reflect more stable amorphous regions or a lower degree of chain branching (218).

The enthalpies and HPSEC (high pressure size exclusion chromatography) profiles of different starch sources are depicted in figure 77.

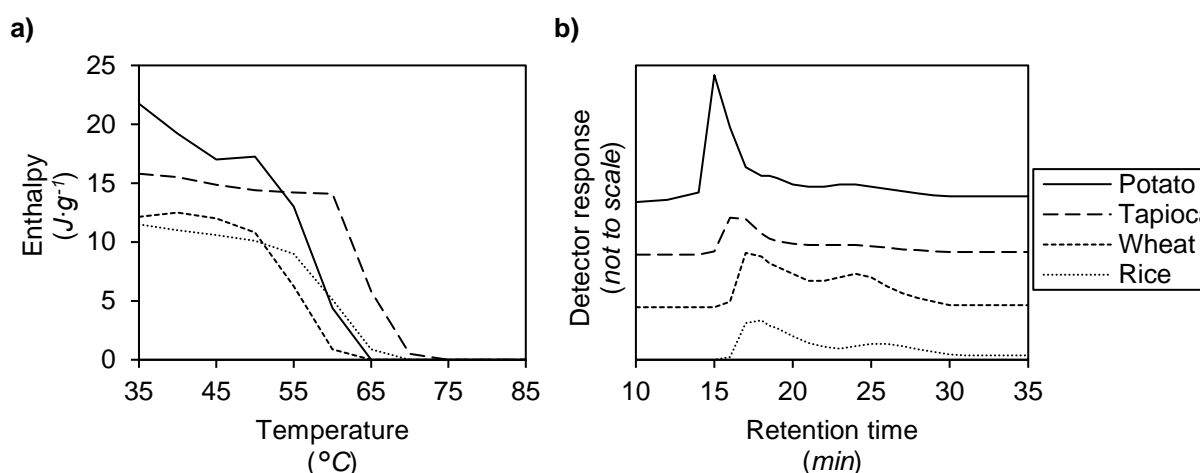


Figure 77. Representative a) DSC enthalpies and b) HPSEC profiles (1st peak: amylopectin, 2nd peak: amylose) for potato, tapioca, wheat and rice starch samples (219)

Therefore, when the starch is heated in water, starch granules become hydrated, swell and are transformed into a paste. The granule structure collapses due to melting of crystallites, unwinding of double helices, and breaking of hydrogen bonds. These changes are collectively referred to as starch gelatinization and are accompanied by the loss of characteristic birefringence of intact granules. On cooling, the disaggregated starch chains retrograde gradually into partially ordered structures that differ from those in native granules and some starch pastes can develop gels (214,221).

The formation of a starch gel from a paste is a result of the interactions between amylose and amylopectin molecules in the granule and the formation of networks to hold water in the swollen granules (214).

Starch retrogradation refers to the recrystallization of the polysaccharides in gelatinized starch. It occurs when the starch-based foods are exposed to freeze/thaw cycles, or when moisture migration occurs in starchy foods, impacting the textural and nutritional attributes of foods increasing hardness and reducing stickiness. In addition to the changes in texture and flavour, retrogradation of starch can also decrease the starch digestibility (222).

9. In vitro digestion of carbohydrates

As it is described in section 8.2, in the recent decades, the prevalence of diabetes has dramatically increased worldwide. This fact increased the need to predict the glycaemic index with accuracy and precision. Since the in vivo are costly, time consuming and imply ethical constraints, the in vitro methods are a good alternative to simulate the human digestion and predict the postprandial blood glucose levels.

Since the early 1990s to the present day, a lot of in vitro methods have been used to study the digestion of carbohydrates. However, the methodologies and conditions used on those methods differ considerably between them, which makes the comparison between the obtained results very difficult or even impossible (189).

The in vitro digestion methods have been used for different objectives: to study the degradation of different kind of carbohydrates, the possibility to modify the speed of the carbohydrate's digestion, the effect of the addition of different substances to the CH digestion, to study the effect of the preparation process, etc. Most of the studies have been performed with static models, for its ease of use and its acceptable cost. Table 10 shows an overview of some of the studies where different methodologies have been used to study CH digestion.

Table 10. Overview of in vitro digestion methods used to study the digestion of carbohydrates

Meal	Methodology	Digestion phase	Conditions			Results	Ref.
			Enzyme	pH	T (°C)		
Arepas	Static	Oral	Physiological conditions				
		Gastric	Pepsin	1.5	37	0.5	Available starch: 56.5±2.6
		Small intestinal	Pancreatin	5.0	40	16	Resistant starch: 35.4±1.2 In vivo: 32.5±0.9
Baguette	Dynamic	Gastric	Pepsin	6 to 2	37	2	Released starch: 83±3
		Small intestinal	Pancreatin, α-amylase	7	37	2	
Banana	Static	Oral	Physiological conditions				
		Gastric	Pepsin	1.5	37	0.5	Available starch: 31.6±3.2
		Small intestinal	Pancreatin	5.0	40	16	Resistant starch: 72.1±5.7 In vivo: 56.6
Beans	Static	Gastric	Pepsin	1.5	40	1	Released starch: 31.66±3.72
		Small intestinal	α-amylase	6.9	37	3	
Biscuits	Static	Oral	Physiological conditions				
		Gastric	Pepsin	1.5	37	0.5	Available starch: 101.4±2.1
		Small intestinal	Pancreatin	5.0	40	16	Resistant starch: 1.0±0.1 In vivo: 2.9±0.9
Biscuits	Static	Gastric	Pepsin	1.5	40	1	Released starch: 62.89±2.09
		Small intestinal	α-amylase	6.9	37	3	
Bread	Static	Oral	Physiological conditions				
		Gastric	Pepsin	1.5	37	0.5	Available starch: 80.2±1.2
		Small intestinal	Pancreatin	5.0	40	16	Resistant starch: 11.4±1.0 In vivo: 9.40
Bread	Static	Gastric	Pepsin	1.5	40	1	Released starch: 76.70±2.16
		Small intestinal	α-amylase	6.9	37	3	
Cereals	Static	Oral	Physiological conditions				
		Gastric	Pepsin	1.5	37	0.5	Available starch: 100.3±2.8
		Small intestinal	Pancreatin	5.0	40	16	Resistant starch: 0.7±0.4 In vivo: 0.66
Chickpeas	Static	Gastric	Pepsin	1.5	40	1	Released starch: 45.08±3.67
		Small intestinal	α-amylase	6.9	37	3	
Fenugreek gum	Static	Gastric	Pepsin	1.8	37	1	57 µg glucose·0.1 ⁻¹ mL
		Small intestinal	Pancreatin	7.8	37	3	

Flaxseed gum	Static	Gastric	Pepsin	1.8	37	1	61 µg glucose·0.1 ⁻¹ mL	(226)
		Small intestinal	Pancreatin	7.8	37	3		
Legume	Static	Oral	Physiological conditions				Available starch: 75.6±5.4 Resistant starch: 23.1±7.7 In vivo: 13.83	(223)
		Gastric	Pepsin	1.5	37	0.5		
Legume	Static	Small intestinal	Pancreatin	5.0	40	16	Released starch: 41.69±4.15	(225)
		Gastric	Pepsin	1.5	40	1		
Peas	Static	Small intestinal	α-amylase	6.9	37	3	Released starch: 18.93±1.89	(225)
		Gastric	Pepsin	1.5	40	1		
Potato	Static	Oral	Physiological conditions				Available starch: 93.5±11.2 Resistant starch: 7.0±1.3 In vivo: 12.20	(223)
		Small intestinal	Pancreatin	5.0	40	16		
Potato (boiled)	Static	Gastric	Pepsin	1.5	40	1	Released starch: 1.00±0.14	(225)
		Small intestinal	α-amylase	6.9	37	3		
Potato (crisp)	Static	Gastric	Pepsin	1.5	40	1	Released starch: 3.27±0.79	(225)
		Small intestinal	Amylase	6.9	37	3		
Rice	Static	Gastric	Pepsin	1.5	40	1	Released starch: 82.22±2.24	(225)
		Small intestinal	Amylase	6.9	37	3		
Spaghetti	Static	Oral	Physiological conditions				Available starch: 94.4±4.0 Resistant starch: 5.1±1.8 In vivo: 4.60	(223)
		Gastric	Pepsin	1.5	37	0.5		
Spaghetti	Dynamic	Small intestinal	Pancreatin	5.0	40	16	Released starch: 32±10	(224)
		Oral	Human saliva		37	0.16		
Spaghetti	Static	Gastric	Pepsin	6 to 2	37	2	Released starch: 74.00±2.24	(225)
		Small intestinal	Pancreatin, α-amylase	7	37	2		
Wheat bread	Static	Gastric	Pepsin	1.5	40	1	Degree hydrolysis: 62.0±6.5	(227)
		Small intestinal	α-amylase	6.9	37	5		
Wheat bread	Static	Gastric	Pepsin	1.5	37	5	Degree hydrolysis: 62.0±6.5	(227)
		Small intestinal	α-amylase	6.9	37	NA		

10. References

1. V.M. Sardesai, *Introduction to Clinical Nutrition*, Taylor & Francis Group, USA, 2012.
2. H.K. Biesakski, S.C. Bischoff and C. Puchstein, *Ernährungsmedizin: Nach dem neuen Curriculum Ernährungsmedizin der Bundesärztekammer*, Thieme, Germany, 2010.
3. M. Elia, *Clinical Nutrition*, ed. M. Elia, O. Ljungqvist, R.J. Stratton and S.A. Lanham-New, John Wiley & Sons, Great Britain, 2nd edn, 2013, **1**, 1 – 14.
4. A. Guerra, L. Etienne-Mesmin, V. Livrelli, S. Denis, S. Blanquet-Diot and M. Alric, Relevance and challenges in modelling human gastric and small intestinal digestion, *Trends in Biotechnol.*, 2012, **30(11)**, 591 – 600.
5. F. Kong and R.P. Singh, Disintegration of solid foods in human stomach, *J. Food. Sci.*, 2008, **73(5)**, R67 – R80.
6. R.R. Seeley, T.D. Stephens and P. Tate, *Anatomy and Physiology*, ed. S.R. Akkaraju, C.M. Eckel, J.L. Regan, A.F. Russo and C.L. VanPutte, The McGraw-Hill Companies, Boston, 6th edn, 2004, **24**, 859 – 910.
7. A.C. Guyton and J.E. Hall, *Textbook of Medical Physiology*, Elsevier, USA, 11th edn, 2006, **65**, 808 – 818.
8. A. Vander, J. Sherman and D. Luciano, *Human physiology: the mechanisms of body function*, The McGraw-Hill Companies, Boston, 8th edn, 2001, **17**, 553 – 591.
9. K. Matsuo and J.B. Palmer, *Principles of deglutition: a multidisciplinary text for swallowing and its disorders*, ed. R. Shaker, P.C. Belafsky, G.N. Postma and C. Easterling, Springer, New York, 1st edn, 2013, **8**, 117 – 131.
10. A. Van der Bilt, L. Engelen, L.J. Pereira, H.W. Van der Glas and J.H. Abbink, Oral physiology and mastication, *Physiol. Behav.*, 2006, **89**, 22 – 27.
11. A.M. Pedersen, A. Bardow, S.B. Jensen and B. Nauntofte, Saliva and gastrointestinal functions of taste, mastication, swallowing and digestion, *Oral Dis.*, 2002, **8**, 117 – 129.
12. C. Fenoll-Palomares, J.V. Muñoz-Montagud, V. Sanchiz, B. Herreros, V. Hernández, M. Minguez and A. Benages, Unstimulated salivary flow rate, pH and buffer capacity of saliva in healthy volunteers, *Rev. Esp. Enferm. Dig.*, 2004, **96(11)**, 773 – 783.
13. F. Kong and R.P. Singh, A human gastric stimulator (HGS) to study food digestion in human stomach, *J. Food Sci.*, 2010, **75(9)**, E627 – E635.
14. A.J. Bredenoord, A. Smout and J. Tack, *A Guide to Gastrointestinal Motility Disorders*, Spring International Publishing, Switzerland, 2016.
15. M.J. Ferrua and R.P. Singh, Modeling the fluid dynamics in a human stomach to gain insight of food digestion, *J. Food Sci.*, 2010, **75(7)**, R151 – R162.
16. S.B. Bhise and A.V. Yadav, *Human Anatomy and Physiology*, Nirali Prakashan, Mumbai, 20th edn, 2008, **13**, 13.1 – 13.9.
17. M. Hamosh, Lingual and gastric lipases, *Nutrition*, 1990, **6(6)**, 421 – 428.
18. C.K. Abrams, M. Hamosh, T.C. Lee, A.F. Ansher, M.J. Collen, J.H. Lewis, S.B. Benjamin and P. Hamosh, Gastric lipase: localization in the human stomach, *Gastroenterology*, 1988, **95**, 1460 – 1464.

19. C. Sauzet, M. Claeys-Bruno, M. Nicolas, J. Kister, P. Piccerelle and P. Prinderre, An innovative floating gastro retentive dosage system: formulation and in vitro evaluation, *Int. J. Pharm.*, 2009, **378**, 23 – 29.
20. D.A. Adkin, S.S. Davis, R.A. Sparrow, P.D. Huckle, A.J. Phillips and I.R. Wilding, The effects of pharmaceutical excipients on small intestinal transit, *Br. J. Clin. Pharmacol.*, 1995, **39**, 381 – 387.
21. C. Shashank, K. Prabha, S. Sunil and A.V. Kumar, Approaches to increase the gastric residence time: floating drug delivery systems – a review, *Asian J. Pharm. Clin. Res.*, 2013, **6(3)**, 1 – 9.
22. G. Hoffman, *Digestive system*, Marshall Cavendish Benchmark, USA, 1st edn, 2009, **2**, 11 – 40.
23. L.K. DeBruyne, K. Pinna and E. Whitney, *Nutrition and diet therapy*, Cengage Learning, USA, 7th edn, 2009, **19**, 531 – 550.
24. L. Sherwood, *Fundamentals of human physiology*, Cengage Learning, USA, 4th edn, 2011, **15**, 437 – 478.
25. D.D. Chiras, *Human Biology*, Jones & Bartlett learning, USA, 7th edn, 2012, **5**, 89 – 117.
26. G.M. Bornhorst, O. Gouseti, M.S.J. Wickham and S. Bakalis, Engineering digestion: multiscale processes of food digestion, *J. Food Sci.*, 2016, **81(3)**, R534 – R543.
27. S.J. Hur, B.O. Lim, E.A. Decker and D.J. McClements, In vitro digestion models for food applications, *Food Chem.*, 2011, **125**, 1 – 12.
28. T. Bohn, F. Carrière, L. Day, A. Deglaire, L. Egger, D. Freitas, M. Golding, S. Le Feunteun, A. Macierzanka, O. Menard, B. Miralles, A. Moscovici, R. Portmann, I. Recio, D. Rémond, V. Santé-Lhoutelier, T.J. Wooster, U. Lesmes, A.R. Mackie and D. Dupont, Correlation between in vitro and in vivo data on food digestion. What can we predict with static in vitro digestion models?, *Crit. Rev. Food Sci. Nutr.*, 2018, **58(13)**, 2239 – 2261.
29. S. Boisen and B.O. Eggum, Critical evaluation of in vitro methods for estimating digestibility in simple-stomach animals, *Nutr. Res. Rev.*, 1991, **4**, 141 – 162.
30. A.C. Longland, *In vitro digestion for pigs and poultry*, CABI publishing, Wisconsin, 1991.
31. T.A. Faber and G.C. Fayer, *Nondigestible carbohydrates and digestive health*, ed. T. Paeschke and W.R. Aimutis, Wiley-Blackwell, USA, 1st edn, 2011, **5**, 97 – 123.
32. M. Minekus, *Development and validation of a dynamic model of the gastrointestinal tract*, Utrecht University, 1998.
33. M. Minekus, M. Alminger, P. Alvito, S. Ballance, T. Bohn, C. Bourlieu, F. Carrière, R. Boutrou, M. Corredig, D. Dupont, C. Dufour, L. Egger, M. Golding, S. Karakaya, B. Kirkhus, S. Le Feunteun, U. Lesmes, A. Macierzanka, A. Mackie, S. Marze, D.J. McClements, O. Ménard, I. Recio, C.N. Santos, R.P. Singh, G.E. Vegarud, M.S. Wickham, W. Weitschies and A. Brodtkorb, A standardized static in vitro digestion method suitable for food – an international consensus, *Food Funct.*, 2014, **5(6)**, 1113 – 1124.
34. A.G. Oomen, A. Hack, M. Minekus, E. Zeijdner, C. Cornelis, G. Schoeters, W. Vertraete, T. Van de Wiele, J. Wragg, C.J.M. Rompelberg, A.J.A.M. Sips and J.H. Van Wijnen, Comparison of five in vitro digestion models to study the bioaccessibility of soil contaminants, *Environ. Sci. Technol.*, 2002, **36**, 3326 – 3334.
35. <http://www.cost-infogest.eu/> (October 2018)
36. <711> Dissolution. In The United States Pharmacopeia and National Formulary USP 41-NF 36. The United States Pharmacopeial Convention, Inc.: Rockville, MD, 2018, 6459 – 6469.

37. J. Mauger, J. Ballard, R. Brockson, S. De, V. Gray and D. Robinson, Intrinsic dissolution performance testing of the USP dissolution apparatus 2 (rotating paddle) using modified salicylic acid calibrator tablets: proof of principle, *Dissolution Technol.*, 2003, **10(3)**, 6 – 15.
38. S.A. Qureshi, Calibration – the USP dissolution apparatus suitable test, *Drug Inf. J.*, 1996, **30**, 1055 – 1061.
39. A.G. Oomen, C.J.M. Rompelberg, M.A. Bruil, C.J.G. Dobbe, D.P.K.H. Pereboom and A.J.A.M. Sips, Development of an in vitro digestion model for estimating the bioaccessibility of soil contaminants, *Arch. Environ. Contam. Toxicol.*, 2003, **44**, 281 – 287.
40. A.I. Mulet-Cabero, N.M. Rigby, A. Brodkorb and A.R. Mackie, Dairy food structures influence the rates of nutrient digestion through different in vitro gastric behaviour, *Food Hydrocolloids*, 2017, **67**, 63 – 73.
41. D. Dupont and A.R. Mackie, Static and dynamic in vitro digestion models to study protein stability in the gastrointestinal tract, *Drug Discovery Today: Dis. Models*, 2015, **17–18**, 23 – 27.
42. K. Verhoeckx, P. Cotter, I. López-Expósito, C. Kleiveland, T. Lea, A. Mackie, T. Requena, D. Swiatecka and H. Wichers, The Impact of Food Bioactives on Health: In Vitro and Ex Vivo Models, *COST Action FA1005*, 2015.
43. M. Vardaku, A. Mercuri, S.A. Barker, D.Q.M. Craig, R.M. Faulks and M.S.J. Wickham, Achieving antral grinding forces in biorelevant in vitro models: comparing the USP dissolution apparatus II and the dynamic gastric model with human in vivo data, *AAPS PharmSciTech*, 2011, **12(2)**, 620 – 626.
44. I. Kobayashi, H. Kozu, Z. Wang, H. Isoda and S. Ichikawa, Development and fundamental characteristics of a human gastric digestion simulator for analysis of food disintegration, *Jpn. Agric. Res. Q.*, 2017, **51(1)**, 17 – 25.
45. L. Chen, Y. Xu, T. Fan, Z. Liao, P. Wu, X. Wu and X.D. Chen, Gastric emptying and morphology of a “near real” in vitro human stomach model (RD-IV-HSM), *J. Food Eng.*, 2016, **183**, 1 – 8.
46. T.A. Tompkins, I. Mainville and Y. Arcand, The impact of meals on a probiotic during transit through a model of the human upper gastrointestinal tract, *Benef. Microbes*, 2011, **2(4)**, 295 – 303.
47. A. Guerra, S. Denis, O.L. Goff, V. Sicardi, O. François, A.F. Yao, G. Garrait, A.P. Manzi, E. Beyssac, M. Alric and S. Blanquet-Diot, Development and validation of a new dynamic computer-controlled model of the human stomach and small intestine, *Biotechnol. Bioeng.*, 2016, **113**, 1325 – 1335.
48. M. Minekus, P. Marteau, R. Havenaar and J.H.J. Huis in’t Veld, A multicompartamental dynamic computer-controlled model simulating the stomach and small intestine, *Altern. Lab. Anim.*, 1995, **23**, 197 – 209.
49. S. Bellmann, J. Lelievelds, T. Gorissen, M. Minekus and R. Havenaar, Development of an advanced in vitro model of the stomach and its evaluation versus human gastric physiology, *Food. Res. Int.*, 2016, **88**, 191 – 198.
50. E. Barroso, C. Cueva, C. Peláez, M.C. Martínez-Cuesta and T. Requena, Development of human colonic microbiota in the computer-controlled dynamic SIMulator of the GastroIntestinal tract SIMGI, *LWT – Food. Sci. Technol.*, 2015, **61**, 283 – 289.
51. T. Cieplak, M. Wiese, S. Nielsen, T. Van de Wiele, F. Van den Berg and D.S. Nielsen, The smallest intestine (TSI) – a low volume in vitro model of the small intestine with increased throughput, *FEMS Microbiol. Lett.*, 2018, **365(21)**, 1 – 8.
52. S. Blanquet-Diot, S. Denis, S. Chalancon, F. Chaira, J.M. Cardot and M. Alric, Use of artificial digestive systems to investigate the biopharmaceutical factors influencing the survival of probiotic yeast during gastrointestinal transit in humans, *Pharm. Res.*, 2012, **29**, 1444 – 1453.

53. M. Wiese, B. Khakimov, S. Nielsen, H. Sørensen, F.W.J. van der Berg and D.S. Nielsen, CoMiniGut – a small volume in vitro colon model for the screening of gut microbial fermentation process, *PeerJ Life & Environment*, 2018, **6**, 1 – 22.
54. M. Minekus, M. Smeets-Peeters, A. Bernalier, S. Marol-Bonnin, R. Havenaar, P. Marteau, M. Alric, G. Fonty and J.H.J. Huis in't Veld, A Computer-controlled system to simulate conditions of the large intestine with peristaltic mixing, water absorption and absorption of fermentation products, *Appl. Microbiol. Biotechnol.*, 1999, **53**, 108 – 114.
55. T. Kuriki and T. Imanaka, The concept of the alpha-amylase family: structural similarity and common catalytic mechanism, *J. Biosci. Bioeng.*, 1999, **87(5)**, 557 – 565.
56. M.J.E.C. Van der Maarel, B. Van der Veen, J.C.M. Uitdehaag, H. Leemhuis and Dijkhuizen, Properties and applications of starch-converting enzymes of the α -amylase family, *J. Biotechnol.*, 2002, **94**, 137 – 155.
57. M. Qian, R. Haser, G. Buisson, E. Duée and F. Payan, The active center of a mammalian α -amylase. Structure of the complex of a pancreatic α -amylase with carbohydrate inhibitor refined to 2.2-Å resolution, *Biochemistry*, 1994, **33**, 6284 – 6294.
58. Y. Nagamine, K. Omichi and T. Ikenaka, Investigation of the active site of human salivary α -amylase from the modes of action on modified maltooligosaccharides, *J. Biochem.*, 1988, **104**, 409 – 415.
59. G.D. Brayer, Y. Luo and S.G. Withers, The structure of human pancreatic α -amylase at 1.8Å resolution and comparisons with related enzymes, *Protein Sci.*, 1995, **4**, 1730 – 1742.
60. N. Ramasubbu, V. Paloth, Y. Luo, G.D. Brayer and M.J. Levine, Structure of human salivary α -amylase at 1.6Å resolution: implications for its role in the oral cavity, *Acta Cryst.*, 1996, **D52**, 435 – 446.
61. E.H. Rydberg, C. Li, R. Maurus, C.M. Overall, G.D. Brayer and S.G. Withers, Mechanistic analysis of catalysis in human pancreatic α -amylase: detailed kinetic and structural studies of mutants of three conserved carboxylic acids, *Biochemistry*, 2002, **41**, 4492 – 4502.
62. R. Zhang, C. Li, L.K. Williams, B.P. Rempel, G.D. Brayer and S.G. Withers, Directed “in situ” inhibitor elongation as a strategy to structurally characterize the covalent glycosyl-enzyme intermediate of human pancreatic α -amylase, *Biochemistry*, 2009, **48**, 10752 – 10764.
63. M. Qian, S. Spinelli, H. Driguez and F. Payan, Structure of a pancreatic α -amylase bound to a substrate analogue at 2.03Å resolution, *Protein Sci.*, 1997, **6**, 2285 – 2296.
64. J.C.M. Uitdehaag, R. Mosi, K.H. Kalk, B.A. Van der Veen, L. Dijkhuizen, S.G. Withers and B.W. Dijkstra, X-ray structures along the reaction pathway of cyclodextrin glycosyltransferase elucidate catalysis in the amylase family, *Nat. Struct. Biol.*, 1999, **6(5)**, 432 – 436.
65. M. Qian, E.H. Ajandouz, F. Payan and V. Nahoum, Molecular basis of the effects of chloride ion on the acid-base catalyst in the mechanism of pancreatic α -amylase, *Biochemistry*, 2005, **44**, 3194 – 3201.
66. S. Numao, R. Maurus, G. Sidhu, Y. Wang, C.M. Overall, G.D. Brayer and S.G. Withers, Probing the role of the chloride ion in the mechanism of human pancreatic α -amylase, *Biochemistry*, 2002, **41**, 215 – 225.
67. H.H. Sky-Peck and P. Thuvasethakul, Human pancreatic alpha-amylase II: effects of pH, substrate and ions on the activity of the enzyme, *Ann. Clin. Lab. Sci.*, 1977, **7(4)**, 310 – 317.
68. Y. Nakamura, M. Ogawa, T. Nishide, M. Emi, G. Kosaki, S. Himeno and K. Matsubara, Sequences of cDNAs for human salivary and pancreatic α -amylases, *Gene*, 1984, **28**, 263 – 270.
69. P.J. Butterworth, F.J. Warren and P.R. Ellis, Human α -amylase and starch digestion: an interesting marriage, *Starch/Stärke*, 2011, **63**, 395 – 405.

70. E. Lebenthal, Role of salivary amylase in gastric and intestinal digestion of starch, *Dig. Dis. Sci.*, 1987, **32**, 1155 – 1157.
71. M. Fried, S. Abramson and J.H. Meyer, Passage of salivary amylase through the stomach in humans, *Dig. Dis. Sci.*, 1987, **32**, 1097 – 1103.
72. J.E. Lennard-Jones, J.F. Cher and D.G. Shaw, Effect of different foods on the acidity of the gastric contents in patients with duodenal ulcer, *Gut*, 1968, **9**, 177 – 182.
73. J.L. Rosenblum, C.L. Irwin and D.H. Alpers, Starch and glucose oligosaccharides protect salivary-type amylase activity at acid pH, *Am. J. Physiol.*, 1988, **254**, G775 – G780.
74. S. Ramachandran, A.K. Patel, K.M. Nampoothiri, S. Chandran, G. Szakacs, C.R. Soccol and A. Pandey, Alpha-amylase from a fungal culture grown on oil cakes and its properties, *Braz. Arch. Biol. Technol.*, 2004, **47**, 309 – 317.
75. P. Bernfeld, *Methods Enzymol.*, ed. N. Kaplan and N. Colowick, Academic Press, United States, 1st edn, 1955, **17**, 149 – 158.
76. http://www.pharmacopeia.cn/v29240/usp29nf24s0_m60270.html#usp29nf24s0_m60270s21 (March 2021).
77. P. Layer, J. Keller and P.G. Lankisch, Pancreatic enzyme replacement therapy, *Curr. Gastroenterol. Rep.*, 2001, **3**, 101 – 108.
78. E. Truscheit, W. Frommer, B. Junge, L. Müller, D.D. Schmidt and W. Wingender, Chemistry and Biochemistry of microbial α -glucosidase inhibitors, *Angew. Chem. Int. Ed. Engl.*, 1981, **20**, 744 – 761.
79. H.P. Lehmann, X. Fuentes-Arderiu and L.F. Bertello, Glossary of terms in quantities and units in clinical chemistry, *Pure & Appl. Chem.*, 1996, **68**, 957 – 1000.
80. <https://www.merriam-webster.com/medical/Somogyi%20unit> (March 2017)
81. R.J. Henry and N. Chiamori, Study of the saccharogenic method for the determination of serum and urine amylase, *Clin. Chem.*, 1960, **6**, 434 – 452.
82. J. A. Rendleman, Hydrolytic action of α -amylase on high-amylose starch of low molecular mass, *Biotechnol. Appl. Biochem.*, 2000, **31**, 171 – 178.
83. L. Engelen, R.A. Wijk, J.F. Prinz, A.M. Janssen, A. Bilt, H. Weenen and F. Bosman, A comparison of the effects of added saliva, α -amylase and water on texture perception in semisolids, *Physiol. Behav.*, 2003, **78**, 805 – 811.
84. S.L. Bellavia, J. Moreno, E. Sanz, E. Picas and A. Blanco, α -amylase activity of human neonate and adult saliva, *Arch. Oral Biol.*, 1979, **24**, 117 – 121.
85. A.B. Acquier, A.K.C. Pita, L. Busch and G.A. Sánchez, Comparison of salivary levels of mucin and amylase and their relation with clinical parameters obtained from patients with aggressive and chronic periodontal disease, *J. Appl. Oral Sci.*, 2015, **23**, 288 – 294.
86. N. Takai, M. Yamaguchi, T. Aragaki, K. Eto, K. Uchihashi and Y. Nishikawa, Effect of psychological stress on the salivary cortisol and amylase levels in healthy young adults, *Arch. Oral Biol.*, 2004, **49**, 963 – 98.
87. M.J. Auvdel, Amylase levels in semen and saliva stains, *J. Forensic Sci.*, 1986, **32**, 426 – 431.
88. J. Hedman, E. Dalin, B. Rasmusson and R. Ansell, Evaluation of amylase testing as a tool for saliva screening of crime scene trace swabs, *Forensic Sci. Int. Genet.*, 2011, **5**, 194 – 198.

89. S.U. Jayasinghe, S.J. Torres, C.A. Nowso, A.J. Tilbrook and A.I. Turner, Physiological responses to psychological stress: importance of adiposity in men aged 50 – 70 years, *Endocr. Connect.*, 2014, **3**, 110 – 119.
90. A.L. Mandel and P.A.S. Breslin, High endogenous salivary amylase activity is associated with improved glycemic homeostasis following starch ingestion in adults, *Nutr. J.*, 2012, **142**, 853 – 858.
91. M. Mahosenaho, F. Caprio, L. Micheli, A.M. Sesay, G. Palleschi and V. Virtanen, A disposable biosensor for the determination of α -amylase in human saliva, *Microchim. Acta*, 2010, **170**, 243 – 249.
92. M.R. Rashkova, L.S. Ribagin and N.G. Toneva, Correlation between salivary α -amylase and stress-related anxiety, *Fol. Med.*, 2012, **54**, 46 – 51.
93. D. Koh, N. Vivian and L. Naing, Alpha amylase as a salivary biomarker of acute stress of venipuncture from periodic medical examinations, *Public Health Front.*, 2014, **2**, 1 – 5.
94. J.M. Braganza, K. Herman, P. Hine, G. Kay and G.I. Sandle, Pancreatic enzymes in human duodenal juice – a comparison of responses in secretin pancreozymin and Lundh Borgström tests, *Gut*, 1978, **19**, 358 – 366.
95. J. Keller and P. Layer, Human pancreatic exocrine response to nutrients in health and disease, *Gut*, 2005, **54**, 1 – 28.
96. H. Holm, L.E. Hanssen, A. Krogdahl and J. Florholmen,) High and low inhibitor soybean meals affect human duodenal proteinase activity differently: In vivo comparison with bovine serum albumin, *Nutr. J.*, 1988, **118**, 515 – 520.
97. J.C. Hafkenschied, M. Hessels and E.W. Van der Hoek, Determination of alpha-amylase, trypsin and lipase in duodenal fluid: comparison of methods, *J. Clin. Chem. Clin. Biochem.*, 1983, **21**, 167 – 174.
98. W. Sheldon, Congenital pancreatic lipase deficiency, *Arch. Dis. Child.*, 1964, **39**, 268 – 271.
99. E.L. McConnell, H.M. Fadda and A.W. Basit, Gut instincts: Explorations in intestinal physiology and drug delivery, *Int. J. Pharm.*, 2008, **364**, 213 – 226.
100. L. Petrakova, B.K. Doering, S. Vits, H. Engler, W. Rief, M. Schedlowski and J.S. Grigoleit, Psychosocial stress increases salivary alpha-amylase activity independently from plasma noradrenaline levels, *PLoS ONE*, 2015, **10**, 1 – 9.
101. K. Barrett, H. Brooks, S. Boitan and S. Barman, *Ganong's review of medical physiology*, McGraw Hill Professional, USA, 23rd edn, 2010, **26**, 429 – 450.
102. D.C. Whitcomb and M.E. Lowe, Human pancreatic digestive enzymes, *Dig. Dis. Sci.*, 2007, **52**, 1 – 17.
103. R.M. Herriott, Pepsinogen and pepsin, *J. Gen. Physiol.*, 1962, **45**, 57 – 76.
104. C. Richter, T. Tanaka and R.Y. Yada, Mechanism of activation of the gastric aspartic proteinases: pepsinogen, progastricsin and prochymosin, *Biochem. J.*, 1998, **335**, 481 – 490.
105. W.H. Brown, C.S. Foote, B.L. Iverson and E.V. Anslyn, *Organic chemistry*, Cengage Learning, USA, 5th edn, 2008, **27**, 1037 – 1072.
106. N.S. Andreeva and L.D. Rumsh, Analysis of crystal structures of aspartic proteinases: on the role of amino acid residues adjacent to the catalytic site of pepsin-like enzymes, *Protein Sci.*, 2001, **10**, 2439 – 2450.

107. N.F. Brás, M.J. Ramos and P.A. Fernandes, The catalytic mechanism of mouse renin studied with QM/MM calculations, *Phys. Chem. Chem. Phys.*, 2012, **14**, 12605 – 12613.
108. J. Eder, U. Hommel, F. Cumin, B. Martoglio and B. Gerhartz, Aspartic proteases in drug discovery, *Curr. Pharm. Des.*, 2007, **13**, 271 – 285.
109. L. Polgár, The mechanism of action of aspartic proteases involves 'push-pull' catalysis, *FEBS Lett.*, 1987, **219**, 1 – 4.
110. N.S. Andreeva and M.N.G. James, *Structure and function of the aspartic proteinases*, ed. B.M. Dunn, Plenum Press, USA, 1st edn, 1991, **4**, 39 – 45.
111. M. Armand, M. Hamosh, J.S. DiPalma, J. Gallagher, S.B. Benjamin, J.R. Philpott, D. Lairon and P. Hamosh, Dietary fat modulated gastric lipase activity in healthy humans, *Am. J. Clin. Nutr.*, 1995, **62**, 74 – 80.
112. E.K. Ulleberg, I. Comi, H. Holm, E.B. Herud, M. Jacobsen and G.E. Vegarud, Human gastrointestinal juices intended for use in in vitro digestion models, *Food Dig.*, 2011, **2**, 52 – 61.
113. B.I. Hirschowitz, A critical analysis with appropriate controls of gastric acid and pepsin secretion in clinical esophagitis, *Gastroenterology*, 1991, **101**, 1149 – 1156.
114. K. Rani, R. Rana and S. Datt, Review on latest overview of proteases, *Int. J. Curr. Life Sci.*, 2012, **2**, 12 – 18.
115. B.J. Haverback, B. Dyce, H. Bundy and H.A. Edmondson, Trypsin, trypsinogen and trypsin inhibitor in human pancreatic juice: mechanism for pancreatitis associated with hyperparathyroidism, *Am. J. Med.*, 1960, **29**, 424 – 433.
116. J.M. Chen, E.S. Radisky and C. Férec, *Handbook of proteolytic enzymes*, ed. A. Barrett, N. Rawlings and J. Woessner, Academic Press, London, 3rd edn, 2013, **576**, 2600 – 2609.
117. W. Appel, *Methods of enzymatic analysis*, ed. H.U. Bergmeyer, Academic Press, USA, 2nd edn, 1974, **3**, 949 – 1080.
118. E. Colomb and C. Figarella, Comparative studies on the mechanism of activation of the two human trypsinogens, *Biochim. Biophys. Acta*, 1979, **571**, 343 – 351.
119. D.C. Whitcomb, Mechanism of disease: advances in understanding the mechanisms leading to chronic pancreatitis, *Nat. Clin. Pract. Gastroenterol. Hepatol.*, 2004, **1**, 46 – 52.
120. T.T. Baird Jr, *Reference Module in Life Sciences*, ed. B.D. Roitberg, Elsevier, Amsterdam, 2nd edn, 2017, **Trypsin**, 1 – 4.
121. T. Sipos, J.R. Merkel, An effect of calcium ions on the activity, heat stability and structure of trypsin, *Biochemistry*, 1970, **9**, 2766 – 2775.
122. R.H. Kretsinger, Evolution and function of calcium-binding proteins, *Int. Rev. Cytol.*, 1976, **46**, 323 – 393.
123. A. Szabó, E.S. Radisky and M. Sahin-Tóth, Zymogen activation confers thermodynamic stability on a key peptide bond and protects human cationic trypsin from degradation, *J. Biol. Chem.*, 2014, **289**, 4753 – 4761.
124. T.T. Baird Jr and C.S. Craik, *Encyclopedia of Genetics*, ed. S. Brenner and J.H. Miller, Elsevier Science, USA, 2001, **Trypsin**, 2071 – 2075.
125. H. Gutfreund, The characterization of the catalytic site of trypsin, *Trans. Faraday Soc.*, 1955, **51**, 441 – 446.

126. M.R. Dukejart, S.K. Dutta and J. Vaeth, Dietary fiber supplementation: effect on exocrine pancreatic secretion in man, *Am. J. Clin. Nutr.*, 1989, **50**, 1023 – 1028.
127. E.P. DiMagno, J.R. Maragelada, L. Vay, W. Go and C.G. Moertel, Fate of orally ingested enzymes in pancreatic insufficiency, *N. Engl. J. Med.*, 1977, **296**, 1318 – 1322.
128. M.E. Lowe, Structure and function of pancreatic lipase and colipase, *Annu. Rev. Nutr.*, 1997, **17**, 141 – 158.
129. M. Armand, Lipases and lipolysis in the human digestive tract: where do we stand?, *Curr. Op. Clin. Nutr. Metab. Care*, 2007, **10**, 156 – 164.
130. A. Roussel, S. Canaan, M.P. Egloff, M. Rivière, L. Dupuis, R. Verger and C. Cambillau, Crystal structure of human gastric lipase and model of lysosomal acid lipase, two lipolytic enzymes of medical interest, *J. Biol. Chem.*, 1999, **274**, 16995 – 17002.
131. Y. Gargouri, G. Pieroni, P.A. Lowe, L. Sarda and R. Verger, Human gastric lipase: the effect of amphiphiles, *Eur. J. Biochem.*, 1986, **156**, 305 – 310.
132. H. Moreau, R. Laugier, Y. Gargouri, F. Ferrato and R. Verger, Human preduodenal lipase is entirely of gastric fundic origin, *Gastroenterology*, 1988, **95**, 1221 – 1226.
133. P. Borel, M. Armand, M. Senft, M. Andre, H. Lafont and D. Lairon, Gastric lipase: evidence of an adaptive response to dietary fat in the rabbit, *Gastroenterology*, 1991, **100**, 1502 – 1509.
134. M. Mukherjee, Human digestive and metabolic lipases – a brief review, *J. Mol. Catal. B: Enzym.*, 2003, **22**, 369 – 376.
135. J. DiPalma, C.L. Kirk, M. Hamosh, A.R. Colon, S.B. Benjamin and P. Hamosh, Lipase and pepsin activity in the gastric mucosa of infants, children and adults, *Gastroenterology*, 1991, **101**, 116 – 121.
136. F. Carrière, C. Renou, V. López, J. de Caro, F. Ferrato, H. Lengsfeld, A. de Caro, R. Laugier and R. Verger, The specific activities of human digestive lipases measured from the in vivo and in vitro lipolysis of test meals, *Gastroenterology*, 2000, **119**, 949 – 960.
137. H. Chahinian, T. Snabe, C. Attias, P. Fojan, S.B. Petersen and F. Carrière, How gastric lipase, an interfacial enzyme with a Ser-His-Asp catalytic triad, acts optimally at acidic pH, *Biochemistry*, 2006, **45**, 993 – 1001.
138. F.I. Khan, D. Lan, R. Durrani, W. Huan, Z. Zhao and Y. Whang, The lid domain in lipases: structural and functional determinant of enzymatic properties, *Front. Bioeng. Biotechnol.*, 2017, **5**, 1 – 13.
139. N. Miled, C. Bussetta, A. de Caro, M. Rivière, L. Berti and S. Canaan, Importance of the lid and cap domains for the catalytic activity of gastric lipases, *Comp. Biochem. Physiol., Part B: Biochem. Mol. Biol.*, 2003, **136**, 131 – 138.
140. A. Aloulou and F. Carrière, Gastric lipase: an extremophilic interfacial enzyme with medical applications, *Cell. Mol. Life Sci.*, 2008, **65**, 851 – 854.
141. P. Reis, K. Holmberg, H. Watzke, M.E. Leser and R. Miller, Lipases at interfaces: a review, *Adv. Colloid Interface Sci.*, 2009, **147 – 148**, 237 – 250.
142. C. Bourlieu, G. Paboeuf, S. Chever, S. Pezennec, J.F. Cavalier, F. Guyomarch, A. Deglaire, S. Bouhallab, D. Dupont, F. Carrière and V. Vié, Adsorption of gastric lipase onto multicomponent model lipid monolayers with phase separation, *Colloids Surf., B: Interfaces*, 2016, **143**, 97 – 106.
143. S. Canaan, A. Roussel, R. Verger and C. Cambillau, Gastric lipase: crystal structure and activity, *Biochim. Biophys. Acta*, 1999, **1441**, 197 – 204.

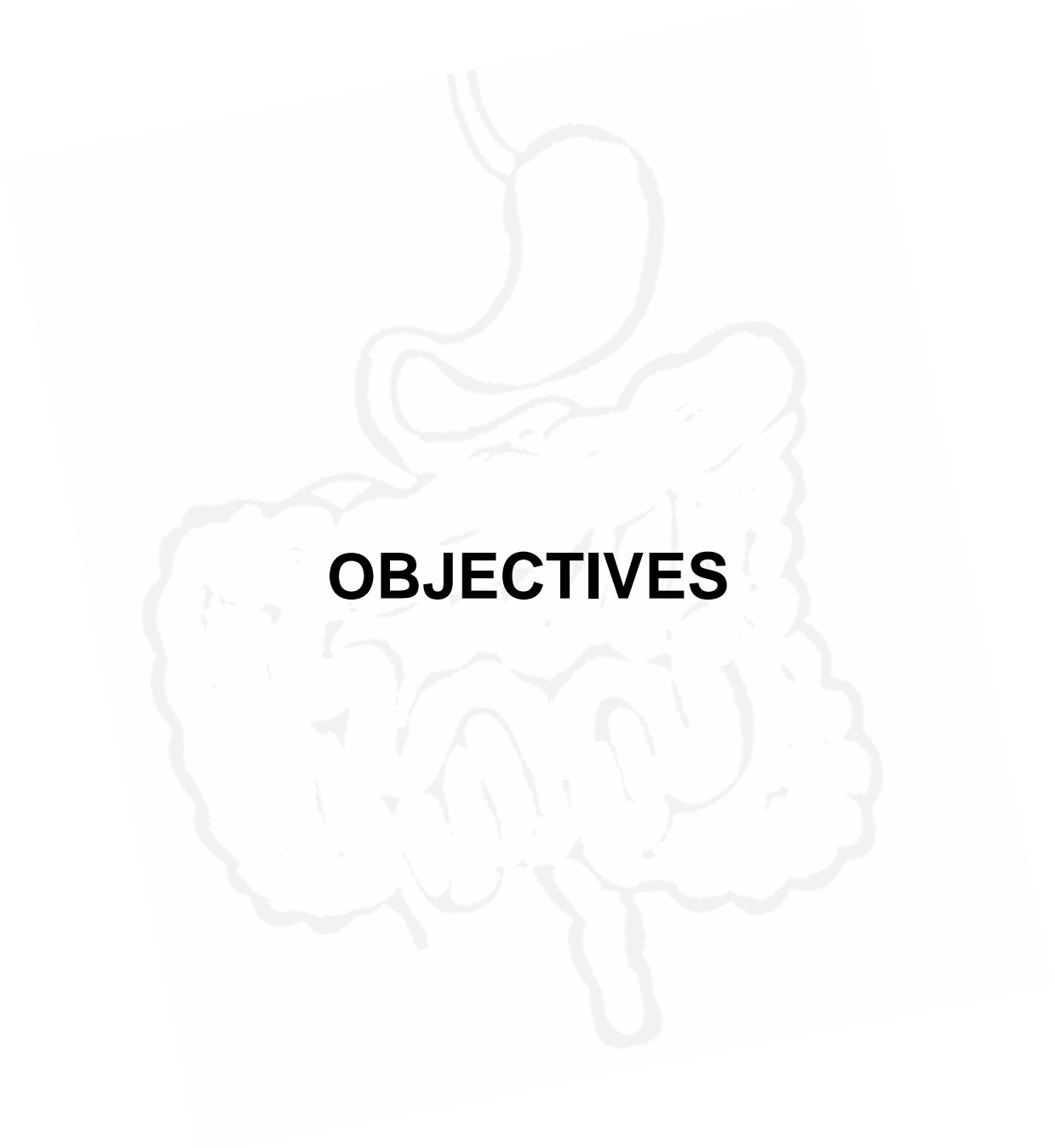
144. L. Casas-Godoy, F. Gasteazoro, S. Duquesne, F. Bordes, A. Marty and G. Sandoval, Lipases: an overview, *Methods Mol. Biol.*, 2018, **1835**, 3 – 38.
145. M. Armand, B. Pasquier, M. André, P. Borel, M. Senft, J. Peyrot, J. Salducci, H. Portugal, V. Jaussan and D. Lairon, Digestion and absorption of 2 fat emulsions with different droplet sizes in the human digestive tract, *Am. J. Clin. Nutr.*, 1999, **70**, 1096 – 1106.
146. F. Carrière, J.A. Barrowman, R. Verger and R. Laugier, Secretion and contribution to lipolysis of gastric and pancreatic lipases during a test meal in humans, *Gastroenterology*, 1993, **105**, 876 – 888.
147. Q. Lüthi-Peng, H.P. Märki and P. Hadváry, Identification of the active-site serine in human pancreatic lipase by chemical modification with tetrahydrolipstatin, *FEBS J.*, 1992, **299**, 111 – 115.
148. D.Y. Colin, P. Deprez-Beauclair, M. Allouche, R. Brasseur and B. Kerfelec, Exploring the active site cavity of human pancreatic lipase, *Biochem. Biophys. Res. Commun.*, 2008, **370**, 394 – 398.
149. M.E. Lowe, The triglyceride lipases of the pancreas, *J. Lipid Res.*, 2002, **43**, 2007 – 2016.
150. P. Benito-Gallo, A. Franceschetto, J.C.M. Wong, M. Marlow, V. Zann, P. Scholes and Gershkovic, Chain length affects pancreatic lipase activity and the extent and pH-time profile of triglyceride lipolysis, *Eur. J. Pharm. Biopharm.*, 2015, **93**, 353 – 362.
151. F. Carrière, P. Grandval, C. Renou, A. Palomba, F. Prière, J. Giallo, F. Henniges, S. Sander-Struckmeier and R. Laugier, Quantitative study of digestive enzyme secretion and gastrointestinal lipolysis in chronic pancreatitis, *Clin. Gastroenterol. Hepatol.*, 2005, **3**, 28 – 38.
152. S.J. Hur, B.O. Lim, E.A. Decker and D.J. McClements, In vitro human digestion models for food applications, *Food Chem.*, 2011, **125**, 1 – 12.
153. A.F. Hofmann, The continuing importance of bile acid in liver and intestinal disease, *Arch. Intern. Med.*, 1999, **159**, 2647 – 2658.
154. L. Kalantzi, K. Goumas, V. Kalioras, B. Abrahamsson, J.B. Dressman and C. Reppas, Characterization of the human upper gastrointestinal contents under conditions simulating bioavailability/bioequivalence studies, *Pharm. Res.*, 2006, **23**, 165 – 176.
155. T.C. Northfield and I. McColl, Postprandial concentrations of free and conjugated bile acids down the length of the normal human small intestine, *Gut*, 1973, **14**, 513 – 518.
156. T.L. Peeters, G. Ventrappen and J. Janssens, Bile acid output and the interdigestive migrating motor complex in normal and in cholecystectomy patients, *Gastroenterology*, 1980, **79**, 676 – 681.
157. D.N. Challacombe, S. Edkins and G.A. Brown, Duodenal bile acids in infancy, *Arch. Dis. Childh.*, 1975, **80**, 837 – 843.
158. L. Humbert, D. Rainteau, N. Tuvignon, C. Wolf, P. Seksik., R. Laugier and F. Carrière, *J. Lipid Res.*, 2018, **59**, 2202 – 2213.
159. X. Gao, S. Jiang, D. Koh and C.Y.S. Hsu, Salivary biomarkers for dental caries, *Periodontol. 2000*, 2015, **70**, 128 – 141.
160. F. Agha-Hosseini, I. Mirzaii-Dizgah, P.P. Moghaddam and Z.T. Akrad, Stimulated whole salivary flow rate and composition in menopausal women with oral dryness feeling, *Oral dis.*, 2007, **13**, 320 – 323.
161. F. Agha-Hosseini, I. Mirzaii-Dizgah and S. Amirkhani, The composition of unstimulated whole saliva of healthy dental students, *J. Contemp. Dent. Pract.*, 2006, **7**, 104 – 111.

162. A. Bardow, J. Madsen and B. Nauntofte, The bicarbonate concentration in human saliva does not exceed the plasma level under normal physiological conditions, *Clin. Oral Investig.*, 2000, **4**, 245 – 253.
163. J.K.M. Aps and L.C. Martens, Review: the physiology of saliva and transfer of drugs into saliva, *Forensic Sci. Int.*, 2005, **150**, 119 – 131.
164. H. Ben-Aryeh, N. Roll, M. Lahav, R. Dlin, N. Hanne-Paparo, R. Szargel, C. Shein-Orr and D. Laufer, Effect of exercise on salivary composition and cortisol in serum and saliva in man, *J. Dent. Res.*, 1989, **68**, 1495 – 1497.
165. J.L. Chicharro, V. Serrano, R. Ureña, A.M. Gutierrez, A. Carvajal, P. Fernández-Hernando and A. Lucía, Trace elements and electrolytes in human resting mixed saliva after exercise, *Br. J. Sports Med.*, 1999, **33**, 204 – 207.
166. W.H. Johnston, Salivary electrolytes in fibrocystic disease of the pancreas, *Arch. Dis. Child.*, 1956, **31**, 477 – 480.
167. W.L. Siqueira, E. Oliveira, Z. Mustacchi and J. Nicolau, Electrolyte concentrations in saliva of children aged 6 – 10 years with Down syndrome, *Oral Surg. Oral Med. Oral Pathol. Oral Radiol. Endod.*, 2004, **98**, 76 – 79.
168. A. Rapoport, B.M. Evans and H. Wong, Observations on electrolytes in human saliva, *Can. Med. Assoc. J.*, 1961, **84**, 579 – 583.
169. A.G. White, P.S. Entmacher, G. Rubin and L. Leiter, Physiological and pharmacological regulation of human salivary electrolyte concentrations with a discussion of electrolyte concentrations of some other exocrine secretions, *J. Clin. Invest.*, 1955, **34**, 246 – 255.
170. C. Dawes, The effects of flow rate and duration of stimulation on the concentrations of protein and the main electrolytes in human parotid saliva, *Arch. Oral Biol.*, 1969, **14**, 277 – 294.
171. A. Almståhl and M. Wikström, Electrolytes in stimulated whole saliva in individuals with hyposalivation of different origins, *Arch. Oral Biol.*, 2003, **48**, 337 – 344.
172. R.A. Winer, M.M. Cohen, R.P. Feller and H.H. Chauncey, Composition of human saliva, parotid gland secretory rate, and electrolyte concentration in mentally subnormal persons, *J. Dent. Res.*, 1965, **44**, 632 – 634.
173. R. Grant, The relation of calcium content to acidity and buffer value of gastric secretions, *Am. J. Physiol.*, 1941, **132**, 467 – 473.
174. J.B. Kirsner and J.E. Bryant, The calcium content of gastric juice, *Am. J. Dig. Dis.*, 1939, **6**, 704 – 706.
175. J.R.C. Gardham and M. Hobsley, The electrolytes of alkaline human gastric juice, *Clin. Sci.*, 1970, **39**, 77 – 87.
176. A. Lambling, J.J. Bernier, Y. Najean and J. Badoz-Lambling, Gastric juice in pernicious anemia: physicochemical composition of gastric juice in complete achlorhydria and composition of primary alkaline secretion of the stomach, *Am. J. Dig. Dis.*, 1961, **6**, 629 – 645.
177. G.M. Makhlof, J.P.A. McManus and W.I. Card, A quantitative statement of the two-compartment hypothesis of gastric secretion, *Gastroenterology*, 1966, **51**, 149 – 171.
178. A. Lindahl, A.L. Ungell, L. Knutson and H. Lennernäs, Characterization of fluids from the stomach and proximal jejunum in men and women, *Pharm. Res.*, 1997, **14**, 497 – 502.
179. M.J. Riddell, J.A. Strong and D. Cameron, The electrolyte concentration of human gastric secretion, *Q. J. Exp. Physiol. Cogn. Med. Sci.*, 1959, **45**, 1 – 11.

180. D.W. Piper and M.C. Stiel, The effect of anticholinergic drugs on the electrolyte content of gastric juice, *Gut*, 1961, **2**, 230 – 232.
181. J.G. Banwell, N.F. Pierce, R.C. Mitra, K.L. Brigham, G.J. Caranasos, R.I. Keimowitz, D.S. Fedson, J. Thomas, S.L. Gorbach, R.B. Sack and A. Mondal, Intestinal fluid and electrolyte transport in human cholera, *J. Clin. Invest.*, 1970, **49**, 183 – 195.
182. G.O. Barbezat and M.I. Grossman, Intestinal secretion: stimulation by peptides, *Science*, 1971, **174**, 422 – 423.
183. H.S. Mekjin, S.F. Phillips and A.F. Hofmann, Colonic secretion of water and electrolytes induced by bile acids: perfusion studies in man, *J. Clin. Invest.*, 1971, **50**, 1569 – 1577.
184. J.G. Temple, A. Birch and R. Shields, Postprandial changes in pH and electrolyte concentration in the upper jejunum after truncal vagotomy and drainage in man, *Gut*, 1975, **16**, 961 – 965.
185. T. Stevens, D.L. Conwell, G. Zuccaro, F. Van Lente, F. Khandwala, E. Purich, J.J. Vargo, S. Fein, J.A. Dumot, P. Trolli and C. O'Laughlin, Electrolyte composition of endoscopically collected duodenal drainage fluid after synthetic porcine secretin stimulation in healthy subjects, *Gastrointest. Endosc.*, 2004, **60**, 351 – 355.
186. K.G. Wormsley, Response to secretin in man, *Gastroenterology*, 1968, **54**, 197 – 209.
187. J.M. Davidson, R.S.T. Linfort and A.J. Taylor, In-mouth measurement of pH and conductivity during eating, *J. Agric. Food Chem.*, 1998, **46**, 5210 – 5214.
188. A.A. Pratha and J. Prabakar, Comparing the effect of carbonated and energy drinks on salivary pH-In vivo randomized controlled trial, *Research J. Pharm. And Tech.*, 2019, **12**, 4699 – 4702.
189. J.W. Woolnough, J.A. Monro, C.S. Brennan and A.R. Bird, Simulating human carbohydrate digestion in vitro: a review of methods and the need for standardization, *Int. J. Food Sci.*, 2008, **43**, 2245 – 2256.
190. S. Baliga, S. Muglikar and R. Kale, Salivary pH: A diagnostic biomarker, *J. Indian Soc. Periodontal.*, 2013, **17**, 461 – 465.
191. L. Sams, J. Paume, J. Giallo and F. Carrière, Relevant pH and lipase for in vitro models of gastric digestion, *Food Funct.*, 2016, **7**, 30 – 45.
192. G.E. Vist and R.J. Maughan, The effect of osmolality and carbohydrate content on the rate of gastric emptying of liquids in man, *J. Physiol.*, 1995, **486**, 523 – 531.
193. J.A.L. Calbet and D.A. MacLean, Role of caloric content on gastric emptying in humans, *J. Physiol.*, 1997, **498**, 553 – 559.
194. J.A.L. Calbet and J.J. Holst, Gastric emptying, gastric secretion and enterogastrone response after administration of milk proteins or other peptide hydrolysates in humans, *Eur. J. Nutr.*, 2004, **43**, 127 – 139.
195. S. Rodriguez-Stanley, K.L. Collings, M. Robinson, W. Owen and P.B. Miner, The effects of capsaicin on reflux, gastric emptying and dyspepsia, *Aliment. Pharmacol. Ther.*, 2000, **14**, 129 – 134.
196. H.P. Simonian, S. Doma, R.S. Fisher and H.P. Parkman, Regional postprandial differences in pH within the stomach and gastroesophageal junction, *Dig. Dis. Sci.*, 2005, **50**, 2276 – 2285.
197. S.P. Mackay and C.G. Wilson, *Pharmaceutical Chemistry*, ed. D.G. Watson, Churchill Livingstone, China, 1st edn, 2011, **8**, 149 – 190.

198. J.R. Malagelada, V.L.W. Go and W.H.J. Summerskill, Different gastric, pancreatic and biliary responses to solid-liquid or homogenised meals, *Dig. Dis. Sci.*, 1979, **24**, 101 – 110.
199. S. Clarysse, J. Tack, F. Lammert, G. Duchateau, C. Reppas and P. Augustijns, Postprandial evolution in composition and characteristics of human duodenal fluids in different nutritional states, *J. Pharm. Sci.*, 2009, **98**, 1177 – 1192.
200. A.Y. Abuhelwa, D.J.R. Foster and R.N. Upton, A quantitative review and meta-models of the variability and factors affecting oral drug absorption-part I: Gastrointestinal pH, *APPS J.*, **18**, 1309 – 1321.
201. R. Giacco, G. Costabile and G. Riccardi, Metabolic effects of dietary carbohydrates: the importance of food digestion, *Food Res. Int.*, 2016, **88**, 336 – 341.
202. B.E. Goodman, Insights into digestion and absorption of major nutrients in humans, *Adv. Physiol. Educ.*, 2010, **34**, 44 – 53.
203. G. Karp, *Cell and Molecular Biology: Concepts and Experiments*, John Wiley & Sons Inc., USA, 6th edn, 2009, **4**, 117 – 172.
204. A.C. Guyton and J.E. Hall, *Textbook of Medical Physiology*, Elsevier, USA, 11th edn, 2006, **78**, 961 – 977.
205. PDB molecule of the month: <https://pdb101.rcsb.org/motm/14> (May 2021, David Goodsell)
206. <https://www.who.int/diabetes/global-report/en/> (Jan 2019)
207. <https://www.cdc.gov/diabetes/data/> (Jan 2019)
208. B.J. Venn and T.J. Green, Glycemic index and glycemic load: measurement issues and their effect on diet-disease relationships, *Euro. J. Clin. Nutr.*, 2007, **61**, S122 – S131.
209. K. Foster-Powell, S. H. A. Holt and J.C. Brand-Miller, International table of glycemic index and glycemic load values: 2002, *Am. J. Clin. Nutr.*, 2002, **76**, 5 – 56.
210. H. Dodd, S. Williams, R. Brown and B. Venn, Calculating meal glycemic index by using measured and published food values compared with directly measured meal glycemic index, *Am. J. Clin. Nutr.*, 2011, **94**, 992 – 996.
211. F.S. Atkinson, K. Foster-Powell and J. Brand-Miller, International tables of glycemic index and glycemic load values: 2008, *Diabetes Care*, 2008, **31**, 2281 – 2283.
212. K. Argyri, A. Athanasatou, M. Bouga and M. Kapsokefalou, The potential of an in vitro digestion method for predicting glycemic response of foods and meals, *Nutrients*, 2016, **8**, 209 – 221.
213. Z. Xie, J. Guan, L. Chen, Z. Jin and Y. Tian, Effect of drying processes on the fine structure of A-, B-, and C-type starches, *Starch/Stärke*, 2017, **70**, 1700218(1 – 8).
214. Y. Ai and J.L. Jane, Gelatinization and rheological properties of starch, *Starch/Stärke*, 2015, **67**, 213 – 224.
215. A. Buleón, P. Colonna, V. Planchot and S. Ball, Starch granules: structure and biosynthesis, *Int. J. Biol. Macromol.*, 1998, **23**, 85 – 112.
216. D.F. Coral, P. Pineda-Gómez, A. Rosales-Rivera and M.E. Rodriguez-Garcia, Determination of the gelatinization temperature of starch presented in maize flours, *J. Phys. Conf. Ser.*, 2009, **167**, 012057(1 – 5).

217. A.A. Karim, L.C. Toon, V.P.L. Lee, W.Y. Ong, A. Fazilah and T. Noda, Effects of phosphorus contents on the gelatinization and retrogradation of potato starch, *J. Food Sci.*, 2007, **72**, C132 – C138.
218. Y.S. Kim, D.P. Wiesenborn, P.H. Orr and L.A. Grant, Screening potato starch for novel properties using differential scanning calorimetry, *J. Food Sci.*, 1995, **60**, 1060 – 1065.
219. W.S. Ratnayake and D.S. Jackson, A new insight into the gelatinization process of native starches, *Carbohydr. Polym.*, 2007, **67**, 511 – 529.
220. R. Hoover, T. Hughes, H.J. Chung and Q. Liu, Composition, molecular structure, properties and modification of pulse starches: a review, *Food Res. Int.*, 2010, **43**, 399 – 413.
221. S. Wang, C. Li, L. Copeland, Q. Niu and S. Wang, Starch: retrogradation: a comprehensive review, *Compr. Rev. Food Sci. F.*, 2015, **14**, 568 – 585.
222. F. Kong and R.P. Singh, *The stability and shelf life of food*, USA, 2nd edn, 2016, **2**, 43 – 76.
223. A. K. Akerberg, H.G. Liljeberg, Y.E. Granfeldt, A.W. Drews and I.M. Björck, An in vitro method, based on chewing, to predict resistant starch content in foods allows parallel determination of potentially available starch and dietary fiber, *J. Nutr.*, 1998, **128**, 651 – 660.
224. D. Freitas and S.L. Feunteun, Oro-gastro-intestinal digestion of starch in white bread, wheat-based and gluten-free pasta: Unveiling the contribution of human salivary α -amylase, *Food Chem.*, 2019, **274**, 566 – 573.
225. I. Goñi, A. García-Alonso and F. Saura-Calixto, A starch hydrolysis procedure to estimate glycemic index, *Nutr. Res.*, 1997, **17**, 427 – 437.
226. H. Fabek, S. Messerschmidt, V. Brulport and H.D. Goff, The effect of in vitro digestive processes on the viscosity of dietary fibres and their influence on glucose diffusion, *Food Hydrocoll.*, 2014, **35**, 718 – 726.
227. C.S. Brennan, D.E. Blake, P.R. Ellis and J.D. Schofield, Effects of Guar Galactomannan on Wheat Bread Microstructure and on the In vitro and In vivo Digestibility of Starch in Bread, *J. Cereal Sci.*, 1996, **24**, 151 – 160.



OBJECTIVES

OBJECTIVES

The main purpose of this thesis was to study the digestion of carbohydrates and how other macronutrients affect their digestibility. The digestibility of different starches has been studied by measuring their degree of hydrolysis during digestion and by the determination of the in vitro glycaemic index of meals containing a variety of starches. Two in vitro digestion methods (static and dynamic) have been used to study the digestion of carbohydrates. Therefore, four main objectives were defined as follows:

Objective 1. Fill the gaps found in the in vitro digestion methods with regards to starch digestion

To mimic human digestion closely and to obtain valuable information from in vitro digestion methods; the first objective consisted of closing the gaps that have been found in in vitro digestion methods, with regards to starch digestion. The following specific objectives for the adaptation of the two in vitro digestion methods were proposed:

- Determine the enzyme activity for α -amylase, pepsin, trypsin and lipase, the unit definition being equal to the unit definition of the reported physiological levels.
- Find potential alternative enzyme sources to mimic the human digestive enzymes.
- Establish adequate methodologies to reach the physiological activities for the four mentioned digestive enzymes and pancreatin.
- Study the effect of the presence of electrolytes on the enzyme activity.
- Evaluate the maximum storage time of the enzymatic solutions.
- Determine the optimal mixing speed in the static digestion method.
- Design an appropriate sampling procedure to be used during the in vitro digestion methods.
- Establish the optimal buffer to keep the pH constant in the static digestion method.

Objective 2. Demonstrate whether the selected in vitro digestion methods provide reliable results

The digestion of three different meals will be studied and the measured glycaemic index will be compared with the reported values.

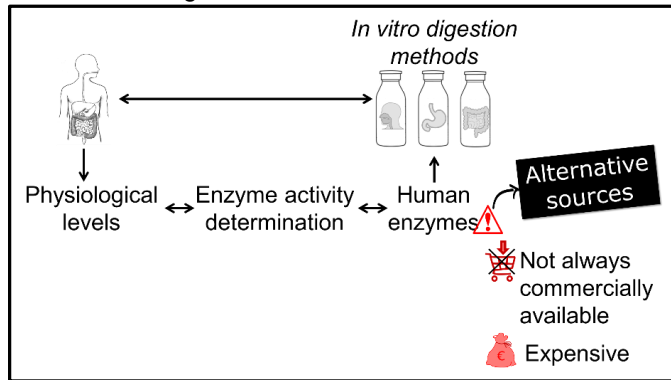
Objective 3. Study of the starch digestion and the effect of other macronutrients on the digestion of carbohydrates

To accomplish this third objective, the following specific objectives were proposed:

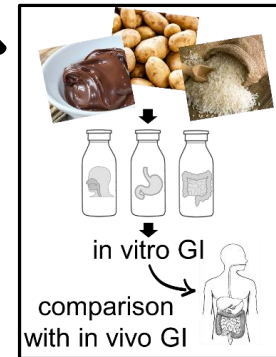
- Evaluate the digestion of two different starch sources to study the digestion of carbohydrates.
- Find out if the individual addition of protein and fat sources to the starchy meals increases or decreases the digestion of the starches.
- Assess the digestion of starches in the presence of both, proteins and fats integrated into complex meals prepared by mixing the three macronutrients.

Objective 4. Compare the results obtained with both in vitro digestion (static and dynamic) methods.

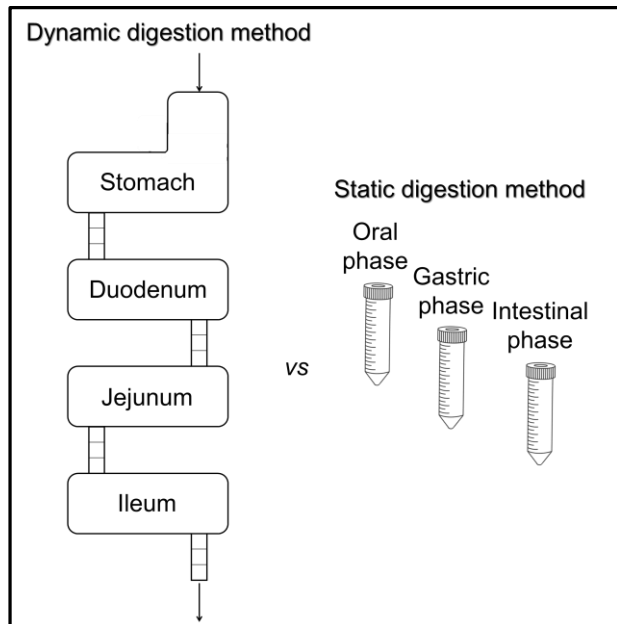
1. Fill the gaps found in the in vitro digestion methods with regards to starch digestion



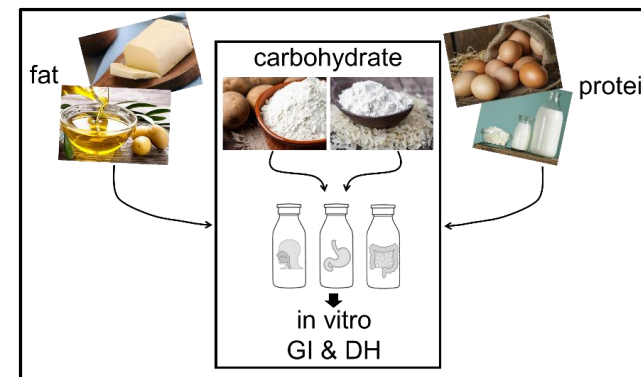
2. Demonstrate whether the selected in vitro digestion methods provide reliable results



In vitro study of the carbohydrate digestion



4. Compare the results obtained with both in vitro digestion (static and dynamic) methods



3. Study of the starch digestion and the effect of other macronutrients on the digestion of carbohydrates



MATERIALS AND METHODS

MATERIALS AND METHODS

1. Chemicals

All the reagents were purchased from Sigma Aldrich Chemie GmbH (Taufkirchen, Germany), unless otherwise is specified.

Table 1. Specifications of chemicals

Chemicals	Article number
3,5-dinitrosalicylic acid	D0550
4-Bromophenylboronic acid	B75956
Ammonium carbonate	207861
Bile bovine	B3883
Bile extract porcine	B8631
Bovine serum albumin	A7030
Calcium chloride dihydrate**	A0775
Casein from bovine milk	C3400
Copper sulphate pentahydrate	C8027
D-(+)-Glucose****	1.08337.1000
D-(+)-maltose monohydrate	M5885
Egg whites from chicken	E0500
Ethanol	32205-M
Glyceryl tributyrat	91010
Haemoglobin from bovine blood	H2625
HEPES	H3375
Hydrochloric acid	30721-M
Iodine	207772
Magnesium chloride hexahydrate	M2670
Methanol	34860
Neocuproine	N1501
N α -p-tosyl-L-arginine methyl ester hydrochloride (TAME)	T4626
Olive oil	O1514
Patent blue V sodium salt	21605
Potassium chloride	P5405
Potassium iodide	60400
Potassium phosphate monobasic	P5655
Potassium sodium tartrate tetrahydrate	S2377
Potato starch	S2004
Sodium bicarbonate	S6297
Sodium carbonate	S7795
Sodium chloride*	S9888
Sodium hydroxide	S8045
Sodium phosphate dibasic	S7907
Sodium taurodeoxycholate	T0875
Soja lecithin***	019192G
Starch from potato	S4251
Starch from rice	S7260
Sudan III	S4131
Tributyrin	W222305
Trichloroacetic acid (TCA)	T0699
Trizma base	T1503
Trizma hydrochloride (Tris-HCl)	T3253
Tween80	-

*from Honeywell Fluka (Stockstadt, Germany)

**from Applichem (Darmstadt, Germany)

***from Fresenius Kabi (Bad Homburg, Germany)

****from Merck (Darmstadt, Germany)

Table 2. Specifications of the enzymes

	Enzymes	Article number
α -amylase	α -amylase from porcine pancreas	A3176
	α -amylase from human saliva	A0521
	α -amylase from bacillus sp.	A6380
Proteases	Pepsin from porcine gastric mucosa	P7012
	Trypsin from bovine pancreas	T9201
Lipase	Lipase from <i>Rhizopus Oryzae</i>	80612
	Lipase from <i>Aspergillus Niger</i>	62301
	Amano lipase from <i>Aspergillus Niger</i>	534781
	Rabbit gastric extract****	RGE
Pancreatin	Pancreatin from porcine pancreas 4USP	P1750
	Pancreatin from porcine pancreas 8USP	P7545
	Pancreatic enzyme for cats and dogs – Pancrex Vet*	-
	Pancreatic enzyme for cats and dogs – Pancrex**	-
	PancZyme***	-
	Pancreatin powder****	N0066397

*from Pfizer (Capelle aan den IJssel, Netherlands)

**from Zoetis (Capelle aan den IJssel, Netherlands)

***from American Laboratories, Inc. (Omaha, United States)

****from Nordmark (Uetersen, Germany)

*****from Lipolytech (Marseille, France)

Different meals were used to perform the in vitro digestion methods, and they were purchased from the supermarket (Rewe):

- Butter (Rewe – BioQualität)
- Potatoes: Kartoffeln Festkochend-belana
- Rice: Original Langkorn Reis (kochbeutel) – Uncle Ben's
- Cocoa cream: Nutella (Ferrero)

The kit "Bile acids" for the measurement of the concentration of bile acids was purchased from DiaSys Diagnostic Systems GmbH (art. n°.:1 2212 99 90 313 – Holzheim, Germany).

The kit "D-Fructose and D-Glucose" for the measurement of the concentration of glucose and fructose was purchased from Megazyme (art. n°.: K-FRUGL 04/18 – Wicklow, Ireland).

2. Simulated digestive fluids

The simulated digestive fluids (SDFs) consist of solutions of electrolytes at a physiological concentration. The composition and procedure to prepare the SDFs were different depending on the in vitro digestion model that was used. Therefore, two different methodologies were used to prepare the SDFs.

The first methodology consists of the preparation of stock solutions of the individual salts, followed by the mixture of the different solutions to reach the physiological concentration during the in vitro digestion method. For that reason, the SDFs were prepared 1.25 times more concentrated than the physiological levels (table 3).

In addition, the pH of those solutions was adjusted depending on the fluid that simulates (pH 7: salivary and intestinal, pH 3: gastric). Due to their lack of stability at room temperature (RT), the SDFs were stored in individual tubes (1 tube per digestive phase, 3 tubes per run) at -20°C for a maximum of 6 months.

Table 3. Composition of the simulated digestive fluids (SDFs) – Method 1 (2)

Electrolyte solution		Simulated digestive fluid (mM)		
<i>Salt</i>	<i>Conc. (M)</i>	<i>Salivary fluid</i>	<i>Gastric fluid</i>	<i>Intestinal fluid</i>
Potassium chloride	0.50	18.88	8.63	8.50
Potassium phosphate	0.50	4.63	1.13	1.00
Sodium bicarbonate	1.00	17.00	31.25	106.25
Magnesium chloride	0.15	0.19	0.13	0.41
Sodium chloride	2.00	0.00	59.00	48.00
Ammonium carbonate	0.50	0.08	0.63	0.00
Hydrochloric acid	1.00	1.38	19.50	10.50
Calcium chloride*	0.30	1.88	0.19	0.75

*Calcium chloride was added just before SDFs use as precipitation may occur

For the second methodology the SDFs were prepared directly as a mixture of the salts, and the preparation of stock solutions for each individual salt was not needed. In this case, the fluids were stored at RT and only the pH of the simulated intestinal fluid was adjusted (pH 7). Table 4 shows the concentration of the salts in the SDFs (method 2).

Table 4. Composition of simulated digestive fluids (SDFs) – Method 2

Salt	Simulated digestive fluid (mM)	
	<i>Gastric fluid</i>	<i>Intestinal fluid</i>
Potassium chloride	300.0	200.0
Sodium chloride	1060.0	2140.0
Calcium chloride	7.3	11.4

3. Enzyme activity methods

3.1. Importance of working with an excess of substrate

To be able to measure the enzyme activity correctly, it is necessary, among other things, to have enough substrate available to be hydrolysed. Therefore, it is important to work under an excess of substrate.

The effect of the enzyme/substrate ratio on the determination of enzyme activity was studied. In the (below) described enzymatic methods, the substrate concentration is constant and for that reason, the variable in this study was the concentration of the enzyme. The selected method to carry out this survey was “3.2.α-amylase”, and the studied enzyme was α-amylase from porcine pancreas (Sigma Aldrich, A3176).

To find the optimal enzyme concentration, two different kinds of experiments were performed. For the first experiment, different enzymatic solutions were prepared and then its activity was measured and depicted versus the concentration.

The second experiment also consisted of preparing enzymatic solutions at different concentrations, but in addition the substrate was incubated with the enzyme for a longer period of time. In the original method (3.2.4.) the incubation last for 3 min, but for this study this incubation was performed also for 6 and 9 min.

In the calculation of the enzyme activity, the obtained activity was corrected in order to express the activity in AU·mg⁻¹ (one unit is the amount of enzyme that is needed to release 1 mg of maltose from starch in 3 min, under assay conditions). Finally, the activity was depicted versus the time of incubation, and the optimal enzyme concentration was selected.

3.2. α-amylase

The selected method for the determination of α-amylase activity was the Bernfeld method, as it is referenced by Minekus et al (1,2). The Bernfeld method determines the reducing sugars released from starch, during its hydrolysis catalysed by α-amylase, by their ability to reduce 3,5-dinitrosalicylic acid (figure 1). This method is based on the following reactions:

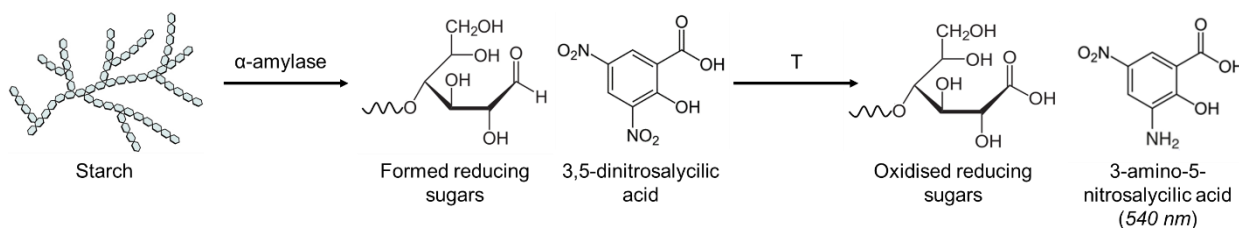


Figure 1. Principle reactions that occur during α -amylase activity determination

With this method, the activity can be expressed as $\text{AU}\cdot\text{mg}^{-1}$ or $\text{AU}\cdot\text{mL}^{-1}$, where one unit is the amount of enzyme that is needed to release 1 mg of maltose from starch in 3 min under assay conditions (20°C , pH 6.9). Which is equivalent to international units (1 μmol product released per min, eq. 1).

$$1 \text{ unit} = \frac{1 \text{ mg maltose}}{3 \text{ min}} \cdot \frac{1 \text{ mmol maltose}}{342.3 \text{ mg maltose}} \cdot \frac{10^3 \mu\text{mol}}{1 \text{ mmol}} = \frac{0.97 \mu\text{mol maltose}}{1 \text{ min}} \sim 1 \text{ IU} \quad \text{Eq. 1}$$

3.2.1. Critical points

3.2.1.1. Starch solution preparation

One of the critical points in the method of α -amylase activity determination is the starch solution preparation, due to its poor solubility at RT.

Starch reacts with iodine in the presence of iodide to form an intensely blue-coloured complex, which is visible at low concentrations of iodine. Because of the low solubility of iodine in DI water, the iodine reagent was prepared by dissolving the iodine in the presence of potassium iodide. This makes a linear triiodide ion complex which is soluble and slips into the coil of the starch (amylose) causing an intense blue-black colour (figure 2). The sensitivity of the colour reaction is such that a blue colour is visible when the iodine concentration is $2 \cdot 10^{-5} \text{ M}$ and the iodine concentration is greater than $4 \cdot 10^{-4} \text{ M}$ at 20°C (3).

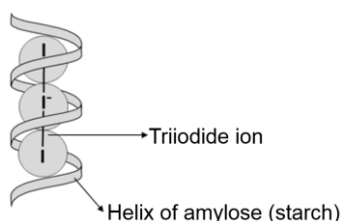


Figure 2. Starch-triiodide ion complex

Different conditions for starch solution preparation were studied. Starch solutions were first prepared by mixing the starch with the buffer (3.2.2.1.) at different temperatures and for different times of mixing, the iodine reagent was added and the absorbance was read at 604 nm (wavelength selected by performing a scan of the iodine-starch complex). The obtained absorbances (data not shown) helped to estimate the degree of starch solubility at the different preparation conditions. However, no conclusive results were obtained from this method.

For that reason, another method was used for the obtention of the best protocol for the starch solution preparation. The starch was mixed with the phosphate buffer (3.2.2.1.) at different temperatures ($50, 60, 70, 80, 90, 100^\circ\text{C}$) for different periods of time (5, 10, 15, 20, 25, 30 min) and at constant mixing (300 rpm). After that, the mixtures were cooled down (fridge: $5 - 8^\circ\text{C}$) to RT, and the volume was adjusted to reach a final concentration of 1 %.

A centrifugation step was executed to remove the remaining insoluble starch (9000 rpm, 20 min, 4°C – Herareus Multifuge X3R, Thermofisher), the supernatant was removed and the precipitate was dried in an oven at 50°C overnight.

Finally, the remaining precipitate was weighed, and the percentage of soluble starch was calculated with the following equation (eq. 2):

$$\% \text{ starch solubilized} = 100 - \left(\frac{\text{insoluble starch (mg)}}{\text{total starch (mg)}} \cdot 100 \right) \quad \text{Eq. 2}$$

3.2.1.2. Enzyme solution preparation

The enzyme solubility could be also a potential critical point in the determination of its activity. The enzyme used to carry out these experiments was “ α -amylase from bacillus sp.” purchased in Sigma Aldrich (A6380). Therefore, to obtain the optimal conditions for the enzymatic solution preparation, different variables were studied:

- *Mixing methodology*: the speed of stirring was studied as the mixing methodology could damage the enzyme or not be enough to completely solubilise the enzyme. For this reason, different speeds of mixing were tested but also two mixing methodologies, the use of magnetic stirrer and the use of ultrasound bath. The studied speeds for the magnetic stirrer were 50, 100, 200 and 300 rpm, a 2x0.6 cm magnet, 50 mL beakers and 25 mL of sample were used. The solutions were prepared, for the magnetic stirrer and ultrasound bath, at RT and mixed for 15 min, using phosphate buffer (3.2.2.1.) as solvent. Finally, α -amylase activity was measured to determine how the mixing process affects the enzyme.
- *Order of addition (1st solvent vs 1st enzyme)*: another factor that could affect the solubility of the enzyme is the order of addition. As an example, when the solvent is added after the solute, a slow wetting of the powder by the solvent could be an obstacle for the solubilization. Moreover, the addition of the powder to the solvent could help the solutes with poor solubility. To study the order of addition, the enzymatic solution was prepared following two different procedures. For one side, the solvent (3.2.2.1.) was added to the enzymatic powder and then mixed at RT, 300 rpm for 15 min. Parallely, the enzymatic powder was added to the solvent while this was in agitation, and then it was mixed at RT, 300 rpm for 15 min. Ultimately, the activity was measured and compared for both procedures.
- *Temperature of mixing*: the temperature at which the enzyme is mixed with the solvent could have different impacts on the enzyme. High temperatures could favour the solubilization but also could influence the stability of the enzyme. For that reason, the enzyme was mixed with the solvent (3.2.2.1.) at 300 rpm and different temperatures (in an ice bath, at RT (~20°C), 25°C and 37°C) for 15 min. After that, α -amylase activity was measured to study how the temperature of solubilization influences the enzyme.
- *Time of mixing*: theoretically, as longer time of mixing, the solubility would be better. However, that could also affect the stability of the enzyme and for that reason, the minimum time of mixing needed to dissolve the enzyme was determined. To carry out this study, the enzyme was mixed with the solvent (3.2.2.1.) at different time periods (5, 10, 15 and 20 min), 300 rpm and RT. Then, the α -amylase activity was measured.

3.2.1.3. Incubation method

Two incubations are involved during α -amylase activity determination, one at 20°C where the enzyme is incubated with the substrate and the hydrolysis of starch takes place, and a second one at 100°C where the redox reaction takes place.

The traditional way to carry out these incubations were the use of baths:

- *Hydrolysis (20°C)*: water bath
- *Redox (100°C)*: boiling water bath or oil bath

For practical reasons, the use of thermoshakers (figure 3) was studied for both incubations. The activity of α -amylase (α -amylase from bacillus sp. – Sigma Aldrich, A6380) was measured using the baths for the incubations, water bath for the hydrolysis and oil bath for the redox reaction. Parallely the method was repeated but using the thermoshakers instead of the baths.

The same batch of enzyme (1333 AU·mg⁻¹) was used for the study of both incubation methods. Two different thermoshakers were studied: 5436 thermomixer and Comfort thermomixer, both from Eppendorf. However, for its temperature limitations, the redox reaction was carried out at 95°C in 5436 thermomixer and 99°C in Comfort thermomixer.

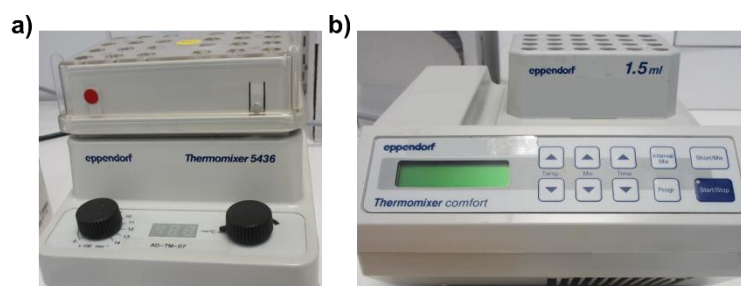


Figure 3. Thermoshakers used for the incubations a) 5436 thermomixer, b) Comfort thermomixer

Finally, it was checked if the activity levels obtained using the thermoshakers were the same as using the traditional baths.

3.2.2. Reagents

3.2.2.1. *Buffer*

The buffer has an important role as the enzyme activity could be affected by a change in the pH. The buffer contains 20 mM sodium phosphate dibasic and 6.7 mM sodium chloride. To prepare the buffer, both salts were dissolved in DI water, then the pH was adjusted to 6.9 and finally, the volume was adjusted to achieve the correct concentrations of the salts.

3.2.2.2. *Substrate*

The substrate used in this method was a solution of 1 % potato starch. Preliminary tests were conducted to determine the best conditions for the substrate preparation (3.2.1.1.).

The substrate was prepared by mixing potato starch with phosphate buffer at 95°C and 350 rpm for at least 5 min (RCT basic, IKA). After that, the solution was cooled down in the fridge (5 – 8°C) to RT, and finally, the volume was adjusted with the phosphate buffer to reach a concentration of 1 %.

3.2.2.3. *Colour reagent*

The colour reagent has two roles, it stops the enzymatic hydrolysis and it is the reagent that contains 3,5-dinitrosalicylic acid needed to measure the α -amylase activity since it is reduced proportionally to the amount of reducing sugars formed during the starch hydrolysis.

This reagent is sensible to the light; therefore, it is important to use opaque material to prepare and store it. This reagent can be stored at RT for a maximum of 3 months.

For the colour reagent preparation, potassium sodium tartrate tetrahydrate was dissolved in 2 M NaOH at 60 – 70°C to obtain a concentration of 5.3 M. In parallel, 96 mM 3,5-dinitrosalicylic acid solution was prepared using DI water as solvent, and heated up to 60 – 70°C. Once both solutions were prepared and heated to 60 – 70°C, they were mixed together with DI water (also at 60 – 70°C), resulting in a yellowish solution that contains 1.06 M sodium potassium tartrate tetrahydrate and 48 mM 3,5-dinitrosalicylic acid. Finally, the mixture was cooled down in the fridge (5 – 8°C) to RT.

3.2.2.4. Standard

Maltose was used as standard. A solution of 0.2 % was prepared, and then diluted at different extend for the construction of the standard curve. The final concentrations of maltose are shown in table 5.

Table 5. Concentration of maltose solutions for the standard curve

Standard	Maltose ($mg \cdot mL^{-1}$)
0	0.0
1	0.2
2	0.4
3	0.6
4	1.0
5	2.0

3.2.3. Sample

The limitation of the method was the enzyme concentration as for the correct use of the method, the enzymatic solution should contain $1 AU \cdot mL^{-1}$ approximately.

However, the specific activity of the enzyme was usually unknown and the procedure explained in “3.1.Importance of working with an excess of substrate” section was followed.

Preliminary tests (3.2.1.2.) were conducted to determine the best conditions for the enzymatic solution preparation. The enzymatic powder was mixed with the solvent (e.g. SDFs: table 3 or 4) at RT and ~350 rpm (speed depends on the volume of the solution and the size of the magnet) for at least 10 min (RCT basic, IKA). After that, the volume was adjusted in a volumetric flask.

In some cases, like the pancreatin, the enzymatic powder was not completely soluble, and a centrifugation step (9000 rpm, 20 min, 4 °C – Herareus Multifuge X3R, Thermofisher) was performed to remove the insoluble part. This step was needed to obtain a homogenous sample but also to mimic the protocol of pancreatin preparation used for the in vitro digestion methods.

3.2.4. Procedure

3.2.4.1. Standard curve

To prepare the standard curve, 200 μL of maltose were mixed with 100 μL of colour reagent and incubated for 15 min at 95°C (5436 thermomixer, Eppendorf). After that, these mixtures were cooled down to RT in an ice bath, 900 μL of DI water were added and the absorbance was read at 540 nm (Sunrise microplate reader, Tecan). Finally, the obtained absorbances (corrected with the blank: standard 0 – table 5) were depicted versus the maltose amount (mg) that was present in each standard tube.

3.2.4.2. Enzyme activity determination

For α -amylase activity determination, 100 μL of the enzymatic solution were mixed with 100 μL of 1 % starch and incubated at 20°C for exactly 3 min with constant stirring (Comfort thermomixer, Eppendorf). Just after the 3 min, the hydrolysis was stopped by the addition of 100 μL of the colour reagent. This mixture was incubated at 95°C for 15 min (5436 thermomixer, Eppendorf) and then cooled down to RT in an ice bath. Once RT was achieved, 900 μL of DI water were added and the absorbance was recorded at 540 nm (Sunrise microplate reader, Tecan).

For the blank, the same procedure was followed, except that the enzymatic solution was added after the incubation of the reagent colour.

The conditions of the method (e.g. pH, temperature ...) were modified only to study how these variables affect enzyme activity. And in all cases, the method conditions were specified in the definition of the enzyme activity unit.

3.2.5. Calculations

As one unit is the amount of enzyme needed to release 1 mg of maltose from starch in 3 min, the corrected absorbance was interpolated into the standard curve in order to calculate the amount of maltose that has been released during the hydrolysis (eq. 3):

$$\text{Activity (AU)} = \frac{\text{Maltose(mg)}}{\frac{t_{\text{hydrolysis}}}{3} \text{ (min)}} = \frac{\left((\text{Abs}_{\text{sample}} - \text{Abs}_{\text{blank}}) - \text{Intercept}_{\text{standard curve}} \right) \cdot 3}{\text{Slope}_{\text{standard curve}} \cdot t_{\text{hydrolysis}}} \quad \text{Eq. 3}$$

Where $\text{Abs}_{\text{sample}}$ and $\text{Abs}_{\text{blank}}$ are the obtained absorbances for the sample and the blank respectively, the Slope and Intercept are the coefficients of the standard curve, $t_{\text{hydrolysis}}$ is the time of incubation for the enzyme and substrate (usually: 3 min) and 3 is the time of incubation specified in the unit definition.

The activity is usually expressed as specific activity ($\text{AU} \cdot \text{mg}^{-1}$), and to calculate that, the obtained activity (AU) was divided by the amount of enzyme (mg) used to carry out the hydrolysis (mg present in a conical tube).

3.3. Pepsin

The selected method to determine pepsin activity was an adaptation of the Anson & Mirsky method, as it is referenced by Minekus et al (2,4,5). In this method, the hydrolysis of haemoglobin is catalysed by pepsin until trichloroacetic acid (TCA) is added and the proteins (unhydrolyzed haemoglobin and pepsin) are denatured. Then, the insoluble part is removed, and the released peptides during the hydrolysis are measured spectrophotometrically.

With this method, the activity can be expressed as $\text{PU} \cdot \text{mg}^{-1}$ or $\text{PU} \cdot \text{mL}^{-1}$, where one unit produce a ΔA_{280} of 0.001 per min under assay conditions, measured as TCA-soluble products (37°C, pH 2.0, total volume: 16 mL, light path: 1 cm). Which is equivalent to 0.0125 IU (eq. 4 – 9):

$$\Delta A_{280} = 0.001$$

$$\epsilon_{\text{tyrosine}} = 1280 \text{ M}^{-1} \text{cm}^{-1} \text{ (6)}$$

$$\text{Light path (b)} = 1 \text{ cm}$$

$$\text{Total volume} = 16 \text{ mL}$$

$$A = \epsilon \cdot b \cdot c \quad \text{Eq. 4}$$

$$A_2 - A_1 = \epsilon_2 \cdot b_2 \cdot c_2 - \epsilon_1 \cdot b_1 \cdot c_1 \quad \text{Eq. 5}$$

$$0.001 = 1280 \cdot 1 \cdot c_2 - 1280 \cdot 1 \cdot c_1 \quad \text{Eq. 6}$$

$$0.001 = 1280 \cdot (c_2 - c_1) \quad \text{Eq. 7}$$

$$\Delta c = \frac{0.001}{1280} = 7.8 \cdot 10^{-7} \text{ mol} \cdot \text{L}^{-1} \quad \text{Eq. 8}$$

$$16 \text{ mL} \cdot \frac{7.8 \cdot 10^{-7} \text{ mol}}{10^3 \text{ mL}} \cdot \frac{10^6 \mu\text{mol}}{1 \text{ mol}} = 0.0125 \mu\text{mol tyrosine} \cdot \text{min}^{-1} \quad \text{Eq. 9}$$

3.3.1. Reagents

3.3.1.1. Substrate

For the substrate preparation, the haemoglobin was mixed vigorously creating a vortex (~700 rpm – RCT basic, IKA) with DI water at 37°C for 15 min to achieve a concentration of 2.5 %. After that, haemoglobin solution was diluted with 300 mM hydrochloric acid to obtain a concentration of 2 % and pH 2.

3.3.1.2. Stop reagent

For the preparation of the stop reagent, the TCA was diluted in a volumetric flask to obtain a concentration of 5 %.

3.3.2. Sample

The limitation of the method was the enzyme concentration, and for the correct use of the method, the enzymatic solution should contain 150 PU·mL⁻¹ approximately.

However, the specific activity of the enzyme was usually unknown and the procedure explained in “3.1.Importance of working with an excess of substrate” section was followed.

The enzymatic powder was mixed with the solvent at RT for at least 10 min (RCT basic, IKA). After that, the volume was adjusted in a volumetric flask.

In general, the supplied pepsin had a high specific activity (~2000 PU·mg⁻¹), for that reason a stock solution was first prepared, and then a dilution step was needed to achieve the proper concentration.

3.3.3. Procedure

For pepsin activity determination, 500 µL of 2 % haemoglobin were added into conical tubes of 1.5 mL (microcentrifuge tubes 3810X, Eppendorf) with a multi-step pipette (multipette M4, Eppendorf).

To equilibrate the temperature, the substrate was incubated at 37°C for around 3 min (Comfort thermomixer, Eppendorf), then 100 µL of the enzymatic solution were added and mixed with the substrate for exactly 10 min at 37°C and 450 rpm (Comfort thermomixer, Eppendorf).

To stop the reaction 1 mL of 5 % TCA was added and mixed in the same thermomixer. The TCA not only stopped the hydrolysis, but also provoked the precipitation of the proteins (pepsin and undigested haemoglobin).

After that, the mixtures were centrifugated (21100 xg, 10 min, 20°C – Heraeus Fresco, Thermo Scientific) to remove the precipitated proteins. Finally, the absorbance of the supernatant was read at 280 nm using quartz cuvettes (1 cm).

For the blank, the enzymatic solution was added after the addition of the TCA.

3.3.3.1. *Precipitate removal method*

In the pepsin activity method, the hydrolysis is stopped by the addition of TCA and this addition triggers the formation of a precipitate. This precipitate needs to be removed for the proper absorbance measurement. Two different methods were studied in order to find the optimal method for the precipitate removal:

- *Centrifugation*: 21100 xg, 10 min, 20°C (Heraeus Fresco, Thermo Scientific)
- *Filtration*: syringe filter (25mm, 0.45 µm, PTFE)

The pepsin activity method was performed parallelly using the centrifugation and filtration steps for the precipitate removal, and then the obtained activity was compared.

3.3.4. Calculations

To calculate the pepsin activity in the defined units, the absorbance was divided by the time and multiplied by a correction factor of the volume. Therefore, the following equation was used (eq. 10):

$$\text{Pepsin activity (PU)} = \frac{\frac{\text{Abs}_{\text{sample}} - \text{Abs}_{\text{blank}}}{0.001}}{\frac{t_{\text{hydrolysis}}}{1} \text{ (min)}} \cdot \frac{V}{16 \text{ mL}} = \frac{(\text{Abs}_{\text{sample}} - \text{Abs}_{\text{blank}}) \cdot 1 \cdot V}{t_{\text{hydrolysis}} \cdot 0.001 \cdot 16 \text{ mL}} \quad \text{Eq. 10}$$

Where Abs_{sample} and Abs_{blank} are the absorbances obtained for the sample and the blank, respectively, 0.001 is the difference of absorbances at 280 nm that is equivalent to one unit. V is the volume of the reaction mixture (in this case: 1.6 mL), 16 mL is the volume that is specified in the unit definition. $t_{hydrolysis}$ is the incubation time of the substrate with the enzyme (usually: 10 min) and 1 is the correction factor of the time that comes from the unit definition (ΔA_{280} of 0.001 in 1 min).

The activity is usually expressed as specific activity ($U \cdot mg^{-1}$), and to calculate that, the obtained activity (PU) was divided by the amount of enzyme (mg) used to carry out the hydrolysis.

3.4. Trypsin

The selected method to determine trypsin activity was an adaption of Hummel method, as it is referenced by Minekus et al (2,7). The release of N-p-tosyl-L-arginine was determined spectrophotometrically during the hydrolysis of TAME. This method is based in the following reaction (figure 4):

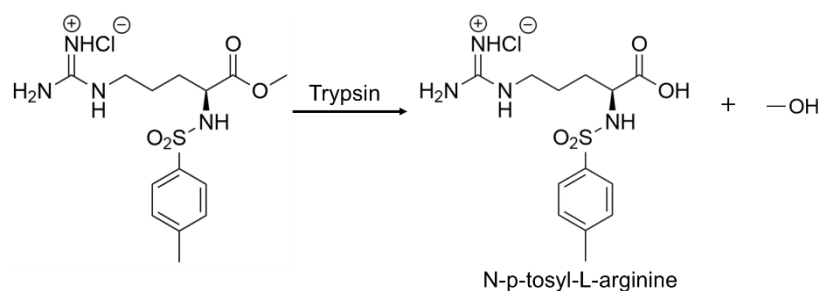


Figure 4. Principle reaction used in the trypsin method

With this method, one unit of trypsin activity (TU) hydrolyses 1 μ mol of TAME per min under assay conditions (25°C, pH 8.1), which is equivalent to IU.

3.4.1. Reagents

3.4.1.1. Substrate

The substrate used in this method was 10 mM p-toluene-sulfonyl-L-arginine methyl ester (TAME). To prepare the substrate, the powder was dissolved in DI water at RT and then the volume was adjusted in a volumetric flask.

3.4.1.2. Buffer

The buffer used to measure trypsin activity contains 46 mM of tris-HCl and 11.5 mM calcium chloride. Both powders were dissolved in DI water at RT, then the pH was adjusted to 8.1 and the volume was adjusted in a volumetric flask to obtain the correct concentration.

3.4.2. Sample

As for the other methods, the enzyme concentration is a critical point in this method, and the enzymatic solution should contain around 3 $TU \cdot mL^{-1}$ for the correct trypsin activity measurement.

However, the specific activity of the enzymatic powder was usually unknown, and different concentrations were tested. The trypsin activity was measured spectrophotometrically with a continuum method, which means that the hydrolysis was followed by measuring the absorbance periodically (e.g. every 30 s). The absorbance was depicted versus time, and the slope of the measurements was calculated. With the value of the slope and intercept it was possible to identify the correct concentration of the enzyme (figure 5).

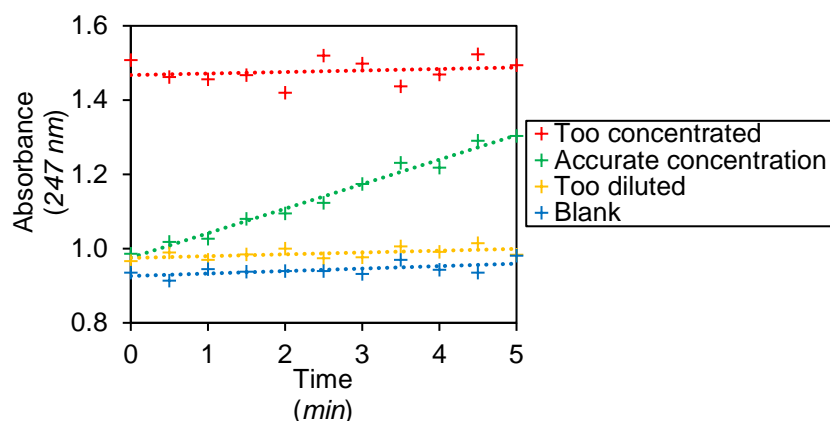


Figure 5. Example of the obtained absorbances for differently concentrated trypsin solutions (too concentrated, accurate concentration, too diluted)

Therefore, the trypsin solution has the optimal concentration for the activity measurement when the slope is higher than 0. When the slope is approximately 0, it could mean that the trypsin solution is too concentrated or too diluted and the intercept should be checked. When the intercept of the sample is much higher than the intercept of the blank, the trypsin solution is too concentrated, as the hydrolysis has been complete before starting the measurements. When the intercept of the sample is close to the intercept of the blank, it means that the trypsin solution is too diluted.

The trypsin solutions were prepared by mixing the enzyme with the solvent at RT and ~350 rpm for at least 10 min and then adjusting the volume to obtain the desired concentration in a volumetric flask.

In some cases, like the pancreatin, the enzymatic powder was not completely soluble, and a centrifugation step (9000 rpm, 20 min, 4 °C – Herareus Multifuge X3R, Thermofisher) was performed to remove the insoluble part. This step was needed to obtain a homogenous sample but also to mimic the protocol of pancreatin preparation used for the in vitro digestion methods.

3.4.3. Procedure

For trypsin activity determination, 2.6 mL of tris-HCl buffer were mixed with 300 µL of substrate directly in a quartz cuvette, the cuvette was covered with a lid (Kartell Labware, art n° 01962), mixed by inversion and incubated at 25°C for around 2 – 3 min (Biospectrometer, Eppendorf).

Then, 100 µL of trypsin solution were added to the cuvette, then it was quickly mixed by inversion and the absorbance measurements started. The increase of the absorbance was recorded at 247 nm in continuum until a plateau was achieved (5 – 10 min).

For the blank, the same procedure was followed but instead of the enzymatic solution, the solvent was mixed with the substrate and buffer.

3.4.4. Calculations

To calculate the trypsin activity, the obtained absorbance was depicted versus the time of hydrolysis. The slope for the sample and the blank was calculated but only from the lineal part of the graph. Then the slope of the sample was corrected by subtracting the slope of the blank (eq. 11):

$$\text{Slope} = \text{Slope}_{\text{sample}} - \text{Slope}_{\text{blank}} \quad \text{Eq. 11}$$

As one unit of trypsin activity hydrolyses 1 µmol of TAME per min, after the slope correction the concentration of N-p-tosyl-L-arginine (obtained product from the TAME hydrolysis) was calculated with the following equation (eq. 12):

$$\text{Slope} (\text{min}^{-1}) = \frac{\Delta A}{\Delta t} = \frac{\epsilon \cdot b \cdot c_2 - \epsilon \cdot b \cdot c_1}{\Delta t} = \frac{\epsilon \cdot b \cdot \Delta c}{\Delta t} \rightarrow \Delta c = \frac{\text{Slope} \cdot \Delta t}{\epsilon \cdot b} \quad \text{Eq. 12}$$

After that, the amount of substrate (μmol) converted into N-p-tosyl-L-arginine was calculated taking into account that 1 mol of substrate is converted into 1 mol of product and multiplying the obtained concentration in eq. 12 for the volume of the mixture.

Finally, the obtained amount of hydrolysed TAME (μmol) was divided by the time of the hydrolysis, as indicated in eq. 13.

$$\text{Trypsin activity (TU)} = \frac{\mu\text{mol TAME}}{1 \text{ min}} = \frac{\Delta c \cdot V}{\frac{t_{\text{hydrolysis}}}{1} \text{ min}} = \frac{\left(\frac{\text{Slope} \cdot \Delta t}{\epsilon \cdot b}\right) \cdot V}{\frac{t_{\text{hydrolysis}}}{1} \text{ min}} = \frac{\text{Slope} \cdot \Delta t \cdot V \cdot 1}{\epsilon \cdot b \cdot t_{\text{hydrolysis}}} \quad \text{Eq. 13}$$

Where *Slope* is the obtained slope for the sample and corrected with the slope of the blank (min^{-1}), Δt is the interval of time in which the slope is calculated (usually: 1 min), V is the volume of the mixture (0.003 L), ϵ is the extinction coefficient of TAME ($0.00054 \text{ L} \cdot \mu\text{mol}^{-1} \cdot \text{cm}^{-1}$ (θ)), b is the light path (1 cm) and $t_{\text{hydrolysis}}$ is the time of the protein hydrolysis (same as Δt).

The activity is usually expressed as specific activity ($\text{TU} \cdot \text{mg}^{-1}$), and to calculate that, the obtained activity (TU) was divided by the amount of enzyme (mg) used to carry out the hydrolysis.

3.5. Lipase

The selected method to determine lipase activity was a pH-titration, as is referenced by Minekus et al (2). In this method, the free fatty acids released by the action of lipase are titrated at a constant pH by 0.1 N sodium hydroxide during the hydrolysis. This method is based on the following reaction (figure 6):

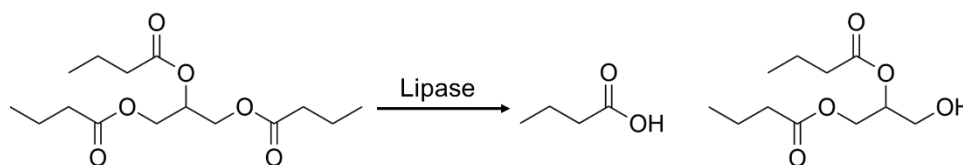


Figure 6. Principle reaction used in the method of lipase activity determination

In this method, one lipase unit (LU) is the amount of enzyme needed to produce 1 μmol of butyric acid per min under assay conditions (37°C , pH 8), which is equivalent to IU.

3.5.1. Reagents

3.5.1.1. Titrant

The selected titrant was 0.1 N sodium hydroxide, which was prepared by mixing the NaOH pellets with DI water at RT and adjusting the volume in a volumetric flask to obtain the desired concentration.

3.5.1.2. Substrate

The substrate used to measure lipase activity was pure tributyrin ($\geq 98.5\%$).

3.5.1.3. Aqueous solution

The composition of the aqueous solution depends on the source of the lipase, for example the fungal lipase could be inhibited by the bile salts while the pancreatic lipase not (as it contains colipase).

For the preparation of the aqueous solution, the different substances were dissolved in DI water, the pH was adjusted just ~ 0.5 units below the pH of the method (gastric lipase: pH 5.5; pancreatic and fungal lipases: pH 8.0) and the volume was finally adjusted to achieve the correct concentration.

The composition of the aqueous solution and the pH of the mixture depending on the source of the lipase are shown in table 6.

Table 6. Composition of the aqueous solution depending on the source of the lipase

Constituent (<i>mg·mL⁻¹</i>)	Gastric lipase	Pancreatic lipase	Fungal lipase
Trizma base	--	0.04	0.04
NaCl	9.00	9.00	9.00
CaCl ₂	--	0.20	0.20
Sodium taurodeoxycholate	1.00	2.10	0.21
Bovine serum albumin	0.10	--	--
pH	~5.0	~7.5	~7.5

3.5.2. Sample

In this case, the enzymatic solution was always prepared with a concentration of 1 mg·mL⁻¹, independently of the activity of the sample, as it has been seen that there is enough substrate to react with. Therefore, the limitation step in this method was not the enzyme/substrate ratio.

The powder was dissolved using cold DI water (~5°C) as solvent. The mixture was mixed with a vortex for about 30 s, and then stored in an ice bath (or in the fridge) until the assay was performed. The sample was always prepared the same day of the measurement.

In some cases, like the pancreatin, the enzymatic powder was not completely soluble, and a centrifugation step (9000 rpm, 20 min, 4 °C – Herereus Multifuge X3R, Thermofisher) was performed to remove the insoluble part. This step was needed to obtain a homogenous sample but also to mimic the protocol of pancreatin preparation used for the in vitro digestion methods.

3.5.3. Procedure

To carry out the experiments that are described in this section, a computer-controlled titrator was used. A description of the device is shown in figure 7a.

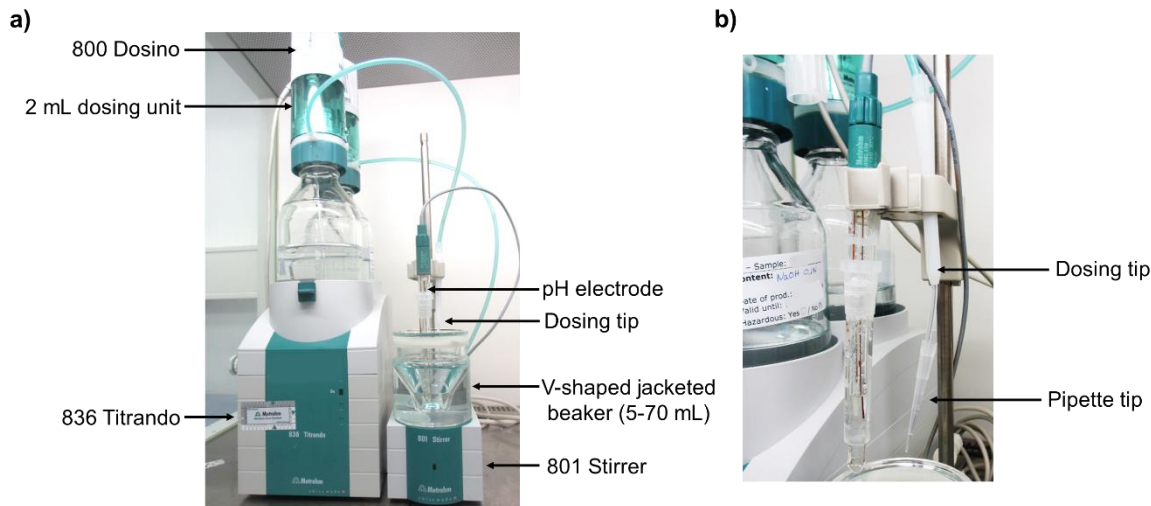


Figure 7. a) Computer-controlled titrator from Metrohm (Software: Tiamo 2.5; beaker ref.: 6.1418.150), b) Dosing tip

To have better control on the flow rate, a tip of 20 – 200 μ L pipette was attached at the end of the dosing tip (figure 7b), as small flow rates were used.

3.5.3.1. *Titrant concentration*

To calculate the lipase activity correctly, the exact concentration of the titrant (0.1 N NaOH) was measured.

To determine the concentration of the sodium hydroxide, 10 mL of 0.1 N NaOH were added into a beaker of 50 mL-high, and then the pH was recorded with the manual mode of the titrator, while 0.1 N HCl was added until the pH over-passes pH 7.0.

3.5.3.2. Lipase activity

A V-shaped jacketed beaker 5 – 70 mL (beaker ref. – 6.1418.150, Metrohm) was connected to a water bath at 37°C. The beaker was filled with 14.5 mL of the adequate aqueous solution (3.5.1.3.) and 500 µL of glyceryl tributyrate (3.5.1.2.).

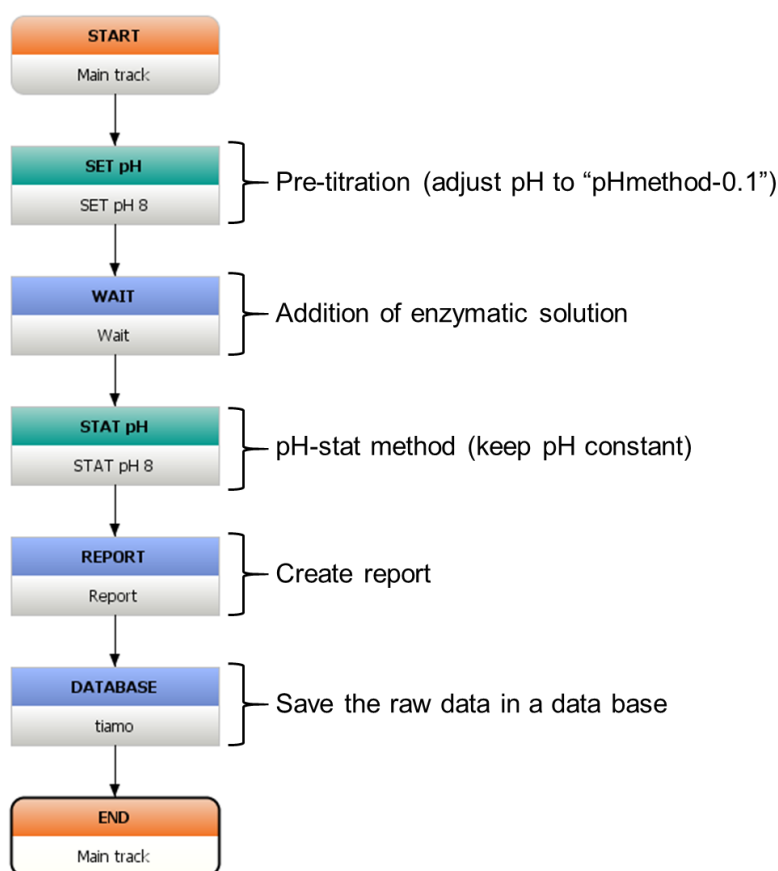
The use of positive displacement pipette, forward and reverse pipetting were studied to assure that the required volume of aqueous solution and substrate were added in the reaction mixture. The volume of both solutions added with the different pipette techniques were checked by weight.

After this study, it was concluded that the aqueous solution, due to its tendency to foam, would be added using reverse pipetting. And to assure that all the required volume of substrate was added and mixed with the aqueous solution, the glyceryl tributyrate would be added dipping the tip of the pipette into the solution and rinsing with the same aqueous solution.

The aqueous solution and the substrate were mixed, using the manual mode of the titrator, at speed 7 (according to the manual, equivalent to ~840 rpm) with a magnet of 2x0.5 cm for at least 10 min, during this time the emulsion was formed, and the temperature was equilibrated to 37°C.

A pH stat method was programmed with the titrator software, which was divided into two steps. First, a pre-titration took place, to adjust the pH to 0.1 units of pH below the pH in which the activity was measured (gastric lipase: pH 5.4; pancreatic and fungal lipase: pH 7.9).

This pre-titration was followed by the addition of 50 – 100 µL (depending on the enzyme activity) of the enzymatic solution and then the pH stat method itself, where the pH was kept constant (gastric lipase: pH 5.5; pancreatic and fungal lipases: pH 8.0) by the addition of 0.1 N NaOH for 400 s. The exact workflow is given in flow chart 1.



Flow chart 1. pH stat method designed in Tiamo 2.5 (titrator software)

As the concentration of the enzyme was always $1 \text{ mg}\cdot\text{mL}^{-1}$, the flow rate of 0.1 N NaOH was carefully adjusted to measure the activity accurately. If the flow rate was too slow, the pH of the reaction mixture was lower than the desired pH because the release of butyric acid was too high compared to the NaOH added into the mixture. However, if the flow rate was too high, then the pH increased too much, and the enzyme did not work at its optimal conditions.

Therefore, for the correct lipase activity measurement the flow rate needed to be adjusted to keep the pH constant by the addition of the correct amount of sodium hydroxide depending on the speed of butyric acid release.

When the method was programmed with the tiemo software, two different flow rates were established. A maximum flow rate when the pH is far from the desired pH and a minimum rate when the experimental pH is close to the desired pH. The issue appeared when the minimum flow rate was too high for some enzymatic solutions or the other way around (max flow rate too slow). Hence, different flow rate combinations were studied to find the optimal flow rate for the correct lipase activity measurement.

After this study, it was concluded that the described flow rates in table 7 were the optimal rates for the cases when the enzyme was highly or poorly active.

Table 7. Flow rate of 0.1 N NaOH for the lipase activity measurement

	<u>Lipase</u>	
	<i>High activity</i>	<i>Low activity</i>
Max rate ($\text{mL}\cdot\text{min}^{-1}$)	2.2	0.3
Min rate ($\mu\text{L}\cdot\text{min}^{-1}$)	5.0	0.2

The adjustment between maximal rate (max rate) and minimum rate (min rate) was automatically controlled by the device.

3.5.4. Calculations

3.5.4.1. *Sodium hydroxide titration*

To calculate the real concentration of the sodium hydroxide, the pH value after each HCl addition was depicted versus the volume of HCl added. After that, a trendline with the values that were near the pH 7 was added (figure 8) and the values of the line equation were obtained.

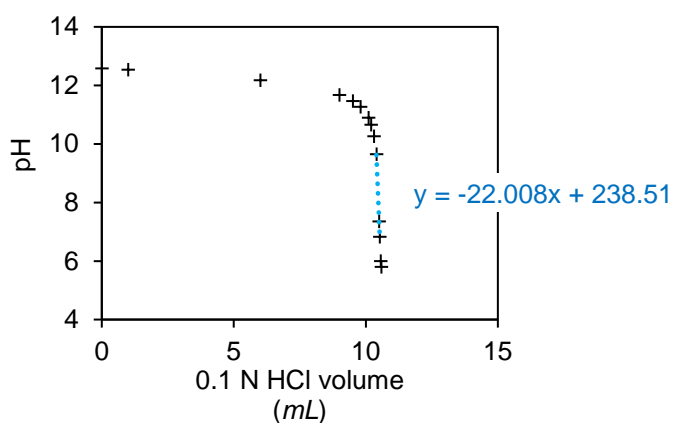


Figure 8. Example of the NaOH titration

The volume of 0.1 N HCl needed to neutralize the pH was calculated with the trendline equation:

$$\text{pH} = \text{slope} \cdot V_{0.1 \text{ N HCl}} + \text{intercept} \rightarrow V_{0.1 \text{ N HCl}} = \frac{\text{pH} - \text{intercept}}{\text{slope}} \rightarrow V_{0.1 \text{ N HCl}}(\text{pH } 7) = \frac{7 - \text{intercept}}{\text{slope}} \quad \text{Eq. 14}$$

Finally, taking in consideration the volume and concentration of HCl it was possible to calculate the real concentration of sodium hydroxide solution:

$$V_{0.1 \text{ N HCl}}(\text{pH } 7) \cdot \frac{0.1 \text{ Eq HCl}}{10^3 \text{ mL}} \cdot \frac{1 \text{ mol HCl}}{1 \text{ Eq HCl}} \cdot \frac{1 \text{ mol NaOH}}{1 \text{ mol HCl}} \cdot \frac{1}{V_{\text{NaOH}}} \cdot \frac{10^3 \text{ mL}}{1 \text{ L}} = 0.1 \cdot \frac{V_{0.1 \text{ N HCl}}}{V_{\text{NaOH}}} \quad \text{Eq. 15}$$

$$C_{\text{NaOH}}(\text{M}) = \frac{0.1 \cdot (7 - \text{intercept})}{V_{\text{NaOH}} \cdot \text{slope}} \quad \text{Eq. 16}$$

Where C_{NaOH} is the experimental concentration of NaOH (M), slope and intercept are the coefficients of the trendline and V_{NaOH} is the NaOH volume (mL) used for the experiment.

3.5.4.2. Lipase activity determination

When the volume of 0.1 N NaOH added during the pH stat method is depicted versus the time, the graph can be divided into two parts (figure 9). The first part is not linear, which means that the enzyme needs some time to reach the substrate, the second part of the graph is linear, and it represents the hydrolysis of the tributyrin as the butyric acid is continuously released.

For that reason, the volume of 0.1 N NaOH used to keep the pH constant needs to be corrected, as the lineal part is the only one that represents the action of the enzyme on the hydrolysis of the substrate.

After some experiments, it could be concluded that the linear NaOH consumption range lies between 160 s and 400 s. Therefore, only the volume of 0.1 N NaOH consumed in that time range was used for the calculation of lipase activity. The following graph is an example of the NaOH volume added during the 400 s of the total method. And, as it can be seen, the lineal part starts at 160 s after the enzymatic solution was added.

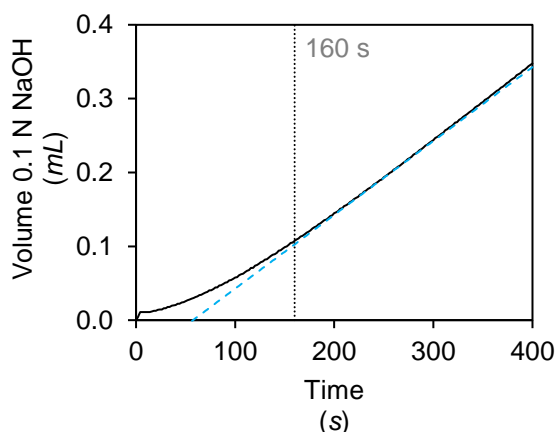


Figure 9. Example of the 0.1 N NaOH added during the lipase activity measurement (black line: NaOH volume, blue line: extended lineal tram of the NaOH volume)

As one unit of lipase is the amount of enzyme needed to release 1 μmol of butyric acid per minute, the amount of NaOH (μmol) was first calculated, then it was transformed into μmol of butyric acid and finally divided by the time of the hydrolysis:

$$V_{\text{corrected}} = V_{400 \text{ s}} - V_{160 \text{ s}} \quad \text{Eq. 17}$$

$$\text{time}_{\text{corrected}} = 400 \text{ s} - 160 \text{ s} = 240 \text{ s} \cdot \frac{1 \text{ min}}{60 \text{ s}} = 4 \text{ min} \quad \text{Eq. 18}$$

$$\mu\text{mol butyric acid} = V_{\text{corrected}} \cdot \frac{C_{\text{NaOH}}}{10^3 \text{ mL}} \cdot \frac{10^6 \mu\text{mol NaOH}}{1 \text{ mol NaOH}} \cdot \frac{1 \mu\text{mol butyric acid}}{1 \mu\text{mol NaOH}} = V_{\text{corrected}} \cdot C_{\text{NaOH}} \cdot 10^3 \quad \text{Eq. 19}$$

$$\text{Lipase activity (LU)} = \frac{\mu\text{mol butyric acid}}{\text{min}} = \frac{V_{\text{corrected}} \cdot C_{\text{NaOH}} \cdot 10^3}{\text{time}_{\text{corrected}}} \quad \text{Eq. 20}$$

$$\text{Lipase activity (LU)} = \frac{V_{\text{corrected}} \cdot C_{\text{NaOH}} \cdot 10^3}{4} = 250 \cdot V_{\text{corrected}} \cdot C_{\text{NaOH}} \quad \text{Eq. 21}$$

Where the $V_{\text{corrected}}$ is the volume (mL) of NaOH added during the action of the lipase on the tributyrin, C_{NaOH} is the real concentration of sodium hydroxide ($\text{mol}\cdot\text{L}^{-1}$) and $t_{\text{corrected}}$ is the time (4 min) in which the hydrolysis takes place.

The activity is usually expressed as specific activity ($\text{LU}\cdot\text{mg}^{-1}$), and to calculate that, the obtained activity (LU) was divided by the amount of enzyme (mg) used to carry out the hydrolysis.

3.5.5. Ring trial

Infogest is a former COST action (2011 – 2015) and is since 2015 an international research network whose objective is to improve the health properties of food by sharing knowledge on the digestive processes. The Infogest network is organized into 6 working groups being working group 4 (WG4) the one dedicated to lipid digestion and digestive lipases (9).

One of the main tasks of WG4 was to validate and standardize lipase assays for gastric and pancreatic lipase, the two main digestive enzymes involved in fat digestion. For that reason, WG4 organized a ring trial in order to validate and standardize a method to determine lipase activity (10).

To perform the ring trial 21 laboratories members of the Infogest network and WG4 group received three sources of lipases (one gastric and two pancreatic lipases) and a detailed protocol to measure lipase activity. This protocol was later used to carry out the experiments for this thesis and is explained in sections 3.5.1. – 3.5.4.

The 21 laboratories followed the detailed protocol and measured the activity of the three lipases. The effect of a possible inhibitor of the lipase was also studied. Lipase inhibition was performed by pre-mixing the lipase solution with boronic acid and then the lipase assay was performed. A 1 M solution of 4-bromophenylboronic acid was prepared in methanol and 5 μL of this stock solution was added to 1 mL of the enzyme solution ($1 \text{ mg}\cdot\text{mL}^{-1}$). The mixture was vortexed and incubated at RT for 10 min before performing the assays of residual lipase activity.

The activity data for the three sources of lipase were analysed by the organisers using SPSS version 24.0 and the coefficients of variation calculated. For all the tests, the significance level was set at $P < 0.05$. Differences between enzyme preparation concentrations were analysed by Student's paired t -test. For each enzyme preparation and concentration tested, 63 measurements of lipase activity were performed, and all were analysed using the Shapiro-Wilk implementation in XLSTAT.

3.6. Study potential alternative sources to human enzymes

Potential alternative sources to human α -amylase, pepsin, trypsin and lipase were studied by measuring the activity with the above methods.

The pH profile was studied for the human enzymes and the potential alternative sources at their optimal temperature (37°C) but also at the temperature in which the activity is measured in the above methods.

For the identification of the best alternative sources, the similarities in the activity profiles (pH, temperature) between both enzymes (human vs alternative sources) were studied.

The different pH and temperatures that were used for the identification of the alternative sources and the selected alternative sources are shown in table 8.

Table 8. Conditions that were used to study their effect on the enzyme activity of the human enzymes and the alternative source

Enzyme	pH	Temperature (°C)	Alternative sources
α-amylase	2, 4, 6, 7, 8, 10, 12	20, 37	porcine, bacterial
Pepsin	1.7, 2, 3, 4, 5	37	porcine
Trypsin	5, 6, 7, 8.1, 9	25, 37	bovine
Lipase	1.7, 2, 3, 4.5, 5.5, 6.5, 7, 7.4, 8	37	fungal

3.7. Effect of electrolytes on enzyme activity

In general, DI water is used as a solvent to prepare the enzymatic solution for the measurement of their activity.

The main objective of the enzyme activity measurement, apart from the identification of the alternative sources, was to calculate the amount of enzyme needed to reach the physiological levels in the in vitro digestion methods.

However, in both in vitro and in vivo digestion processes, the enzymes are surrounded by other substances like electrolytes, which could affect their activity. Therefore, to be able to mimic human digestion, it is important to know how the electrolytes present in the gastrointestinal tract at their physiological concentration, affect the activity of the digestive enzymes.

To study the effect of the electrolytes on enzyme activity, the identified alternative sources of the enzymes were dissolved in DI water and parallelly, in the corresponding simulated digestive fluids (2.Simulated digestive fluids) depending on in which part of the gastrointestinal tract the enzymes are secreted.

3.8. Pancreatin

The reported activities for α-amylase, trypsin and lipase in the small intestine are $183.9 \pm 28.9 \text{ AU}\cdot\text{mL}^{-1}$ (11–16), $100.8 \pm 31.7 \text{ TU}\cdot\text{mL}^{-1}$ (11,12,17–20) and $1704.3 \pm 566.7 \text{ LU}\cdot\text{mL}^{-1}$ (12,21–23), respectively. Therefore, the approximate ratio of these enzymes in the small intestine is approximately 2:1:20 (α-amylase : trypsin : lipase), which means that for each trypsin unit, there are two α-amylase units and 20 lipase units present.

There are two options to mimic the human digestion of carbohydrates, proteins and fats in the small intestine; one is the option to use individual enzymes and the other would be the use of the mixture of enzymes called pancreatin.

The advantage of the use of individual enzymes is that the physiological levels of the enzymes can be reached by mixing the adequate amount of each enzyme. However, its main disadvantage is that the lipase may be inhibited by the presence of bile acids and the colipase is needed to restore lipase activity. However, commercially available colipase is very expensive in the case of a large number of in vitro digestion experiments.

On the other hand, the advantage of the use of pancreatin is that this product already contains enough amount of colipase for the proper lipolytic function, and no extra addition of colipase is needed. The drawback of the use of pancreatin is that a similar enzyme ratio to the human is needed for the correct intestinal digestion imitation, and the enzyme ratio in the pancreatin is fixed and different depending on the commercial product.

In general, the described in vitro digestion methods only take into consideration the activity of the enzyme that catalyses the hydrolysis of the substrate of interest. However, it would be more accurate to find a solution to mimic the pancreatin with the same ratio of enzymes.

3.8.1. Pancreatic powders

Different commercial pancreatins have been studied to find a commercial pancreatin that mimics the enzyme ratio present in the human intestine during digestion. The selected commercial pancreatins to carry out this study were:

- P1: Pancreatic enzyme for cats and dogs – Pancrex Vet (Pfizer)
- P2: Pancreatic enzyme for cats and dogs - Pancrex (Zoetis)
- P3: Pancreatin from porcine pancreas 4xUSP (Sigma Aldrich)
- P4: Pancreatin from porcine pancreas 8xUSP (Sigma Aldrich)
- P5: PancZyme (American Laboratories inc.)
- P6: Pancreatin powder (Nordmark)

It is reported that the best alternative for the human pancreatin is from porcine source (2). For that reason, the selected pancreatins are all from porcine source, therefore the differences between them depend on the supplier preparation. The specific activity given by the supplier were:

Table 9. Specific activities of different commercial pancreatins

	α-amylase	Proteases	Lipase
P1 – Pfizer	30 BP·mg ⁻¹	1.4 BP·mg ⁻¹	25 BP·mg ⁻¹
P2 – Zoetis	30 PhEur·mg ⁻¹	1.4 PhEur·mg ⁻¹	30 PhEur·mg ⁻¹
P3 – 4xUSP	100 USP·mg ⁻¹	100 USP·mg ⁻¹	8 USP·mg ⁻¹
P4 – 8xUSP	200 USP·mg ⁻¹	200 USP·mg ⁻¹	16 USP·mg ⁻¹
P5 – PancZyme	250 USP·mg ⁻¹	285 USP·mg ⁻¹	46.1 USP·mg ⁻¹
P6 – Nordmark	89 PhEur·mg ⁻¹	4.9 PhEur·mg ⁻¹	89.4 PhEur·mg ⁻¹

The commercial products from table 9 gives the protease activity as a mixture of the action of trypsin and chymotrypsin.

The activities specified by the supplier are given in different units, which makes the comparison between the different pancreatins difficult. For that reason, the given activities were converted to AU, TU and LU for α -amylase, trypsin and lipase, respectively.

The BP (British Pharmacopeia) units and Ph.Eur. (European Pharmacopeia) units are equivalent, and their equivalence to USP (United States Pharmacopeia) are for α -amylase 1 BP/PhEur unit = 4.15 USP units, for proteases 1 BP/PhEur unit = 62.5 USP units and for lipase 1 BP/PhEur unit = 1 USP unit (24).

The FIP (International Pharmaceutical Federation) units are equivalent to BP and PhEur units. For α -amylase one FIP unit is defined as the amount of enzyme which, under assay conditions, splits starch at such an initial rate that 1 μ Eq of glycosidic linkage is hydrolysed per minute (25). For proteases one FIP unit is defined as the amount of enzyme which can to turn over 1 μ mol of substrate in 1 min, under assay conditions (26). For lipase one FIP unit is defined as the quantity of lipase which liberates the equivalent of 1 μ mol of fatty acid per minute, under assay conditions (27). Therefore, the FIP units are equivalent to the described AU, TU and LU for α -amylase, trypsin and lipase.

The unit definition according to the United States Pharmacopeia is different for the three kinds of enzymes present in the pancreatin. One USP unit of α -amylase activity contained in the amount of pancreatin that decomposes starch at an initial rate such that 0.16 μ Eq of glycosidic linkage is hydrolysed per minute under the assay conditions.

One USP unit of protease activity is contained in the amount of pancreatin that under the conditions of the assay hydrolyses casein at an initial rate such that there is liberated per minute an amount of peptides not precipitates by trichloroacetic acid that gives the same absorbance at 280 nm as 15 nmol of tyrosine. And one USP unit of lipase activity is contained in the amount of pancreatin that liberates 1 μ Eq of acid per minute under assay conditions (28).

To calculate the theoretical enzyme ratio that is present in the commercial pancreatins, the activities from table 9 were converted to the defined AU, TU and LU (table 10):

Table 10. Activities of α -amylase, proteases and lipase in the commercial pancreatin (corrected units)

	<u>α-amylase</u> (AU·mg ⁻¹)	<u>Proteases</u> (TU·mg ⁻¹)	<u>Lipase</u> (LU·mg ⁻¹)
P1 – Pfizer	30	1.4	25
P2 – Zoetis	30	1.4	30
P3 – 4xUSP	24	1.6	8
P4 – 8xUSP	48	3.2	16
P5 – PancZyme	60	4.6	46
P6 – Nordmark	89	4.9	89

According to table 10, the theoretical enzyme ratio of the commercial pancreatins is different compared with the human ratio.

To be able to calculate the experimental enzyme ratio of the different pancreatins, the pancreatic solutions were first prepared by mixing the different powders in DI water. The concentration of the pancreatic solutions was adapted to the optimal concentration for the enzyme activity method. To find the optimal pancreatic concentration for the enzymatic methods, different concentrations were studied as it is explained in section “3.1.Importance of working with an excess of substrate”.

As the pancreatin was not completely soluble, a centrifugation step (9000 rpm, 20 min, 4 °C – Herareus Multifuge X3R, Thermofisher) was performed to remove the insoluble part. This step was needed to obtain a homogenous sample but also to mimic the protocol of pancreatin preparation used for the in vitro digestion methods.

Once the pancreatic solutions were prepared, the activity was measured by following the described methods (3.2., 3.4., 3.5.). Finally, the experimental enzyme ratio was calculated for each commercial pancreatin and compared with the human ratio.

3.8.2. Mixture of pancreatin and individual enzymes

The drawback of the use of pancreatin was that its enzyme ratio is fixed, and what could happen is that when the pancreatin concentration is based on the activity of one enzyme, the levels of the other enzymes would not be physiological.

A solution to that problem could be the addition of the individual enzymes to the pancreatin. Thus, the combination of the pancreatin with individual enzymes was studied in order to find the optimal enzyme mixture and be able to reach the physiological levels to mimic the digestion of the small intestine.

To carry out this study, the enzyme activity present in the pancreatin was first measured and then the amount of individual enzymes needed to reach the physiological levels was calculated. Finally, the enzyme activity of the mixture was measured and the levels of the different enzymatic products were modified until the optimal combination (pancreatin and individual enzymes) was found.

3.8.3. Effect of electrolytes

The effect of the electrolytes on the enzyme activity was also studied for the pancreatic samples. For this study, the pancreatic solutions were prepared by dissolving the commercial powders in simulated intestinal fluid (table 3) instead of DI water. After that, the solutions were also centrifugated (9000 rpm, 20 min, 4 °C – Herareus Multifuge X3R, Thermofisher) and then the enzyme activity was measured. The selected pancreatins for this study were: P3 – P6 (4xUSP, 8xUSP, PancZyme and Nordmark), except for the α -amylase where all the pancreatins were included in the study.

3.9. Determination of maximum storage time of enzymatic solutions

A stability study was performed to determine the maximum storage time of the prepared enzymatic solutions at -20°C at constant activity.

To carry out this study, a stock solution of each enzyme (α -amylase, pepsin, trypsin and lipase) was prepared using DI water and SDFs (table 3) as solvent. Aliquots of 1 mL were stored at -20°C and the activity of the solution was measured every week during the first month and then, once a month until one year of storage time. Each measurement was done with separate aliquots avoid differences due to freeze-thaw cycles that could damage the enzymes and falsify the results.

4. Determination of bile acids concentration

The concentration of bile acids was measured using the commercial kit "Bile acids" from Diagnostic systems (article n $^{\circ}$: 1 2212 99 90 313).

The measurement of the bile acids in this kit is based on the following reactions (figure 10):

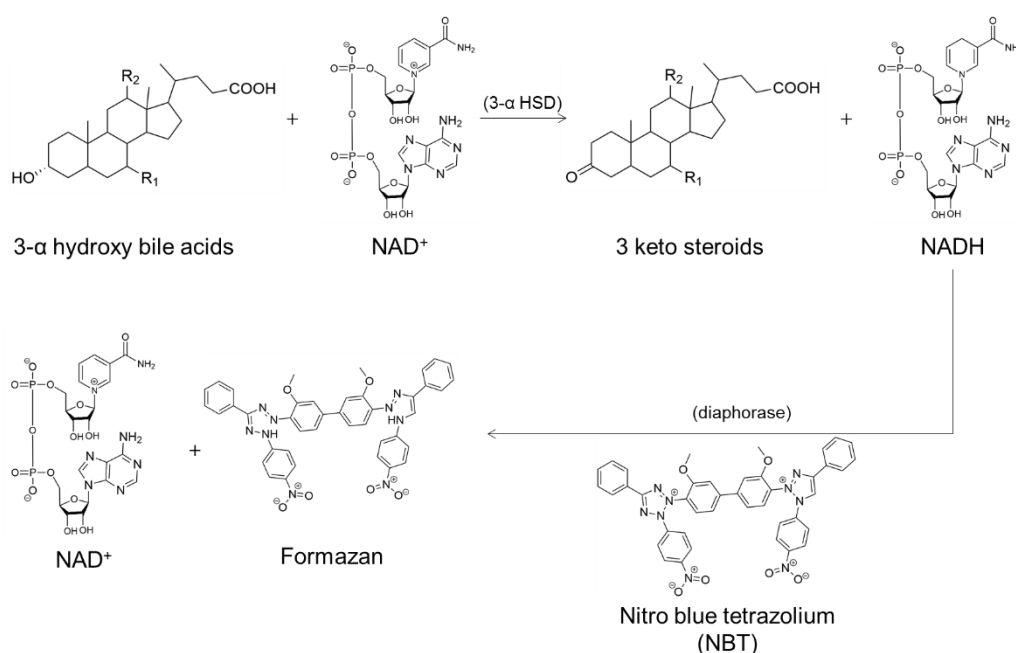


Figure 10. Principle of the method (enzymes are in brackets)

The position 3- α of the bile acids is oxidized by the enzyme 3- α hydroxysteroid dehydrogenase and in the presence of NAD^+ , which is reduced and converted into NADH .

After that, nitro blue tetrazolium reacts with the obtained NADH which is oxidized while the nitro blue tetrazolium reduced. This reaction occurs in the presence of a diaphorase enzyme.

A formazan dye is formed, and the formation of this dye is monitored spectrophotometrically at 540 nm. The bile acids concentration can be calculated because the formation of the dye is directly proportional to the bile acids concentration in the sample.

4.1. Reagents

4.1.1. Standard

The kit contains a standard that consists of a solution of bile acids with a concentration of $35 \mu\text{mol}\cdot\text{L}^{-1}$.

4.1.2. Buffer

The buffer is a phosphate buffer that contains EDTA in a concentration of $100 \text{mmol}\cdot\text{L}^{-1}$.

4.1.3. Enzyme solution

The enzymatic solution consists of a solution of 3- α hydroxysteroid dehydrogenase that contains 60 U·L⁻¹, and the enzyme is dissolved in a 50 mmol·L⁻¹ TRIS buffer.

4.1.4. Mixture of reagents

The mixture of reagents contains 50 U·L⁻¹ diaphorase, 1 mmol·L⁻¹ NAD⁺ and 0.2 mmol·L⁻¹ NBT. This mixture is sold as a mixture of powders, and before its use, the powder mixture needs to be dissolved with the buffer (4.1.2.).

4.2. Sample

The bile solution was prepared by mixing the powder in DI water at RT and ~350 rpm for at least 10 min.

The kit can measure bile acids concentrations up to 150 $\mu\text{mol}\cdot\text{L}^{-1}$. As the optimal concentration for the method was unknown, a stock solution was prepared (1 mg·mL⁻¹), and then different dilutions were prepared (10, 25 and 50 $\mu\text{g}\cdot\text{mL}^{-1}$).

To find the optimal alternative source, two different sources (bovine and porcine) were analysed.

4.3. Procedure

To measure the concentration of bile acids 80 μL of the sample and 600 μL of the “mixture of reagents” (4.1.4.) were added in a plastic cuvette (light path: 1 cm) and the cuvette was covered with a lid (Kartell Labware, art n° 01962). The substances were mixed by inversion and incubated at 37°C for 4 min in the spectrophotometer (Biospectrometer, Eppendorf). After this incubation step, the absorbance was read at 540 nm and recorded as “A1”.

Subsequently, 120 μL of the enzymatic solution (4.1.3.) were added to the mixture, which was then incubated at 37°C for 5 min. Finally, the absorbance was read at 540 nm and recorded as “A2”.

For the blank and standard, the same procedure was followed but instead of the use of sample, DI water was used for the blank and standard solution (4.1.1.) for the standard.

4.4. Calculations

To calculate the concentration of bile acids, the formation of formazan was spectrophotometrically monitored. The reactions started when the enzymatic solution (4.1.3.) was added, thus the recorded “A1” was the measurement of the matrix. Therefore, to calculate the amount of formazan that was formed, the recorded “A2” was corrected by subtracting the absorbance of the matrix (A1).

However, a dilution factor was taken into account as the sample was slightly diluted by the addition of the enzymatic solution to the mixture.

$$\text{dilution factor} = \frac{\text{Volume}_{\text{sample}} + \text{Volume}_{\text{mixture of reagents}}}{\text{Volume}_{\text{Total}}} = \frac{680 \mu\text{L}}{800 \mu\text{L}} = 0.85 \quad \text{Eq. 22}$$

$$A_{\text{corrected}} = A2 - 0.85 \cdot A1 \quad \text{Eq. 23}$$

This correction was applied, not only to the sample but also to the blank and standard. After that, the blank was subtracted from the corrected absorbance of the sample and standard.

The samples that had an $A_{\text{corrected}}$ lower than 0.1 were discarded as it was considered that the prepared concentration was too low for the correct measurement.

As the concentration of the standard was known (35 $\mu\text{mol}\cdot\text{L}^{-1}$), the concentration could be calculated as follows:

$$C_{\text{sample}} (\mu\text{mol}\cdot\text{L}^{-1}) = \frac{((A2 - 0.85 \cdot A1)_{\text{sample}} - (A2 - 0.85 \cdot A1)_{\text{blank}}) \cdot C_{\text{Standard}}}{(A2 - 0.85 \cdot A1)_{\text{standard}} - (A2 - 0.85 \cdot A1)_{\text{blank}}} \quad \text{Eq. 24}$$

Once the concentration in $\mu\text{mol}\cdot\text{L}^{-1}$ was calculated, was then converted into $\text{mmol}\cdot\text{L}^{-1}$ and knowing the concentration in $\text{mg}\cdot\text{L}^{-1}$, it was possible to calculate a virtual "molecular weight" of the bile acids, which was later on used to calculate the amount of bile needed for the in vitro digestion methods.

$$\text{"molecular weight" (mg}\cdot\text{mmol}^{-1}) = \frac{\text{Bile acids (mg}\cdot\text{L}^{-1})}{\text{Bile acids (mmol}\cdot\text{L}^{-1})} \quad \text{Eq. 25}$$

5. Determination of the mixing speed

In the case of the static digestion method, a thermoshaker (New Brunswick Innova 40/40R, Eppendorf) was used to agitate and incubate the digestion mixtures.

The agitation speed with the thermoshaker was studied to find the minimum speed needed to completely mix the digestive mixtures during the static in vitro digestion method.

For that study, 40 μL of tributyrin were mixed with a few drops of 0.01 % Sudan III and parallelly 40 μL of DI water were mixed with a few drops of 25 % patent blue solution. After that, 20 μL of reddish tributyrin and 20 μL blueish DI water were added in a 50 μL tube. Two tests were performed simultaneously, one without emulsifier and another one in the presence of an emulsifier (Tween80).

The tubes were incubated and mixed at 37°C and at different speeds (0, 50, 100, 150, 200, 250, 300, 400, 450 and 500 rpm) for 1 min, just after that the tube was placed on the bench and a picture was taken.

6. Method to stop digestion

To be able to follow the digestion of a meal in the in vitro digestion methods, the hydrolysis reactions must be stopped after each sampling point.

Different methods were studied in order to find the most effective method to stop the digestion. The first method was based on the physical removal of the enzymes from the samples, and for that reason, different kind of filters were studied. The second method was based on stopping the enzyme activity by denaturing the digestive enzymes thermally. The denaturation was performed by placing the sample in a boiling water bath for 5 min.

To check if the method was effective, the enzyme activity was measured after filtration or the heat treatment, and the remaining activity was calculated according to eq. 26:

$$\text{Remaining activity (\%)} = \frac{\text{Enzyme activity}_{\text{after treatment}}}{\text{Enzyme activity}_{\text{before treatment}}} \cdot 100 \quad \text{Eq. 26}$$

7. Buffer for static digestion method

During the intestinal phase, the lipase catalyses the hydrolysis of fats provoking the release of free fatty acids which decrease the pH. When the pH decreases too much, the enzymes cannot carry out the catalysis at their optimal conditions, which means that the human digestion would not be properly mimicked. During the static digestion method no secretion would compensate for the decrease of pH. For that reason, the use of a buffer is needed to keep the pH constant.

To find the optimal buffer, the digestion of tributyrin was performed using the protocol of the static digestion method. To study the efficiency of the buffers, the pH of the intestinal phase was monitored when different buffers were used. The studied buffers were bicarbonate buffer (1 M) and HEPES buffer (0.4, 0.8, 1.2 and 1.5 M) at pH 7.

8. Meal

8.1. Composition (%)

The nutrient intake goals recommended by the German Nutrition Society (DGE) were used to calculate the composition of the meals used to study the carbohydrate digestion in the in vitro digestion methods. The nutrient intake goals recommended by DGE are given in percentage of energy as figure 11 shows (29):

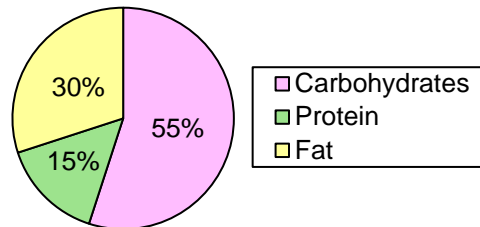


Figure 11. Nutrient intake goals (% energy) (29)

Assuming a 100 kcal meal and taking into account the energy content of the nutrients (30) it was possible to re-calculate the nutrient intake goals in mass (g):

$$100 \text{ kcal meal} \cdot \frac{55 \text{ kcal CH}}{100 \text{ kcal meal}} \cdot \frac{1 \text{ g CH}}{4.1 \text{ kcal CH}} = 13.4 \text{ g CH} \quad \text{Eq. 27}$$

$$100 \text{ kcal meal} \cdot \frac{15 \text{ kcal P}}{100 \text{ kcal meal}} \cdot \frac{1 \text{ g P}}{4.1 \text{ kcal P}} = 3.7 \text{ g P} \quad \text{Eq. 28}$$

$$100 \text{ kcal meal} \cdot \frac{30 \text{ kcal F}}{100 \text{ kcal meal}} \cdot \frac{1 \text{ g F}}{9.3 \text{ kcal F}} = 3.2 \text{ g F} \quad \text{Eq. 29}$$

Figure 12, the nutrient intake goals in percentage of mass would be:

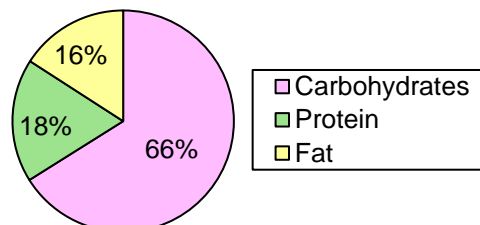


Figure 12. Nutrient intake goals (% mass)

However, the food does not only contain dry matter but also contains moisture, being the water sometimes the major component of the food products. For that reason, the moisture content of the food was taken into account, and the nutrient intake goals were "corrected". Each food has a different moisture content, but the average of it is found to be around 70 %, as it is depicted in the following figure (figure 13):

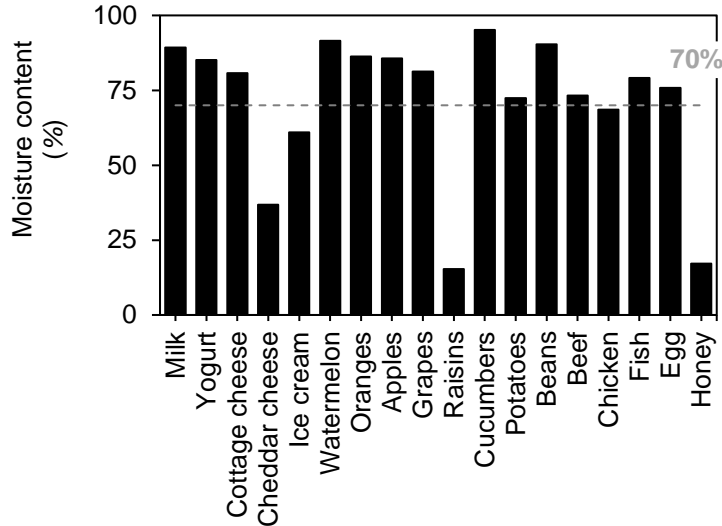


Figure 13. Moisture content of selected foods (31)

Therefore, to perform the *in vitro* digestions and to mimic the composition of the real meals, the final content of water and dry matter were 70 % and 30 %, respectively.

On the other hand, the presence of an emulsifier was also needed for the integration of the fat component into the meal. To calculate the emulsifier concentration, its presence was checked in three different products intended for clinical nutrition.

The following figures (figure 14) are a representation of the meal composition used to carry out the *in vitro* digestions; taking into consideration the ratio of carbohydrates, protein and fat, plus the amount of emulsifier and the moisture content. When one of the nutrients was absent, it was substituted by water.

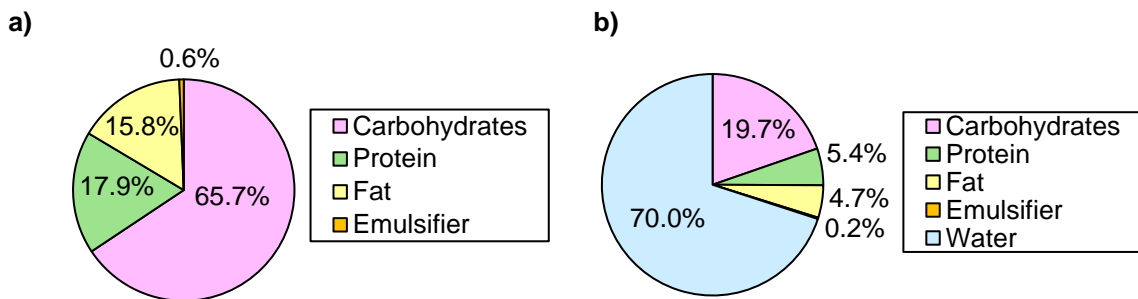


Figure 14. Meal composition (% mass), a) dry matter, b) complete meal

8.2. Starch sources

To study the digestion of carbohydrates, the consumption of the main sources of this nutrient was checked. The daily consumption of carbohydrate sources in Germany are depicted in the following figure (figure 15):

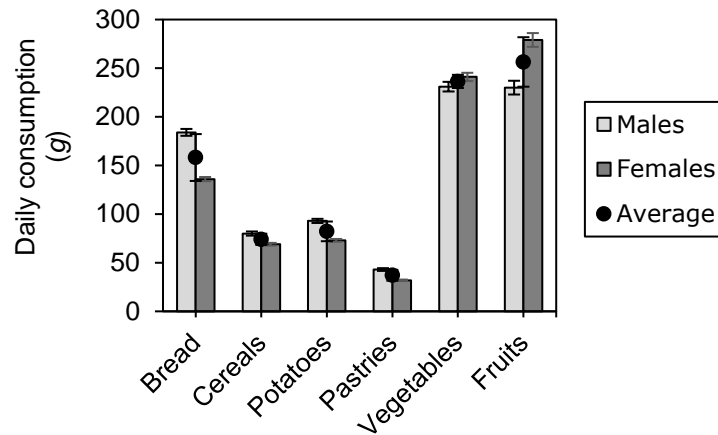


Figure 15. Daily consumption of different sources of carbohydrates (32,33)

The previous figure refers to the amount of the entire food that is daily consumed. However, the carbohydrate concentration is different in each kind of food (figure 16a). This fact was taken into consideration and the bread turned out to be the most consumed carbohydrate source in Germany (figure 16b).

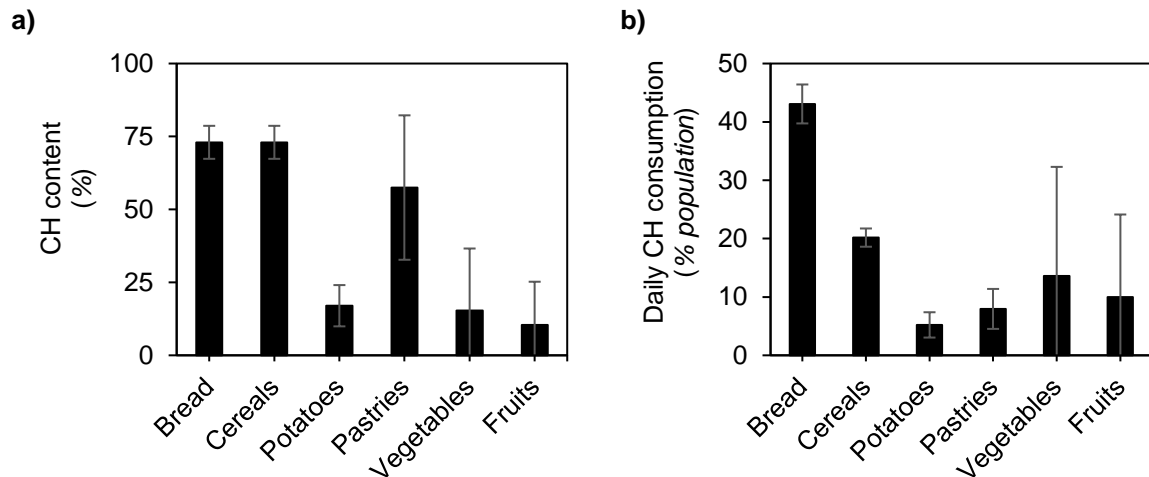


Figure 16. a) Carbohydrate content of the different sources (34–39), b) Daily CH consumption in Germany

Based on the depicted data in figure 16b, the main sources of carbohydrates that are consumed in Germany are bread, cereals and pastries (or some vegetables). However, the type of carbohydrate that is present in pastries is not of interest in the scope of this thesis as is mainly sugar. Therefore, the three sources selected as possible sources of carbohydrates to study its digestion were:

- *Bread*: starch from wheat
- *Cereals*: starch from rice
- *Potato/vegetables*: starch from potato

Some properties of these three types of starch are given in the following table:

Table 11. Properties of three different starches (mean \pm SD^{n° references}) (40–65)

	Starch from wheat	Starch from rice	Starch from potato
Structure	A-type	A-type	B-type
Mw (Da·10 ⁸)	1.4 \pm 0.8 ¹	10.1 \pm 0.2 ¹	8.5 \pm 0.2 ¹
Density (g·cm ⁻³)	1.5 \pm 0.0 ²	1.5 \pm 0.0 ¹	1.6 \pm 0.1 ³
Particle size (μ m)	43 \pm 6 ⁴	16 \pm 4 ⁴	5 \pm 1 ⁵
Composition			
Amylose (%)	22 \pm 2 ⁸	27 \pm 3 ⁸	25 \pm 6 ⁸
Amylopectin (%)	78 \pm 2 ³	72 \pm 0 ¹	
P (ppm)	812 \pm 59 ⁶	539 \pm 43 ⁴	406 \pm 250 ⁴
Protein (%)	0.11 \pm 0.06 ³	0.3 \pm 0.1 ³	0.6 \pm 0.3 ⁴
Lipids (%)	0.08 \pm 0.04 ²	0.8 \pm 0.2 ³	0.7 \pm 0.4 ²
Moisture (%)	15 \pm 3 ⁴	14 \pm 1 ²	10.8 \pm 0.1 ²
Gelatinization parameters			
Enthalpy (J·g ⁻¹)	15 \pm 2 ⁴	11 \pm 2 ⁵	12 \pm 3 ⁷
Onset	60 \pm 2 ⁶	55 \pm 2 ⁶	66 \pm 5 ⁸
T (°C) Peak	64 \pm 2 ⁷	63 \pm 9 ⁷	72 \pm 4 ⁸
Final	70 \pm 3 ⁴	67 \pm 4 ⁵	79 \pm 2 ⁷

Rice and potato starch were finally chosen to study the digestion of carbohydrates because they show the bigger difference in the particle size and they also belong to two different types of structure: A- and B-type starch. The used starches were purchased from Sigma Aldrich, and the properties from table 11 are the specific properties of these commercial starches.

The chosen carbohydrate sources to study its digestion were:

- Starch from rice (Sigma Aldrich - S7260)
- Starch from potato (Sigma Aldrich - S4251)

8.3. Protein sources

As meals usually not only contains carbohydrates, the effect of proteins on the digestion of carbohydrates was another objective of this thesis. In order to select the protein sources the daily consumption of the principal proteins in Germany was checked. Figure 17 shows the daily consumption of protein in Germany.

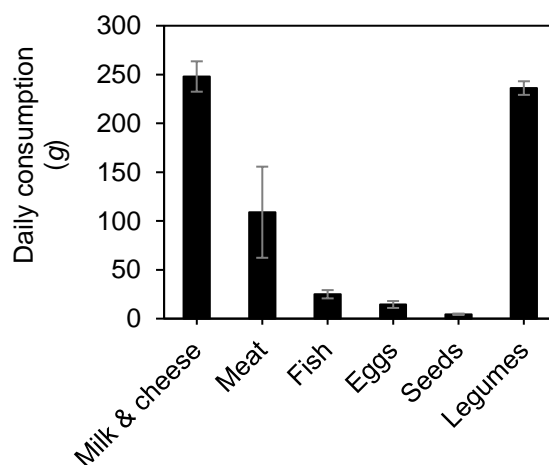


Figure 17. Daily consumption of different protein sources in Germany (32)

For the selection of the protein sources, the content of protein in those foods (figure 17) was taken into consideration. Figure 18 shows the protein content in each source and the consumption of protein depending on the protein sources.

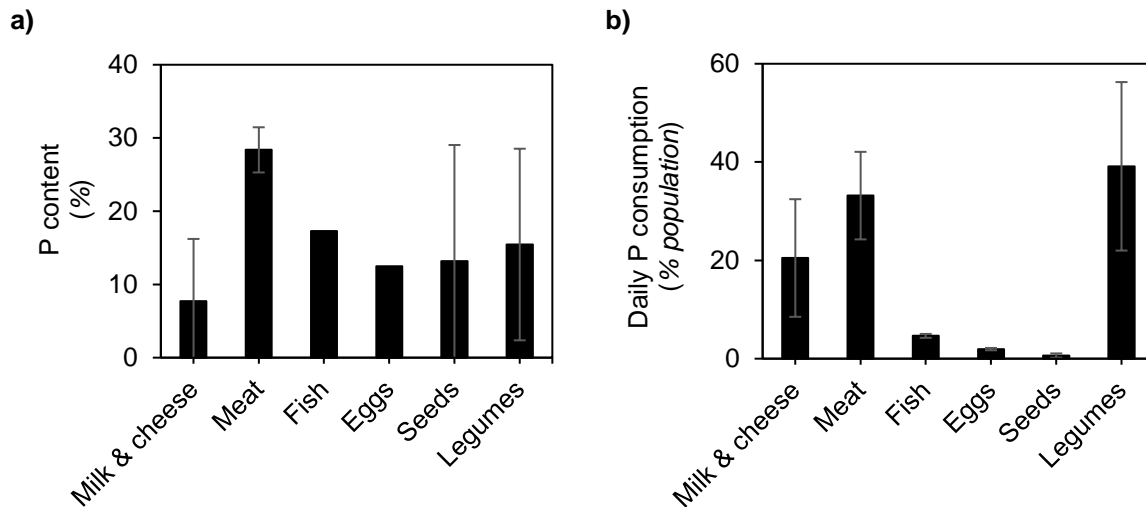


Figure 18. a) Protein content of the different sources, b) Daily protein consumption in Germany (34)

According to figure 18, the most consumed protein sources are meat, legumes and milk & cheese. However, the selected protein sources were chosen by taking into consideration the daily protein consumption but also by its commercial availability.

The chosen protein sources to study its effect on the carbohydrate digestion were:

- Egg whites from chicken (Sigma Aldrich - E0500)
- Casein from bovine milk (Sigma Aldrich - C3400)

8.4. Fat sources

The effect of fats on the digestion of carbohydrates was studied as they are also an important macronutrient in the human diet. Fats contain different degrees of saturation; saturated, monounsaturated and polyunsaturated fats (figure 19).

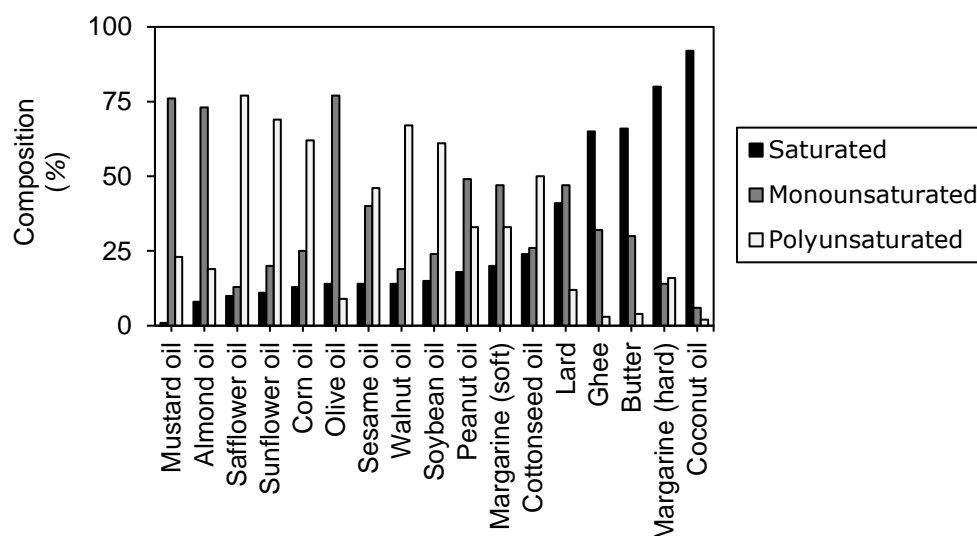


Figure 19. Percentage of saturated, monounsaturated and polyunsaturated fats in different fat sources (66)

Therefore, the fats depicted in figure 19 could be classified by their major kind of saturation:

- *Saturated fat*: ghee, butter, margarine (hard), coconut oil
- *Monounsaturated fat*: mustard oil, almond oil, olive oil, peanut oil, margarine (soft), lard
- *Polyunsaturated fat*: safflower oil, sunflower oil, corn oil, sesame oil, walnut oil, soybean oil, cottonseed oil

Olive oil and butter were selected as fat sources as they belong to two different groups of fats; olive oil is rich in monounsaturated fat and butter in saturated fats. The commercial fats used for this study are:

- Olive oil (Sigma Aldrich – O1514)
- Butter (Rewe Bio – 4388844071070)

In the case of the fat source, an emulsifier is needed for its solubility in water. The selected emulsifier to perform this study was soja lecithin and it was provided internally (Fresenius Kabi).

8.5. Real meal

To validate the method for the calculation of the glycaemic index, the in vitro digestion was also performed by using three different kinds of meals with reported glycaemic index. The selected meals were rice, potatoes and cocoa cream, as they belong to different levels of the glycaemic index. Rice and potatoes were chosen because they are rich in carbohydrates but also to compare their glycaemic index with the glycaemic index obtained for the selected starches (from rice and potato). Finally, cocoa cream was chosen because is a mixture of different macronutrients, and it could be comparable with the prepared mixture of starch, protein and fat.

The reported glycaemic index of the selected meals is expressed in the following table (table 12):

Table 12. Reported glycaemic index of the selected meals (all were purchased from the German supermarket "Rewe") (67)

	Name	Glycaemic index
Potato	Kartoffeln Festkochend – Belana	80 ± 15
Rice	Original Langkorn Reis (Kochbeutel) – Uncle Ben's	48 ± 5
Mixture (cocoa cream)	Nutella (Ferrero)	25 ± 4

8.6. Meal preparation

To perform the in vitro digestion methods, the meal needs to be prepared and cooked in the most similar way as it would be prepared for its human consumption.

8.6.1. Real meal

8.6.1.1. Rice

For the rice preparation (figure 20), DI water was heated to 100°C first with the use of a kettle and then this temperature was kept by using a magnetic stirrer with temperature control under constant stirring. Once the water was at 100 ± 5°C, the rice was added and cooked for 20 min at this temperature and 800 rpm.

After that, the rice was separated from the water by using a strainer mesh. Then, the rice was placed on a tissue for at least 15 min, to cool down to RT and to dry it.

The amount of rice needed to meet the intake goals of carbohydrates (%CH_{intake goals}: %) was first calculated (eq. 30) by taking into consideration the carbohydrate content in rice (%CH_{rice}: %):

$$m_{\text{rice}} = \frac{\%CH_{\text{intake goals}} \cdot m_{\text{meal}}}{100} \cdot \frac{100}{\%CH_{\text{rice}}} \quad \text{Eq. 30}$$

The rice was weighed before and after cooking to calculate the amount of water that the rice absorbed ($m_{\text{water absorbed rice: g}}$) during its cooking process (eq. 31):

$$m_{\text{water absorbed rice}} = m_{\text{rice}} \cdot \left(\frac{m_{\text{cooked rice}} - m_{\text{uncooked rice}}}{m_{\text{uncooked rice}}} \right) \quad \text{Eq. 31}$$

The amount of water needed to prepare the meal for the in vitro digestion method was calculated (eq. 32) by taking into account the intake goals (figure 14b), carbohydrate content in rice and the water absorbed by the rice during its cooking process:

$$m_{\text{water corrected rice}} = m_{\text{meal}} - m_{\text{rice}} - m_{\text{water absorbed rice}} \quad \text{Eq. 32}$$

Finally, the human mastication was mimicked by mixing the cooked rice ($m_{\text{rice: g}}$) with the correct amount of water ($m_{\text{water corrected: g}}$) by using a kitchen blender at its maximum speed for 5 min. Just before adding the mixture to the in vitro digestion method, it was pre-warmed to 37°C, the temperature at which the digestion takes place.

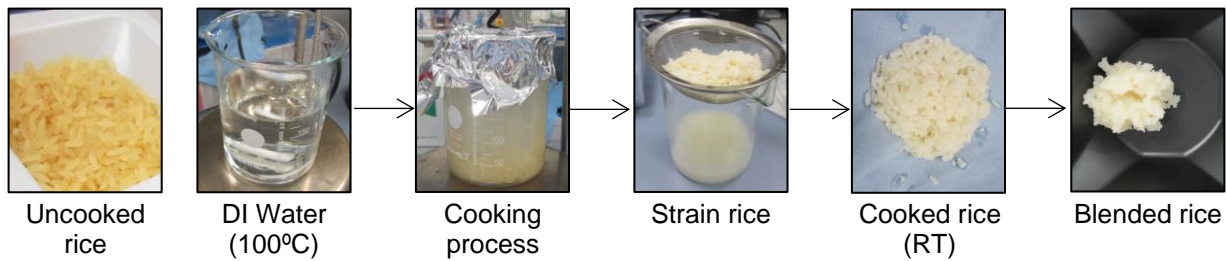


Figure 20. Rice preparation

8.6.1.2. Potato

For the preparation of the potato meal (figure 21), the potato was first cleaned with water and dried with a tissue, to remove the soil. After that, the potato was placed (one potato) in a beaker full of DI water (RT) without peeling, and it was heated to $100 \pm 5^\circ\text{C}$ for 40 min (20 min to reach $100 \pm 5^\circ\text{C}$ and 20 min to cook). Finally, the potatoes were dried with a tissue and cooled down to RT.

The carbohydrate content of the potato ($\%CH_{\text{potato: \%}}$) was taken into account to calculate the amount of potato ($m_{\text{potato: g}}$) needed to meet the intake goals of carbohydrates ($\%CH_{\text{intake goals: \%}}$) (eq. 33):

$$m_{\text{potato}} = \frac{\%CH_{\text{intake goals}} \cdot m_{\text{meal}}}{100} \cdot \frac{100}{\%CH_{\text{potato}}} \quad \text{Eq. 33}$$

The potatoes were weighed after cleaning ($m_{\text{uncooked potato: g}}$) and after cooking ($m_{\text{cooked potato: g}}$) to be able to calculate the amount of water that was absorbed by the potatoes ($m_{\text{water absorbed potato: g}}$) (eq. 34).

$$m_{\text{water absorbed potato}} = m_{\text{potato}} \cdot \left(\frac{m_{\text{cooked potato}} - m_{\text{uncooked potato}}}{m_{\text{uncooked potato}}} \right) \quad \text{Eq. 34}$$

The amount of water needed to prepare the potato meal ($m_{\text{water corrected potato: g}}$) was calculated taking into account the intake goals, carbohydrate content in potatoes and the water absorbed by the potatoes during its cooking process (eq. 35):

$$m_{\text{water corrected potato}} = m_{\text{meal}} - m_{\text{potato}} - m_{\text{water absorbed potato}} \quad \text{Eq. 35}$$

The boiled potato was first peeled, cut into small pieces with a spatula and mixed with the corrected amount of DI water. Finally, it was blended with a kitchen blender at its maximum speed for 5 min. Just before adding the mixture to the in vitro digestion method, it was pre-warmed to 37°C, the temperature at which the digestion takes place.

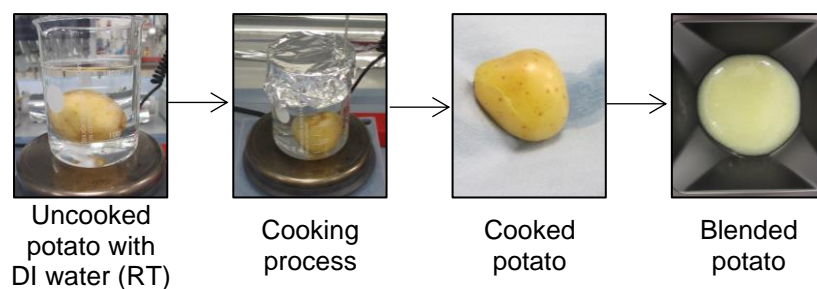


Figure 21. Potato meal preparation

8.6.1.3. Cocoa cream

To prepare the cocoa cream meal, the correct amount of cocoa cream (Nutella) was mixed with DI water at RT and 300 rpm until complete homogenisation. The correct amount of cocoa cream ($m_{\text{cocoa cream}}$: g) was calculated (eq. 36) taking in consideration the intake goals of carbohydrates ($\%CH_{\text{intake goals}}$: %) and its content in cocoa cream ($\%CH_{\text{cocoa cream}}$: %).

$$M_{\text{cocoa cream}} = \frac{\%CH_{\text{intake goals}} \cdot m_{\text{meal}}}{100} \cdot \frac{100}{\%CH_{\text{cocoa cream}}} \quad \text{Eq. 36}$$

$$m_{\text{water}} = m_{\text{meal}} - m_{\text{cocoa cream}} \quad \text{Eq. 37}$$

Just before adding the mixture (cocoa cream and DI water) to the in vitro digestion method, it was pre-warmed to 37°C, the temperature in which the digestion takes place.

8.6.1.4. Measurement of carbohydrate content

The carbohydrate content of the raw material was measured in order to prepare the meals with the same levels of carbohydrates: 19.7 % CH (figure 14b).

To measure the carbohydrate content of the meals, first, the meal was prepared by following the explained procedures in the previous sections (8.6.1.1, 8.6.1.2, 8.6.1.3 **Error! Reference source not found.**).

Then, 500 μL of the meal were mixed with 500 μL 1.4M HCl in a conical tube of 1.5 mL. The mixture was incubated at 95°C for 5 h at constant stirring in a thermo-shaker, after that, it was cooled down to RT and the pH was neutralised by adding 500 μL 1.4M NaOH. During this step the available carbohydrates were hydrolysed and converted to glucose.

The carbohydrate content was calculated by measuring the glucose concentration after the hydrolysis with the Megazyme kit (K-FRUGL) and taking into account that the hydrolysis efficiency with this method is 99.1 %.

8.6.2. “Artificial” meal

The protocol for the “artificial” meal preparation was divided into two steps:

- Step 1: mix all the ingredients
- Step 2: pasteurization of the meal

8.6.2.1. Mixing process

Four different protocols were studied to find the best method to mix the raw ingredients. The devices that have been checked for the meal preparation are the magnetic stirrer (IKA RET basic) with thermocouple (IKA ETS D5) and the turbotest evo Rayneri (VMI) with the emulsifier rotor/stator with a diameter of 55 mm.

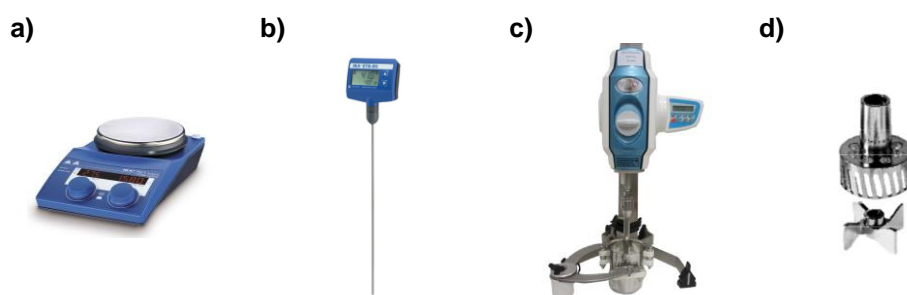


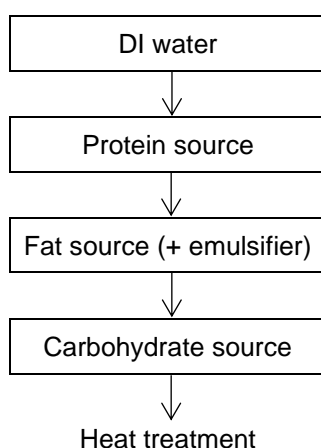
Figure 22. Different devices used for the meal preparation a) magnetic stirrer (D1), b) thermocouple (D2), turbotest evo Rayneri (D3), d) emulsifier rotor/stator (D3)

The conditions of the different protocols studied for the meal preparation are specified in the following table (table 13):

Table 13. Conditions of the protocols for the meal preparation

	Protocol 1	Protocol 2	Protocol 3	Protocol 4
Device	D1	D1, D2	D3	D1,D2,D3
Speed (rpm)	550	550 – 700	2500 – 3300	2500 – 3300
Temperature (°C)	RT	60	RT	60
Time (min)	30	30	9	9

The ingredients of the meal were mixed at different speeds (550 – 3300 rpm) and temperatures (RT, 60°C) for different periods of time (9 – 30 min), and different devices (figure 22) were studied. The method to mix the ingredients was selected based on the degree of homogenisation obtained after mixing. The order in which the ingredients were mixed was generally as it is explained in the following flow chart:



Flow chart 2. Order to mix the ingredients

As it is shown in flow chart 2, the protein source was first mixed with DI water, once the mixture was homogenised the fat source, including the emulsifier, was slowly added. The fat source was previously mixed with the emulsifier with a spatula (olive oil: RT, butter: ~40°C). Finally, the carbohydrate source was added and mixed to complete homogenisation.

However, this protocol was slightly modified in the absence or presence of some ingredients. For example, in the absence of the fat source, the protein was added at the end as it was the way to obtain the maximum hydration of the carbohydrate source. On the other hand, when the butter was used, both the water and butter were pre-warmed to ~40°C using a water bath and the emulsifier was added to the melted butter. In that case, the fat source (butter and emulsifier) was the first ingredient to be mixed

with DI water to avoid its solidification. When one of the macronutrients was missing, it was substituted by DI water.

In the case of the casein being used as the protein source, the protocol was also slightly modified. The casein was first dissolved at 35°C on a temperature-controlled magnetic stirrer using 1.2M NaHCO₃ as solvent, then it was cooled down to RT. Once the casein solution was prepared, the correct amount of casein solution was mixed with the carbohydrate and fat sources with the general protocol.

8.6.2.2. Heat treatment

After the mixing step, the mixtures went through a heating step to mimic the conditions that would suffer the nutritional products during its preparation. The purpose of this treatment is to reduce or destroy the microbial/enzyme activity and make the chemical changes needed to produce edible food.

Pasteurisation is a form of thermal processing, for both bulk liquids and foods in containers, which uses moderate temperatures to extend shelf life by days, or at most a few weeks, but causes the minimum changes to the sensory properties or nutrient value of the food. The temperature/time combination used in pasteurisation depends to a degree upon the pH of the product concerned. For acidic foods, defined as those with a pH below 4.5, the main purpose is the inactivation of enzymes (e.g., in fruit juices) or the destruction of spoilage organisms. In low-acid foods, at pH greater than 4.5, the purpose is the destruction of particular pathogens (68).

There are different possible combinations of temperature-time to perform the heat treatment (table 14):

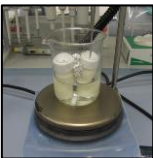
Table 14. Parameters of different heat treatments (69,70)

Treatment		Temperature (°C)	Time
Low temperature – long time	(LTLT)	63 – 66	30 – 32 min
High temperature – short time I	(HTST I)	72 – 75	15 – 30 s
High temperature – short time II	(HTST II)	85	2 – 3 s
Extended shelf life	(ESL)	123 – 127	1 – 5 s
Ultra-high temperature	(UHT)	136 – 138	5 – 8 s
Sterilization	(ST)	107 – 115	20 – 40 min

Considering that the gelatinization temperature of starches varies from 48 to 72°C, the chosen method to perform the heat treatment is the “High temperature – short time I”.

To carry out the selected heat treatment different protocols were studied, and the conditions of that protocols are specified in the following table (table 15):

Table 15. Protocols to perform the heat treatment

	Protocol 1	Protocol 2	Protocol 3
Method	Oil bath	Water bath	Water bath
Container	25 mL vial	50 mL beaker	25 mL vial
Temperature (°C)	(heat)	135	135
	(measured)	72 (extern)	72
Speed (rpm)	0	350	350
Picture			

Oil bath (device: memmert ONE 7-45, oil: WNB7 BO2686)

Water bath (device: magnetic stirrer IKA RET basic, water: DI water)

Thermocouple (extern: Testo 720, attached to magnetic stirrer: IKA ETS D5)

The three protocols were performed and the time needed to reach the desired temperature and the stability of the temperature of the meal was checked to choose the heat treatment conditions.

8.7. Viscosity measurements

Depending on the objective that was checked, the composition of the meal was slightly different, these differences in the composition could affect its viscosity. Furthermore, the viscosity of the meal could have an impact on its digestibility, and as one of the objectives of this thesis was to study if/how the proteins or/and fats affect the digestion of carbohydrates, the differences in the meal viscosity could disturb the obtained conclusions.

For that reason, the viscosity of four kinds of meals was measured in order to check if the meal composition affected its viscosity. The composition of the meals was:

- Meal 1: Carbohydrates
- Meal 2: Carbohydrates and proteins
- Meal 3: Carbohydrates and fats
- Meal 4: Carbohydrates, proteins and fats

The device used for the viscosity measurement was the Haake Mars Modular advanced rheometer system (Mars III, Thermo Fischer) with the geometry DIN Z20 (figure 23a, 23b).

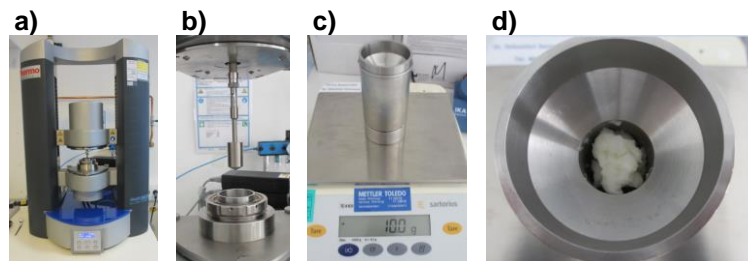


Figure 23. Rheometer and geometry Z20

For the viscosity measurement, the zero of the rheometer was manually done and the temperature was set to 50°C. Then, 10.0 g of the meal was weighed in situ (figure 23c) and the geometry was placed with a gap of 4.2 mm from the sample. The meal was let inside the device approximately for one minute to equilibrate the temperature. Finally, the measurement was performed following the next configurations depicted in figure 24.

1		ID 3: Set Temperature	CS τ 0,000 Pa	t 120,00 s	T 37,00 °C
2		ID 4: Set Temperature	CS τ 0,000 Pa	t < 120,00 s	T 37,00 °C $\leq \pm 0,10$ °C
3		ID 5: Rot Steps	CR $\dot{\gamma}$ 0,1000 1/s - 1000, 1/s log	t 990,00 s	#30 T 37,00 °C
4		ID 8: Curvefit	Ostwald de Waele (Visc) (5)		
5		ID 7: Lift	Lift apart [Message]		
<u>End of job</u>					

Figure 24. Steps of the selected 'job' for the viscosity measurement

The meal was prepared and the viscosity was measured, three repetitions of the measurement were performed. Then, the shear viscosity (Pa·s) was depicted versus the shear rate (s^{-1}). The obtained curves for the different meals were compared and checked if there were significant differences between them. In case some differences were found, a thickener was added to the meals with lower viscosity in order to have all the meals with the same viscosity.

9. In vitro digestion method

Two different in vitro digestion methods were used to study the digestion of the selected carbohydrate sources and the effect of the other macronutrients on the digestion of carbohydrates. The selected in vitro digestion methods were a static digestion method, the Infogest protocol (2), and a dynamic digestion method, the TIM-1 system (71).

The Infogest protocol was selected as it is a widely used protocol, which makes the comparison between different studies possible. On the other hand, the dynamic digestion method was chosen as it is one of the most advanced devices to mimic human digestion.

10. Static digestion method

10.1. Pre-digestion

To be able to perform the static digestion method, some preparation procedures needed to be done before the digestion method itself.

The first step was to measure the enzyme activity of the commercial enzymatic powders (individual enzymes and pancreatin). Once the enzyme activity was known, the enzymatic solutions of the individual enzymes were prepared and stored in the freezer, the enzymatic solutions were prepared to meet the physiological levels during the in vitro digestion method (stock solutions: 1500 AU·mL⁻¹ α-amylase, 1325 LU·mL⁻¹ lipase, 40000 PU·mL⁻¹). Before each enzymatic solution preparation, the enzyme activity of the powders was checked.

Apart from the preparation of the enzymatic solution, the simulated digestive fluids (only electrolytes) were also prepared before the day of the performance of the in vitro digestion method. The composition of the simulated digestive fluids is specified in table 3. To prepare the concentrated digestive fluids, the individual salts were first dissolved in DI water at RT and 350 rpm (except sodium bicarbonate that was prepared at ~65°C), and then the volume was adjusted to obtain the desired concentration of each salt. After that, the different electrolyte solutions were mixed to obtain the concentrated simulated digestive fluid. But, before adjusting the volume of the simulated digestive fluid, the pH of the mixture was adjusted to the appropriate pH value:

- *Simulated salivary fluid (SSF)*: pH 7.0 ± 0.1
- *Simulated gastric fluid (SGF)*: pH 3.0 ± 0.1
- *Simulated intestinal fluid (SIF)*: pH 7.0 ± 0.1

Calcium chloride was the only solution that was not mixed with the simulated fluids as it may precipitate during its storage. This solution was mixed with the simulated fluids just before its use in the in vitro digestion method.

The simulated digestive fluids were prepared 1.25 times more concentrated as the physiological levels, because when it would be mixed with the enzymes and meal will be diluted. The final concentration of the simulated digestive fluids is specified in the following table (table 16):

Table 16. Final concentration of the simulated digestive fluids

Salt	Simulated digestive fluid (mM)		
	Salivary fluid	Gastric fluid	Intestinal fluid
Potassium chloride	15.10	6.90	6.80
Potassium phosphate	3.70	0.90	0.80
Sodium bicarbonate	13.60	25.00	85.00
Magnesium chloride	0.15	0.10	0.33
Sodium chloride	0.00	47.20	38.40
Ammonium carbonate	0.06	0.50	0.00
Hydrochloric acid	1.10	15.60	8.40
Calcium chloride	1.50	0.15	0.60

Both, the enzymatic solutions and simulated digestive fluids were stored at -20°C and they were frozen in aliquots, those aliquots had enough volume to perform one run of the in vitro digestion method. In that way, the stability of the solutions was not damaged by freeze-thaw cycles.

Before the day of the run, the virtual “molecular weight” of the commercial bile was also measured.

The Infogest protocol (2) is divided into three different phases; oral, gastric and small intestinal phase. Since it is a static digestion method, the pH needed to be adjusted before the start of each digestive phase, and the pH should be kept constant during all the phases:

- *Oral phase:* pH 7.0 ± 0.1
- *Gastric phase:* pH 3.0 ± 0.1
- *Small intestinal phase:* pH 7.0 ± 0.1

Another aspect that was taken into account was the time needed to mix all the ingredients to perform each phase of the in vitro digestion. That is important because the digestion starts when the meal is mixed with the enzymes, and if the time needed to mix the ingredients is too long or/and different between experiments, this it would affect the obtained results and distort the conclusions.

The pH adjustment could highly affect the time needed to prepare each digestive phase. A pre-trial was performed, not only to check the amount of 1M HCl or 1M NaOH needed to adjust the pH but also to assure that the pH was kept constant during each digestive phase.

Checking the amount of acid or base needed to adjust the pH of each phase helps to standardise and reduce the time needed to mix all the substances.

To perform the pre-trial, the protocol of the static digestion method was followed with the only difference that the pH was constantly measured during the digestion of the meal. At least two pre-trials for each kind of meal were carried out, in order to precisely check the amount of acid/base needed to adjust the pH.

10.2. Digestion

To perform the in vitro digestion with the static method, the buffer, pancreatin and bile were prepared the same day of the run. The pancreatin was prepared as a mixture of pancreatic powder and individual enzymes, and the mass composition was different depending on the specific activity of each powder. This mixture was prepared to obtain a stock that contains 1600 AU·mL⁻¹ of α-amylase, 1600 LU·mL⁻¹ of lipase and 800 TU·mL⁻¹ of trypsin.

To prepare the pancreatin, the different powders were weighed and mixed (650 rpm) at RT with DI water for at least 10 min. after that, the mixture was centrifugated (9000 rpm, 20 min, 4 °C – Herareus Multifuge X3R, Thermofisher) to remove the insoluble parts. Finally, it was stored in the fridge (5 – 8°C) until its usage.

To prepare the bile solution (200 mM), the powder was slowly added to DI water as it is slightly insoluble. For its solubilization, after the complete addition it was mixed at RT and 650 rpm for at least 10 min, until it was completely solubilised. The bile solution was also stored in the fridge until its usage.

The other reagents (buffer, simulated digestive fluids and DI water) were pre-warmed in a water bath to 37°C, the temperature that the digestion takes place (both, in vivo and in vitro).

The enzymatic solutions were let at RT to slowly defrost; these solutions were not pre-warmed to 37°C as they could lose part of its activity, and as the volume of enzymatic solutions needed to perform the in vitro digestion was small, it would not have a big impact on the temperature of the digestive mixture.

As the temperature is an important variable for the enzymes to catalyse the hydrolysis at its optimal conditions, the thermoshaker was pre-warmed to 37°C.

While the ingredients were pre-warmed and the enzymes defrost, the meal was prepared. After the meal preparation, a sample of the meal was taken and the rest was also pre-warmed to 37°C.

50 mL plastic tubes were used to perform the in vitro digestion, and a single tube was used for each sample that was taken from the digestion. As 6 samples were taken during the digestion, 6 different tubes were used per run. In that way, the sampling was simpler and more reproducible.

Once all the reagents were prepared and achieved the desired temperature, the in vitro digestion was started. The static digestion method is divided into 3 phases, oral, gastric and small intestinal phases.

10.2.1. Oral phase

For the oral phase, the meal was added into each plastic tube, and depending on the state of the meal it was added in differently as follows:

The liquid meal (5 mL per tube) was added using a multistep pipette. In contrast, the solid meal (5 g per tube) was added with a 60 mL syringe, creating a spaghetti shape. The “spaghetti” was created directly into the tube, and after the 5 g were added, the tube was bounced against the bench to bring the meal to the bottom of the tube. That was also important, as the total volume of the oral phase was 10 mL and the meal needed to be completely submerged into the simulated fluid.

The solid meal was added with this shape to homogenise the size and shape between the different samples/runs. The size and shape of the meal are important properties to take into account as they affect the accessibility of the enzymes and therefore could affect the digestibility of the meal. An example of the addition of the solid meal is depicted in the following figure (figure 25):

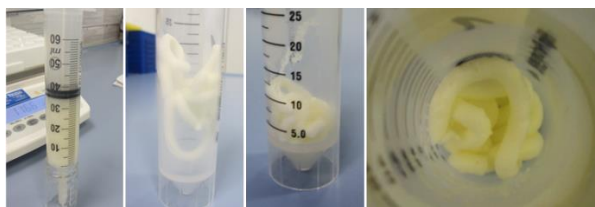


Figure 25. "Spaghetti" shape created for the solid meal

The meal was first added into the plastic tubes and then it was pre-incubated in the thermoshaker at 37°C for at least 10 min, to stabilise the temperature of the meal to the physiological temperature.

After that, 3.5 mL of the simulated salivary fluid (table 3) and 100 μ L of 75 mM calcium chloride were added to the plastic tube that contains the meal. Then, the acid or base needed to adjust the pH to 7.0 ± 0.1 (in vivo pH in saliva: Introduction_figure 61) were added (this amount was checked during the pre-trial), and the volume was adjusted to 9.5 mL with DI water. Finally, 0.5 mL of α -amylase (physiological activity: Introduction_figure 26a) were added to the mixture and it was incubated at 37°C and 400 rpm (Results and discussion_Section 4) for exactly 2 min, in the thermoshaker (New Brunswick Innova 40/40R, Eppendorf).

Figure 26 is an in vitro – in vivo comparison of the electrolytes and enzymes levels used in the oral phase of the static digestion method.

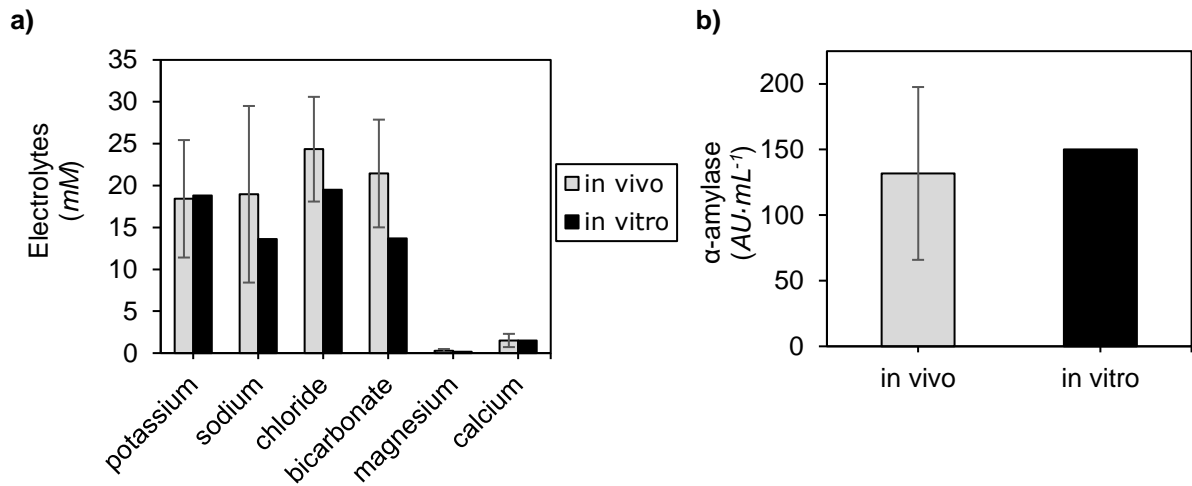


Figure 26. Comparison of the physiological levels with the levels used in the oral phase of the in vitro digestion method a) Some of the used electrolytes (Introduction_figure 57), b) α-amylase (Introduction_figure26a)

After the incubation time, one of the tubes (1st sample) was placed in a boiling water bath for 5 min to stop the enzyme activity (Results and discussion_Section 5.2). After that, the sample was filtered with a sieve and the amount of undigested meal was weighed to be able to calculate the percentage of the meal that was solubilised. Finally, the token sample was split into 3 aliquots and frozen in conical tubes of 5 mL. The sample was divided into 3 aliquots to avoid a large number of freeze-thaw cycles that could damage the sample.

After the 2 min of incubation, the rest of the tubes were used to carry out the other phases of the digestion.

10.2.2. Gastric phase

Just after the oral phase was incubated for 2 min at 37°C, the oral bolus was mixed with 7.5 mL of simulated gastric fluid and 20 μL of 75 mM calcium chloride. After that, the acid was added to adjust the pH of the mixture to 3.0 ± 0.1 . This reduction in the pH induced the denaturation of the α-amylase added in the oral phase, and the catalysis of the hydrolysis of carbohydrates stopped.

Figure 27 is an in vitro – in vivo comparison of the electrolytes and enzymes levels used in the gastric phase of the static digestion method.

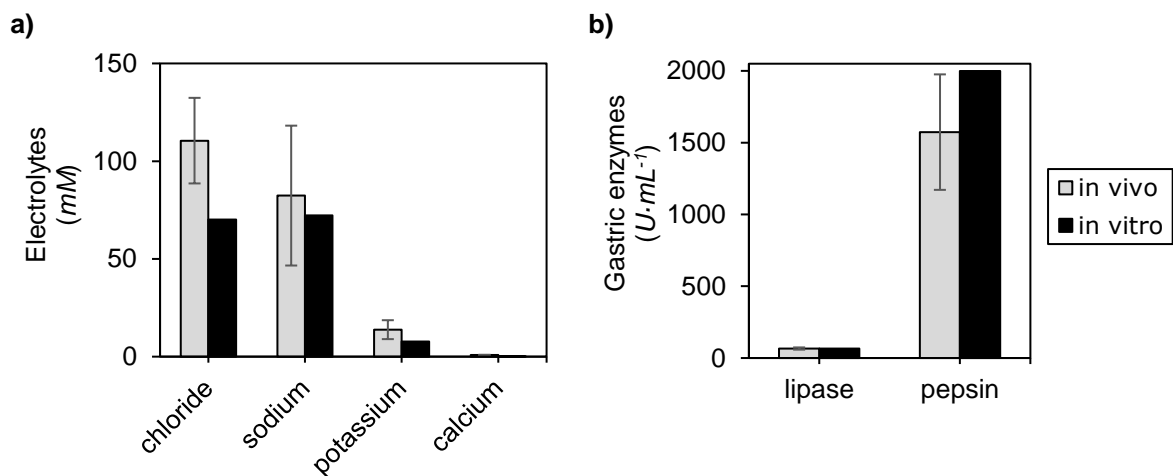


Figure 27. Comparison of the physiological levels with the levels used in the gastric phase of the in vitro digestion method a) Some of the used electrolytes (Introduction_figure 58), b) gastric enzymes (Introduction_figures 26a, 50)

After that, the volume of the gastric phase was adjusted to 18 mL with DI water. Finally, the gastric enzymes (1 mL of pepsin and 1 mL of lipase) were added. The gastric phase was incubated at 37°C and 400 rpm for exactly 2 h, in the thermoshaker.

Only one sample was taken after the gastric phase, after the 2 h of incubation. The sample was treated in the same manner as the sample taken after the oral phase (heat treatment, filtration, aliquoting and freezing). The other tubes were used to carry out the small intestinal phase.

10.2.3. Intestinal phase

To carry out the small intestinal phase, 20 mL of the chyme were mixed with 11 mL of simulated intestinal fluid, 2 mL 200 mM bile and 1 mL 1M bicarbonate buffer. Then, the needed amount of acid (1M HCl) or base (1M NaHCO₃) to adjust the pH to 7.0 ± 0.1 was added and the volume of the intestinal phase was adjusted to 35 mL with DI water. Ultimately, 5 mL of pancreatin were added and the mixture incubated at 37°C and 400 rpm for 2 h, in the thermoshaker.

Figure 28 is an in vitro – in vivo comparison of the electrolytes and enzymes levels used in the small intestinal phase of the static digestion method.

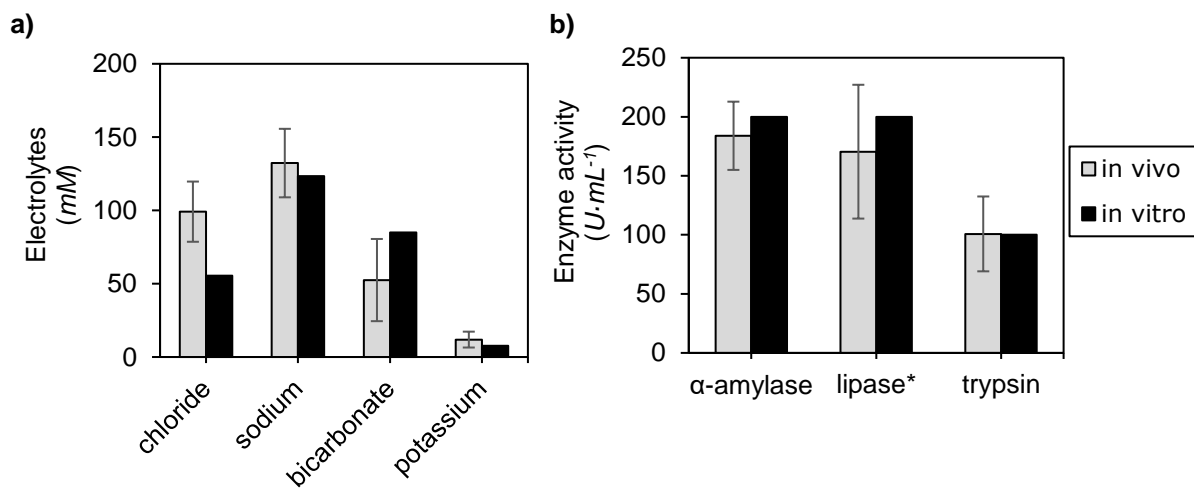


Figure 28. Comparison of the physiological levels with the levels used in the intestinal phase of the in vitro digestion method a) some of the used electrolytes (Introduction_figure 59), b) gastric enzymes (Results and discussion_figure 33)

Four samples were taken during the intestinal phase, one every 30 min. Each sample underwent the same treatment, they were incubated in a boiling water bath for 5 min, then filtered with a sieve to calculate the percentage of solubilised meal, aliquoted in three conical tubes of 5 mL and frozen at -20°C (freezer).

11. Dynamic digestion method

The in vitro dynamic model used for this study (TIM-1) consists of four successive compartments simulating the stomach and small intestine (duodenum, jejunum and ileum), as is shown in figure 29.

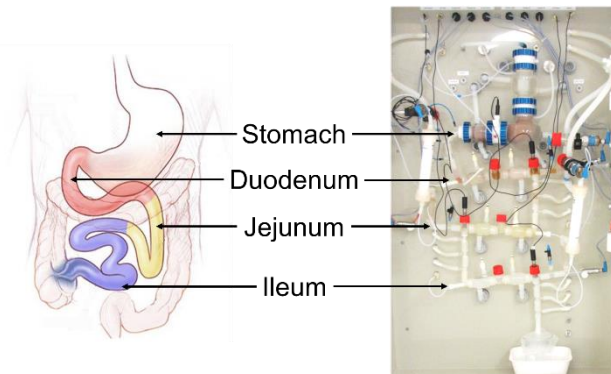


Figure 29. Schematic comparison of the human GIT and TIM-1 system

The digestion with the TIM-1 system can be performed with two kinds of stomachs; the standard and the advanced gastric compartment. For this thesis, the advanced gastric compartment (TIMagc) was used as it better mimics the shape and motility of the human stomach.

The TIMagc consists of three different parts, each presenting a specific gastric region: body, bottom and antrum (figure 30). The bottom and antrum of the TIMagc mimic the proximal and distal antrum, respectively. And a valve, placed directly after the antrum, represents the pyloric sphincter.

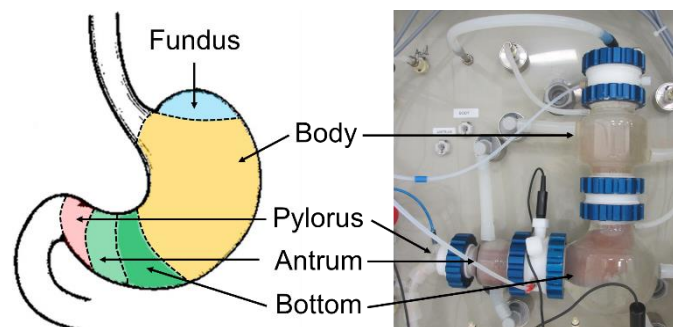


Figure 30. Schematic comparison of the human stomach and TIMagc

On the other hand, each compartment of the small intestine is formed by two connected basic units. The units that form the stomach and small intestine consist of a glass jacket with a flexible wall inside. Water is pumped from a water bath into the glass jackets around the flexible walls to control the temperature inside the units but also the pressure on the flexible walls. This is the method to mimic the peristaltic movements that occur in the human gastrointestinal tract by alternate compression and relaxation of the flexible walls. All contractile movements and the resulting mixing and pressure profiles are accurately computer-controlled and synchronized.

The compartments are connected by peristaltic valve pumps consisting of three connected T-tubes, each with a separate tube-like flexible wall inside. If pressure is applied to the outside of the flexible wall, the valve is closed, leaving minimal dead space inside. In the open position, the flexible walls facilitate unhindered passage of the chyme through the valves. Peristaltic pumping is achieved by regulating the sequence of opening and closing of the three parts of the valve pump. During each peristaltic cycle, a volume of chyme is transferred.

The frequency of peristaltic cycles is dictated by the computer, allowing the flow rate of the chyme to be controlled. The volume in each compartment (except for the stomach) is monitored with a level sensor connected to the computer (71,72).

All the compartments are equipped with pH electrodes, the pH values are controlled via the computer by screening either water or HCl into the stomach, or by screening either water or sodium bicarbonate into the small intestine.

In the stomach the acid/water could be secreted in the upper part of the stomach or close to the pH electrode, and it was decided to attach the acid/water tube close to the electrode and the secretion tube in the upper part of the stomach. In that way, when the pH was different from the pH curve, the acid was secreted and it was quickly adjusted. If the acid/water tube would be attached to the upper part of the stomach, then it would need some time to reach the pH electrode. The secretions of the GIT are regulated by using computer-controlled syringe pumps.

Digestion products are removed by dialysis (NIPRO Sureflux 07L dialyser) through membranes with a molecular weight cut-off of approximately 10 kDa, connected to the jejunum and ileum. The digestion products that were removed by dialysis was the bioaccessible fraction, the fraction of meal that is available for intestinal absorption (figure 31).

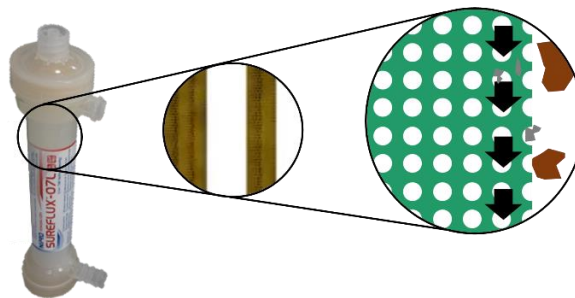


Figure 31. NIPRO Sureflux 07L dialyser

To avoid the blockage of the dialysers, a prefilter was connected between the jejunal and ileal compartments and the dialysers (figure 32).

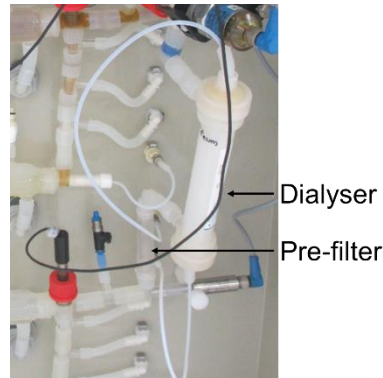


Figure 32. Connection of the dialysers and pre-filters to the system

11.1. Calculations

One of the objectives of this thesis was the comparison of the static and dynamic digestion methods, and to be able to compare both methods, the levels of the enzymes, electrolytes and meal used in the dynamic digestion model needed to be the same as the ones used in the static digestion method. For that reason, the concentration of the stock solutions had to be calculated taking into consideration their final concentration in the lumen of the dynamic digestion method.

For the meal preparation, the enzyme-meal ratio used to perform the gastric phase in the static digestion method was mimicked in the stomach of the TIM-1 system. To calculate the enzyme-meal ratio, the units, in absolute value, of α -amylase (750 AU), pepsin (40000 PU) and lipase (1325 LU) present in the gastric phase was divided by the amount of meal used in the static digestion method (5 g), then the units of the enzymes present in the stomach of the dynamic system were divided into the obtained enzyme-meal ratio used for the static digestion method (eq. 38):

$$\text{meal}_{\text{Dynamic system}}(\text{g}) = \frac{\text{enzyme activity}_{\text{Dynamic system}}(\text{U})}{\text{enzyme-meal ratio}_{\text{Static method}}(\text{U} \cdot \text{g}^{-1})} = 35 \text{ g meal} \quad \text{Eq. 38}$$

The mass balance was used to calculate the concentration of the electrolytes, bile and enzymes in the lumen of the dynamic digestion model (TIM-1 system). Therefore, it was taken into account the amount of substance that enters and leaves each compartment.

The digestion with the dynamic system was performed for 5 h and, as the model is a dynamic model the concentration varies by time, for that reason the composition of the chyme was calculated each 30 min.

The volume of each substance present in each compartment in each time point was first calculated, and then taking into account the concentration of the stock solution, the concentration in the lumen was calculated. However, to be able to calculate the volume of each substance in each compartment, the total volume that enters, remains and leaves each compartment was calculated.

11.1.1. Total volume

To calculate the total volumes of the compartments during the in vitro digestion, it was taken in consideration the initial volume of each compartment, the secretions delivered during the digestion and the emptying profile of each compartment.

To perform a run, 300 mL of intake (meal and secretions) were initially introduced into the stomach. And the small intestine was filled with secretions; the duodenum with a mixture of pancreatin, bile and electrolytes (50 mL), and the jejunum/ileum with electrolytes (100 mL each).

On the other hand, during the digestion, some secretions were delivered into the lumen of the in vitro GIT. These secretions contained electrolytes, enzymes and bile, but also DI water, acid or base for the correct pH adjustment. The flow rates of these secretions are specified in the following table (table 17):

Table 17. Secretion flow rates
(*the individual flow rate of acid/base and DI water/SIES depends on the lumen pH)

Compartment	Secretion	Flow rate (mL·min ⁻¹)
Stomach	Gastric enzyme solution	0.25
	HCl/DI water*	0.25
Duodenum	Bile	0.50
	Pancreatin	0.25
	NaHCO ₃ /SIES*	0.25
Jejunum	NaHCO ₃ *	0.02
Ileum	NaHCO ₃ *	0.03

SIES: diluted simulated intestinal fluid

Finally, the emptying profile of each compartment was taken into account. The stomach was emptied following an equation that mimics the behaviour of the human stomach (73):

$$f = IN \cdot \left(1 - 2^{-\left(\frac{t}{t_{1/2}}\right)^\beta} \right) \quad \text{Eq. 39}$$

Where f represents the volume that leaves the stomach (mL), IN is the amount of meal and secretions that enters into the stomach (mL), t is the time point of the digestion (min), $t_{1/2}$ is the time from the start until 50 % of the meal has emptied from the stomach (80 min), and β determines the shape of the curve of the stomach emptying ($\beta: 2$). The differences in the curve profile depend on the status of the meal, for example a solid meal needs some time to be divided into particles that are small enough to leave the stomach, and this time is represented by a lag phase (figure 33).

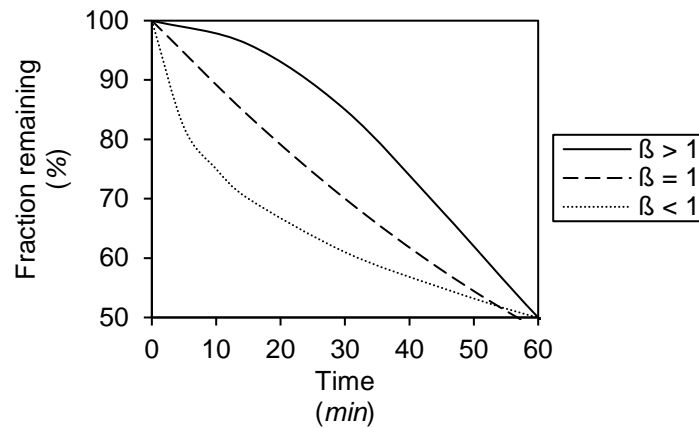


Figure 33. Differences in the emptying curves ($t_{1/2} = 60 \text{ min}$) for meals that has a rapid initial emptying followed by a slower emptying phase ($\beta < 1$), liquid meals that are constantly emptying ($\beta = 1$) and meals that need some time to be disintegrated ($\beta > 1$)

On the other hand, the different compartments of the small intestine are emptied when the liquid reached the level sensors, therefore their volumes are constant.

The calculation of the chyme volume that leaves each compartment is specified in table 18, and it is based on the written values in flow chart 3.

Table 18. Equations used to calculate the volumes of chyme that were delivered from each compartment (t: time point of the digestion, $t_{1/2}$: 80 min, β : 2, Absorption bottle 1,2: the volume depends on the time point)

Chyme A Chyme delivered from the stomach	$(0.25 \cdot t + 0.25 \cdot t + 300) \cdot \left(1 - 2^{-\left(\frac{t}{t_{1/2}}\right)^\beta}\right)$	Eq. 40
Chyme B Chyme delivered from the duodenum	$(2 \cdot (0.25 \cdot t) + 300) \cdot \left(1 - 2^{-\left(\frac{t}{t_{1/2}}\right)^\beta}\right) + (0.25 \cdot t + 0.25 \cdot t + 0.50 \cdot t)$	Eq. 41
Chyme C Chyme delivered from the jejunum	$(0.50 \cdot t + 300) \cdot \left(1 - 2^{-\left(\frac{t}{t_{1/2}}\right)^\beta}\right) + t + (\sim 0.02 \cdot t) - \text{Absorption bottle 1}$	Eq. 42
Ileum efflux Chyme delivered from the ileum	$(0.50 \cdot t + 300) \cdot \left(1 - 2^{-\left(\frac{t}{t_{1/2}}\right)^\beta}\right) + (1.02 \cdot t) - \text{Absorption bottle 1} + (\sim 0.03 \cdot t) - \text{Absorption bottle 2}$	Eq. 43

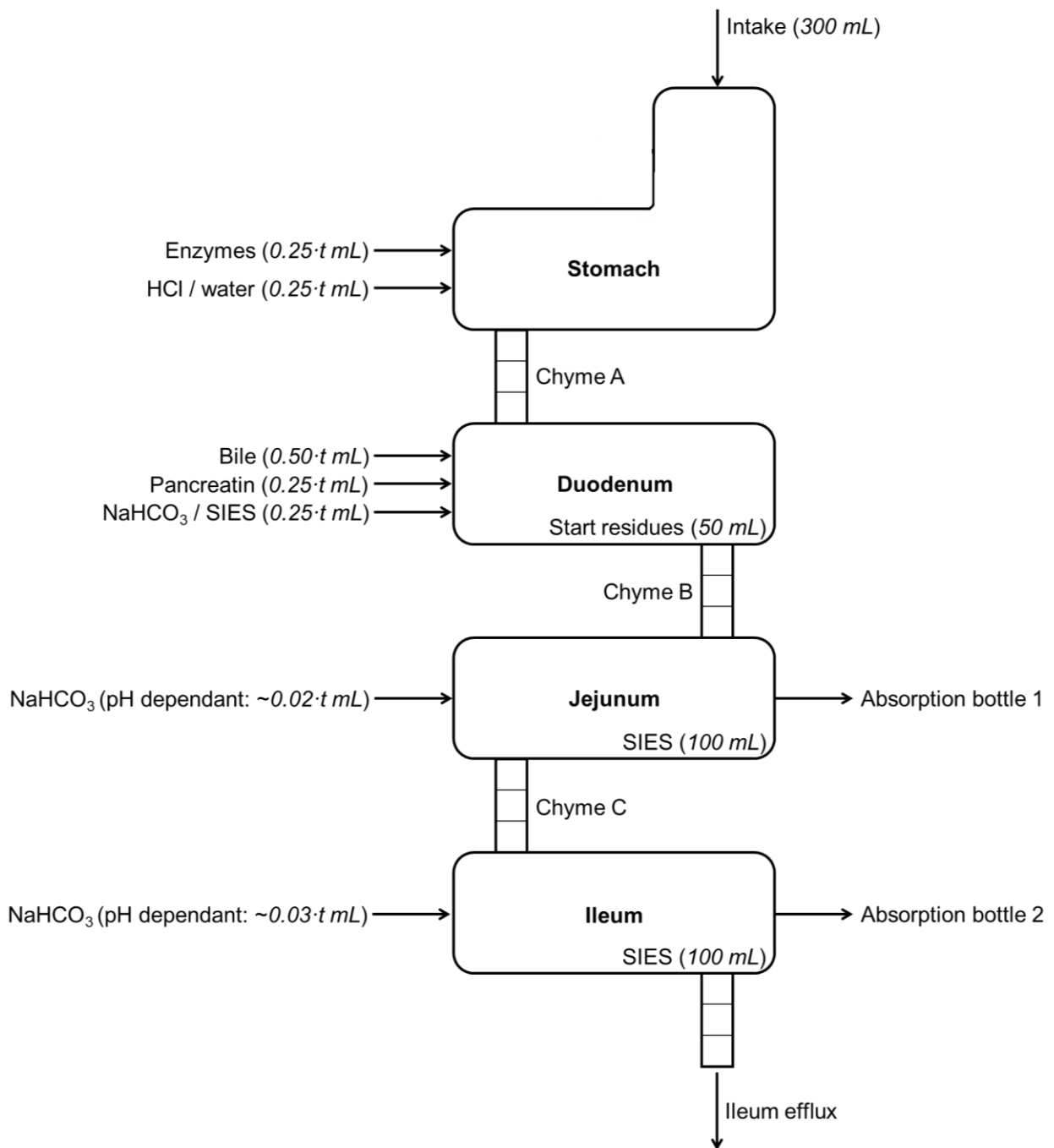
The amount of chyme (mL) that remains in the stomach in each time point (except t: 0 min) was calculated by using eq. 44.

$$\text{Chyme}_{\text{stomach}} = (0.25 \cdot t + 0.25 \cdot t + 300) - (0.25 \cdot t + 0.25 \cdot t + 300) \cdot \left(1 - 2^{-\left(\frac{t}{t^{1/2}}\right)^{\beta}}\right) \quad \text{Eq. 44}$$

The volume of chyme that is delivered to the absorption bottles are specified in table 19, these volumes are an average of experimental volumes (average of 10 runs).

Table 19. Chyme volumes in absorption bottles vs digestion time

Time (min)	Absorption bottle 1 (mL)	Absorption bottle 2 (mL)
30	45.6	11.9
60	130.3	24.6
90	147.9	38.8
120	202.1	52.1
150	235.6	65.3
180	240.6	77.9
210	241.1	90.6
240	241.3	103.0
270	241.6	116.0
300	241.9	127.8



Flow chart 3. Volumes used in the dynamic digestion method

The chyme volumes that leave each compartment were calculated at different time points (every 30 min from 0 to 300 min), depicted versus digestion time and compared with the experimental emptying profile (figure 34). This comparison was made to prove that the calculated volumes were a good approximation to what is happening in the dynamic digestion method.

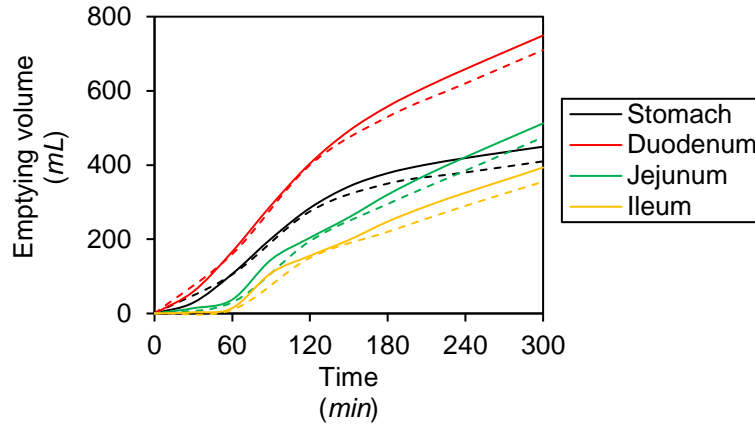


Figure 34. Comparison of the calculated and experimental emptying profile (solid line: calculated, dashed line: experimental)

11.1.2. Individual volumes

The individual volume of each substance (gastric enzymes, bile, pancreatin and electrolytes) could be calculated once the total volumes were known. However, the interval volume in each time point was first calculated by subtracting the volume of the previous from the current time point:

$$\text{Chyme}_{\text{interval}}(t) = \text{Chyme}_{\text{cumulative}}(t) - \text{Chyme}_{\text{cumulative}}(t-30) \quad \text{Eq. 45}$$

Where t is the time point and $t-30$ is the previous time point, both expressed in minutes.

To calculate the individual volumes, it was taken into account if the molecules pass through the dialysers or not. As the cut-off of the dialysers was bigger than the molecular weight of the electrolytes, it was concluded that they pass through the dialysers. On the other hand, it was proved that the dialysers retain the enzymes as no activity (α -amylase, trypsin, lipase, pepsin) was found after the enzymatic solutions passed through the dialysers. Finally, it was considered that the solubilised bile also passes through the dialysers.

Taking into account that only the enzymes were retained by the dialysers, the volume of each kind of substance was calculated in each time point and compartment by using the equations 46 – 49.

Stomach & duodenum

$$V_X^{\text{molecule}} = \frac{V_{\text{from previous compartment}}^{\text{molecule}} + V_{\text{inside}}^{\text{molecule}} + V_{\text{secretions}}^{\text{molecule}}}{V_{\text{from previous compartment}}^{\text{total}} + V_{\text{inside}}^{\text{total}} + V_{\text{secretions}}^{\text{total}}} \cdot V_X^{\text{total}} \quad \text{Eq. 46}$$

Jejunum & ileum (pass)

$$V_X^{\text{molecule}} = \frac{V_{\text{from previous compartment}}^{\text{molecule}} + V_{\text{inside}}^{\text{molecule}} + V_{\text{secretions}}^{\text{molecule}} - V_{\text{dialyzer}}^{\text{molecule}}}{V_{\text{from previous compartment}}^{\text{total}} + V_{\text{inside}}^{\text{total}} + V_{\text{secretions}}^{\text{total}} - V_{\text{dialyzer}}^{\text{total}}} \cdot V_X^{\text{total}} \quad \text{Eq. 47}$$

$$V_{\text{dialyzer}}^{\text{molecule}} = \frac{V_{\text{from previous compartment}}^{\text{molecule}} + V_{\text{inside}}^{\text{molecule}} + V_{\text{secretions}}^{\text{molecule}}}{V_{\text{from previous compartment}}^{\text{total}} + V_{\text{inside}}^{\text{total}} + V_{\text{secretions}}^{\text{total}}} \cdot \left(V_{\text{dialyzer}}^{\text{total}} + \frac{V_{\text{inside}}^{\text{total}}}{2} \right) \quad \text{Eq. 48}$$

Jejunum & ileum (do not pass)

$$V_X^{\text{molecule}} = \frac{V_{\text{from previous compartment}}^{\text{molecule}} + V_{\text{inside}}^{\text{molecule}} + V_{\text{secretions}}^{\text{molecule}}}{V_{\text{from previous compartment}}^{\text{total}} + V_{\text{inside}}^{\text{total}} + V_{\text{secretions}}^{\text{total}} - V_{\text{dialyzer}}^{\text{total}}} \cdot V_X^{\text{total}} \quad \text{Eq. 49}$$

Where V^{molecule} is the individual volume of the substance, V^{total} is the no cumulative total volume of chyme, V_X is the volume that remains inside or leaves the compartment, $V_{\text{from previous compartment}}$ is the volume that comes from the previous compartment (e.g. the volume of pepsin that goes from the stomach to the duodenum), V_{inside} is the volume that was inside the compartment in the previous time point, $V_{\text{secretions}}$ is the volume that comes from the secretions and V_{dialyzer} is the volume that leaves the dialyzer. All the volumes were expressed in mL.

11.1.3. Lumen concentration

Finally, the concentration of each substance and the enzyme activity in the lumen was calculated with the following equation:

$$\text{concentration or activity} = \frac{(V_{\text{molecule}} \cdot C_{\text{stock solution}})_{\text{input 1}} + (V_{\text{molecule}} \cdot C_{\text{stock solution}})_{\text{input 2}} + \dots}{V_{\text{compartment}}} \quad \text{Eq. 50}$$

Where C is the concentration of the molecule (mM) or the activity of the enzyme ($\text{U} \cdot \text{mL}^{-1}$), and *input 1/input 2...* refers to the stock solution where the molecule is initially present (e.g. amylase is present in the intake and pancreatin or trypsin is added in the start residues of the duodenum and pancreatin), V_{molecule} is the calculated individual volume (mL) and $V_{\text{compartment}}$ is the total volume of the compartment (mL).

An excel template was prepared for each substance, taking into account the above equations. The composition of the stock solutions was calculated by comparing the calculated concentration/activity in the lumen of the dynamic system with the reported physiological levels and the levels used in the static digestion method.

11.1.3.1. α -amylase

On one hand, the reported saliva flow rate was taken into account to mimic the α -amylase levels in the stomach: $192.0 \pm 47.6 \text{ mL} \cdot \text{h}^{-1}$ (74–77). It was also considered that the saliva secretion lasts for 30 min when a meal is eaten. Finally, both the activity in the saliva used in the static digestion method ($150 \text{ AU} \cdot \text{mL}^{-1}$) and the intake volume (300 mL) used for the dynamic system were considered for the calculation of the α -amylase activity in the stomach:

$$\alpha\text{-amylase}_{\text{Stomach}} = 30 \text{ min} \cdot \frac{192 \text{ mL}}{60 \text{ min}} \cdot \frac{150 \text{ AU}}{1 \text{ mL}} \cdot \frac{1}{300 \text{ mL}} = 48 \text{ AU} \cdot \text{mL}^{-1} \quad \text{Eq. 51}$$

On the other hand, the activity during the gastric phase is $37.5 \text{ AU} \cdot \text{mL}^{-1}$. However, it should be taken into account that during the gastric phase of the static method the pH is 3.0 ± 0.1 . Therefore, the enzyme is probably denatured and without activity. In contrary to the most likely denatured α -amylase in the static digestion method, in the dynamic digestion method, the α -amylase activity was adjusted to the expected remaining activity at the pH of the gastric compartment (pH curve used in the dynamic digestion method: table 20; pH effect on α -amylase activity: Results and discussion_figure 10).

Finally, it was important to take into account that the biggest difference between both methods is that the Infogest protocol is a static method, while TIM-1 system is a dynamic digestion method. Therefore, while in the Infogest protocol the pH and the activity remain constant during each digestive phase, in the TIM system, the pH and activity vary during the digestion.

The pH of the stomach content at the beginning of the digestion with the dynamic system is 5.5, at this pH the α -amylase activity is around 51 % lower compared with the activity at pH 7, and from the minute 60, the pH of the stomach content is 3. Therefore α -amylase is inactivated from minute 60 of the digestion. The comparison of the physiological activity, the activity used in the static digestion method and the activity used in the dynamic system is depicted in the following graph (figure 35):

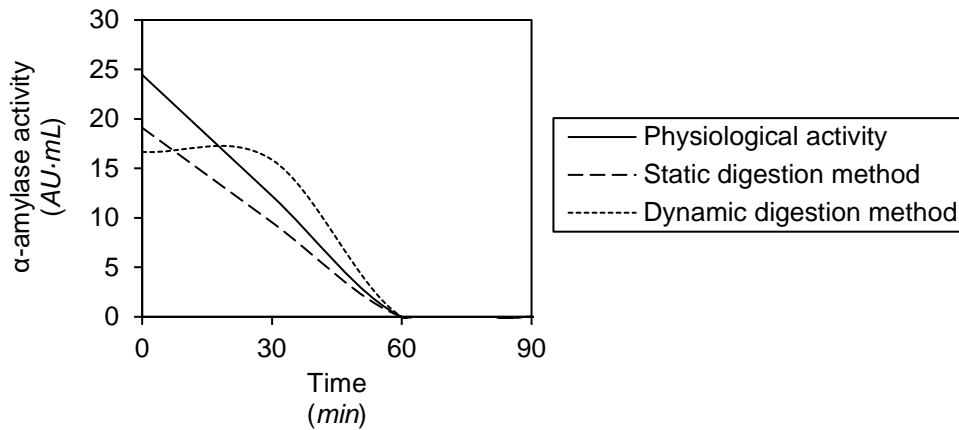


Figure 35. Comparison of the α -amylase activity in the stomach (human, static and dynamic methods) (74–77)

α -amylase is also secreted in the small intestine as pancreatin, a mixture of enzymes (figure 36). The physiological level is $183.9 \pm 28.0 \text{ AU}\cdot\text{mL}^{-1}$ (Introduction_Figure 26), and the α -amylase activity levels used in the small intestinal phase during the static digestion method is $200 \text{ AU}\cdot\text{mL}^{-1}$.

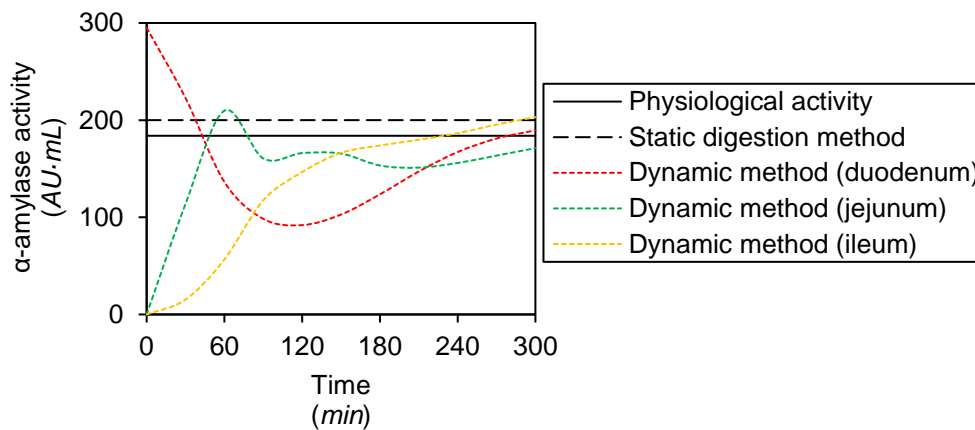


Figure 36. Comparison of the α -amylase activity in the small intestine (human, static and dynamic methods)

11.1.3.2. Lipase

The lipase activity in the stomach of the dynamic digestion method was calculated by taking into account the physiological activity (Introduction_Figure 50), the levels of lipase used in the gastric phase of the static digestion method and the solubility of the commercial powder. The optimal pH of the gastric lipase is 5.5. Therefore, at the beginning of the digestion in the dynamic system the lipase acts at its 100 % activity.

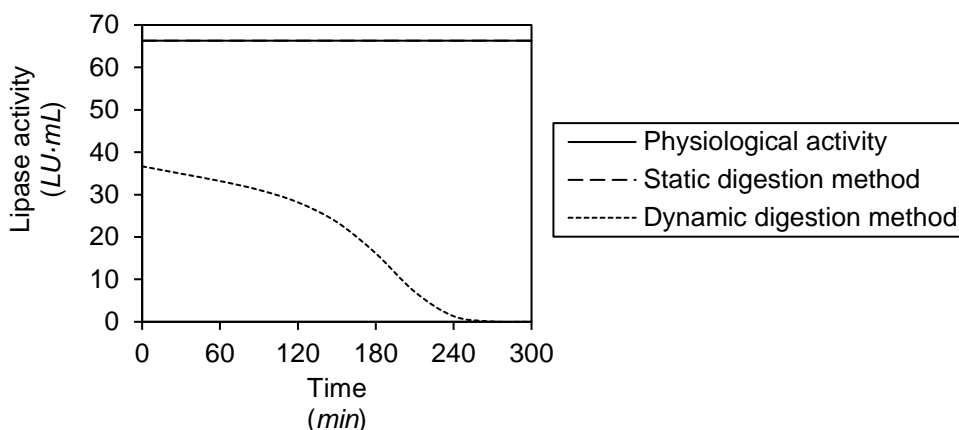


Figure 37. Comparison of the lipase activity in the stomach (human, static* and dynamic methods)
 *the activity used in the static digestion method is the same as the physiological activity

As figure 37 shows, the lipase levels used in the stomach of the dynamic system is much lower than the physiological activities and the lipase activity used in the gastric phase of the static method. This difference is because of the solubility of the commercial powder. When a more concentrated stock solution was prepared, the lipase was not completely solubilised.

On the other hand, the comparison of the lipase activity in the small intestine of the human, dynamic and static digestion methods is depicted in figure 38. As it is explained in section 2.6.2. in ‘Results and discussion’, the lipase is secreted in excess in the small intestine, for the static digestion method the physiological level can be decreased 10-fold. The minimum amount of lipase needed to digest a fatty meal with the dynamic system was also calculated. It was taken into account that the maximum volume of meal present in the small intestine was 10 mL, the volume of the jejunum and ileum is 100 mL, the first time point was at 30 min, the molecular weight of butyric acid is $88.11 \text{ g}\cdot\text{mol}^{-1}$ and its density is $0.95 \text{ g}\cdot\text{mL}^{-1}$.

$$\frac{10 \text{ mL meal}}{100 \text{ mL small intestine}} \cdot \frac{1 \text{ mL butyric acid}}{1 \text{ mL meal}} \cdot \frac{0.9528 \text{ g butyric acid}}{1 \text{ mL butyric acid}} \cdot \frac{1 \text{ mol butyric acid}}{88.11 \text{ g butyric acid}} \cdot \frac{10^6 \mu\text{mol}}{1 \text{ mol}} \cdot \frac{1}{30 \text{ min}} = 36.05 \frac{\mu\text{mol butyric acid}}{\text{mL}\cdot\text{min}} \quad \text{Eq. 52}$$

Therefore, the lipase activity could be also decreased 10-fold for the dynamic digestion method.

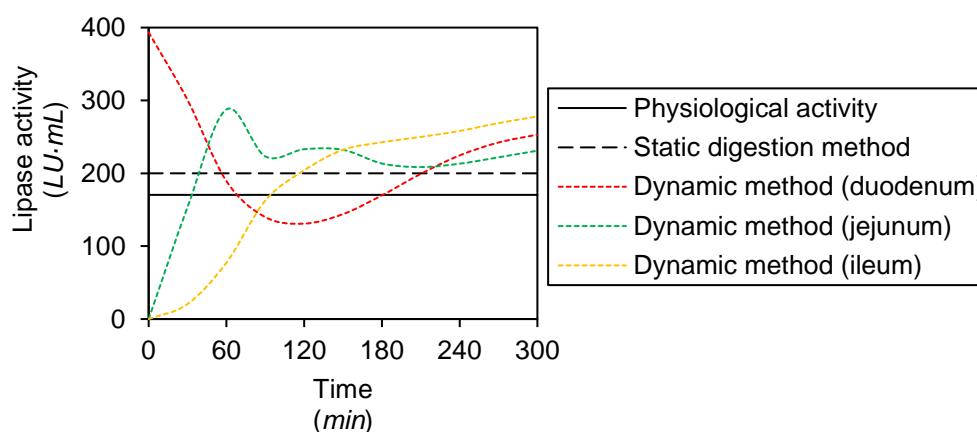


Figure 38. Comparison of the lipase activity in the small intestine (human, static and dynamic methods)

11.1.3.3. Pepsin

Figure 39 shows the pepsin activity used in the stomach of the dynamic digestion method compared with the pepsin levels used in the static method and human stomach. At the beginning of the digestion, the pepsin activity was lower than the physiological activity, but then the pepsin activity increases until it reaches a 'steady state' that was higher than the physiological activity. However, it was taken into account that the stomach of the dynamic system was empty at 160 min ($t_{1/2}$ 80 min).

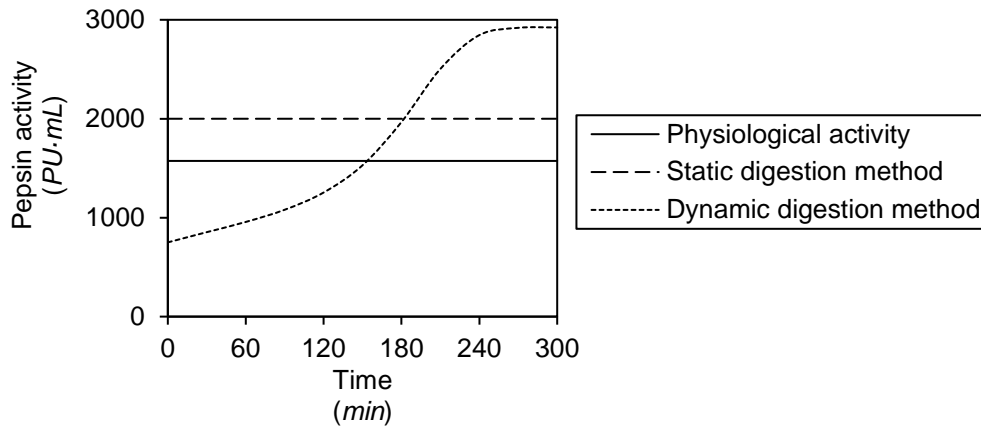


Figure 39. Comparison of the pepsin activity in the stomach (human, static and dynamic methods)

11.1.3.4. Trypsin

The trypsin was secreted into the duodenum of the dynamic system as pancreatin, but it was also added at the beginning of the digestion, in the start residues of the duodenum as individual enzyme and pancreatin. Therefore, two different sources of trypsin were used in the dynamic digestion method (individual enzyme and mixture of enzymes).

The trypsin activity present in the dynamic digestion method is compared with the physiological levels and the activity present in the static digestion method (figure 40).

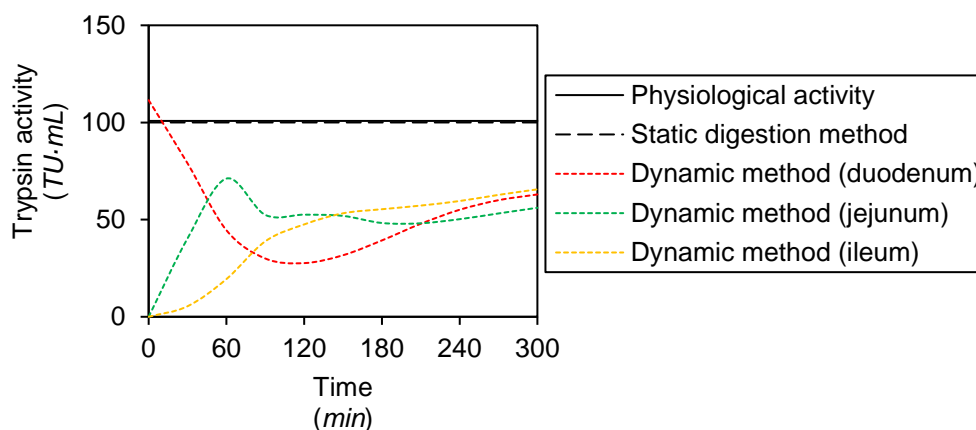


Figure 40. Comparison of the trypsin activity in the small intestine (human, static and dynamic methods)

The trypsin activity used in the small intestine of the dynamic system was lower than the physiological levels. The activity of trypsin solution ($TU \cdot mL^{-1}$) increase with the mass concentration ($mg \cdot mL^{-1}$) until it reaches a steady state, where when more trypsin was solubilised, the activity remained almost constant. Therefore, the amount of trypsin needed to reach the physiological levels in the small intestine was too high and it would be too expensive. For that reason, a compromise between activity and price was decided.

11.1.3.5. Bile

Figure 41 shows the comparison among the bile concentration in the human small intestine, the concentration used in the static digestion method and in the dynamic model. In the dynamic system, the bile concentration in the duodenum reached the physiological concentration. However, the concentration in the jejunum and ileum was lower than the physiological level. This can be explained by the fact that the bile was secreted only to the duodenum and the presence of bile in the jejunum and ileum is due to the duodenum emptying.

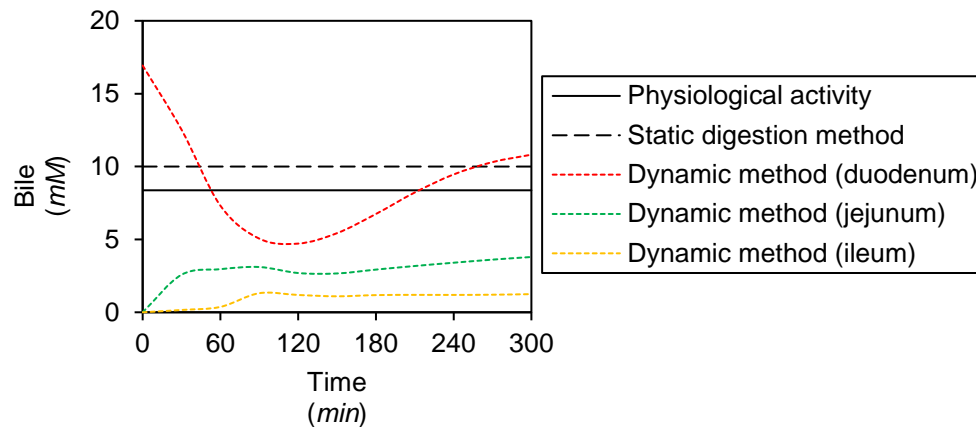


Figure 41. Comparison of the bile concentration in the small intestine (human, static and dynamic methods)

11.1.3.6. Electrolytes

Figure 42 shows the comparison of some of the electrolytes that are involved in human digestion. Its physiologic concentration is compared with the concentration of these electrolytes used in the in vitro digestion methods (static and dynamic). In the first column of graphs (left) the electrolyte concentration in the stomach is depicted and in the second column (right) the concentration in the small intestine. In general, the concentration of electrolytes used in the dynamic and static system mimics the concentration in the human GIT, except for the sodium concentration in the small intestine. The concentration of the solution is lower in the in vitro methodology (dynamic). The sodium was added as sodium chloride. Therefore, an increase in the concentration of the stock solution of sodium implies an increase in the concentration of chloride, which with the current concentration fits the concentration used in the static digestion method. For that reason, the concentration of sodium chloride in the stock solution was not increased.

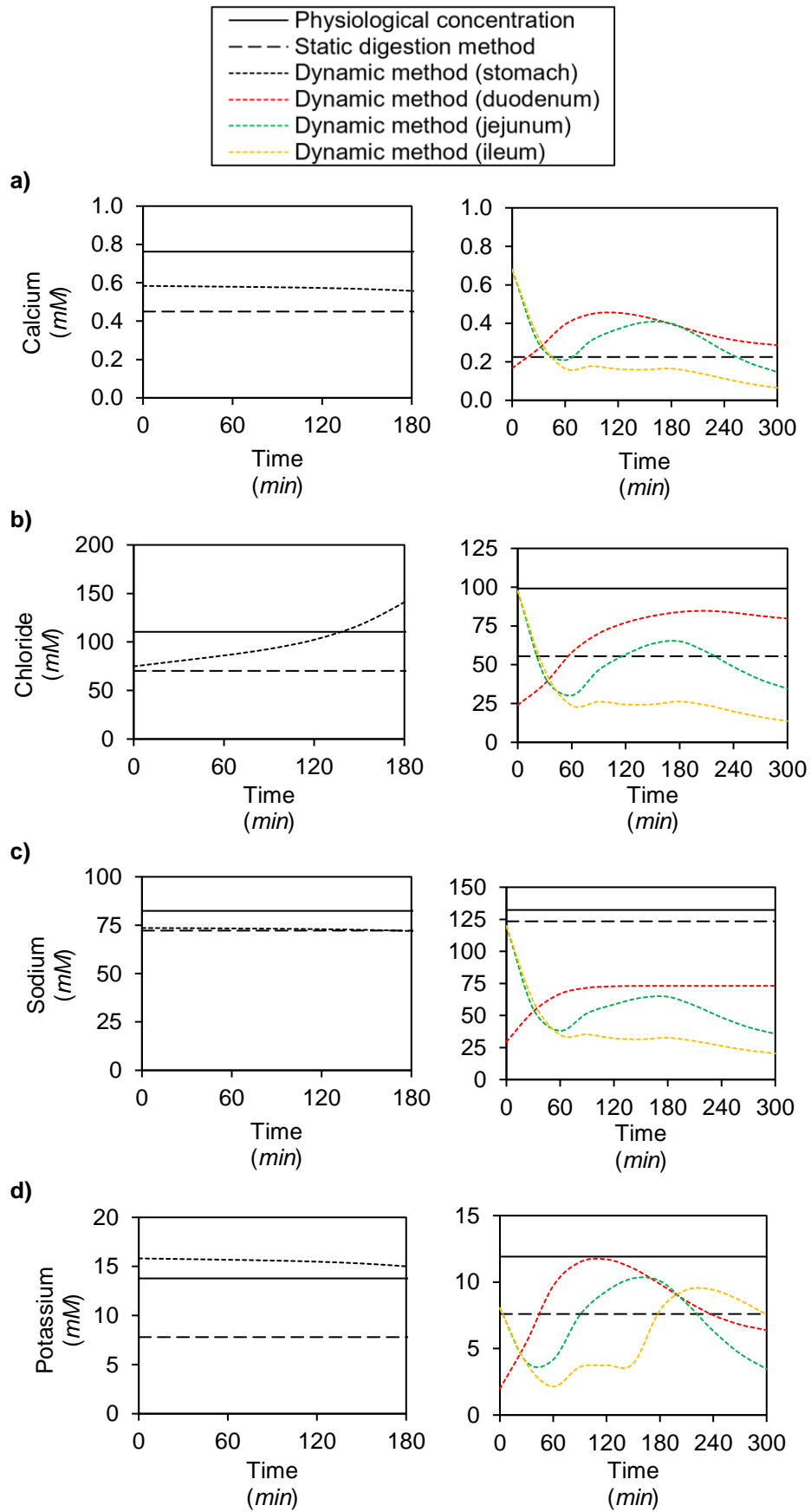


Figure 42. Comparison of the concentration of some of the electrolytes involved in the digestion (left: stomach, right: small intestine)

11.2. Software – protocol

The dynamic system (TIM-1) is a computer-controlled apparatus, and the program has been designed to mimic parameters and data obtained from in vivo studies. Human digestion depends on a wide range of variables, and depending on the type of meal (solid, liquid, rich in fats, ...) and the status of the human that is mimicked (young/old, sick/healthy, ...), the script used would have different values to mimic the in vivo conditions.

For this thesis, it was considered that the carbohydrates were the macronutrient of interest and that the component of interest was ingested with a meal. That means that not only the secretion concentrations and flow rates but also the pH curves used in TIM-1 mimicked the “fed” conditions. On the other hand, it was considered that the poly-/di- and monosaccharides released from the meal were solubilised in water, not in fats.

Therefore, the protocol settings that were chosen are described in table 20:

Table 20. Simulated gastro-intestinal parameters - Protocol settings

Stomach																		
Elashoff parameters	a = 80 b = 2 c = 100	$t_{1/2} = 80$ min $\beta = 2$ 100 % meal																
pH curve	<table border="1"> <thead> <tr> <th><u>Time (min)</u></th> <th><u>pH</u></th> </tr> </thead> <tbody> <tr><td>0</td><td>5.5</td></tr> <tr><td>30</td><td>4.5</td></tr> <tr><td>60</td><td>3.0</td></tr> <tr><td>120</td><td>2.0</td></tr> <tr><td>180</td><td>1.7</td></tr> <tr><td>182</td><td>9.0</td></tr> <tr><td>360</td><td>9.0</td></tr> </tbody> </table>	<u>Time (min)</u>	<u>pH</u>	0	5.5	30	4.5	60	3.0	120	2.0	180	1.7	182	9.0	360	9.0	<p>The pH decreases with the time until minute 182, where the target pH is 9.0. This “increase” in the pH is to stop the acid secretion as the stomach is almost empty.</p>
	<u>Time (min)</u>	<u>pH</u>																
0	5.5																	
30	4.5																	
60	3.0																	
120	2.0																	
180	1.7																	
182	9.0																	
360	9.0																	
Secretions (mL·min ⁻¹)	<table border="1"> <thead> <tr> <th><u>Enzymes</u></th> <th>0.25</th> </tr> <tr> <th><u>Acid/Water</u></th> <th>0.25</th> </tr> </thead> </table>	<u>Enzymes</u>	0.25	<u>Acid/Water</u>	0.25	<p>The acid/water is secreted in a total flow rate of 0.25 mL·min⁻¹, and the HCl (acid) or DI water is secreted to adjust the gastric pH to the pH curve.</p>												
<u>Enzymes</u>	0.25																	
<u>Acid/Water</u>	0.25																	
Mixing profile	<p>1=c,80,60,3,1, 2=c,50,60,5,1, 3=s,0,0,0,0, 4=c,50,10,4,1, 5=c,66,10,3,1,</p>	<p>The first item after the equal refers to the body volume (compensates the total volume), the second item is the bottom volume (e.g. 80=0.8·(meal volume – antrum volume)), the third item is the antrum volume (e.g. 60 mL), the time</p>																
Minvol (mL)	40	Is the left volume at the end of the digestion																
Small intestine																		
Mixing profile	<p>1=-----**-----***** 2=**_*****_***** s=-----*-----</p>																	

Duodenum		
Volume (mL)		50
pH		5.9
Secretions (mL·min ⁻¹)	<i>Bile</i>	0.50
	<i>Pancreatin</i>	0.25
	<i>Base/SIES</i>	0.25

The base/SIES is secreted in a total flow rate of 0.25 mL·min⁻¹, and the HCl (acid) or SIES (electrolyte solution) is secreted to adjust the pH to 5.9.

Jejunum		
Volume (mL)		100
pH		6.5
Dialysate (mL·min ⁻¹)		10

Ileum		
Volume (mL)		100
pH		7.4
Dialysate (mL·min ⁻¹)		10
Absorption (mL·min ⁻¹)		0.4
Minil (%)		1

11.3. In vitro digestion

The different parts of the TIM-1 are depicted in figures 43 and 44.

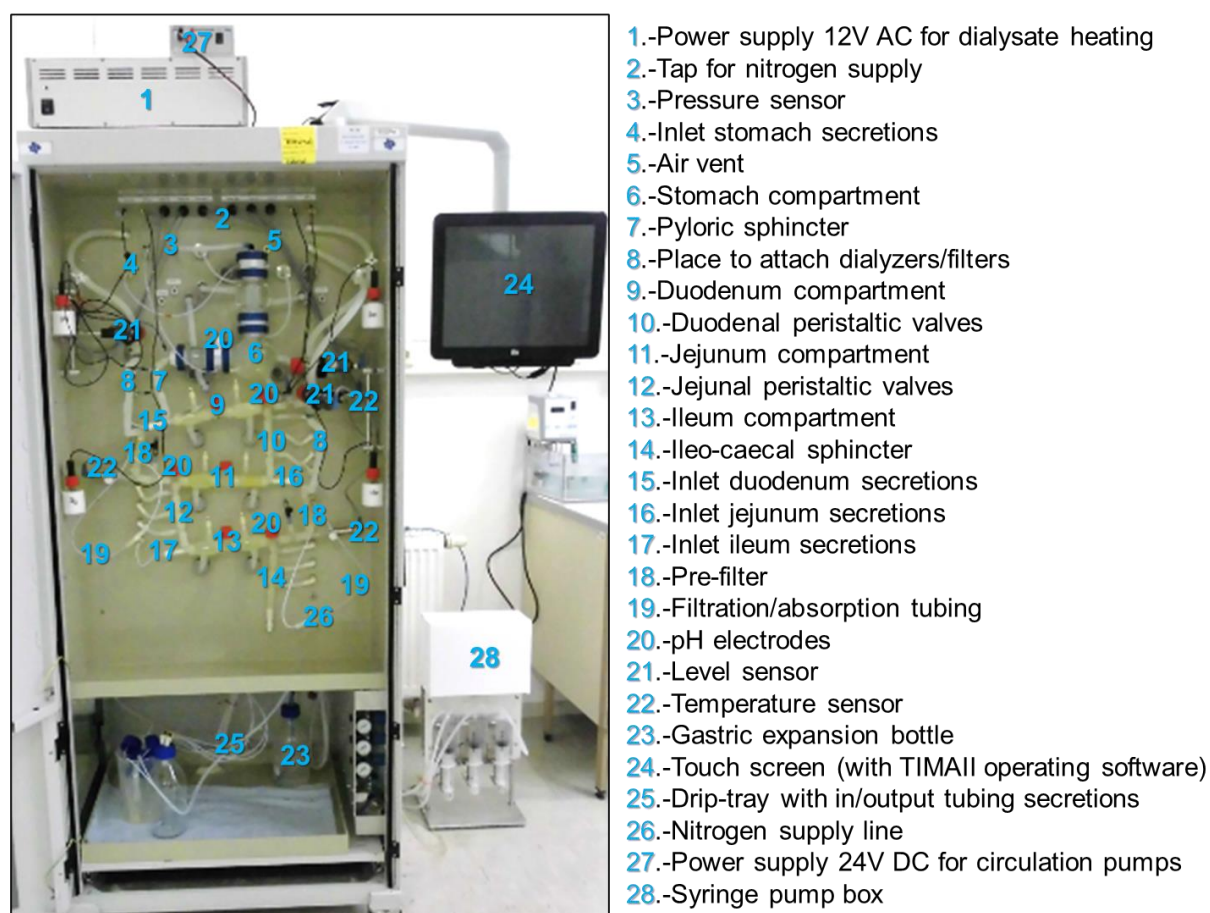


Figure 43. Frontal view of TIM-1 (dynamic digestion method)

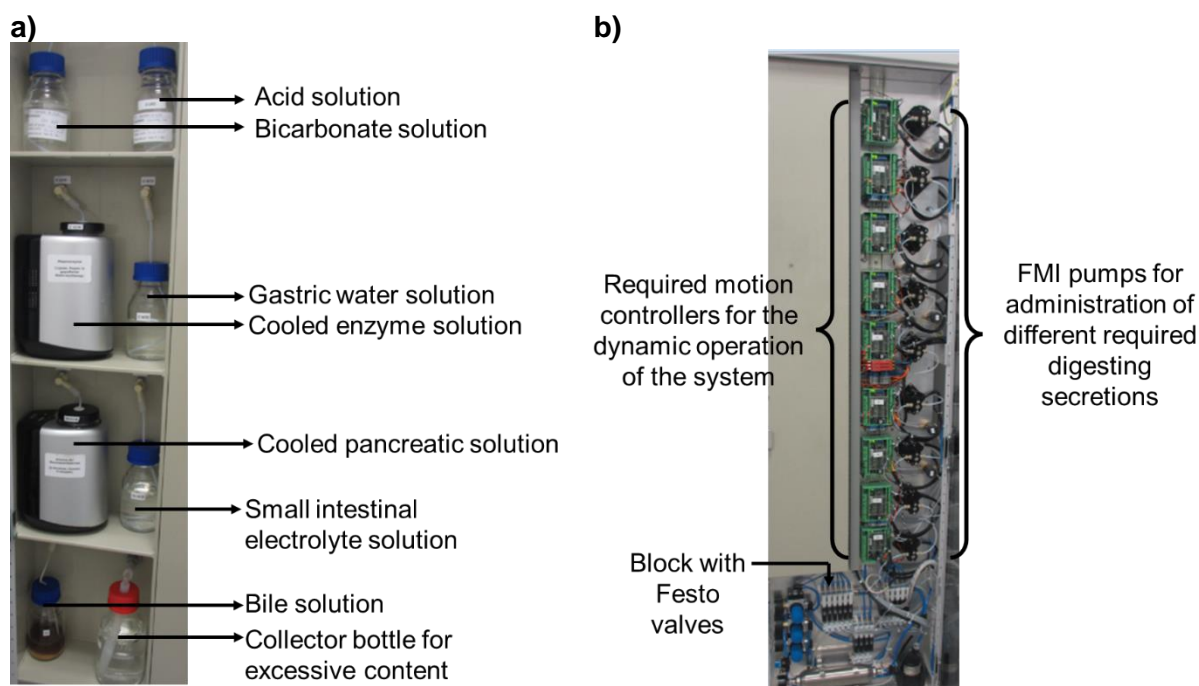


Figure 44. a) lateral secretion side of TIM-1, b) hardware lateral side

11.3.1. Pre-digestion

As for the static digestion method, some of the preparation procedures needed to be done before the digestion method itself.

The enzyme activity of the commercial enzymes (individual and mixture of enzymes) was measured. Then, the enzymatic solutions of the individual enzymes were prepared and stored in aliquots at -20°C (stock solutions: $2000 \text{ AU}\cdot\text{mL}^{-1}$ α -amylase, $5500 \text{ LU}\cdot\text{mL}^{-1}$ lipase, $600000 \text{ PU}\cdot\text{mL}^{-1}$, $800 \text{ TU}\cdot\text{mL}^{-1}$).

The simulated electrolyte fluids (gastric and small intestinal) were also prepared before the day of the run, the composition of these electrolyte solutions is specified in table 4. For the preparation of those electrolyte solutions, the commercial powders were mixed and dissolved with DI water at RT. The sodium bicarbonate (needed for the pH adjustment in the small intestine) was prepared by mixing the powder and DI water at $\sim 65^{\circ}\text{C}$ and 350 rpm. Then, the pH of the simulated intestinal fluid was adjusted to 7.0 ± 0.1 . And finally, the volume was adjusted to obtain the desired concentration of each salt in a volumetric flask.

The simulated gastric fluid was prepared ten times concentrated and the simulated intestinal fluid was prepared 25 times more concentrated (table 4). The electrolyte solutions were stored at RT.

The calculations with the simulated electrolyte solutions were done in volume (mL). However, to perform the *in vitro* digestion, the amount of electrolytes solution was measured in weight (g). For that reason, the densities of the simulated electrolyte solutions (gastric and small intestinal) were measured.

Finally, the virtual “molecular weight” of the bile was measured.

11.3.2. Start-up and preparation

For the start-up and preparation of the dynamic digestion method, the enzymatic solutions were brought out to defrost (at RT). Then, the meal, pancreatin and bile solutions were prepared. The meal was prepared as it is explained in section 8.6 and then it was pre-warmed to 37°C . For the pancreatic solution, the powders were mixed (individual enzymes and pancreatin) with DI water at RT and 600 rpm for at least 10 min, and then a centrifugation step was performed (9000 rpm, 20 min, 4°C – Heraeus Multifuge X3R, ThermoFisher) to remove the insoluble part as it could block the tubes of the dynamic system. A bile solution of 70 mM was prepared by adding the powder slowly to DI water at RT and constant mixing (600 rpm) until complete solubilization.

After that, the simulated fluids were diluted to reach the physiological concentrations, 53 g of simulated gastric fluid were mixed with 450 g of DI water (GELS) and 88 g of simulated intestinal fluid with 1920 g DI water (SIES). The gastric enzyme solution was prepared by mixing 151 g GELS, 1.5 mL sodium acetate buffer pH 5, 1.5 mL pepsin and 500 μ L DI water.

Finally, the start residues were prepared, and their composition is described in table 21:

Table 21. Composition of the start residues

Compartment	Solution	Amount
Stomach	DI water	99.2 g
	GELS	153.3 g
	Gastric enzyme solution	7.7 g
	α -amylase	2.5 mL
	Lipase	2 mL
	Pepsin	300 μ L
Duodenum	Bile	30.0 \pm 0.5 g
	Pancreatin	15.0 \pm 0.5 g
	Trypsin	1 mL
	SIES	15.0 \pm 0.5 g
Jejunum	SIES	100 g
Ileum	SIES	100 g

The pH of the start residue of the stomach was adjusted to 5.5 ± 0.5 . The start residues of the stomach and duodenum were kept at 5-8°C due to the presence of the enzymes, and before its use it was prewarmed to 37°C. The start residues of jejunum and ileum were kept at 37°C in a water bath.

Then, the dialysers were rinsed with DI water with the following flow rates and times:

- *Dial side*: max 240 mL·min⁻¹ (20 s)
- *Lumen side*: max 600 mL·min⁻¹ (10 min)

The TIM-1 system, when is not in use, is filled with a “cleaning solution” (mixture of 0.1 M NaOH and RBS: detergent). Therefore, the system was emptied and rinsed before its use. After the emptying, the compartments were rinsed with DI water for 10 min and the tubes with 50 mL of DI water. Then, the secretion tubes were filled with 10 mL of the secretion fluids, and the dialysers were filled with 40 mL of simulated intestinal fluid (only electrolytes). The dialysers were attached to the system just before filling them with the simulated fluid.

During this filling process, it was checked if the pumps suck/secrete the desired volume. The amount of secretion that was sucked by the pumps was weighed and compared with the theoretical volume (considering a density of ~ 1). When the difference between the experimental and theoretical values was lower than 5 % it was considered that the pumps work properly.

Once the dialysers were filled with the secretion fluid, they were disconnected from the system to check the pumps but also to avoid that the secretion fluid would go to the lumen of the compartment. This was important to be able to calculate the mass balance at the end of the run.

After that, the 4 pH electrodes were calibrated and placed in each compartment. The dialysis bottles were prepared (air removal) and placed below the system (figure 45).

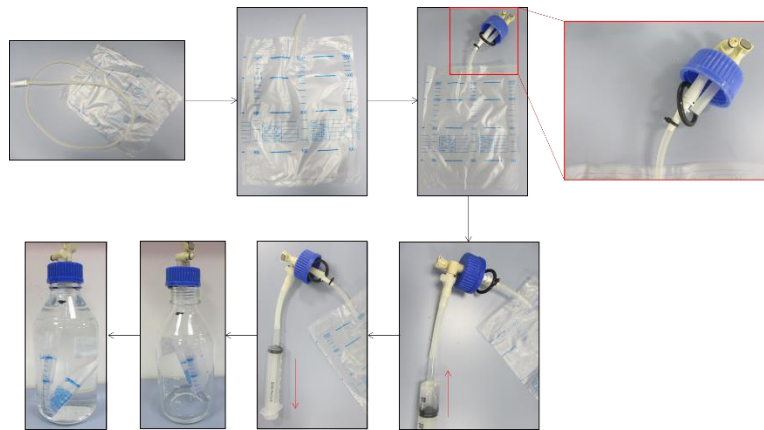


Figure 45. Protocol to check and empty the urine bags

In order to have the system ready for the dynamic digestion method, the compartments were emptied and the system was prewarmed to 37°C to have the TIM-1 ready for the dynamic digestion method. After that, to assure the correct mixing in the small intestine, the air from the water circulation was removed.

The secretion bottles were placed and connected to the system, the pancreatin and gastric enzyme solution were kept in coolers during the run because of the presence of the enzymes.

Finally, all the PVP valves were closed to not mix the start residues of the different compartments, the dialysers were attached to the system (figure 46) and a beaker in an ice bath was placed below the ileum compartment.

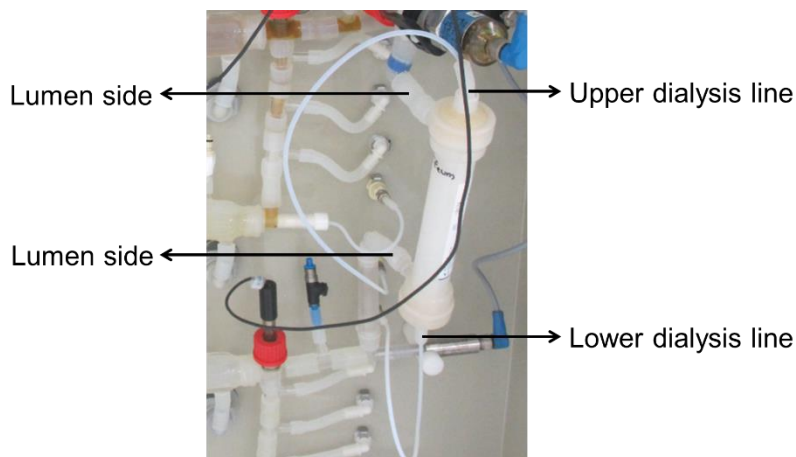


Figure 46. Connection of the dialysers with the system

11.3.3. Performance of the in vitro digestion

The system was filled always in the same order, from the ileum to the stomach. The start residues of the small intestine were introduced from the side of the compartment (left: duodenum and ileum, right: jejunum). The start residues were introduced into the duodenum, jejunum and ileum until they reached the level sensor, and the volume added were approximately 50, 100 and 100 g, respectively.

35 g of the meal was introduced using spatulas. The amount of meal that was added mimics the meal:enzyme ratio used in the static digestion method. Unlike the static digestion method, the spaghetti-shape was not used for the dynamic model as the meal was squeezed and well mixed with the secretions in the stomach. Just before starting the run, 265 g of the gastric start residue was introduced with a beaker, from the upper part of the stomach (figure 47).

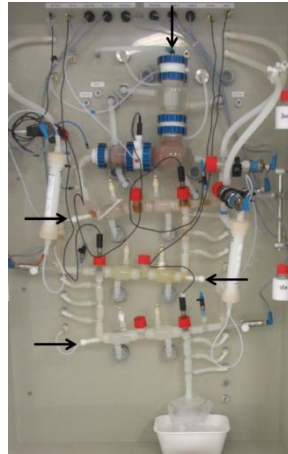


Figure 47. Places to introduce the start residues

The time needed to introduce the meal to the stomach was different each time and it could last for 2-3 min. To homogenise the time when the meal was in contact with the enzymes, the meal was introduced before the gastric start residue.

The intake filled in each part of the stomach was established by the first motility protocol (table 20). And the followed steps for the stomach filling were:

- Disconnect the pressure sensor
- Empty the stomach and check that the inside pressure is 0.1 bar
- Increase the volume of the body by about 80 mL
- Increase the volume of the bottom by 50 mL
- Increase the volume of the antrum by 60 mL
- Add the meal (35 g)
- Add ~150 mL of the start residues
- Empty the antrum to remove the air bubbles
- Increase the volume of the antrum to 60 mL again
- Increase the volume of the bottom by 50 mL
- Add ~50 mL of start residues
- Increase the volume of the bottom by 50 mL
- Add ~50 mL of start residues
- Increase the volume of the bottom by 42 mL
- Add ~15 mL of start residues
- Close the stomach
- Connect the pressure sensor

The run was started just after the stomach was filled with the meal and secretions. The dynamic *in vitro* digestion was run for five hours. During the run, the system was checked to assure that the digestion was performed properly. Among other checks, the secretion bottle levels, coolers function, pH and temperature, syringe pistons were checked during the run.

The dialysis bottles were exchanged each 30 min for the first 2 h and every 1 h the next 3 h, to be able to take samples and to follow the digestion of the meal over time (section 11.4).

After 5 h of digestion, the run was stopped. Then, the system was emptied compartment by compartment, from the stomach to the ileum, and at the end, the absorption/dialysis bottles were disconnected from the system.

To collect the end residues, the compartments were rinsed with the diluted simulated digestive fluids (GELS and SIES) and mixed with the end residue (see “11.4.Sampling times” section).

To check if the run was correctly performed or not, a mass balance was calculated, and the run was considered good when “delta IN” was less than 3 %:

$$IN(g) = \text{Start residues} + \text{Meal} + \text{Secretions} + \text{Rinse} \quad \text{Eq. 53}$$

$$\text{OUT(g)} = \text{End residues} + \text{Rinse} + \text{Absorption bottle} + \text{Ileum Efflux} \quad \text{Eq. 54}$$

$$\% \text{ delta IN} = \frac{\text{IN} - \text{OUT}}{\text{IN}} \cdot 100 \quad \text{Eq. 55}$$

The amount of start residues, secretions, end residues, and the ileum efflux were weighed check the mass balance and the run was considered good when the difference between the input and output was less than 3 %.

11.4. Sampling times

A total of 20 samples were taken during the in vitro digestion (TIM-1). To analyse the contents of the meal, a sample was taken before and after the heat treatment.

In the first 2 h of the run, a sample of the jejunum and ileal dialysates were taken every 30 min followed by hourly samples in the last 3 h. Those samples were collected after the lumen travelled through the dialysers. The bioaccessible fraction was obtained from these samples. As the enzymes could not pass through the dialysers, the digestion of the meal was stopped once the chyme passed the dialysers, then these samples could be collected at RT.

Two other samples were collected from the outlet of the ileum, which represent the chyme that would go to the large intestine, and it was assumed that it would not be available for absorption. During the digestion, the ileum was emptied in a beaker that was placed in an ice bath. The ice bath was used to stop the enzyme activity and therefore to stop the digestion.

At the end of the run, the device protocol was stopped and all the residues (from the stomach to the ileum) were collected. The stomach content was mixed with the duodenum content, and the jejunum was mixed with the ileum content. To take the end residues, the compartment was emptied and then it was rinsed with the simulated digestive fluid, the rinse was also mixed with the chyme.

To be able to compare the results from the static digestion method with the obtained results from the dynamic digestion method, the procedure to take the samples was kept identical. After the sampling point, the samples were treated in a boiling water bath to stop the enzyme activity, and then they were stored at -20°C.

12. In vitro digestion runs

Both, the static and dynamic digestion methods were used to perform in vitro digestions for different objectives, and depending on the objective, the performed runs were divided into different groups. Table 22 shows the composition of the 26 meals prepared for the in vitro digestion methods, where 10 of them were used in both methods, 15 of them were used only in the static method, and only one in the dynamic method.

Table 22. Meal composition used to perform the in vitro digestion methods

Ingredient	Blank runs			Positive control		Real meal			CH digestion		Matrix effect								Effect of protein				Effect of fat				
	1	2	3	4	5	6	7	8	9	10	11	12	13	14	15	16	17	18	19	20	21	22	23	24	25	26	
DI water	b																										
Xanthan					d																						
Carbohydrates																											
Glucose				b	d																						
Starch from rice									b		b	s	s	s					b	s			b	s			
Starch from potato										s					s	s	s	s			s	s			s	s	
Protein																											
Egg whites from chicken		b									b	s			s	s			b		s						
Casein			s										s	s			s	s		s		s					
Fat																											
Olive oil											b		s		s		s						b		s		
Butter												s		s		s		s						s		s	
Real meal																											
Rice						b																					
Potato							b																				
Cocoa cream								b																			

s: meal used in static digestion method, d: meal used in dynamic digestion method, b: meal used in both methods

The blank, water and only protein runs, were performed to verify the settings and to qualify the analytical methods (section 13.1).

The positive control runs were carried out to assure that the used concentration was correct to be analysed, to guarantee that all the meal added to the digestion method can be analysed. But also, to have an idea of the meal distribution in the digestive tract, mainly in the dynamic digestion method. The positive control was first performed with a solution of glucose (the same concentration as the carbohydrate source used for the other runs). However, the prepared meals had a higher viscosity than the glucose solution. As the viscosity of the meal could have an impact on the digestibility (e.g., would affect the stomach emptying), a mixture of glucose and xanthan gum was prepared and used in the dynamic digestion method. The xanthan gum was used as it would not be digested during the run and would only contribute to the viscosity of the meal. And the amount of xanthan added to the glucose solution was selected to mimic the viscosity of the prepared meals.

The real meals were used to check if the in vitro digestion methods used in this thesis were a good alternative for the in vivo methods to calculate the glycaemic index.

Then, the digestion of two different sources of starch was studied to check, if the starch type had an impact on its digestibility. But, as the meals usually not only contains carbohydrates, the effect of the matrix was also studied. Finally, it was checked, if the proteins or fats would affect the carbohydrate digestion.

Three repetitions with the static digestion method were performed, and due to limited access two repetitions with the dynamic method.

13. Analytical methods

Three aliquots of each sample were frozen, one aliquot was used to measure the reducing sugars, another one for the glucose and starch content measurement. The third aliquot was kept as back up.

Therefore, each sample was frost/defrost just once for each analytical measurement, and the possible differences obtained between runs would not be due to frozen/thaws cycles. The day before the analytics, the samples were placed in the fridge to be slowly defrosted.

13.1. Reducing sugars

The selected method for the determination of the degree of hydrolysis is the neocuproine method (figure 48) as it was proven to have a higher sensitivity and precision than the widely used dinitrosalicylic acid colorimetric method. The neocuproine method is based on the Cu(II) reduction by reducing sugars and the complexation of reduced transition metal ion with neocuproine (78).

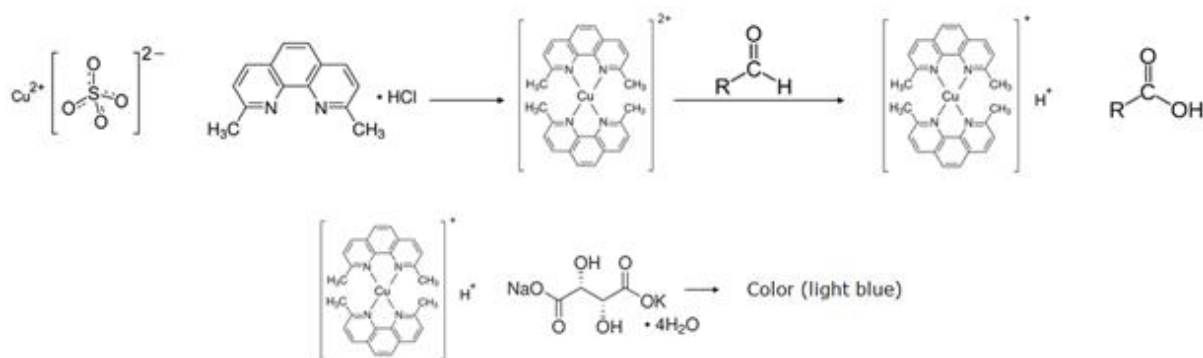


Figure 48. Principle reactions that occur during neocuproine method

With this method it was possible to calculate the amount of reducing ends, which represents the amount of cuts that the starch suffered during its digestion. Therefore, with the amount of reducing ends together with the analysed/calculated starch content (section 13.3), it was possible to calculate the degree of hydrolysis (section 0).

For the determination of reducing sugars, the reagents were prepared the same day of their usage. And the samples, once defrosted, were properly diluted with DI water to fit the concentration range of the method (5 – 75 μM).

10 mM copper sulphate was prepared by mixing 25 mg of the powder with ~8 mL of DI water at RT, 350 rpm until complete solubilisation, and then the volume was adjusted to 10 mL in a volumetric flask. The 15 mM neocuproine solution was prepared by mixing 31.2 mg of neocuproine with ~8 mL of ethanol at RT, 350 rpm until complete solubilization, and the volume was then adjusted to 10 mL with ethanol in a volumetric flask.

The alkaline tartrate solution was prepared by weighing 200 mg of sodium carbonate, 200 mg of sodium hydroxide and 282.2 mg of potassium sodium tartrate, the powders were dissolved in ~8 mL of DI water at RT, 350 rpm and the volume was adjusted to 10 mL in a volumetric flask.

A stock solution of 2 mM glucose was prepared by mixing 9 mg of glucose in ~20 mL of DI water at RT, 350 rpm until complete solubilisation, and the volume was then adjusted to 25 mL with DI water in a volumetric flask.

A standard curve was prepared, preparing different dilutions from 2 mM glucose solution (table 23):

Table 23. Glucose concentration of the standard curve

Standard	Glucose (μM)
1	150
2	100
3	50
4	20
5	10
6	2

For the measurement of the reducing sugars, 200 μL copper sulphate were mixed in a 1.5 mL conical tube with 200 μL alkaline tartrate, 200 μL neocuproine and 400 μL of sample at RT. Then, it was incubated at 60°C for exactly 20 min (Comfort thermomixer, Eppendorf), after the incubation, it was quickly placed in an ice bath to stop the reaction and the colour development. Finally, the absorbance was read at 460 nm (Sunrise microplate reader, Tecan).

For the standard curve and blank, the same protocol was followed except that the sample was substituted by the standard solutions and DI water, respectively.

This method measures the amount of reducing ends, and as the glucose was used as standard, the obtained glucose concentration was equivalent to reducing ends.

For the calculation of the reducing sugars content, the obtained absorbance was first corrected with the blank (eq. 56). To construct the standard curve, the corrected absorbance was depicted versus the glucose concentration of the standards.

Then, for the calculation of the reducing sugars content (μM) in the digestive samples, the corrected absorbance of the samples was interpolated in the standard curve (eq. 57).

$$\text{Absorbance}_{\text{corrected}} = \text{Absorbance} - \text{Absorbance}_{\text{blank}} \quad \text{Eq. 56}$$

$$[\text{Reducing sugars}]_{\text{sample}} (\mu\text{M}) = \frac{\text{Absorbance}_{\text{corrected}} - \text{Intercept}}{\text{Slope}} \cdot \text{df} \quad \text{Eq. 57}$$

Eq. 57 gives the amount of reducing ends (cuts) in μM , however for the degree of hydrolysis calculation, the reducing ends needed to be expressed in mg (eq. 58).

$$V_{\text{sample}}(\text{mL}) \cdot \frac{\mu\text{mol glucose}}{10^3 \text{mL}} \cdot \frac{1 \text{mmol}}{10^3 \mu\text{mol}} \cdot \frac{180.16 \text{ mg glucose}}{1 \text{ mmol glucose}} = \text{mg glucose in samples} \quad \text{Eq. 58}$$

The obtained amount (mg) of reducing ends present in the samples of a run was corrected with the amount of reducing ends found in the blank runs.

The protein and its digestive products also contain reducing ends; therefore, they could interfere the obtained results. For that reason, experiments with a blank with DI water and a blank with the protein source were carried out with the *in vitro* digestion methods.

13.2. Glucose

To be able to calculate the glycaemic index, the glucose and fructose content in the samples were measured with the D-Fructose and D-Glucose assay kit from Megazyme (K-FRUGL 04/18). The content of the kit was one bottle of 15 mL of buffer pH 7.6, a bottle of NADP⁺, ATP and PVP (mixture of powders), 2.25 mL of hexokinase plus glucose-6-phosphate dehydrogenase suspension (HK/G6P-DH), 2.25 mL of phosphoglucose isomerase suspension (PGI) and 5 mL of standard solution (0.2 mg·mL⁻¹ D-glucose and 0.2 mg·mL⁻¹ D-fructose).

All the reagents were used as supplied except for the NADP⁺, ATP and PVP bottle, which needed to be dissolved with 12 mL of DI water.

With this method, the glucose and fructose were phosphorylated by the hexokinase enzyme (HK) and ATP (adenosine-5'-triphosphate) to glucose-6-phosphate (G6P) and fructose-6-phosphate (F6P) with the simultaneous formation of adenosine-5'-diphosphate (ADP) (figure 49):

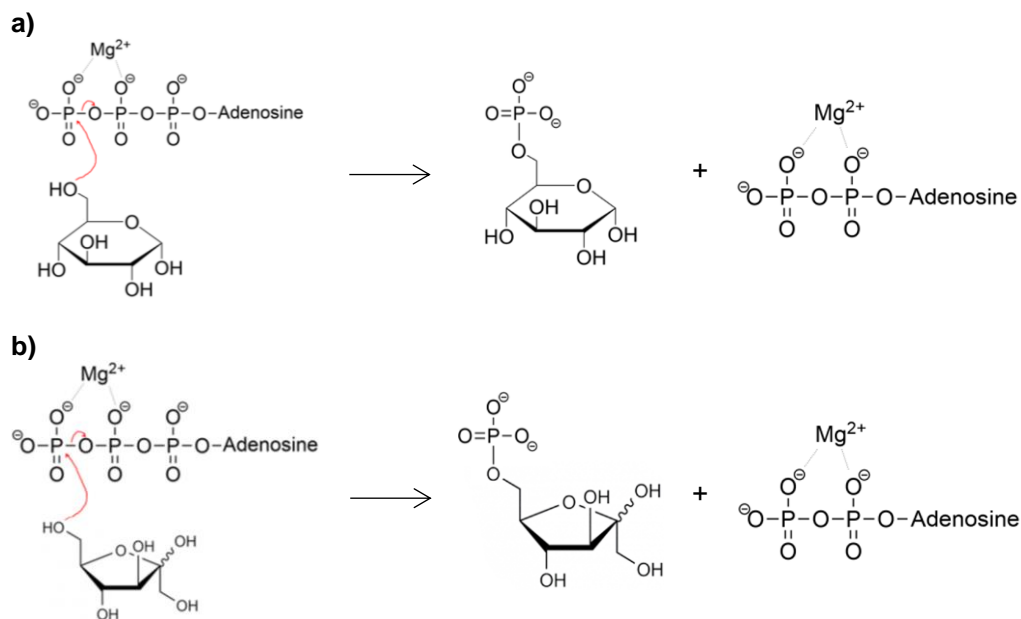


Figure 49. Phosphorylation of a) glucose and b) fructose

For one side, the phosphorylated glucose was oxidized with the presence of NADP⁺ (figure 50):

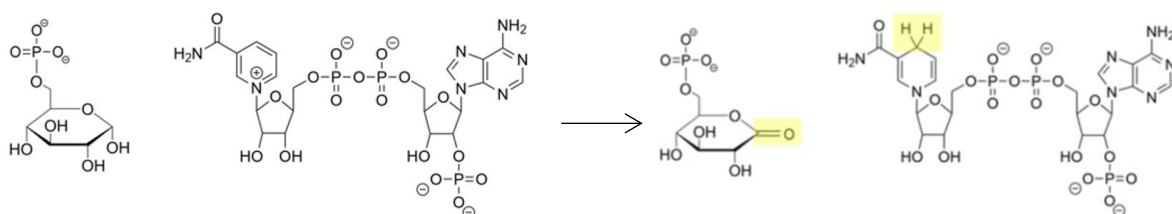
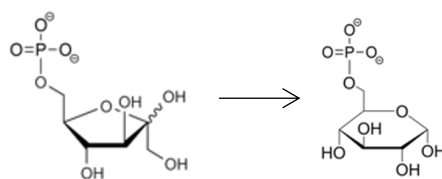


Figure 50. Oxidation of the phosphorylated glucose

And on the other side, the phosphorylated fructose was first converted to phosphorylated glucose due to the presence of PGI, and then underwent the same oxidation as the phosphorylated glucose (figure 51).

a)



b)

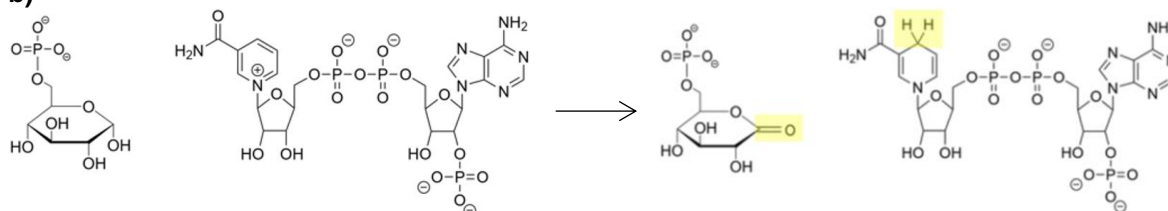


Figure 51. a) Conversion of the phosphorylated fructose to phosphorylated glucose, b) Oxidation of phosphorylated glucose

For the measurement of the glucose and fructose content, the samples were diluted based on the previously analysed reducing ends, and a solution of around $500 - 1000 \mu\text{g}\cdot\text{mL}^{-1}$ of reducing ends were prepared.

The standard curve was only prepared periodically (not before each measurement) to assure the linearity of the method.

For the glucose/fructose measurement, $200 \mu\text{L}$ of DI water were added into a plastic microcuvette ($50 - 1000 \mu\text{L}$ Uvette Eppendorf) and mixed with $10 \mu\text{L}$ of the diluted sample, $10 \mu\text{L}$ of the buffer and $10 \mu\text{L}$ of the NADP+/ATP mixture. It was mixed by inversion with the help of a plastic lid that fitted into the cuvette.

It was let for approximately 3 min at RT and then the absorbance was read at 340 nm (Absorbance 1) (Biospectrometer, Eppendorf). After that, $2 \mu\text{L}$ of the HK/G6P-DH suspension were added to the mixture, it was mixed by inversion and it was let for at least 5 min at RT. The absorbance was then read also at 340 nm (Absorbance 2).

To measure the fructose content, $2 \mu\text{L}$ of PGI were added to the previous mixture, mixed and let at RT for 10 min. Finally, the absorbance was read at 340 nm (Absorbance 3).

For the standard curve and blanks, the standard solutions and DI water were substituted for the sample in the protocol.

For the calculation of the glucose content, the absorbance was first corrected applying eq. 59:

$$\text{Absorbance}_{\text{corrected}} = \text{Absorbance 2} - \text{Absorbance 1} \quad \text{Eq. 59}$$

Then, the glucose concentration present in the digestive samples was calculated with the following equation:

$$\text{glucose} (\text{mg}\cdot\text{mL}^{-1}) = \frac{V_{\text{final}} \cdot MW_{\text{glucose}} \cdot \text{Absorbance}_{\text{corrected}} \cdot df}{\epsilon_{\text{NADPH}} \cdot b \cdot V_{\text{sample}}} \quad \text{Eq. 60}$$

Where V_{final} is the final volume of the reaction mixture (0.232 mL), MW_{glucose} is the molecular weight of the glucose ($180.16 \text{ g}\cdot\text{mol}^{-1}$), $\text{Absorbance}_{\text{corrected}}$ the obtained absorbance in eq. 59, df is the dilution factor, ϵ_{NADPH} is the extinction coefficient of NADPH ($6300 \text{ L}\cdot\text{mol}^{-1}\cdot\text{cm}^{-1}$), b is the light path (1 cm) and V_{sample} is the volume of the sample in the reaction mixture (0.01 mL).

After that, the glucose amount (mg) in the digestive samples was calculated by multiplying the glucose concentration ($\text{mg}\cdot\text{mL}^{-1}$) for the total volume of the sample (e.g., volume of the oral phase: 10 mL).

The fructose content was calculated applying eq. 60, except for the final volume (0.234 mL) and the corrected absorbance (calculated in eq. 61).

$$\text{Absorbance}_{\text{corrected}} = \text{Absorbance 3} - \text{Absorbance 2} \quad \text{Eq. 61}$$

The glucose and fructose content (mg) obtained for the digestive samples, was corrected with the glucose/fructose obtained in the blank runs (DI water as meal) of the in vitro digestion methods.

13.3. Starch

To be able to calculate the degree of hydrolysis or the percentage of meal that has been converted into glucose, the starch content in each sample needed to be measured.

In the static digestion method, the amount of starch (mg) was the same amount that was added with the 5 g of meal:

$$M_d \cdot \frac{CH_m}{M_t} \cdot \frac{S_p}{100} = S_{ds} \quad \text{Eq. 62}$$

Where M_d is the exact amount of meal (g) added for static digestion method (~5 g), CH_m is the amount of starch added for the meal preparation (e.g., 29.5 g), M_t is the total amount of meal prepared (e.g., 150 g), S_p the starch purity of the commercial powder (e.g., 88.2 %) and S_{ds} is the amount of starch used for the static digestion method (e.g., 873.3 mg).

In the dynamic digestion method, the amount of meal present in the bioaccessible samples could not be calculated, and for that reason, the starch content needed to be measured. The method for the starch measurement was based on the complete hydrolysis of the meal followed by the glucose measurement.

The starch could be digested by two different methods; enzymatic and acid hydrolysis. Among other reasons, the enzymatic hydrolysis was discarded as the maximum hydrolysis achieved with this kind of hydrolysis was 77 %.

The protocol used for the acidic hydrolysis was based on the work done by Haebel et al (79). In their protocol, the starch was suspended in 0.7 M HCl and incubated for 3h at 95°C, following neutralization with an equal volume of 0.7 M NaOH.

However, when these conditions were checked, the hydrolysis was not complete. For that reason, the incubation time was slightly modified (figure 52).

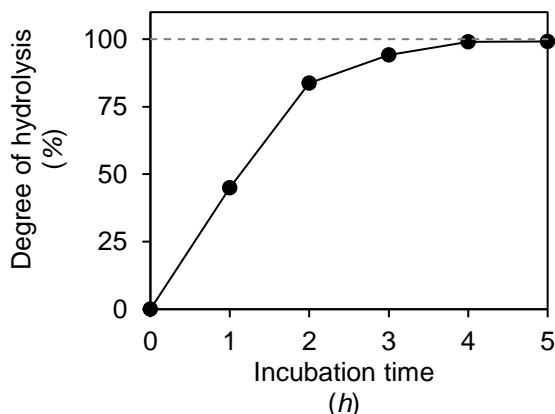


Figure 52. Effect of the incubation time on the degree of hydrolysis of the starch

For the starch hydrolysis, 500 µL of the digestive sample were mixed with 500 µL of 1.4 M HCl (final concentration: 0.7 M) and incubated at 95°C for 5h (Comfort thermomixer, Eppendorf). After that, it was cooled down to RT and the pH of the mixture was neutralised with the addition of 1.4 M NaOH.

With this hydrolysis, the starch was converted into glucose, which was then measured with the Megazyme kit (section 13.2). With these conditions, the achieved efficiency of the hydrolysis was 99.1 %, which was taken into account for the starch content calculation (eq. 66).

For the starch content calculations, the measured starch was converted into the commercial powder taking into account the impurities of the starch (eq. 63 – 65).

$$\text{Starch}_{\text{pure}} \text{ (mg)} = \text{Starch}_{\text{impure}} \text{ (mg)} - \text{Impurities (mg)} \quad \text{Eq. 63}$$

$$\text{Impurities (mg)} = \text{Starch}_{\text{impure}} \text{ (mg)} \cdot \frac{\text{Impurities (\%)}}{100} \quad \text{Eq. 64}$$

$$\text{Starch}_{\text{impure}} \text{ (mg)} = \frac{100 \cdot \text{Starch}_{\text{pure}} \text{ (mg)}}{100 - \text{Impurities (\%)}} \quad \text{Eq. 65}$$

$$\text{Starch}_{\text{impure corrected}} \text{ (mg)} = \text{Starch}_{\text{impure}} \text{ (mg)} \cdot \frac{\text{Hydrolysis}_{\text{efficiency}} \text{ (\%)}}{100} \quad \text{Eq. 66}$$

Where $\text{Starch}_{\text{pure}}$ is the measured glucose after the hydrolysis, $\text{Starch}_{\text{impure}}$ is the commercial powder of starch, Impurities are the impurities present in the commercial powder and $\text{Starch}_{\text{impure corrected}}$ is the starch content of the sample corrected with the hydrolysis efficiency (99.1 %).

The meal recovery was calculated to know if the amount of starch added to the system was recovered after the run. The recovery could be different to 100 % as part of the samples would be lost or not completely recovered from the system, but also could be due to the analytical methods. Therefore, the recovery was also considered for the starch determination (eq. 67):

$$\text{Meal}_{\text{corrected}} = \text{Starch}_{\text{impure corrected}} \text{ (mg)} \cdot \frac{\text{IN (mg)}}{\text{OUT (mg)}} \quad \text{Eq. 67}$$

Where $\text{Meal}_{\text{corrected}}$ is the amount of starch present in the digestive samples corrected with the recovery of the run, $\text{Starch}_{\text{impure corrected}}$ is the starch content calculated in eq. 66, IN is the amount of starch that was added to the stomach of the dynamic system and OUT is the total amount of starch recovered after the run.

13.4. Degree of hydrolysis calculation

The digestibility of the meals was given as the degree of hydrolysis, which was calculated by dividing the number of cuts that starch suffered by the amount of meal present in each sample. The number of cuts was measured as it is explained in section 13.1 (reducing sugars), and the meal was calculated/measured as it is calculated in equation eq. 67 (section 13.3.).

$$\text{Degree of hydrolysis (\%)} = \frac{\text{Reducing sugars (mg)}}{\text{Starch (mg)}} \cdot 100 \quad \text{Eq. 68}$$

13.5. Glycaemic index calculation

For the glycaemic index calculation, the amount of fructose and glucose released from the meal was measured (section 13.2). The fructose was also taken into account as it has been demonstrated that 42 % of the fructose is converted into glucose in the small intestine and therefore it has an impact on the glycaemic index (80).

Therefore, the total glucose ($Glucose_T$) was first calculated with the following equation:

$$\text{Total glucose (mg)} = \text{Glucose (mg)} + 0.42 \cdot \text{Fructose (mg)} \quad \text{Eq. 69}$$

The glycaemic index was calculated as the incremental area under the curve (iAUC) for glucose released from the test food divided by the iAUC of a reference food (glucose) containing the same amount of carbohydrate.

Unlike the in vivo systems, the used in vitro digestion method did not take into account the insulin secretion, which has a direct impact on blood glucose levels. However, the insulin was absent for both, the run with the reference food and the run with the test food. And as for the in vivo glycaemic index calculation the iAUC of the test food was divided by the iAUC of the test food.

However, to assure that it was a good method to predict the glycaemic index, meals with known glycaemic index were checked with both methods (static and dynamic digestion methods).

The amount of meal used in the in vitro digestion methods was not exactly the same for all the runs, therefore this would bring to small differences in the obtained amount of glucose released. As a correction measure, the iAUC was calculated using the percentage of glucose instead of the mg of glucose. Therefore, before the calculation of the area under the curve, the percentage of glucose was calculated.

The released glucose in the small intestine phase was considered for the GI calculation in the static digestion method. As the digestive products were not removed during the digestion of the static method, the measured glucose (eq. 60, 61 and 69) and the calculated starch (eq. 62) were expressed as cumulative values. Therefore, the percentage of glucose could be directly calculated as follows:

$$\text{Glucose (\%)} = \frac{\text{Glucose}_T (S)}{\text{Starch} (S)} \cdot 100 \quad \text{Eq. 70}$$

Where $Glucose_T (S)$ and $Starch (S)$ are the total glucose and starch present in the samples of the static method.

In the dynamic digestion method, only the bioaccessible fraction (cumulative) was taken into account for the GI calculation:

$$\text{Glucose}_{BA} = \text{Glucose}_T (\text{jejunum}) + \text{Glucose}_T (\text{ileum}) \quad \text{Eq. 71}$$

$$\text{Starch}_{BA} = \text{Meal}_{\text{corrected}} (\text{jejunum}) + \text{Meal}_{\text{corrected}} (\text{ileum}) \quad \text{Eq. 72}$$

$$\text{Glucose}_{CUM}(D) = \text{Glucose}_{BA} (t) + \text{Glucose}_{BA} (t-1) \quad \text{Eq. 73}$$

$$\text{Starch}_{CUM}(D) = \text{Starch}_{BA} (t) + \text{Starch}_{BA} (t-1) \quad \text{Eq. 74}$$

$$\text{Glucose(\%)} = \frac{\text{Glucose}_{CUM}(D)}{\text{Starch}_{CUM}(D)} \cdot 100 \quad \text{Eq. 75}$$

Where $Glucose_{BA}$ is the amount of glucose in the bioaccessible fraction, $Glucose_T (\text{jejunum})$ and $Glucose_T (\text{ileum})$ are the total amount of glucose in the jejunum and ileum, respectively. $Starch_{BA}$ is the starch content in the bioaccessible fraction, $Meal_{\text{corrected}} (\text{jejunum})$ and $Meal_{\text{corrected}} (\text{ileum})$ are the starch content in jejunum and ileum. $Glucose_{CUM} (D)$ and $Starch_{CUM} (D)$ are the cumulative glucose and starch content in the bioaccessible fraction of the dynamic system, t represents the sample in the current time point and $t-1$ the sample in the previous time point.

The trapezoid method was used for the iAUC calculation. This method is based on the division of the area in different strips of equal width, as it is shown in figure 53:

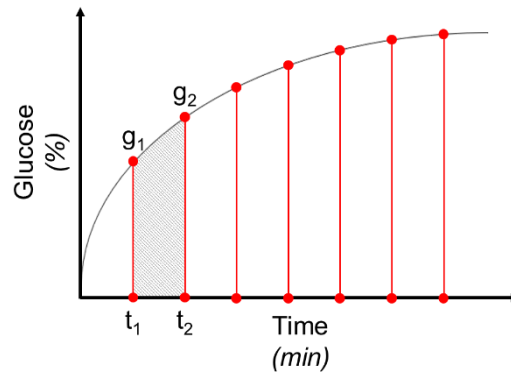


Figure 53. Representation of the trapezoid method

Then, approximate the area of each strip to the area of the trapezium, and the total sum of these approximations gives the final area under the curve.

$$AUC = \sum \left(\frac{g_1 + g_2}{2} \cdot (t_2 - t_1) \right) \quad \text{Eq. 76}$$

After the AUC calculation, the glycaemic index (GI) could be calculated:

$$GI(\%) = \frac{AUC_{\text{test food}}}{AUC_{\text{reference food}}} \cdot 100 \quad \text{Eq. 77}$$

Where $AUC_{\text{test food}}$ is the area under the curve of the test food and the $AUC_{\text{reference food}}$ is the area under the curve of the reference food, which is the glucose (in vitro digestion performed with the positive control).

14. References

1. P. Bernfeld, *Methods Enzymol.*, ed. N. Kaplan and N. Colowick, Academic Press, United States, 1st edn, 1955, **17**, 149 – 158.
2. M. Minekus, M. Alminger, P. Alvito, S. Ballance, T. Bohn, C. Bourlieu, F. Carrière, R. Boutrou, M. Corredig, D. Dupont, C. Dufour, L. Egger, M. Golding, S. Karakaya, B. Kirkhus, S. Le Feunteun, U. Lesmes, A. Macierzanka, A. Mackie, S. Marze, D.J. McClements, O. Ménard, I. Recio, C.N. Santos, R.P. Singh, G.E. Vegarud, M.S. Wickham, W. Weitschies and A. Brodkorb, A standardized static in vitro digestion method suitable for food – an international consensus, *Food Funct.*, 2014, **5(6)**, 1113 – 1124.
3. G.H. Jeffery, J. Bassett, J. Mendham and R.C. Denney, *Vogel's textbook of quantitative chemical analysis*, John Wiley & Sons Inc, United States, 1989.
4. M.L. Anson, The estimation of pepsin, trypsin, papain and cathepsin with haemoglobin, *J. Gen. Physiol.*, 1938, **22**, 79 – 89.
5. M.L. Anson and A.E. Mirsky, The estimation of pepsin with haemoglobin, *J. Gen. Physiol.*, 1932, **16**, 59 – 63.
6. K. Żamojć, D. Kamrowski, M. Zdrowowicz, D. Wyrzykowski, W. Wiczak, L. Chmurzyński and J. Makowska, A pentapeptide with tyrosine moiety as fluorescent chemosensor for selective nanomolar-level detection of copper(II) ions, *Int. J. Mol. Sci.*, 2020, **21**, 743 – 759.
7. B.C.W. Hummel, A modified spectrophotometric determination of chymotrypsin, trypsin and thrombin, *Can. J. Biochem. Physiol.*, 1959, **37**, 1393 – 1399.
8. R.M. Broadway, Are insects resistant to plant proteinase inhibitors, *J. Insect Physiol.*, 1995, **41**, 107 – 116.
9. <http://www.cost-infogest.eu/> (March 2021)
10. M.M.L. Grundy, E. Abrahamse, A. Almgren, M. Alminger, A. Andres, R.M.C. Ariëns, S. Bastiaan-Net, C. Bourlieu-Lacanal, A. Brodkorb, M.R. Bronze, I. Comi, L. Couëdelo, D. Dupont, A. Durand, S.N. El, T. Grauwet, C. Heerup, A. Heredia, M.R. Infantes Garcia, C. Jungnickel, I. E. Klosowska-Chomiczweska, M. Létisse, A. Macierzanka, A.R. Mackie, D.J. McClements, O. Menard, A. Meynier, M.C. Michalski, A.I. Mulet-Cabero, A. Mullertz, F.M. Payeras Perelló, I. Peinado, M. Robert, S. Secouard, A.T. Serra, S.D. Silva, G. Thomassen, C. Tullberg, I. Undeland, C. Vaysse, G.E. Vegarud, S.H.E. Verkempinck, M. Viau, M. Zahir, R. Zhang and F. Carrière, INFOGEST inter-laboratory recommendations for assaying gastric and pancreatic lipases activities prior to in vitro digestion studies, *J. Funct. Foods*, 2021, **82**, 104497 (1 – 13).
11. J. Keller and P. Layer, Human pancreatic exocrine response to nutrients in health and disease, *Gut*, 2005, **54**, 1 – 28.
12. J.M. Braganza, K. Herman, P. Hine, G. Kay and G.I. Sandle Pancreatic enzymes in human duodenal juice – a comparison of responses in secretin pancreozymin and Lundh Borgström tests, *Gut*, 1978, **19**, 358 – 366.
13. J. A. Rendleman, Hydrolytic action of α -amylase on high-amylose starch of low molecular mass, *Biotechnol. Appl. Biochem.*, 2000, **31**, 171 – 178.
14. W. Sheldon, Congenital pancreatic lipase deficiency, *Arch. Dis. Childh.*, 1964, **39**, 268 – 271.
15. H. Holm, L.E. Hanssen, A. Krogdahl and J. Florholmen, High and low inhibitor soybean meals affect human duodenal proteinase activity differently: In vivo comparison with bovine serum albumin, *J. Nutr.*, 1988, **118**, 515 – 520.
16. J.C.M. Hafkenschied, M. Hessels and E.W. van der Hoek, Determination of α -amylase, trypsin and lipase in duodenal fluid: Comparison of methods, *J. Clin. Chem. Clin. Biochem.*, 1983, **21**, 167 – 174.

17. E.L. McConnell, H.M. Fadda and A.W. Basit, Gut instincts: Explorations in intestinal physiology and drug delivery, *Int J Pharm*, 2008, **364**, 213 – 226.
18. M.R. Dukejart, S.K. Dutta and J. Vaeth, Dietary fiber supplementation: effect on exocrine pancreatic secretion in man, *Am. J. Clin. Nutr.*, 1989, **50**, 1023 – 1028.
19. E.P. DiMagno, J.R. Maragelada, L. Vay, W. Go and C.G. Moertel, Fate of orally ingested enzymes in pancreatic insufficiency, *N. Engl. J. Med.*, 1977, **296(23)**, 1318 – 1322.
20. B.J. Haverback, B. Dyce, H. Bundy and H.A. Edmondson, Trypsin, trypsinogen and trypsin inhibitor in human pancreatic juice, *The American Journal of Medicine*, 1960, **29**, 421 – 433.
21. M. Armand, Lipases and lipolysis in the human digestive tract: where do we stand, *Curr. Opin. Clin. Nutr. Metab. Care*, 2007, **10**, 156 – 164.
22. M. Armand, B. Pasquier, M. André, P. Borel, M. Senft, J. Peyrot, J. Salducci, H. Portugal, V. Jaussan and D. Lairon, Digestion and absorption of 2 fat emulsions with different droplet sizes in the human digestive tract, *Am. J. Clin. Nutr.*, 1999, **70(6)**, 1096 – 1106.
23. F. Carrière, P. Grandval, C. Renou, A. Palomba, F. Priéri, J. Giallo, F. Henniges, S. Sander-Struckmeier and R. Laugier, Quantitative study of digestive enzyme secretion and gastrointestinal lipolysis in chronic pancreatitis, *Clin. Gastroenterol. Hepatol.*, 2005, **3**, 28 – 38.
24. P. Layer, J. Keller and P.G. Lankisch, Pancreatic enzyme replacement therapy, *Curr. Gastroenterol. Rep.*, 2001, **3**, 101 – 108.
25. E. Truscheit, W. Frommer, B. Junge, L. Müller, D.D. Schmidt and W. Wingender, Chemistry and Biochemistry of microbial α -glucosidase inhibitors, *Angew. Chem. Int. Ed. Engl.*, 1981, **20**, 744 – 761.
26. G. Lorkowski, Gastrointestinal absorption and biological activities of serine and cysteine proteases of animal and plant origin: review an absorption of serine and cysteine proteases, *Int. J. Physiol. Pathophysiol. Pharmacol.*, 2012, **4**, 10 – 27.
27. O. Prykhodko, S.G. Pierzynowski, E. Nikpey, E.A. Sureda, O. Fedkiv and B.R. Weström, Pancreatic and pancreatic-like microbial proteases accelerate gut maturation in neonatal rats, *PLoS One*, 2015, **10**, e0116947 (1 – 14).
28. http://www.pharmacopeia.cn/v29240/usp29nf24s0_m60270.html#usp29nf24s0_m60270s21 (March 2021).
29. H.K. Biesakski, S.C. Bischoff and C. Puchstein, *Ernährungsmedizin: Nach dem neuen Curriculum Ernährungsmedizin der Bundesärztekammer*, Thieme, Germany, 2010.
30. E.M. Widdowson, Assessment of the energy value for human foods, *P. Nutr. Soc.*, 1955, **14**, 142 – 154.
31. S.S. Nielsen, *Food analysis*, Springer Science & Business Media, Boston, 2010.
32. T. Heuer, C. Krems, K. Moon, C. Brombach and I. Hoffmann, Food consumption of adults in Germany: results of the German National Nutrition Survey II based on diet history interviews, *Br. J. Nutr.*, 2015, **113**, 1603 – 1614.
33. A. Straßburg, M. Eisinger-Watzl, C. Krems, A. Roth and I. Hoffmann, Comparison of food consumption and nutrient intake assessed with three dietary assessment methods: results of the German National Nutrition survey II, *Eur. J. Clin. Nutr.*, 2019, **58**, 193 – 210.
34. M. Allman-Farinelli, *Essentials of human nutrition*, ed. J. Mann and A.S. Truswell, Oxford University Press, Oxford, 2nd edn, 2002, **22**, 383 – 414.

35. <https://www.gov.uk/government/publications/nutrient-analysis-survey-of-biscuits-buns-cakes-and-pastries> (November 2019)
36. M. Carocho, J.C.M. Barreira, L. Barros, A. Bento, M. Cámara, P. Morales and I.C.F.R. Ferreira, Traditional pastry with chestnut flowers as natural ingredients: An approach of the effects on nutritional value and chemical composition, *J. Food Compos. Anal.*, 2015, **44**, 93 – 101.
37. J.Y. Chen, Y. Miao, H. Zhang and R. Matsunaga, Non-destructive determination of carbohydrate content in potatoes using near infrared spectroscopy, *J. Near Infrared Spec.*, 2004, **12**, 311 – 314.
38. K.M. Gupta, *Engineering Materials: Research, applications and advances*, CRC Press, Florida, 1st edn, 2015, **7**, 165 – 192.
39. J.A. Woolfe, *The potato in the human diet*, Cambridge University Press, Cambridge, 1st edn, 1987, **2**, 19 – 57.
40. D.G. Stevenson, A. Biswas, J.L. Jane and G.E. Inglett, Changes in structure and properties of starch of four botanical sources dispersed in the ionic liquid, 1-butyl-3-methylimidazolium chloride, *Carbohydr. Polym.*, 2007, **67**, 21 – 31.
41. B.W. Kong, J.I. Kim, M.J. Kim and J.C. Kim, Porcine pancreatic alpha-amylase hydrolysis of native starch granules as a function of granule surface area, *Biotechnol. Prog.*, 2003, **19**, 1162 – 1166.
42. K.H. Jung, M.J. Kim, S.H. Park, H.S. Hwang, S. Lee, J.H. Shim, M.J. Kim, J.C. Kim and H. Lee, The effect of granule surface area on hydrolysis of native starches by pullulanase, *Starch/Stärke*, 2013, **65**, 848 – 853.
43. H.N. Dengate, D.W. Baruch and P. Meredith, The density of wheat starch granules: A tracer dilution procedure for determining the density of an immiscible dispersed phase, *Starch/Stärke*, 1978, **30**, 80 – 84.
44. A.C. Reyes, E.L. Albano, V.P. Briones and B.O. Juliano, Varietal differences in physicochemical properties of rice starch and its fractions, *J. Agric. Food Chem.*, 1965, **13**, 438 – 442.
45. D. Simková, J. Lachman, K. Hamouz and B. Vokál, Effect of cultivar, location and year on total starch, amylose, phosphorus content and starch grain size of high starch potato cultivars for food and industrial processing, *Food Chem.*, 2013, **141**, 3872 – 3880.
46. I.S.M. Zaidul, N. Norulaini, A.K.M. Omar, H. Yamauchi and T. Noda, RVA análisis of mixtures of wheat flour and potato, sweet potato, yam, and cassava starches, *Carbohydr. Polym.*, 2007, **69**, 784 – 791.
47. M.S. Hossen, I. Sotome, M. Takenaka, S. Isobe, M. Nakajima and H. Okadome, Effect of particle size of different crop starches and their flours on pasting properties, *Japan J. Food Eng.*, 2011, **12**, 29 – 35.
48. T. Sasaki and J. Matsuki, Effect of wheat starch structure on swelling power, *Cereal Chem.*, 1998, **75**, 525 – 529.
49. H.S. Kim and K.C. Huber, Physicochemical properties and amylopectin fine structures of A- and B-type granules of waxy and normal soft wheat starch, *J. Cereal Sci.*, 2010, **51**, 256 – 264.
50. M. Peng, M. Gao, E.S.M. Abdel-Aal, P. Hucl and N. Chibbar, Separation and characterization of A- and B-type starch granules in wheat endosperm, *Cereal Chem.*, 1999, **76**, 375 – 379.
51. J.C. Shannon, D.L. Garwood and C.D. Boyer, *Starch: Chemistry and Technology*, ed. J. BeMiller and R. Whistler, Academic Press, Oxford, 3rd edn, 2009, **3**, 23 – 82.

52. B.O. Juliano, *Starch: Chemistry and Technology*, ed. R.L. Whistler, J.N. Bemiller and E.F. Paschall, Academic Press, California, 2nd edn, 1984, **16**, 507 – 528.
53. J. Jane, Y.Y. Chen, L.F. Lee, A.E. McPherson, K.S. Wong, Radosavljevic and T. Kasemusawan, Effects of amylopectin branch chain length and amylose content on the gelatinization and pasting properties of starch, *Cereal Chem.*, 1999, **76**, 629 – 637.
54. M.A. Elgadir, J. Bakar, I.S.M. Zaidul, A. Rahman, K.A. Abbas, D.M. Hashim and R. Karim, Thermal behavior of selected starches in presence of other food ingredients studied by differential scanning calorimetry (DSC)-Review, *Compr. Rev. Food Sci. Food Saf.*, 2009, **8**, 195 – 201.
55. J.J.M. Swinkels, Composition and properties of commercial native starches, *Starch/Stärke*, 1985, **37**, 1 – 5.
56. J. Waterschoot, S.V. Gomand, E. Flerens and A.J. Delcour, Production structure physicochemical and functional properties of maize cassava wheat potato and rice starches, *Starch/Stärke*, 2014, **66**, 1 – 16.
57. M.Ö. Raeker, C.S. Gaimes, P.L. Finney and T. Donelson, Granule size distribution and chemical composition of starches from 12 soft wheat cultivars, *Cereal Chem.*, 1998, **75**, 721 – 728.
58. Y. Nakamura, A. Sakurai, Y. Inaba, K. Kimura, N. Iwasawa and T. Nagamine, The fine structure of amylopectin in endosperm from Asian cultivated rice can be largely classified into two classes, *Starch/Stärke*, 2002, **54**, 117 – 131.
59. S. Pancha-arnon and D. Uttapap, Rice starch vs rice flour: differences in their properties when modified by heat-moisture treatment, *Carbohydr. Polym.*, 2013, **91**, 85 – 91.
60. L. Qin-lu, X. Hua-xi, F.U. Xiang-jin, T. Wie, L.I. Li-hu and Y.U. Feng-xiang, Physico-chemical properties of flour starch and modified starch of two rice varieties, *Agric. Sci. China*, 2011, **10**, 960 – 968.
61. G.E. Vandeputte, R. Vermeylen, J. Geeroms and J.A. Delcour, Rice starches I Structural aspects provide insight into crystallinity characteristics and gelatinization behavior of granular starch, *J. Cereal Sci.*, 2003, **38**, 43 – 52.
62. N. Singh, J. Singh, L. Kaur, N.S. Sodhi and B.S. Gill, Morphological thermal and rheological properties of starches from different botanical sources, *Food Chem.*, 2003, **81**, 219 – 231.
63. T. Woggum, P. Sirivongpaisal and T. Wittaya, Properties and characteristics of dual-modified rice starch based biodegradable films, *Int. J. Biol. Macromol.*, 2014, **67**, 490 – 502.
64. I.S.M. Zaidul, N. Absar, S.J. Kim, T. Suzuki, A.A. Karim, H. Yamauchi and T. Noda, DSC study of mixtures of wheat flour and potato sweet potato casava and yam starches, *J. Food Eng.*, 2008, **86**, 68 – 73.
65. P.H. Zaal, H.A. Schols, J.H. Bitter and P.L. Buwalda, Ismalto/malto-polysaccharide structure in relation to the structural properties of starch substrates, *Carbohydr. Polym.*, 2018, **185**, 179 – 186.
66. C. Milan, Oil, Ghee, Cheese, Butter, Cholesterol and Atherosclerosis ... What should we know?, *Gujarat Med. J.*, 2010, **65**, 60 – 65.
67. F.S. Atkinson, K. Foster-Powell, J.C. Brand-Miller, International tables of glycemic index and glycemic load values: 2008, *Diabetes Care*, 2008, **31**, 2281 – 2283.
68. P.G. Smith, *Introduction to food process engineering*, Springer, Boston, 2nd edn, 2011, **10**, 235 – 273.
69. H.D. Belitz, W. Grosh, P. Schieberle, *Food Chemistry*, Springer, Germany, 3rd edn, 2004, **10**, 504 – 550.

70. H. Deeth, Optimum thermal processing for extended shelf life (ESL) milk, *Foods*, 2017, **6**, 102 – 122.
71. M. Minekus, P. Marteau, R. Havenaar and J.H.J. Huis in't Veld, A multicompartmental dynamic computer-controlled model simulating the stomach and small intestine, *Altern. Lab. Anim.*, 1995, **23**, 197 – 209.
72. S. Bellmann, J. Lelieveld, T. Gorissen, M. Minekus and R. Havenaar, Development of an advanced in vitro model of the stomach and its evaluation versus human gastric physiology, *Food Res. Int.*, 2016, **8**, 191 – 198.
73. J.D. Elashoff, T.J. Reedy and J.H. Meyer, Analysis of gastric emptying data, *Gastroenterology*, 1982, **83**, 1306 – 1312.
74. C.T. Richardson and M. Feldman, Salivary response to food in humans and its effect on gastric acid secretion, *Am. J. Physiol.*, 1986, **250**, G85 – G91.
75. P. Del Vigna de Almeida, A.M. Trindade Grégio, M.A. Naval Machado, A.A. Soares de Lima, L.R. Azevedo, Saliva composition and functions: a comprehensive review, *J. Contemp. Dent. Pract.*, 2008, **9**, 72 – 80.
76. N. Rohleder, J. M. Wolf, E.F. Maldonado and C. Kirschbaum, The psychosocial stress-induced increase in salivary alpha-amylase is independent of saliva flow rate, *Psychophysiology*, 2006, **43**, 645 – 652.
77. C. Dawes, Physiological factors affecting salivary flow rate, oral sugar clearance, and the sensation of dry mouth in man, *J. Dent. Res.*, 1987, **66**, 648 – 653.
78. K.S. Baskan, E. Tütem, E. Akyüz, S. Özen and R. Apak, Spectrophotometric total reducing sugars assay based on cupric reduction, *Talanta*, 2016, **147**, 162 – 168.
79. S. Haebel, M. Hejazi, C. Frohberg, M. Heydenreich and G. Ritte, Mass spectrometric quantification of the relative amounts of C6 and C3 position phosphorylated glycosyl residues in starch, *Anal. Biochem.*, 2008, **379**, 73 – 79.
80. C. Jang, S. Hui, W. Lu, A.J. Cowan, R.J. Morscher, G. Lee, W. Liu, G.J. Tesz, M. J. Bimbaum and J.D. Rabinowitz, The small intestine converts dietary fructose into glucose and organic acids, *Cell Metab.*, 2017, **27**, 351 – 361.



RESULTS AND DISCUSSION

RESULTS AND DISCUSSION

1. Introduction

In this chapter, the most relevant results obtained in this thesis have been presented and discussed. The obtained results could be divided into two parts: adaptation of the in vitro digestion methods and the results obtained with the in vitro digestion methods.

Related to the digestive enzymes, the critical points of the enzyme activity methods, the effect of electrolytes on the enzyme activity and the determination of its maximum storage time, were studied. To mimic the human carbohydrate digestion adequately, alternative sources to the human enzymes were also checked. Among other factors, a method to stop the digestion and the mixing speed used during the in vitro digestion were determined.

Finally, the obtained results of the in vitro digestion methods for the different meals are exposed and discussed.

2. Enzyme activity methods

2.1. Importance of working with an excess of substrate

As it is important to work under an excess of substrate, enzyme/substrate ratio is an important factor to take into consideration for the correct determination of the enzyme activity. As the amount of substrate is constant for the applied methods, the variable of the methods is the concentration of the enzymatic solutions.

To find the optimal enzyme concentration, solutions were prepared with different enzyme concentrations, and checked for enzyme activity. The obtained results are depicted in the following graph (figure 1):

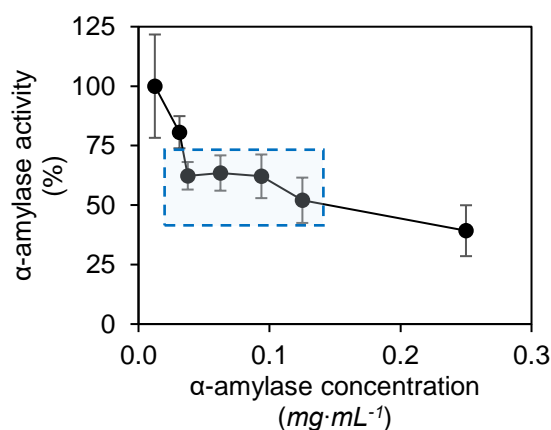


Figure 1. α -amylase activity obtained for different enzyme concentrations

The enzyme concentration range was considered correct when the amount of enzyme varies but the specific activity remains constant (blue box in figure 1: in this case from 0.04 to 0.13 $\text{mg}\cdot\text{mL}^{-1}$).

Specific activity is referred to the enzyme activity expressed as the number of units per milligram of powder (or protein): $\text{U}\cdot\text{mg}^{-1}$. When the obtained activity was higher than the “*steady-state*” it means that the recorded absorbance was below the detection limits (< 0.1), and when the activity had a lower value than the “*constant*” activity, it was considered that the amount of substrate was insufficient for the amount of enzyme present in the reaction and that not all the enzyme, could participate in the hydrolysis.

Additionally, three solutions at different enzyme concentration were prepared and incubated (with the substrate) for a longer period of time (6 and 9 min). The concentrations of the α -amylase solutions were selected according to the depicted curve in figure 1, and the chosen enzyme concentration ranges were:

- Too diluted: $< 0.04 \text{ mg}\cdot\text{mL}^{-1}$
- Accurate concentration: $0.04 - 0.13 \text{ mg}\cdot\text{mL}^{-1}$
- Too concentrated: $> 0.13 \text{ mg}\cdot\text{mL}^{-1}$

The effect of the incubation time on enzyme activity can be seen in figure 2:

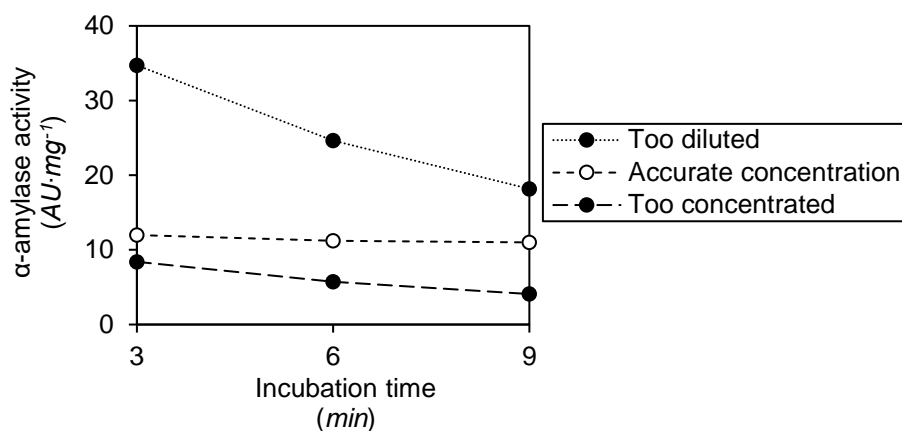


Figure 2. Effect of the incubation time on enzyme activity for three different enzyme concentrations

Figure 2 shows the obtained activity after incubating α -amylase with starch for 3, 6 and 9 min. The activity is expressed as specific activity, the units in figure 2 are defined as the amount of enzyme needed to release 1 mg of maltose in 3 min.

In figure 2, the measured activity of the “Too diluted” solution decreased from ~ 35 to $\sim 20 \text{ AU}\cdot\text{mg}^{-1}$ when it was incubated for 3 or 9 min, respectively. The obtained activity for the “Accurate concentration” solution was constant around $11 \text{ AU}\cdot\text{mg}^{-1}$ when the enzyme was incubated with the substrate for 3, 6 or 9 min. The activity measured for the “Too concentrated” solution also decreased from 8 to $4 \text{ AU}\cdot\text{mg}^{-1}$ when the enzyme was incubated for 3 or 9 min, respectively.

According to the results shown in figure 2, the enzyme concentration was considered to be correct when the specific activity ($\text{AU}\cdot\text{mg}^{-1}$) remained constant even when the hydrolysis incubation was performed for a longer period of time. When the specific activity remains constant, it means that the enzyme can work at its maximum capacity because there is enough substrate to be hydrolysed.

2.2. α -amylase

2.2.1. Critical points

The selected method to determine α -amylase activity comprises some critical points, which are:

- Starch solution preparation
- Enzyme solution preparation
- Incubation method

2.2.1.1. *Starch solution preparation*

Due to the lack of solubility of the starch, the conditions in which the starch is mixed with the solvent were studied and two tests were performed. The temperature test consisted of mixing the starch with the solvent at different temperatures for 15 min and 300 rpm. On the other hand, the time of the heating test was performed at 100°C and 300 rpm using different times of heating.

The percentage of solubilised starch is depicted versus the temperature (figure 3a) and versus the time of heating (figure 3b).

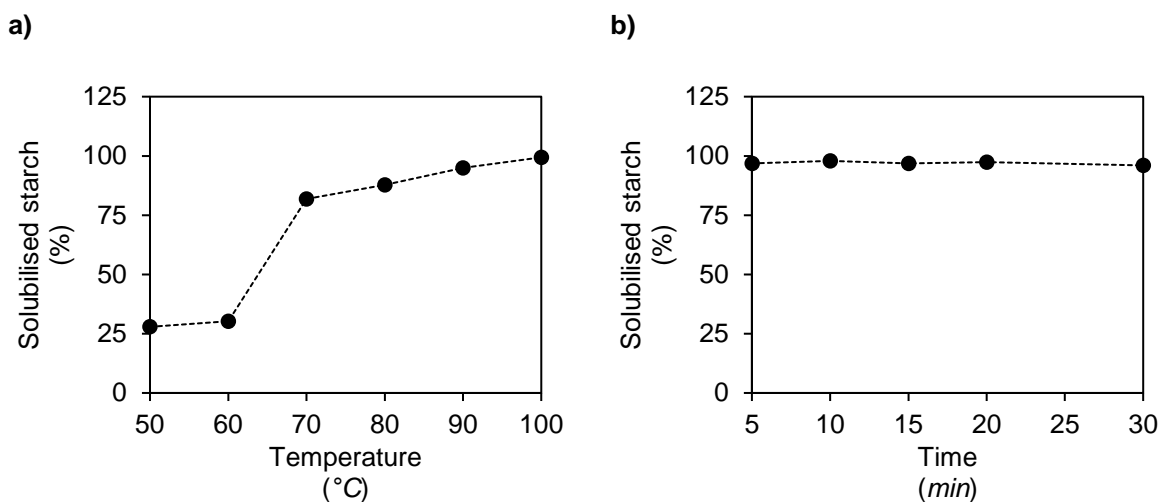


Figure 3. Percentage of solubilised starch after heating the mixture a) at different temperatures, b) for different times

The obtained results of the temperature test (figure 3a) demonstrated low solubility of the starch at 50 – 60°C with only ~25 % solubilised starch, the starch solubility increased drastically when it was prepared at 70°C reaching values of 82 % of solubilised starch. At higher temperatures, the starch solubility slightly increased proportionally with the temperature reaching values of > 95 % solubilised starch at 90 – 100°C.

Figure 3b shows a constant solubility of starch of ≥ 96 % for each studied heating time between 5 and 30 min. The solubility of starch, once 100°C was reached and kept for at least 5 min, is 97.0 ± 0.7 %.

Based on these findings it can be considered that for providing maximum starch solubility, the most critical point in the starch solution preparation is the temperature. For that reason, the conditions in which the starch solution was prepared for the α -amylase activity determination were 95°C, 300 rpm for at least 5 min. The starch was prepared at 95°C and not at 100°C to avoid the water boiling temperature and the resulting moisture loss.

2.2.1.2. Enzyme solution preparation

As the preparation of the enzymatic solution could be also a critical point in the measurement of its activity, different variables that could affect its solubility were studied. The enzyme activity was measured in each case and the activity given by the supplier was established as 100 % ($1333 \text{ AU}\cdot\text{mg}^{-1}$):

- *Mixing methodology:* two different methodologies were studied for the enzyme solution preparation; magnetic stirrer at different speeds and ultrasonic bath. For the magnetic stirrer, four different speeds of stirring were checked and then the obtained activity was compared. The enzymatic solution was also prepared by immersing the beaker that contained the enzymatic powder and solvent in an ultrasonic bath for 15 min RT. The effect of the mixing methodology and speed of mixing on the enzyme activity is depicted in figure 4.

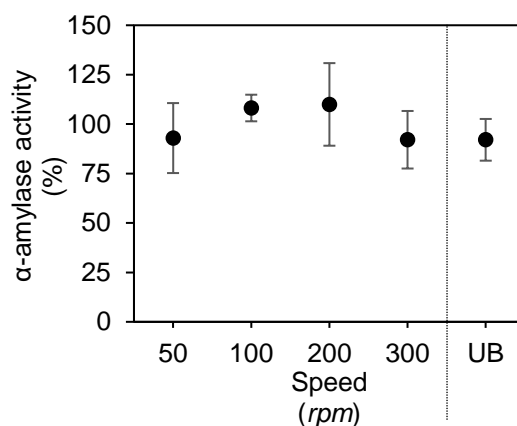


Figure 4. Effect of the mixing methodology on enzyme activity (UB: ultrasonic bath)

As it can be seen in figure 4, the obtained activities for the different speeds were similar for the magnetic stirring with $93 \pm 18 \%$, $108 \pm 7 \%$, $110 \pm 21 \%$ and $92 \pm 15 \%$ for 50, 100, 200 and 300 rpm, respectively.

Therefore, the speed at which the enzyme was mixed with the solvent on the magnetic stirrer did not affect the enzyme activity. Also, the activity obtained using the ultrasonic bath for the mixing ($92 \pm 11 \%$) was not different to the activity obtained when the enzymatic solution was prepared using the magnetic stirrer. Therefore, the mixing methodology studied did not influence the enzyme activity.

- *Order of addition (1st solvent vs 1st solute):* the enzymatic solution was prepared with both protocols (addition of the enzyme to the solvent and vice versa), the α-amylase activity was measured and the comparison of the obtained activities (%) is depicted in figure 5:

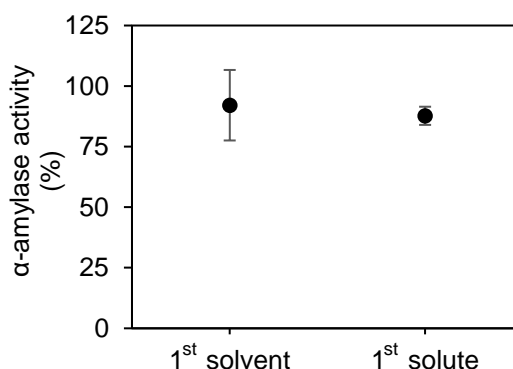


Figure 5. Effect of the addition order of enzyme and solvent on the enzyme activity

When the enzyme was added to the solvent (1st solvent) the measured activity was $92.1 \pm 14.6 \%$, while when the solvent was added to the enzymatic powder (1st solute) the obtained activity was $87.7 \pm 3.8 \%$. These findings demonstrate that the order in which the solvent and solute are mixed do not alter the final activity, obtaining ~100 % of its activity. Therefore, it can be concluded that the order of mixing does not have an impact on the solubilisation process. The enzymatic solutions subsequently used in this thesis were prepared by adding the solvent to the powder followed by mixing it until complete solubilisation.

- *Temperature of mixing:* for the study of the effect of the temperature on the enzyme activity during the enzyme solubilization process, the enzymatic powder was mixed with the solvent at different temperatures, and then the activity was measured.

The obtained results are depicted in figure 6:

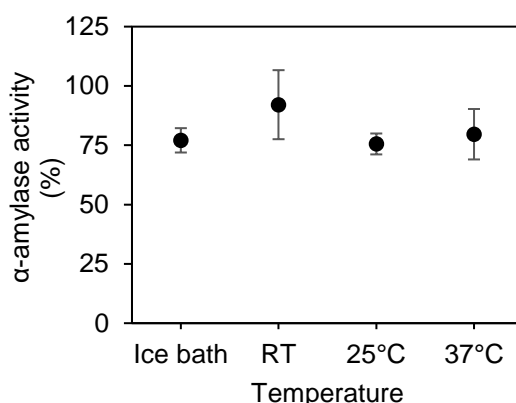


Figure 6. Effect of the temperature during solubilisation on enzyme activity

As it can be seen in figure 6, the measured activities for all temperatures were similar. When the solution was prepared in an ice bath, the activity was 77 ± 5 %, while when it was prepared at RT the activity was 92 ± 15 %. The obtained activity when the α -amylase solution was prepared at 25 or 37°C was 76 ± 4 % and 80 ± 11 %, respectively. Therefore, the temperature at which the enzymatic solution was prepared did not affect the enzyme activity and consequently its solubilization. Therefore, it was concluded that the optimal temperature for the enzyme solution preparation was at RT, which was approximately 20°C, as here the obtained levels were closest to 100 %.

- *Time of mixing*: the time of mixing needed for the enzyme solution preparation was also studied, and its effect on α -amylase activity is depicted in figure 7:

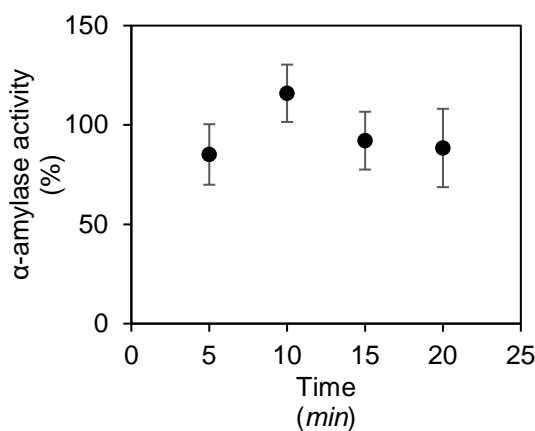


Figure 7. Effect of the mixing time during enzyme solution preparation on enzyme activity

The obtained activities when the α -amylase was mixed with the solvent for 5, 10, 15 or 20 min were 85 ± 15 %, 116 ± 14 %, 92 ± 15 % and 88 ± 20 %. Figure 7 reveals that the studied enzymatic powder was completely solubilised after being mixed with the solvent for at least 5 min. But it also demonstrated that the enzyme keeps its activity after being in solution at RT for 20 min. For that reason, the chosen mixing time was 5 min.

2.2.1.3. Incubation method

During α -amylase activity determination, first, the hydrolysis of the starch is performed at 20°C and then the released reducing sugars are oxidised at 100°C. The optimal incubation method for both reactions was studied as follows:

- *Starch hydrolysis (20°C)*: the use of a water bath (motionless) and a thermoshaker (Comfort thermomixer, Eppendorf) were studied as potential incubation methods to carry out the starch hydrolysis at controlled conditions: 20°C (water bath and thermoshaker), 1000 rpm (only for the thermoshaker).

For this study, the α -amylase activity obtained using both methods were compared and depicted in the following graph (figure 8):

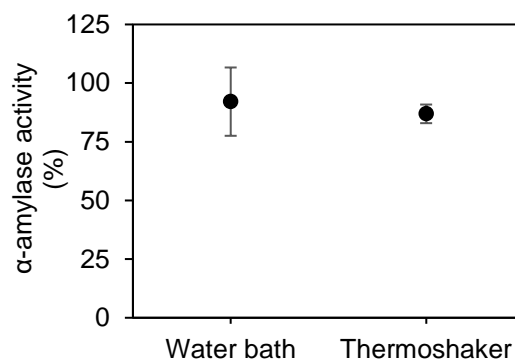


Figure 8. α -amylase activity obtained using water bath and thermoshaker to carry out starch hydrolysis at controlled temperature

When the incubation was performed with the water bath, the measured activity was $92 \pm 15 \%$, while the obtained activity was $87 \pm 4 \%$ when the thermoshaker was used. Thus, both settings let to similar activity levels but with a lower variation for the thermoshaker. This reveals that the thermoshaker could be used to carry out the incubation at 20°C and an advantage of the use of the thermoshaker is that the enzyme-substrate mixture could be mixed during the incubation, providing more reproducible results.

- *Redox reaction (100°C)*: Two different thermoshakers were studied as a potential alternative to the use of an oil bath for the incubation at 100°C. However, due to the type of thermoshakers, the following temperatures were studied for each incubation methodology:
 - Oil bath: 100°C
 - TS1-5436 thermomixer: 95°C
 - TS2-Comfort thermomixer: 99°C

The obtained activities in each case are depicted in figure 9:

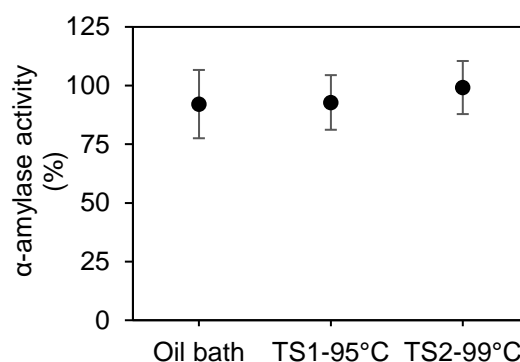


Figure 9. Comparison of α -amylase activity when the oil bath and thermoshakers (TS: thermoshaker) were used to carry out the incubation of the reducing sugars with the 3,5-dinitrosalysilic acid

As shown in figure 9, no differences between the obtained activities were found when the redox reaction took place in an oil bath ($92 \pm 15 \%$) or in any of the thermoshakers (TS1-95°C: $93 \pm 12 \%$, TS2-99°C: $99 \pm 11 \%$). Therefore, a thermoshaker could be used to carry out both incubations, the hydrolysis and redox reactions.

Additionally, the obtained results demonstrate that even when the incubation is done at 95°C the same level of enzyme activity was achieved, therefore there is no need to operate at 100°C.

Based on the findings in this section, for a most accurate and reproducible α -amylase activity determination the following conditions were defined and used subsequently in this thesis: preparing enzyme and substrate solutions by mixing the commercial powder with the solvent at 300 rpm for at least 5 min at RT (enzymatic solution) or at 95°C (substrate solution) to assure their complete solubilization. The selected method for the two incubations was the use of a thermoshaker at 20°C and 1000 rpm to carry out the starch hydrolysis and the use of a motionless thermoshaker at 95°C for the redox reaction.

2.3. Pepsin

2.3.1. Precipitate removal method

The selected method to determine pepsin activity is a colourimetric method, and a clean solution (without precipitates) is needed in this kind of methods, as the precipitates could alter the result. The use of centrifugation and filtration techniques have been studied as possible methods for the precipitate removal (figure 10).

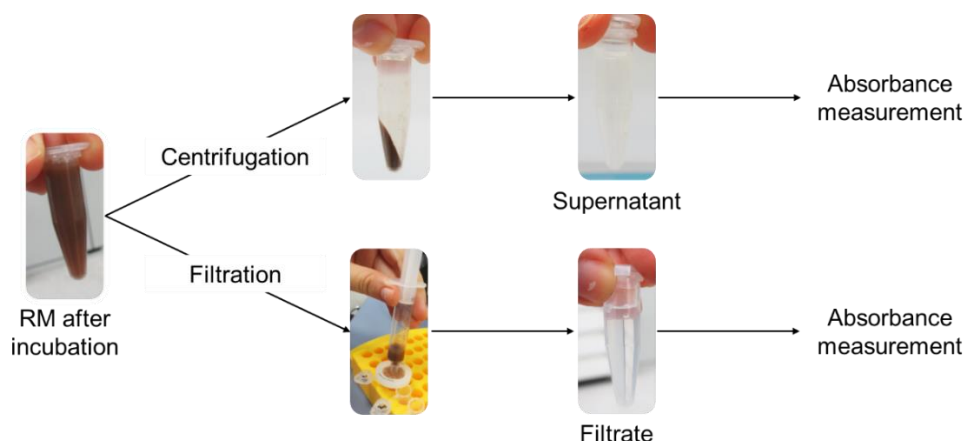


Figure 10. Studied techniques for precipitate removal (RM: reaction mixture)

Pepsin activity was measured by using both methods and the obtained results are depicted in the following figure (figure 11):

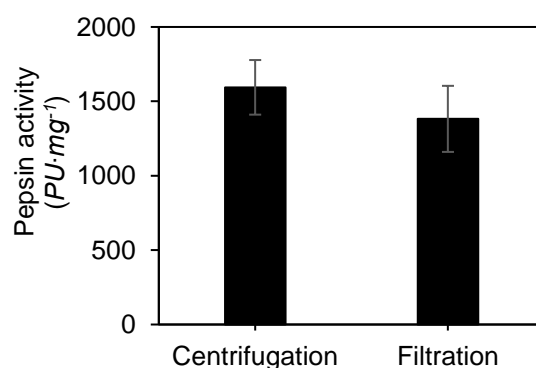


Figure 11. Comparison of the obtained activities when centrifugation or filtration are used for precipitate removal

Figure 11 demonstrates that both methods could be used to clean the reaction mixture for the pepsin activity determination, as no significant (α 0.05) difference between the activities was observed (centrifugation: 1594.1 ± 183.6 PU·mg⁻¹, filtration: 1382.1 ± 222.1 PU·mg⁻¹). However, for ease of use, centrifugation was selected to remove the precipitates in pepsin activity determination.

2.4. Lipase

2.4.1. Critical points

The selected method for the determination of lipase activity presents two critical points:

- Reagent addition methodology
- Flow rate

2.4.1.1. *Reagent addition methodology*

The amount of tributyrin added to the reaction mixture could be affected by its viscosity, for that reason, different addition methodologies were studied.

The addition methodology of tributyrin was studied by adding 500 μ L in a tared weighing boat, the added tributyrin was weighed. Then, the experimental weight was converted into volume (μ L) taking into consideration the tributyrin density (according to the supplier: 1.032 g·mL⁻¹).

The comparison of the experimental volume with the theoretical 500 μ L in dependence of pipetting mode is depicted in the following figure (figure 12):

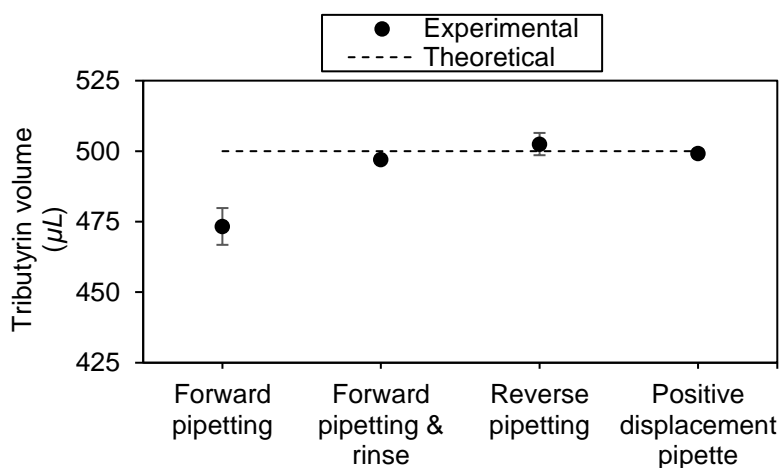


Figure 12. Experimental volume of tributyrin compared to the theoretical 500 μ L (n = 3)

The measured volumes sucked with the different methodologies were 473.3 ± 6.5 μ L, 497.0 ± 1.5 μ L, 502.5 ± 3.9 μ L and 499.2 ± 1.5 μ L for the forward pipetting, forward pipetting and rinse, reverse pipetting and the use of the positive displacement pipette, respectively. Figure 12 demonstrates that the forward pipetting followed by rinse, reverse pipetting and the use of the positive displacement pipette are the best options for the measurement of the tributyrin volume, as the experimental volume is equal to the theoretical and the experimental volume has a small standard deviation, demonstrating that the three pipetting techniques are reproducible methods for the tributyrin volume measurement.

On the other hand, figure 12 also shows that the forward pipetting is not the optimal way for the measurement of the tributyrin volume as the experimental volume is lower than the desired one, and the experimental volume has a higher standard deviation compared with the other pipetting techniques.

The addition methodology of the aqueous solution was also studied by weighing 14.5 mL and comparing the experimental volumes with the theoretical 14.5 mL (figure 13):

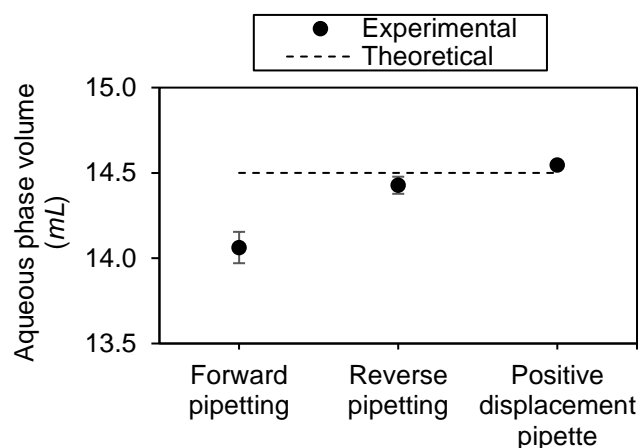


Figure 13. Comparison of pipette techniques for the addition of aqueous phase (n = 3)

As shown in figure 13, the optimal pipette technique for the addition of the aqueous phase is the reverse pipetting and the use of positive displacement pipette, as with the forward pipetting only 96 % of the volume is added compared with the > 99 % obtained with the other techniques.

In conclusion, the tributyrin volume was measured by forward pipetting and then a rinse was performed to assure that all the substrate was added but also to help to its emulsification with the aqueous phase.

The aqueous phase was measured and added to the beaker by reverse pipetting as it was one of the optimal pipette techniques for this solution. The positive displacement pipette was discarded as there was not an available tip for the total addition of 14.5 mL needed for the method.

2.4.1.2. Flow rate

As the same amount of enzyme is always used for the determination of lipase activity, the titrant flow rate is the limitation of the method. Different flow rates of NaOH were checked to find the optimal flow rate for the lipases with high or low activity.

The effect of the use of a slow flow rate on the pH in the reaction mixture during the tributyrin hydrolysis is depicted in figure 14. It can be seen that when the flow rate was too slow the addition of 0.1 N NaOH was not enough to counter the release of the butyric acid from the tributyrin and the pH did not reach the desired pH. In this example, and ignoring the first 160 s (Materials and methods_Figure 10), the pH range for the lipase activity determination was 7.78 – 7.94, therefore the reaction mixture never reached the required pH 8.0 of the method.

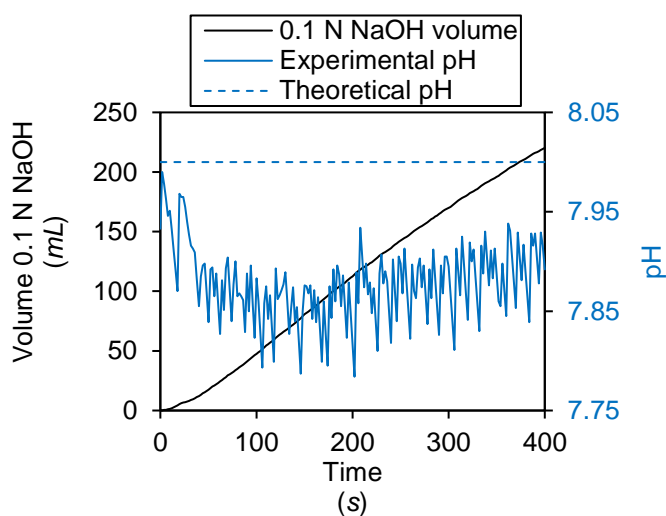


Figure 14. Effect of the low flow rate on the pH of the mixture

On the other hand, when the flow rate was too fast, then the pH of the solution was too high. At this pH, the enzyme was not at the conditions of the method (e.g., pH 8.0) which decreased the speed of the catalysis. Therefore, the volume of 0.1 N NaOH needed to counteract the butyric acid released would be unreal, which lead to the obtention of false activities.

The effect of a fast flow rate on the pH of the solution is depicted in figure 15:

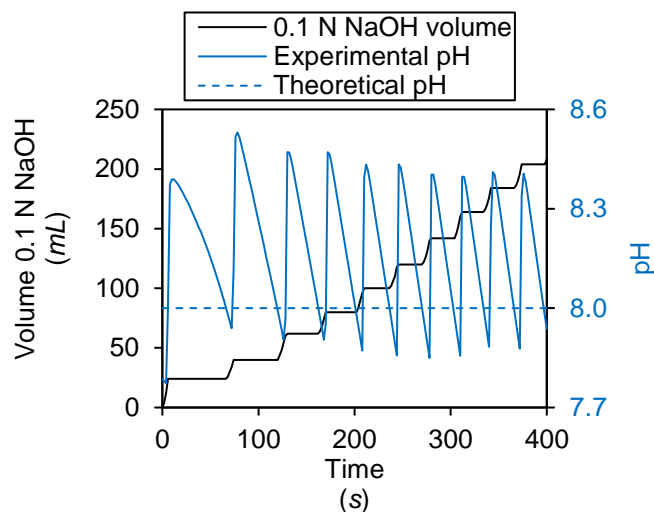


Figure 15. Effect of the high flow rate on the pH of the mixture

In this case, and ignoring the first 160 s, the pH range for the lipase activity determination was 7.85 – 8.47, the reaction mixture is most of the time at a higher pH than the pH of the method (pH 8.0).

As it can be seen in figure 15, when the pH is slightly lower than the set pH (pH 8.0), the NaOH is quickly added, resulting in an excess of NaOH, which provokes a drastic increase in the pH. Thereby, the enzyme is not at the desired pH for most of the time, which cause a decrease in the hydrolysis speed and it takes time to release enough butyric acid to obtain the desired pH (pH 8.0). For that reason, the number of NaOH additions are lower than the additions done in figure 14, and the stairs-shape of the NaOH volume is also more visible in figure 15 compared with figure 14.

When the lipase activity method is performed at the optimal flow rate, the pH of the solution is practically constant at the desired pH. Therefore, the enzyme is at the pH of the method, which leads to the accurate NaOH addition and lipase activity measurement. The effect of working at the optimal flow rate on the pH of the solution is depicted in the following graph:

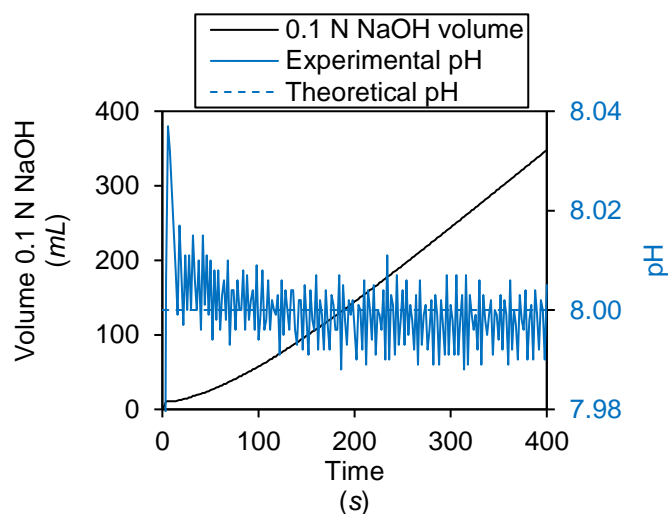


Figure 16. Effect of the use of the optimal flow rate on the pH of the mixture

Figure 16 demonstrates that when there is a small decrease in the pH of the mixture, due to the release of butyric acid, the amount of NaOH added suits the needed volume of 0.1 N NaOH to readjust the pH to 8.0. In those conditions, the enzyme can catalyse the tributyrin hydrolysis at the desired conditions, and therefore, the lipase activity is calculated correctly.

In this example, the pH range of the reaction mixture (ignoring the first 160 s) goes from pH 7.99 to pH 8.01, which proves that the enzyme is mainly at the conditions of the method.

When comparing NaOH additions at different flow rates, it can be seen that the number of additions is much higher when the accurate flow rate is used, and lower when the flow rate is too high.

The selected titrator operated with two different flow rates: maximum rate and minimum rate. In addition, lipases at different activity levels (with high and low activity) were studied in this thesis. For that reason, the accurate combination of flow rates (max and min) for the different lipases was checked by measuring the activity at different flow rate combinations (max and min flow rate).

The identified optimal combination of flow rates obtained for the correct measurement of lipase activity are described in table 1 for lipases with high and low activities.

Table 1. Flow rate of 0.1 N NaOH for the lipase activity measurement

	Lipase	
	<i>High activity</i>	<i>Low activity</i>
Max rate (mL·min ⁻¹)	2.2	0.3
Min rate (μL·min ⁻¹)	5.0	0.2

2.4.2. Ring trial

2.4.2.1. *Specific activities of the lipase preparations*

A ring trial to measure the lipase activities of one batch of RGE (lyophilized rabbit gastric extracts) and two different batches of porcine pancreatin (from Sigma Aldrich and Nordmark) was carried out involving 21 laboratories. The assays were performed in triplicate using 3 different amounts of enzyme preparation in each case.

This ring trial was used as an additional reference to assure that lipase activity measurements used for this thesis are carried out correctly. The results of all participating laboratories were analysed and the conclusions were taken by the organisers (1). The major findings will be summarised in the text below and set in relation to own results (that are also included in the ring trial).

Only one of the 21 laboratories deviated from the average CV for all repeated replicates and the values of this lab were therefore removed from the mean calculation.

From the results obtained from the labs, for RGE and Sigma pancreatin the mean specific activities obtained for the three amounts tested (50, 100 and 200 μg) did not vary with the amount of enzyme. However, for Nordmark pancreatin the specific activity measured with the highest amount tested (200 μg) was lower than with the other amounts (50 and 100 μg). This behaviour is depicted in figure 17, where the results obtained from all the laboratories (black) is compared with the own obtained results (blue). This observed decrease in the specific activity at the highest concentration tested indicates that this amount was outside the range allowed for measuring a constant specific activity.

When the results obtained for own measurements are compared with the overall results it can be seen that in general, the results obtained fit with the activities measured by the other laboratories. Therefore, it can be concluded that the conditions used for own measurements and the followed procedure performed was adequate for the correct lipase activity measurement.

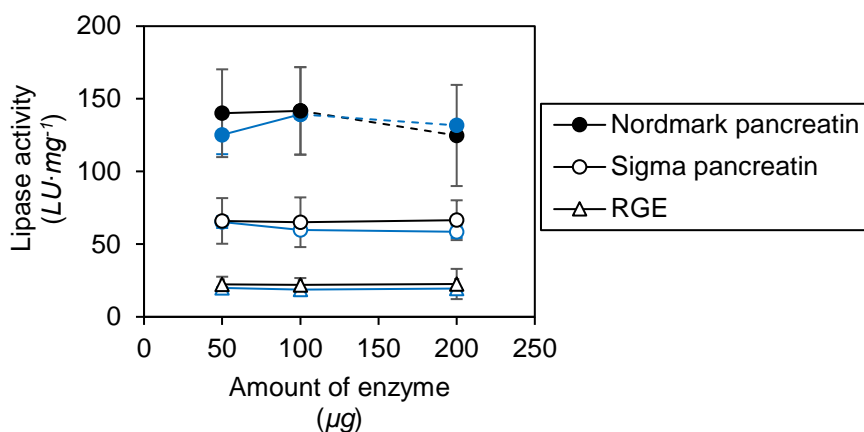


Figure 17. Specific activities of the lipase sources as a function of the amount of enzyme preparation used in the assay (black: all laboratories, blue: own results)

The intra-laboratory CVs were overall acceptable with mean values < 10 %, regardless of the enzyme source. On the other hand, the inter-laboratory variabilities were too large (> 21 %) to reach international standards for bioanalytical method validation according to which CV values should not exceed 15 %.

The inter-laboratory variability was not reduced by removing data from the outlier laboratory the potential sources of variability between laboratories involved were checked and special attention was given to the various pH-stat devices and their respective characteristics used by the laboratories used. The following properties of the pH-stat devices were identified to show high variety maximum volume of the reaction vessel, the vessel shape, the stirring mode, the stirring speed and the maximum burette volume for the delivery of NaOH. Some aspects will be discussed in more depth in the following paragraph.

2.4.2.2. Overview of the equipment used

Instruments from 8 different brands and/or models were used by the 21 laboratories: Titrino and Titrando from Methrom, Mettler Toledo, Radiometer Copenhagen Meterlab, Kyoto Electronics Manufacturing, Orion, Dasgip Eppendorf and Cerko Lab System (1).

Conical reaction vessels were more widely found than cylindrical vessels, and magnetic stirrers than propellers. Diversity was also observed in the maximum volume (from 25 up to 200 mL) of the reaction vessel and the maximum volume (5, 10 or 20 mL) of the automated burette used for NaOH delivery. However, one laboratory (lab 16) used a Dasgip Eppendorf bioreactor system instead of a classical pH-stat. This device had no burette and was based on a different principle (pump) for the NaOH delivery.

The ring trial confirmed that the mixing conditions in the pH-stat vessel are critical to obtain accurate and reproducible lipase activities (1). This is influenced by the shape and size of the reaction vessel, the stirrer type and the stirring rate. Using a reaction vessel with a conical shape appeared as the most important variable influencing the interlaboratory variability.

The maximum volume of the reaction vessel had a limited influence, but the concluding recommendation is to use a thermostated conical vessel with a 70 mL maximum capacity. The type of stirrer (propeller vs magnetic bar) had also a limited influence, the highest activity was recorded with the propeller. It is generally recommended to use a propeller because it allows better monitoring of the stirring rate with viscous reaction mixtures.

Specific activities were found to increase with increasing stirring rate. However, it is worth noting that the rates provided by the laboratories were often rough estimations of rates found in the instruction manuals. Indeed, most pH-stat instruments are equipped with stirrers having a few pre-set rates and it is not possible to finely adjust the stirring rate. If possible, the authors would recommend using a stirring rate between 700 and 800 rpm, a range in which the specific activities measured are close to the mean specific activities measured by all laboratories.

The last variable of importance identified is the volume of the burette used for the automated delivery of NaOH, where higher specific activities were recorded with the smallest burettes. The authors assume it is due to the precision of NaOH delivery to keep the pH of the system at the set value, the smallest burettes being the most precise at adding small volumes of NaOH into the reaction vessel.

The equipment used for the thesis was the 836 titrator and a V-shaped jacketed beaker 5 – 70 mL, a magnetic stirrer connected to the titrator, 2 mL burette from Metrohm. And according to the conclusions obtained after the ring trial, it was proved that the equipment used in our laboratory was appropriate for the accurate lipase activity measurements.

2.4.2.3. Inhibition of lipases by 4-bromophenylboronic acid

Among other things, an inhibitor would be useful to stop the enzyme activity after each sampling point in the in vitro digestion methods. The use of 4-bromophenylboronic acid was studied as a possible lipase inhibitor.

In the first series of inhibition assays performed with 100 µg of each enzyme preparation with a fixed amount of inhibitor the 21 laboratories were involved. From the results obtained from all the laboratories, the specific activities of the two pancreatin sources were significantly reduced (α 0.0001) when they were mixed with 4-bromophenylboronic acid, with only 8 % and 6 % of residual activity for Sigma and Nordmark pancreatins, respectively. On the other hand, 34 % of gastric lipase from the RGE was still active when using the same quantity of inhibitor.

Inhibition assays of gastric lipase were therefore repeated for RGE with higher amounts of 4-bromophenylboronic acid (10, 25 and 50 µL of 1 M solution) in the second series of experiments involving only 8 laboratories out of the 21 (including own results). The addition of 50 µL of inhibitor solution, (equivalent to an extremely high inhibitor to lipase molar ratio of 135100) resulted in a remaining activity of 12 ± 8 %, which was still higher than the residual activities measured for the other two pancreatins using a 10-folds lower inhibitor to lipase molar ratio of 13500. The effect of the inhibitor on the lipase activity is depicted in figure 18, where it can be seen the residual activity versus the ratio inhibitor:enzyme obtained own measurements (blue) and the average of all laboratories (black) can be seen.

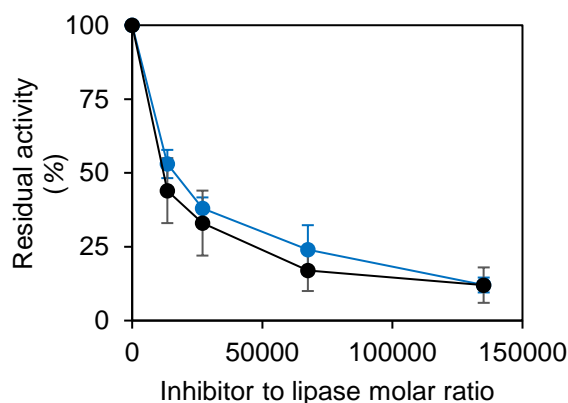


Figure 18. Inhibition of gastric lipase after mixing RGE with 4-bromophenylboronic acid (black: all laboratories, blue: own results)

As it can be seen in this figure, the behaviour of the inhibitor observed as an average for all the laboratories was also seen for own measurements having similar residual activity patterns (decrease with increasing inhibitor to lipase ratio). In summary, the authors confirmed that 4-bromophenyl boronic acid significantly inhibits lipase present in Sigma and Nordmark pancreatin but it is a weak inhibitor of gastric lipase even at high inhibitor concentrations.

3. Adaptation of enzymes used in in vitro methods to physiological levels

3.1. α -amylase

3.1.1. Alternative source to human α -amylase

α -amylase is secreted in the mouth (pH 6.2 – 7.6) and small intestine (pH 5.5 – 8.0); therefore, α -amylase is present throughout the GIT (gastrointestinal tract) (2 – 4). The pH varies over time and place during the digestion depending, among other factors, on the buffer capacity of the meal and the section of the GIT where the α -amylase driven digestion takes place. In contrast, the temperature is relatively constant at around 37°C.

Physiological activities are reported at 20°C and pH 6.9, whereas the human α -amylase acts in vivo at 37°C and various pH values. The enzyme activity difference between these two temperatures might not be linear for all relevant pH values. To screen potential alternative α -amylase sources for their suitability for the application in in vitro digestions, their activity profiles (temperature, pH) need to be determined and compared to the activity profile of human α -amylase.

Therefore, the effect of the pH at 20°C and 37°C on α -amylase activity was studied for human α -amylase (figure 19) and two alternative α -amylase sources (figures 20 and 21) by a slight modification of the enzyme activity method. The two alternative sources were chosen for different reasons, a bacterial α -amylase was chosen because it is a cost-effective alternative, and a porcine α -amylase due to its reported characteristics that hypothesized that it could mimic the human α -amylase closely (5). Moreover, both sources are commercially available.

To study the effect of the pH, the standard buffer used to prepare the substrate and the enzymes was adjusted to different pH values (pH 2.0, 4.0, 6.0, 7.0, 8.0, 10.0, 12.0). To study the temperature effect, the hydrolysis was additionally performed at 37°C.

The results are depicted in figures 19 – 21, where for ease of comparison α -amylase activity is presented in relative values.

The maximum activity obtained for the studied sources of α -amylase were $153.3 \pm 3.7 \text{ AU}\cdot\text{mg}^{-1}$ for human α -amylase, $1663.1 \pm 250.8 \text{ AU}\cdot\text{mg}^{-1}$ for the bacterial α -amylase and $29.0 \pm 4.3 \text{ AU}\cdot\text{mg}^{-1}$ for the porcine α -amylase. These activities were set as 100 %, respectively and used for the graphical representations (figures 19 – 21).

For all studied pH values and enzymes, where enzymatic activity could be detected, the activity at 37°C (closed circles) was found to be higher than the activity determined at 20°C (open circles) (figures 19 – 21). The obtained activity profiles (20 and 37°C) for the human α -amylase are depicted in figure 19, where the maximum activity was obtained at 37°C and a pH of 7.0. This is in agreement with previously reported optimal conditions for human α -amylase (pH 7.0) (6).

No activity was detected at pH 4.0 or lower for both temperatures. At pH 6.0 the human α -amylase showed medium activity (36 % at 20°C, 65 % at 37°C). At pH values higher than 7.0, the activity decreased until a pH of 12.0 where no more activity was observed. The activity at pH 6.0 and 7.0 obtained at 20°C was ~55 % of the activity at 37°C. While, the activity at pH 8.0 and 10.0 obtained at 20°C were 60 and 70 % of the activity at 37°C, respectively.

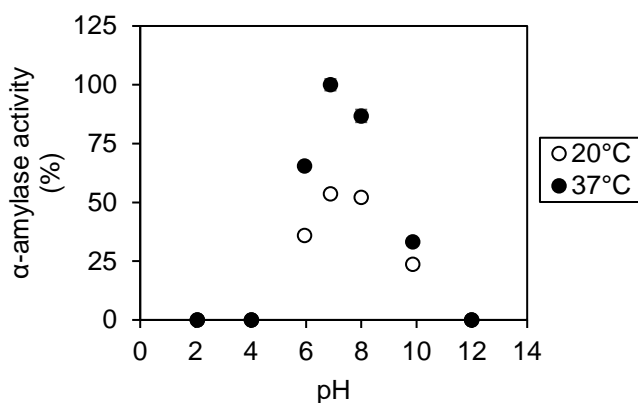


Figure 19. pH profile at 20°C and 37°C for human α -amylase (Sigma Aldrich, A0521)

Based on the above results, a good alternative for the human α -amylase, should not show activity at pH values of 4.0 or lower, while at pH 7.0 the activity at 20°C should be close to 55 % of the activity at 37°C. The factor at higher pH values is less relevant for this thesis as the digestion rarely reaches those pH values.

Figure 20 shows the pH profile at 20 and 37°C of the α -amylase from bacillus sp., a possible alternative to human α -amylase. In this case, the maximum activity was found at 37°C and pH 6.0 and 7.0, while the reported optimal conditions are at 65°C and pH 5.9 (7). Unlike the human α -amylase, the pH range where the bacterial α -amylase is active was wider at 37°C ranging from pH 4.0 to 10.0 (human α -amylase: pH 6.0 – 10.0) and tighter at 20°C ranging from pH 6.0 – 8.0 (human α -amylase: pH 6.0 – 10.0). Another difference, which can be observed in the figure, is that the activity at pH 6.0 and 7.0 obtained at 20°C is ~70 % of the activity at 37°C (human α -amylase: ~55 %).

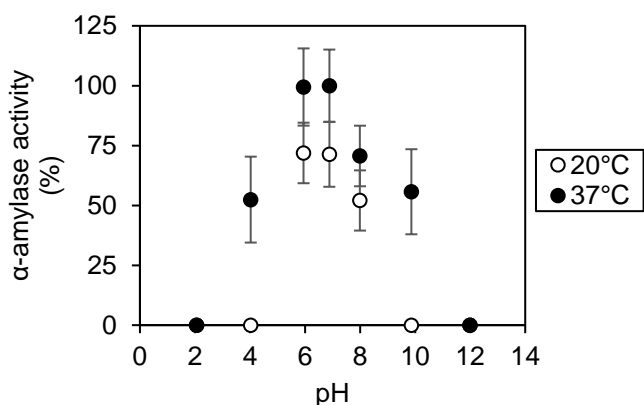


Figure 20. pH profile at 20°C and 37°C for bacterial α -amylase (Sigma Aldrich, A6380)

Taking these results into consideration, major differences were obtained in the activity profile of bacterial α -amylase compared to human α -amylase. If the amount of α -amylase used to mimic the human digestion is calculated with the activity measured at 20°C, the resulting activity at 37°C will be lower than its human counterpart. This is because the differences in the activities between the two temperatures (test and performance) for the bacterial α -amylase are smaller than for the human α -amylase.

On the other hand, when the human α -amylase passes the stomach, it decreases or fully loses its activity. In contrast, the bacterial α -amylase would still show ~50 % of its activity, which would lead to false results. Therefore, it can be concluded that this source of α -amylase is not an ideal alternative to carry out in vitro digestion methods.

A second alternative source, α -amylase from porcine pancreas has been studied, and the obtained results are depicted in figure 21.

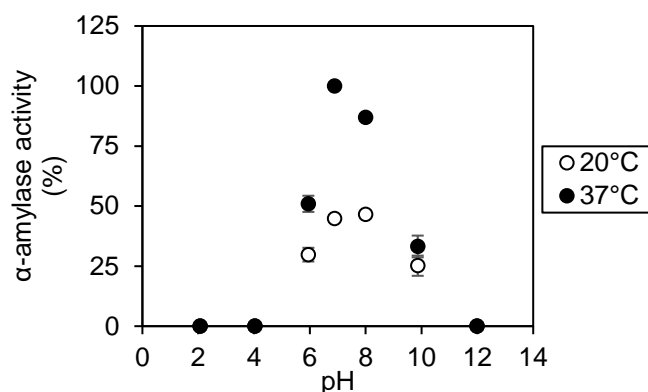


Figure 21. pH profile at 20°C and 37°C for porcine α-amylase (Sigma Aldrich, A3176)

This source was selected due to its potential to closely mimic the behaviour of the human α-amylase as it has been reported that they show an 84 % similarity in their sequence (5,8). Furthermore, the reported optimal conditions are also pH 7.0 and 37°C.

As shown in figure 21, the pH range where the enzyme is active is the same as for the human α-amylase (pH 6.0 – 10.0), showing a maximum activity at pH 7.0 and 37°C. The factor between the two temperatures matched with the factor obtained for the human α-amylase in the range of pH 7.0 – 10.0. However, at pH 6.0 and 37°C the enzyme showed only 50 % of its maximum activity while the human α-amylase showed 65 % of its maximum activity. It can be concluded that the porcine α-amylase differs slightly at this pH value.

Based on the results above it can be stated that α-amylase from porcine pancreas is a good alternative to human α-amylase.

3.1.2. Effect of electrolytes on α-amylase activity

The enzyme activity not only depends on the pH and temperature of the media but is also affected by the solvent or the compounds surrounding the enzyme. Therefore, it is needed to measure the enzyme activity at the same conditions as being present during the digestion. To study the effect of the electrolytes, α-amylase from porcine pancreas (A3176) was dissolved in the presence and absence of the electrolytes that are present in the digestive fluids and the enzyme activity was measured at pH 6.9 at both temperatures, 20 and 37°C.

The obtained results are depicted in figure 22, where it can be seen that at 20°C α-amylase was less active in the absence of electrolytes ($6.8 \pm 0.3 \text{ AU}\cdot\text{mg}^{-1}$; DI water), while in presence of simulated salivary fluid (SSF), the enzyme was significantly ($\alpha 0.05$) more active ($10.0 \pm 0.5 \text{ AU}\cdot\text{mg}^{-1}$).

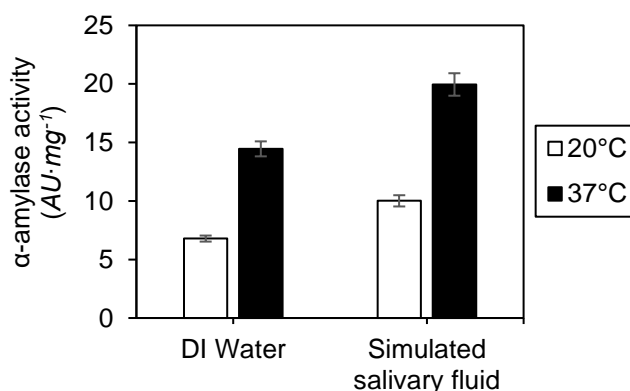


Figure 22. α-amylase activity in dependence of solvent type (n = 3; pH 6.9)

That means that at 20°C the enzyme increased its activity to $148 \pm 7 \%$ in the presence of the oral electrolytes. This increase was also observed at 37°C where the activity increased to $138 \pm 7 \%$. Moreover, the activity of α -amylase for both solvents at 20°C was $\sim 50 \%$ of the activity that it showed at 37°C (DI Water: 47 %, SSF: 50.2 %).

Therefore, when the enzyme activity is measured to calculate the concentration ($\text{mg}\cdot\text{mL}^{-1}$) of enzyme needed to mimic the human digestive fluids, it is important to prepare it in the most similar conditions as being present during the in vitro digestion method.

3.2. Pepsin

3.2.1. Alternative source to human pepsin

Pepsin is secreted in the stomach, where the pH varies from pH 1.4 to pH 6.6, thus it is present also in subsequent GIT regions but not in the mouth and oesophagus (9,10).

The effect of temperature was not studied for pepsin because the physiological and experimental activities are expressed in PU at 37°C, which is the same temperature at which the digestion takes place. As mentioned in the α -amylase section, the pH is not constant over time and place during digestion. Therefore, a good alternative to mimic human protein digestion should follow the same pH profile at 37°C as the human pepsin.

A potential alternative to human pepsin could be the porcine pepsin because it has been reported that it displays similar structural and biochemical properties and it is also commercially available (11).

To study if the pepsin from porcine gastric mucosa is a good alternative to replace human pepsin in in vitro studies, the porcine pepsin was incubated at different pH values (1.7, 2.0, 2.7, 4.2, 5.2) using a buffer to prepare both, the enzyme and the substrate solution. The obtained results are depicted in figure 23, and compared to the reported pH profile of the human pepsin at pH 1.5, 2.1, 2.5, 3.0, 4.0, 5.0 and 6.0 according to Rey et al (12).

The activity of the human pepsin at different pH was not measured because it is not commercially available.

In figure 23, the maximum specific activity for both sources of pepsin was individually set as 100 %.

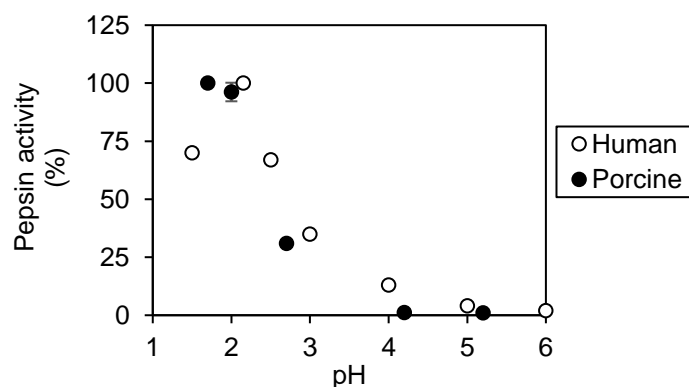


Figure 23. Effect of pH on the activity of porcine pepsin (n=2, 37°C) in comparison to literature data for human pepsin at 37°C (12)

Figure 23 shows that both pepsin sources are active at acidic conditions, showing the maximum activity at pH 1.7 for the porcine pepsin and at pH 2.1 for the human pepsin. This difference in the pH of the maximum activity could be because the human activity at pH 1.7 is not available in the work of Rey et al (12) and therefore could not be compared.

With increasing the pH, the activity decreases showing activity of 30 and 35 % at pH ~ 3.0 for the porcine and human pepsin, respectively. And almost no activity was found at pH ~ 4.0 (porcine $\sim 1 \%$, human $\sim 10 \%$) and pH ~ 5.0 (porcine $\sim 1 \%$, human $\sim 4 \%$).

The pepsin activity was not measured at pH values higher than 5.2 because it has been reported that the tertiary structure of pepsin becomes extremely unstable, and it denatures irreversibly at pH values greater than 6.5 (13). Therefore, when the pepsin reaches the small intestine and the pH is neutralised with the intestinal secretions to pH 5.5 – 8.0, the enzyme loses its activity (2 – 4).

Based on the above results, the pepsin from porcine gastric mucosa can be considered an alternative to mimic the gastric proteolysis in in vitro methods because it shows only slight differences to the human pepsin. Moreover, there are only a few alternative sources to the human pepsin that are commercially available and at an adequate price.

3.2.2. Effect of electrolytes on pepsin activity

In the GIT, pepsin is surrounded by other substances, like electrolytes, which can affect the enzyme activity. Therefore, the porcine pepsin activity was measured with and without the simulated gastric fluid (SGF) and the obtained results are depicted in figure 24. The porcine pepsin did not show an increase in its activity in the presence of electrolytes ($2239.0 \pm 283.1 \text{ PU}\cdot\text{mg}^{-1}$) when compared to the preparation with DI water ($2520.5 \pm 100.7 \text{ PU}\cdot\text{mg}^{-1}$). This is in contrast to the findings obtained with the porcine α -amylase.

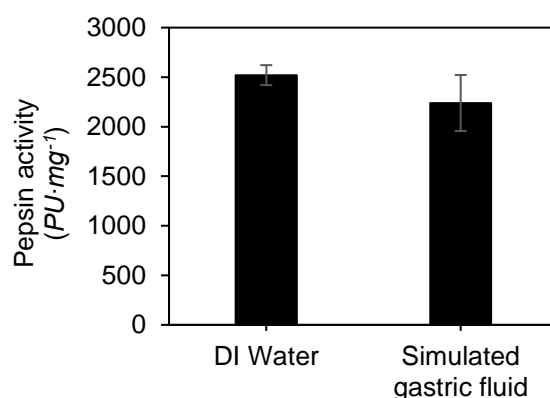


Figure 24. Pepsin activity in dependence of solvent type (n=16; 37°C; pH 2.0)

3.3. Trypsin

3.3.1. Alternative source to human trypsin

Trypsin is secreted in the small intestine where the pH varies from pH 5.5 to pH 8.0 (2 – 4) and it is active at around 37°C. However, the physiological activities are dominantly reported at 25°C and pH 8.1, except e.g., by Goldberg et al (14), where the activity was measured at 37°C and different pH values. A potential alternative to the human trypsin should mimic the pH-dependent activity profile at 25 and 37°C.

Deng et al (15) compared the degree of hydrolysis obtained for porcine, bovine and human trypsin and the authors concluded that there are no big differences between them. However, the obtained degree of hydrolysis and the initial hydrolysis rate constants were more similar between the human and bovine trypsin than between the human and the porcine trypsin. For that reason, bovine trypsin was chosen to be studied as a possible alternative to human trypsin.

The effect of pH at 25 and 37°C was studied for the bovine trypsin by a slight modification of the enzymatic method. To study the effect of pH, the buffer used to carry out the method was adjusted to pH 5.0, 6.0, 7.0, 8.1 and 9.0, and to study the effect of temperature, the incubation of the enzyme with the substrate was carried out at 25 and 37 °C. The enzymatic solution was prepared using DI water as solvent.

Figure 25 shows the comparison of the reported pH profile for the human trypsin at 37°C (14) with the experimental profile of the bovine trypsin at 37°C. The maximum activity was set as 100 %, which was found at pH 8.1 and 37°C, for both trypsin sources.

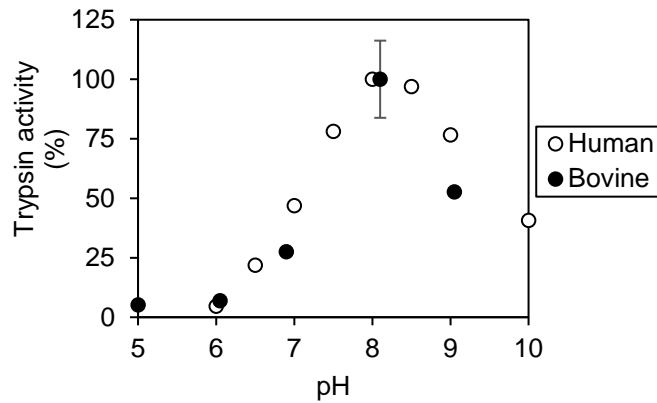


Figure 25. Effect of the pH on the activity of bovine trypsin (37°C) in comparison to literature data for human trypsin at 37°C (14)

When the pH values were different to pH 8.1, the trypsin activity decreased drastically. At pH 7.0, the human trypsin shows only 47 % of the activity at pH 8.1, while the bovine trypsin shows only 28 % of the activity at the optimal pH. And at lower pH values, the trypsin activity continues decreasing, showing at pH 6.0 only 5 and 7 % of the activity at pH 8.1 for the human and bovine trypsin sources, respectively.

When the pH is higher than the optimal, the activity also decreases but to a lower extent. At pH 9.0, the bovine trypsin shows 53 % of the activity at pH 8.1, and the human trypsin shows 77 %.

As a good alternative to the human trypsin, the bovine trypsin should also mimic the behaviour at 25°C, as most of the reported activity levels are expressed at 25°C. Mckeehan et al (16) demonstrated that the human activity at 25°C is around 84 % of the activity that is found at 37°C and pH 8.1, while the bovine trypsin at 25°C shows 71 % of the activity at 37°C and pH 8.1.

According to the obtained results, bovine trypsin has a similar pH-profile as the human trypsin at 37°C, showing more analogy when the pH is lower than 8.1. And, the factor at pH 8.1 between 25 and 37°C is ~10 % lower for the bovine trypsin, compared to the human trypsin.

3.3.2. Effect of electrolytes on trypsin activity

Like the other enzymes, trypsin is surrounded by electrolytes during human digestion. The effects of some electrolytes on trypsin activity were studied by several authors (17,18).

Haverback et al (17) demonstrated that the addition of calcium increases the trypsin activity, but at the same time the addition of potassium oxalate has a negative effect on the activity. Therefore, the expected impact of electrolytes (present in digestion processes) on the trypsin activity was studied at the physiological concentrations of the electrolytes and the obtained results are depicted in figure 26.

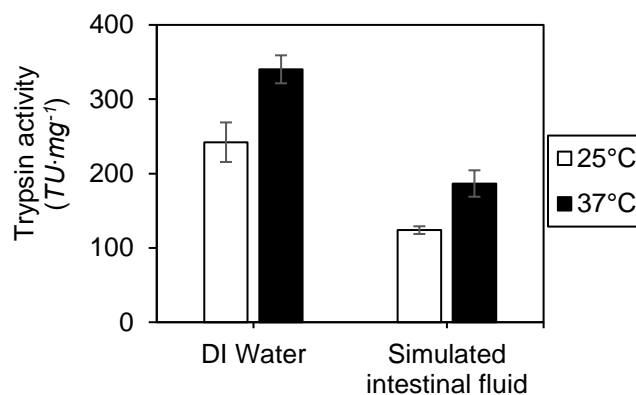


Figure 26. Trypsin activity in dependence of solvent type (n = 3; pH 8.1)

The obtained results (figure 26) demonstrated that at 25°C and 37°C, the trypsin activity was significantly (α 0.05) lower in the presence of electrolytes than when the enzymatic solution was prepared in DI water. This decrease in activity was of 51 % at 25°C and of 55 % at 37°C.

The effect of temperature on trypsin activity was similar when the enzyme was dissolved in DI Water (71 % increase at 25°C) or in simulated intestinal fluid (SIF) (66 % increase at 25°C).

3.4. Lipase

3.4.1. Alternative source to human gastric lipase

Gastric lipase is secreted in the stomach where the pH varies from pH 1.4 to pH 6.6 (9,10). Among the commercially available lipases, the rabbit gastric lipase is the alternative source that could best mimic the human gastric lipase (HGL) because it generates the same lipolytic products as the HGL (19).

However, this lipase source is expensive to carry out in vitro digestion methods periodically. For that reason, other sources like fungal lipases were studied in this thesis.

The physiological and experimental activities are expressed at 37°C, the same temperature at which the in vivo digestion takes place. Therefore, the effect of temperature was not included in the study to find an adequate alternative to the HGL.

However, as the pH varies during the digestion the effect of pH on the lipase activity for two fungal lipases was studied. The selected lipases as potential alternative sources to HGL were lipase from *Rhizopus Oryzae* (source I) and *Aspergillus Niger* (source II). To study the effect of the pH on the lipase activity, the aqueous phase of the emulsion was adjusted to different pH values between pH 1.7 – 8.0, except for source II where the studied pH range was pH 1.7 – 5.5 (corresponds to pH curve used in the dynamic digestion method). The results are depicted in figure 27.

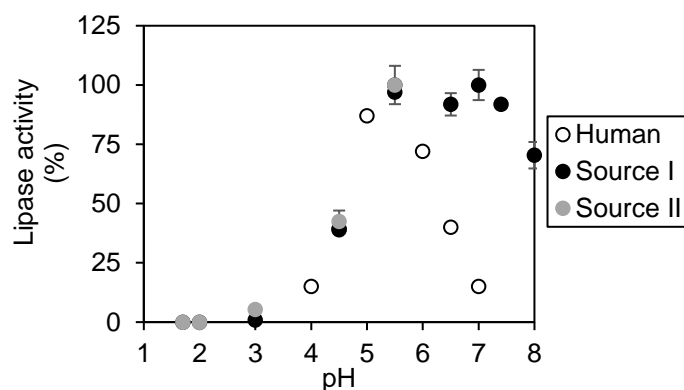


Figure 27. Effect of the pH on the activity of lipase from *Rhizopus Oryzae* (source I) and lipase from *Aspergillus Niger* (source II) (37°C) in comparison to literature data for HGL at 37°C (20)

As shown in figure 27, the maximum activity for both fungal lipases was obtained at pH 5.5 which matches the optimal pH of the HGL. However, while the activity of HGL decreased above the optimal pH, the activity of the source I remained constant until pH 7.5. Thus, above the optimal pH, the pH profile for the human and fungal lipases is different. At pH 7.0 the fungal lipase still showed 100 % of their activity whereas the HGL only showed 15 %. Therefore, at pH 6.0 or higher the fungal lipase is not a good alternative to the HGL.

On the other hand, at acidic conditions the potential alternative lipases mimic the HGL activity closely, e.g., the activity of the HGL at pH 4.5 was 39 % of the activity at the optimal pH, while the potential alternatives showed 39.4 (source I) and 42.5 % (source II) of the activity at pH 5.5.

The experimental activities showed that the pH profile of the two proposed fungal lipases at 37°C is similar, but the commercial product of source I was of higher purity than the one of source II. Besides, gastric lipase from rabbit (19), fungal lipase from source I could be an economic solution to carry out the gastric phase of the in vitro digestion methods.

3.4.2. Effect of electrolytes on lipase activity

During digestion, the lipase acts in contact with electrolytes, therefore the effect of the electrolytes present in the gastric juice on the lipase activity was studied for source I and the obtained results are depicted in figure 28:

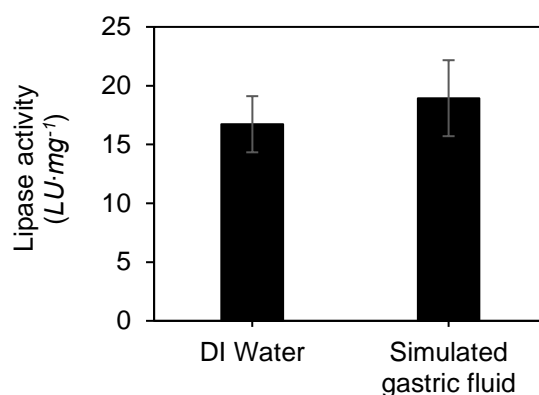


Figure 28. Lipase activity (source I) in dependence of solvent type (n = 15; 37 °C; pH 8.0)

The results (figure 28) do not show significant (α 0.05) differences in lipase activity in the absence or presence of gastric electrolytes. The activity changes from 16.7 ± 2.4 LU·mg⁻¹ (no electrolytes) to 18.9 ± 3.2 LU·mg⁻¹ (electrolytes) at 37°C.

3.5. Pancreatin

3.5.1. Pancreatic powders

It is reported that the best alternative source for the human pancreatin is a porcine pancreatin (21). However, there are a lot of commercial products available for this alternative and each of them exhibits a different enzyme-ratio (α -amylase : trypsin : lipase). For that reason, the activity of the main enzymes present in the pancreatin was measured. The commercial pancreatins tested for this study are:

- P1: Pancreatic enzyme for cats and dogs – Pancrex Vet (Pfizer)
- P2: Pancreatic enzyme for cats and dogs – Pancrex (Zoetis)
- P3: Pancreatin from porcine pancreas 4xUSP (Sigma Aldrich)
- P4: Pancreatin from porcine pancreas 8xUSP (Sigma Aldrich)
- P5: PancZyme (American Laboratories inc.)
- P6: Pancreatin powder (Nordmark)

3.5.1.1. α -amylase activity

Pancreatic solutions at different concentrations were prepared for the correct enzyme activity measurement. The α -amylase activity levels present in the different pancreatins (P1 – P6) are depicted in figure 29, where the experimental activities (AU·mg⁻¹) are compared with the activities given by the supplier (partially converted data).

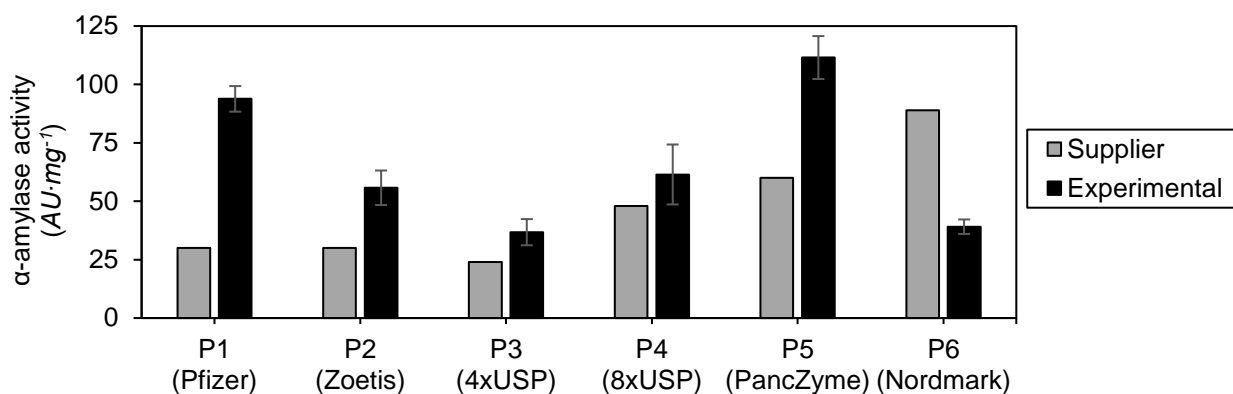


Figure 29. α -amylase activity present in the commercial pancreatic powders (supplier vs experimental activities)

The highest α -amylase activity levels were experimentally found for P1 and P5 and lowest for P3 and P6. The experimental α -amylase activities of the different commercial pancreatins vary from $36.8 \pm 5.6 \text{ AU}\cdot\text{mg}^{-1}$ (P3 – 4xUSP) to $111.5 \pm 9.2 \text{ AU}\cdot\text{mg}^{-1}$ (P5 – PancZyme). Thus, revealing that α -amylase levels in the pancreatic powders are different depending on the supplier.

Major differences to supplier data were obtained for P1, P5 and P6, while for P2, P3 and P4 only minor differences were obtained (considering the SD). And in contrary to all other materials for P6 the activity given by the supplier is higher than the experimentally determined activity.

The activities given by the suppliers were expressed in the same units as defined for the experimentally determined activities. However, the assay conditions were different. These differences in the conditions of the activity measurements could explain the differences between the supplier activities and the experimentally found activities.

Another aspect that could affect the activity is that in some of the pancreatins (P1 – P4) the supplier activity was not related to the specific batch, but a general activity level of their product. And it is known that the activity can differ from batch to batch but also the same batch could show a difference in its activity depending on the storage time and conditions.

To reach the physiological activity of α -amylase in vitro experiments, the concentration ($\text{g}\cdot\text{mL}^{-1}$) of the pancreatin would be much higher for the pancreatins with lower activity like P3 (4xUSP) than for pancreatins with higher activity like P5 (PancZyme).

Besides, the pancreatic powders are not completely soluble for that reason it is important to also take the mass concentration for the selection of the commercial pancreatin into consideration, as the activity may decrease when the mass concentration increase.

However, the optimal pancreatin should be chosen by taking into account the combination of the activity of the three enzymes (enzyme-ratio) more than the activity of a single enzyme. Therefore, protease and lipase activity were compared in the subsequent sections.

3.5.1.2. Protease (trypsin) activity

The pancreatin contains proteases like trypsin and chymotrypsin, these proteases are responsible for the catalysis of protein hydrolysis in the small intestine, but also for the possible degradation of the pancreatin itself.

The suppliers give the protease activity as a combination of, mainly, two enzymes, trypsin and chymotrypsin. However, the experimental activities are only referred to the trypsin activity.

The comparison of the given activities by the supplier (partially converted data) with the experimental activities ($\text{TU}\cdot\text{mg}^{-1}$) for the different commercial pancreatins is depicted in figure 30:

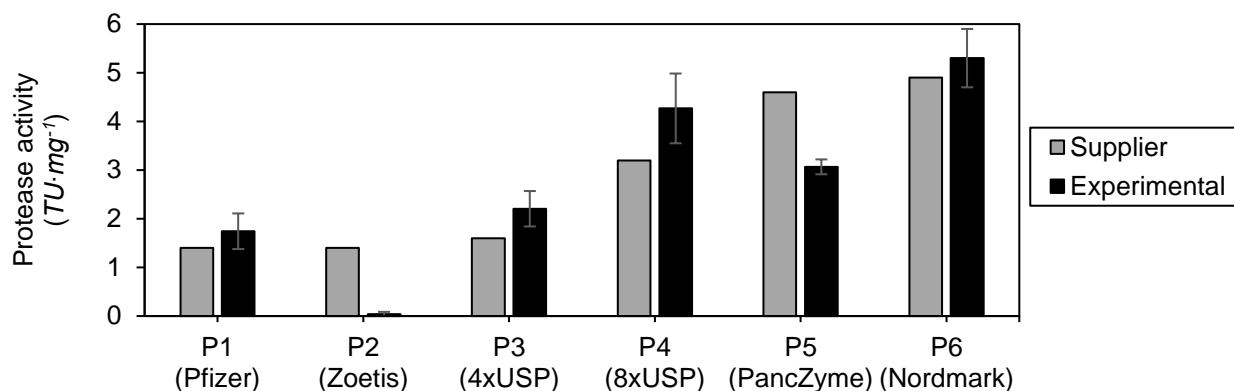


Figure 30. Protease activity present in the commercial pancreatic powders (supplier vs experimental activities)

The main differences between the supplier and experimental activities were found for the P2-Zoetis and P5-PancZyme pancreatins, where the experimental activities are lower than the activities provided by the supplier. Concretely, the biggest difference belongs to P2-Zoetis where almost no proteolytic activity was found. For P1, P3, P4 and P6 supplier activity is lower than experimental activities. Apart from P2-Zoetis, the range of trypsin activity in these pancreatins goes from $1.7 \pm 0.4 \text{ TU}\cdot\text{mg}^{-1}$ for P1-Pfizer to $5.3 \pm 0.6 \text{ TU}\cdot\text{mg}^{-1}$ for P6-Nordmark.

The differences found for P2 and P5 could be explained, by the existent differences between batch to batch (data for P1-P4 were only available for the general product but not for the specific batch). Furthermore, it needs to be considered, that the supplier activity combines trypsin and chymotrypsin while the experimental activity is only referring to the trypsin activity.

Although a narrow range of trypsin activity was obtained for the tested pancreatins, it is important to take into consideration the differences in the activity between the products for the selection of the optimal pancreatin, as these activity levels are low compared with the other enzymes.

3.5.1.3. Lipase activity

The pancreatic lipase is the enzyme responsible for the catalysis of the fat hydrolysis in the small intestine. Due to its inhibition by the also present bile, the presence of colipase is important to retain the pancreatic lipase activity. Enough colipase is present in the pancreatic powders.

The lipase activity levels present in the studied commercial pancreatins (P1 – P6) are depicted in figure 31, where the experimental activities ($\text{LU}\cdot\text{mg}^{-1}$) are compared with the activities given by the supplier (partially converted data).

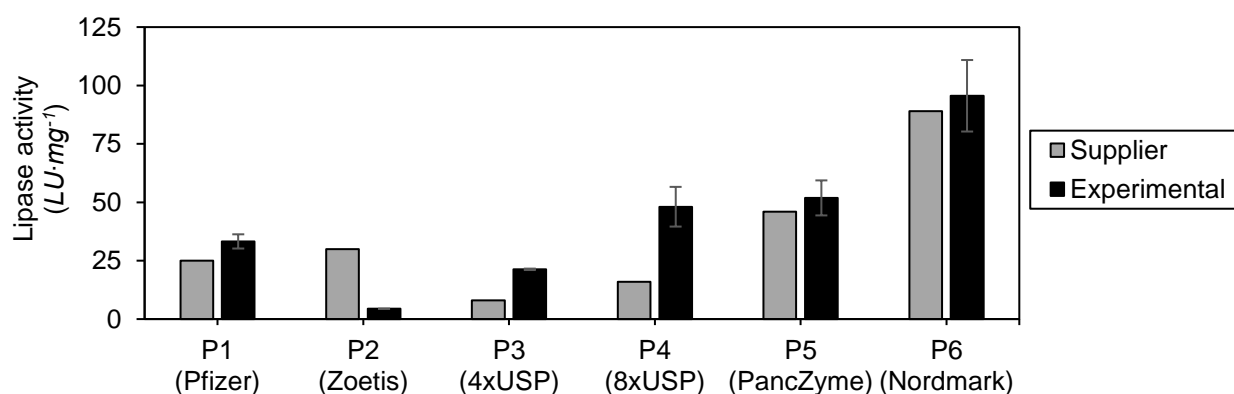


Figure 31. Lipase activity present in the commercial pancreatic powders (supplier vs experimental activities)

As depicted in figure 31, the analysed pancreatins could be classified as pancreatin with low, moderate and high lipolytic activity, except for P2 (Zoetis):

- Low activity: P1 – Pfizer ($33.3 \pm 3.0 \text{ LU}\cdot\text{mg}^{-1}$), P3 – 4xUSP ($21.3 \pm 0.3 \text{ LU}\cdot\text{mg}^{-1}$)
- Moderate activity: P4 – 8xUSP ($48.1 \pm 8.5 \text{ LU}\cdot\text{mg}^{-1}$), P5 – PancZyme ($51.9 \pm 7.5 \text{ LU}\cdot\text{mg}^{-1}$)
- High activity: P6 – Nordmark ($95.6 \pm 15.3 \text{ LU}\cdot\text{mg}^{-1}$)

For pancreatin P2 (Zoetis) a lower experimental lipase activity compared to the supplier was obtained and also compared to the other pancreatins. As already discussed for the trypsin activity, this low activity may be due to the storage effect.

The experimental activities found for the powders P3 – 4xUSP and P4 – 8xUSP are higher than the activity given by the supplier, where the activity given by the supplier only reaches values of ~35 % of the experimental activity (P3 – 4xUSP: 37 %, P4 – 8xUSP: 33 %). This could be explained by the fact that this supplier only specifies the minimum activity that these products would contain but not the actual activity.

Due to the obtained differences in lipolytic activity, the studied pancreatin was revealed to have different fat-digesting capacities. This is despite the fact that all studied commercial products are from porcine origin.

After all major enzyme activities were detected individually, the results will be set in relation to each other in the text section to identify an adequate pancreatin to carry out in vitro digestions.

3.5.1.4. Enzyme ratio

When a pancreatic solution is used (for digestion experiments) the three major enzymes (α -amylase, trypsin, lipase) are present. For the selection of the optimal pancreatin it is important to take the enzyme ratio (α -amylase to trypsin to lipase) into account that is present in the specific pancreatin.

The enzyme-ratio was based on the trypsin activity, as it is the enzyme with the lowest activity in all the pancreatins.

To calculate the enzyme ratio, the experimental α -amylase and lipase activities displayed in figures 29 and 31 were set in relation to the experimental trypsin activities depicted in figure 30 (eq. 1, 2), and considering a solution of $1 \text{ mg}\cdot\text{mL}^{-1}$, to be able to compare the commercial pancreatins with the human pancreatin which activity is reported as $\text{U}\cdot\text{mL}^{-1}$.

$$\text{Enzyme ratio } (\alpha\text{-amylase}) = \frac{\alpha\text{-amylase activity}_{\text{Pancreatin 1}} (\text{AU}\cdot\text{mL}^{-1})}{\text{trypsin activity}_{\text{Pancreatin 1}} (\text{TU}\cdot\text{mL}^{-1})} \quad \text{Eq. 1}$$

$$\text{Enzyme ratio (lipase)} = \frac{\text{lipase activity}_{\text{Pancreatin 1}} (\text{LU}\cdot\text{mL}^{-1})}{\text{trypsin activity}_{\text{Pancreatin 1}} (\text{TU}\cdot\text{mL}^{-1})} \quad \text{Eq. 2}$$

The calculated enzyme-ratio for the different commercial pancreatins compared with the enzyme-ratio of the human pancreatin ($\text{U}\cdot\text{mL}^{-1}$) (Introduction_Figures 26b, 42, 53) are depicted in the following graph:

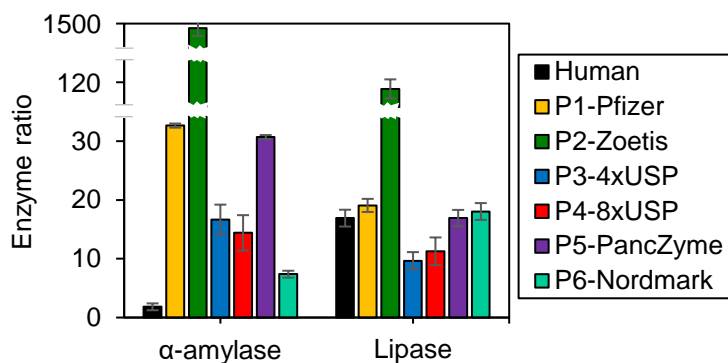


Figure 32. Enzyme-ratio for the commercial pancreatins compared with the human pancreatin (based on trypsin; trypsin = 1)

The enzyme-ratio of the human pancreatin was also calculated by applying the eq. 1, 2 with the physiological activities (Introduction_Figures 26b, 42, 53), and the obtained enzyme-ratio was $1.8 (\pm 0.3) : 1 : 16.9 (\pm 5.6)$ for α -amylase, trypsin and lipase, respectively. However, later on an approximate enzyme-ratio ($2 : 1 : 20 - \alpha$ -amylase : trypsin : lipase) was used as a ratio goal to correctly mimic the human pancreatic digestion.

As it can be seen in figure 32, very high α -amylase ratio was found for P2 (Zoetis) while high ratios were found for P1 (Pfizer) and P5 (PancZyme) and medium ratios for P3 (4xUSP) and P4 (8xUSP). On the other hand, very high lipase ratio was found for P2 (Zoetis) while low ratios were found for P3 (4xUSP) and P4 (8xUSP) and for P1 (Pfizer), P5 (PancZyme) and P6 (Nordmark) similar results as for human were found.

When the amount of pancreatin needed for the in vitro digestion method is calculated based on the lipase or trypsin activity, there would be an excess of α -amylase. This excess of α -amylase in the small intestine of the in vitro digestion methods could result in the obtention of an overestimated prediction of carbohydrates digestibility. Or, on the other hand, the pancreatic concentration could be calculated based on the α -amylase activity and then, it would result in the obtention of an underestimation of the protein and fat digestibility.

As seen in figure 32, for all non-human pancreatins α -amylase activity would be too high when trypsin and lipase activities are adjusted to the physiological levels.

The commercial pancreatin with an enzyme-ratio that differs most from the human pancreatin is P2 (Zoetis), which has an enzyme-ratio of $1394 : 1 : 110$ (α -amylase : trypsin : lipase). The obtained enzyme-ratio of P2 (Zoetis) is that high because of its low trypsin activity, which was almost inexistent. Therefore, this commercial pancreatin was not considered for the use in the small intestine of the in vitro digestion methods.

The commercial pancreatins P3 (4xUSP) and P4 (8xUSP) from Sigma Aldrich showed similar enzyme-ratio between them, but slight differences when compared to the human enzyme-ratio. Both pancreatins were rejected for their use during intestinal digestion in in vitro digestion methods due to their low lipase activity.

Based on the above results, two other pancreatins were also rejected as potential alternatives: P1 (Pfizer) and P5 (PancZyme). The main reason for its exclusion was their high ratio obtained for α -amylase, which was ~ 15 -folds higher than the human α -amylase ratio. Even though, the obtained lipase ratios for both pancreatins were similar to the human one.

In the case of the pancreatin from Nordmark (P6), the obtained enzyme ratio for lipase matched with its human analogous. Therefore, it could be a good alternative to mimic the fat digestion in the small intestine. However, the calculated enzyme-ratio for α -amylase was slightly higher (4-folds) compared with the human α -amylase ratio but the lowest compared to all other pancreatins.

When the obtained enzyme-ratios for the 6 commercial pancreatins were compared, it was concluded that the pancreatin that contains the most similar enzyme-ratio to the human ratio was the P6-Nordmark pancreatin.

3.5.2. Mixture of pancreatin and individual enzymes

Although a commercial pancreatin with a similar enzyme-ratio as the human pancreatin was found, it still implies the limitation of the high α -amylase ratio (4-fold). Therefore, none of the available products mimics the ratio of the major enzymes present in the human small intestine precisely. As it is commented in the previous section, this leads to the point that when the amount of pancreatin is added based on the activity of one enzyme, the levels of the other enzymes would not be physiological.

It is reported that the human lipase is secreted in large excess into the small intestine and it would be sufficient to use lower amounts of the enzyme (22). For that reason, the minimum amount of pancreatic lipase needed for an in vitro digestion method was determined. Which was calculated to still assure that a 100 % fat meal is completely digested before the first sample is taken (e.g., 15 min). The following equation is an example of this calculation for the harmonised static digestion method (21).

$$\frac{5 \text{ mL meal}}{40 \text{ mL intestinal sample}} \cdot \frac{1 \text{ mL butyric acid}}{1 \text{ mL meal}} \cdot \frac{0.9528 \text{ g butyric acid}}{1 \text{ mL butyric acid}} \cdot \frac{1 \text{ mol butyric acid}}{88.11 \text{ g butyric acid}} \cdot \frac{10^6 \mu\text{mol}}{1 \text{ mol}} \cdot \frac{1}{15 \text{ min}} = 90.11 \frac{\mu\text{mol butyric acid}}{\text{mL}\cdot\text{min}} \quad \text{Eq. 3}$$

In eq. 3 it is considered that a meal consisting of 100 % fat would be completely digested and converted into butyric acid before the first sample is taken, at 15 min. For that reason, the 5 mL of meal that would be present in the “*small intestine*” (total volume: 40 mL) are transformed to molar concentration ($\mu\text{mol}\cdot\text{mL}^{-1}$) of butyric acid the in “*small intestine*” taking into account its density ($0.9528 \text{ g}\cdot\text{mL}^{-1}$) and molecular weight ($88.11 \text{ g}\cdot\text{mol}^{-1}$) of butyric acid. Finally, the calculated butyric acid concentration is divided by the time of the first sample to be taken (here 15 min). The butyric acid concentration is divided by the time of the first sampling point to consider the worst scenario, where all the meal would be completely digested before the first sample is taken.

For the calculation of the required lipase, the unit definition for the lipase activity was taken into consideration: one lipase unit is defined as the amount of enzyme needed to release 1 μmol of butyric acid per minute. Therefore, the minimum lipase activity needed to digest the 5 mL in the intestinal phase would be $90.11 \text{ LU}\cdot\text{mL}^{-1}$ (eq. 4):

$$1 \text{ LU} = 1 \frac{\mu\text{mol butyric acid}}{\text{min}} \rightarrow 90.11 \frac{\mu\text{mol butyric acid}}{\text{mL}\cdot\text{min}} = 90.11 \frac{\text{LU}}{\text{mL}} \quad \text{Eq. 4}$$

Considering that the physiological activity of the lipase in the small intestine is $1704.3 \pm 566.7 \text{ LU}\cdot\text{mL}^{-1}$ (23–26), the required activity is ~ 18 -fold lower.

The amount of lipase needed to mimic the fat digestion in the small intestine could therefore be securely decreased by ~ 8.5 -folds, being the adapted physiological activity $200 \text{ LU}\cdot\text{mL}^{-1}$.

Apart from the lipase, for the standardization of the in vitro digestion methods, the physiological activity in the small intestine was set for trypsin and α -amylase as $100 \text{ TU}\cdot\text{mL}^{-1}$ (reported activity: $100.8 \pm 31.7 \text{ TU}\cdot\text{mL}^{-1}$ (17, 23, 27 – 30) and $200 \text{ AU}\cdot\text{mL}^{-1}$ (reported activity: $183.9 \pm 28.9 \text{ AU}\cdot\text{mL}^{-1}$ (23, 27,31 – 34)), respectively. These activities of trypsin and α -amylase were also recommended by Minekus et al (21).

Considering the specific activity of the selected pancreatin in the previous section (P6-Nordmark), the amount of pancreatin needed for the in vitro digestion method was calculated to reach the physiological levels in the small intestine.

Since, the commercial pancreatin P6 (Nordmark) did not match the enzyme-ratio with the human pancreatin, the mass concentration was calculated based on the lipase activity, as it is the enzyme with the highest activity in the pancreatin. After considering the adapted lipase activity, the α -amylase and trypsin activities will be lower than in vivo.

For that reason, there was the need to also add these enzymes as individual enzymes until the physiological pancreatic levels were reached.

The effect of the addition of individual enzymes to the pancreatin on the activity was subsequently studied. The comparison of the physiological activities and the use of pancreatin alone or with the addition of individual enzymes is depicted in the following figure:

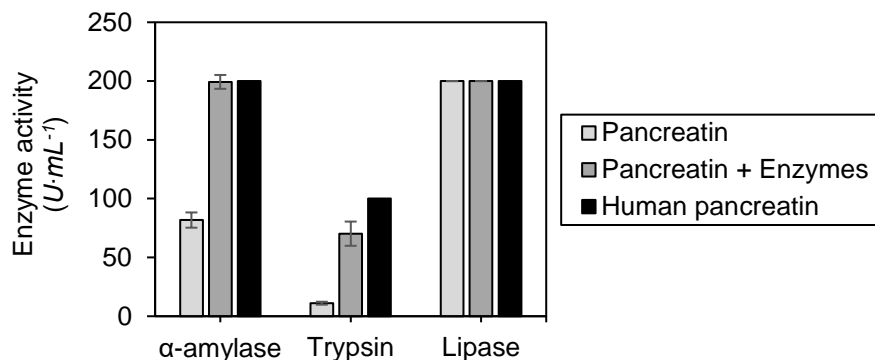


Figure 33. Enzyme activity of the human pancreatin (lipase activity adapted) compared to that of the prepared pancreatic solution and the mixture of pancreatin and individual enzymes

The activities shown in figure 33 are expressed as U·mL⁻¹, where the unit definition is different depending on the enzyme, being AU for α-amylase, TU for trypsin and LU for lipase. The physiological lipase activity that appears in this figure is the adapted lipase activity: 200 LU·mL⁻¹.

Figure 33 revealed that when the porcine pancreatin was used alone (no addition of individual enzymes), the activity of trypsin (11.1 ± 1.3 TU·mL⁻¹) and α-amylase (81.8 ± 8.2 AU·mL⁻¹) did not reach the selected physiological levels.

However, with the addition of individual enzymes to the pancreatin, the determined α-amylase activity in the intestinal phase (199.3 ± 5.9 AU·mL⁻¹) was equal to the physiological one. The overall trypsin activity was slightly lower (70.2 ± 10.3 TU·mL⁻¹).

In this study it was seen that the amount of the enzymes needed to reach the physiological activities could not be calculated by measuring the activity of the individual enzymes and then mixing it directly with the pancreatin. In contrast, the individual enzymes were mixed with the pancreatin and then the activity of the mixture was measured. The amount (in mg) of the individual enzymes was modified until a final pancreatic solution with the “physiological” activities was achieved.

Figure 34 is an example of the difference in the calculated activity taking into account the specific activities of the pancreatin and trypsin independently or when they were first mixed and then the activity experimentally measured:

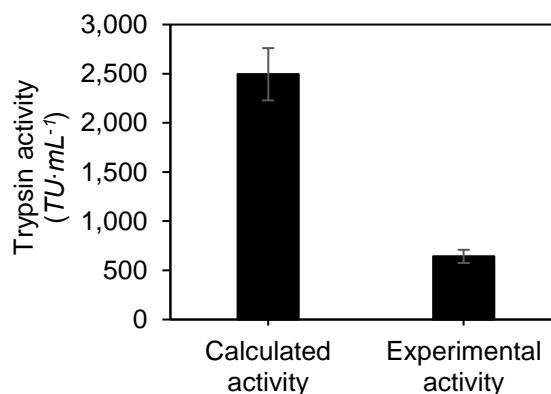


Figure 34. Differences between the theoretical and experimental trypsin activity

The “Calculated activity” was calculated (eq. 5, 6) taking into account the mass concentration and specific activity of the pancreatin and trypsin:

$$350.7 \text{ mg Pancreatin} \cdot \frac{5.3 \text{ TU}}{1 \text{ mg}} = 1858.7 \text{ TU}; \quad 249.8 \text{ mg Trypsin} \cdot \frac{242.2 \text{ TU}}{1 \text{ mg}} = 60501.6 \text{ TU} \quad \text{Eq. 5}$$

$$\frac{1858.7 \text{ TU} + 60501.6 \text{ TU}}{25 \text{ mL}} = 2494.4 \text{ TU} \cdot \text{mL}^{-1} \quad \text{Eq. 6}$$

In summary, it was concluded that the use of a combination of pancreatin and individual enzymes is preferential to the use of pancreatin alone.

3.5.3. Effect of electrolytes

The effect of the electrolytes on the pancreatic activity was expected to be similar to that for the individual enzymes. Thus, the activity would increase for α -amylase, decrease in the case of trypsin and remain constant for the lipase.

The obtained activity of the three enzymes of interest from the pancreatin is depicted in figures 35 – 37, in the presence and absence of the electrolytes present in the gastrointestinal tract at the physiological concentrations.

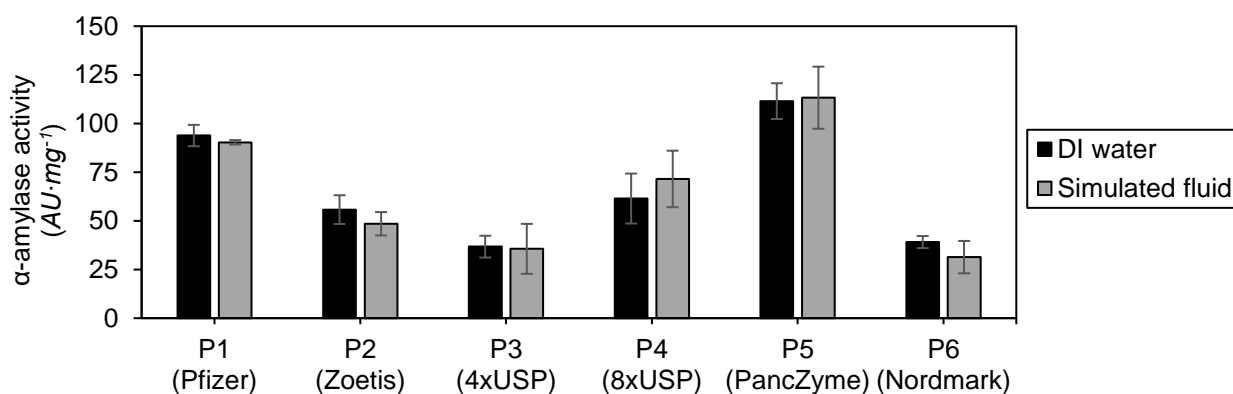


Figure 35. Effect of the electrolytes present in the small intestine on the α -amylase activity

Figure 35 revealed that, in contrast to the expectations, when the pancreatic solution was prepared in presence of the simulated intestinal fluid no increase or decrease of α -amylase activity was obtained. The individual enzyme studied in section 3.1.2. (A3176) is also from porcine origin. Therefore, the activity increasing effect of the electrolytes was expected to be the same or similar for the pancreatin products.

However, the pancreatic powders also contain some electrolytes (e.g., P1-Pfizer contains $10.1 \text{ mg} \cdot \text{g}^{-1}$ of Ca^{2+} – experiment not shown) that might already lead to an increase in α -amylase activity in contrast to a scenario in the absence of electrolytes. While a further increase of electrolytes in the simulated fluid do not lead to a further increase in activity.

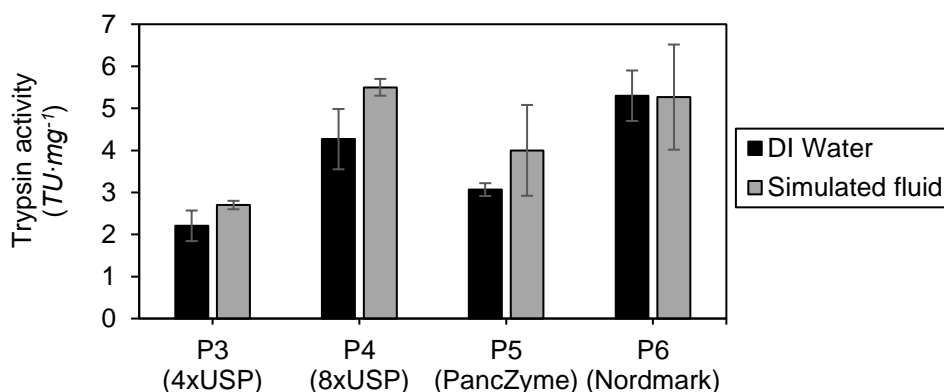


Figure 36. Effect of electrolytes present in the small intestine on the trypsin activity

In the case of trypsin activity, the commercial pancreatins P4 (8xUSP) and P5 (PancZyme) show slightly but insignificant lower activity in the absence of electrolytes. Also, for P3 (4xUSP) and P6 (Nordmark) no major differences for resulting trypsin activity was found in the presence of electrolytes. Those findings are in contrast to the results obtained for the individual enzyme in section 3.3.2, where a decreasing activity was found in the presence of electrolytes. Apart from the electrolytes present in the pancreatic powders that might impact the trypsin activity, it needs to be noted that the pancreatins are of porcine source while the trypsin used in section 3.3.2 is from bovine origin. Therefore, the source of the enzyme could also account for the difference in its behaviour in the absence/presence of electrolytes.

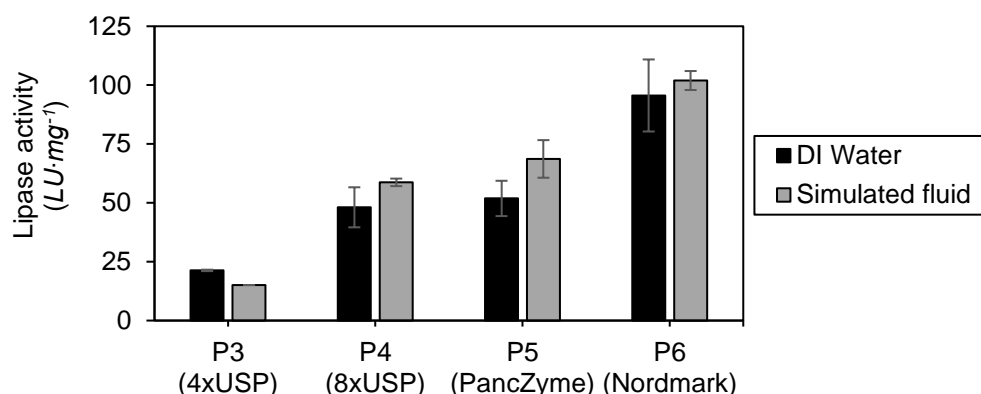


Figure 37. Effect of electrolytes present in the small intestine on the lipase activity

The commercial pancreatin P3 (4xUSP) shows slightly lower activity in the presence of the simulated fluid, while P4 (8xUSP), P5 (PancZyme) and P6 (Nordmark) show insignificant higher activity when they were dissolved in simulated fluid.

The lipase from the pancreatin is the only enzyme that maintains its behaviour compared to the study carried out in section 3.4.2., and is not affected by the presence of the electrolytes that the simulated intestinal fluid consists of. Besides, it is important to note that the individual enzyme used in section 3.4.2., has a different source as it is a fungal lipase while pancreatin is from pork.

The only exception would be pancreatin P3-4xUSP where the activity obtained in the absence of electrolytes is slightly higher than in the presence. However, taking into account the results for the other pancreatins, this was not considered a significant difference.

In conclusion, unlike the results obtained for the individual enzymes, the presence of the electrolytes from the SIF did not affect the enzyme activity of pancreatin. This could be explained by the fact that pancreatin already contains electrolytes, but also by the fact that the commercial pancreatins are from porcine source while the individual enzymes studied (except α -amylase) are from a different source (bovine trypsin and fungal lipase).

3.6. Determination of maximum storage time of enzymatic solutions

As the enzymatic products are powders, they need to be dissolved to carry out the in vitro digestion methods. Ideally, all the enzymatic solutions needed to carry out the in vitro digestion method should be prepared just before use, but this is time-consuming and sometimes not applicable. To be able to use enzyme stock solutions, it is necessary to demonstrate their stability in terms of remaining activity.

The stability of the individual enzymes α -amylase, pepsin, trypsin and lipase in solution was tested for up to 12 months. The effect of storage on the enzyme activity was studied by dissolving the enzymatic powders in DI water (figure 38) but also in the corresponding simulated digestive fluid (figure 39), to additionally check the effect of the electrolytes on the enzyme activity during storage at -20°C .

Figure 38 shows the remaining enzyme activity (%) during storage at -20°C , when the enzymes were dissolved in DI Water.

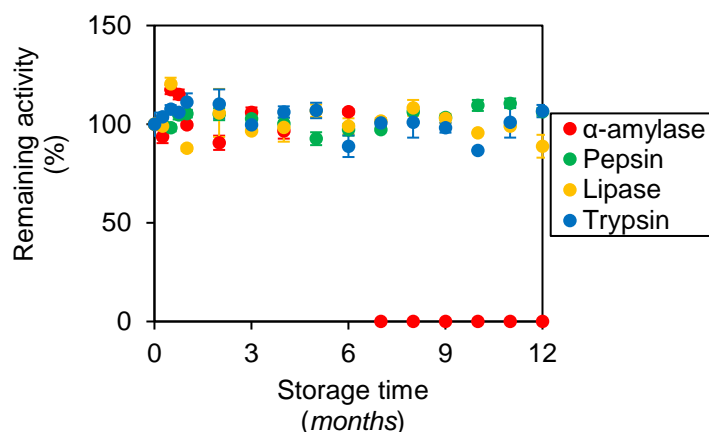


Figure 38. Effect of storage time on enzyme activity (solvent: DI water, temperature: -20°C)

The results depicted in figure 38 demonstrate that the enzymatic solutions were stable for a long period of time, showing $\sim 100\%$ of its initial activity after 12 months for all the cases except for α -amylase. In the absence of electrolytes, the α -amylase solution maintained its activity for 6 months. After 6 months, the remaining activity was found to be 0% which means that the enzyme solution completely lost its enzyme activity. This could be explained by the fact that, in the absence of electrolytes, α -amylase already had a low specific activity (figure 22).

Therefore, the α -amylase solution could only be used for the in vitro digestion methods during the first 6 months after its preparation, since beyond that time it lost its activity. On the other hand, the proteases and lipase solutions could be used for 1 year after its preparation, since after this time they still showed $\sim 100\%$ of their activity.

Figure 39 represents the remaining activity (%), when the enzymatic solutions were prepared in the respective simulated digestive fluids, during storage at -20°C .

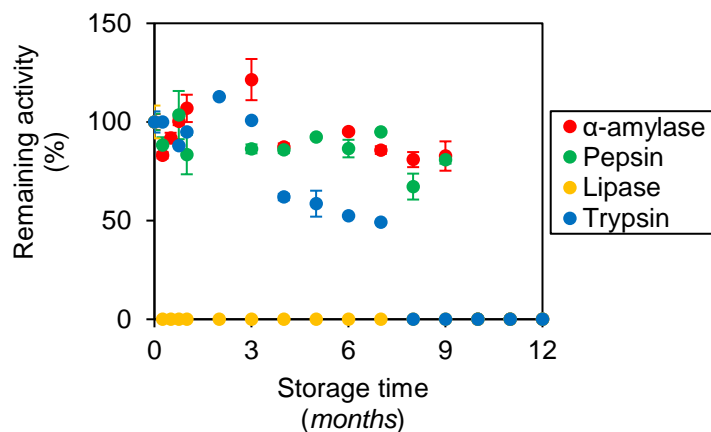


Figure 39. Effect of storage time on enzyme activity (solvent: SDF)

In the case of α -amylase high remaining activity was found up to 9 months and from that time onwards no activity. The same behaviour was found for the pepsin, the pepsin solution kept some activity until 9 months, and then from 9 to 12 months no activity was found. For the trypsin, high remaining activity was found during the first 3 months, then the activity slightly decreased until 7 months of storage and no activity was found between the 8th and 12th month of storage. The lipase lost its activity from the 1st month as no activity could be measured.

In contrast to the previous figure, more differences were found in the remaining activity between the enzymes in the presence of electrolytes. Thus, the presence of electrolytes has an impact on the stability of the enzyme solutions.

In the case of α -amylase, the fact that the enzyme was prepared in SSF made the solution stable for 3 months longer than when prepared using DI water as solvent. Therefore, the α -amylase solution could be stored for 9 months, since up to this time the enzyme was active, meaning that it could be used for performing *in vitro* digestion studies.

On the other hand, the preparation of the enzymatic solutions with simulated digestive fluids had a negative effect on storage stability for the proteases and lipase. This reduction in the solution stability for pepsin and lipase could be explained by the fact their solution was prepared using SGF, which had a pH of 3.0, and this low pH could account for the loss of activity. This effect was much more accentuated for lipase than for pepsin, since the solution of lipase lost its activity already during the first month, whereas the pepsin solution maintained its activity for 9 months.

The trypsin solution was prepared with SIF (pH 7.0), and the solution maintained its activity for 3 months, and then the activity started to decrease until it completely lost its activity after 8 months of its preparation.

In conclusion, the results obtained suggest that the enzymatic solutions were stable for a long period of time. However, individual stability differences were obtained. Furthermore, the stability depended on the type of solvent used to dissolve the enzyme as well as the pH of the solution. In summary, the α -amylase is more stable in the presence of electrolytes, whereas the other enzymes are more stable when dissolved in DI water.

4. Adaptation of non-enzymatic key parameters of *in vitro* methods

4.1. Bile acids concentration

To achieve the physiological concentration of bile, it was necessary to measure the concentration of the prepared bile solution. Two different bile sources were studied for their use in the *in vitro* digestion methods, one porcine and one bovine bile. Both commercial bile products were purchased in powder form, requiring a solubilization step.

After solubilization (using DI water as solvent), the kit “Bile acids” from Diagnostic systems was used to measure the molar concentration (μM) of the bile solution. The measured concentration was $45.2 \pm 0.4 \mu\text{M}$ for bovine bile and $45.4 \pm 1.6 \mu\text{M}$ for the porcine bile solution (data not shown).

To reach the reported physiological bile concentration required in the solution a recalculation of the required powder is needed. To do so a molecular weight is needed. As bile consists of a mixture of substances, a so-called virtual molecular weight was used. To know the amount (in mg) of bile needed to mimic the human concentration, a virtual molecular weight was calculated. It is a virtual molecular weight since bile is a mixture of substances.

The virtual molecular weight calculated (Materials and methods_Section 5.4.) for the used batch of both biles were $1141.1 \pm 10.7 \text{ g}\cdot\text{mol}^{-1}$ for bovine bile and $1247.9 \pm 44.7 \text{ g}\cdot\text{mol}^{-1}$ for porcine bile.

As the alternative source to human bile, the bovine bile was selected to carry out the in vitro digestion methods for two reasons. The first and most important reason is that the composition in bile acids for the bovine bile is reported to be more similar to the human bile (35). The second reason is related to its solubility. While the bovine bile was completely soluble, the porcine bile solution always revealed remaining precipitate that was insoluble (data not shown).

4.2. Determination of the mixing speed

During human digestion, the meal is mixed with the secretions along the gastrointestinal tract by peristaltic movements. To mimic this movement in the static digestion method described by Minekus et al (21), the New Brunswick Innova 40/40R thermoshaker was used for this thesis. This thermoshaker allows mixing the meal with the secretions but also incubating the digestive mixtures at the desired temperature (37°C).

It is important to use the correct mixing speed, because if the speed used is too slow the meal and the secretions would not mix properly, which could lead to an underestimated digestibility of the meal of interest. But, if the speed used is too fast then the meal is likely to disintegrate faster than it would in the human body, which would induce an overestimated digestibility.

Therefore, the minimum speed necessary to completely mix the meal with the secretions was studied and the obtained results are depicted in figure 40:

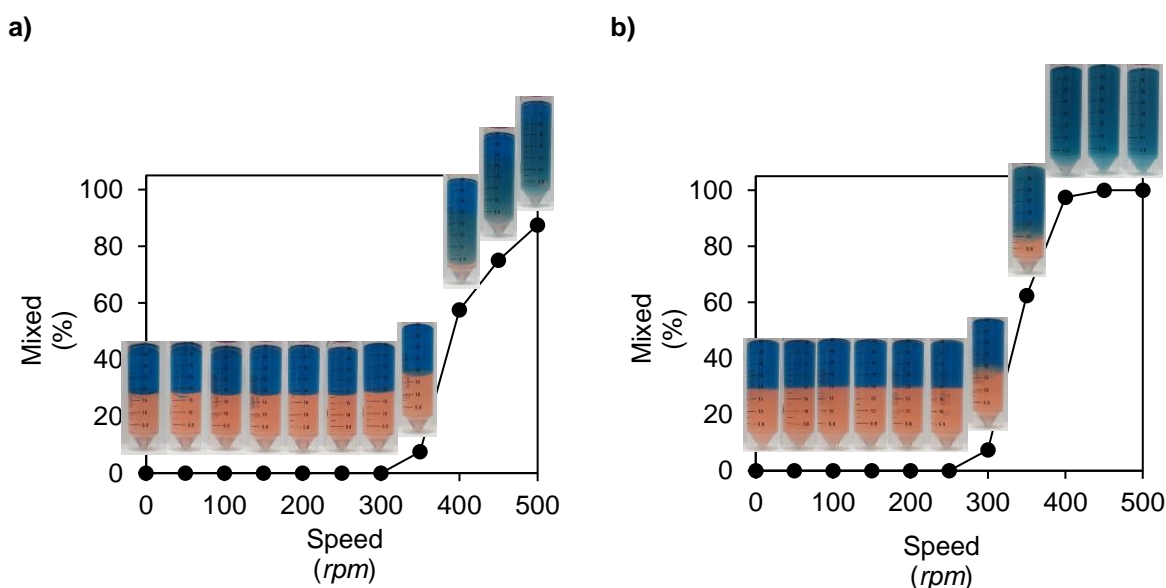


Figure 40. Effect of the shaking speed on the mixing process a) without emulsifier, b) with emulsifier

Figure 40 shows the percentage of the tributyrin mixed with DI water in the absence (a) and presence (b) of an emulsifier. In the absence of an emulsifier, ~90 % of tributyrin is mixed with water when the maximum speed of 500 rpm is used. Thus, even when the solutions were mixed at the fastest rate it was insufficient for complete mixing.

During both in vivo and in vitro digestion bile is present, which acts as an emulsifier. Thus, the results depicted in figure 40b are more representative for finding the optimal speed for the thermoshaker.

Figure 40b reveals that the slowest speed at which, shaking started to affect on the mixing process was at 300 rpm, 50 rpm less than in the absence of the emulsifier. At 350 rpm the amount of the fat mixed with water increased (~60 %) but it is not until the shaking reaches speeds of 400 rpm that the mixing of both substances was complete.

Based on the above results, the speed selected for the proper mixing with the thermoshaker was 400 rpm, as it was the minimum speed necessary to completely mix the fat and the water.

4.3. Method to stop digestion

In order to follow the digestion of a meal in in vitro digestion methods, a method to stop the action of enzymes was needed. For that reason, different techniques were tested to find the best method to stop the hydrolysis.

4.3.1. Physical removal

One way to stop the hydrolysis was the physical removal of the enzymes through the use of filters. Two types of filtration were studied as potential methods to physically remove the enzymes from the digestive mixtures and leave the samples free of enzymes.

The specifications of the filters used to physically remove the enzymes are described in table 2:

Table 2. Specification of the filtration techniques
(PTFE: polytetrafluoroethylene, PES: polyethersulfone, CA: cellulose acetate)

Filtration technique	Material filter	Pore size (μm)
Syringe filter	PTFE	0.45
	PES	0.20
Vacuum filter	CA	0.45
	PES	0.22

The most effective filter should have a pore size large enough for the analyte (glucose in this thesis) to pass through the filter, but small enough to be able to remove the enzymes. Therefore, the radii of the glucose and the digestive enzymes were calculated as:

$$\text{Volume of a molecule} = \frac{\text{Partial specific volume} \cdot \text{Molecular weight}}{\text{Avogadro constant}} \quad \text{Eq. 7}$$

$$V_{\text{sphere}} = \frac{4 \cdot \pi \cdot r^3}{3} \rightarrow r = \left(\frac{3 \cdot V}{4 \cdot \pi} \right)^{\frac{1}{3}} = \left(\frac{3 \cdot \frac{\text{Partial specific volume} \cdot \text{Molecular weight}}{\text{Avogadro constant}}}{4 \cdot \pi} \right)^{\frac{1}{3}} \quad \text{Eq. 8}$$

The partial specific volumes and molecular weight of the glucose and the digestive enzymes are summarised in table 3:

Table 3. Partial specific volumes and molecular weight of glucose and digestive enzymes (36–40)

	Partial specific volume ($cm^3 \cdot g^{-1}$)	Molecular weight (kDa)
Glucose	0.622	0.18
α -amylase	0.725	51 - 54
Pepsin	0.725	34.6
Lipase	0.725	32
Trypsin	0.725	24

The values of partial specific volume for most proteins lie between 0.700 and 0.750 cm³·g⁻¹, from which a value of 0.725 cm³·g⁻¹, is commonly used (36).

First, the volume of the molecule was calculated and expressed in nm³, then the radius could be calculated, and the values obtained are shown in table 4:

Table 4. Calculated radius of glucose and digestive enzymes

	<u>Volume</u> (nm ³)	<u>Radius</u> (nm)
Glucose	0.2	0.4
α-amylase	63.2	2.5
Pepsin	41.6	2.2
Lipase	38.5	2.1
Trypsin	28.9	1.9

The calculated radius from table 4 shows that in principle both glucose and enzymes are too small and would pass through the selected filters (0.20 – 0.45 μm), so filtration would not be a useful technique for the removal of these enzymes. However, not only the pore size is important for filtration, but the filter material also plays an important role. For that reason, the efficiency of filtration was studied by testing the remaining activity after filtration.

An enzymatic solution was prepared for each individual enzyme (α-amylase, pepsin, trypsin and lipase), and its activity was measured before and after the filtration to check whether the selected filters were the appropriate method for the enzyme removal.

The efficiency of the syringe filters for the enzyme removal is depicted in figure 41:

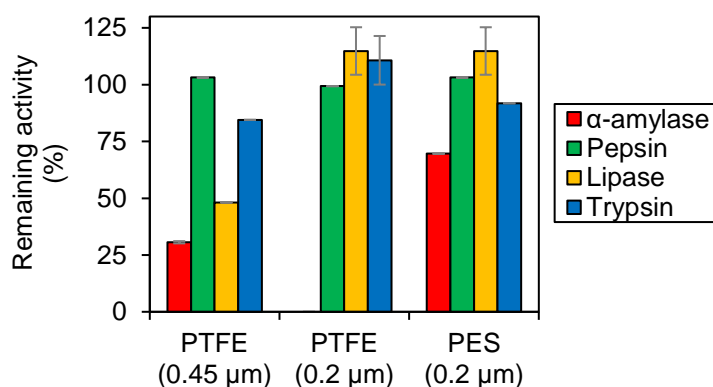


Figure 41. Remaining activity after filtration with the syringe filters

For α-amylase no activity was found when the solution was filtered with PTFE (0.2 μm) filter, while only a fraction of the initial activity could be measured when the solution was filtered with PTFE (0.45 μm) or PES (0.2 μm). For the pepsin, the remaining activity after its filtration was close to 100 % with the three tested filters. The lipase solution showed only a decrease in its activity when it was filtered with the PTFE (0.45 μm) filter, as with the other filters around 100 % was recovered after filtration. And according to the obtained results, the trypsin solution also kept almost all its activity after filtration.

Figure 41 demonstrates that filtration using syringe filters was not a good option for removing the enzymes as in general they were still active after filtration. However, the level of remaining activity obtained after filtration was different depending on the enzyme, filter material and pore size.

In the case of proteases (pepsin, trypsin) filtration did not affect on their activity as their solutions had close to 100 % of the activity they had before filtration.

The remaining activity obtained for the lipase suggested that the PTFE-0.45 μ m filter retained part of the enzyme as it only showed ~50 % of its activity after filtration. However, the remaining activity after the solution was filtered with the PTFE-0.2 μ m and PES-0.2 μ m was ~100 %.

Finally, in the case of the α -amylase there was a variation in the remaining activities depending on the filter used. All three filters retained part of the enzyme and there was a difference in the remaining activity depending on the material but also on the pore size of the filter. The PTFE filter was better than the PES filter as it retained more of the enzyme and at the same time, the filter with the 0.2 μ m pore size was more effective than the 0.45 μ m filter showing no activity after filtration with the PTFE-0.2 μ m filter.

In summary, it was concluded that the syringe filters were not a good technique to stop the digestion after sampling in in vitro digestion methods.

Therefore, the effectiveness of vacuum filters for the enzyme removal was studied and the results obtained are depicted in figure 42.

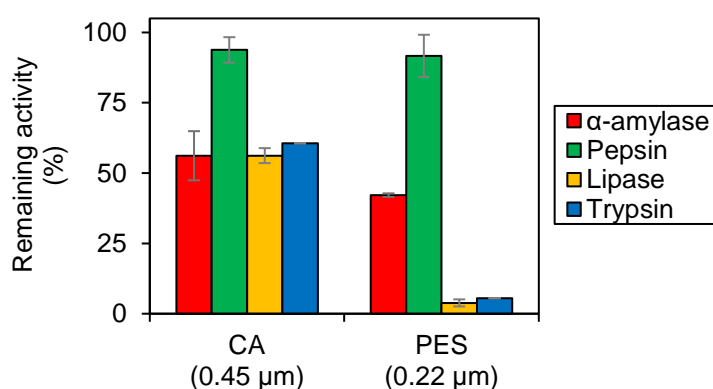


Figure 42. Remaining activity after filtration with the vacuum filters

For α -amylase, the activity decreased around 50 % after filtration with both filters, while the pepsin activity found after filtration was close to 100 %. The lipase and trypsin activities after filtration with the CA (0.45 μ m) decreased around 50 %, but almost no activity was found when those solutions were filtered with the PES (0.22 μ m) filter.

The filter made of PES and with a pore size of 0.22 μ m had very similar specifications to the PES-0.2 μ m filter used as a syringe filter (figure 41) but with the difference that in this case it was vacuum filtration. This difference already brought some differences in the remaining activity after filtration mainly for lipase and trypsin, which show almost no remaining activity. Pepsin still shows almost 100 % of the activity after the filtration and α -amylase solution had ~45 % activity remaining, which is just slightly less activity than that obtained with the syringe filter (~70 %).

When the CA-0.45 μ m filter was used, pepsin could pass through it as it shows ~100 % of the activity after filtration. However, the other three enzymes showed around ~60 % of the activity in the CA-0.45 μ m filtrate compared to before filtration.

Although vacuum filtration provided better results than using syringe filters, filtration was not effective enough, and therefore was not considered as an option to stop digestion.

4.3.2. Enzyme denaturation

Another method that was tested to stop the digestion after the sampling was the denaturation of the enzymes by applying a thermal treatment. The sample (enzymatic solution for the test) was incubated in a boiling water bath (100°C) for 5 min. The enzyme activity was measured before and after the thermal treatment to check its effectiveness.

Almost no activity was found for the enzymatic solutions after the thermal treatment (data not shown). This treatment was an effective method to stop α -amylase and pepsin activity as the enzymes were totally deactivated after the treatment.

The remaining lipase activity (%) found after the treatment was 4.0 ± 0.2 %, which is a very low percentage. Moreover, it should be noted that during the lipase activity measurement, the total volume of 0.1 N NaOH needed to counteract the released butyric acid was 7 μ L, and this small volume of titrant could be neglected and leave the remaining activity as 0 %.

Finally, the remaining trypsin activity found after the thermal treatment was about 15 %, therefore it was the enzyme that resisted most the heat treatment. Although some activity was found after the treatment, the percentage of the enzyme that was deactivated was high.

In conclusion, the thermal treatment was considered to be the optimal method to deactivate the enzymes after each sampling point of the in vitro digestion methods. But, as some activity for trypsin was found after treatment and to assure that the digestion of the macronutrients was stopped just after the sample collection, the samples were placed in an ice bath after the thermal treatment. Furthermore, all samples were stored in the freezer (at -20°C) until analysis.

4.4. Buffer for static digestion method

In the intestinal phase the action of lipase causes the release of fatty acids that could lead to a decrease in pH. This would affect the action of the intestinal enzymes and, therefore, the digestion of the meal. For that reason, different buffers were studied to keep the pH constant during the intestinal phase of the static digestion method (21).

The static digestion method was performed with a fatty meal (olive oil 50 %) and the pH of the intestinal phase was measured to study the effectiveness of the different buffers. The pH of the buffers was adjusted to 7 before its addition to the intestinal phase. The pH curves of the intestinal phase as a function of the buffer used are depicted in figure 43:

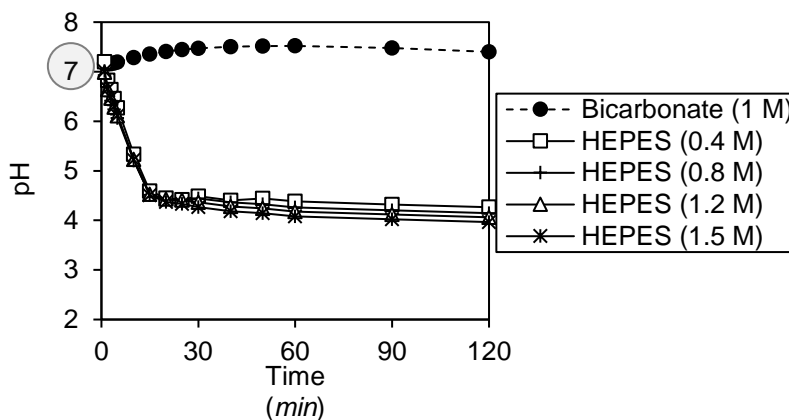


Figure 43. Buffer capacity during intestinal phase of a fatty meal

When bicarbonate buffer was used (closed circles) the pH of the intestinal phase remained at 7 for the total experimental time of 120 min. For all concentrations of HEPES buffer used an almost linear decrease in pH was observed in the first 15 min, followed by a plateau phase at pH ~ 4.5 (lipase activity minimised at these conditions, no more release of fatty acids leading to lower pH values beyond this).

The results demonstrate that the best option to keep the pH constant during the intestinal phase was the bicarbonate buffer since none of the studied concentrations of HEPES buffer was enough powerful to counteract the fatty acid release from the fatty meal.

4.5. Meal viscosity comparison

The viscosity of the meal could have an impact on its digestibility, and differences in meal viscosity could affect the obtained results and therefore the extracted conclusions.

For that reason, the viscosity of the following meals was measured to study the possible differences in their viscosities:

- *CH*: Starch from rice
- *CH+P*: Starch from rice and egg whites from chicken
- *CH+F*: Starch from rice and olive oil
- *CH+P+F*: Starch from rice, egg whites from chicken and olive oil

Figure 44 shows the viscosity curves (shear viscosity vs shear rate) obtained for the above meals:

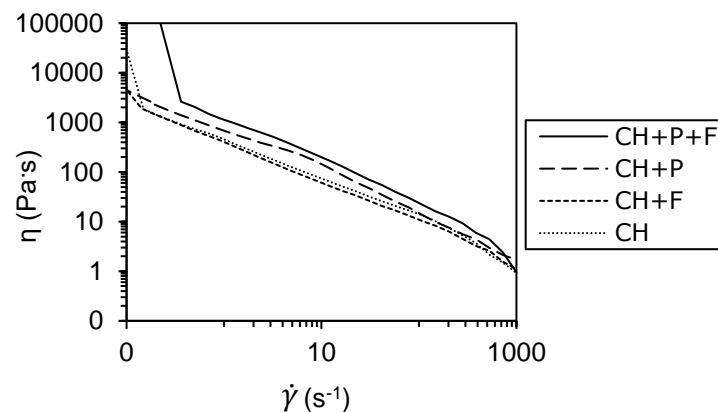


Figure 44. Comparison of the measured viscosity of four types of meals

The shear viscosity decreased with the shear rate, and at low shear rate this decrease was higher for the complete meal (CH+P+F) compared with the shear viscosity obtained for the other meals. However, from 0.4 s^{-1} shear rate the decrease of shear viscosity was analogous for all meals.

As it can be seen in figure 44, the viscosities of the meals are slightly different depending on their composition. The meals that contain the carbohydrate source and the mixture of carbohydrate and fat sources do not show differences in their viscosities. The measured viscosity of the meal that contains the carbohydrate and protein sources is slightly higher than the viscosity of the meal that only contains the carbohydrate source. And finally, the meal that contains the three macronutrients is the meal with the highest viscosity, but it is only moderately higher compared to the viscosity of the other meals.

Although the differences in the viscosities were not very large, the addition of a thickener (guar) was studied to equalise the viscosities of the meals.

Guar gum was selected because is widely used as a thickener for dysphagia products. One of its advantages is that it cannot be hydrolysed by salivary α -amylase, therefore it would not disturb the results obtained during the digestion of the starchy meals (41).

Solutions with different guar concentrations (0.10 – 0.75 %) were prepared, their viscosity was measured and the obtained results are depicted in figure 45. As expected, the solutions with higher concentrations show the highest viscosity.

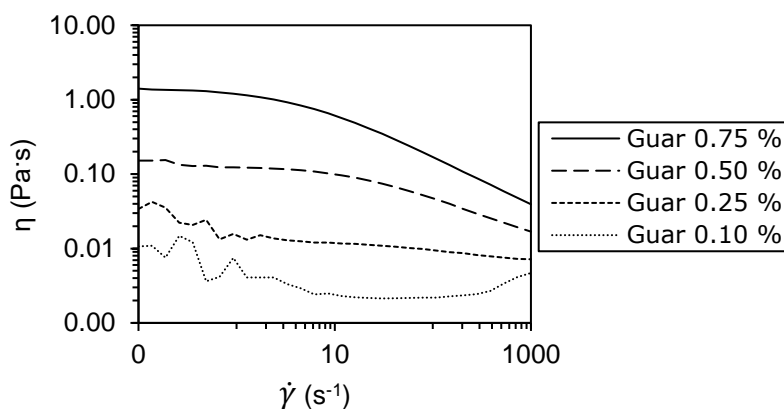


Figure 45. Viscosities measured of guar solutions (0.10 – 0.75 %)

When figures 44 and 45 are compared, it can be seen that the degree of viscosity of the meals is much higher compared with the obtained viscosity of the guar solutions.

In figure 44, the greatest difference in viscosity was found between the complete meal (CH+P+F) and the meal containing only carbohydrate or carbohydrate with fat. To check which guar concentration should be used to equalise the viscosity of the meals, the guar was mixed with the CH meal, the viscosity was measured and compared with the viscosity of the complete (CH+P+F) and CH meals (figure 46).

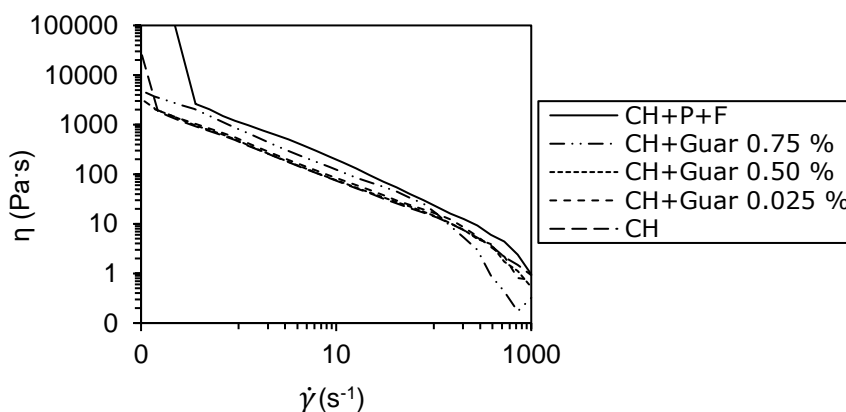


Figure 46. Effect of the guar on the meal's viscosity

The obtained viscosities in figure 46 show that the only guar concentration that promotes an increase in the meal viscosity is 0.75 %, but even that concentration is not sufficient to reach the viscosity of the complete meal. An increase in the guar concentration implied slight insolubility of the starch or the guar itself, for that reason a higher concentration of guar was not considered.

Xanthan gum was also studied as a thickener of the starchy meals. Xanthan gum was chosen as a second candidate because it is also widely used as additive in the food industry. And it has been seen that, both, guar and xanthan gums hasten the onset of initial paste viscosity and substantially increase the final peak viscosity of starch, starch-guar and starch-xanthan dispersions display synergistic viscosity (42, 43).

The starch was mixed with the xanthan to get a final concentration of 0.75 % of xanthan, and after the meal preparation, the viscosity was measured. The effect of the xanthan on the viscosity of the meal is shown in figure 47.

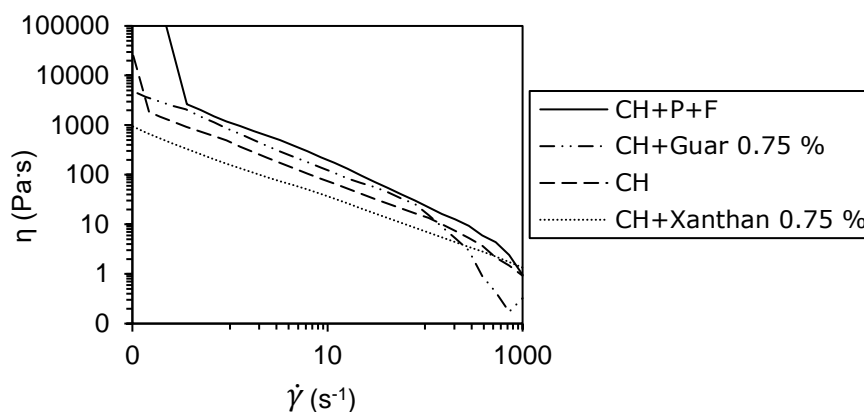


Figure 47. Effect of xanthan and guar (0.75 %) on the meal viscosities

As figure 47 shows, it was not possible to reach the viscosity of the complete meal (CH+P+F). And as the addition of thickeners at a higher concentration could have an undesirable impact on the meal, it was decided not to use thickeners.

5. Verification of carbohydrate adapted in vitro methods with real foods

Both, the static and the dynamic digestion methods shall be used in the further course of this thesis to study if and how the macronutrients protein and fat could affect the digestion of carbohydrates. To assure that these in vitro digestion methods, that were adapted to carbohydrate digestion in the previous chapters, would provide a reasonable prediction on the starch digestion, three test foods were studied. After the in vitro digestion of these foods, the in vitro glycaemic index was calculated and compared with the reported human in vivo glycaemic index (GI). The test meals were rice, potato and cocoa cream and results are shown in the following sections for the static and the dynamic method as well as for the relation to reported in vivo GI data.

The starch content of the meals was measured and compared with the written values on the label or literature. The comparison is depicted in figure 48.

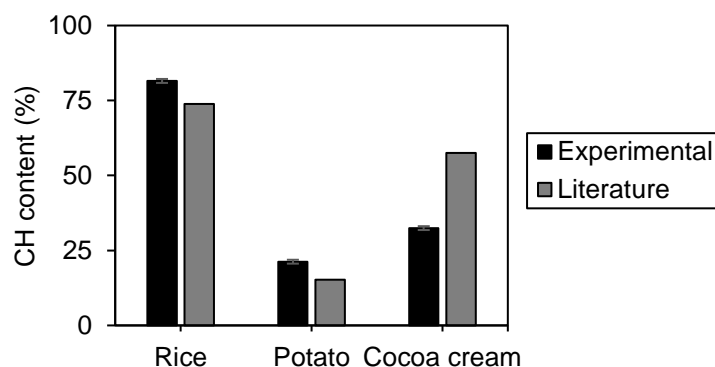


Figure 48. Carbohydrate content in rice, potato and cocoa cream (experimental vs literature)

5.1. In vitro digestion of rice

5.1.1. Static in vitro digestion of rice

The release of glucose from the rice (Original Langkorn Reis (Kochbeutel) – Uncle Ben's) was followed during the static in vitro digestion and the results are depicted in figures 49, 51.

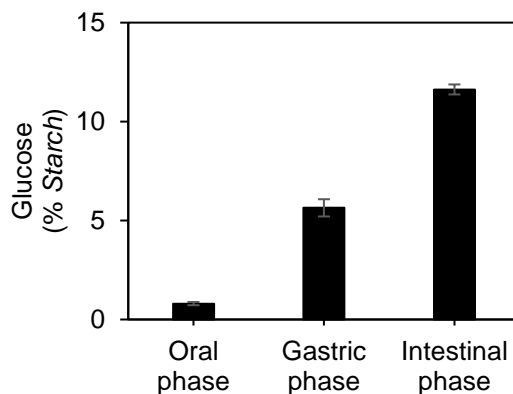


Figure 49. Glucose (% Starch) after the oral, gastric and intestinal phase of the static digestion method

Figure 49 shows the amount of glucose (in percentage of starch present in the used amount of rice) released from rice after each digestive phase in the static digestion method. A steady increase of glucose can be seen from the oral phase to the intestinal phase. While only 0.8 ± 0.1 % were released during the oral phase (2 min), 5.6 ± 0.4 % and 11.6 ± 0.3 % were released after the gastric phase (2 h) and intestinal phase (2 h), respectively.

During the oral phase, the α -amylase is present at its optimal conditions (pH 7). Still, only a minor fraction of glucose was released during that phase. This could be explained by the fact that the rice needs some time to be disintegrated before the α -amylase can act and catalyse the hydrolysis of the accessible starch. After the oral phase, the oral bolus is mixed with the gastric secretions which are not optimal for the activity of the α -amylase (pH 3). However, the α -amylase still hydrolysed the starch to some extent. The fact that α -amylase was not completely inactivated at the acidic conditions of the gastric phase could be due to a protective effect of the rice or starch (44). Furthermore, while the rice was further disintegrated by acid and pepsin, additional starch was solubilised and could be accessed by the α -amylase.

The amount of starch that was disintegrated and solubilised during its in vitro digestion is shown in figure 50. The percentage of rice solubilised was calculated by weighing the remaining solid meal after each sampling point. After the oral phase, more than 50 % of the rice was still insolubilized, therefore it could not be hydrolysed, which explains the low percentage of glucose measured after the oral phase. During the gastric phase, around 15 % of the starch was additionally disintegrated and solubilised, and the glucose released increased to around 5 %. Then, during the intestinal phase the solubilisation of the rice increased until its complete solubilisation at the end of the digestion.

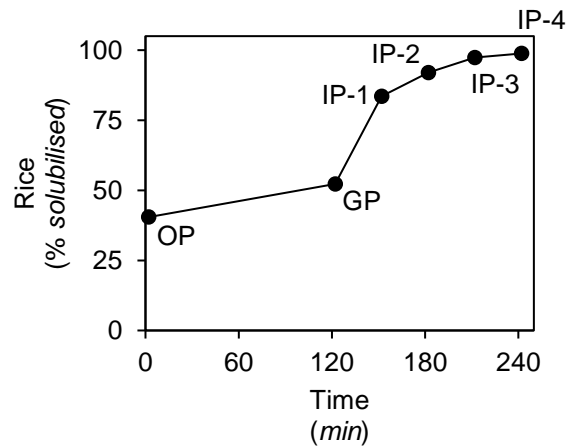


Figure 50. Rice solubilised during the in vitro digestion (OP: oral phase; GP: gastric phase; IP-1, IP-2, IP-3, IP-4: intestinal phase samples)

Figure 51 shows the release of glucose during the intestinal phase, which is expressed in percentage of starch. The time “0” h represents the amount of glucose released at the end of the gastric phase. Furthermore, the release of glucose is compared with the rice solubilisation (right axis), that is the amount of rice that was disintegrated and dissolved (grey solid line).

As shown in figure 51, the release of glucose during the intestinal phase is gradual and directly proportional to the solubilisation of the rice.

After 1.5 h of the intestinal phase, almost all the rice was already dissolved (97 %). Therefore, the enzyme could access the entire starch and catalyse its hydrolysis.

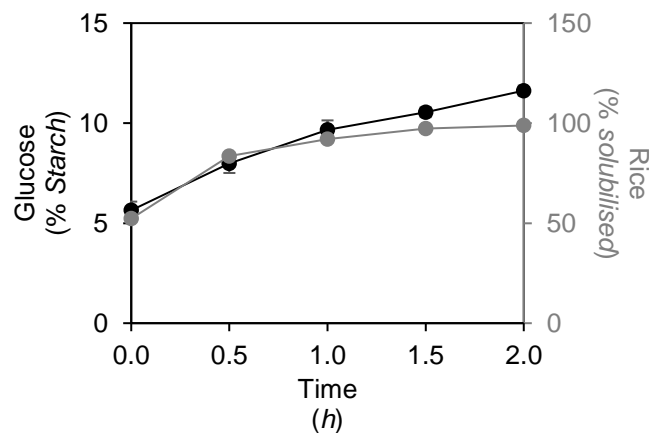


Figure 51. Glucose (% starch) released during the intestinal phase and amount of solubilized rice

Furthermore, the area under the curve (AUC) was calculated for the starch release (figure 51) and was used for the calculation of the in vitro glycaemic index (GI) (*Materials and methods_ Section 14.5*). The obtained GI for the rice in the static digestion method was 9.2 ± 0.4 % (data not shown). This is around 5 times lower compared to the reported GI in humans (48.0 ± 5.0 %) (45).

The differences obtained between the in vivo and in vitro GI could be due to the simplicity of the static digestion method compared with the complexity of the digestion of the meal in the human gastrointestinal tract. For example, the presence of brush border enzymes that are present in the small intestine that were not used in the in vitro digestion method.

5.1.2. Dynamic in vitro digestion of rice

The distribution of the rice (starch) throughout the gastrointestinal tract during its digestion could be followed in the dynamic in vitro digestion method. The final state is depicted in figure 52a. Furthermore, the amount of starch (% intake) was measured in the dialysate samples (jejunum and ileum) over time, and it is depicted in figure 52b.

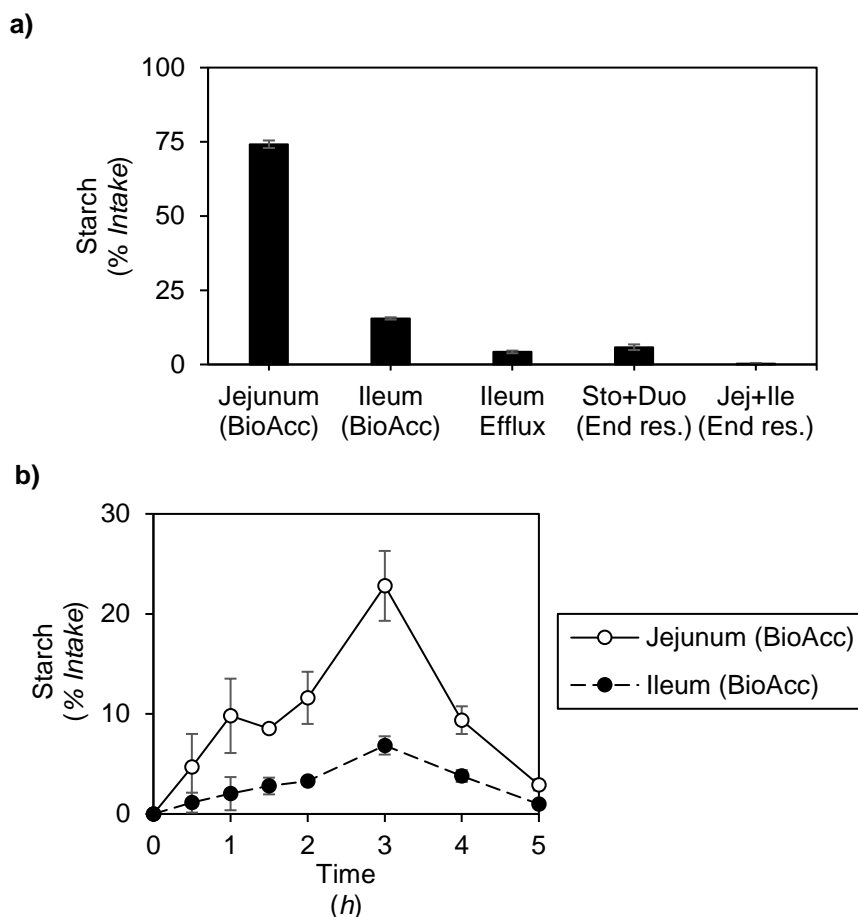


Figure 52. Starch (rice) distribution in the dynamic digestion method a) by compartment, b) bioaccessible fraction by time

Figure 52a shows that, at the end of the digestion, around 75 % of the starch added to the dynamic method were found in the bioaccessible fraction of the jejunum and 15 % in the bioaccessible fraction of the ileum. The remaining 10 % were found in the lumen (final residues) of the stomach, duodenum, jejunum and ileum, but also in the ileum efflux (chyme that would be passed to the colon).

In figure 52b, the amount of meal (starch) present in the bioaccessible fraction (jejunum and ileum) during digestion can be seen. A peak was observed for both compartments after 3 h of digestion. The amount of meal found in the bioaccessible fraction increases with the digestion time until it reaches a peak, and then it decreases until the end of the digestion. The initial slope could be explained by the fact that the rice needed some time to be disintegrated and solubilised with the gastric secretions and be able to cross the “pyloric sphincter” present after the stomach.

From the amount of starch that reached the bioaccessible fraction, the percentage of glucose released from the starch during its digestion was measured and depicted in figure 53.

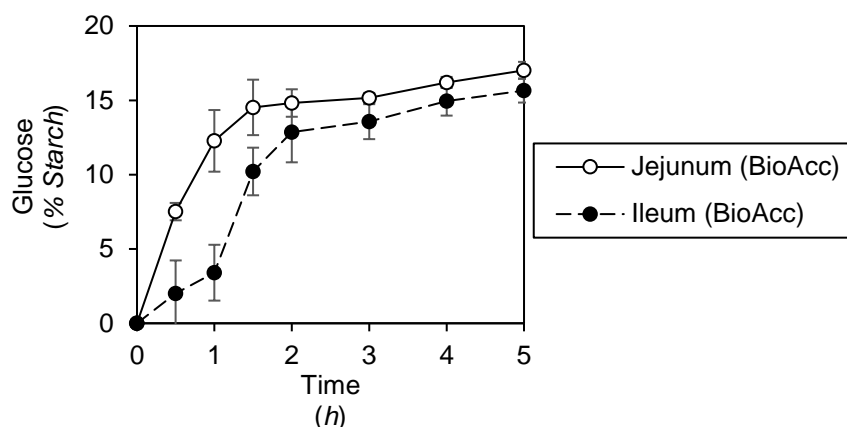


Figure 53. Glucose release from rice in the jejunum and ileum (bioaccessible fraction)

The amount of glucose released in the jejunum had a linear increase until 1.5 h to ~15 % and then it reached a plateau with a maximum of 17.0 ± 0.6 %. The amount of glucose released in the ileum had a linear increase during the first hour to ~3 %, then it increased in the next hour to ~13 % followed by a plateau reaching a maximum of 15.7 ± 0.8 % at the end of the digestion.

As figure 53 shows, the amount of glucose released from the starch during the two first hours was higher in the jejunum than in the ileum. This can be explained by the fact that, the rice, after leaving the stomach reached first the jejunum. Therefore, only a minor fraction of the starch reached the ileum in the time of the first sampling points.

On the other hand, it has to be taken into account that the pancreatin (contains α -amylase) is secreted into the duodenum. Also, the enzyme would need some time to reach the ileum to be able to catalyse the starch hydrolysis of the starch present in the ileum.

Finally, the glycaemic index (GI) of the bioaccessible fraction (jejunum + ileum) was calculated being of 13.8 ± 0.7 %. The reported *in vivo* GI for this type of rice (Original Langkorn Reis (Kochbeutel) – Uncle Ben's) is 48.0 ± 5.0 % (45). Therefore, the obtained GI is around 3.5 times lower compared with the *in vivo* GI.

The GI obtained for the rice with the dynamic *in vitro* digestion method also differs from the *in vivo* GI, but at a lower extent compared with the differences obtained with the static *in vitro* digestion method. This could be explained by the fact that the dynamic *in vitro* digestion method mimics in a closer way the physiological conditions than the static *in vitro* digestion method. But it still shows some differences when is compared with the complexity of human digestion.

A comparison of static and dynamic digestion of rice is provided in the following section.

5.1.3. In vitro digestion method comparison for the digestion of rice

To check if the used *in vitro* digestion method had an impact on the rice digestion, the amount of glucose released in both methods are compared in figure 54. As the digestion time in both methods was different, the digestion time of the static method was adapted to the time used in the dynamic method by taking into account the total digestion time in both methods.

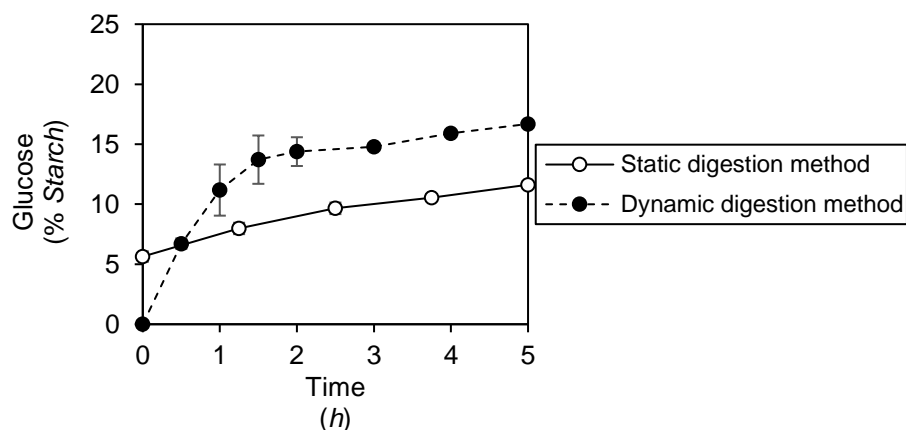


Figure 54. Comparison of the glucose released in the static and dynamic models

The glucose levels depicted in figure 54 are the glucose released in both the bioaccessible fraction (jejunum and ileum) for the dynamic digestion method and the small intestinal phase of the static digestion method.

The first difference that can be seen in figure 54 is the glucose level at time 0 h. While in the dynamic digestion method no glucose was found, in the static digestion method 5.6 ± 0.4 % of glucose was already released. For both methods, it is represented only the intestinal phase (no oral or gastric phase), but for the dynamic method the time 0 h is the time when the digestion started, while for the static method the meal was already in contact with the α -amylase during the oral and gastric phase before it reaches the intestinal phase.

The other big difference that can be noticed in this figure is the shape of the curves. The release of glucose in the static digestion method is gradual during the digestion, however, in the dynamic digestion method the graph could be divided into two parts: the first 1.5 h when the meal is quickly digested, and the second part (from 1.5 h until the end of the digestion) when the digestion is slower and gradual.

A further difference between methods is the obtained degree of hydrolysis (glucose) at the end of the digestion. The amount of glucose released at the end of the digestion with the dynamic model (16.7 ± 0.3 %) is higher than the glucose level obtained with the static digestion method (11.6 ± 0.3 %).

It has been seen that the measurement of the digestion of rice is slightly different depending on the in vitro digestion method used, and these differences were higher when the results were compared with the in vivo data. Therefore, it could be concluded that, in principle, the used in vitro digestion method has an impact on the digestion of the rice.

5.2. In vitro digestion of potato

5.2.1. Static in vitro digestion of potato

The selected potato to study its digestion with the in vitro digestion methods was Kartoffeln Festkochend – Belana. And the amount of glucose released during their digestion with the static digestion method is depicted in figure 55.

The amount of glucose released after each digestive phase is shown in figure 55a, while in figure 55b the release of glucose during the intestinal phase can be seen.

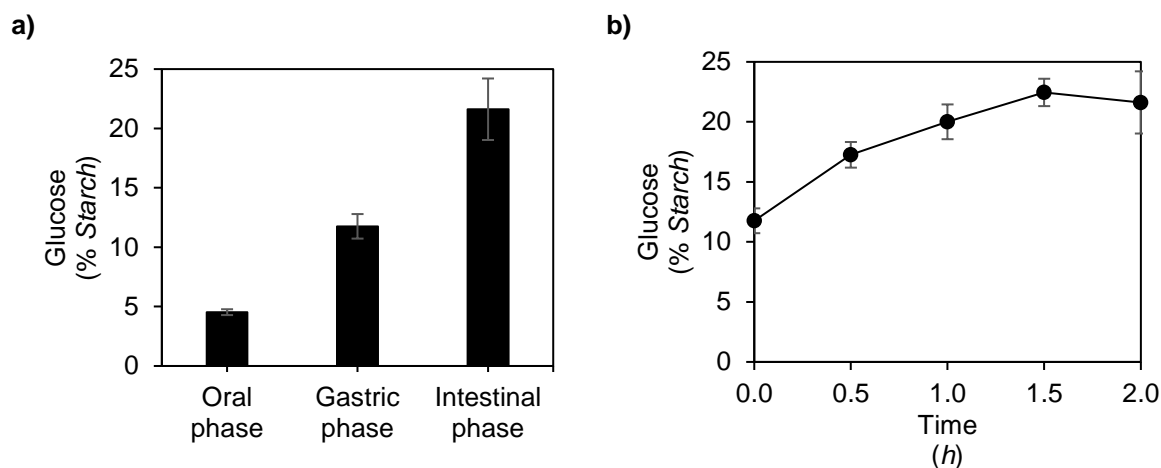


Figure 55. Glucose released during potato digestion with the static method

The amount of glucose released gradually increased after each digestive phase. The digestion of the potato during the intestinal phase was faster during the first 1.5 h and then it reached a steady state for the last 30 min.

When the amount of glucose released in each digestive phase is compared, it can be seen that the digestion of potato increased throughout the gastrointestinal tract (GIT) and that the acidic conditions of the gastric phase do not slow down the hydrolysis. This may be because the α -amylase was protected by the potato and the gastric secretions could not completely denature the enzyme.

During the intestinal phase the meal was also digested gradually with the time, but it seems that during the first 30 min the speed of hydrolysis was slightly higher compared with the rest of the digestion, as the rate of glucose released in this first step is $\sim 11 \text{ \%}\cdot\text{h}^{-1}$. Then, the digestion speed decreased to $\sim 5 \text{ \%}\cdot\text{h}^{-1}$ for the next hour and in the last step of the intestinal phase the amount of glucose released was constant, no more glucose was released.

The in vitro GI for the potato was calculated from the curve depicted in figure 55b being of $19.1 \pm 1.0 \text{ \%}$. The in vitro GI obtained with the static digestion method was around 4 times lower compared with the reported in vivo GI (human), $80.0 \pm 15.0 \text{ \%}$ (45).

The differences obtained between the in vivo and in vitro GI could be due to the simplicity of the static digestion method compared with the complexity of the digestion of the meal in the human gastrointestinal tract.

5.2.2. Dynamic in vitro digestion of potato

The distribution of the potato throughout the gastrointestinal tract of the dynamic model was also studied, and the results are depicted in figure 56.

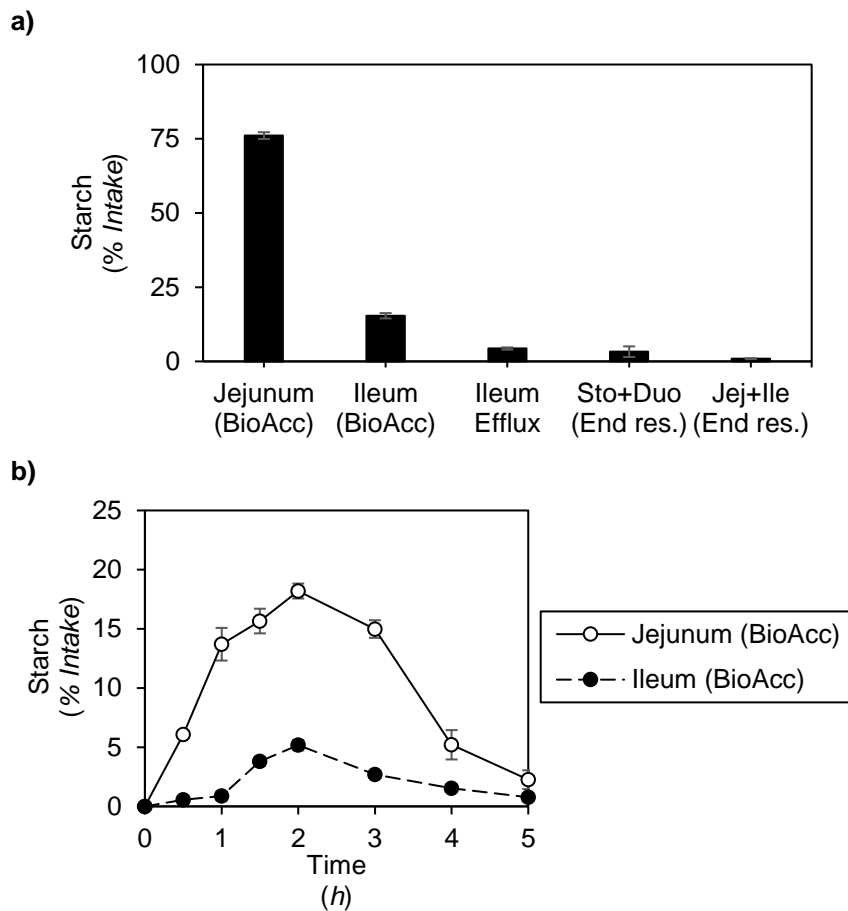


Figure 56. Distribution of the potato throughout the dynamic model

As figure 56a shows, most of the starch (~75 %) was found in the jejunal dialysate samples. In the ileum (bioaccessible fraction) it was only found ~15 % of the potato added into the system. The remaining 10 % was found mainly in the ileum efflux and the end residues of the stomach and duodenum. Only a small percentage (~1 %) of the potato could be found in the lumen of the jejunum and ileum.

The highest amount of potato was found in the bioaccessible fraction (jejunum and ileum) because when the starch was digested, it could pass through the dialysers and it was removed from the lumen, therefore it could not be found in the end residues.

Figure 56b shows the distribution of the potato during the digestion in the bioaccessible fraction (jejunum and ileum). In the jejunum, the amount of potato increases with the time until it reaches a maximum after 2 h of digestion, and then the percentage of potato present in the jejunal dialysate slowly decreases until the end of the digestion.

On the other hand, the amount of starch present in the dialysate fraction of the ileum during the first hour is very low. Thus, could be because the starch reached first the jejunum and it was removed from the system, therefore only a small part reached the ileum. When the amount of meal in the jejunum was high enough that it was not completely removed through the dialysers, it could reach the ileum, thus, an increase in the amount of meal in the ileum (bioaccessible fraction) can be observed. The maximum of starch in both compartments was reached after 2 h of digestion.

After the peak the amount of meal present in the dialysates gradually decreased until the end of the digestion in both compartments. In the jejunum, it can be seen that the decrease was faster during the third and fourth hour and then during the fifth hour it slows down.

The degree of hydrolysis of the potato, taking into account only the glucose, is depicted in figure 57.

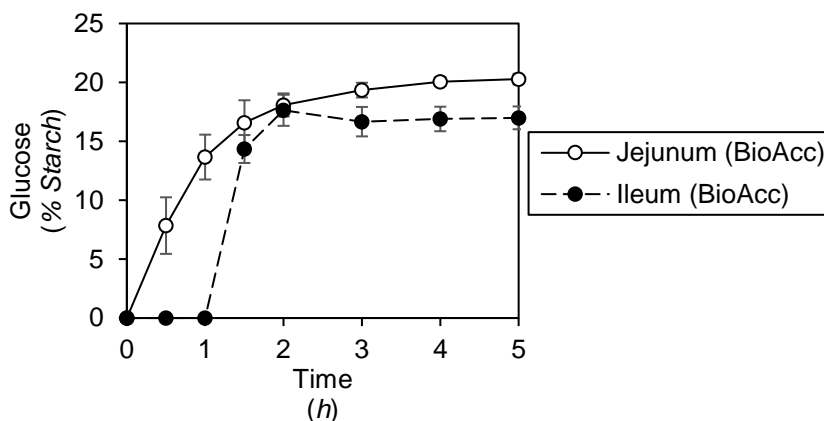


Figure 57. Glucose release from rice in the jejunum and ileum (bioaccessible fraction)

The amount of glucose released in the jejunum (bioaccessible fraction) during digestion is increasing until it reaches a steady-state. The glucose was released at high speed ($\sim 11\% \cdot h^{-1}$) for the first 1.5 h and then it slowed down ($\sim 1\% \cdot h^{-1}$) until the end of the digestion.

In the case of the ileum, no glucose was found during the first hour, which could be explained by the fact that almost no meal reached this compartment at this time point. After the first hour, the amount of glucose released from the potato rapidly increased and reached the values found in the jejunum. However, the degree of hydrolysis (glucose) remained constant from the third to the fifth hour of the digestion. The differences that can be seen, from the second to the fifth hour between the jejunum and ileum could arise from experimental errors during the sample collection or the analytics (glucose and starch measurements).

The measured GI with the dynamic digestion method of the potato was found to be $16.8 \pm 0.8\%$, which is almost 5 times lower than the reported GI found in humans ($80.0 \pm 15.0\%$) (45).

A comparison of static and dynamic digestion of potato is provided in the following section.

5.2.3. In vitro digestion method comparison for the digestion of potato

The release of glucose from potato during the digestion with both methods (static and dynamic) is compared in figure 58.

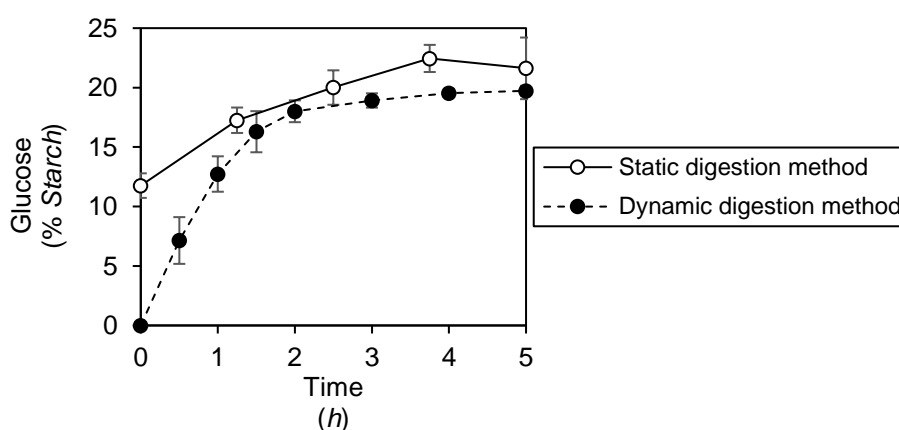


Figure 58. Comparison of the glucose released in the static and dynamic models

The amount of glucose released rapidly increased during the first 2 h of digestion for both methods, and then the digestion of the potato slowed down until the end of the digestion.

The main differences are found at the beginning of the digestion. The depicted data for the static digestion method only belongs to the intestinal phase, therefore the meal was previously slightly digested in the oral and gastric phases. However, these differences also come from the fact that in the static method all the meal and digestive products are all the time in contact with the secretions, but in the dynamic digestion method the meal is added into the stomach and it needs some time to reach the small intestine, and the digestive products are removed from the lumen through the dialysers.

The final percentage of glucose found in both methods is similar; in fact, the amount of glucose found in both methods is similar from the 1.5 h of digestion onwards.

5.3. In vitro digestion of cocoa cream

5.3.1. Static in vitro digestion of cocoa cream

The cocoa cream was used, as an example of a mixture of macronutrients (6.7 % protein, 32.6 % fat, 32.5 % carbohydrate), to evaluate if the in vitro digestion methods could predict the glycaemic index properly.

Both, the percentage of glucose in the different digestive phases, and the amount of glucose released during the intestinal phase are depicted in figure 59.

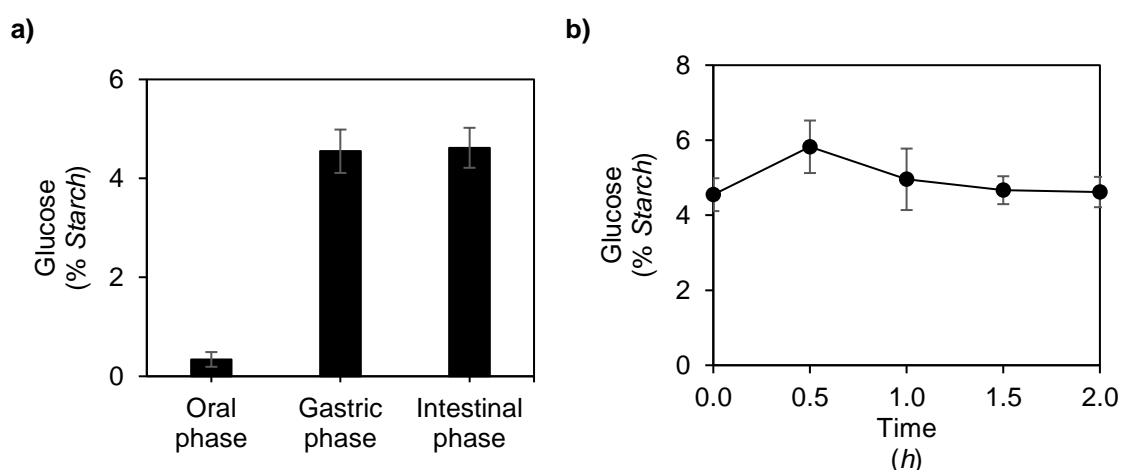


Figure 59. Glucose released during the cocoa cream digestion with the static method

The cocoa cream was almost not digested during the oral phase, but then during the gastric phase the amount of glucose released drastically increased. And during the intestinal phase no more glucose was released. It can be seen in figure 59b that the amount of glucose released from the cocoa cream slightly increased during the first 30 min but then the glucose levels kept constant.

As can be seen in figure 59a, almost no glucose was released from the cocoa cream during the oral phase. However, during the gastric phase, a high amount of glucose was released which could be due to the fact that the acidic conditions of the gastric phase aided the disintegration of the meal, and as the cocoa cream contains a big amount of sugar, this could be released and dissolved.

Almost no differences can be found between the glucose levels of the gastric and intestinal phase, which means that no more glucose was released from the cocoa cream (digested or liberated). This can be observed when plotting the percentage of glucose found in the intestinal phase versus digestion time, where the shape of the curve is almost a horizontal line.

However, the maximum degree of hydrolysis (glucose) was low: 4.6 ± 0.4 %, therefore, a large amount of starch could not be hydrolysed by the end of the digestion in the static digestion method.

The calculated GI of the cocoa cream in the static digestion method was $5.0 \pm 0.4 \%$, which was around five times lower than the reported human GI ($25.0 \pm 4.0 \%$) (45). This could be explained by the limitations of the static in vitro digestion method, which cannot perfectly mimic the complexity of human digestion.

5.3.2. Dynamic in vitro digestion of cocoa cream

The distribution of the cocoa cream in the dynamic digestion method at the end of the digestion is depicted in figure 60a, and in figure 60b the amount of starch (% intake) present in the dialysate samples (jejunum and ileum) during the digestion is shown.

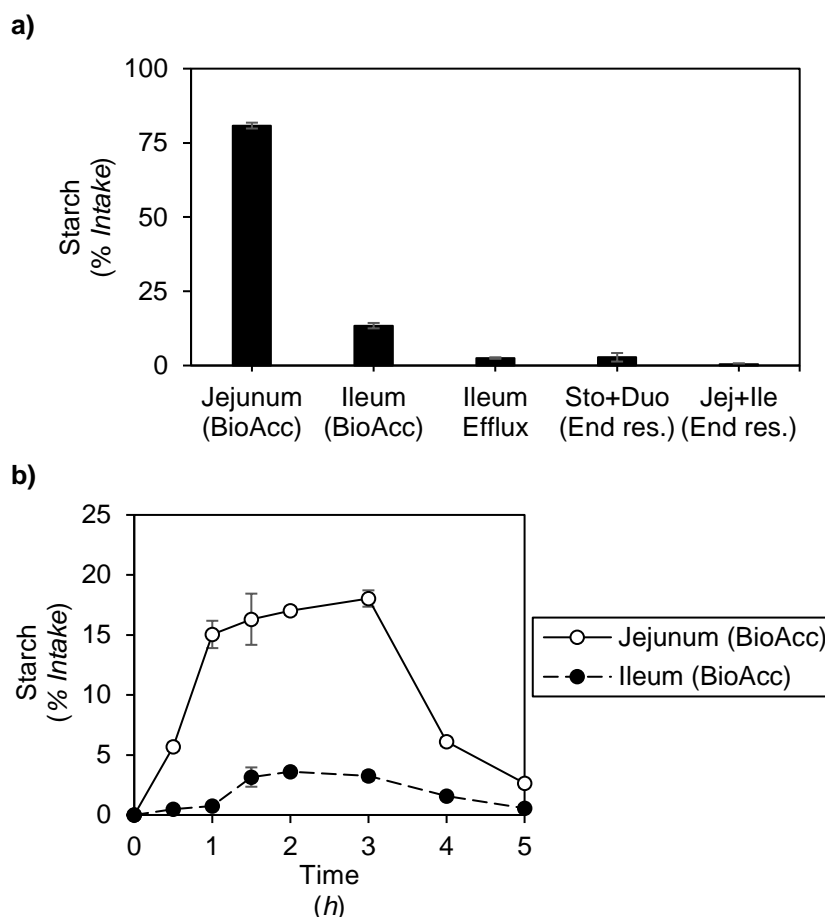


Figure 60. Distribution of the cocoa cream throughout the dynamic model

Most of the cocoa cream added into the system was found in the bioaccessible fraction of the jejunum at the end of the run (~81 %), while only ~13 % of the starch was found in the bioaccessible fraction of the ileum. Therefore, only a small part of the starch was found in the lumen of the compartments (~3 % stomach and duodenum and ~0.5 % in the jejunum and ileum) or in the ileum efflux (2.5 %).

Consequently, around ~94 % of the cocoa cream added to the system was found in the bioaccessible fraction, which means that it would be accessible for absorption and it could reach the bloodstream.

The distribution of the cocoa cream in the jejunum could be divided into three parts, during the first part (0 – 1 h), the amount of starch collected from the system in the jejunum quickly increased until it reached values of around 15 %, this first part was mainly influenced by the stomach emptying. The second part last from the first to the third hour of digestion, and in this part the amount of starch present in the jejunum increased very slowly until it reached the maximum of 18 %, during this time, the stomach was practically empty and all the meal was distributed throughout the system.

Finally, the last part of the graph belongs to the last 2 h of digestion, when the amount of starch present in the jejunal dialysate quickly decreased. This decrease in the starch content can be explained by the fact that most of the meal has been already removed from the lumen and as no more starch is added to the system, the amount of cocoa cream that could pass through the dialysers is smaller.

In the first hour of digestion, almost no starch was found in the ileal dialysate, as the starch did not have time to reach that compartment. After that the amount of starch present in the bioaccessible fraction of the ileum slightly increased until it reaches its maximum at 3.6 % (2 h), however from 1.5 to 3 h, the amount of starch that passed through the dialyser was almost constant (~3.5 %). Finally, the amount of starch found in the ileum decreased until the end of the digestion.

Taking into account only the bioaccessible fraction, it can be seen in figure 60b the differences of the starch distribution between the jejunum and ileum. The level of the starch (from cocoa cream) found in the jejunum is much higher than the amount of starch found in the ileum. And, as explained in the previous sections, it could be because the meal first reaches the jejunum where it is slowly removed through the dialysers and what is not removed can finally travel to the ileum, where it is also removed from the lumen through the ileal dialyser.

The percentage of the starch that was converted into glucose in the bioaccessible fraction (jejunum and ileum) is depicted in figure 61.

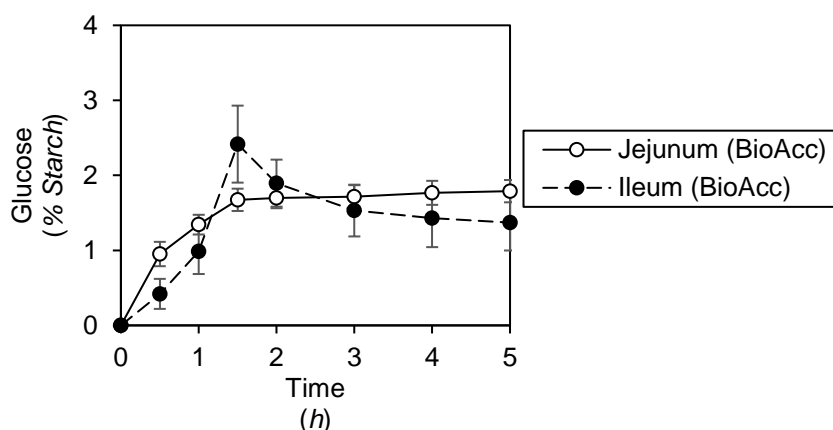


Figure 61. Glucose release from rice in the jejunum and ileum (bioaccessible fraction)

In both compartments, the amount of glucose released from the available starch slowly increased during the first 1.5 h and then it reached a plateau until the end of the digestion.

Almost no differences were found in the percentage of glucose between the jejunum and ileum. As figure 61 shows, the amount of glucose released from the cocoa cream during the digestion reached only values of around 2 %, therefore the carbohydrates present in the cocoa cream were almost not digested. This low digestibility could be due to the preparation methodology used for the cocoa cream, which protects the carbohydrate source.

The GI calculated for the dynamic digestion method was of 1.6 ± 0.1 %, almost 16 times lower than the reported human GI (25.0 ± 4.0 %) (45). Among other reasons, like the differences between the in vivo and in vitro conditions, one reason that could trigger this difference on the in vitro and in vivo GI could be that the cocoa cream was stuck in the pre-filter that was placed prior to the dialyser, and therefore partially or completely cocoa cream digestion could not pass through the dialysers and reach the bioaccessible fraction.

A comparison of static and dynamic digestion of cocoa cream is provided in the following section.

5.3.3. In vitro digestion method comparison for the digestion of cocoa cream

The amount of glucose released from cocoa cream during both in vitro digestion methods (static and dynamic) is depicted in figure 62.

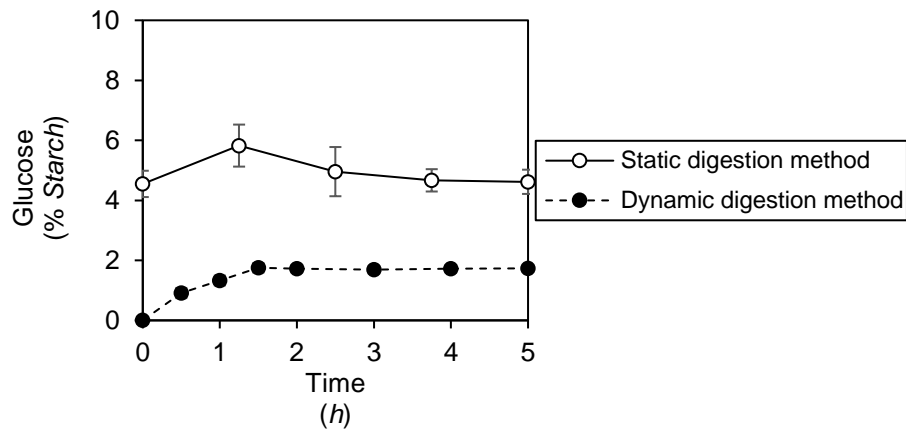


Figure 62. Comparison of the released glucose from cocoa cream in the static and dynamic digestion methods

During the intestinal phase of the static digestion method, the glucose levels were more or less constant. However, in the dynamic digestion method the amount of glucose released increased during the first 1.5 h and then it reached a steady state until the end of the digestion.

It can be seen in figure 62 that there is a big difference in the behaviour of cocoa cream in the static method compared to the behaviour of cocoa cream in the dynamic digestion method. The meal was able to be more digested in the static method than in the dynamic system, even though the enzyme : meal ratio was practically equal in both methods.

Apart from the differences in the level of digestibility between the methods, another difference can be found in the first part of the digestion. The release of glucose in the dynamic system is gradually increased during the first 1.5 h and then it remained constant, while in the static digestion method the release of glucose took place during the gastric phase, and almost no glucose was released during the intestinal phase.

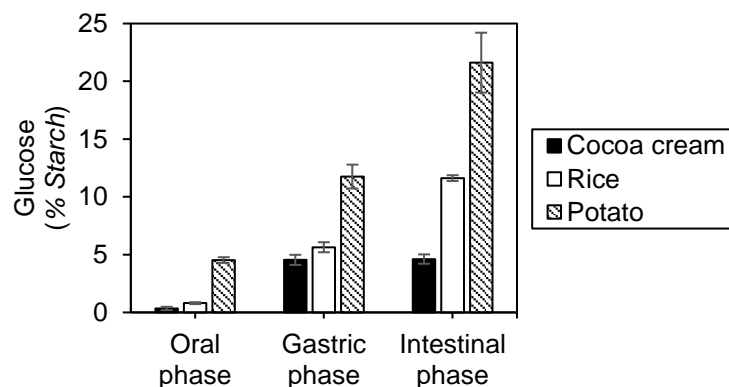
A comparison of all three foods tested with in vitro digestion methods will be provided in the next section.

5.4. Comparison of in vitro digestion of rice, potato and cocoa cream

5.4.1. Static in vitro digestion of rice, potato and cocoa cream

The amount of glucose released for the three studied meals using the static digestion meal is compared in figure 63.

a)



b)

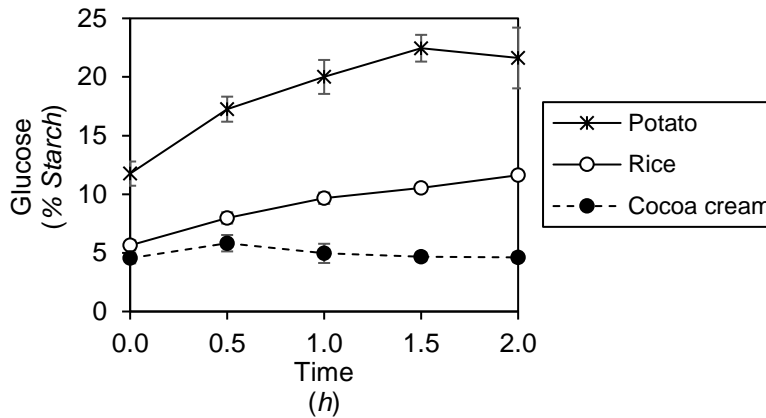


Figure 63. Comparison of the glucose released from rice, potato and cocoa cream using the static digestion method a) glucose levels at the end of the oral, gastric and intestinal phase, b) release of glucose during the small intestinal phase

As it can be seen in figure 63a, the rice and potato have similar behaviour but different from cocoa cream. The glucose was gradually released during the three phases of the digestion for the rice and potato, while the cocoa cream had a small glucose release during the oral phase, then the release of glucose increased during the gastric phase and finally almost no glucose was released during the intestinal phase. Therefore, while for the rice and potato the digestion is continuous during the static method, the cocoa cream was mainly digested during the gastric phase.

Figure 63a also shows that the meal that can release the biggest amount of glucose is the potato followed by the rice and finally the cocoa cream.

The behaviour shown in figure 63a can also be seen in figure 63b, as the digestion of the rice and potato is continuous with time (the amount of glucose released increases), while the digestion of the cocoa cream somehow stopped after the gastric phase and almost no more glucose was released during the intestinal phase.

The rate at which the potato was digested is higher ($\sim 7\% \cdot h^{-1}$) compared with the digestion of the rice ($\sim 3\% \cdot h^{-1}$). And while the digestion of the rice is more or less constant with time, the release of glucose from potato increases with the time until it reaches a steady-state at 1.5 h of the intestinal phase.

The measured glycaemic index for the three meals is depicted in figure 64.

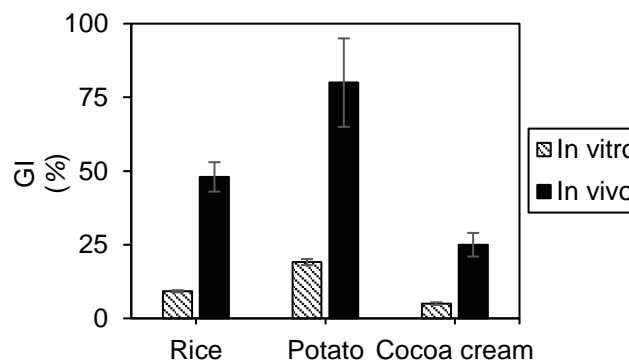


Figure 64. Comparison of the in vitro and in vivo (45) glycaemic index

As it can be seen in figure 64, the in vitro GI is much lower than the reported GI for humans (45). However, the factor between the in vitro and in vivo GI (taking into account the standard deviations) is around 4.5. Therefore, it could be applied a factor of 4.5 to the obtained GI with the static digestion method to predict the human GI.

This factor (4.5) was applied to the measured GI and the obtained GI are depicted and compared with the in vivo GI in figure 65.

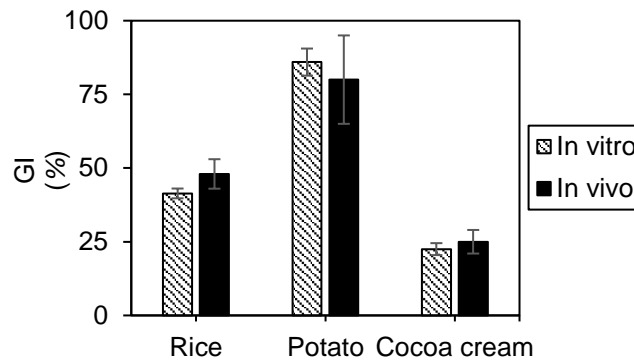


Figure 65. Comparison of the in vivo GI (45) with the recalculated in vitro GI

Figure 65 shows that by applying the 4.5 factor the in vitro GI reaches the reported GI, therefore the static digestion method would be a good tool for the GI prediction. This calculated factor was used for the calculation of the GI of other meals with the static digestion method.

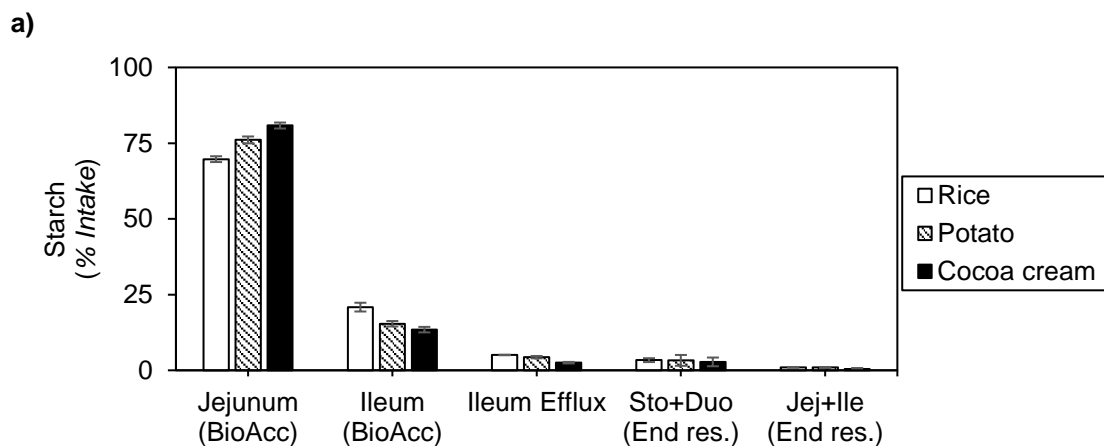
5.4.2. Dynamic in vitro digestion of rice, potato and cocoa cream

The distribution of the three different meals in the dynamic system is depicted in figure 66. And it shows that the general distribution is similar for the three meals, and only small differences between them can be noticed, and they are mainly found in the bioaccessible fraction.

According to the figure 66a, a bigger amount of rice reached the ileum compared with the other meals. This may be because the rice needed more time to be disintegrated and dissolved in the secretions than the other meals. This could also explain why the cocoa cream is the meal that was found in a bigger amount in the jejunum, as it did not need too much time to be dissolved.

And the differences found in the jejunum are also found in the ileum, but in the other way around, therefore the meal that could not pass through the jejunal dialysate went to the ileum, where it could pass through the dialyser.

The amount of meal found in the lumen at the end of the digestion (end residues) and in the ileum efflux is equal when the three meals are compared. Therefore, the main differences in their digestion were found in the bioaccessible fraction (jejunum and ileum).



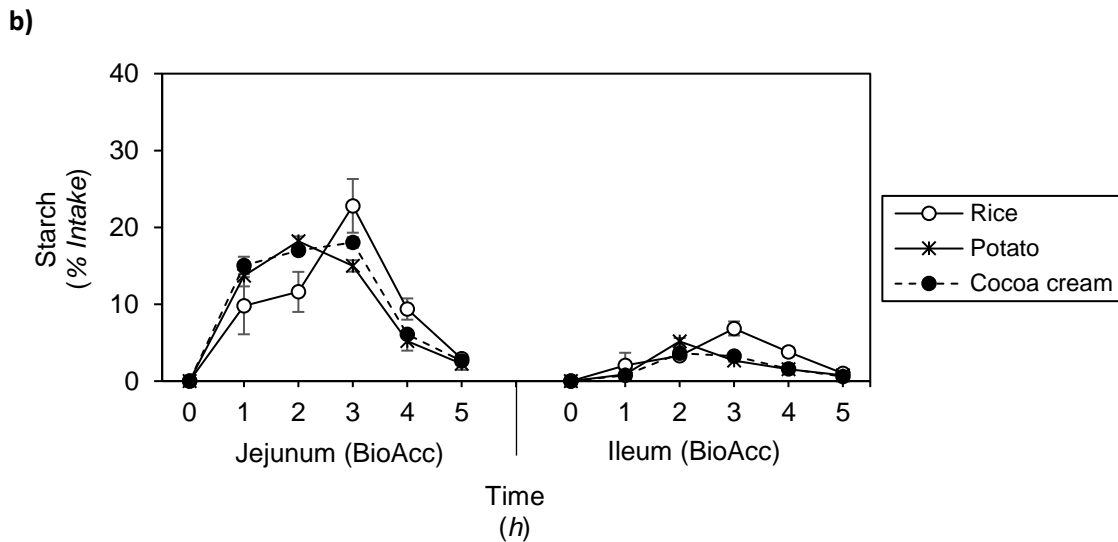


Figure 66. Comparison of the meal distribution (rice vs potato vs cocoa cream)

Figure 66b shows the distribution of the different meals in the bioaccessible fraction (jejunum and ileum).

The distribution of the potato and cocoa cream in the jejunum during the digestion is similar, showing an increase during the first hour then the amount of starch found in the jejunum kept between 15-18 % for the next 2 h and the maximum of starch was found around 18 % at 2 h in the case of the potato and at 3 h for the cocoa cream. During the last 2 h, the amount of starch found in the jejunum decreased from 15-18 % to ~2.5 %.

On the other hand, the distribution of the rice was slightly different showing a maximum of 22.8 ± 3.5 % at 3 h. Therefore, the maximum of rice was found at the same time as the cocoa cream but with a higher percentage of starch.

The behaviour of the rice and potato was similar in the ileum, but with a lower amount of meal. But, the behaviour of the potato was different in the ileum compared with the jejunum, as the maximum of meal was found after 2 h of digestion while in the jejunum was found at 3 h.

The glycaemic index (GI) measured with the dynamic digestion method compared with the human GI is depicted in figure 67.

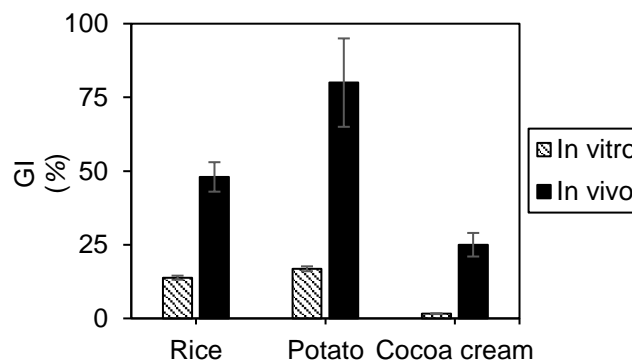


Figure 67. Comparison of the GI between the dynamic digestion method and the human

For the three meals, the measured GI with the dynamic system, was much lower compared with the in vivo values. The measured GI of rice and potato was very similar, while the measured GI of cocoa cream was much lower compared with rice and potato.

The factor between the in vitro and in vivo methodologies is around 4 for the rice and potato, while the in vitro GI of the cocoa cream was almost 16 times the in vivo GI. Therefore, the dynamic digestion method could be used for the prediction of the glycaemic index by applying a factor of 4 for meals with in vivo GI > 45 %.

The factor of 4 was applied to the measured GI and this “corrected” GI is compared with the in vivo GI in figure 68. This calculated factor was used for the calculation of the GI of other meals with the dynamic digestion method.

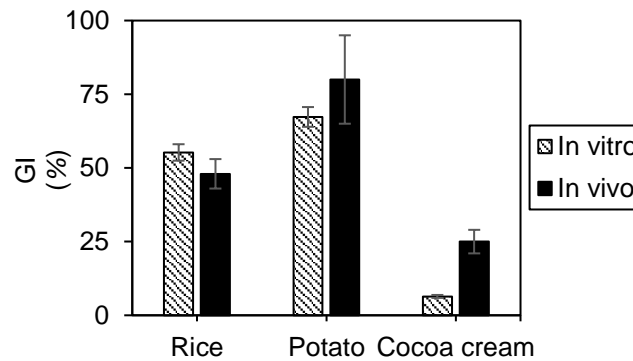


Figure 68. Comparison of the corrected in vitro GI with the in vivo GI

And as it can be seen in figure 68, the calculated GI with the dynamic digestion method reached the in vivo GI except for the cocoa cream, which it was still lower compared with the in vivo GI.

5.4.3. In vitro digestion method comparison for the digestion of rice, potato and cocoa cream

The obtained glycaemic index (GI) with both in vitro methods (static and dynamic) is compared with the reported in vivo GI in figure 69.

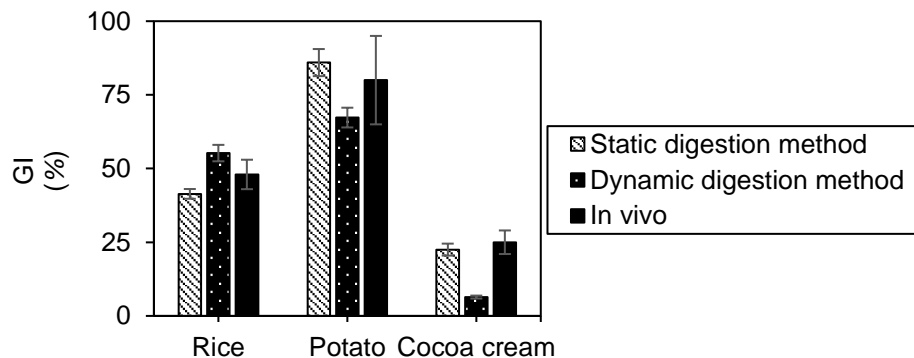


Figure 69. Glycaemic index measured with the static and dynamic digestion methods compared with the in vivo GI

As it can be seen in figure 69, the calculated GI matches the in vivo GI except for the cocoa cream. When the GIs of the meals are compared, it can be seen that the potato had the highest GI and the cocoa cream the lowest.

Therefore, the in vitro digestion methods (static and dynamic) predict the glycaemic index of the rice and potato accurately, then both methods could be used for the measurement of the in vitro glycaemic index. On the other hand, the GI predicted for the cocoa cream with the static digestion method was accurate but it was too low with the dynamic digestion method.

6. In vitro digestion of starch

The digestion of carbohydrates was studied by using starch from rice and starch from potato as meal in the in vitro digestion methods.

6.1. In vitro digestion of starch from rice

6.1.1. Static in vitro digestion of starch from rice

The total degree of hydrolysis (DH) and the amount of glucose released from the starch from rice after oral, gastric and intestinal phase are depicted in figure 70.

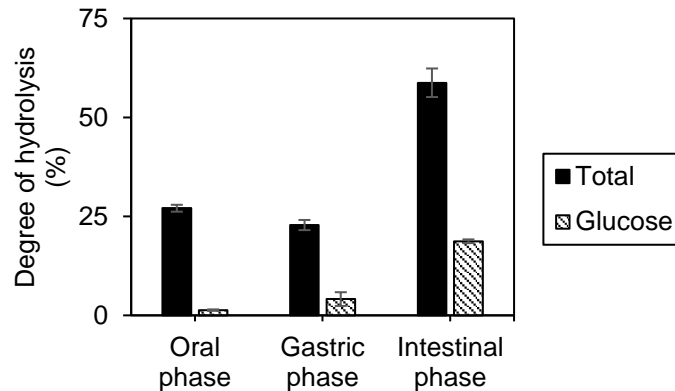


Figure 70. Comparison of the total DH (%) and glucose (%) after each digestive phase

As figure 70 shows, the total DH did not increase during the gastric phase and then it highly increased during the intestinal phase. Moreover, the amount of starch converted into glucose gradually increased during digestion.

Around 25 % of the starch from rice was digested during the oral phase, but only 1.3 ± 0.2 % of the starch was converted into glucose.

On the other hand, and according to the depicted results in figure 70, the starch could not be digested further during the gastric phase. During the gastric phase the oral bolus is incubated in the presence of the salivary α -amylase at acidic conditions, therefore the low pH could deactivate the enzyme. However, it seems that the salivary α -amylase was partially active as the percentage of glucose increased from 1.3 ± 0.2 % to 4.1 ± 1.7 %.

The digestion of the starch from rice continued during the intestinal phase thanks to the pancreatic α -amylase. The pH/temperature conditions during the intestinal phase were optimal for the α -amylase, and the enzyme could catalyse the hydrolysis of the starch and the total DH increased ~ 260 %, while the amount of glucose released also increased reaching a value of 18.7 ± 0.5 %.

The degree of hydrolysis (DH) of the starch from rice during the intestinal phase is depicted in figure 71, where it can be seen the total DH compared with the amount of starch converted into glucose.

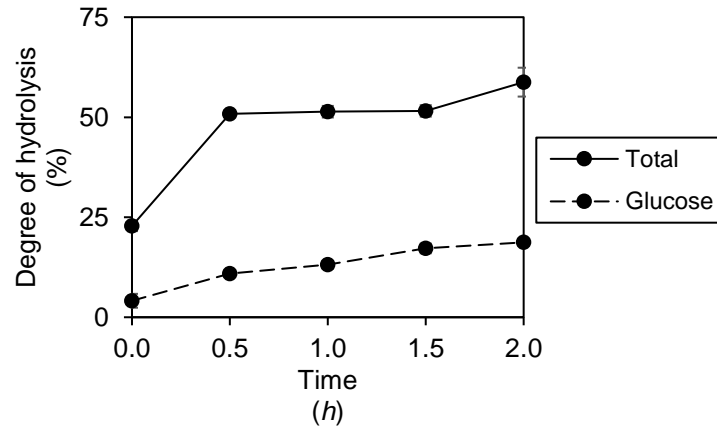


Figure 71. Degree of hydrolysis of the starch from rice (total of DH vs glucose)

According to the results depicted in figure 71, the total DH increases during the first 30 min of the intestinal phase from 23 % to 51 %. The total DH kept constant the next hour, which means that the starch from rice was not further digested between the 30 min and 1.5 h of the intestinal phase. And during the last 30 min of the intestinal phase the DH slightly increased reaching a final DH of 58.8 ± 3.6 %.

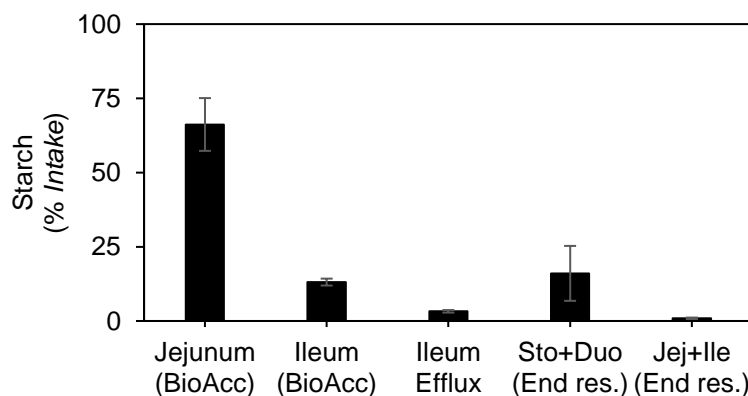
Unlike the total DH, the amount of glucose released increased with time. During the first 30 min, the percentage of glucose increased from ~4 % to ~11 % and after that, the glucose was released at $\sim 5.5 \text{ \%}\cdot\text{h}^{-1}$. Therefore, the digestion of the starch from rice mainly occurred during the first 30 min of the intestinal phase, which is the moment where the chyme that comes from the gastric phase is mixed with the pancreatic α -amylase, among other secretions.

The glycaemic index was calculated with the AUC (area under the curve) calculated from the DH-glucose curve depicted in figure 71 and taking into account the factor between in vitro-in vivo methodologies found in section 5.4. The measured GI of the starch from rice is 59.3 ± 2.3 %, which is higher compared with the measured GI for the rice (41.4 ± 1.7 %).

6.1.2. Dynamic in vitro digestion of starch from rice

The distribution of the starch from rice through the dynamic system (TIM-1) is shown in figure 72a, and figure 72b shows the amount of meal in the bioaccessible fraction (jejunum and ileum) during its digestion.

a)



b)

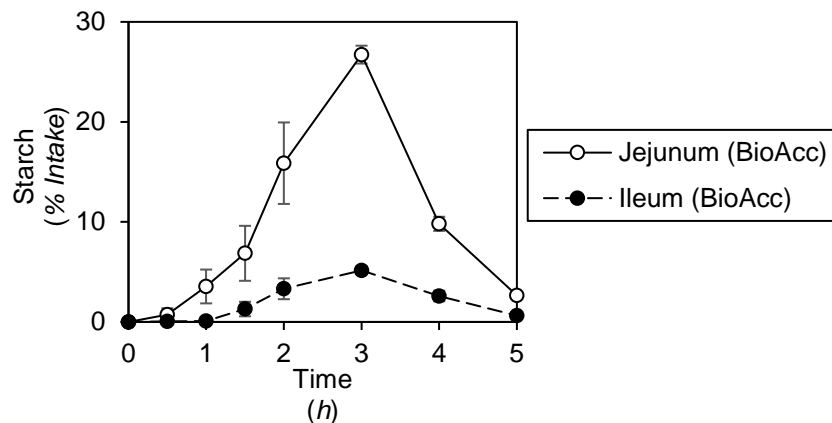


Figure 72. Distribution of the starch from rice in the dynamic digestion method (TIM-1)

As it can be seen in figure 72a, the starch from rice was mainly distributed between the bioaccessible fraction and in the lumen of the stomach and duodenum at the end of the digestion. However, almost 75 % of the meal was found in the jejunal dialysate, which means that a big part of the starch from rice was accessible for absorption at the middle part of the small intestine.

Around 15 % of the starch added to the system was found in the stomach and duodenum. This amount of meal was found at the end of the digestion in the upper part of the gastrointestinal tract because the viscosity of the meal slowed down the stomach emptying and part of the meal did not have time to reach the jejunum or ileum.

The meal distribution in the bioaccessible fraction during the digestion is shown in figure 72b, and it can be seen that the meal reached both compartments, jejunum and ileum, slowly until it reached a maximum after 3 h of digestion. During the first 30 min, almost no starch was found in the dialysate samples, after one hour it gets through to the jejunum but not to the ileum. However, after 1.5 h of digestion the amount of starch found in the bioaccessible fraction increased at a higher speed compared with the first 1.5 h. The amount of starch from rice found in the jejunal and ileal dialysates was mainly influenced by the rate of stomach emptying.

In the last 2 h of digestion, the percentage of starch found in the bioaccessible fraction drastically decreased as most of the meal was already removed from the system through the dialysers or ileum efflux. This effect can be seen mainly in the jejunum than in the ileum, but this is because the amount of meal that reached the jejunum was much higher than in the ileum.

The degree of hydrolysis (DH) of the starch from rice found in the dynamic digestion method is depicted in figure 73, where it is compared the total DH with the amount of starch converted into glucose.

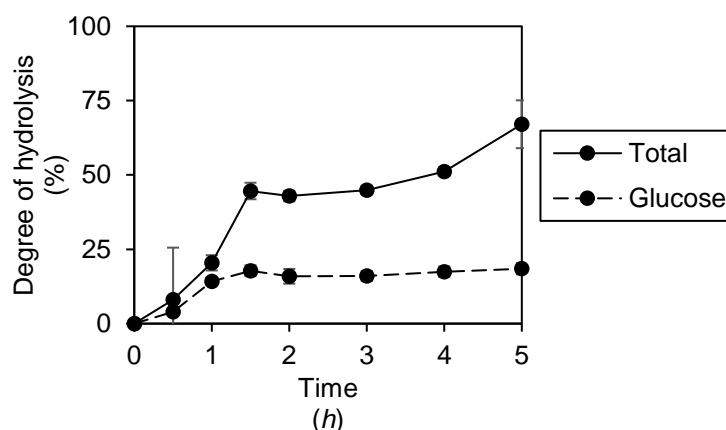


Figure 73. Degree of hydrolysis of the starch from rice

The total DH increased during the first 1.5 h, then the increase slowed down but it kept increasing until the end of the digestion. The amount of glucose released from the starch also increased during the first 1.5 h, but after that the glucose levels kept constant until the end of the digestion.

According to the depicted results in figure 73, during the first hour, the digested starch was mainly glucose. But it should be taken into account that the amount of meal that reached the bioaccessible fraction was very low (figure 72b), therefore the amount of glucose released from the total amount of meal was not too high (< 1 %).

In general, the starch was mainly digested during the first 90 min and then the hydrolysis of the starch slowed down. The amount of starch converted into glucose increased during the first 90 min and then it remained constant, therefore the glucose was only released at the beginning of the digestion.

Although the conversion of starch to glucose stopped after the 90 min of digestion, the digestion of the starch from rice slowed down but it did not stop and the total DH slightly increased until it reached 67.1 ± 8.0 %.

The glycaemic index calculated with the area under the curve is depicted in figure 73 (dashed line), and the obtained GI is 61.2 ± 4.7 %.

A comparison of static and dynamic digestion of starch from rice is provided in the following section.

6.1.3. In vitro digestion method comparison for the digestion of starch from rice

The degree of hydrolysis obtained with both methods is represented in figure 74.

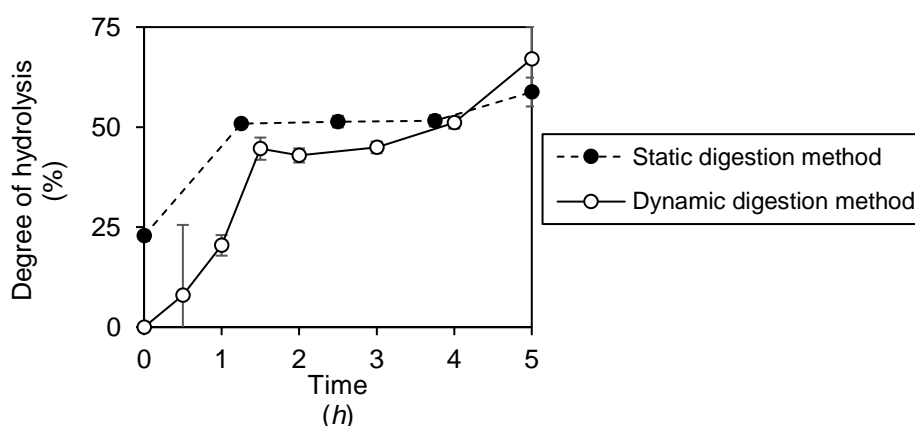


Figure 74. Degree of hydrolysis measured with the static and dynamic digestion methods in the small intestine

The DH increased during the first 1.5 h in both methods, and then it reached a steady state in the static digestion method while in the dynamic digestion method the DH slightly increased until the end of the digestion. Figure 74 shows that the shape of the curve of both in vitro digestion methods is slightly different. However, the DH measured at the end of the digestion was similar between methods.

Although the shape of the curve is different between methods, in both cases the DH increased during the first 1.5 h until it reaches values of ~50 % and then the digestion of the starch slowed down until the last hour where the rate of hydrolysis slightly increased in both cases.

The DH in the small intestine is represented in figure 74, but while the time 0 h of the dynamic digestion method is referred to the starting point of the digestion, in the static method the meal was already in contact with the oral secretions for 2 min and with the gastric secretions for 2 h. Therefore, this could explain why the DH of the static digestion method in the small intestine starts already at almost 25 % while the DH found in the dynamic digestion method is 0 %. The glycaemic index of the starch from rice measured with both the static and dynamic digestion methods is depicted in figure 75.

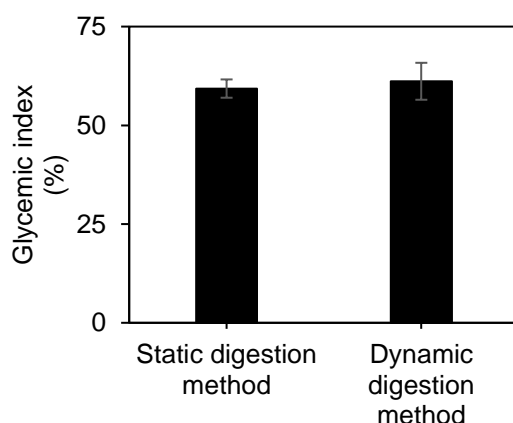


Figure 75. Glycaemic index of starch from rice obtained with both, the static and dynamic digestion method

As it can be seen in figure 75, the same glycaemic index (α 0.05) is found with both methods for the starch from rice.

The obtained results are not far from the in vitro glycaemic index measured by Frei et al (46) from six indigenous Philippine rice cultivars, which ranges between 68 and 109 for cooked rice.

6.2. In vitro digestion of starch from potato

The in vitro digestion of the starch from potato was only studied with the static digestion method, and the obtained degree of hydrolysis is depicted in figure 76.

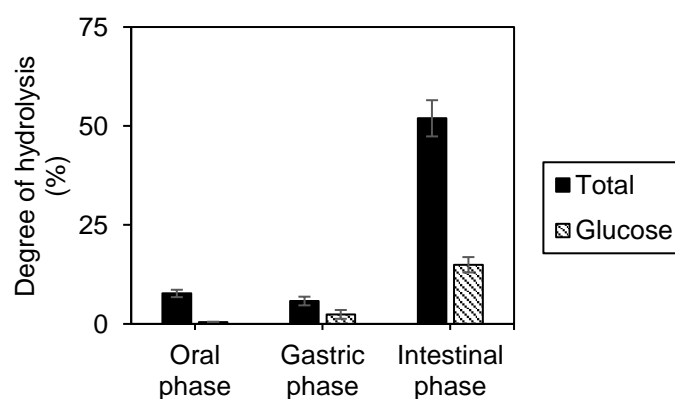


Figure 76. Measured DH (total vs glucose) for starch from potato with the static digestion method

As it can be seen in figure 76, the amount of starch that was digested during the oral and gastric phases was very low, only ~7 %. On the other hand, only 2.4 ± 1.1 % was converted into glucose during the gastric phase but almost no glucose was released during the oral phase.

When the gastric chyme was incubated with the intestinal secretions, the digestion of the starch increased reaching a DH of 51.9 ± 4.6 %, and the amount of glucose released at the end of the in vitro digestion was 14.9 ± 1.9 %.

The low DH obtained at the beginning of the digestion (oral and gastric phases) could be explained by the fact that the starch from potato needs some time to be disintegrated and dissolved with the secretions and be available for its digestibility. Once it was dissolved and in contact with the pancreatic α -amylase, the DH increased almost 10-folds.

The DH vs time during the intestinal phase is depicted in figure 77.

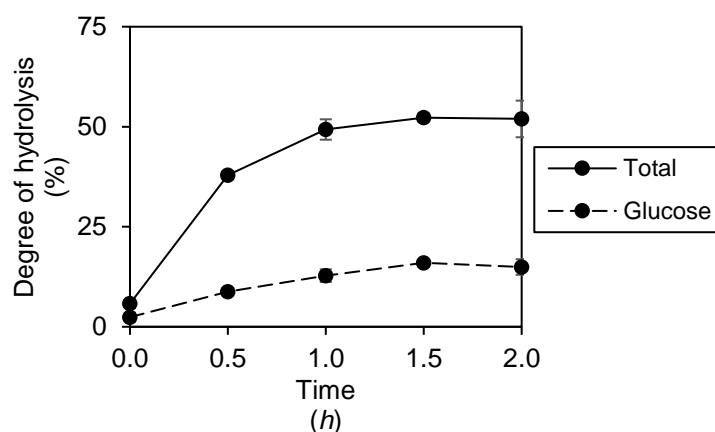


Figure 77. Degree of hydrolysis of the starch from potato (total of DH vs glucose)

Where it can be seen that the hydrolysis of the starch increased mainly during the first 30 min, and then the digestion of the starch slowed down until it reached a steady state. This first increase can only be seen for the total DH, as the amount of glucose released during the intestinal phase increased gradually with the time of digestion until it also reached a steady state.

The glycaemic index was calculated for the starch from potato by taking into account the amount of glucose released during the intestinal phase (figure 77), and the obtained GI for this kind of starch is 52.0 ± 3.6 %.

In the next section, a comparison of the digestion of starch from rice and starch from potato tested with both in vitro digestion methods will be provided.

6.3. Comparison of in vitro digestion of starch from rice and starch from potato

As is explained in the previous sections, two different starch sources have been used to perform the static digestion method and their hydrolysis has been studied during the digestion. The comparison of the DH obtained for both starches after each digestive phase is depicted in figure 78, which shows the total DH (figure 78a) but also the amount of starch converted into glucose (figure 78b).

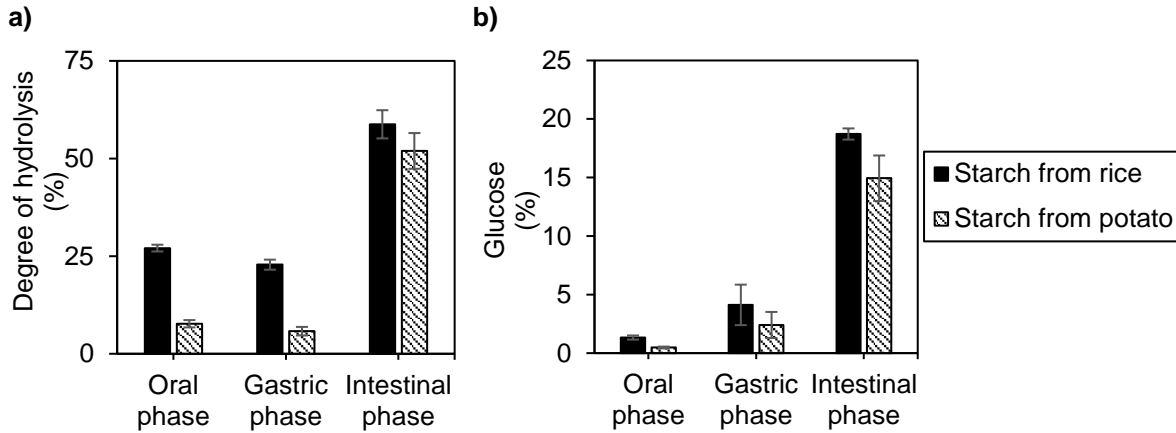


Figure 78. DH (%) and Glucose (%) obtained during the digestion of starch from rice and starch from potato

Figure 78a shows that the measured DH for the starch from rice was higher than the DH of the starch from potato, showing a higher difference after the oral and gastric phase than after the intestinal phase. Figure 78b shows that the amount of glucose released from the starch from rice or potato was similar after the oral and gastric phase, but the percentage of glucose obtained after the intestinal phase was higher for the starch from rice compared with the glucose released from the starch from potato.

The main differences in the degree of hydrolysis are found after the oral and gastric phases. Where the amount of starch that has been hydrolysed is much higher in the case of the rice than for the potato source. Figure 79 could explain these differences on the DH, as it shows the percentage of starch that was solubilised after each sampling point. The graph illustrates that the starch from potato was almost not solubilised after the oral and gastric phases, while more than 80 % of the starch from rice was already solubilised after the oral phase and completely dissolved after the gastric phase. Therefore, it is understandable that, after the oral and gastric phases, the DH obtained for the starch from potato was lower compared with the one obtained for the rice starch.

On the other hand, both starches were completely dissolved during the intestinal phase and almost no differences can be seen on the measured DH after the intestinal phase.

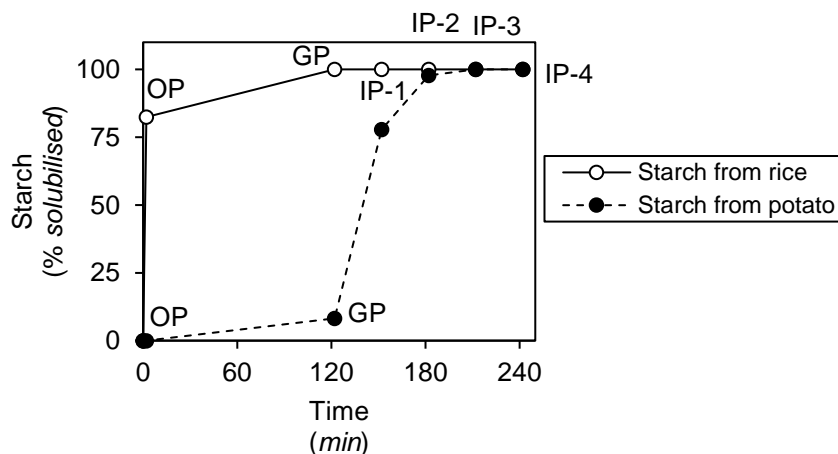


Figure 79. Starch solubilized during the static digestion method (OP: oral phase; GP: gastric phase; IP-1, IP-2, IP-3, IP-4: intestinal phase samples)

In figure 78b, it can be seen that the differences observed on the DH are not present in the glucose released (%). The amount of glucose released from the starch from potato is slightly lower than the glucose released from the starch from rice, but they are not statically different (α 0.05).

The degree of hydrolysis and the released glucose from the starches during the intestinal phase are depicted in figure 80.

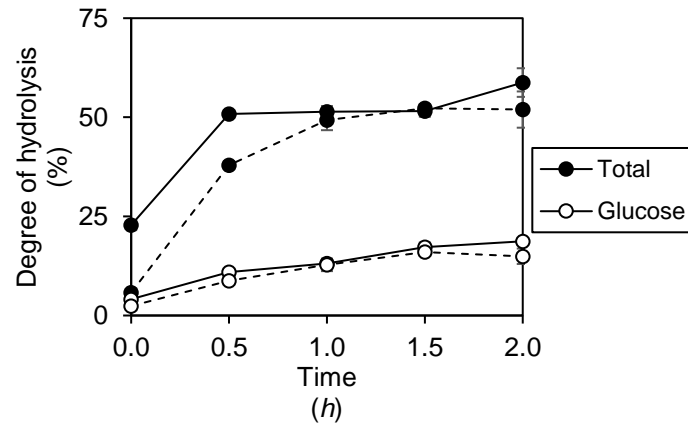


Figure 80. Degree of hydrolysis and glucose released from rice starch (solid line) and potato starch (dashed line)

The obtained DH for the starch from rice is slightly higher during the first hour of intestinal digestion, compared with the DH measured for the starch from potato. However, after that the DH obtained for both starches equalise and therefore it can be concluded that the DH during the intestinal phase is not different between starches (α 0.05).

Although the amount of glucose seems to be equal for both starches during the intestinal phase, it has been proved that they are statically different (α 0.05) and that the obtained glucose levels are higher for the starch from rice, compared with the starch from potato.

The comparison of the measured GI for the rice and potato starches is depicted in figure 81, which shows that the obtained GI for the rice starch is not different from the GI obtained for the starch from potato.

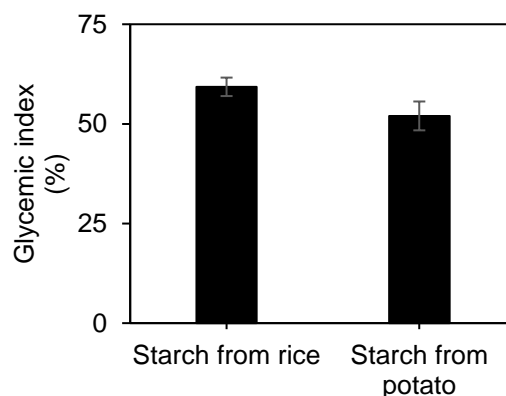


Figure 81. GI obtained for the starch from rice and starch from potato

In the next section, a comparison of the commercial starch vs rice and potato tested with both in vitro digestion methods will be provided.

6.3.1. Comparison of in vitro digestion of commercial starch vs rice and potato

The DH and the GI were measured for the starch from rice and potato but also for the rice and potato (complete food). The comparison of the DH and GI between the starch and the complete food, for both rice and potato, is depicted in figure 82.

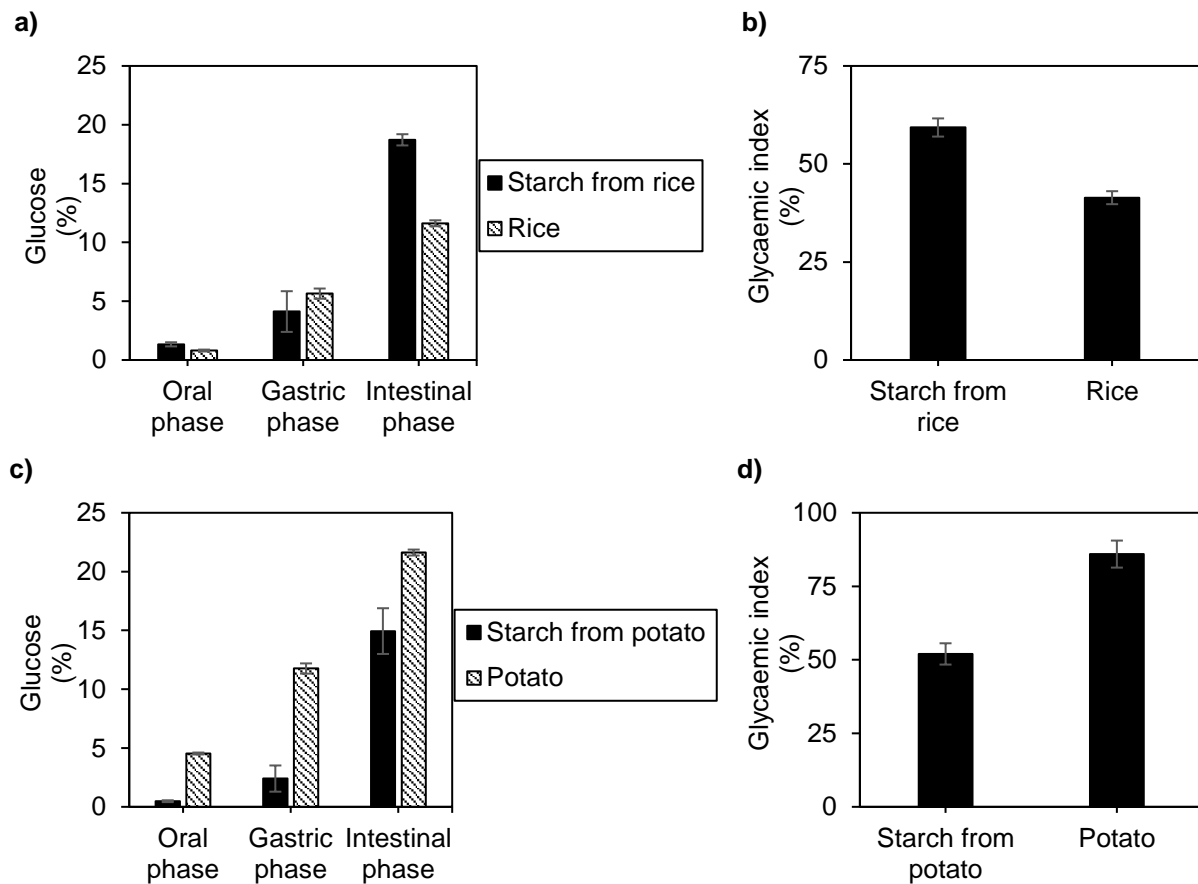


Figure 82. Comparison of the obtained DH and GI for the starches and complete food (rice and potato)

Figure 82a shows that the digestion during the oral and gastric phases is not different for the rice or the starch from rice. However, during the intestinal phase the starch from rice could be more hydrolysed and converted into glucose than the rice. The difference in the release of glucose during the intestinal phase could be because the starch in the rice is more protected than the prepared meal with the commercial starch. Therefore, the commercial starch could be more accessible for the pancreatic α -amylase and for that reason it was more digested. These differences during the intestinal phase are also reflected in the measured GI (figure 82b), which is higher for the commercial starch than for the rice.

The behaviour of the potato is different from that of the rice, as figure 82c shows the amount of glucose released during all the digestion is much higher for the potato than for the commercial starch. However, it seems that during the intestinal phase the difference between both meals slightly decreased. This could be because the prepared meal with the starch had a higher viscosity compared with the meal prepared with the potato, and therefore the starch needed more time to be mixed with the secretions and be available for the enzyme. The comparison of the appearance of both potato meals is shown in figure 83.

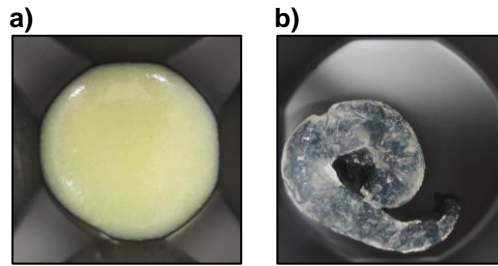


Figure 83. Prepared meals with a) potato, b) commercial starch from potato

Therefore, the obtained GI for the potato is higher than the GI measured for the starch from potato (figure 82d). Besides the texture of the meal, it has to be taken into account that even both are potatoes (or potato source), there are a lot of kinds of potatoes, and each kind of potato has a different GI (table 6). And the same happens with the rice, that each kind of rice releases a different amount of glucose and therefore has a different GI (table 5).

Table 5. GI of different kind of rice

Rice	
Type	GI
Risotto	69 ± 7
Type NS (Italy)	94
Type NS (India)	43
Long grain white	50
Rice porridge (China)	19 ± 1

Table 6. GI of different kind of potatoes

Potato	
Type	GI
White with skin	69 ± 5
Irish potato	83 ± 6
Desiree (Australia)	101 ± 15
Type NS (India)	23
Sweet potato	46 ± 5

Selma-Gracia et al (47) studied the thermal and pasting properties of starches from various botanic origins but also their connection with enzyme digestibility were evaluated. An in vitro digestion method was used to study, among others, the digestibility of rice and potato starches. The calculated in vitro GI for rice starch was 99.3 ± 4.0 %, which is much higher compared with the depicted results in figure 82. On the other hand, the calculated in vitro GI for the potato starch was 74.0 ± 3.5 %. Their calculated GI is slightly higher compared to the measured GI of the potato starch, but slightly lower than the measured GI of the potato (complete meal). Those differences may be triggered mainly by the differences on the conditions of the in vitro digestion method but also on the specific source of the starches (47).

7. Impact of protein on starch digestion

The effect of two protein sources on carbohydrate digestion was studied with the in vitro digestion methods.

7.1. Impact of egg whites on starch from rice digestion

7.1.1. Static in vitro digestion of starch from rice mixed with egg whites

A meal prepared with the starch from rice and the commercial powder made of egg whites from chicken was used to perform the static digestion method. The obtained degree of hydrolysis (total and glucose) after each digestive phase is depicted in figure 84.

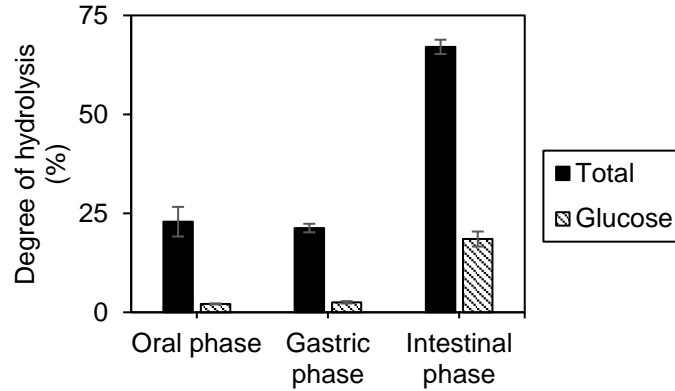


Figure 84. DH and glucose released from the starch in the presence of egg whites from chicken

Figure 84 shows that the total DH did not increase during the gastric phase, but after the intestinal phase the measured DH drastically increased. The glucose levels during the oral and gastric phases were similar, and then it increased during the intestinal phase.

According to the depicted results, the starch was mainly digested during the oral and intestinal phases. The carbohydrate-protein mixture was mixed with the oral secretions, and almost 25 % (22.9 ± 3.7 %) of the starch was hydrolysed. Then, during the gastric phase, the salivary α -amylase would be inactivated by the acidic conditions and for that reason, the digestion of the starch was stopped. Finally, when the gastric chyme was incubated with the intestinal secretions, the starch was further hydrolysed reaching a degree of hydrolysis of 67.1 ± 1.8 %.

Figure 84 also shows the amount of starch converted into glucose, and it can be seen that only 2.1 ± 0.1 % of glucose was released during the oral phase. The release of glucose was also ceased during the gastric phase and then, during the intestinal phase, the formation of glucose continued achieving values of 18.5 ± 1.9 %. Therefore, only a small portion of the hydrolysates that were formed during the digestion of the mixture of starch and protein was glucose (27.6 ± 2.8 % hydrolysed starch).

The hydrolysis of the starch in the presence of egg whites was followed during the intestinal phase, and the obtained DH is depicted in figure 85.

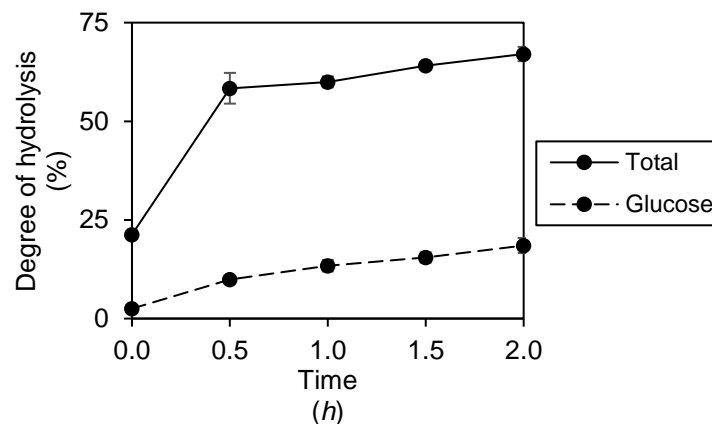


Figure 85. DH (total and glucose) obtained during the intestinal phase

The total DH highly increased during the first 30 min of the intestinal phase, and then it reached a steady state. However, the measured glucose gradually increased during the intestinal phase.

As figure 85 shows, when the chyme was mixed with the intestinal secretions, the starch was highly hydrolysed reaching a DH of 58.4 ± 3.9 % after 30 min of intestinal digestion. After that, the hydrolysis of the starch slowed down obtaining a final DH of 67.1 ± 1.8 %. Therefore, almost 40 % of the starch

was digested during the first 30 min of the intestinal phase, while during the last 1.5 h only ~9 % of the starch was hydrolysed.

Unlike the total DH, the release of glucose, which mainly occurred during the intestinal phase, increased constantly with time, and the total amount of starch converted into glucose was 18.5 ± 1.9 %.

The glycaemic index of this meal was calculated with the curve of glucose depicted in figure 85, and the obtained GI is 55.5 ± 4.8 %.

7.1.2. Dynamic in vitro digestion of starch from rice mixed with egg whites

The meal (starch) distribution found in the dynamic system (TIM-1) after the digestion is depicted in figure 86a, and its distribution in the bioaccessible fraction during the digestion is shown in figure 86b.

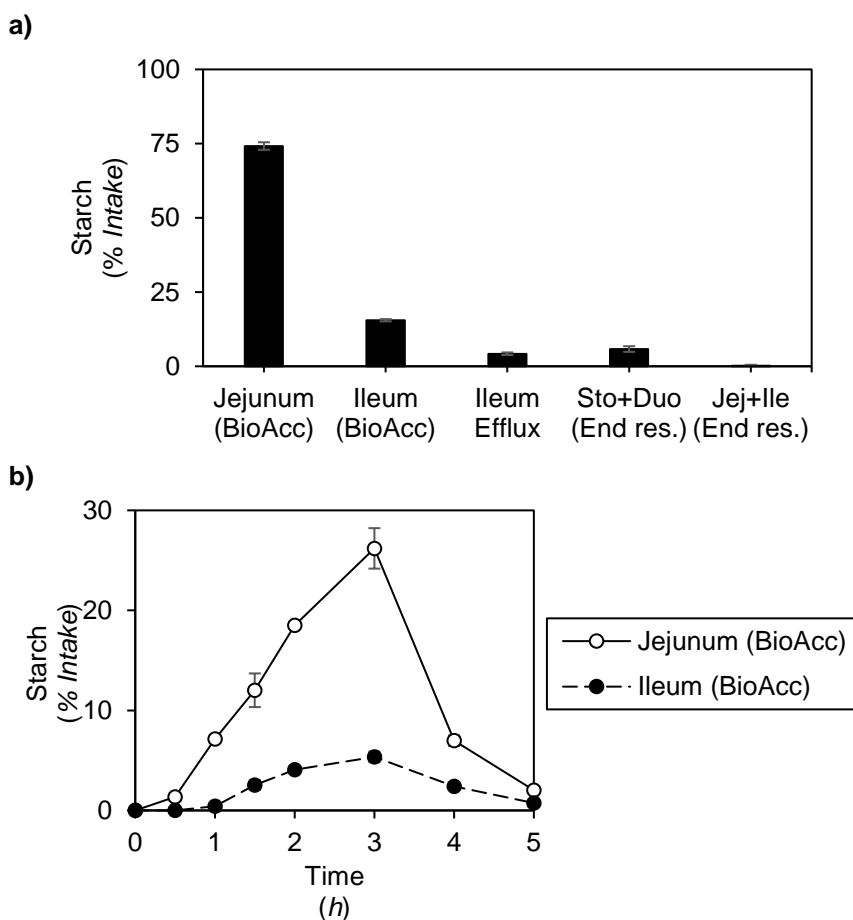


Figure 86. Distribution of the mixture of starch from rice and egg whites throughout the dynamic system (TIM-1)

As figure 86a shows, the meal was mainly found in the bioaccessible fraction of the jejunum, the other 25 % of the meal was found in the bioaccessible fraction of the ileum, ileum efflux and in the end residues. And, at the end of the digestion, almost no meal was found in the lumen of the jejunum and ileum.

According to figure 86b, the amount of starch that was recollected in the jejunal dialysate increased with the time until it reached a maximum at 3 h of digestion, and then it decreased until the end of the digestion. The same behaviour can be seen in the ileum bioaccessible fraction, but with a lower amount of starch. Moreover, during the first hour of digestion almost no starch could be found in the dialysate sample.

The distribution of the starch during the first 3 h of digestion was mainly influenced by the stomach emptying, which mainly depends on the ease of disintegration of the meal.

The obtained degree of hydrolysis of the starch is depicted in figure 87.

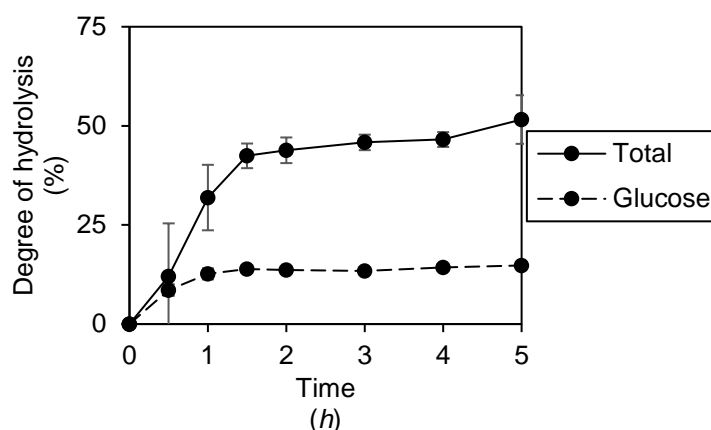


Figure 87. DH (total and glucose) observed during the in vitro dynamic digestion method for the meal that contains starch from rice and egg whites from chicken

The total DH increased during the first 1.5 h of the in vitro digestion and then it reached a steady state until the end of the digestion. The glucose levels also increased during the first hour and after that it kept constant.

Figure 87 shows that the digestion of the starch occurred mainly during the first 1.5 h, but the starch was able to be converted into glucose only during the first hour. After that, the hydrolysis of the starch slowed down, almost ceased until the end of the digestion.

The measured GI with the dynamic digestion method of the meal that contains rice starch and egg whites from chicken is 53.0 ± 2.2 %.

A comparison of both static and dynamic digestion of starch from rice with egg whites is provided in the following section.

7.1.3. In vitro digestion method comparison for the digestion of starch from rice mixed with egg whites

The measured DH of the starch from rice mixed with egg whites, with both methods (static and dynamic) is depicted in figure 88.

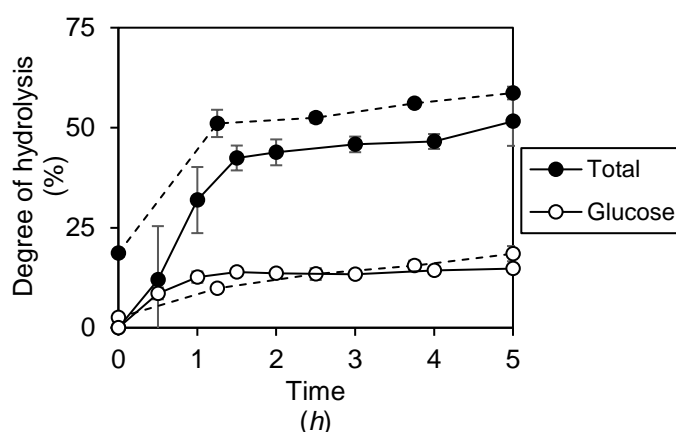


Figure 88. Comparison of the obtained DH for the same meal for both methods (static digestion methods: dashed line, dynamic digestion method: solid line)

As figure 88 shows, the obtained DH in the small intestine with the static method is higher than with the dynamic digestion method. However, the glucose levels measured with both in vitro digestion methods

are not different (α 0.05). And consequently, the in vitro GI obtained with both methods is also equal (figure 89).

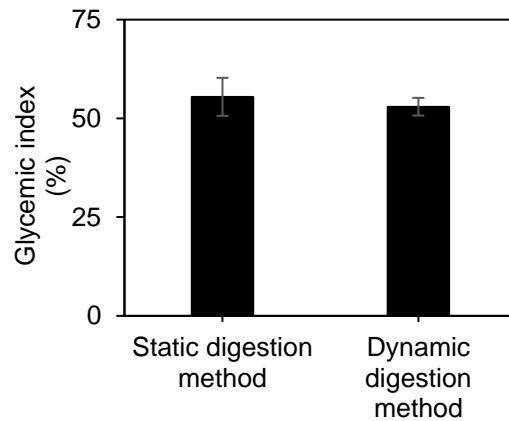
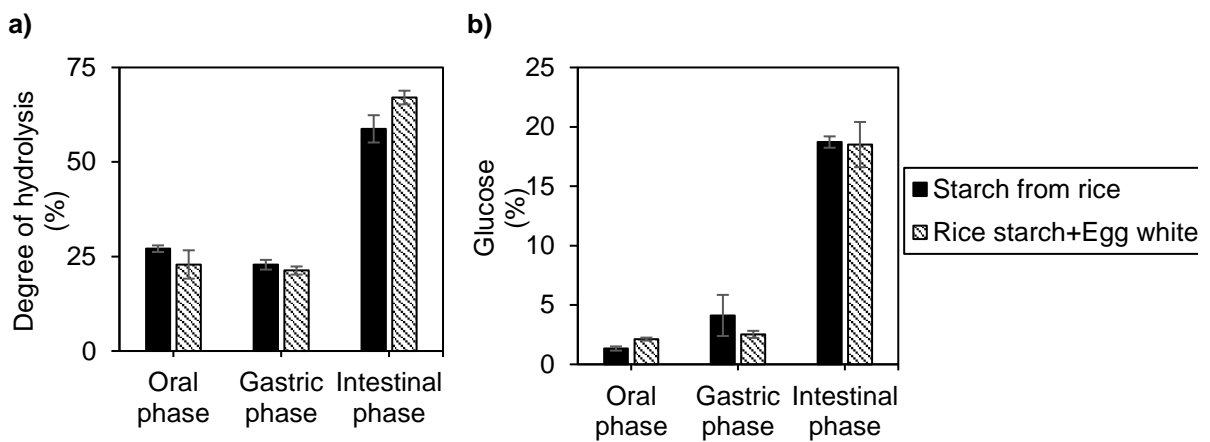


Figure 89. Calculated GI of starch from rice with egg whites with the static and dynamic digestion methods

A comparison of the starch from rice and starch from rice with egg whites tested with in vitro digestion methods will be provided in the next section.

7.1.4. Comparison of in vitro digestion of starch from rice and starch from rice with egg whites

To check the effect of the egg protein on the digestion of the starch from rice, the DH obtained with both meals is depicted in figure 90.



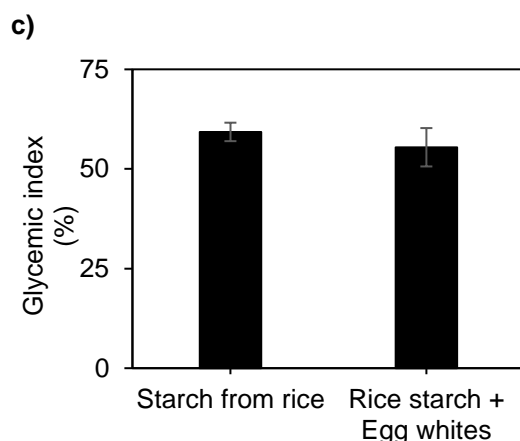


Figure 90. a) Total DH, b) glucose released and c) GI measured for the starch and the mixture of starch and egg whites

Figure 90a shows that there were no differences between the DH measured after the oral and gastric phases for the starch from rice, but also for the starch from rice with egg whites. And the DH measured after the intestinal phase drastically increased for both meals. It can be seen in figure 90b that the amount of glucose released from both meals was not different after each digestive phase. And figure 90c shows that the same GI was obtained for the starch from rice and the starch from rice with egg whites.

As it can be seen in figure 90, there are no differences between the digestion of both meals. Therefore, the addition of egg whites from chicken does not have an impact on the digestion of starch from rice. This is in agreement with the results obtained from a randomised, controlled, non-blind, cross-over study, where the authors studied the effect of egg whites on the digestion of rice by measuring their glycaemic index. They concluded that no significant differences were observed between the test meal (egg whites and rice) compared with the control meal (rice). The effect of some proteins on the postprandial blood glucose levels can be seen in figure 91, this figure also shows that there are no significant differences on the AUC₁₂₀ when the egg white was added to the rice starch (48).

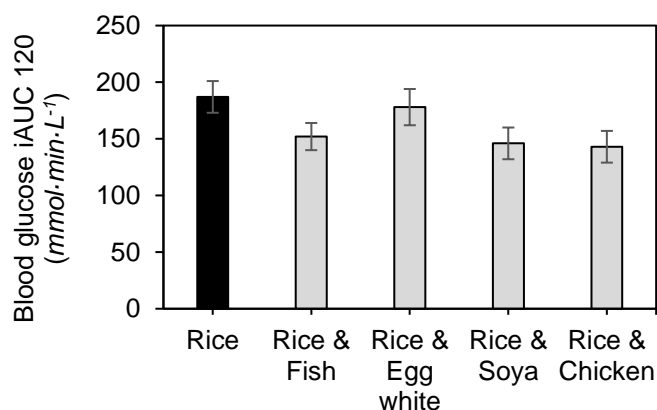


Figure 91. Effect of the protein on the digestion of rice (48)

7.2. In vitro digestion of starch from potato with egg whites

The starch from potato was mixed with the egg whites from chicken, and its digestion was studied with the static digestion method. The obtained degree of hydrolysis after each digestive phase is depicted in figure 92.

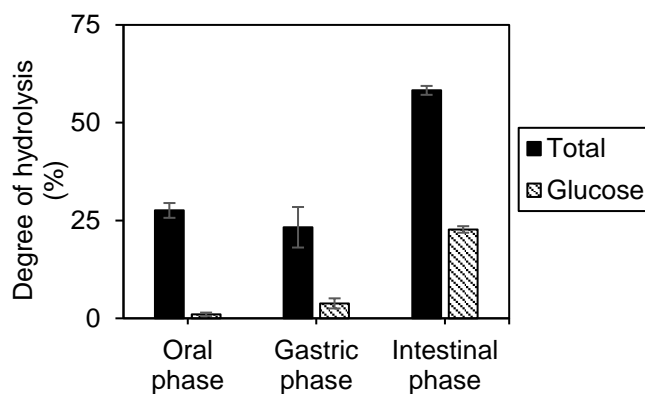


Figure 92. DH and glucose released during the in vitro digestion

During the oral phase, more than 25 % of the starch intaken was hydrolysed, but only 1.0 ± 0.4 % was converted into glucose. During the gastric phase, the starch was almost not hydrolysed, while the amount of glucose released from the starch slightly increased. Therefore, the meal may have protected the enzyme and for that reason, the α -amylase was slightly active during the gastric phase. Finally, during the intestinal phase the starch was further hydrolysed reaching values of DH of 58.3 ± 1.1 % and 22.7 ± 0.8 % of glucose.

The digestion of this meal was studied during the intestinal phase, and the obtained DH (total and glucose) is depicted in figure 93.

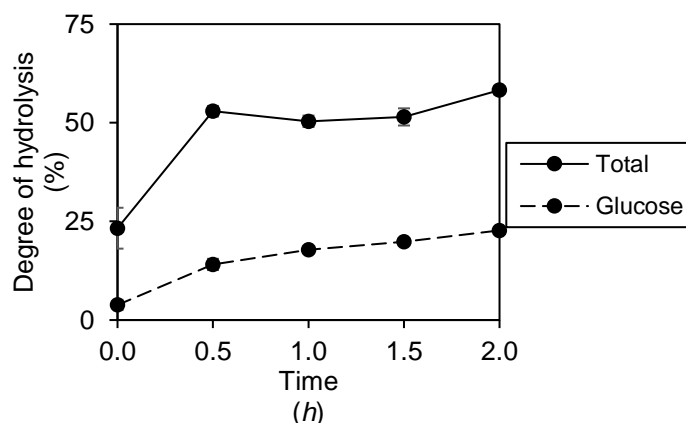


Figure 93. Total DH and glucose released during the intestinal phase

Figure 93 shows how the total DH increased from 23.3 ± 5.2 % to 52.9 ± 1.3 % during the first 30 min of the intestinal phase. After that, the total DH almost did not vary until the last 30 min of digestion, when the DH slightly increased.

Figure 93 also shows a higher increase in the glucose release during the first 30 min of the intestinal phase, compared with the rest of the intestinal digestion. However, the glucose formation during the last 1.5 h was larger compared with the total DH at the same time points.

The calculated GI with the static digestion method is 73.1 ± 2.8 % for the meal that contains starch from potato and egg whites from chicken.

A comparison of the starch from potato and starch from potato with egg whites tested with in vitro digestion methods will be provided in the next section.

7.2.1. Comparison of in vitro digestion of starch from potato and starch from potato with egg whites

The comparison of the measured DH and glucose released of both meals after each digestive phase is depicted in figure 94.

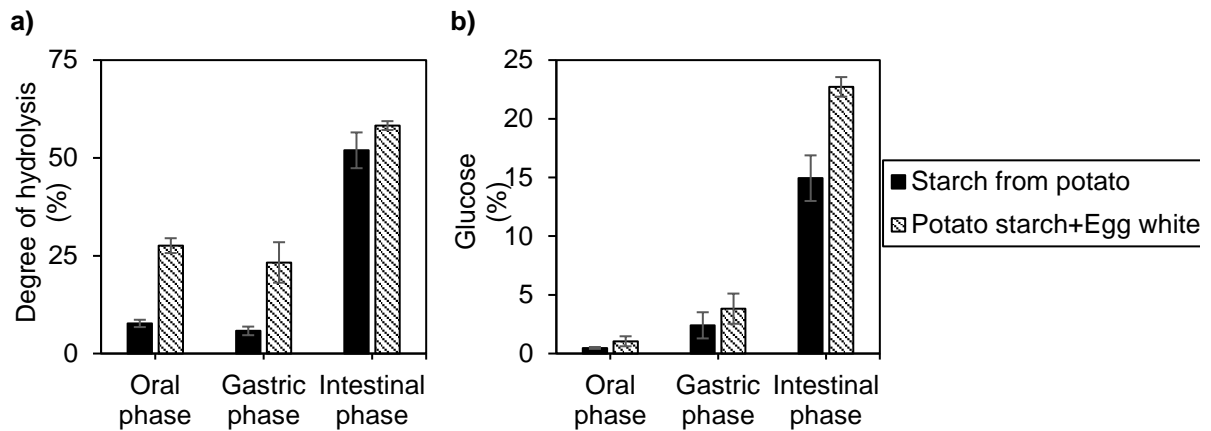


Figure 94. Effect of the egg whites on the potato starch digestion, a) total DH, b) glucose released

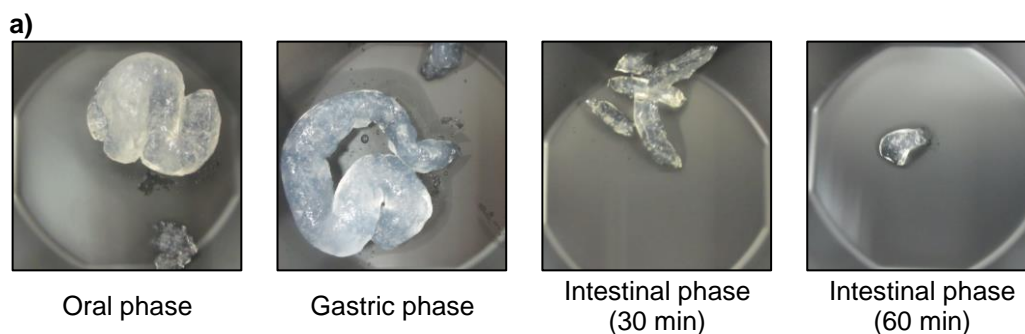
In general, the total DH of the starch from potato was lower than the DH measured for the starch from potato with egg whites, the differences being bigger after the oral and gastric phases.

As figure 94b shows, no significant differences can be seen in the glucose release after the oral and gastric phases between meals. However, a higher amount of glucose was released during the intestinal phase for the starch from potato with egg whites compared with the glucose released from the starch from potato.

Unlike expected, as figure 94 shows, the addition of the protein (egg whites from chicken) to the starch from potato favours the digestion of the potato starch. The differences in the digestion of both meals can be seen mainly on the total DH after the oral and gastric phase and on the glucose released after the intestinal phase.

The increase in digestion could be triggered by the differences in the physical properties of the meals, as the meal that contains only the potato starch is more viscous than the meal that also contains the protein. And as the viscosity of the starch from potato is higher, it needs more time to be disintegrated and accessible for the enzyme.

Figure 95 shows the meal left after the oral, gastric and after different time points of the intestinal phase. And as it can be seen, the presence of egg whites favours the disintegration and solubilization of the meal, which helps to its digestion. One of the main differences is that the starch from potato keeps the “spaghetti” shape after the digestive phases.



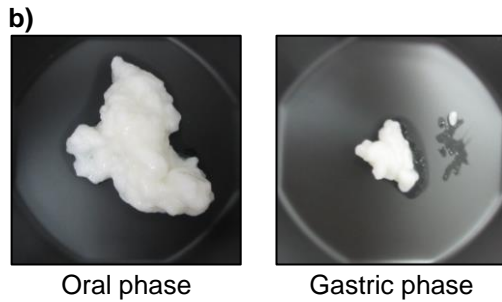


Figure 95. Differences in the appearance of the digested meal after the digestive phases, a) starch from potato, b) starch from potato with egg whites from chicken

The differences in the glucose release from the potato starch in the presence or absence of egg whites could only be appreciated after the intestinal phase. This may be because the starch needs more time to be converted into glucose rather than into bigger molecules.

The comparison of the calculated GI of both meals is depicted in figure 96.

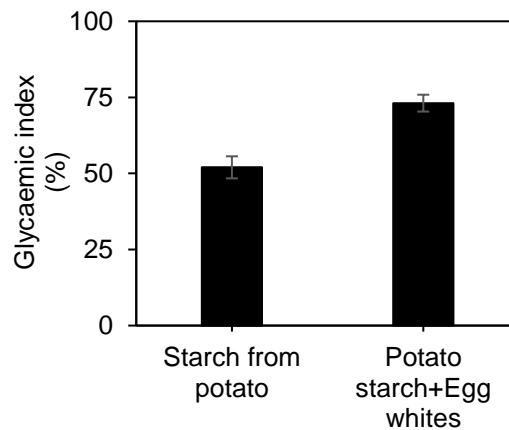


Figure 96. GI measured with the static digestion method for potato starch in the absence or presence of egg whites

As it can be seen in figure 96, the addition of the egg whites to the potato starch increases the GI almost 1.5-folds. This may be affected by the initial disintegration of the meal, as the potato starch would have less time to be completely digested and converted into glucose.

Gulliford et al (49) studying the impact of the addition of protein to potato on the glycaemic index, it found that the addition of protein slightly reduced the glycaemic index response to mashed potato, as the insulin response greatly increased. It was concluded that this might have been caused by an increase in the osmolality of the stomach contents reducing the rate of gastric emptying. Those results are in disagreement with the measured GI depicted in figure 96, where the addition of egg whites caused an increase of the GI measured for the potato starch alone. The differences obtained between both studies could be due to the potato and protein origins, besides the conditions of the meal preparation which could lead to structural differences between the carbohydrates.

7.3. In vitro digestion of starch from rice and casein

The casein was used to study the effect of another protein source on the digestion of starch from rice. To do that, the starch was first mixed with the casein, and then olive oil or butter was added to this mixture. The obtained results for these meals are depicted in figure 97. Where it can be seen that, in all the meal combinations, the addition of casein to the meal decreases the digestion of starch from rice. The casein effect is bigger on the glucose release rather than the total DH.

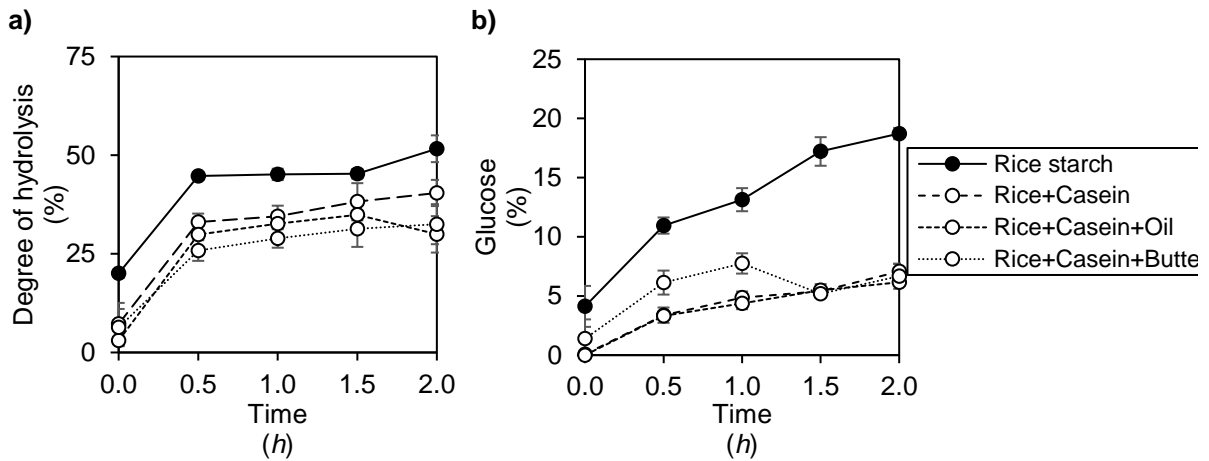


Figure 97. DH and glucose released from the rice starch in the presence or absence of casein

And therefore, the GI of the meals that contain casein is also lower compared with the GI measured for the starch from rice. The obtained values are depicted in figure 98.

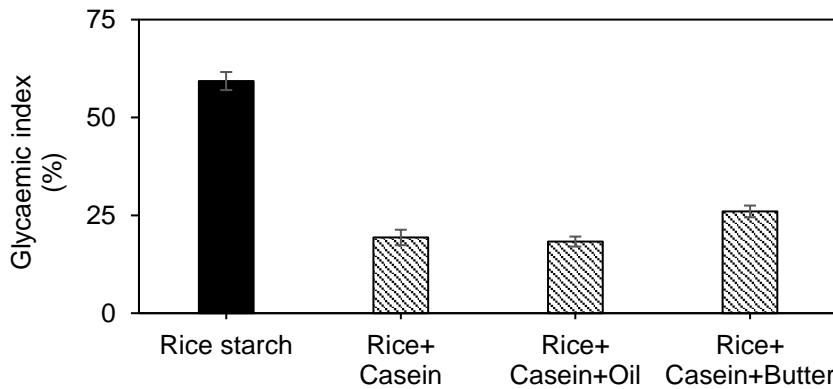


Figure 98. Measured GI of the starch from rice and its comparison with the meals that contains casein

The decrease in the starch digestion was not triggered by the casein, but by the sodium bicarbonate used to dissolve the casein. During the digestion, the sodium bicarbonate was released and the pH of the solution increased. Therefore, the enzymes catalyse the hydrolysis at different conditions, compared with the digestion of the starch from rice. Moreover, those conditions were not optimal for the enzymes triggering the decrease in the digestion of the meal. Figure 99 shows the comparison of the conditions used in the static digestion method with the pH values measured during the digestion of the casein meals.

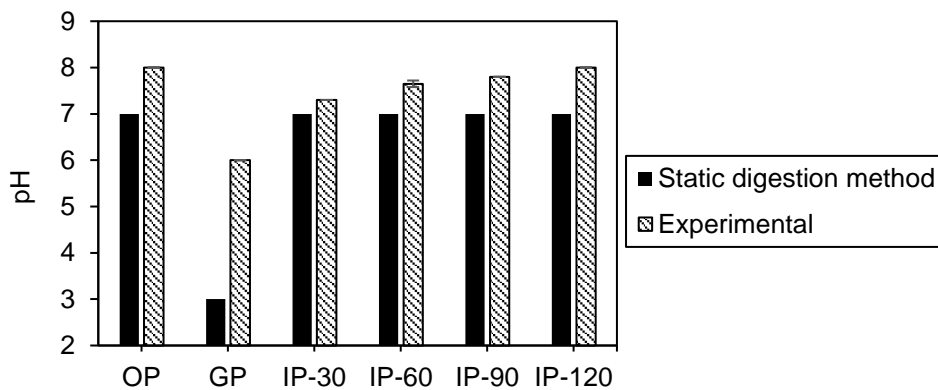


Figure 99. Effect of the casein on the pH of the digestive phases (OP: oral phase, GP: gastric phase, IP: intestinal phase)

As it was not possible to add HCl to adjust the pH during the digestion with the static method, it was concluded that this method was not appropriate to study the effect of the casein. The effect of casein was also studied with the dynamic digestion method. The advantage of this method is that there is a constant secretion of HCl and NaHCO₃ to adjust the pH of the lumen. The pH in the lumen of the different compartments was checked during the digestion, and the measured values of one of the runs are depicted in the following figure (figure 100).

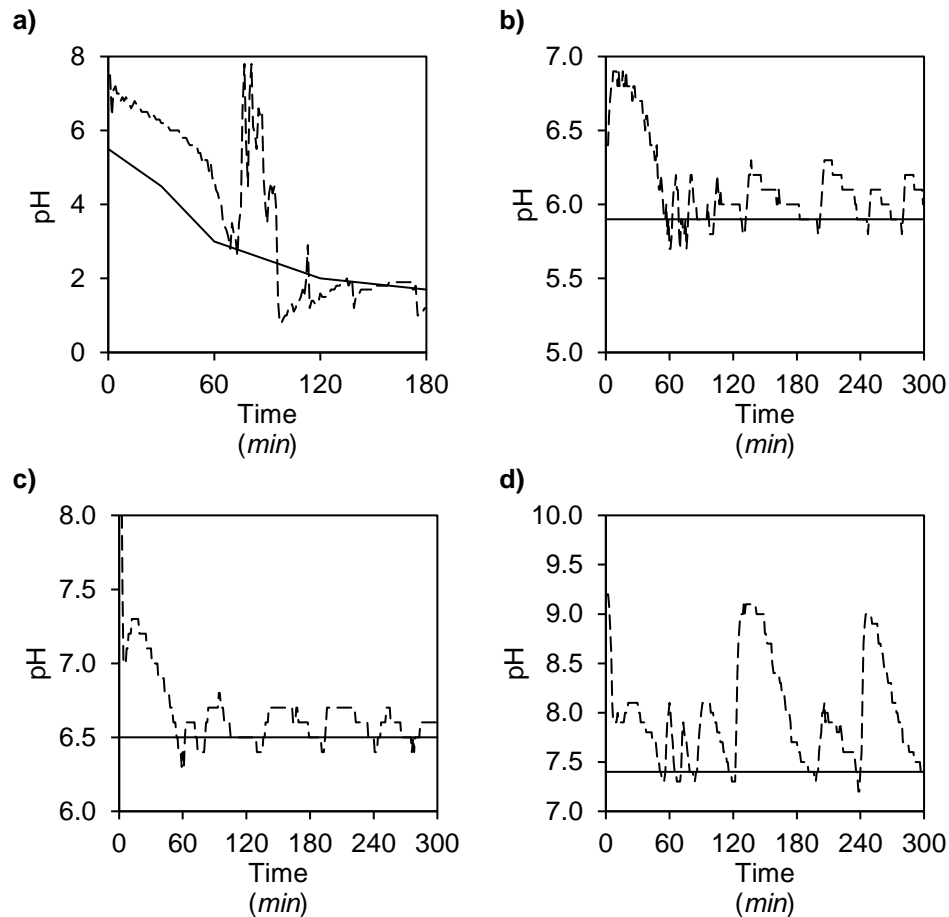


Figure 100. pH values measured in the a) stomach, b) duodenum, c) jejunum, d) ileum during the digestion of starch from rice in the presence of casein (solid line: theoretical, dashed line: experimental)

As it can be seen in figure 100, the NaHCO₃ released from the meal has an impact on the pH of the lumen content. The release of NaHCO₃ can be seen in the stomach, where the pH is slightly higher than the theoretical one, and at 1 h there is a peak. This peak in the pH may be due to the disintegration of the meal, as after 1 h the meal started to be completely disintegrated.

During the digestion, the meal was solubilised with the secretions and left the stomach. The chyme that left the stomach travels throughout the system and therefore, the pH is also slightly higher in the other compartments. The acid secretion was only available in the stomach, but for the small intestine TIM-1 does not have any system to decrease the pH.

For that reason, a higher concentration of HCl (5 M instead of 1 M) was used as acid secretion in the stomach. However, when 5 M HCl was used the casein present in the stomach precipitated and the precipitate blocked some of the tubes of the system.

Therefore, it was decided not to use the casein to study how this kind of protein affects the digestion of the starch because the obtained results would not be realistic and could lead to wrong conclusions.

8. Impact of fat on starch digestion

The effect of two different fat sources on the digestion of starch was also studied, with both, the static and dynamic digestion methods.

8.1. In vitro digestion of starch from rice with olive oil

8.1.1. Static in vitro digestion of starch from rice with olive oil

The static digestion method was used to check the possible effect of olive oil on the digestion of the starch from rice.

The measured DH (total and glucose) after each digestive phase is depicted in figure 101.

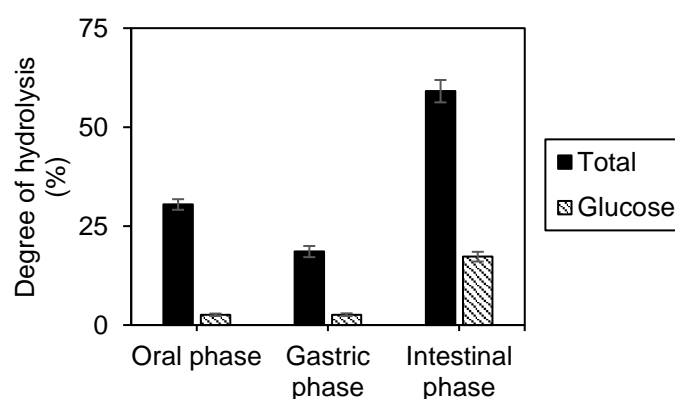


Figure 101. DH (total and glucose) after each digestive phase

It can be seen in figure 101 that 30.5 ± 1.3 % of the starch was already hydrolysed after the oral, but only 2.6 ± 0.3 % of the starch was converted into glucose. After that, the measured DH after the gastric phase seems to be slightly lower than after the oral phase. But this may come from experimental errors during the in vitro digestion or its analytics. However, the differences are very small and it could be considered that the meal was not further digested during the gastric phase. The amount of glucose released after the gastric phase is equal to after the oral phase, which could confirm that during the gastric phase the starch could not be hydrolysed.

Then, the pancreatic α -amylase seems to have an important role in the digestion of the starch, as both the total DH and glucose released increase from the gastric to the intestinal phase. The DH measured at the end of the digestion is 59.1 ± 2.8 %, while the total amount of starch converted into glucose is 17.3 ± 1.2 %.

The digestion was followed during the intestinal phase, and the measured DH vs digestion time is depicted in figure 102. The figure shows that almost no glucose was released when the intestinal phase started, but it was continuously released until the end of the digestion. The DH increased significantly during the first 30 min of the intestinal phase, going from 18.6 ± 1.4 % to 52.2 ± 3.0 %. After that, the hydrolysis of the starch slowed down obtaining a final DH of 59.1 ± 2.8 %, only ~ 7 % higher than the DH measured at 30 min of IP (intestinal phase).

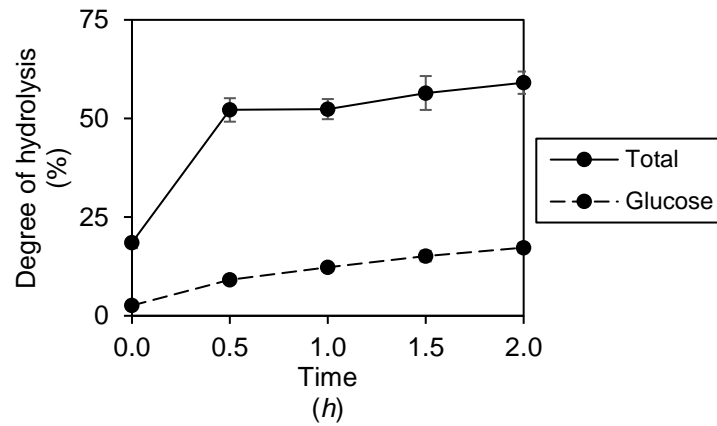


Figure 102. Digestion of the starch from rice mixed with olive oil during the intestinal phase

The measured GI with the static method for the meal that contains starch from rice and olive oil is 52.3 ± 2.3 %.

8.1.2. Dynamic in vitro digestion of starch from rice with olive oil

The effect of olive oil on the digestion of the starch from rice was also studied with the dynamic digestion method. The distribution of the meal (starch) throughout the system at the end of the digestion and at the bioaccessible fraction during the digestion are depicted in figure 103.

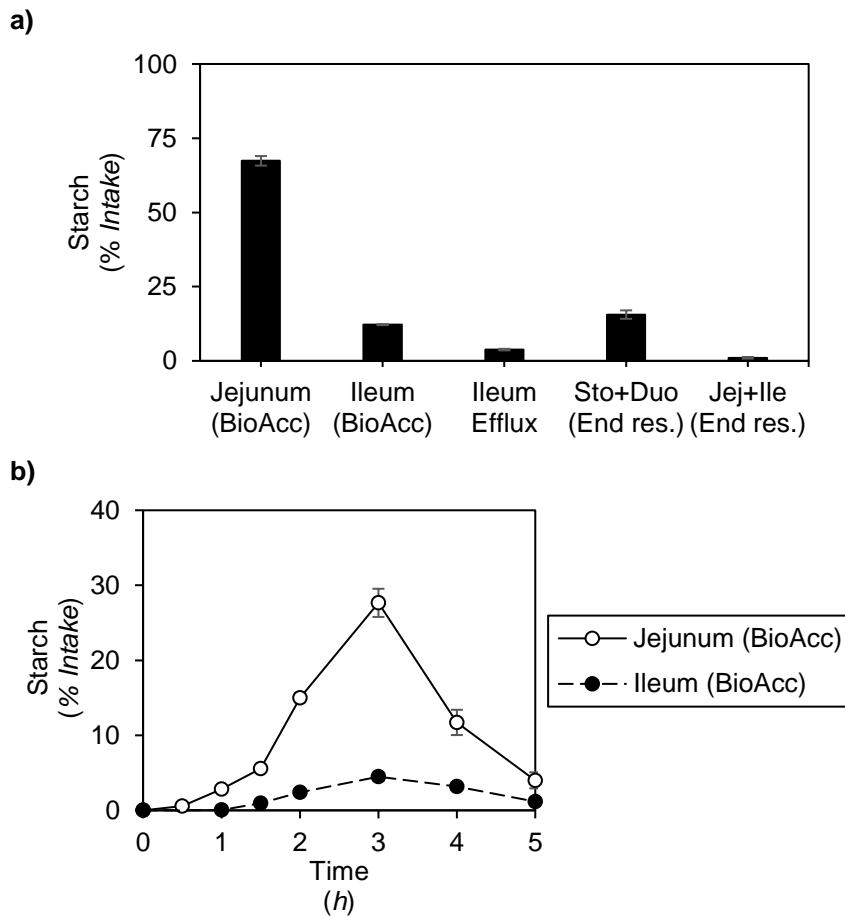


Figure 103. Distribution of the starch from rice throughout the TIM-1 system in the presence of olive oil

The major part of the meal was collected in the jejunum bioaccessible fraction (~70 %), around 15 % of the starch was found in the ileum bioaccessible fraction and ~15 % in the lumen of the stomach and duodenum. At a lower extent, around 1 – 4 % of the starch was found in the ileum efflux and in the lumen of the jejunum and ileum.

The amount of meal found in the jejunum bioaccessible fraction slightly increased during the first 1.5 h and then it significantly increased until it reached a maximum at 3 h of digestion. Finally, the amount of starch found in the jejunum decreased until the 5th h of digestion.

In figure 103b, it can be seen that the meal did not reach the ileum until after 1 h of digestion. Then, the amount of starch found in the ileum slightly increased until the 3rd h, where it reached a maximum. After that, the percentage of starch decreased until the end of the digestion.

The amount of starch found in the bioaccessible fraction during the first 1.5 h was low because it was the time that the meal needed to be disintegrated and leave the stomach. After 1.5 h the meal was almost completely disintegrated, and for that reason, there is a change on the slope of the curve, and the amount of meal found in the bioaccessible fraction drastically increased until it reached the maximum.

The measured DH (total and glucose) with the dynamic digestion method is depicted in figure 104.

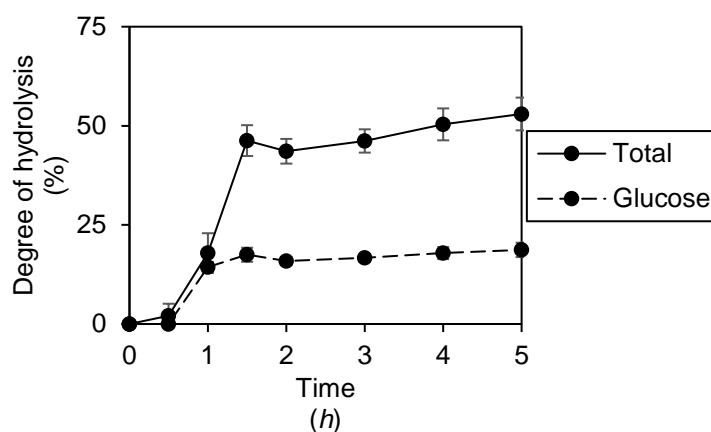


Figure 104. DH (total and glucose) of the starch from rice in the presence of olive oil, measured with the dynamic digestion method

The total DH slightly increased during the first 30 min, then the DH drastically increased for the next hour and then it reached a plateau. The same behaviour was observed for the amount of glucose released, except that it reached the plateau after 1 h of digestion.

Figure 104 shows that during the first hour, the starch that was hydrolysed was converted into glucose. But it has to take into account that the amount of meal that reached the bioaccessible fraction during the first hour was really small, only 2.9 ± 0.3 %. For the next 30 min, the starch was highly hydrolysed but almost no glucose was released. And from the 1.5 h, the meal was only slightly hydrolysed reaching a final DH of 53.0 ± 4.1 %.

The glucose curve from figure 104 was used to calculate the in vitro GI, and the obtained value was 60.4 ± 4.8 %.

A comparison of static and dynamic digestion of starch from rice with olive oil is provided in the following section.

8.1.3. In vitro digestion method comparison for the digestion of starch from rice with olive oil

Both methods were used to study the digestion of the starch from rice in the presence of olive oil. The measured DH (total and glucose) in the small intestine with both the static and dynamic digestion methods is depicted in figure 105.

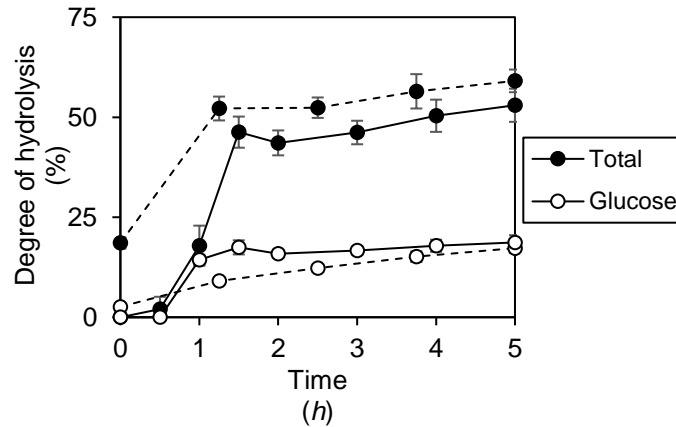


Figure 105. Measured DH (total, glucose) of starch from rice mixed with olive oil with the static (dashed line) and dynamic (solid line) digestion methods

The figure shows that the main differences are found at the beginning of the digestion. After 30 min of digestion the DH obtained with the dynamic method was much lower than the DH obtained with the static method. One of the big differences is that with the dynamic method the time “0” means the beginning of the digestion, while in the static method the meal was already incubated with the oral and gastric secretions. In the dynamic digestion method, the meal needed some time to be disintegrated and be able to leave the stomach, for that reason the measured DH is very low.

After that, the measured DH increases with both methods, but the hydrolysis of the starch is faster with the dynamic digestion method. This could be because with the dynamic method the released products are removed from the system, while in the static method it is not. The removal of the released products favours the catalysis of the enzymes, as the products may inhibit their activity.

From the 1.5 h of digestion and with both methods, the hydrolysis of the meal slowed down and the measured DH slightly increased until the end of the digestion.

The final DH measured with both methods does not show differences, therefore the same end point was achieved with the two methods.

The comparison of the measured GI with the static and dynamic digestion methods is depicted in figure 106. And as it can be seen in the figure, there are no differences when the GI was measured with the static or dynamic methods (α 0.05).

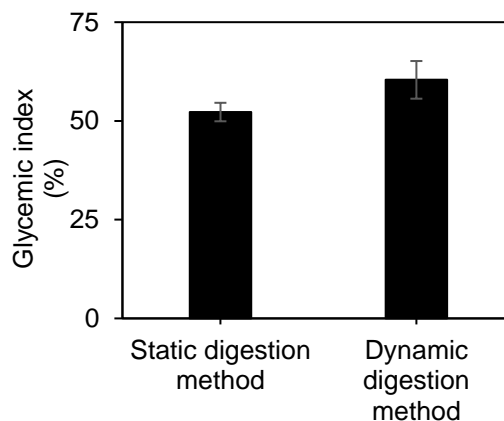


Figure 106. Measured GI for starch from rice mixed with olive oil with the static and dynamic digestion methods

A comparison of the starch from rice and starch from rice with olive oil tested with in vitro digestion methods will be provided in the next section.

8.1.4. Comparison of in vitro digestion of starch from rice and starch from rice with olive oil

To study the effect of olive oil on the digestion of the starch from rice, the DH (total and glucose) measured with the static digestion method is depicted in figure 107.

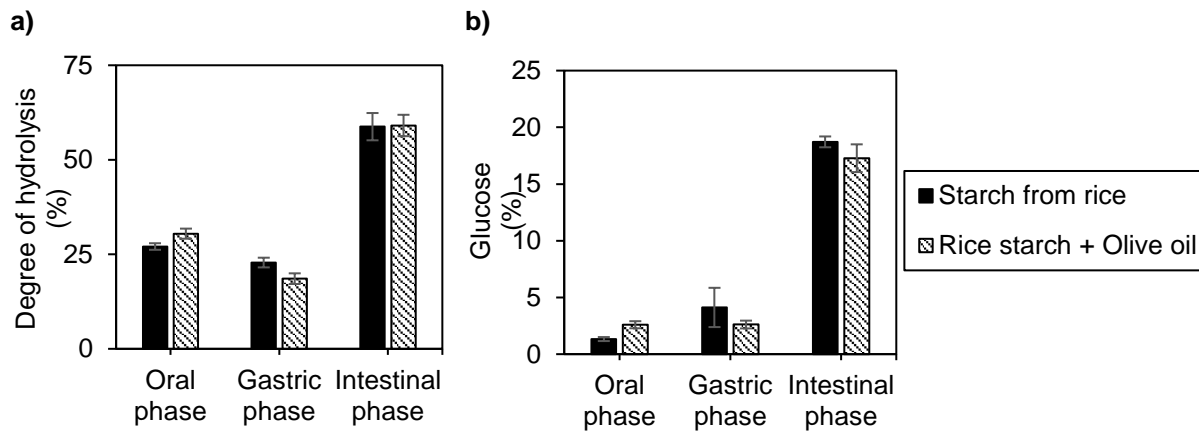


Figure 107. DH of the starch from rice in the absence and presence of olive oil, a) total, b) glucose

Figure 107 shows that there are no differences between the measured DH for the starch from rice and the meal that contains starch from rice and olive oil. Therefore, it demonstrates that olive oil does not have any effect on the digestion of the starch from rice.

The GI calculated for both meals is depicted in figure 108. Where it can also be seen that the addition of olive oil to the starch from rice does not have any effect on the glucose release from the starch.

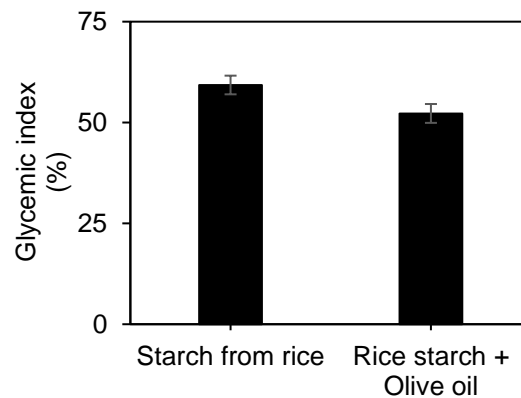


Figure 108. Measured GI for starch from rice and starch from rice with olive oil

A meta-analysis study tested the hypothesis of whether olive oil consumption would improve glycaemic indices. Thirteen trials were reviewed and the results showed that those glycaemic indices slightly reduced in the groups receiving olive oil compared with their control groups, although these reductions were not statistically significant (50). Therefore, it was concluded that olive oil did not have an impact on the glycaemic index of the control meal, which is in harmony with the obtained results in this thesis.

Kim et al (51) studied whether different macronutrients in a meal significantly affect the postprandial glucose response and the validity of calculated GI and GL values for mixed meals. 12 healthy subjects consumed different meals, which included 1) rice, or 2) rice plus olive oil, among others. The postprandial blood glucose levels are depicted in figure 109, where it can be seen that there is a drastic increase until 30 min of digestion, followed by a slightly decrease until the end of the digestion. Those results show that there were no significant differences on the glucose response when the oil was added to the rice, which is in agreement with the results depicted in figure 108.

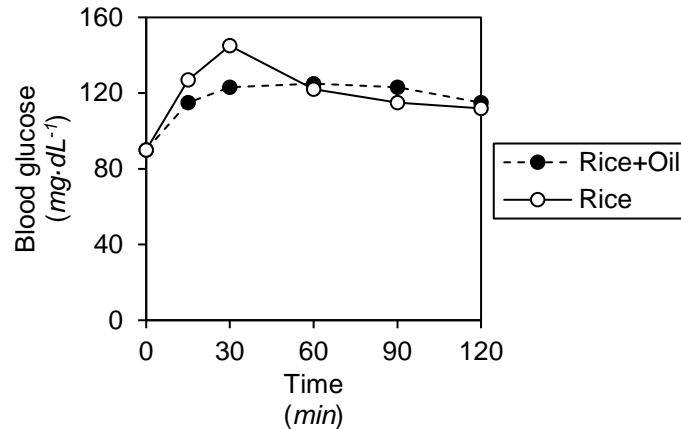


Figure 109. Temporal changes in subjects' postprandial blood glucose responses to the test meals (12 subjects, 2 meals) (51)

8.2. In vitro digestion of starch from rice with butter

Butter was another fat source used to study the impact of fats on the digestion of carbohydrates.

The measured DH (total and glucose) of the meal that is composed of starch from rice and butter is depicted in figure 110. The digestion of this meal was studied with the static digestion method, and the depicted DH are the measured DH after each digestive phase.

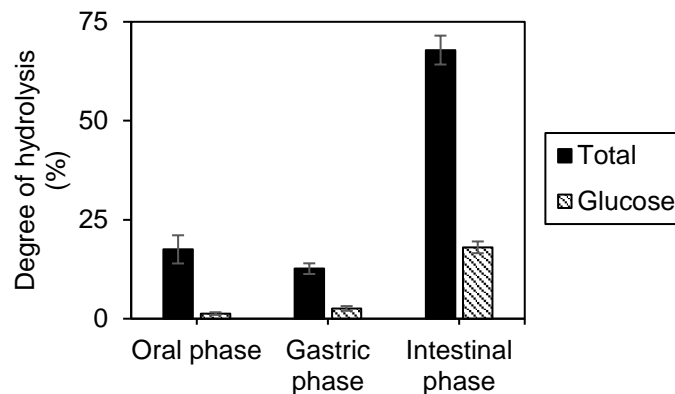


Figure 110. Measured DH (total and glucose) after each digestive phase of the starch from rice and butter

As figure 110 shows, the starch from rice in the presence of the butter was slightly digested during the oral phase reaching a DH of $17.5 \pm 3.6\%$. However, only a small portion of the starch ($1.3 \pm 0.3\%$) was able to be converted into glucose.

During the gastric phase, the total DH did not increase ($12.6 \pm 1.3\%$) which means that the oral α -amylase was deactivated due to the acidic conditions. Nonetheless, the amount of glucose released slightly increased during the gastric phase ($2.6 \pm 0.6\%$). Therefore, some of the enzyme was somewhat protected by the meal and could be slightly active in the acidic conditions.

Figure 110 also shows that the digestion of the starch considerably increased during the intestinal phase. This increase could be attributed to the time needed for the meal to be dissolved and be accessible for the enzymes. And once the meal was completely dissolved, the pancreatic α -amylase could catalyse the hydrolysis of the starch. The percentage of starch converted into glucose also increased during the intestinal phase, reaching a final value of $18.0 \pm 1.5\%$.

The DH measured during the intestinal phase is depicted in figure 111.

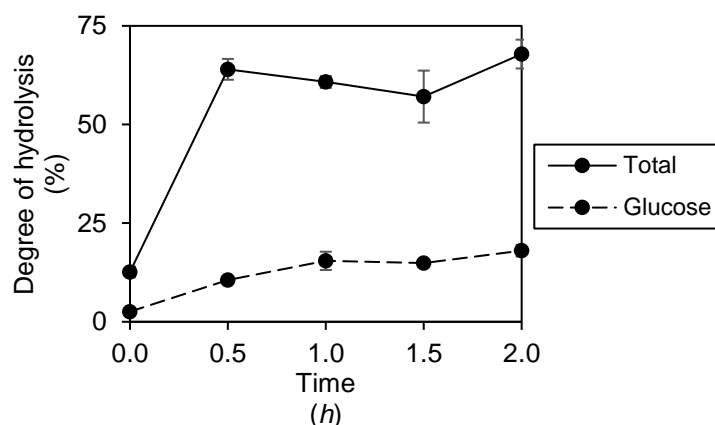


Figure 111. DH (total and glucose) measured during the intestinal phase for the starch from rice and butter

The figure shows that the increase in the hydrolysis occurred mainly during the first 30 min, as it went from 12.6 ± 1.3 % after the gastric phase to 64.0 ± 2.6 % at the 30 min of the intestinal phase. After that, the total DH remained nearly constant, with a final DH of 67.9 ± 3.6 %.

On the other hand, the amount of glucose released during the intestinal phase increased during the first hour (15.4 ± 2.3 %) and then it nearly reached a steady state. The measured percentage of glucose at the end of the digestion was 18.0 ± 1.5 %.

A comparison of the starch from rice and starch from rice with butter tested with in vitro digestion methods will be provided in the next section.

8.2.1. Comparison of in vitro digestion of starch from rice and starch from rice with butter

The effect of the butter on the digestion of the starch from rice can be seen in figure 112. Figure 112a shows that the total DH of the starch from rice was slightly higher than in the presence of the butter, which means that the butter provokes a decrease in the digestion of the starch from rice (α 0.05) during the oral and gastric phases. However, during the intestinal phase the final DH of the starch with the butter reached the DH of the starch from rice (α 0.05).

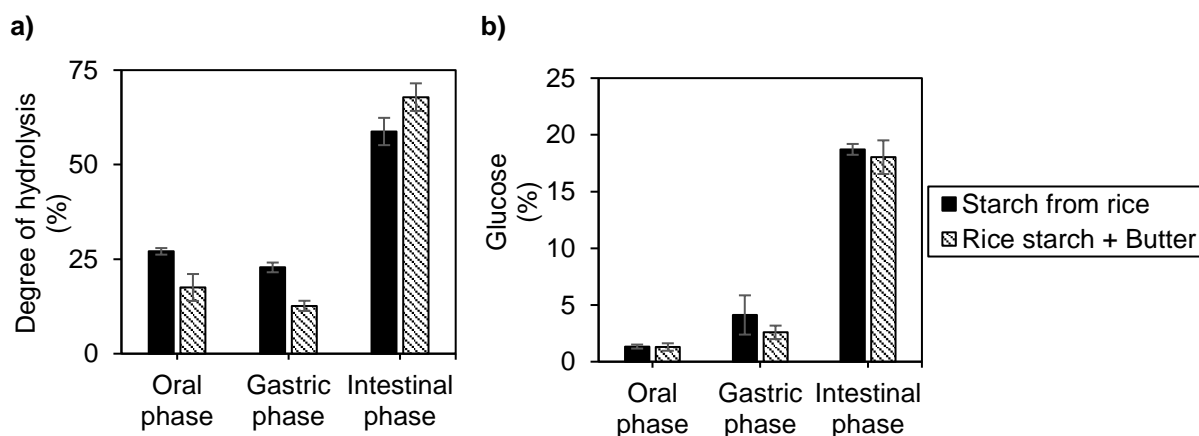


Figure 112. Comparison of the DH measured for the starch from rice with and without butter, a) total, b) glucose

Figure 112b shows the amount of glucose released from the rice starch in the presence or absence of butter. The depicted results demonstrate that the butter does not affect the conversion of the starch into glucose, as no differences in the % glucose could be appreciated.

The comparison of the measured GI with the static method of both meals is depicted in figure 113. And it demonstrates that the butter does not have an impact on the digestion of the starch from rice and consequently there are no differences in the GI.

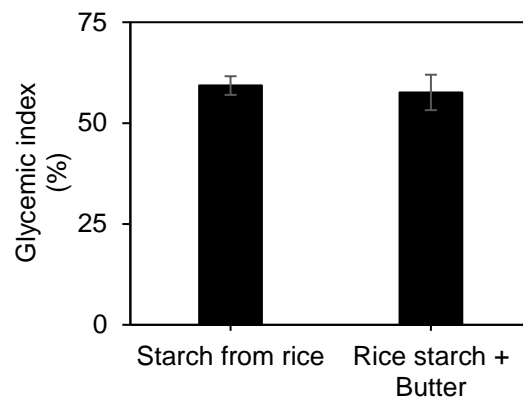


Figure 113. GI comparison between meals (starch from rice vs starch from rice with butter)

Vidrasco et al (52) studied the impact of butter on the digestion of rice and their results led to the conclusion that the combination of boiled rice with butter significantly reduces the GI of rice. However, it was also seen that the addition of butter at the stage of serving was preferable to reduce the GI of the preparation than its incorporation during the boiling process. The explanation could be that butter added at the stage of rice boiling hydrolyses in the heat treatment process could cause faster digestion and absorption of nutrients than in the case of butter added at the stage of serving. Their results are not in agreement with the obtained in this thesis, which could be due to the differences in the rice starch origin or in the meal preparation.

In the study of Sun et al (53), twenty healthy Chinese men were recruited and were asked to ingest different kind of meals (rice or rice cooked with butter, among others). Fingerprick capillary and venous blood samples were collected every 15 min during the first hour and every 30 min during the next 3 hours. The glucose levels were measured, and the results revealed that the different types of dietary fat did not differentially affect glucose and insulin responses to meal ingestion. Which is in line with the reported results in this thesis.

8.3. In vitro digestion of starch from potato with olive oil

The effect of olive oil on the digestion of carbohydrates was also studied with the starch from potato. The measured DH after each digestive phase of the static digestion method is depicted in figure 114.

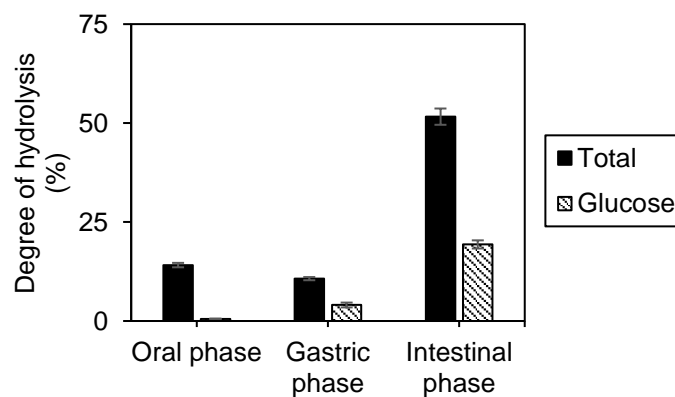


Figure 114. Measured DH (total and glucose) after each digestive phase of the starch from potato and olive oil

The figure shows that the meal was slightly digested during the oral phase, reaching a total DH of 14.1 ± 0.6 %. Although the starch from potato started to be digested with the oral secretions, only a

small amount of the starch was hydrolysed and converted into glucose (0.6 ± 0.1 %). This could be because the meal needed some time to be dissolved with the secretions, and it only have time to start the digestion of the starch but not to be converted into glucose.

According to the depicted results, the amount of glucose released from the starch slightly increased during the gastric phase, reaching a value of 4.0 ± 0.6 %. Therefore, the percentage of glucose only increased around 3 %, which means that only a small amount of α -amylase was still active. This was confirmed with the total DH measured after the gastric phase, which is not different from the total DH measured after the oral phase.

The obtained DH after the intestinal phase shows that the total DH and glucose released increased during this digestive phase. Both, the total DH and percentage of glucose increased almost 5-folds during the intestinal phase reaching values of 51.6 ± 2.1 % and 19.3 ± 1.0 %, respectively.

The DH (total and glucose) measured during the intestinal phase are depicted in figure 115, where it can be seen that even though both, the total DH and glucose, increased around 5-folds during the intestinal phase, that increase occurred differently. While the starch was slowly converted into glucose during the last phase of the digestion method. The total DH increased mainly during the first 30 min of the intestinal phase, increasing around 4-folds, compared with the total DH after the gastric phase. After that, the digestion of the starch from potato in the presence of olive oil slowed down and it only increase from 41.4 ± 1.2 %, at 30 min of intestinal phase to 51.6 ± 2.1 % at the end of the digestion.

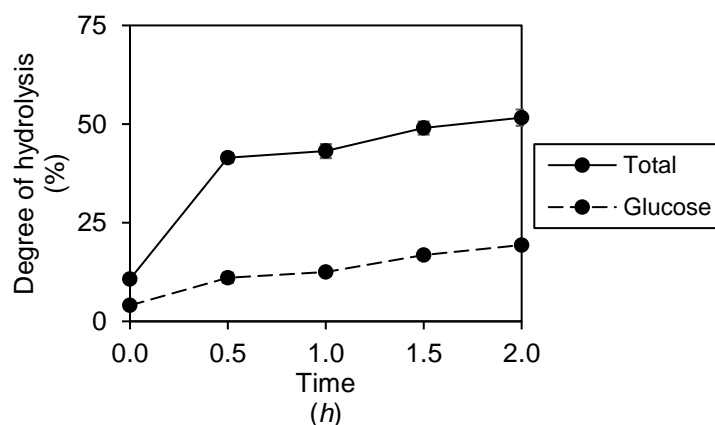


Figure 115. DH (total and glucose) measured during the intestinal phase for the starch from potato and olive oil

A comparison of the starch from potato and starch from potato with olive oil tested with in vitro digestion methods will be provided in the next section.

8.3.1. Comparison of in vitro digestion of starch from potato and starch from potato with olive oil

The total DH and glucose (%) measured for the starch from potato and for the mixture of potato starch and olive oil are depicted in figure 116. According to the depicted results in figure 116a, even though it seems that the olive oil favours the digestion of the potato starch, the obtained DH with both meals is not different (α 0.05). On the other hand, the amount of glucose released from the potato starch in the presence or absence of olive oil is depicted in figure 116b. The obtained results show that the olive oil does not have any effect on the digestion of the starch from potato.

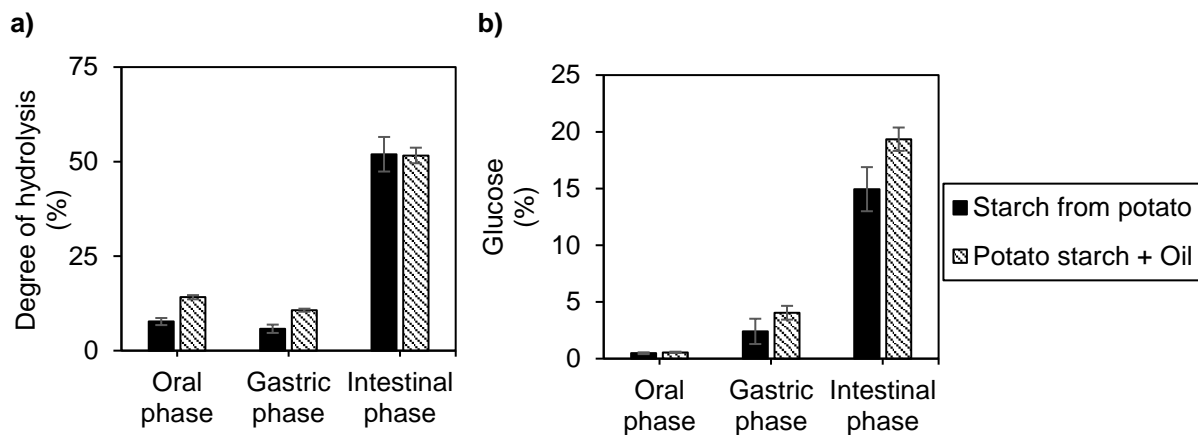


Figure 116. Comparison of the DH measured for the starch from potato with and without olive oil, a) total, b) glucose

The no-effect that is depicted in figure 116, can also be seen in figure 117. Where the GI calculated for both meals are depicted.

Therefore, the conclusion that could be extracted from these results is that the addition of olive oil to the starch from potato does not have any influence on the digestion of this kind of starch.

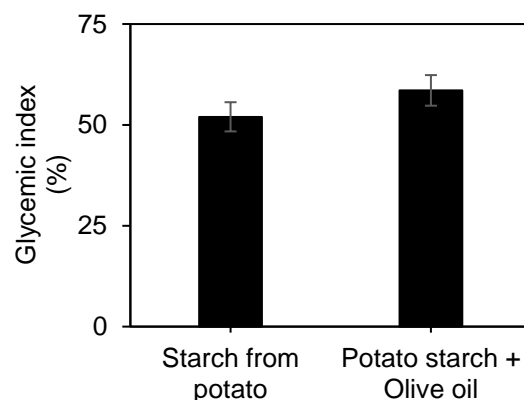


Figure 117. GI comparison between meals (starch from potato vs starch from potato with olive oil)

The impact of fats on GI values of potato was assessed by Muldoon A. (54), who could see that the addition of fat causes a slight increase in the GI compared to the control (potato). However, this value was not significantly different to potato. This is also seen in figure 117, where no differences between the measured GI were obtained.

This is also in agreement with the results obtained for the Leeman et al (55) group. Fourteen healthy subjects participated in the study, where they were requested to ingest different kinds of meals. Two of the meals were composed of boiled potatoes served either with or without the addition of sunflower oil. Finger-prick capillary blood samples were taken and analysed to measure the postprandial blood glucose levels. Their results are depicted in figure 118, where it can be seen an increase on the blood glucose levels just after the meal ingestion, and then there is a soft decrease until the end of the digestion. They concluded that there were no significant differences between both curves, therefore that the oil did not affect the glucose release.

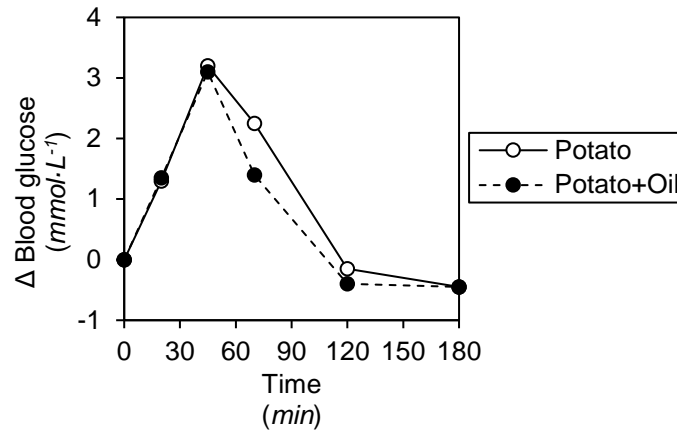


Figure 118. Mean blood glucose responses in healthy subjects

8.4. In vitro digestion of starch from potato with butter

The effect of butter on the digestion of the potato starch was also studied. The measured DH after the oral, gastric and intestinal phases are depicted in figure 119.

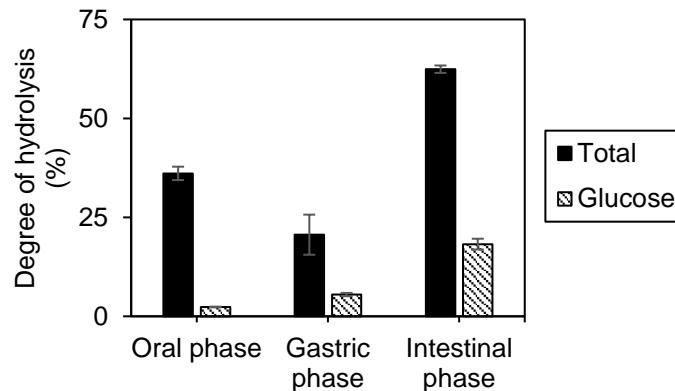


Figure 119. Measured DH (total and glucose) after each digestive phase of the starch from potato and butter

The figure shows that the starch was able to be highly digested during the oral phase, as after the incubation with the oral secretions 36.1 ± 1.7 % of the starch was already hydrolysed. According to the obtained results, during the gastric phase the starch was not further digested, which may be because the salivary α-amylase was deactivated due to the low pH of the gastric secretions. Finally, during the intestinal phase the digestion of the potato starch, mixed with butter, continued obtaining a final DH of 62.4 ± 0.9 %.

On the other hand, the amount of glucose released from the potato starch, mixed with butter, was measured. The behaviour of the glucose released was different compared with the total degree of hydrolysis of the starch. During the oral phase only a small part of the starch could be completely hydrolysed and converted into glucose (2.4 ± 0.1 %). Then, during the gastric phase, the percentage of glucose increased around 2.5-folds. Therefore, unlike it was thought with the total DH, it seems that the salivary α-amylase was still slightly active during the gastric phase. Finally, when the chyme was mixed with the intestinal secretions the amount of glucose released increased, showing a final DH (glucose) of 18.2 ± 1.4 %.

The digestion of the starch from potato when is mixed with butter it was studied during the intestinal phase. The measured glucose and total DH are depicted in figure 120.

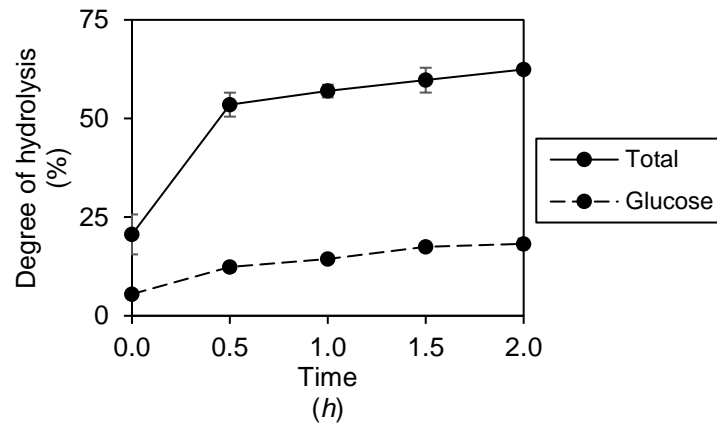


Figure 120. DH (total and glucose) measured during the intestinal phase for the starch from potato and butter

As can be seen in the figure the meal was highly digested during the first 30 min as it increased from 20.6 ± 5.1 % to 53.5 ± 3.0 %. After that, the digestion of the potato starch slowed down and slightly increased with the time of digestion. The curve that belongs to the glucose released shows that during the first 30 min, the amount of glucose increased at a higher rate compared with the rest of the intestinal phase.

In general, the total DH increased a lot when the meal was mixed with the intestinal secretions and then it reached a steady state. The same behaviour was seen for the percentage of glucose but at a lower extent, showing a gradual release of glucose with the time until the end of the digestion. The glucose curve depicted in figure 120, was used to calculate the glycaemic index of the meal that contains starch from potato and butter. The obtained GI with the static digestion method was 63.1 ± 2.7 %.

A comparison of the starch from potato and starch from potato with butter tested with in vitro digestion methods will be provided in the next section.

8.4.1. Comparison of in vitro digestion of starch from potato and starch from potato with butter

The measured total DH and glucose released from the potato starch when is mixed with butter and when is ingested alone are compared in figure 121 to check if the addition of the butter to the meal affected the digestion of the potato starch.

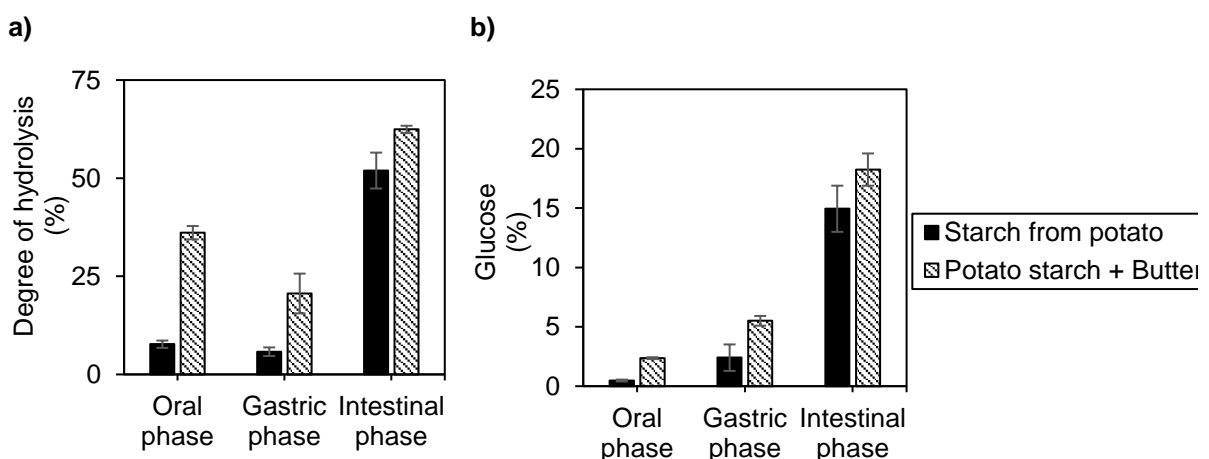


Figure 121. Comparison of the DH measured for the starch from potato with and without butter, a) total, b) glucose

Figure 121 shows that the addition of butter to the meal triggers an increase in the digestion of the starch from potato. This increase could be provoked due to the ease of the meal disintegration. The butter could difficult the cohesiveness of the potato starch when the meal was prepared. For that reason, the meal that contained the starch from potato and butter could be solubilised easier and faster than

potato starch alone. The solubilisation of both meals is depicted in figure 122, where it can be seen that the main differences in the meal solubilisation were found during the oral and gastric phases. This is in concordance with the depicted DH (total and glucose) in figure 121, where the main differences are also found after the oral and gastric phases. On the other hand, in both figures, no differences can be seen after the intestinal phase. This confirms that the digestion of the starch was mainly influenced by the rate of disintegration and solubilisation.

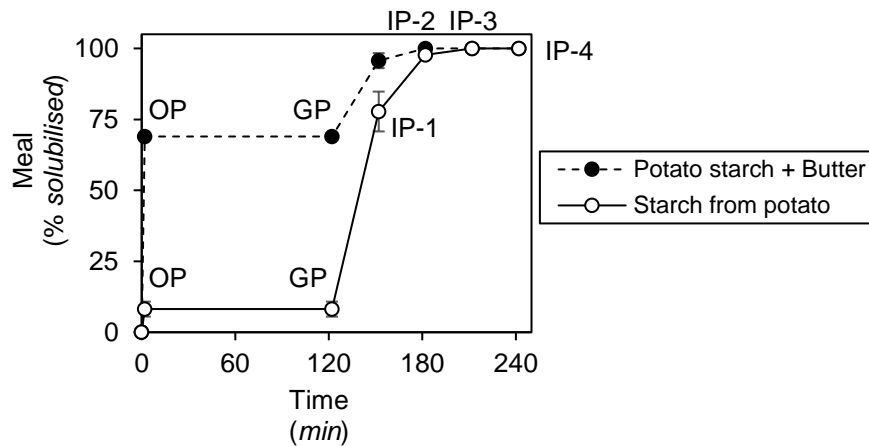


Figure 122. Meal solubilized during the static digestion method (OP: oral phase; GP: gastric phase; IP-1, IP-2, IP-3, IP-4: intestinal phase samples)

The measured glycaemic index for both meals is depicted in figure 123. Where it can be seen that, despite the differences found on the DH (total), the addition of the butter to the starch from potato does not affect the GI of the meal.

This can be explained by the fact that the GI was calculated with the AUC of the curve during the intestinal phase, and there were no differences in the digestion of the meal during the intestinal phase.

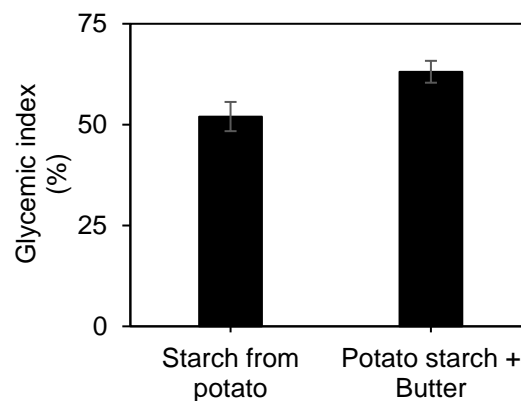


Figure 123. GI comparison between meals (starch from potato vs starch from potato with butter)

As it was seen in the previous section, the addition of butter did not have an impact on the GI of the potato starch, which was also seen in the work of Muldoon A. (54).

MacIntosh et al (56) studied the effect of different types of fat on glycaemic index of the mashed potato. Ten healthy men received portions of mashed potato with butter, sunola oil or sunflower oil. Capillary blood samples were taken, and GI calculated. The obtained GI values ranged from 68 ± 8 to 74 ± 10 , and fat type did not affect the GI. However previous studies have produced conflicting findings, Gatti et al (57) reported a reduction in the postprandial glucose responses to white bread after the addition of olive oil and corn oil but not butter.

In contrast, Pederson et al (58) found no differences in glucose responses to meals containing rapeseed oil, sunflower oil or palm oil. The contrast in findings among studies may be related to methodology, including the use of venous versus capillary blood, the timing of blood samples and the type and amount of fats and carbohydrates studied.

9. Impact of food matrix on starch digestion

9.1. In vitro digestion of starch from rice with egg whites and olive oil

9.1.1. Static in vitro digestion of starch from rice with egg whites and olive oil

The digestion of the starch from rice, when it was mixed with egg whites and olive oil, was studied with the static digestion method, and the measured results are depicted in figure 124.

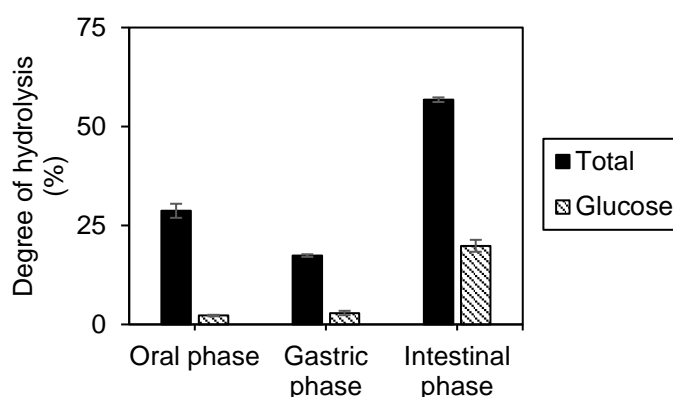


Figure 124. Measured DH (total and glucose) after each digestive phase of the starch from rice, egg whites and olive oil

As can be seen in figure 124, more than 25 % of the meal was already digested after the oral phase. Then, it seems that the total DH after the gastric phase is slightly lower than after the oral phase, but this difference could be due to experimental errors. But most probably the meal was not further digested during the gastric phase because the α -amylase was deactivated due to the acidic conditions of the gastric phase. Then, the meal continued to digest during the intestinal phase, obtaining a final DH of 56.8 ± 0.6 %.

On the other hand, almost no glucose was released during the oral and gastric phases. The percentage of glucose after the gastric phase was equal to the % glucose after the oral, which corroborates that the meal was not further digested during the gastric phase. Finally, during the intestinal phase the % glucose increased from 2.9 ± 0.6 % to 19.9 ± 1.5 %.

The digestion of the meal was also studied during the intestinal phase and the measured DH (total and glucose) are depicted in figure 125, where it can be seen that the glucose was continuously released from the starch during the intestinal phase. While the total DH suffered a high increase during the first 30 min of the intestinal phase and then the digestion of the meal slowed down until the end of the digestion.

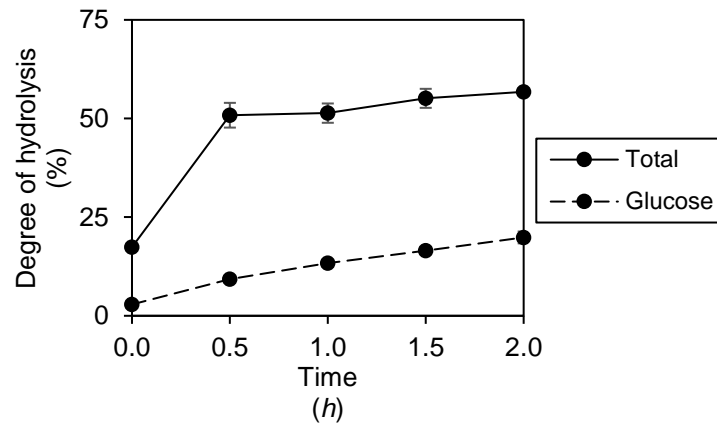


Figure 125. Measured DH (total and glucose) during the intestinal phase of the starch from rice, egg whites and olive oil

The glucose curve depicted in figure 125, was used to calculate the GI of this meal, and the obtained GI was 65.0 ± 4.0 %.

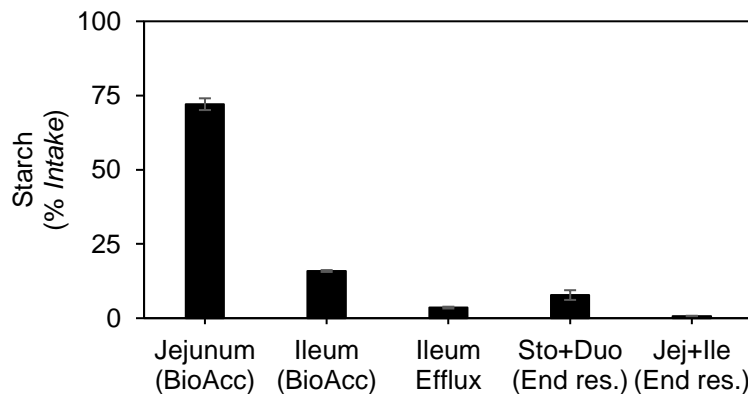
9.1.2. Dynamic in vitro digestion of starch from rice with egg whites and olive oil

The digestion of the meal (starch) that contains starch from rice, egg whites and olive oil was also studied with the dynamic digestion method.

The distribution of the meal throughout the system is depicted in figure 126. In figure 126a it can be seen that almost all of the meal (72.1 ± 2.0 %) was found in the bioaccessible fraction of the jejunum. The rest of the meal was found in the bioaccessible fraction of the ileum, ileum efflux and in the lumen of the stomach and duodenum. Almost no meal was found in the lumen of the jejunum and ileum at the end of the digestion.

Figure 126b shows the amount of meal present in the bioaccessible fraction, jejunum and ileum, during digestion. It can be seen that almost no meal reached the bioaccessible fraction during the first 30 min. Then the meal started to be disintegrated and therefore a bigger amount of meal reached the bioaccessible fraction during the next hour. Finally, the disintegration of the meal was even at a higher rate and for that reason the amount of meal found in the bioaccessible fraction increased until it reached a maximum at the 3rd hour of digestion. During the last 2 h of digestion, the amount of starch present in the bioaccessible fraction decreased because almost all the meal already left the stomach and the meal was removed from the system.

a)



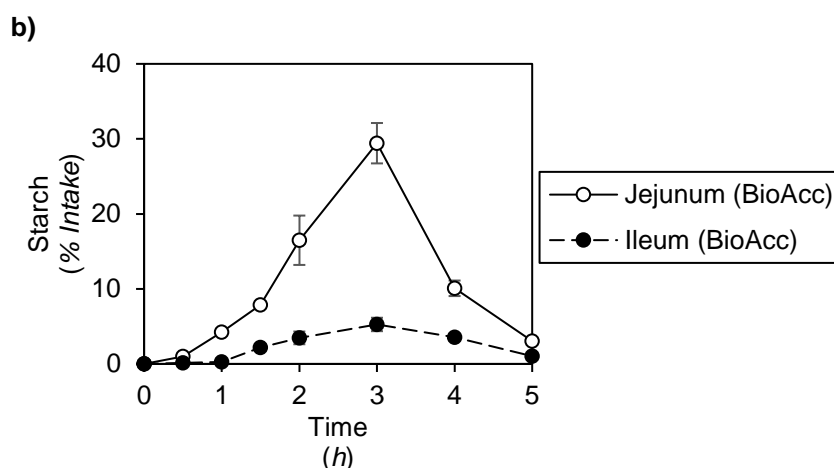


Figure 126. Meal distribution throughout the dynamic system (TIM-1), a) all the compartments after the digestion, b) bioaccessible fraction during the digestion

The measured DH (total and glucose) of the meal with the dynamic digestion method is depicted in figure 127, where it can be seen that there is an increase in the release of the digestive products during the first 1.5 h. At 1.5 h of digestion the total DH was 41.4 ± 3.1 %, while the amount of glucose released at this time point was 13.5 ± 0.5 %.

After that and until the end of the digestion the DH kept more or less constant, obtaining a final DH of 44.5 ± 3.4 % and a total amount of glucose released from the starch of 12.4 ± 0.2 %. therefore, the hydrolysis of the starch in the presence of egg whites and olive oil slowed down and almost stopped after 1.5 h of digestion.

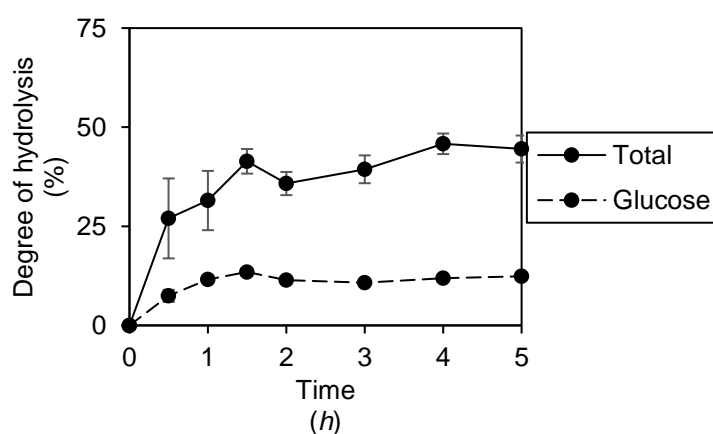


Figure 127. DH (total and glucose) of the starch measured in the bioaccessible fraction (jejunum and ileum)

The glycaemic index of this meal was also measured with the dynamic digestion method, which was calculated with the glucose curve depicted in figure 127. And the obtained GI was 56.6 ± 1.9 %.

A comparison of static and dynamic digestion of starch from rice with egg whites and olive oil is provided in the following section.

9.1.3. In vitro digestion method comparison for the digestion of starch from rice with egg whites and olive oil

The digestion of the starch from rice mixed with olive oil and egg whites was studied with both methods, static and dynamic digestion methods. The comparison of the measured DH in both methods is depicted in figure 128.

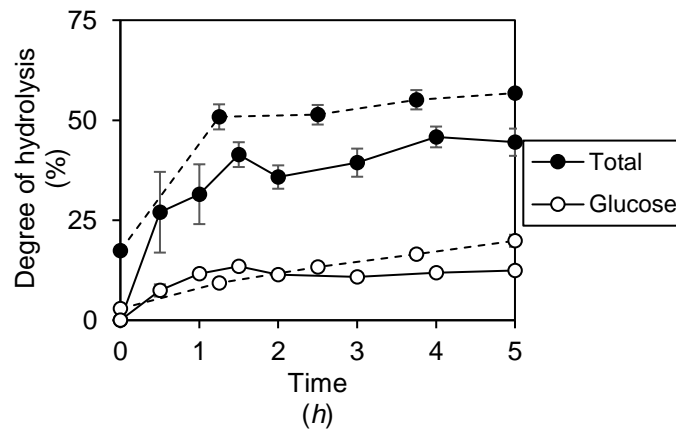


Figure 128. Measured DH (total, glucose) of starch from rice mixed with olive oil and egg whites with the static (dashed line) and dynamic (solid line) digestion methods

Figure 128 shows the total degree of hydrolysis and the glucose release in the small intestine during digestion. The shape of the glucose curve was slightly different for both methods, the glucose levels obtained with the static method constantly increased during the intestinal phase going from $2.9 \pm 0.6 \%$ at the beginning of the digestive phase to $19.9 \pm 1.5 \%$ at the end of the digestion. On the other hand, the glucose levels measured in the dynamic system (TIM-1) had an increase during the first 1.5 h and then it kept constant. Therefore, the glucose release was continuous with the static method, while with the dynamic method it happened mainly at the beginning of the digestion.

The total DH curves measured with both methods have a similar shape. However, the measured DH with the dynamic method was slightly lower compared with the DH measured with the static digestion method ($\alpha 0.05$).

The measured GI with both in vitro digestion methods is depicted in figure 129. The figure shows that the glucose levels obtained with the dynamic digestion method are equal to the GI measured with the static digestion method ($\alpha 0.05$).

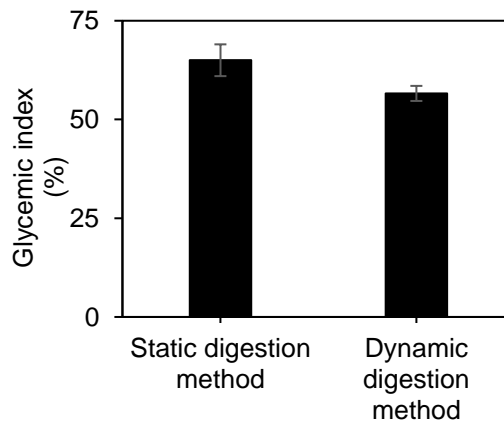


Figure 129. GI of the starch from rice mixed with egg whites and olive oil measured with the static and dynamic digestion methods

A comparison of the starch from rice and starch from rice with egg whites and olive oil tested with in vitro digestion methods will be provided in the next section.

9.1.4. Comparison of in vitro digestion of starch from rice with egg whites and olive oil

To study the effect of the meal matrix (olive oil and egg whites) the measured DH (total and glucose) of the meal that contains only starch from rice and the meal where the starch was mixed with the olive oil and egg whites are depicted in figure 130.

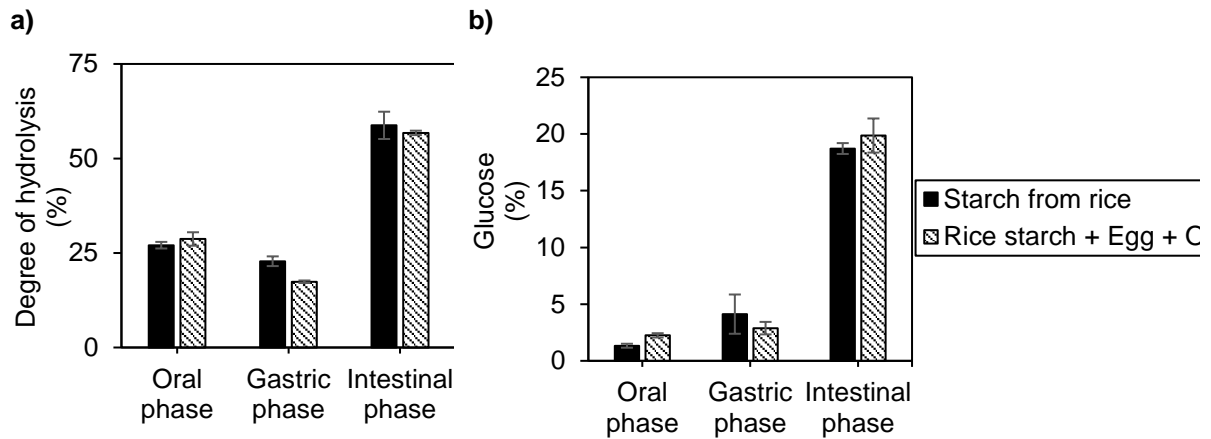


Figure 130. Comparison of the DH measured for the starch from rice with and without egg whites and olive oil, a) total, b) glucose

Figure 130a shows the total DH obtain for both meals, and it demonstrated that the addition of the egg whites and olive oil does not affect the digestion of the starch from rice. On the other hand, figure 130b also demonstrated the no effect of the matrix on the rice starch digestion.

The matrix effect was also checked on the measured GI, and the comparison of the GI obtained for both meals is depicted in figure 131, where it can be seen that there are no differences between the GIs. Thus, the conclusion that can be extracted could be that the addition of the egg whites and olive oil to the starch from rice does not affect the glucose release from the starch from rice.

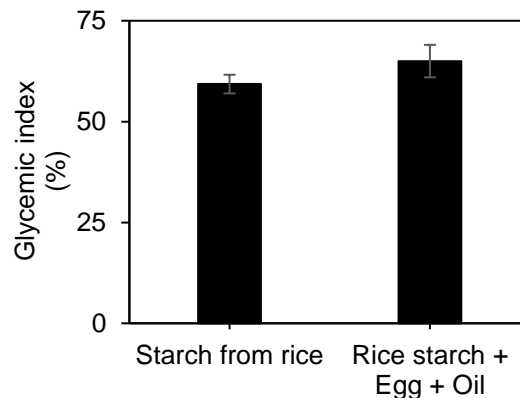


Figure 131. GI measured of the starch from rice compared with the GI measured of the starch from rice mixed with egg whites and olive oil

Kim et al (51) also studied the effect of egg, oil and bean sprouts to the digestibility of rice. 12 healthy subjects consumed both meals (only rice and rice combined with egg, oil, bean sprouts) and the postprandial blood glucose levels determined. Figure 132 shows that the blood glucose levels after the ingestion of the complex meal were significantly lower at the 30, 60 and 120 min time points, compared with the blood glucose levels after the ingestion of rice. Which is in disagreement with the depicted results in figure 131, where no differences were found between the GI obtained for both meals. These differences could be triggered by the differences on the methodology or because the complex meal in the Kim et al work also contained bean sprouts.

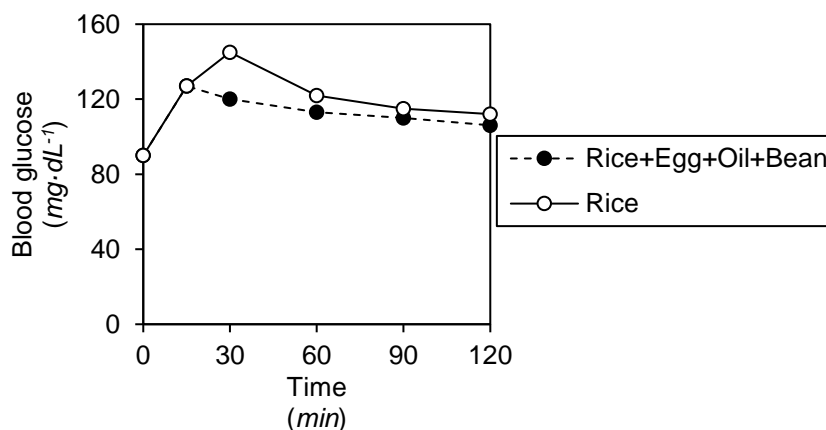


Figure 132. Temporal changes in subjects' postprandial blood glucose responses to the test meals

9.2. In vitro digestion of starch from potato with egg whites and olive oil

The digestion of the meal composed of starch from potato, egg whites and olive oil, was studied with the static digestion method. And the obtained DH (total and glucose) after each digestive phase is depicted in figure 133.

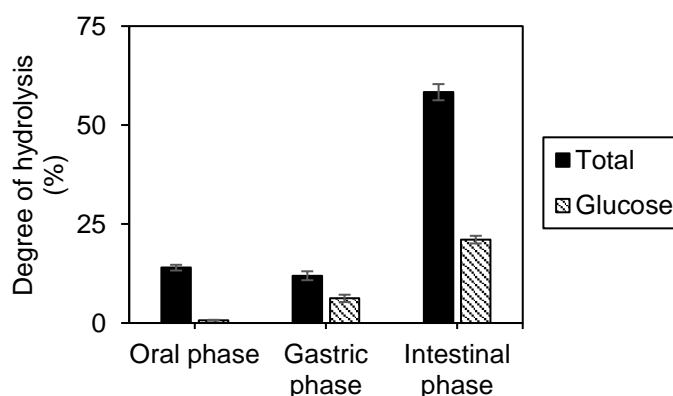


Figure 133. DH (total and glucose) measured after each digestive phase for the meal that contains potato starch, egg whites and olive oil

Figure 133 shows that 14.0 ± 0.7 % of the starch was hydrolysed during the oral phase, but only 0.7 ± 0.1 % of the starch was converted into glucose. After that, the total DH measured after the gastric phase was not different from the DH measured after the oral phase. But the amount of glucose released after the gastric phase was ~9-folds higher compared with the percentage of glucose released after the oral phase. Therefore, it seems that during the gastric phase the salivary α -amylase was slightly deactivated due to the acidic conditions.

The digestion of the meal was followed during the intestinal phase, and the measured DH (total and glucose) is depicted in figure 134. The total DH highly increased during the first 30 min of the intestinal phase, as it went from 11.9 ± 1.1 % at time 0 to 41.5 ± 3.9 % after 30 min. After that, the digestion slowed down and the total DH only slightly increased, obtaining a final DH of 58.3 ± 2.0 %.

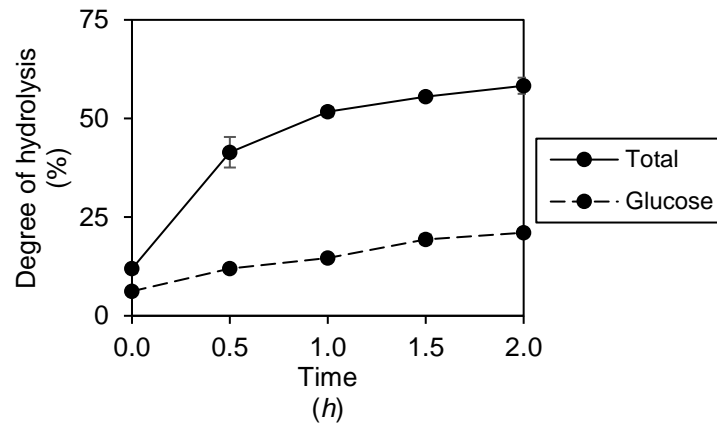


Figure 134. DH (total and glucose) measured during the intestinal phase of the meal that contains potato starch, egg whites and olive oil

On the other hand, the glucose was constantly released during the intestinal phase and increased from 6.2 ± 0.9 % measured after the gastric phase to 21.1 ± 1.0 % at the end of the digestion.

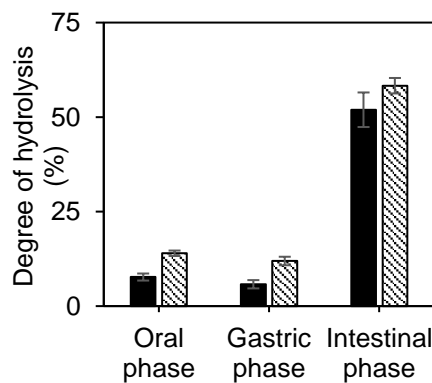
The glycaemic index was obtained with the AUC calculated from the glucose curve depicted in figure 134, and the measured GI was 76.7 ± 3.9 %.

A comparison of the starch from potato and starch from potato with egg whites and olive oil tested with in vitro digestion methods will be provided in the next section.

9.2.1. Comparison of in vitro digestion of starch from potato and starch from potato with egg whites and olive oil

The digestion of the starch from potato mixed with egg whites and olive oil was compared with the digestion of the starch from potato, and the depicted results are shown in figure 135. The total DH is depicted in figure 135a, while the amount of glucose released is depicted in figure 135b. Figure 135a shows that the starch from potato suffered higher hydrolysis in the presence of egg whites and olive oil (α 0.05). It can also be seen in figure 135b that a higher amount of glucose was released from the starch in the presence of protein and fat sources (α 0.05).

a)



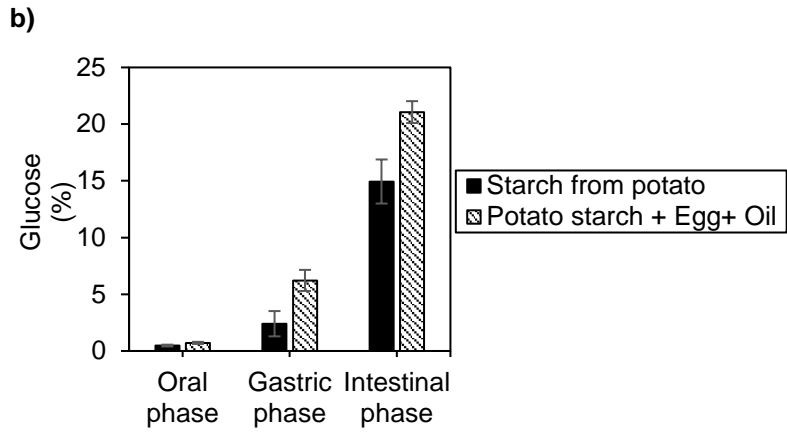


Figure 135. Comparison of the DH measured for the starch from potato in the absence and presence of egg whites and olive oil, a) total DH, b) glucose

The effect of the matrix on the digestion of the starch from potato is also reflected in the measured GI, which is depicted in figure 136. This increase in the digestion of the starch in the presence of protein and fat sources may be due to the viscosity of the meal. Therefore, when the egg whites and olive oil were added to the potato starch the viscosity of the meal was lower compared with the viscosity of the potato starch. Those differences in the viscosities of the meal provoked differences in its solubility. For that reason, the enzymes could reach the complex meal faster and therefore it could be further digested than the starch alone.

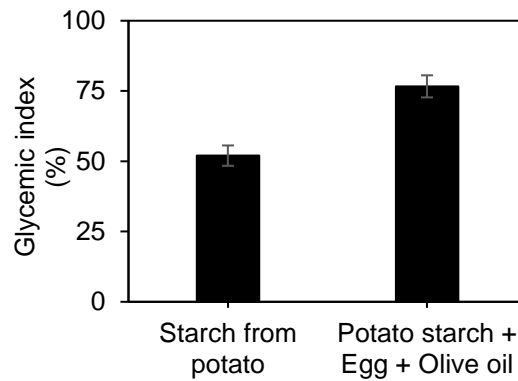


Figure 136. GI measured for the potato starch and potato starch mixed with egg whites and olive oil

9.3. In vitro digestion of starch from rice with egg whites and butter

The digestion of the starch from rice mixed with egg whites and butter was studied with the static digestion method. The obtained DH (total and glucose) is depicted in figure 137.

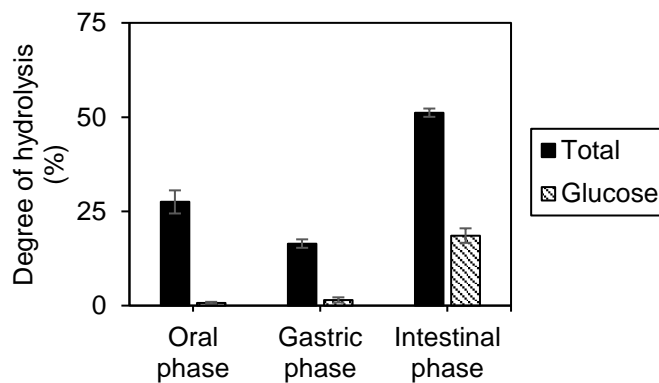


Figure 137. DH (total, glucose) measured after each digestive phase for starch from rice mixed with egg whites and butter

Figure 137 shows that during the oral phase the starch from rice started to be digested in the presence of egg whites and butter, obtaining a total DH of 27.5 ± 3.1 % at the end of the oral phase. However, only 0.7 ± 0.3 % of the starch was converted into glucose.

When the oral bolus was mixed with the gastric secretions, the salivary α -amylase was deactivated. For that reason, the DH (total, glucose) measured after the gastric phase did not increase, compared with the DH measured after the oral phase. In fact, the measured total DH “decreased” a little bit, but this difference could be triggered by experimental errors during the *in vitro* digestion method or the analytical determinations.

Finally, during the intestinal phase, the pancreatic α -amylase reactivated the digestion of the meal obtaining a total DH of 51.2 ± 1.1 % at the end of the digestion. And the amount of starch that was converted into glucose was 18.6 ± 1.9 % after the intestinal phase.

The digestion of this meal was studied not only after each digestive phase but also during the intestinal phase, and the obtained results are depicted in figure 138, where it can be seen in this figure that the glucose was continuously released from the starch during the intestinal phase. On the other hand, the total DH increased mainly during the first 30 min, increasing from 16.5 ± 1.1 % to 42.9 ± 5.6 %. After that, the digestion slowed down until the end of the digestion, reaching the final DH of 51.2 ± 1.1 %.

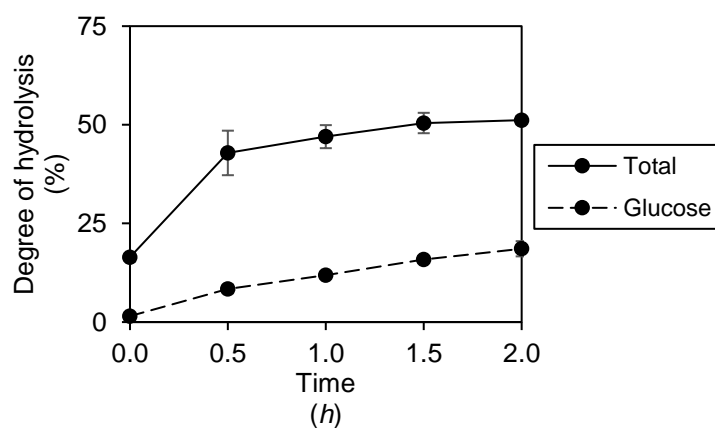


Figure 138. DH (total, glucose) measured after each digestive phase for starch from rice mixed with egg whites and butter

The glucose curve depicted in figure 138 was used to calculate the GI of the meal that contains starch from rice, egg whites from chicken and butter, and the obtained GI was 59.4 ± 4.2 %.

A comparison of the starch from rice and starch from rice with egg whites and butter tested with *in vitro* digestion methods will be provided in the next section.

9.3.1. Comparison of *in vitro* digestion of starch from rice and starch from rice with egg whites and butter

To study the effect of the egg whites and butter on the digestion of the starch from rice, the measured DH (total and glucose) for this meal was compared with the DH (total and glucose) obtained for the meal that only contains starch from rice. The comparison is shown in figure 139 (a) total DH, (b) glucose).

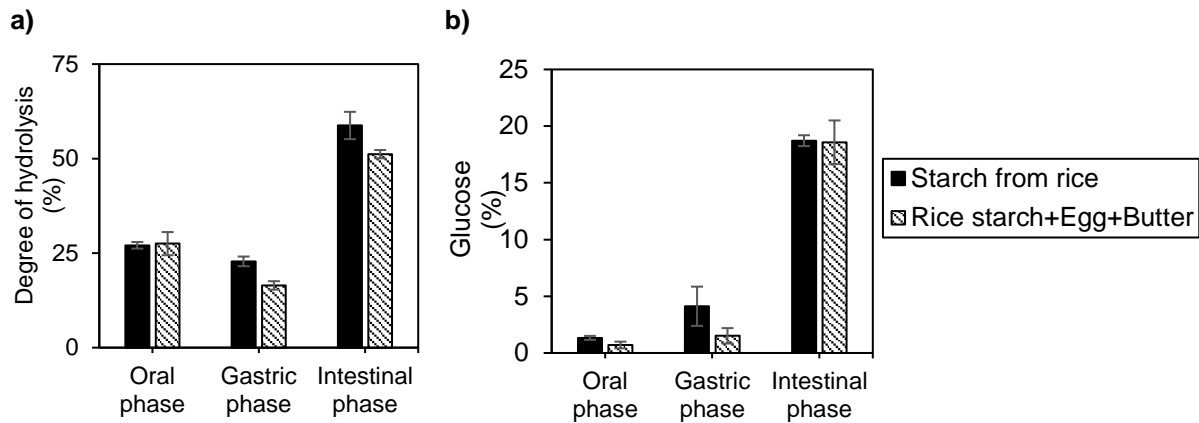


Figure 139. Comparison of the measured DH of the starch from rice in the absence and presence of egg whites and butter

The results depicted in figure 139 demonstrates that the egg whites and butter did not affect the digestion of the starch from rice, as no differences were found neither in the total DH nor in the glucose released. The no-effect of the matrix on the digestion of the starch from rice was also seen on the calculated GI for both meals, and its comparison is shown in figure 140.

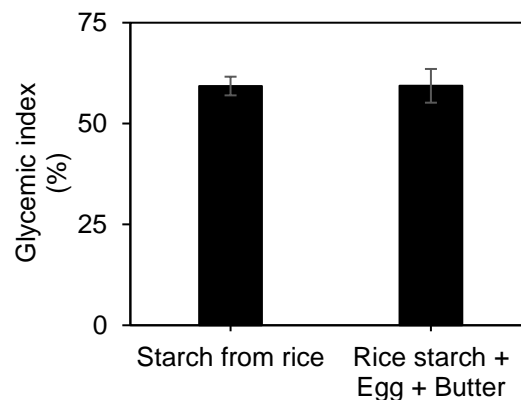


Figure 140. Comparison of the GI obtained for starch from rice and starch from rice mixed with egg whites and butter

9.4. In vitro digestion of starch from potato with egg whites and butter

The digestion of the starch from potato in the presence of egg whites and butter was studied with the static digestion method and the obtained results are depicted in figures 141 and 142.

The measured DH (total and glucose) after each digestive phase is depicted in figure 141. It can be seen that only a small part of the starch could be digested during the oral phase (13.4 ± 0.8 %), and that the amount of glucose released from the starch was only 0.8 ± 0.1 %.

During the gastric phase the salivary α -amylase was slightly active as the total DH did not increase but the amount of starch that was converted into glucose increased from 0.8 ± 0.1 % to 6.4 ± 0.4 %. Finally, when the gastric chyme was mixed with the intestinal secretions the total DH increased 5-folds, while the amount of glucose released was 3.5-folds.

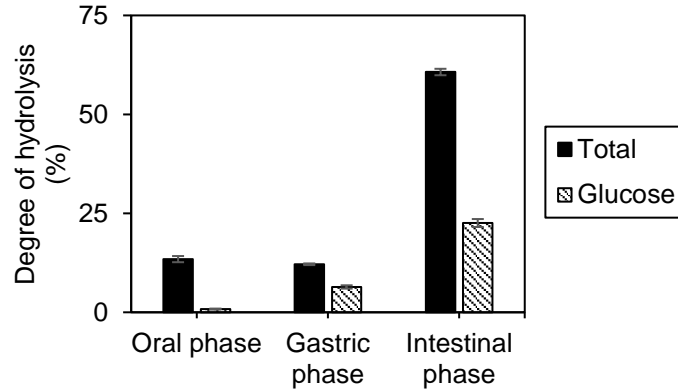


Figure 141. Measured DH after each digestive phase of the starch from potato mixed with egg whites and butter

The degree of hydrolysis was measured during the intestinal phase, and the obtained results are depicted in figure 142. Where it can be seen that the digestion of the meal was faster at the beginning of the meal and then it slowed down until the end of the digestion. The measured DH increased with the time of digestion going from 12.1 ± 0.2 % (total) and 6.4 ± 0.4 % (glucose) to 60.7 ± 0.8 % (total) and 22.6 ± 1.0 % (glucose).

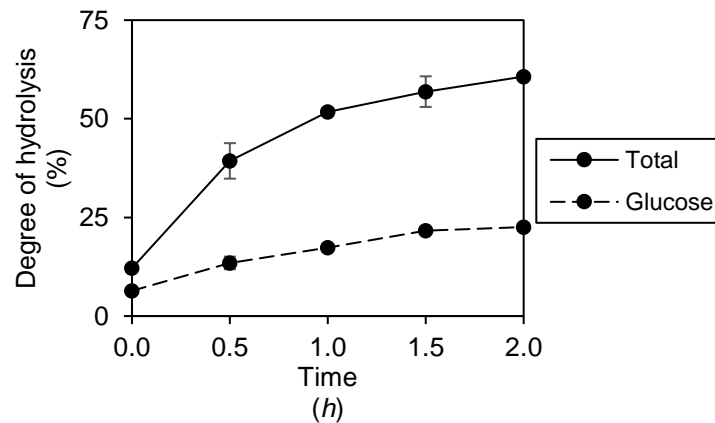


Figure 142. Measured DH during the intestinal phase of the starch from potato mixed with egg whites and butter

The measured GI for the meal that contains starch from potato, egg whites and butter was 86.1 ± 3.5 %.

A comparison of the starch from potato and starch from potato with egg whites and butter tested with in vitro digestion methods will be provided in the next section.

9.4.1. Comparison of in vitro digestion of starch from potato and starch from potato with egg whites and butter

The previous results are compared in figure 143 with the DH (total and glucose) measured for the starch from potato. The obtained results demonstrate that the addition of the egg whites and butter facilitates the digestion of the potato starch. This may be due to the ease of the meal solubilization in the digestive secretions (α 0.05).

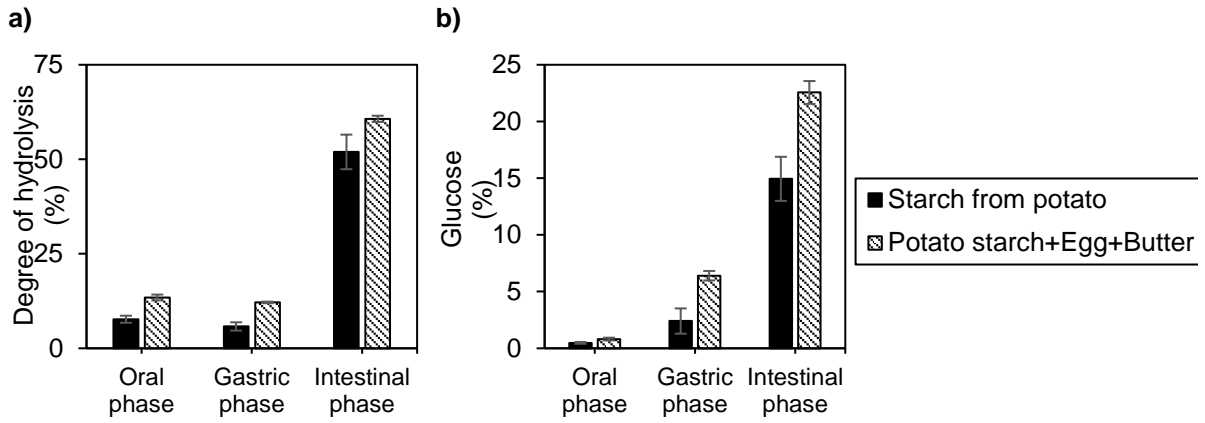


Figure 143. Comparison of the measured DH of the starch from potato in the absence and presence of egg whites and butter

The matrix effect seen in figure 143 is also seen in figure 144, where the measured GI for the starch from potato is lower compared with the GI measured for the meal that contains potato starch, egg whites and butter.

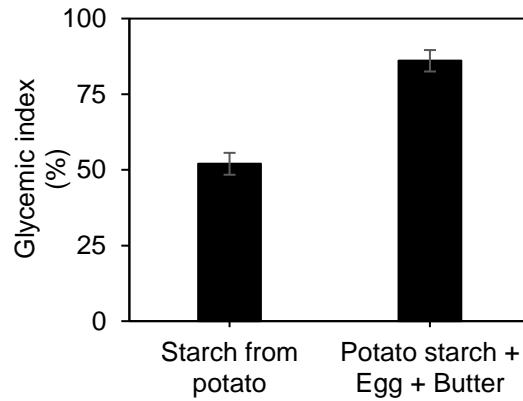


Figure 144. Measured GI of the starch from potato in the absence and presence of egg whites and butter

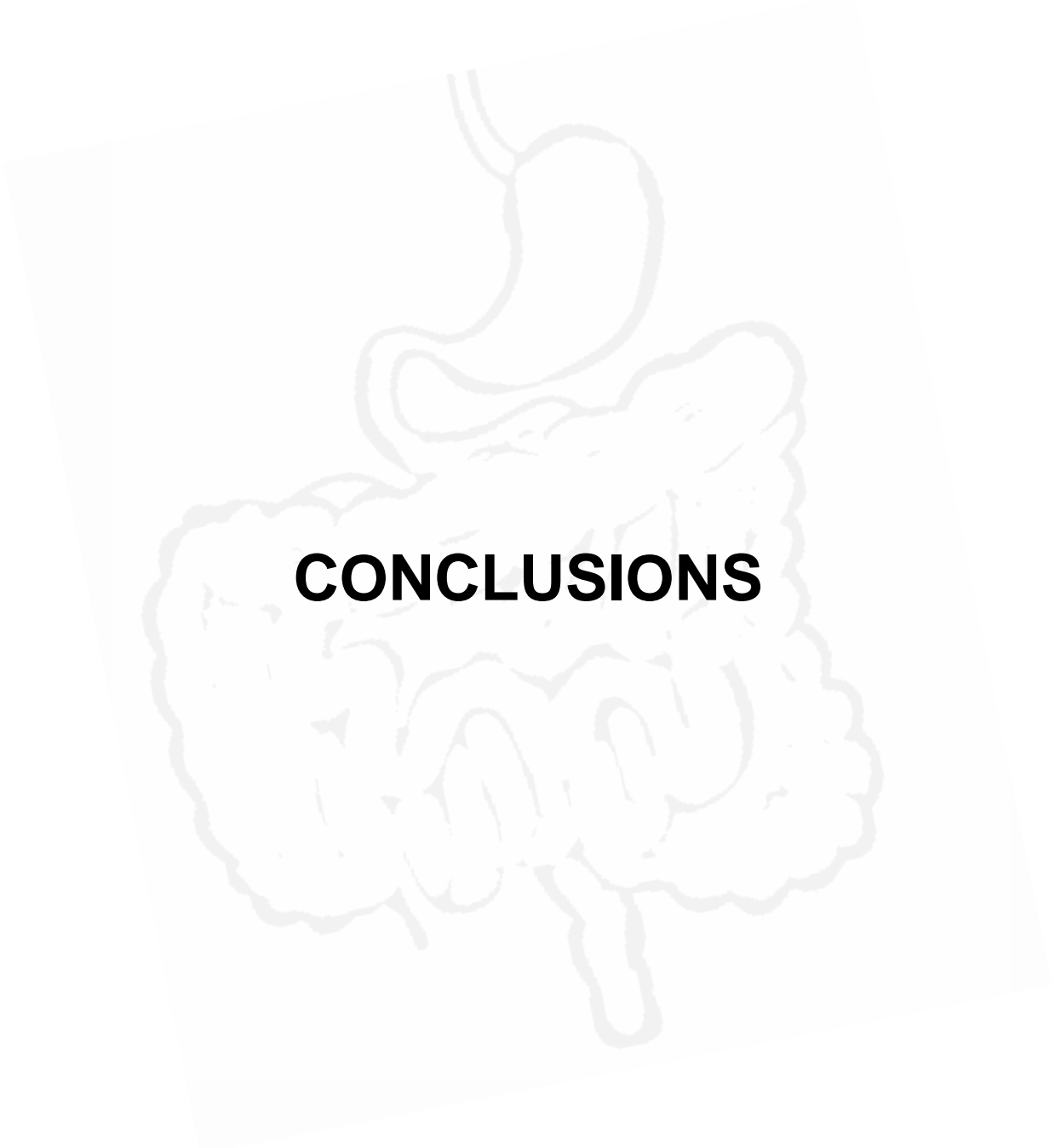
10. References

1. M.M.L. Grundy, E. Abrahamse, A. Almgren, M. Alminger, A. Andres, R.M.C. Ariëns, S. Bastiaan-Net, C. Bourliew-Lacanal, A. Brodkorb, M.R. Bronze, I. Comi, L. Couëdelo, D. Dupont, A. Durand, S.N. El, T. Grauwet, C. Heerup, A. Heredia, M.R. Infantes Garcia, C. Jungnickel, I. E. Klosowska-Chomiczweska, M. Létisse, A. Macierzanka, A.R. Mackie, D.J. McClements, O. Menard, A. Meynier, M.C. Michalski, A.I. Mulet-Cabero, A. Mullertz, F.M. Payeras Perelló, I. Peinado, M. Robert, S. Secouard, A.T. Serra, S.D. Silva, G. Thomassen, C. Tullberg, I. Undeland, C. Vaysse, G.E. Vegarud, S.H.E. Verkempinck, M. Viau, M. Zahir, R. Zhang and F. Carrière, INFOGEST inter-laboratory recommendations for assaying gastric and pancreatic lipases activities prior to in vitro digestion studies, *J. Funct. Foods*, 2021, **82**, 104497 (1 – 13).
2. S. Baliga, S. Muglikar and R. Kale, Salivary pH: A diagnostic biomarker, *J. Indian Soc. Periodontol.*, 2013, **17**, 461 – 465.
3. A. Nokhodchi, S. Raja, P. Patel and K. Asare-Addo, The role of oral controlled release matrix tablets in drug delivery systems, *BiolImpacts*, 2012, **2**, 175 – 187.
4. L. Kalantzi, K. Goumas, V. Kalioras, B. Abrahamsson, J.B. Dressman and C. Reppas, Characterization of the human upper gastrointestinal contents under conditions simulating bioavailability/bioequivalence studies, *Pharm. Res.*, 2006, **23**, 165 – 176.
5. M. Qian, R. Haser, G. Buisson, E. Duée and F. Payan, The active center of a mammalian α -amylase. Structure of the complex of a pancreatic α -amylase with a carbohydrate inhibitor refined to 2.2Å resolution, *Biochemistry*, 1994, **33**, 6284 – 6294.
6. H.H. Sky-Peck and P. Thuvasethakul, Human pancreatic alpha-amylase II: Effects of pH, substrate and ions on the activity of the enzyme, *Ann. Clin. Lab. Sci.*, 1977, **7**, 310 – 317.
7. N.E. Welker and L.L. Campbell, Comparison of the α -amylase of bacillus subtilis and bacillus amyloliquefaciens, *J. Bacteriol.*, 1967, **94**, 1131 – 1135.
8. N. Ramasubbu, V. Paloth, Y. Luo, G.D. Brayer and M.J. Levine, Structure of human salivary α -amylase at 1.6Å resolution: implications for its role in the oral cavity, *Acta Crystallogr.*, 1996, **D52**, 435 – 446.
9. J.A.L. Calbet and J.J. Holst, Gastric emptying, gastric secretion and enterogastrone response after administration of milk proteins or their peptide hydrolysates in humans, *Eur. J. Nutr.*, 2004, **43**, 127 – 139.
10. J.E. Lennard-Jones and N. Babouris, Effect of different foods on the acidity of the gastric contents in patients with duodenal ulcer, *Gut*, 1965, **6**, 113 – 117.
11. M.R. Islam, N.S. Kim, J.W. Jung, H.B. Kim, S.C. Han and M.S. Yang, Spontaneous pepsin C-catalyzed activation of human pepsinogen C in transgenic rice cell suspension culture: Production and characterization of human pepsin C, *Enzyme Microb. Technol.*, 2018, **108**, 66 – 73.
12. M. Rey, M. Yang, L. Lee, Y. Zhang, J.G. Sheff, C.W. Sensen, H. Mrazek, P. Halada, P. Man, J.L. McCarville, E.F. Verdu and D.C. Schriemer, Addressing proteolytic efficiency in enzymatic degradation therapy for celiac disease, *Sci. Rep.*, 2016, **6**, 1 – 13.
13. N.S. Andreeva and M.N.G. James, *Structure and Function of the Aspartic Proteinases*, ed. B.M. Dunn, Springer US, New York, 1st edn, 1991, **4**, 39 – 45.
14. D.M. Goldberg, R. Campbell and A.D. Roy, Fate of trypsin and chymotrypsin in the human small intestine, *Gut*, 1969, **10**, 477 – 483.
15. Y. Deng, H. Gruppen and P.A. Wierenga, Comparison of protein hydrolysis catalyzed by bovine, porcine and human trypsins, *J. Agric. Food Chem.*, 2018, **66**, 4219 – 4232.

16. W.L. McKeehan, The effect of temperature during trypsin treatment on viability and multiplication potential of single normal human and chicken fibroblasts, *Cell Biol. Int. Rep.*, 1977, **1**, 335 – 343.
17. B.J. Haverback, B. Dyce, H. Bundy and H.A. Edmondson, Trypsin, trypsinogen and trypsin inhibitor in human pancreatic juice, *The American Journal of Medicine*, 1960, **29**, 421 – 433.
18. M. Castaneda-Agulló, L. M. del Castillo, J.R. Whitaker and A.L. Tappel, Effect of ionic strength on the kinetics of trypsin and alpha chymotrypsin, *J. Gen. Physiol.*, 1961, **44**, 1103 – 1120.
19. P. Capolino, C. Guérin, J. Paume, J. Giallo, J.M. Ballester, J.F. Cavalier and F. Carrière, In vitro gastrointestinal lipolysis: replacement of human digestive lipases by a combination of rabbit gastric and porcine pancreatic extracts, *Food Dig.*, 2001, **2**, 43 – 51.
20. F. Schonheyder and K. Volqvartz, The gastric lipase in man, *Acta Physiol. Scand.*, 1946, **11**, 349 – 360.
21. M. Minekus, M. Alminger, P. Alvito, S. Ballance, T. Bohn, C. Bourlieu, F. Carrière, R. Boutrou, M. Corredig, D. Dupont, C. Dufour, L. Egger, M. Golding, S. Karakaya, B. Kirkhus, S. Le Feunteun, U. Lesmes, A. Macierzanka, A. Mackie, S. Marze, D.J. McClements, O. Ménard, I. Recio, C.N. Santos, R.P. Singh, G.E. Vegarud, M.S. Wickham, W. Weitschies and A. Brodkorb, A standardized static in vitro digestion method suitable for food – an international consensus, *Food Funct.*, 2014, **5**, 1113 – 1124.
22. F. Carrière, C. Renou, V. Lopez, J. de Caro, F. Ferrato, H. Lengsfeld, A. de Caro, R. Laugier and R. Verger, The specific activities of human digestive lipases measured from the in vivo and in vitro lipolysis of test meals, *Gastroenterology*, 2000, **119**, 949 – 960.
23. J.M. Braganza, K. Herman, P. Hine, G. Kay and G.I. Sandle, Pancreatic enzymes in human duodenal juice – a comparison of responses in secretin pancreozymin and Lundh Borgström tests, *Gut*, 1978, **19**, 358 – 366.
24. M. Armand, Lipases and lipolysis in the human digestive tract: where do we stand, *Curr. Opin. Clin. Nutr. Metab. Care*, 2007, **10**, 156 – 164.
25. M. Armand, B. Pasquier, M. André, P. Borel, M. Senft, J. Peyrot, J. Salducci, H. Portugal, V. Jaussan and D. Lairon, Digestion and absorption of 2 fat emulsions with different droplet sizes in the human digestive tract, *Am. J. Clin. Nutr.*, 1999, **70**, 1096 – 1106.
26. F. Carrière, P. Grandval, C. Renou, A. Palomba, F. Priéri, J. Giallo, F. Henniges, S. Sander-Struckmeier and R. Laugier, Quantitative study of digestive enzyme secretion and gastrointestinal lipolysis in chronic pancreatitis, *Clin. Gastroenterol. Hepatol.*, 2005, **3**, 28 – 38.
27. J. Keller and P. Layer, Human pancreatic exocrine response to nutrients in health and disease, *Gut*, 2005, **54**, 1 – 28.
28. E.L. McConnell, H.M. Fadda and A.W. Basit, Gut instincts: Explorations in intestinal physiology and drug delivery, *Int J Pharm*, 2008, **364**, 213 – 226.
29. M.R. Dukejart, S.K. Dutta and J. Vaeth, Dietary fiber supplementation: effect on exocrine pancreatic secretion in man, *Am. J. Clin. Nutr.*, 1989, **50**, 1023 – 1028.
30. E.P. DiMagno, J.R. Maragelada, L. Vay, W. Go and C.G. Moertel, Fate of orally ingested enzymes in pancreatic insufficiency, *N. Engl. J. Med.*, 1977, **296(23)**, 1318 – 1322.
31. J. A. Rendleman, Hydrolytic action of α -amylase on high-amylose starch of low molecular mass, *Biotechnol. Appl. Biochem.*, 2000, **31**, 171 – 178.
32. W. Sheldon, Congenital pancreatic lipase deficiency, *Arch. Dis. Childh.*, 1964, **39**, 268 – 271.

33. H. Holm, L.E. Hanssen, A. Krogdahl and J. Florholmen, High and low inhibitor soybean meals affect human duodenal proteinase activity differently: In vivo comparison with bovine serum albumin, *J. Nutr.*, 1988, **118**, 515 – 520.
34. J.C.M. Hafkenscheid, M. Hessels and E.W. van der Hoek, Determination of α -amylase, trypsin and lipase in duodenal fluid: Comparison of methods, *J. Clin. Chem. Clin. Biochem.*, 1983, **21**, 167 – 174.
35. K. Verhoeckx, P. Cotter, I. López-Expósito, C. Kleiveland, T. Lea, A. Mackie, T. Requena, D. Swiatecka and H. Wichers, *The Impact of Food Bioactives on Health: In Vitro and Ex Vivo Models*, Springer Open, COST Action FA1005, 2015.
36. M.S. Lewis and R.P. Junghans, *Methods in enzymology: Numerical computer methods*, ed. M.L. Johnson and L. Brand, Academic Press, United States, 1st edn, 2000, **8**, 136 – 148.
37. X. Cai, J. Yu, L. Xu, R. Liu and J. Yang, The mechanism study in the interactions of sorghum procyanidins trimer with porcine pancreatic α -amylase, *Food Chem.*, 2015, **174**, 291 – 298.
38. S. Yenjai, P. Malaikaew, T. Liwporcharoenwong and A. Buranaprapuk, Selective cleavage of pepsin by molybdenum metalloproteinase, *Biochem. Biophys. Res. Commun.*, 2012, **419**, 126 – 129.
39. S. Minning, A. Serrano, P. Ferrer, C. Solà, R.D. Schmid and F. Valero, Optimization of the high-level production of Rhizopus Oryzae lipase in Pichia pastoris, *J. Biotechnol.*, 2001, **86**, 59 – 70.
40. B. Ásgeirsson, J.W. Fox and J.B. Bjarnason, Purification and characterization of trypsin from the poikilotherm Gadus morhua, *Eur. J. Biochem.*, 1989, **180**, 85 – 94.
41. C. Gallegos, M. Turcanu, G. Assegehegn and E. Brito-de la Fuente, Rheological Issues on Oropharyngeal Dysphagia, *Dysphagia*, 2021.
42. D.D. Christianson, J.E. Hodge, D. Osborne and R.W. Detroy, Gelatinization of Wheat and Starch as Modified by Xanthan Gum, Guar Gum, and Cellulose Gum, *Cereal Chem.*, 1981, **58(6)**, 513 – 517.
43. M. Chaisawang and M. Suphantharika, Effects of guar gum and xanthan gum additions on physical and rheological properties of cationic tapioca starch, *Carbohydr. Polym.*, 2005, **61**, 288 – 295.
44. J.L. Rosenblum, C.L. Irwin and D.H. Alpers, Starch and glucose oligosaccharides protect salivary-type amylase activity at acid pH, *Am. J. Physiol.*, 1988, **254**, 775 – 780.
45. F.S. Atkinson, K. Foster-Powell and J.C. Brand-Miller, International tables of glycemic index and glycemic load values: 2008, *Diab. Care*, 2008, **31**, 2281 – 2283.
46. M. Frei, P. Siddhuraju and K. Becker, Studies on the in vitro starch digestibility and the glycemic index of six different indigenous rice cultivars from the Philippines, *Food Chem.*, 2003, **83**, 395 – 402.
47. R. Selma-Gracia, J.M. Laparra and C.M. Haros, Potential beneficial effect of hydrothermal treatment of starches from various sources on in vitro digestion, *Food Hydrocoll.*, 2020, **103**, 105687.
48. R. Quek, X. Bi and C.J. Henry, Impact of protein-rich meals on glycaemic response of rice, *Br. J. Nutr.*, 2016, **115**, 1194 – 1201.
49. M.C. Gulliford, E.J. Bicknell and J.H. Scarpello, Differential effect of protein and fat ingestion on blood glucose responses to high- and low-glycemic-index carbohydrates in noninsulin-dependent diabetic subjects, *Am. J. Clin. Nutr.*, 1989, **50**, 773 – 777.
50. F. Dehghani, M. Morvaridzadeh, A.B. Pizarro, T. Rouzitalab, M. Khorshidi, A. Izadi and J. Heshmati, Effect of extra virgin olive oil consumption on glycemic control: A systematic review and metanalysis, *Nutr. Metab. Cardiovasc. Dis.*, 2021, **31**, 1953 – 1961.

51. J.S. Kim, K. Nam and S.J. Chung, Effect of nutrient composition in a mixed meal on the postprandial glycemic response in healthy people: a preliminary study, *Nutr. Res. Pract.*, 2019, **13**, 126 – 133.
52. A. Vidrasco and L. Cosciug, The effect of technological processing on the glycaemic index of rice porridge, *Modern Technologies*, 2016, 329 – 332.
53. L. Sun, K.W.J. Tan, J.Z. Lim, F. Magkos, C.J. Henry, Dietary fat and carbohydrate quality have independent effects on postprandial glucose and lipid responses, *Eur. J. Nutr.*, 2018, **57**, 243 – 250.
54. A. Muldoon, The glycaemic index of fresh and processed potatoes, University College Cork, 2020
55. M. Leeman, E. Östman and I. Björck, Glycaemic and satiating properties of potato products, *Eur. J. Clin. Nutr.*, 2008, **62**, 87 – 95.
56. C.G. MacIntosh, S.H.A. Hold and J.C. Brand-Miller, The degree of fat saturation does not alter glycemic, insulinemic or satiety responses to a starchy staple in healthy men, *J. Nutr.*, 2003, **133**, 2577 – 2580.
57. E. Gatti, D. Noe, F. Pazzucconi, G. Gianfranceschi, M. Porrini, G. Testolin and C.R. Sirtori, Differential effect of unsaturated oils and butter on blood glucose and insulin response to carbohydrate in normal volunteers, *Eur. J. Clin. Nutr.*, 1992, **46**, 161 – 166.
58. A. Pederson, P. Marckmann and B. Sandstrom, Postprandial lipoprotein, glucose and insulin responses after two consecutive meals containing rapeseed oil, sunflower oil or palm oil with or without glucose at the first meal, *Br. J. Nutr.*, 1999, **82**, 97 – 104.



CONCLUSIONS

CONCLUSIONS

This research aimed to fill the gaps found in in vitro digestion methods with regards to starch digestion to obtain a strong in vivo-in vitro correlation, and also to study the starch digestion and the effect of other macronutrients on the digestion of carbohydrates.

Two in vitro digestion methods were selected for the study of carbohydrate digestion; static and dynamic methods. Four digestive enzymes (α -amylase, pepsin, trypsin, lipase) were chosen to carry out these methods.

Based on the results obtained in this work, the following conclusions can be stated:

1. The main critical points of the methods for the enzyme activity determination were identified and solved. The importance of working with an excess of substrate for the correct enzyme activity determination was proved by measuring the specific activity ($\text{mg}\cdot\text{mL}^{-1}$) at different enzyme:substrate ratios.
 - For α -amylase activity determination, the best conditions for the complete solubilization of the enzyme and substrate were found (enzyme: RT, 300 rpm, 5 min; substrate: 95°C, 300 rpm, 5 min). The incubation method to perform the hydrolysis and colour development was also identified by measuring the activity with different devices (hydrolysis: thermoshaker at 20°C, 1000 rpm; colour development: thermoshaker at 95°C, motionless).
 - The critical point studied for the correct pepsin activity determination was the precipitate removal that is formed when the hydrolysis is stopped. Although both, centrifugation and filtration provided similar results, centrifugation was chosen for its simplicity.
 - The best methodology for the reagent addition (critical point) in the lipase activity measurement was forward pipetting and then a rinse, which also helped its emulsification in the aqueous phase. The optimal flow rate was different depending on the kind of lipase that was analysed; lipase with high (max flow rate: $2.2 \text{ mL}\cdot\text{min}^{-1}$, min flow rate: $5.0 \mu\text{L}\cdot\text{min}^{-1}$) or low activity (max flow rate: $0.3 \text{ mL}\cdot\text{min}^{-1}$, min flow rate: $0.2 \mu\text{L}\cdot\text{min}^{-1}$).
 - The participation in a ring trial (21 international laboratories) on the lipase activity determination organised by the working group 4 of the Infogest group helped to identify some critical points of the lipase activity which were studied and solved. A final detailed protocol was reached and published (1).
2. Alternative sources to human digestive enzymes were successfully identified for their suitability to be used in in vitro digestion methods.
 - α -amylase from porcine pancreas is a good alternative to human α -amylase; it was less active in the absence of electrolytes ($6.8 \pm 0.3 \text{ AU}\cdot\text{mg}^{-1}$), while in the presence of simulated salivary fluid at 20°C, the enzyme activity increased ($10.0 \pm 0.5 \text{ AU}\cdot\text{mg}^{-1}$).
 - Pepsin from porcine gastric mucosa is a good alternative to human pepsin; pepsin activity was not affected by the presence ($2239.0 \pm 283.1 \text{ PU}\cdot\text{mg}^{-1}$) or absence ($2520.5 \pm 100.7 \text{ PU}\cdot\text{mg}^{-1}$) of electrolytes.
 - Trypsin from bovine pancreas is a good alternative to human trypsin; trypsin activity decreased in the presence of electrolytes, showing only 51% and 55% of the activity in the absence of electrolytes at 25 and 37°C, respectively.
 - The rabbit gastric lipase, a usual alternative source to mimic human gastric lipase, is expensive. Lipase from *Rhizopus Oryzae* was selected as an alternative to the human gastric lipase; the presence or absence of electrolytes did not affect lipase activity (no electrolytes: $16.7 \pm 2.4 \text{ LU}\cdot\text{mg}^{-1}$; electrolytes: $18.9 \pm 3.2 \text{ LU}\cdot\text{mg}^{-1}$).

- Porcine pancreatin (from Nordmark) mixed with individual enzymes (α -amylase from porcine pancreas, trypsin from bovine pancreas) with a final specific ratio (α -amylase : trypsin : lipase – 2 : 1 : 2) was chosen to mimic the physiological levels of the enzymes in the small intestine.
 - The presence of electrolytes did not affect the activity of the α -amylase, trypsin or lipase present in the pancreatin.
 - The maximum storage time of the enzymatic solutions was identified.
 - The α -amylase solution prepared with deionized (DI) water as the solvent could be used for the in vitro digestion methods only during the first 6 months after its preparation (stored at -20°C). Beyond that time it lost its activity. However, when it was dissolved in simulated salivary fluid (pH 7), its activity was about 100 % during 9 months after its preparation.
 - When the proteases (pepsin, trypsin) and the lipase were dissolved in DI water, the activity remained constant for one year (stored at -20°C). However, when the solutions were prepared using the simulated digestive fluids, they partly or completely ceased to be active. Pepsin activity prepared using the simulated gastric fluid (pH 3) remained constant for 8 months. Lipase also dissolved in simulated gastric fluid (pH 3), lost all its activity during the first month. Finally, the trypsin solution prepared in simulated intestinal fluid (pH 7) remained active for 3 months.
3. Non-enzymatic key parameters of in vitro methods were also defined.
- For the static in vitro digestion method, the optimal speed of the thermoshaker where the in vitro digestion took place was defined: 400 rpm.
 - A method to stop the starch digestion after each sampling point was identified: thermal treatment (5 min at 100°C (boiling water bath)) followed by sample freezing.
 - For the static in vitro digestion method, a buffer and its optimal concentration were selected to keep the pH of the intestinal phase constant (physiological pH): bicarbonate buffer 1 M.
 - No significant differences were found between the viscosity of the meals.
4. The in vivo-in vitro correlation of the selected in vitro digestion methods (static and dynamic) was proven for different foods (rice, potato, cocoa cream) by comparing the measured glycaemic index with the reported values. The correlation only failed for the cocoa cream when the glycaemic index was determined with the dynamic digestion method, as the measured value was lower compared with the reported glycaemic index.
5. The glycaemic index (GI) and the degree of hydrolysis (DH) were obtained for different starchy meals.
- In vitro digestion of starch:
 - The differences between the digestion of two starch sources (starch from rice and starch from potato) were identified. In the static digestion method, the differences observed after the oral and gastric phases (DH of the starch from rice was higher than DH of starch from potato) were triggered by the differences in the solubilization of the meals with the secretions during the first part of the digestion. Once it reached the intestinal phase the measured DH was similar in both the starches (starch from rice: $58.8 \pm 3.6 \%$; starch from potato: $51.9 \pm 4.6 \%$). No significant differences were found between the GI measured for the starch from rice ($59.3 \pm 2.3 \%$) and starch from potato ($52.0 \pm 3.6 \%$).

- Impact of protein on starch digestion:
 - When the DH and GI for the rice starch and for the meal containing rice starch and chicken egg whites (DH: 67.1 ± 1.8 %; GI: 55.5 ± 4.8 %) were compared, no effect of the protein was observed, leading to the conclusion that the selected protein source did not affect the digestion of rice starch.
 - When the protein source (chicken egg whites) was added to the potato starch, the digestion was faster and the measured GI was higher (73.1 ± 2.8 %) compared with the meal that only contained the starch (52.0 ± 3.6 %). This difference could be due to the higher consistency of potato starch compared with the meal that contained starch and chicken egg whites.
- Impact of fat on starch digestion:
 - No differences were observed when olive oil was added to rice starch: the measured DH (rice starch and olive oil: 59.1 ± 2.8 %) or GI (rice starch and olive oil: 52.3 ± 2.3 %).
 - A small DH decrease after the oral and gastric phases was observed when butter was added to rice starch. During the intestinal phase, the DH obtained for both meals (without and with butter) were not different (rice starch with butter: 67.9 ± 3.6 %). The amount of glucose released during the in vitro digestion was the same for both meals, and therefore no fat-effect was seen on the measured GI (rice starch with butter: 57.6 ± 4.4 %).
 - The olive oil did not exhibit any effect on the digestion of potato starch (DH: 51.6 ± 2.1 %; GI: 58.6 ± 3.8 %).
 - Butter caused an increase in potato starch digestion, mainly during the oral and gastric phases (DH: 62.4 ± 0.9 %), which could be triggered by the disintegration of the meal with the secretions. Almost 75 % of potato starch mixed with butter was solubilised with saliva after the oral phase, but only about 10 % of the potato starch alone. However, the addition of butter to the potato starch did not affect the GI (63.1 ± 2.7 %), which could be explained because the GI was calculated only with the amount of glucose released during the intestinal phase.
- Impact of food matrix on starch digestion:
 - The effect of the complex matrix on the digestion of starch was studied by mixing the three macronutrients (protein, fat and carbohydrate). The effect of olive oil and egg whites on the digestion of rice starch was checked. The selected matrix did not exhibit any effect on the digestion of the rice starch as no differences between DH (56.8 ± 0.6 %) or GI (65.0 ± 4.0 %) were found.
 - The addition of egg whites and olive oil caused an increase in the potato starch digestion DH (58.3 ± 2.0 %) and GI (76.7 ± 3.9 %). This could be explained by the decrease in viscosity when the protein and fat sources were added, which favoured the dissolution of the meal in the secretions.
 - The egg whites and butter did not affect the digestion of the rice starch (DH: 51.2 ± 1.1 %, GI: 59.4 ± 4.2 %).
 - The matrix obtained by mixing butter and egg whites with starch potato favoured the digestion, as the measured DH (60.7 ± 0.8 %) and GI (86.1 ± 3.5 %) for the complex meal was higher compared with the DH and GI measured for the potato starch.

- In vitro digestion method comparison for the digestion of starchy meals
 - o No differences were found between the DH/GI measured with both methods. Taking into account that the static digestion method is faster and easier to use, it could be concluded that this method is a useful tool to screen a large number of meals or to measure end-points like GI. As digestion can be followed through the gastrointestinal tract with the dynamic digestion method, this method could be used to gain more detailed information on the digestion of the selected meals.

1. M.M.L. Grundy, E. Abrahamse, A. Almgren, M. Alminger, A. Andres, R.M.C. Ariëns, S. Bastiaan-Net, C. Bourlieu-Lacanal, A. Brodkorb, M.R. Bronze, I. Comi, L. Couëdelo, D. Dupont, A. Durand, S.N. El, T. Grauwet, C. Heerup, A. Heredia, M.R. Infantes Garcia, C. Jungnickel, I. E. Klosowska-Chomiczweska, M. Létisse, A. Macierzanka, A.R. Mackie, D.J. McClements, O. Menard, A. Meynier, M.C. Michalski, A.I. Mulet-Cabero, A. Mullertz, F.M. Payeras Perelló, I. Peinado, M. Robert, S. Secouard, A.T. Serra, S.D. Silva, G. Thomassen, C. Tullberg, I. Undeland, C. Vaysse, G.E. Vegarud, S.H.E. Verkempinck, M. Viau, M. Zahir, R. Zhang and F. Carrière, INFOGEST inter-laboratory recommendations for assaying gastric and pancreatic lipases activities prior to in vitro digestion studies, *J. Funct. Foods*, 2021, **82**, 104497 (1 – 13).